

**Influence of Kinematics on the Calculation of Hip
Joint Reaction Forces in Patients with
Symptomatic Leg Length Inequality following
Total Hip Replacement**

Ammar Wahid

Submitted in accordance with the requirements for the
degree of Doctor of Philosophy

The University of Leeds
School of Mechanical Engineering

August 2016

The candidate confirms that the work submitted is his own and that appropriate credit has been given where reference has been made to the work of others.

This copy has been supplied on the understanding that it is copyright material and that no quotation from the thesis may be published without proper acknowledgement.

©2016 The University of Leeds and Ammar Wahid

The right of Ammar Wahid to be identified as Author of this work has been asserted by him in accordance with the Copyright, Designs and Patents Act 1988.

Acknowledgements

I would like to express my gratitude to my supervisor Dr. Todd Stewart for his continued support, patience and enthusiasm for the subject area throughout the course of my research. In particular I am thankful for the immense amount of knowledge he has given me in the field of engineering and the critical thinking skills he has helped me develop.

I appreciate the help of Dr. Neil Messenger during my PhD in understanding the complexities of human biomechanics. Neil was instrumental in critiquing both my methods and research results and I am thankful for the time he spent supervising me.

My thanks also extend to Dr. Junyan Li and Dr. Bobin Varghese for the support and resources they provided whilst they were students at The University of Leeds. I greatly appreciate the help of Dr. Graham Chapman from Chapel Allerton Hospital for his meticulous approach to research and his tutoring on Visual3D. I would like to also make special mentions to Professor Anthony Redmond, Mr. Martin Stone, Michael Ferrandino and Brendan McDermott.

I am grateful to my Doctoral Training Centre colleagues who made my time in Leeds enjoyable and also to the EPSRC for funding my PhD. In particular, I am grateful of the opportunity given to me by the Doctoral Training Centre to study at the interface of biology, chemistry, biomechanics and engineering. I am also thankful for the opportunities I had to travel to Griffith University in Australia and Aalborg University in Denmark to further explore my research area.

Lastly, I would like to say thank you to my family who have always been there supporting me during the ups and downs of my PhD. Without your support and encouragement, I would not be where I am today.

Abstract

Up to 10% of patients following Total Hip Replacement (THR) are symptomatic for a Leg Length Inequality (LLI), commonly being up to 20mm longer on the operated side. With 100,000 patients undergoing THR in 2015, 8.7% of all errors in the NHS being attributed to an LLI and malpractice claims being frequent, understanding why certain patients are symptomatic whilst others remain asymptomatic is of great importance.

Anthropometric and demographic measurements together with gait analysis results were compared between a group of 26 symptomatic LLI patients following THR, 14 asymptomatic THR patients and 38 healthy individuals using Plug-in-Gait. Statistically significant results were found for height, with LLI patients generally being 6% shorter than their THR counterparts. Gait analysis results using Visual3D and AnyBody found LLI patients demonstrated reductions in peak joint forces, ground reaction forces, moments and knee flexion relative to the THR and healthy group. This was linked to LLI patients walking 20% and 59% slower than their THR and healthy counterparts respectively. Wear analysis found that LLI patients had 9% greater sliding distances than THR patients per stride together with more unidirectional motion paths.

A thorough critique of Plug-in-Gait found the clinical results were generally reliable. Further sensitivity analyses however highlighted the weaknesses of the model if used improperly, with a 45mm error in lateral thigh marker positioning leading to a 10% change in hip flexion angle. The choice of hip joint centre regression equation, errors in joint width measurement and the use of CAST over PiG were also found to have a profound effect on kinematic results.

It was concluded that LLI patients were symptomatic due to a combination of a greater LLI magnitude to height ratio, leading to greater pelvic obliquity in smaller individuals, and weakened muscles/soft tissues at the hip causing an asymmetric gait.

Contents

List of Figures	xii
List of Tables	xxxii
1 <u>Introduction</u>	1
2 <u>Literature Review</u>	4
2.1 Normal People	4
2.1.1 Hip Anatomy	4
2.1.2 Muscles at the Hip	5
2.1.3 Gait	7
2.1.4 Measuring Gait	8
2.1.5 Gait Kinematics	11
2.1.6 Gait Kinetics	14
2.1.7 Temporal-Spatial Parameters	19
2.2 Total Hip Replacement Patients	23
2.2.1 Etiology	23
2.2.2 Gait	23
2.2.3 Gait Kinematics	24
2.2.4 Gait Kinetics	27
2.2.5 Temporal-Spatial Parameters	30
2.3 Leg Length Inequality Patients	32
2.3.1 Etiology	32
2.3.2 Risk Factors, Clinical Symptoms and Treatment	34
2.3.3 Radiographic Measurement of LLI	36
2.3.4 Hip Joint Centre	37
2.3.5 Gait Kinematics	38
2.3.6 Gait Kinetics	39
2.3.7 Temporal-Spatial Parameters	40
2.4 Computational Modelling of Gait	41
2.4.1 The Conventional Gait Model	41
2.4.2 Hip Joint Centre Estimation	42
2.4.3 Soft Tissue Artefact	45

2.5	Rigid Body Modelling	46
2.5.1	Muscle Recruitment	48
2.5.2	Muscle Geometry	50
2.5.3	Sensitivity	52
2.5.4	Model Comparison	53
2.6	Biotribology	55
2.6.1	Archard Equation	55
2.6.2	Hertz Contact Theory	56
2.6.3	Cross Shear	57
2.6.4	Contact Surface Motion Paths	58
2.6.5	Aspect Ratios	60
2.6.6	Lubrication	61
2.7	Summary of Literature	64
2.8	Study Objectives	67
3	<u>Generic Methods - Implementing PiG in Visual3D and AnyBody</u>	69
3.0.1	Plug-in-Gait	69
3.0.2	Visual3D	77
3.0.3	AnyBody	85
3.0.4	Statistics	89
4	<u>Anthropometrics & Demographics</u>	90
4.1	Aims & Objectives	90
4.2	Methodology	90
4.2.1	Initial Clinical Method	90
4.2.2	Non-Clinical Method	92
4.2.3	Clinical Method	92
4.3	Results - Anthropometrics	97
4.3.1	Femoral Offset	97
4.3.2	Inter-Hip Centre Distance	98
4.3.3	Cup Inclination Angle	98
4.3.4	Leg Length Difference	99
4.4	Results - Demographics	101
4.5	Discussion	101

4.5.1	Leg Length Difference	101
4.5.2	Height	103
4.6	Conclusion	104
5	<u>Kinematics & Temporal-Spatial Parameters</u>	105
5.1	Aims & Objectives	105
5.2	Methodology	105
5.2.1	Initial Clinical Method	105
5.2.2	Non-Clinical Method	106
5.3	Results - Dynamic Joint & Segment Angles	110
5.3.1	Pelvic Obliquity	110
5.3.2	Pelvic Rotation	112
5.3.3	Hip Flexion-Extension	114
5.3.4	Hip Abduction-Adduction	117
5.3.5	Knee Flexion-Extension	120
5.3.6	Ankle Dorsi-Plantar Flexion	123
5.4	Results - Gait Events	126
5.4.1	Heel Strike	126
5.4.2	Mid-Stance	127
5.4.3	Toe Off	128
5.5	Results - Standing Joint Angles	129
5.6	Results - Temporal-Spatial Parameters	130
5.6.1	Raw Results	130
5.6.2	Temporal-Spatial Symmetry	131
5.7	Discussion	131
5.7.1	Dynamic Joint & Segment Angles	131
5.7.2	Temporal-Spatial Parameters	139
5.7.3	Standing Joint Angles	140
5.7.4	Errors in Results	140
5.8	Conclusion	141
6	<u>Kinetics</u>	142
6.1	Aims & Objectives	142
6.2	Methodology	142

6.2.1	Initial Clinical Method	142
6.2.2	Non-Clinical Method	142
6.3	Results - Ground Reaction Force	145
6.4	Results - Hip Joint Reaction Force	150
6.5	Results - Joint Moments	156
6.5.1	Hip Flexion-Extension	156
6.5.2	Hip Abduction-Adduction	158
6.5.3	Knee Flexion-Extension	160
6.5.4	Ankle Dorsi-Plantar Flexion	162
6.6	Results - Gait Events (Moments)	164
6.6.1	Heel Strike	164
6.6.2	Mid-Stance	164
6.6.3	Toe Off	165
6.7	Discussion	166
6.7.1	Comparing to Literature I	167
6.7.2	Comparing to Literature II	169
6.7.3	Vertical Ground Reaction Force	170
6.7.4	Hip Joint Reaction Force	173
6.7.5	Joint Moments	175
6.7.6	Errors in Results	178
6.8	Conclusion	178
7	<u>Critiquing Clinical Results</u>	180
7.1	Rationale	180
7.2	Aims & Objectives	181
7.3	Methodology	182
7.3.1	Subject	182
7.3.2	Gait Analysis	182
7.3.3	Body Model	182
7.4	Results - Standing Segment Angles	184
7.5	Methodology II	185
7.5.1	Subject	185
7.5.2	Gait Analysis	185
7.5.3	Body Model	185

7.6	Results - Effect on Kinematics & Kinetics	185
7.7	Discussion	197
7.8	Conclusion	198
8	<u>A Critique of PiG - I</u>	200
8.1	Aims & Objectives	200
8.2	Methodology	200
8.2.1	Subject	200
8.2.2	Gait Analysis	200
8.2.3	Body Model	200
8.2.4	Hip Joint Centre	201
8.2.5	Joint Radius	201
8.3	Results - Hip Centre Regression Equation - Standing Trial	202
8.4	Results - Hip Centre Regression Equation - Dynamic Trial	203
8.4.1	Hip	203
8.4.2	Knee	205
8.4.3	Ankle	208
8.5	Discussion I	210
8.6	Results - Knee Joint Radius Standing Trial	215
8.7	Results - Knee Joint Radius Dynamic Trial	217
8.7.1	Hip	217
8.7.2	Knee	218
8.7.3	Ankle	219
8.8	Discussion - II	221
8.9	Results - Ankle Joint Radius Standing Trial	222
8.10	Results - Ankle Joint Radius Dynamic Trial	223
8.10.1	Hip & Knee	223
8.10.2	Ankle	223
8.11	Discussion - III	225
8.12	Conclusion	226
9	<u>A Critique of PiG - II</u>	228
9.1	Aims & Objectives	228
9.2	Methodology	228

9.2.1	Subject	228
9.2.2	Gait Analysis	228
9.2.3	Body Model	229
9.2.4	Processing	229
9.3	Results - Lateral Thigh Marker	231
9.3.1	Hip	231
9.3.2	Knee	232
9.3.3	Ankle	235
9.4	Results - Lateral Shank Marker	237
9.4.1	Hip	237
9.4.2	Knee	237
9.4.3	Ankle	238
9.5	Discussion	240
9.6	Conclusion	242
10	<u>A Comparison between PiG & CAST</u>	243
10.1	Aims & Objectives	243
10.2	Methodology I	243
10.2.1	Subject	243
10.2.2	Gait Analysis	243
10.2.3	Body Model	245
10.3	Results	246
10.3.1	Hip	246
10.3.2	Knee	247
10.3.3	Ankle	250
10.4	Discussion I	252
10.5	Methodology II	254
10.5.1	Subject	254
10.5.2	Gait Analysis	254
10.5.3	BodyModel	255
10.6	Results - Joint Reaction Forces	255
10.7	Discussion II	256
10.8	Conclusion	257

11 <u>Contact Surface Motion Paths</u>	259
11.1 Aims & Objectives	259
11.2 Methodology	259
11.2.1 Clinical Method	259
11.2.2 Non-Clinical Method	259
11.3 Results - Wear	265
11.4 Results - Motion Paths	268
11.5 Results - Film Thickness	271
11.6 Discussion	271
11.6.1 Sliding Distance/Sliding Velocity	271
11.6.2 Cross Shear/Aspect Ratio	272
11.6.3 Lubrication	273
11.7 Conclusion	274
12 <u>Discussion</u>	275
12.1 Background	275
12.2 Objective 1	275
12.3 Objective 2	277
12.4 Objective 3	283
12.5 Objective 4	286
12.6 Concluding Remarks	288
12.6.1 Proposition 1	288
12.6.2 Proposition 2	289
12.6.3 Proposition 3	290
12.6.4 Proposition 4	292
12.7 Summary	293
12.8 Future Work	293
13 <u>Conclusion</u>	295
14 References	296
15 Appendix I	339
16 Appendix II	341

List of Figures

1	Three different hip prosthesis femoral offsets. A femoral offset is defined as the perpendicular distance between the centre of hip rotation and the line passing through the long axes of the femoral stem.	1
2	Hip Joint Anatomy	4
3	The hip abductors from the posterior and lateral views	5
4	The derivation of a muscle moment arm	6
5	The gait cycle	8
6	Two different marker sets. A marker set based on a combination of individual markers and clusters (left) and a marker set consisting of only individual markers (right)	9
7	A typical laboratory setup with the PiG marker set	10
8	The three planes of motion	13
9	GRFs in the vertical, medial-lateral and anterior-posterior directions	15
10	Hip joint forces during gait with S-I (Superior-Inferior), A-P (Anterior-Posterior), M-L (Medial-Lateral) and Resultant forces represented - Paul (1967)	17
11	Total Hip Replacement Components	23
12	A schematic showing the anterior, lateral and posterior incision sites for a THR	26
13	The black line denotes the average THR force computed by Li et al. whilst all other lines denote individual patient results during gait at a self-selected speed by Bergmann et al.	28
14	The typical stance adopted by an individual with an LLI with the longer leg flexed to accommodate its change in length	33
15	Two of the commonly used leg length measuring techniques on radiographs	37
16	ISB recommended joint coordinate axes	41
17	The CAST model as originally defined by Benedetti et al.	43
18	Lines used to represent muscles in AnyBody	51
19	An illustration of the contact area between the femoral head and acetabular cup. The contact area will change overtime with the varying levels of joint force.	57
20	The Great Circle illustrated together with two smaller circles which cannot be classified as Great Circles	58
21	Image (A) shows where the Ramamurti points are located relative to the shape of the femur whilst (B) shows how the points are located with respect to each other on the femoral head viewed from directly above the apex of the femoral head	59

22	Image (a) shows motion paths over the femoral head produced computationally (b) shows motion paths as produced by a hip simulator when a method is used to track the loci during the gait cycle	60
23	A typical image of the aspect ratio. This image shows a 2D representation of a 3D motion path	61
24	A schematic demonstrating fluid entrainment and the dragging of fluid into the contact area between the surfaces	62
25	The Stribeck curve	63
26	The Plug-in-Gait marker set with the marker names which are conventionally used. The left image gives the front view of the marker positions whilst the right image the back view.	69
27	(a) - The KJC is computed using the HJC, lateral thigh marker and lateral knee marker plane together with the knee width via the chord function. (b) - The AJC is computed using the KJC, lateral shank marker and lateral ankle marker plane together with the ankle width via the chord function.	71
28	A patient with a KAD. A virtual knee marker is assumed to exist equidistant from the 3 markers on the device. The direction formed by the line passing through the virtual knee marker and the knee wand marker(both circles) is the knee flexion-extension axis	71
29	The effects of thigh marker positioning on the KJC. A more anterior thigh marker leads to a more posterior KJC whilst a more posterior thigh marker leads to a more anterior KJC. The same could be said for the relationship between the lateral shank marker and the AJC.	72
30	Schematic representing the potential positions of the KJC/AJC in the knee/ankle joint as viewed from above the joint. The edges of the sphere represent all the positions that the KJC/AJC can take through the joint width measurement. The effects of the plane which is used to compute the distal joint centre can be seen, with a joint centre which is more anterior also moving laterally due to the clinically measured joint width.	73

-
- 31 Schematic representing the potential positions of the KJC/AJC in the knee/ankle joint as viewed from the front of the joint. The edges of the sphere represent all the positions that the KJC/AJC can take through the joint width measurement. The effects of the plane which is used to compute the distal joint centre can be seen, with a joint centre which is more anterior also moving either superior or inferior due to the clinically measured joint width. 73
- 32 The symbols Φ and Ψ represent angles formed between the lateral knee marker and different KJC's, which is equivalent to the rotation of the thigh. As can be seen, a more anterior KJC leads to a greater angle between the KJC and lateral knee marker (measured between the anterior-posterior directions), causing external rotation of the thigh. The same could be said of the lateral shank marker and AJCs positions. . . . 74
- 33 The leg in the diagram is assumed to be a left leg. (A) represents an internally rotated thigh due to anterior positioning of the lateral thigh marker, (C) represents a externally rotated thigh due to posterior placement of the lateral thigh marker, (B) represents a natural joint axes orientation. The red axes represents flexion-extension, with an anterior rotation of the axes being flexion and a posterior rotation being extension. The green axes represents abduction-adduction, with a medial rotation of the axes being adduction and a lateral rotation being abduction. The blue axes represents internal-external rotation. Changes in the orientation of the axes redefine where each motion is measured from and hence leads to cross-talk between axes. . . . 75
- 34 The effects of joint centre offset on kinematics and kinetics. A more medial KJC in the standing trial leads to an adduction offset at the distal portion of the thigh and an abduction offset at the proximal portion. 76

35	A top view of the foot, with ankle, toe and AJC markers. The foot is defined from the AJC/AJC2 to the toe marker. An AJC positioned more medial, lateral, anterior or posterior to the original position will alter the amount of foot rotation. A more medial AJC, such as AJC2 in schematic B relative to AJC1, leads to greater external rotation whilst a more lateral AJC would lead to a more internally rotated foot. Likewise, a more anterior or posterior AJC is also likely to lead to errors in rotation but is itself dependent on the amount of medial or lateral error. For instance in schematic (A), an error in only the anterior or posterior directions will have no effect as the AJC and toe marker are parallel. If they were not parallel, an anterior or posterior offset would cause a change in foot rotation. Changes in the position of the AJC/AJC2 also effect the foots relationship with the heel marker, which defines the foot medial-lateral tilt.	76
36	A static trial in Visual3D with segment definitions of the pelvis, thigh, shank and foot	79
37	The Davis pelvis as defined in Visual3D	79
38	A schematic of a pelvis with the pelvic marker placements and the origin as defined as half way between RASI and LASI	80
39	Measurements of ASIS distance are taken as the medial-lateral distance of the centre of the RASIS (Right Anterior Superior Iliac Spine) marker and the centre of the LASIS (Left Anterior Superior Iliac Spine) marker. Pelvic depth is computed as the average distance between the RASIS and RPSIS (Right Posterior Superior Iliac Spine) markers and the LASIS and LPSIS (Left Posterior Superior Iliac Spine) markers	81
40	Schematic demonstrating the anthropometric measurements used by Davis in formulating their HJC equation	82
41	The creation of the thigh segment, with the RTHI and RKNE markers coloured yellow.	83
42	The creation of the shank segment, with the lateral shank and lateral ankle markers coloured yellow.	84
43	The creation of the foot segment, with the ankle centre, heel and toe markers coloured yellow.	85
44	Model marker and experimental marker positions in the loaded AnyBody model . .	86
45	A radiograph of a LLI patient with the calibration ball labelled.	93

46	Derivation of the HJC through the use of bisecting lines over the femoral head of the hip implant. The horizontal line crosses from the most medial to the most lateral portion of the femoral head whilst the vertical line crosses from the most superior to the most inferior. Image analysis undertaken for this illustration in Coreldraw and represents what occurred in PACS	94
47	Calculation of inter-hip distance on a radiograph using Coreldraw, representative of PACS.	94
48	Calculation of femoral offset on a radiograph. The HJC position was computed first, with a line then drawn from the HJC to the line passing through the long axis of the femur, meeting at a right angle. In this Figure, the green line denotes the femoral offset.	95
49	Calculation of cup inclination angle on a radiograph using CorelDraw, representing how measurements were undertaken in PACS.	95
50	Calculation of leg length using the McWilliams method on a radiograph. C^A and S^A represent artificial cup and stem length respectively with C^N and S^N representing the natural cup and stem length. O^A and O^N represent the overall length found through the addition of the C^A and S^A and C^N and S^N measurements.	96
51	Average femoral offset compared between the LLI and Happy THR groups together with standard errors.	97
52	Average inter HJC distance compared between the LLI and Happy THR groups together with standard errors	98
53	Average cup inclination angles compared between the LLI and Happy THR groups together with standard errors	99
54	Comparison of the leg length differences of the LLI group to the Happy THR group, where the latter is split into results with an increase in operated leg length and a decrease. Standard errors are included.	100
55	Average absolute differences in cup height and stem length between the operated and non-operated sides of each group. Standard errors are included.	100
56	Pelvic obliquity levels when there is zero obliquity (A) and when there is positive obliquity (B) with the operated side lifted upwards.	101
57	The effect that varying the leg length difference has on pelvic obliquity angle as a function of inter-hip distance	102

58	The effect that varying leg length differences have on pelvic obliquity angle for both the LLI and Happy THR groups	103
59	The image on the left shows the identification of heel strike on the force plate with the initial force vector produced. The image on the right shows the identification of toe off with the terminal force vector produced.	108
60	Average pelvic operated side superior obliquity (+) & inferior obliquity (-) angles together with 95% confidence intervals over a normalised gait cycle between consecutive heel strikes of the same foot. The dashed lines represent the associated confidence intervals for each sample.	110
61	Raw pelvic operated side superior(+) and inferior(-) obliquity angle results for all three groups over a normalised gait cycle between consecutive heel strikes of the same foot. (A) Operated side LLI patients (B) Operated side Happy THR patients (C) Normal Healthy Patients. The blue curve in each graph is the same and represents the average pelvic obliquity for the Normal group	111
62	Schematic demonstrating the physical characteristics of pelvic internal-external rotation. Positive internal rotation (a) was taken to be the anterior rotation of the operated sided pelvis whilst external rotation (b) was posterior rotation of the operated sided pelvis	112
63	Average pelvis operated side anterior rotation (+) & posterior rotation (-) angles together with 95% confidence intervals over a normalised gait cycle between consecutive heel strikes of the same foot. The dashed lines represent the associated confidence intervals for each sample.	113
64	Raw operated side anterior rotation (+) & posterior rotation (-) angle results for all three groups over a normalised gait cycle between consecutive heel strikes of the same foot. (A) Operated side LLI patients (B) Operated side Happy THR patients (C) Normal healthy patients. The blue curve in each graph is the same and represents the average pelvic rotation for the Normal group	113
65	Schematic demonstrating the physical characteristics of hip flexion-extension. Anterior movement of the thigh relative to the pelvis was referred to as hip flexion whilst posterior movement of the thigh relative to the pelvis was referred to as hip extension.	114
66	Average hip flexion (+) extension (-) angles together with 95% confidence intervals over a normalised gait cycle between consecutive heel strikes of the same foot. The dashed lines represent the associated confidence intervals for each sample.	115

67	Raw hip flexion (+)-extension (-) angle results for all three groups over a normalised gait cycle between consecutive heel strikes of the same foot. (A) Operated side LLI patients (B) Non-operated side LLI patients, (C) Operated side Happy THR patients (D) Non-operated side Happy THR patients (E) Normal healthy patients. The blue curve in each graph is the same and represents the average hip flexion-extension for the Normal group	116
68	Schematic demonstrating the physical characteristics of hip abduction-adduction. The lateral movement of the thigh with respect to the pelvis away from the mid-line of the body was referred to as hip abduction. The medial movement of the thigh with respect to the pelvis towards the mid-line of the body was referred to as hip adduction.	117
69	Average hip abduction (+) adduction (-) angles together with 95% confidence intervals over a normalised gait cycle between consecutive heel strikes of the same foot. The dashed lines represent the associated confidence intervals for each sample. . . .	118
70	Raw hip abduction (+)-adduction (-) angle results for all three groups over a normalised gait cycle between consecutive heel strikes of the same foot. (A) Operated side LLI patients (B) Non-operated side LLI patients, (C) Operated side Happy THR patients (D) Non-operated side Happy THR patients (E) Normal healthy patients. The blue curve in each graph is the same and represents the average hip abduction-adduction for the Normal group	119
71	Schematic demonstrating the physical characteristics of knee flexion-extension. The posterior movement of the shank relative to the thigh is referred to as flexion and the anterior movement of the shank relative to the thigh is referred to as extension. . . .	120
72	Average knee (+) extension (-) angles together with 95% confidence intervals over a normalised gait cycle between consecutive heel strikes of the same foot, The dashed lines represent the associated confidence intervals for each sample.	121
73	Raw knee flexion (+)-extension (-) angle results for all three groups over a normalised gait cycle between consecutive heel strikes of the same foot. (A) Operated side LLI patients (B) Non-operated side LLI patients, (C) Operated side Happy THR patients (D) Non-operated side Happy THR patients (E) Normal healthy patients. The blue curve in each graph is the same and represents the average knee flexion-extension for the Normal group	122

74	Schematic demonstrating the physical characteristics of ankle dorsi-plantar flexion. The pointing of the toes upwards towards the shank is classed as dorsiflexion and the pointing downwards away from the shank is referred to as plantarflexion	123
75	Average ankle dorsiflexion (+) plantarflexion (-) angles together with 95% confidence intervals over a normalised gait cycle between consecutive heel strikes of the same foot. The dashed lines represent the associated confidence intervals for each sample.	124
76	Raw ankle dorsi (+)-plantar (-) flexion angle results for all three groups over a normalised gait cycle between consecutive heel strikes of the same foot. (A) Operated side LLI patients (B) Non-operated side LLI patients, (C) Operated side Happy THR patients (D) Non-operated side Happy THR patients (E) Normal healthy patients. The blue curve in each graph is the same and represents the average ankle dorsi-plantar flexion for the Normal group	125
77	Average heel strike joint angles together with standard errors for the operated (LLI OS) and non-operated (LLI NOS) sides of the Symptomatic LLI group, the operated (Happy THR OS) and non-operated (Happy THR NOS) sides of the Happy THR group together with the results of the Normal patient group	126
78	Average mid-stance joint angles together with standard errors for the operated (LLI OS) and non-operated (LLI NOS) sides of the Symptomatic LLI group, the operated (Happy THR OS) and non-operated (Happy THR NOS) sides of the Happy THR group together with the results of the Normal patient group	127
79	Average toe off joint angles together with standard errors for the operated (LLI OS) and non-operated (LLI NOS) sides of the Symptomatic LLI group, the operated (Happy THR OS) and non-operated (Happy THR NOS) sides of the Happy THR group together with the results of the Normal patient group	128
80	Standing joint angles together with standard errors	129
81	Average pelvic superior (+) - inferior obliquity (-) (A), pelvic anterior (+) - posterior (-) rotation (B), hip flexion (+) - extension (-) (C), hip abduction (+) - adduction (-) (D), knee flexion (+) - extension (-) (E) and ankle dorsi (+)-plantar (-) flexion (F) angle comparison between the Normal patient results to that of Bovi et al. over consecutive heel strikes normalised to 100 percentiles. Error intervals of ± 1 standard deviation are also plotted for each group.	133

82	Comparing the results of Pospischill et al. to the experimental results of the operated sides of the Symptomatic LLI and Happy THR groups in terms of hip flexion-extension over a normalised gait cycle between consecutive heel strikes of the same foot . Pospischil et al. have results for both MIS (Minimally Invasive Surgery) THR and standard THR at 10 days and 3 months post-surgery together with the preoperative results.	136
83	Comparing VGRF between the operated and non-operated sides of the LLI and THR groups to that of the average Normal healthy individuals together with 95% confidence intervals over a normalised gait cycle between consecutive heel strikes of the same foot. Results have been normalised for bodyweight.	145
84	Average VGRF 1 st peak, 2 nd peak and trough for Normal, LLI Operated Side (LLI OS), LLI Non-Operated Side (LLI NOS), Happy THR Operated Side (Happy THR OS) and the Happy THR Non-Operated Side (Happy THR NOS) groups together with standard errors.	147
85	VGRF Symmetry Index results following normalisation for bodyweight for all patient groups at 0%, 20%, 40% and 60% gait intervals together with standard errors. . . .	148
86	VGRF results following normalisation for bodyweight for all patient groups at mid-stance for Normal, LLI Operated Side (LLI OS), LLI Non-Operated Side (LLI NOS), Happy THR Operated Side (Happy THR OS) and the Happy THR Non-Operated Side (Happy THR NOS) groups together with standard errors.	148
87	Raw VGRF results for all three groups over a normalised gait cycle between consecutive heel strikes of the same foot. (A) Operated side LLI patients (B) Non-operated side LLI patients, (C) Operated side Happy THR patients (D) Non-operated side Happy THR patients (E) Normal Healthy Patients. Average lines are added to each graph for the particular group being studied together with the average Normal patient result. Results have been normalised for bodyweight.	149
88	Comparing hip JRFs between the operated and non-operated sides of the LLI and THR groups to that of the average Normal healthy individuals together with 95% confidence intervals over a normalised gait cycle between consecutive heel strikes of the same foot. Results have been normalised for bodyweight.	150

89	Average hip JRF 1 st peak, 2 nd peak and trough for Normal, LLI Operated Side (LLI OS), LLI Non-Operated Side (LLI NOS), Happy THR Operated Side (Happy THR OS) and the Happy THR Non-Operated Side (Happy THR NOS) groups together with standard errors	152
90	Hip JRF symmetry index results following normalisation for bodyweight for all patient groups at 0%, 20%, 40% and 60% gait intervals together with standard errors .	153
91	Hip JRF results following normalisation for bodyweight for all patient groups at heel strike, mid-stance and toe off for Normal, LLI Operated Side (LLI OS), LLI Non-Operated Side (LLI NOS), Happy THR Operated Side (Happy THR OS) and the Happy THR Non-Operated Side (Happy THR NOS) groups together with standard errors	154
92	Raw hip JRF results for all three groups over a normalised gait cycle between consecutive heel strikes of the same foot. (A) Operated side LLI patients (B) Non-operated side LLI patients, (C) Operated side Happy THR patients (D) Non-operated side Happy THR patients (E) Normal healthy patients. Average lines are added to each graph for the particular group being studied together with the average Normal patient result. Results have been normalised for bodyweight.	155
93	Average hip flexion (+)-extension (-) moments during gait for all patient groups together with 95% confidence intervals over a normalised gait cycle between consecutive heel strikes of the same foot. Results have been normalised for bodyweight.	156
94	Peak hip flexion (+)-extension (-) moments in terms of averaged raw results between consecutive heel strikes of the same foot over a normalised gait cycle for all patients in each group. Results have been adjusted for bodyweight. Standard errors are included.	157
95	Raw hip flexion (+)-extension (-) moment results for all three groups over a normalised gait cycle between consecutive heel strikes of the same foot. (A) Operated side LLI patients (B) Non-Operated side LLI patients (C) Operated side Happy THR patients (D) Non-Operated side Happy THR patients (E) Normal Healthy Patients. Average lines are added to each graph for the particular group being studied together with the average Normal patient result. Results have been normalised for bodyweight.	157
96	Hip abduction (+)-adduction (-) moments during gait for all patient groups together with 95% confidence intervals over a normalised gait cycle between consecutive heel strikes of the same foot. Results have been normalised for bodyweight.	158

-
- 97 Peak hip abduction (+) - adduction (-) moments in terms of averaged raw results between consecutive heel strikes of the same foot over a normalised gait cycle for all patients in each group. Results have been adjusted for bodyweight. Standard errors are included. 159
- 98 Raw hip abduction (+)-adduction (-) moment results for all three groups over a normalised gait cycle between consecutive heel strikes of the same foot. (A) Operated side LLI patients (B) Non-Operated side LLI patients (C) Operated side Happy THR patients (D) Non-Operated side Happy THR patients (E) Normal Healthy Patients. Average lines are added to each graph for the particular group being studied together with the average Normal patient result. Results have been normalised for bodyweight. 159
- 99 Knee flexion (-)-extension (+) moment during gait for all patient groups together with 95% confidence intervals over a normalised gait cycle between consecutive heel strikes of the same foot. Results have been normalised for bodyweight. 160
- 100 Peak knee flexion-extension moments in terms of averaged raw results between consecutive heel strikes of the same foot over a normalised gait cycle for all patients in each group. Results have been adjusted for bodyweight. Standard errors are included.161
- 101 Raw knee flexion (-)-extension (+) moment results for all three groups over a normalised gait cycle between consecutive heel strikes of the same foot. (A) Operated side LLI patients (B) Non-Operated side LLI patients (C) Operated side Happy THR patients (D) Non-Operated side Happy THR patients (E) Normal Healthy Patients. Average lines are added to each graph for the particular group being studied together with the average Normal patient result. Results have been normalised for bodyweight.161
- 102 Ankle dorsi (+)-plantar (-) flexion moments during gait for all patient groups together with 95% confidence intervals over a normalised gait cycle between consecutive heel strikes of the same foot. Results have been normalised for bodyweight. 162
- 103 Peak ankle dorsi (+)-plantar (-) flexion moments in terms of averaged raw results between consecutive heel strikes of the same foot over a normalised gait cycle for all patients in each group. Results have been adjusted for bodyweight. Standard errors are included. 163

104	Raw ankle dorsi (+)-plantar (-) flexion moment results for all three groups over a normalised gait cycle between consecutive heel strikes of the same foot. (A) Operated side LLI patients (B) Non-Operated side LLI patients (C) Operated side Happy THR patients (D) Non-Operated side Happy THR patients (E) Normal Healthy. Average lines are added to each graph for the particular group being studied together with the average Normal patient result. Results have been normalised for bodyweight.	163
105	Average heel strike joint moments with standard errors for the Normal, Happy THR and Symptomatic LLI groups. Results have been normalised for bodyweight.	164
106	Average mid-stance joint moments with standard errors for the Normal, Happy THR and Symptomatic LLI groups. Results have been normalised for bodyweight.	165
107	Average toe off joint moments with standard errors for the Normal, Happy THR and Symptomatic LLI groups. Results have been normalised for bodyweight.	166
108	Average VGRFs (A), hip flexion (+) - extension (-) moments (B), hip abduction (+) - adduction (-) moments (C), knee flexion (+) - extension (-) moments (D) and ankle dorsi (+)-plantar (-) flexion moments (E) comparison between the Normal patient results to that of Bovi et al. over consecutive heel strikes normalised to 100 percentiles. Error intervals of ± 1 standard deviation are also plotted for each group. Results are normalised for bodyweight	168
109	Resultant Hip JRF during gait for the average Normal group patient against Paul (1967) together with ± 1 standard error intervals over a normalised gait cycle between consecutive heel strikes of the same foot for the former. Results were normalised for bodyweight.	169
110	Normalised VGRF gait cycle results at the 1 st peak (A), 2 nd peak (B) and trough (C) between consecutive heel strikes of the same foot for all clinically measured data together with lines of best fit.	172
111	Normalised hip JRF results at the 1 st peak (A), 2 nd peak (B) and trough (C) between consecutive heel strikes of the same foot for all clinically measured data together with lines of best fit.	175

-
- 112 Image from Visual3D demonstrating excessive hip axes rotation due to poor lateral thigh marker positioning on both the left and right sides. The centre axes are of the pelvis whilst the axes on the left and right hand sides represent the hip. The green axis (anterior-posterior) represents abduction-adduction, the red axis (medial-lateral) flexion-extension and the blue internal-external rotation. It would be expected that the anterior-posterior axis in a subject is rotated such that it generally faces the direction that the individual is standing. This was not the case for this particular patient for either hip, with there instead being excessive external rotation. 180
- 113 Image from Visual3D demonstrating excessive knee axes external rotation on both the left and right sides due to poor lateral shank marker positioning. Typically, the axes would be rotated such that the green axis (anterior-posterior) is facing in the same direction as the subject is standing. At both of the knees shown, the green axis was excessively externally rotated indicating that the lateral shank marker which defines the rotation of the axes was placed too posterior. 181
- 114 Image from Visual3D demonstrating both an excessively rotated foot (left) and a correctly rotated foot (right). The foot in Visual3D was defined to exist between the toe marker and the AJC with the medial-lateral rotation of the joint axes, defined at the AJC, being dependent on the position of the heel marker relative to the foot. A heel marker which is incorrectly placed leads to there being either an inversion or eversion offset in the results. 181
- 115 Image from Visual3D demonstrating the pose of a single subject volunteer during the standing trial. Segment axes were measured against the laboratory axes in terms of computing segment rotation. 183
- 116 Segment rotations of the pelvis, thigh, shank and foot for all clinical groups together with Pilot data. Positive (+) angles depict internal rotation and negative (-) angles depict external rotation. Standard errors are included. 184
- 117 The effect of varying initial thigh standing angles when measured against the laboratory axes to maximum hip flexion- extension, hip abduction-adduction, knee flexion-extension and ankle dorsi-plantar flexion joint angles. 186
- 118 The effect of varying initial thigh standing angles when measured against the laboratory axes to hip flexion-extension, abduction-adduction, knee flexion-extension and ankle dorsi-plantarflexion RoM. 187

119	The effect of varying initial shank standing angles when measured against the laboratory axes to maximum hip flexion-extension, hip abduction-adduction, knee flexion-extension and ankle dorsi-plantarflexion joint angles.	188
120	The effect of varying initial shank standing angles when measured against the laboratory axes to hip flexion-extension, abduction-adduction, knee flexion-extension and ankle dorsi-plantarflexion RoM.	189
121	The effect of varying initial foot standing angles when measured against the laboratory axes to maximum hip flexion- extension, hip abduction-adduction, knee flexion-extension and ankle dorsi-plantar flexion joint angles.	190
122	The effect of varying initial foot standing angles when measured against the laboratory axes to hip flexion-extension, abduction-adduction, knee flexion-extension and ankle dorsiflexion-plantarflexion RoM.	191
123	The effect of varying initial thigh standing angles when measured against the laboratory axes to maximum hip flexion-extension, hip abduction-adduction, knee flexion-extension and ankle dorsi-plantar flexion moments.	192
124	The effect of varying initial thigh standing angles when measured against the laboratory axes to range of moment in terms of hip flexion-extension, hip abduction-adduction, knee flexion-extension and ankle dorsi-plantar flexion.	193
125	The effect of varying initial shank standing angles when measured against the laboratory axes to maximum hip flexion-extension, abduction-adduction, knee flexion-extension and ankle dorsi-plantarflexion moments.	194
126	The effect of varying initial shank standing angles when measured against the laboratory axes to range of moment in terms of hip flexion-extension, hip abduction-adduction, knee flexion-extension and ankle dorsi-plantar flexion.	195
127	The effect of varying initial foot standing angles when measured against the laboratory axes to maximum hip flexion-extension, hip abduction-adduction, knee flexion-extension and ankle dorsi-plantar flexion moments.	196
128	The effect of varying initial foot standing angles when measured against the laboratory axes to maximum knee flexion-extension and ankle dorsi-plantarflexion moments	197
129	The effect of different HJC regression equations on orientation of thigh, shank and foot segments.	202
130	The effect of different HJC regression equations on the positions of the HJC, KJC and AJC.	203

131	Average hip flexion (+)-extension (-) angles (A) and moments (B), abduction (+) adduction (-) angles (C) and moments (D), internal (+) external rotation (-) angles (E) and moments (F) for the Davis, Harrington and Bell HJC regression equations over 5 normalised gait cycle trials between consecutive heel strikes of the same foot	205
132	Average knee flexion (+)-extension (-) angles (A) and flexion (-)-extension (+) moments (B), abduction (+) adduction (-) angles (C) and moments (D), internal (+) external rotation (-) angles (E) and moments (F) for the Davis, Harrington and Bell HJC regression equations over 5 normalised gait cycle trials between consecutive heel strikes of the same foot	207
133	Average ankle dorsiflexion (+)-plantarflexion (-) angles (A) and moments (B), eversion (+) inversion (-) angles (C) and moments (D), internal (+) external rotation (-) angles (E) and moments (F) for the Davis, Harrington and Bell HJC regression equations over 5 normalised gait cycle trials between consecutive heel strikes of the same foot	209
134	The sum of the percentage difference between the Bell, Davis and Harrington HJC calculation methods across all joints when analysing the average gait cycle joint angle and joint moment.	212
135	The sum of the percentage difference between the Bell, Davis and Harrington HJC calculation methods when comparing joints using the average gait cycle joint angle and joint moment. Hip results include hip flexion-extension, abduction-adduction and internal-external rotation. Knee results include knee flexion-extension, abduction-adduction and internal-external rotation whilst foot results include ankle dorsi-plantar flexion, ankle eversion-inversion and ankle internal-external rotation.	213
136	The sum of the percentage difference between the Bell, Davis and Harrington HJC calculation methods when comparing movement planes using the average gait cycle joint angle and joint moment. Sagittal results include hip flexion-extension, knee flexion-extension and ankle dorsi-plantar flexion. Frontal results include hip abduction-adduction, knee abduction-adduction and ankle eversion-inversion. Transverse results include hip, knee and ankle rotation.	214
137	KJC medial-lateral displacement following increasing levels of knee width calculation error.	215
138	KJC and AJC displacement following increasing levels of knee width calculation error	216
139	AJC displacement following increasing levels of ankle width calculation errors. . . .	216

140	Average hip abduction (+)-adduction (-) angle at original knee width level and errors of 5mm and 10mm together with 95% confidence intervals for original knee width	217
141	Average knee flexion (+)-extension (-) angles (A) and flexion (-)-extension (+) moments (B), abduction (+) adduction (-) angles (C) and moments (D), internal (+) external rotation (-) angles (E) and moments (F) for varying knee width errors over 5 normalised gait cycle trials between consecutive heel strikes of the same foot	219
142	Average ankle dorsiflexion (+)-plantarflexion (-) angles (A) and moments (B), eversion (+) inversion (-) angles (C) and moments (D), internal (+) external rotation (-) angles (E) and moments (F) for varying knee width errors over 5 normalised gait cycle trials between consecutive heel strikes of the same foot	220
143	Sum of angles and moments across joints (hip, knee, ankle) and planes (sagittal, frontal, transverse) with regards to the average angle/moment change with a 10mm error in knee width during a normalised gait cycle between consecutive heel strikes of the same foot. Standard errors are also included.	222
144	AJC displacement following increasing levels of ankle width calculation errors.	222
145	Average ankle eversion (+) inversion (-) angles (A) and moments (B) and internal (+) external rotation (-) angles (C) and moments (D) for varying ankle width errors over 5 normalised gait cycle trials between consecutive heel strikes of the same foot	225
146	Sum of angles and moments across joints (hip, knee, ankle) and planes (sagittal, frontal, transverse) with regards to the average angle/moment change with a 10mm error in ankle width during a normalised gait cycle between consecutive heel strikes of the same foot. Standard errors are also included.	226
147	Custom market set with two columns of lateral segment markers running from the greater trochanter to the lateral ankle markers.	229
148	The definition of proximal, distal, anterior and posterior markers on the custom marker set. This image represents the thigh but the same method was applied to the shank	230
149	Average hip flexion (+)-extension (-) angles (A) and moments (B), abduction (+) adduction (-) angles (C) and moments (D), internal (+) external rotation (-) angles (E) and moments (F) for anterior-proximal, posterior-proximal, anterior-distal and posterior-distal positioned lateral thigh markers over 10 normalised gait cycle trials between consecutive heel strikes of the same foot	232

-
- 150 Average knee flexion (+)-extension (-) angles (**A**) and flexion (-)-extension (+) moments (**B**), abduction (+) adduction (-) angles (**C**) and moments (**D**), internal (+) external rotation (-) angles (**E**) and moments (**F**) for anterior-proximal, posterior-proximal, anterior-distal and posterior-distal positioned lateral thigh markers over 10 normalised gait cycle trials between consecutive heel strikes of the same foot 234
- 151 Average ankle dorsiflexion (+)-plantarflexion (-) angles (**A**) and moments (**B**), eversion (+) inversion (-) angles (**C**) and moments (**D**), internal (+) external rotation (-) angles (**E**) and moments (**F**) for anterior-proximal, posterior-proximal, anterior-distal and posterior-distal positioned lateral thigh markers over 10 normalised gait cycle trials between consecutive heel strikes of the same foot 236
- 152 Average knee flexion (+)-extension (-) angles (**A**) and flexion (-)-extension (+) moments (**B**), abduction (+) adduction (-) angles (**C**) and moments (**D**), internal (+) external rotation (-) angles (**E**) and moments (**F**) for anterior-proximal, posterior-proximal, anterior-distal and posterior-distal positioned lateral shank markers over 10 normalised gait cycle trials between consecutive heel strikes of the same foot 238
- 153 Demonstration of Gimbal Lock. In this example, the green circle represents the sagittal plane, the red circle the frontal plane and the blue the transverse plane. Image (A) is of a non-Gimbal locked axes whilst image (B) is of a Gimbal locked axes, where two gimbals have overlapped 239
- 154 Average ankle dorsiflexion (+)-plantarflexion (-) angles (**A**) and moments (**B**), eversion (+) inversion (-) angles (**C**) and moments (**D**), internal (+) external rotation (-) angles (**E**) and moments (**F**) for anterior-proximal, posterior-proximal, anterior-distal and posterior-distal positioned lateral shank markers over 10 normalised gait cycle trials between consecutive heel strikes of the same foot 240
- 155 The customised lateral segment (thigh and shank) markers used in this study. A marker was secured at the centre of each cluster and used to represent PiG, whilst the four remaining markers were used to represent CAST. 244
- 156 Average hip flexion (+)-extension (-) angles (**A**) and moments (**B**), abduction (+) adduction (-) angles (**C**) and moments (**D**), internal (+) external rotation (-) angles (**E**) and moments (**F**) for the PiG and CAST marker sets over 10 normalised gait cycle trials between consecutive heel strikes of the same foot 247

157	Average knee flexion (+)-extension (-) angles (A) and flexion (-)-extension (+) moments (B), abduction (+) adduction (-) angles (C) and moments (D), internal (+) external rotation (-) angles (E) and moments (F) for the PiG and CAST marker sets over 10 normalised gait cycle trials between consecutive heel strikes of the same foot	250
158	Average ankle dorsiflexion (+)-plantarflexion (-) angles (A) and moments (B), eversion (+) inversion (-) angles (C) and moments (D), internal (+) external rotation (-) angles (E) and moments (F) for the PiG and CAST marker sets over 10 normalised gait cycle trials between consecutive heel strikes of the same foot	252
159	Hip joint forces comparing the PiG and CAST models between consecutive heel strikes of the same foot over a normalised gait cycle. Forces have been normalised for bodyweight. Results are plotted together with 95% confidence intervals	256
160	Image (A) shows where the Ramamurti points are located relative to the shape of the femur whilst (B) shows how the points are located with respect to each other on the femoral head viewed from directly above the apex of the femoral head	261
161	Motion paths produced by 20 loci on the femoral head computed via the in-house Matlab program	263
162	The calculation of the Aspect Ratio. The (x,y) coordinate values for the maximum and minimum anterior, posterior, medial and lateral points of each of the 20 motion paths were found. The Aspect Ratio was subsequently found using Equations 65-68. This image is from Budenberg et al. and is a 2D rendition of the 3D Aspect Ratio calculation.	264
163	Average sliding distances for each of the clinical groups per stride length together with standard errors.	266
164	Average Kang cross shear ratio for each patient group together with standard errors over the Hertz Contact Area	267
165	Normalised wear rate calculation for each group using the Archard Equation	267
166	Contact surface motion paths as computed using an in-house Matlab code for all clinical groups at 20 Ramamurti points using the XYZ Cardan angle sequence	268
167	Contact surface motion paths as computed using an in-house Matlab code for all clinical groups at 20 Ramamurti points using the YZX Cardan angle sequence	269
168	Calculated Aspect Ratios for each group together with standard errors for the XYZ and YZX cardan angle sequences	270

169	Comparing the motion paths on a 14mm femoral head between PiG and CAST when using the same motion trials. 20 Ramamurti points are used.	270
170	Average entraining lubrication fluid film thickness at peak hip JRFs over the course of the gait cycle using the Hamrock & Dowson Equations for entraining lubrication. Standard errors are also plotted.	271
171	An image from Visual3D of an LLI patient with the lateral thigh markers on the left and right sides placed at different superior-inferior positions	282

List of Tables

1	Hip muscles and the moments they can generate	7
2	Demographics for the LLI and Happy THR groups with average results and standard errors together with t-test results	101
3	Table showing segment motions in 6DOF Visual3D model. X measured anterior (flexion)-posterior (extension) motion, Y medial (adduction)-lateral (abduction) motion and Z rotation	107
4	Maximum angle, minimum angle and RoM in terms of averaged results for the raw pelvic operated side superior(+) and inferior obliquity(-) for all patients in each group. * and † represent statistical significance. Comparisons are made in columns. All values are in degrees.	111
5	Maximum angle, minimum angle and RoM in terms of averaged results for the raw pelvic operated side internal(+) and external(-) rotation for all patients in each group. * represents statistical significance for Maximum and Minimum Values. Comparisons are made in columns. All values are in degrees.	114
6	Maximum angle, minimum angle and RoM in terms of averaged results for the raw hip flexion (+)-extension (-) angle compared between hips for all patients in each group. *, †, ▷ and ◊ represent statistical significance for Maximum and Minimum Values. Comparisons are made in columns. All values are in degrees.	115
7	Maximum angle, minimum angle and RoM in terms of averaged results for the raw hip abduction (+)-adduction (-) angles compared between hips for all patients in each group. *, †, ▷ and ◊ represent statistical significance for Maximum and Minimum Values. Comparisons are made in columns. All values are in degrees.	118
8	Maximum angle, minimum angle and RoM in terms of averaged results for the raw knee flexion (+)-extension (-) angles compared between knees for all patients in each group. * and † represent statistical significance for Maximum and Minimum Values. Comparisons are made in columns. All values are in degrees.	121
9	Maximum angle, minimum angle and RoM in terms of averaged results for the raw ankle dorsi(+)-plantar(-) flexion angles compared between ankles for all patients in each group. *, †, ▷ and ◊ represent statistical significance for Maximum and Minimum Values. All values are in degrees.	124
10	Temporal-spatial data for all patient groups with * and † used to represent statistically significant differences at the 5% significance level across columns	130

11	Temporal-spatial parameters for all patient groups with * and † used to represent statistically significant differences at the 5% significance level across columns	131
12	Temporal-spatial parameter symmetry index values for all patient groups with * and † used to represent statistically significant differences at the 5% significance level across columns. Results rounded to nearest integer	131
13	Table showing how moments and forces were measured in AnyBody	143
14	Percentage difference between the average hip flexion (+)-extension (-) angles (FE) and moments (FE), abduction (+) adduction (-) angles (AA) and moments (AA), internal (+) external rotation (-) angles (IER) and moments (IER) for the Davis, Harrington and Bell HJC regression equations over 5 normalised gait cycle trials between consecutive heel strikes of the same foot	204
15	Percentage difference between the average knee flexion (+)-extension (-) angles (FE) and flexion (-)-extension (+) moments (FE), abduction (+) adduction (-) angles (AA) and moments (AA), internal (+) external rotation (-) angles (IER) and moments (IER) for the Davis, Harrington and Bell HJC regression equations over 5 normalised gait cycle trials between consecutive heel strikes of the same foot	207
16	Percentage difference between the average ankle dorsiflexion (+)-plantarflexion (-) angles (FE) and moments (FE), eversion (+) inversion (-) angles (EI) and moments (EI), internal (+) external rotation (-) angles (IER) and moments (IER) for the Davis, Harrington and Bell HJC regression equations over 5 normalised gait cycle trials between consecutive heel strikes of the same foot	209
17	Percentage difference between the average hip flexion (+)-extension (-) angles (FE) and moments (FE), abduction (+) adduction (-) angles (AA) and moments (AA), internal (+) external rotation (-) angles (IER) and moments (IER) for varying knee width errors over 5 normalised gait cycle trials between consecutive heel strikes of the same foot	217
18	Percentage difference between the average knee flexion (+)-extension (-) angles (FE) and flexion (-)-extension (+) moments (FE), abduction (+) adduction (-) angles (AA) and moments (AA), internal (+) external rotation (-) angles (IER) and moments (IER) for varying knee width errors over 5 normalised gait cycle trials between consecutive heel strikes of the same foot	219

19	Percentage difference between the average ankle dorsiflexion (+)-plantarflexion (-) angles (FE) and moments (FE), eversion (+) inversion (-) angles (EI) and moments (EI), internal (+) external rotation (-) angles (IER) and moments (IER) for varying knee width errors over 5 normalised gait cycle trials between consecutive heel strikes of the same foot	220
20	Percentage difference between the average hip/knee/ankle flexion (+)-extension (-) angles (FE) and moments (FE), abduction (+) adduction (-) angles (AA) and moments (AA), internal (+) external rotation (-) angles (IER) and moments (IER) for varying ankle width errors over 5 normalised gait cycle trials between consecutive heel strikes of the same foot	223
21	Percentage difference between the average ankle eversion (+) inversion (-) angles (IE) and moments (IE) and internal (+) external rotation (-) angles (IER) and moments (IER) for varying ankle width errors over 5 normalised gait cycle trials between consecutive heel strikes of the same foot	224
22	A comparison of the differences in peak joint angles between LLI/Normal patients and the differences between PiG and CAST	254
23	Average sliding distances and velocities for each clinical group together with standard deviations	265
24	LLI and Happy THR patients demographics and anthropometrics	339
25	Normal patients demographics and anthropometrics	340

Abbreviations

AJC - Ankle Joint Centre
ANOVA - Analysis of Variance
CAST- Calibrated Anatomical Systems Technique
CGM - Conventional Gait Model
CNS - Central Nervous System
CT - Computed Tomography
EMG - Electromyograph
GRF - Ground Reaction Force
HJC - Hip Joint Centre
ISB - International Society of Biomechanics
JRF - Joint Reaction Force
KAD - Knee Alignment Device
KG - Kilogram
KJC - Knee Joint Centre
LANK - Left Ankle
LASIS - Left Anterior Superior Iliac Spine
LHEE - Left Heel
LKNE - Left Knee
LLI - Leg Length Inequality
LPSIS - Left Anterior Superior Iliac Spine
LTHI - Left Thigh
LTIB - Left Tibia
LTOE - Left Toe
MRI - Magnetic Resonance Imaging
N-m - Newton Metre
PACS - Picture Archiving and Communication System
PCSA - Physiological Cross Sectional Area
PiG - Plug-in-Gait
PMO - Principal Molecular Orientation
RANK - Right Ankle
RASIS - Right Anterior Superior Iliac Spine
RHEE - Right Heel

RKNE - Right Knee

RoM - Range of Motion

RPSIS - Right Posterior Superior Iliac Spine

RTHI - Right Thigh

RTIB - Right Tibia

RTOE - Right Toe

SPSS - Statistical Programme for the Social Sciences

SRCC - Spearmans Rank Correlation Coefficient

STA - Soft Tissue Artefact

THA - Total Hip Arthroplasty

THR - Total Hip Replacement

UHMWPE - Ultra-High Molecular Weight Polyethylene

VGRF - Vertical Ground Reaction Force

1 Introduction

Total Hip Replacement (THR) has emerged as one of the most successful operative procedures with over 100,000 patients in the UK having their hips replaced in 2015 [1]. It has been stated that after a period of a year, the hip becomes the "forgotten joint" with many patients not noticing any differences from a natural hip [2]. The femoral offset is a key controlled variable during THR defined as the perpendicular distance between the centre of the hip and the line passing through the long axis of the stem. Figure 1 illustrates this definition. Historically postoperative hip instability and dislocation was a considerable issue, however, implant design variations have provided surgeons with more options for femoral offset to allow adjustment of soft tissue tension to reduce ligament laxity. Whilst patient satisfaction is now high with 90% of patients satisfied post-surgery[3], a large proportion of patients may still end up with a LLI (Leg Length Inequality).

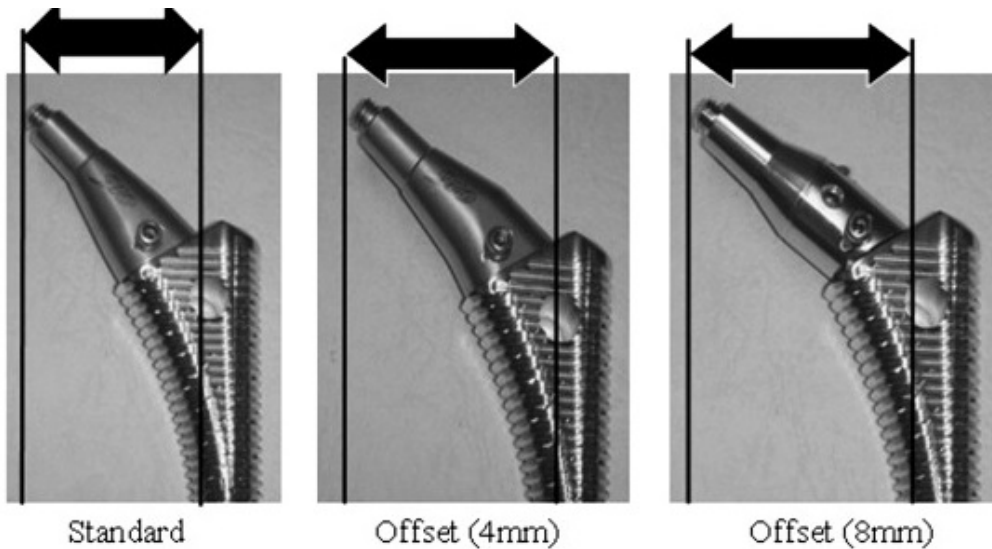


Figure 1: Three different hip prosthesis femoral offsets. A femoral offset is defined as the perpendicular distance between the centre of hip rotation and the line passing through the long axes of the femoral stem.

[4]

An anatomic LLI following THR is dependent on the selection of femoral offset, with an increase in leg length on the operated side being more common. This results from the surgeon attempting to compromise between patient satisfaction levels and implant stability. A longer leg through the use of a larger femoral offset increases the soft tissue tension at the joint and hence increases stability. A longer leg however leads to an LLI, with discrepancies as little as 6mm known to cause clinical symptoms [5]. Approximately 10% of patients following THR are symptomatic for an anatomic LLI [6].

There does not exist a consensus in the literature for a minimum threshold in discrepancy that cannot be tolerated, although discrepancies of less than 10mm are generally thought of as acceptable [7]. A significant increase in leg length can lead to the development of nerve palsy, limp, osteoarthritis in the shorter limb, spinal deficiencies, implant instability and the need for revision surgery [8–10]. Pain is also common in both the operated and non-operated sided hip, knee and ankle [11]. This has led LLI to become one of the leading causes of litigation following THR [8, 9, 12] with patients unhappy in wearing a shoe lift despite research showing its benefits in terms of maintaining a regular posture, increasing mobility and providing substantial pain relief [13–15]. Liability issues exist due to the absence of a standard which determines what an acceptable LLI is [16], with frequent malpractice claims occurring [17, 18] and LLI representing 8.7% of all medical errors in the NHS [19]. Due to the difficulty in ascertaining the number of cases where the condition leads to clinical symptoms and the lack of a systematic data collection process, the causes and effects of this condition have yet to be thoroughly analysed from an engineering perspective despite there being a clear need.

The purpose of this research was to meet this need and can be defined using the study aim:

Aim - To understand why certain patients following a Total Hip Replacement are symptomatic for a Leg Length Inequality whilst others remain asymptomatic.

A symptomatic LLI patient was defined as a individual who post-THR perceived a change in leg length which they were troubled to such an extent that they required revision surgery. These patients did not have a difference in leg length pre-operatively which caused clinical symptoms. This thesis addressed the aim through a series of experimental measures and study objectives. These included examining whether there was a particular anthropometric (femoral offset, leg length magnitude) or demographic (age, height, BMI) variable which increased the risk of being symptomatic for a LLI. Another objective examined how symptomatic LLI patients, who have symptoms of leg lengthening post-THR severe enough to require clinical referral, differ to asymptomatic THR and Normal patients in terms of the gait. A series of sensitivity analyses were also undertaken and attempted to answer whether the use of the PiG (Plug-in-Gait) measuring system was accurate enough to measure gait in THR patients. The final objectives was to study the effects of being symptomatic for an LLI on durability of the hip implant through predicting wear and lubrication levels. Both individually and collectively, these studies would enable a greater understanding of the

typical characteristics of a symptomatic LLI patient and aid in identifying patients most at risk both preoperatively and postoperatively. The study objectives are:

Objective 1 - Understand whether differences exist in both anthropometric measurements and demographics between Symptomatic LLI and asymptomatic Happy THR patients

Objective 2 Examine whether LLI patients show a characteristic gait pattern in their kinematic, kinetic and temporal-spatial results together with comparing them to asymptomatic Happy THR and Normal patients

Objective 3 - Compute how error using the PiG model may have effected the variability seen in the clinical gait analysis results

Objective 4 - Analyse how differences in kinematics, kinetics and temporal-spatial parameters effect the Symptomatic LLI, Happy THR and Normal groups in terms of predicted wear rates and lubrication thickness

In answering the study aim through each of the objectives, this thesis can be broadly split into 3 sections which comprise of 13 chapters. The 1st section comprises of a single chapter review of the literature relevant to this research and a generic methods section. The 2nd section covers 8 chapters and deals with both the specific methods and experimental results of each of the studies undertaken. Following this, the 3rd section comprises of 2 chapters of which the first is an overall discussion of the results and their clinical interpretations. This is followed by a conclusion which summaries the findings of this thesis and attempts to answer the initial study aim.

2 Literature Review

2.1 Normal People

2.1.1 Hip Anatomy

The hip is the region of the body where the pelvis and thigh meet to form a ball and socket joint called the hip joint. The ball is called the femoral head and is located at the top of the thigh, while the socket is called the acetabulum and is located on the pelvis. Both the femoral head and acetabulum are covered in articular cartilage which provides greater stability through its smooth low friction surface [20]. A ring of fibrous cartilage surrounds the acetabulum called the labrum which serves to increase depth and provide greater stability [21].

The hip joint is used in everyday activities such as walking, running, climbing stairs and jumping through being able to withstand forces up to 7-8 times that of bodyweight [22]. It is also one of the most flexible joints providing rotation in the sagittal, frontal and transverse planes. In the sagittal plane the hip can flex normally up to 120° and extend to around 20° , move 45° in abduction and adduction together with internal-external rotation totalling 90° [23]. This is enabled by the orientation of the femur and the elongated femoral neck which connects the head and shaft at an angle of 125° [23]. The structure of the hip joint can be seen in Figure 2.

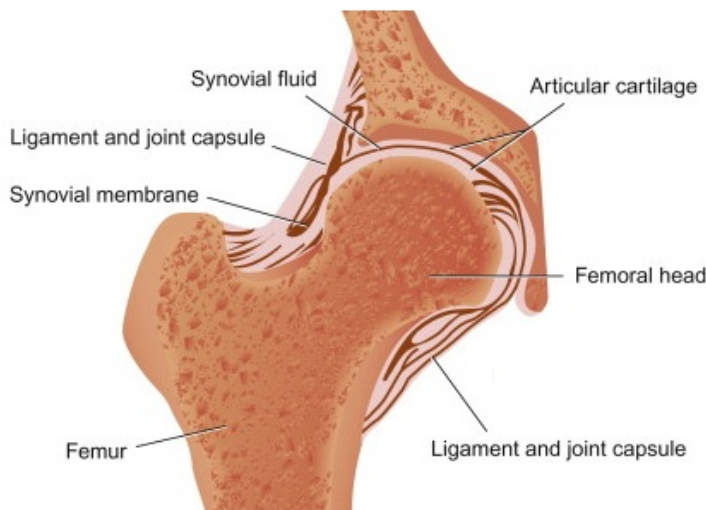


Figure 2: Hip Joint Anatomy
[24]

The primary role of the hip joint is to provide stability during static and dynamic tasks. The deep structure of the acetabulum encompasses the whole of the femoral head making it less likely that a dislocation will occur. It also has a role in distributing forces around the joint [25]. The hip

capsule provides extra stability through its thick structure [26] which on the outside is attached to a number of ligaments. These ligaments aid in the stabilisation of the hip through connecting bones to each other and minimising movement [27].

2.1.2 Muscles at the Hip

A total of 22 muscles at the hip joint provide stability, mobility and strength and can be grouped according to their functions and locations. These include the anterior femoral muscles on the front of the thigh, the posterior femoral muscles at the back of the thigh and the medial femoral muscles which are located to the side [28]. The muscles on the anterior portion of the thigh are the Quadriceps Femoris, which in itself consists of distinct muscular regions, and the Sartorius. Collectively the Quadriceps Femoris flexes the knee with the subset region of the Rectus Femoris muscle additionally providing hip flexion. The Hamstrings, which are the posterior muscles, are biarticular in their action through working both at the hip and the knee. For instance, the Biceps Femoris muscle at the Hamstrings contributes to hip flexion and external rotation and likewise with the knee [28]. The medial thigh muscles work to adduct the hip. Figure 3 shows the anatomy of the hip with the location of the abductors (Gluteus Medius and Gluteus Maximus) shown.

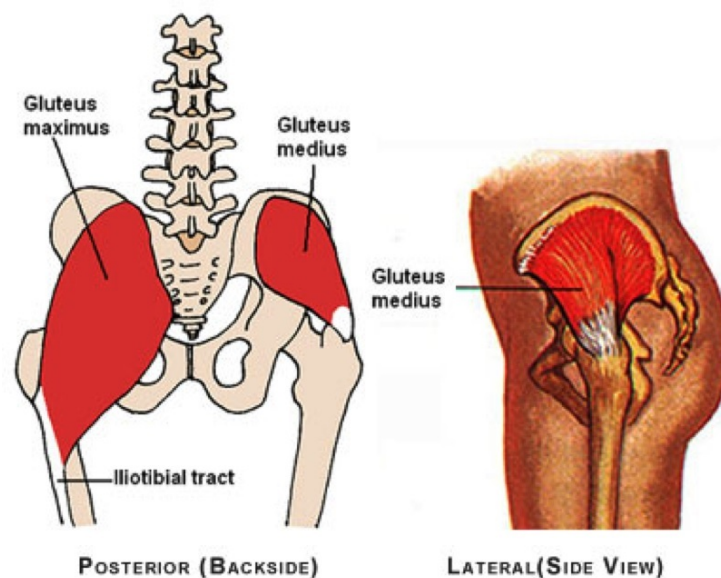


Figure 3: The hip abductors from the posterior and lateral views [29]

Muscles are often attached to bone over a significant area, however for simplicity a single geometric path called the line of action which is normally the centroid of the area is assumed [30]. The more proximal attachment point of the muscle is referred to as the origin site and the more distal as the insertion.

Moments are the tendency of a force to rotate a body around its axis. Muscles produce moments of forces across the hip joint during a variety of tasks and can be calculated using Equation 1 where M is moment, F is force and D is the moment arm (perpendicular distance from the line of action of the muscle to the hip joint). The moment arms of muscles change as a consequence of joint angle changes and are assumed to be the shortest path between the muscle and the joint. A schematic of how a moment arm is derived is shown in Figure 4. The moments which can be generated by the muscles at the hip can be seen in Table 1.

$$M = F \times D \quad (1)$$

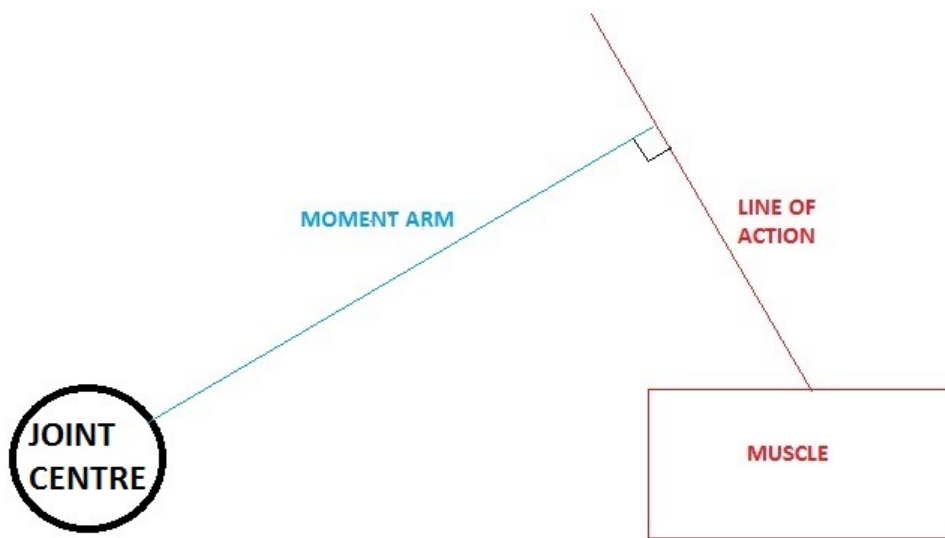


Figure 4: The derivation of a muscle moment arm

Out of the 22 muscles acting at the hip joint, six work to rotate the femur of the hip and are all relatively small in size leading them to have a smaller contribution in terms of moments and forces when compared to more larger muscles [31]. The magnitude of a force on the femoral head can be calculated as the ratio between the body weight moment arm (distance between the femur and the centre of gravity) and the abductor muscle moment arm, known commonly as the lever arm ratio [32]. When walking, the lever arm ratio is around 2.5 [25].

Table 1: Hip muscles and the moments they can generate

<i>Muscle</i>	Flexion	Extension	Abduction	Adduction	Int-Rotation	Ext-Rotation
Gluteus Medius I	✓		✓		✓	
Gluteus Medius II		✓	✓			✓
Gluteus Maximus I		✓	✓			✓
Gluteus Maximus II		✓		✓		✓
Biceps Femoris		✓				✓
Semitendinosus		✓				✓
Semimembranosus		✓			✓	
Tensor Fasciae Latae	✓		✓		✓	
Iliopsoas	✓					✓
Pectineous	✓			✓		✓
Adductor Brevis	✓			✓		✓
Adductor Longus	✓			✓		
Adductor Magnus		✓		✓		✓
Gracilis	✓			✓	✓	
Sartorius	✓		✓			✓
Rectus Femoris	✓					
Obturator Externus						✓
Piriformis						✓
Gemellus Inferior						✓
Quadratus Femoris						✓

2.1.3 Gait

Gait is the locomotion performed in order to move the lower limbs forward while its quantitative description is referred to as gait analysis. The gait cycle is defined as the sequence of events where a set of regular repeating set of locomotive phases are completed. This is most often defined to occur between the initial contact on the ground of one foot, referred to as heel strike, to the next initial contact of the same foot. This would be defined as one gait cycle [33]. Kinetics and kinematics are all based upon the gait cycle. Temporal-spatial parameters, defined as metric calculations based upon time and space, are also measured during the gait cycle. Temporal parameters include cycle time and swing phase time whilst spatial parameters include stride length. Gait is important in understanding the manner of walking in a healthy person and in detecting pathological conditions of the lower limb [34]. The gait cycle is split into two phases; the stance phase and the swing phase, with their ratios split approximately 60:40 for healthy individuals.

The stance phase refers to the period of time when the foot is in contact with the ground and

is where the lower regions of the leg support the weight of the body through distributing the load to supporting structures, thus allowing the advancement of the opposite limb [35]. Traditionally the stance phase has been further broken up into 5 smaller stages; initial contact, loading response, mid-stance, terminal stance and pre-swing. The instant of initial contact is the weight acceptance period of the stance leg and accounts for the first 10% of the gait cycle [35]. Subsequently, the limb goes into loading response and mid-stance which together make up around 40% of the gait cycle and are where the stance leg supports the entire weight of the body whilst the opposite leg is in swing phase. The next 10% of the stance phase is made up of the terminal stance and pre-swing phases where the stance leg is unloading the body weight onto the opposite limb and is preparing to enter swing phase [36].

The swing phase occurs when the foot is not in contact with ground and hence not weight bearing. Like the stance phase, the swing phase is also subdivided into smaller gait instances ;initial swing, mid-swing and terminal swing. Initial swing is defined as the instant when the foot is lifted from the floor and is where knee flexion and ankle dorsiflexion occur to accelerate the forward motion of the limb [33]. This phase lasts for approximately 1/3 of the swing phase [36]. During midswing, the swing leg appears adjacent to the opposite stance leg which is in mid-stance. The swing phase completes when the leg decelerates at terminal swing in preparation for initial contact. The whole gait cycle is approximated to last for 1 second in healthy individuals and can be seen in Figure 5.

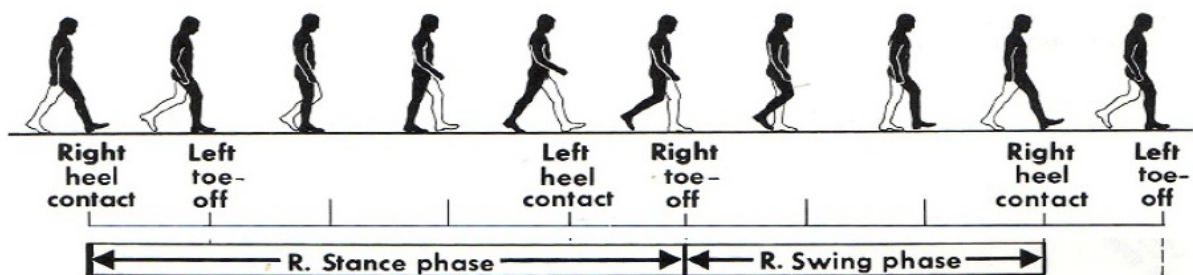


Figure 5: The gait cycle [37]

2.1.4 Measuring Gait

With the rapid development of computer technology in the last century, it has now become possible to capture 3D motion images to obtain quantitative rather than qualitative data regarding joint

kinematics, kinetics and temporal-spatial parameters [38]. Today marker based motion capture systems are widely used in gait analysis laboratories despite their disadvantages in preparation time and potential to produce artefacts [39, 40]. These systems require a number of small reflective sphere shaped markers to be attached to several key points such as the pelvis, legs and feet which are captured by infrared cameras placed strategically around the room [41]. Markers are placed following a set laboratory protocol such as Vicon's PiG model [42, 43] with the order of marking commonly being pelvis, thigh, knees, shank and foot. Alternatively, a combination of markers and clusters can be used where the latter consists of 3 or more skin markers attached to a shell. Skin markers are usually attached via double sided tape to anatomical positions on the body whilst clusters are fastened into position using a strap. Both types of marker set can be seen in Figure 6.

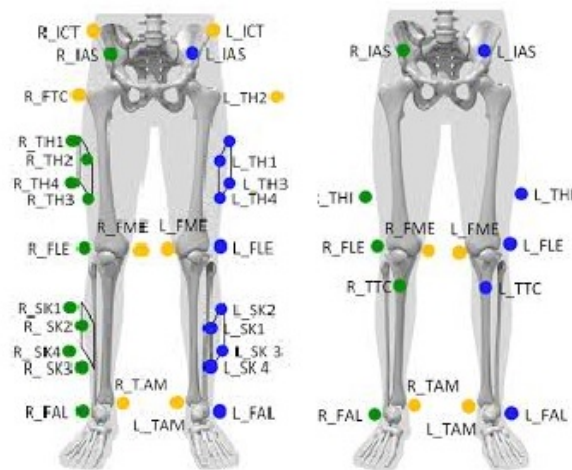


Figure 6: Two different marker sets. A marker set based on a combination of individual markers and clusters (left) and a marker set consisting of only individual markers (right)

[44]

Subsequently, the infrared cameras are calibrated and focus onto the force plate/s at the centre of the gait laboratory which the subject will be required to step on during analysis. These plates have a transducer at each corner which can capture the magnitude of the forces placed onto it [45]. A motion capture system converts the data into a video feed which can be exported for biomechanical analysis at a later stage. The system uses a series of cameras to follow the position of the reflective spheres which are attached to the lower extremities of the body. Figure 7 demonstrates a typical laboratory setup.



Figure 7: A typical laboratory setup with the PiG marker set [46]

Some of the biggest sources of error in modern gait analysis are in regards to anthropometry and compensating for soft tissue movement [47, 48]. During gait the markers which are attached to the skin do not move with the underlying bone that they are attempting to represent [49]. This error term is labelled as STA (Soft Tissue Artefact) and occurs due to skin movement and muscle contraction. There are numerical models that have tried mapping out marker movement in relation to skin; however as of yet there is no gold standard method due to the disparity between results [47].

Subject specific factors can also confound results. During gait analysis, subjects are required to wear suitable clothing which are tight fitting. Most of the lower limbs must be exposed in order for the markers to be placed accurately [47]. The wearing of loose garments may cause some of the markers to move positions and mask the true motion of the segments. At other times, some markers on the subjects body can be restricted from view and not processed whilst reflection of light by markers may cause false readings [50].

Other errors produced in the results can be down to the equipment used; these errors however have been shown by Leardini et al. [51] to be smaller than that caused by STA. This includes capturing accurate times for foot contact for slower walking patients, such as those following THR [52]. The camera systems used are prone to the production of residual values which can negatively effect the results. This is especially true for cameras which are located furthest away from the subjects. Each camera has a fixed number of pixels and must compromise between the optimum field of view and pixel resolution size [50]. The subject is therefore asked to complete a number of trials in order to gain as much data as possible in order to increase accuracy. A down side to this is that it can lead to fatigue which may cause the patient to alter the gait pattern [50].

Errors are also present with the use of the force platform, which are used to measure GRFs (Ground Reaction Forces). As the force platform is often fixed in the laboratory, the subject may have to adjust their motion in order to target a clean strike of the force plate with a particular foot [53]. Wearing et al. [54] found little effect on temporal-spatial parameters. The phase of data processing using the optical system can also produce errors through some markers being unintentionally excluded from the data, having markers which are overlapping or others that are partially included. To compensate for this, interpolation of the data points occurs which may not simulate the laboratory conditions. Other sources of error include motion marker noise, body segment inertial parameters and force plate measurement noise [55].

Temporal-spatial data obtained via gait analysis are very sensitive to walking speed which consequently makes comparisons between studies difficult [56]. Differences are often due to factors such as height, cadence and step length [57]. There are studies which have however overcome the walking speed problem by making patients walk on a treadmill which has been pre-defined at a set speed [58]. These results may on the other hand alter the regular gait pattern and thus make results unreliable. Some of the differences observed during gait analysis can be down to gender [59] and age [60].

2.1.5 Gait Kinematics

Gait kinematics is the study of velocities, positions, angles and accelerations of joints and body segments when dynamic. Kinematics provide a description of motion with the absence of the forces involved. Common outputs include temporal, linear and angular measurement data [61]. The study of angular segment displacements, also known as joint angles, are commonly used in biomechanics.

Measurement of segment displacements in gait rely on two reference systems; the global reference system which is fixed in space and the local reference system which is located on the proximal end of a segment. Joint angles are relative angles and are calculated from absolute angles which are the orientations of segments in space using Equations 2, 3 and 4 for 2D motion. Calculation of 3D angles involves the use of other techniques such as inverse kinematics.

$$\theta_{hip} = \theta_{trunk} + (180 - \theta_{thigh}) \quad (2)$$

$$\theta_{knee} = \theta_{shank} + (180 - \theta_{thigh}) \quad (3)$$

$$\theta_{ankle} = \theta_{shank} + (180 - \theta_{foot}) \quad (4)$$

During gait, 3D kinematics can be used to describe the motions of the pelvis, hip, knee and ankle in three planes of motion; the sagittal, frontal and transverse. The sagittal plane is vertical and passes through the middle of the body splitting it into left and right halves. The frontal plane is such that it passes through and divides the body into front and back sections whilst the transverse divides the body into inferior superior parts.

Anterior motion in the sagittal plane for the hip and the knee is called flexion whilst posterior motion is called extension. Sagittal plane motion for the pelvis can be described as either forwards or backwards (anterior-posterior) tilt. At the ankle, dorsiflexion refers to the curling of the toes towards the shank whilst plantarflexion refers to the curling of the toes away from the shank. Frontal plane motion towards the body is referred to as adduction whilst movement away is abduction for the hip and knee.

Frontal plane motion at the pelvis is called obliquity, with superior (upwards) obliquity referring to the upwards tilting of one side of the pelvis whilst the other side of the pelvis goes into inferior (downwards) obliquity. At the ankle, the tilting of the foot towards the mid-line of the body is referred to as inversion whilst that away from the body is called eversion. Motion in the transverse plane is referred to as rotation, with rotation towards the mid-line of the body being internal rotation and that away from the mid-line being external rotation. All three planes of motion can be seen in Figure 8.

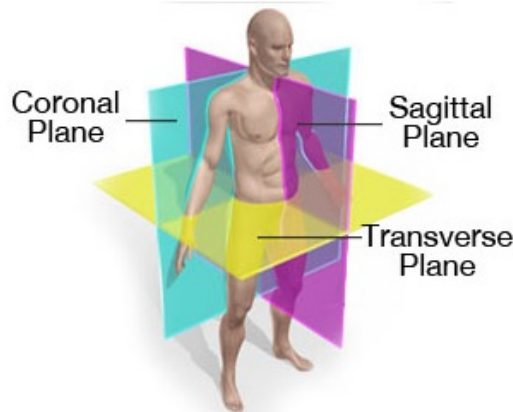


Figure 8: The three planes of motion
[62]

There are many variables which have been studied in the analysis of normal human gait including age, gender, weight, laboratory setup, injury, footwear and gait velocity [63]. Their interlinking nature however makes analysis of how each of these variables individually effects gait difficult to interpret. There however have been a considerable number of investigations which have attempted to understand how these variables can affect gait kinematics.

Younger patients generally show less variability in pelvic motions when compared to older patients [64]. Studies have determined that elderly individuals walk with a smaller amount of hip [65–67] and knee extension [68, 69] together with reduced ankle plantarflexion [67, 70] during the stance phase. The amount of anterior pelvic tilt has also been shown to increase with age when walking [65, 71]. Its coupling with a reduction in peak hip extension has been associated with hip flexion contractures [65] and a reduction in abductor muscle strength [71]. Knee flexion has been reported to decrease together with ankle plantarflexion during the swing phase in older individuals [72] which may be linked to decreased foot clearance levels. Ankle dorsiflexion has however been shown to be greater in older individuals during the swing phase [71].

In general, elderly peoples have a smaller gait velocity compared to younger individuals which may be the underlying cause for kinematic differences in joint angles. Graf et al. [67] however demonstrated that elderly patients maintained the loss of hip extension and ankle plantarflexion during gait independent of velocity. Lelas et al. [73] found that sagittal plane kinematics shared a weak relationship to gait velocity. However, Crownshield et al. [74] found that the RoM (Range of Motion) in the sagittal plane of the hip shared a linear relationship to velocity. Differences in kinematics may however also be linked to lifestyle choices with Graf et al. demonstrating that less

active elderly individuals show less hip extension, greater hip flexion in swing phase, greater pelvic rotation and reduced ankle dorsiflexion in stance phase compared to more active elderly individuals.

Authors in the analysis of obese or overweight individuals during gait have been inconsistent in their conclusions. There have been studies which observed no changes in kinematics [75], a change only in frontal plane kinematics [76], a decrease [77] or no change in knee flexion during stance [78], or many changes such as decreases in hip flexion together with an increase in ankle plantarflexion [77]. Changes in hip motion in the frontal plane have been observed as either being an increase in hip abduction [79, 80] or adduction [76] which is accompanied by an increase in the RoM. Likewise, Lai et al. [76] determined that obese patients show more knee adduction during stance whilst Mcmillan et al. [81] observed greater knee abduction. It must be noted however that gait velocity was not controlled in many of the studies which may have contributed to the conflicting results.

Gender differences exist when walking. The most in depth study was that of Cho et al. [82] who analysed and compared the kinematics of 98 adults. They showed that females demonstrate a greater pelvic anterior tilt during gait than their male counterparts. At the hip they observed greater hip flexion, adduction and more internal rotation for females. The results for adduction and internal rotation have been corroborated by Chumanov et al. [83] whilst Kerrigan et al. [84] observed greater peak hip flexion angles for females before initial contact. The greater hip flexion in females could be a result of a greater stride length in relation to height. Cho et al., Chumanov et al. and Kerrigan et al. [82–84] all agree that males show less knee flexion during stance phase of the gait cycle. Kerrigan et al. in addition observed smaller ankle plantarflexion angle values for males when compared to females during pre-swing. These differences are carried through the ageing process which suggests anatomy being the underlying cause in terms of factors such as muscle strength and activation [85].

2.1.6 Gait Kinetics

In engineering and classical mechanics, kinetics is the term used to describe the relationship between motions of a segment to forces and torques. In the analysis of the kinetics of gait, forces and torques are measured in terms of JRFs (Joint Reaction Forces), GRFs, joint moments and muscle moments.

A GRF is an opposite and equal force produced by the ground in response to the force produced by the placement of the foot on the ground [86] which complies with Newton's 3rd law of motion.

For instance, the GRF for a person standing still would be equal to bodyweight [87]. GRFs are measured using either a force plate or a securely mounted dynamometer. These forces have an inferior-superior, anterior-posterior and medial-lateral component and pass through the foot to produce movement in every lower extremity joint [88].

Kirtley [33] stated that GRFs are in reality an average of all forces or pressures under the foot with the distribution of these pressures being unevenly distributed, with the majority being at the metatarsophalangeal joints. This however contradicts the notion put forward by Watkins [89] who stated that the GRF is distributed evenly across the foot. Figure 9 demonstrates the typical GRF curves produced by a healthy person when walking.

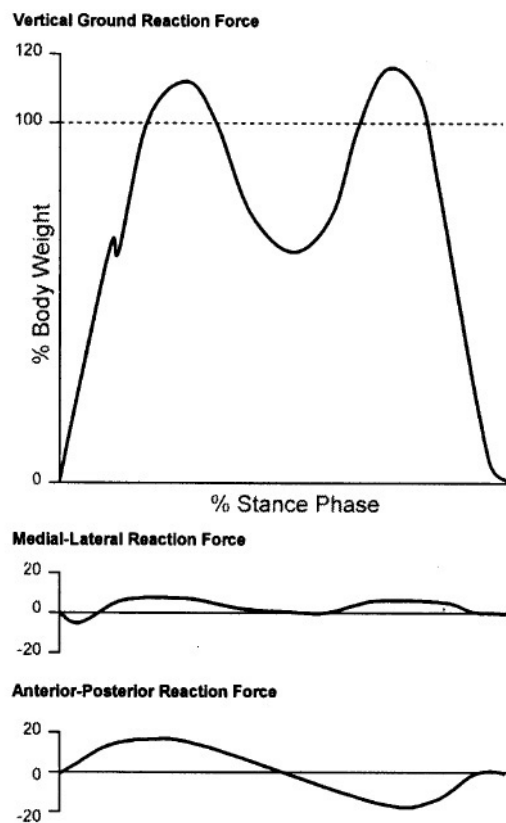


Figure 9: GRFs in the vertical, medial-lateral and anterior-posterior directions [90]

When walking, the medial-lateral component of GRF is very small and causes little side-to-side movement of the body [89]. The vertical component has the greatest magnitude and has a characteristic double peak shape during single limb support of the stance phase. Anterior-posterior components of GRF similarly show two peaks which coincide with those of the vertical. All of the components of the GRF are characterised by single or multiple spikes of force during heel strike which represent the impact of the heel on the ground [89]. The effect of the force is assumed to

occur through a single theoretical point called the centre of pressure [89] which in normal standing is approximately 5cm anterior of the ankle joint [33].

GRFs of healthy individuals during gait have been studied from a variety of perspectives. These include comparisons between healthy individuals and professional sports players [91], genders [92, 93], opposing limbs [94, 95], varying gait velocities [75, 93, 96–98], BMI (Body Mass Index) levels [75, 76] and muscle strength [99]. Jansen et al. [92] found a small statistically significant difference which was not clinically relevant between genders whilst Chiu & Wang [93] demonstrated that females produce greater VGRFs (Vertical Ground Reaction Forces) than males during the stance phase. The results of Jansen et al. may however be a better comparison between the genders as they allowed individuals to walk at a self-selected speed whilst Chiu & Wang made females walk faster to match the speed of males and hence did not take into account the differences in natural velocity between the genders. Vanzant et al. [94] found no statistically significant differences between the dominant and non-dominant foot in terms of GRFs. Likewise, Burnett et al [95] found the dominant and non-dominant limbs to have a symmetry index value of 1 implying that no difference exists in terms of GRF's.

A greater walking velocity causes an increase in VGRF during mid-stance and resultant force during loading response (occurs at approximately the 20% stage of the gait cycle) [93]. This increase is thought to be linear [97] and is linked to Newton's 2nd Law as seen in Equation 5:

$$\text{Force} = \text{Mass} \times \text{Acceleration} \quad (5)$$

Browning & Kram [75] observed that GRFs during gait increased proportionally with body-weight in their analysis of obese individuals. They also demonstrated that with an increase in walking speed, obese patients produced VGRFs which were up to 60% greater than normal individuals. Similarly, peak anterior-posterior and medial-lateral GRFs were on average 63% and 85% greater respectively for obese individuals when compared to normal individuals. La Roche et al. [99] have shown that diminishing energy levels when subjects get older are correlated to smaller VGRFs.

JRFs are produced in response to external forces acting at the joint. At the hip, these forces occur between the femoral head and the acetabulum. These forces can be calculated computationally using inverse dynamics techniques or experimentally using transducers placed inside implants. As

the latter is not possible when studying normal healthy individuals, most investigations use computational means in calculating JRFs. A thorough study of hip JRFs during gait was carried out by Paul [100] using GRF and muscle moment data via a nine-point double differentiation formula based upon a least square fit regression model [23]. Paul reported hip JRFs in the region of 2.3-5.8 times body weight during gait, which can be seen in Figure 10 .

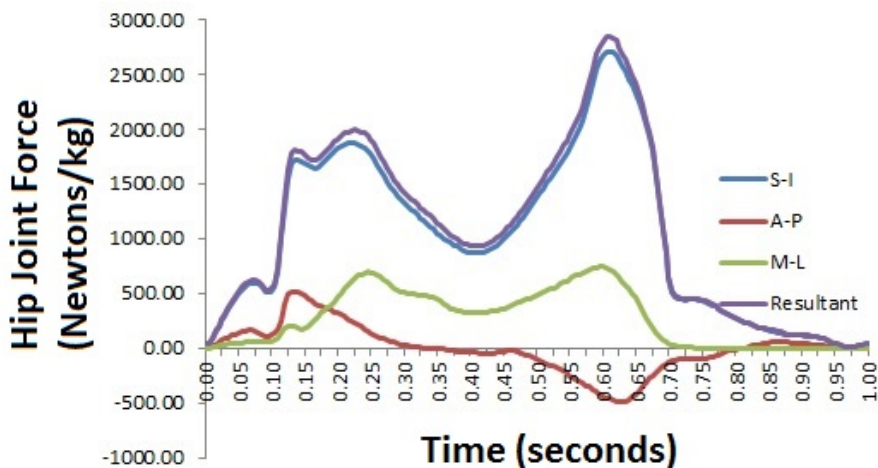


Figure 10: Hip joint forces during gait with S-I (Superior-Inferior), A-P (Anterior-Posterior), M-L (Medial-Lateral) and Resultant forces represented - Paul (1967)

Sanford et al. [101] used AnyBody (AnyBody Technology, Aalborg) to calculate JRFs for healthy, overweight and obese patients. They found that an approximate linear relationship existed between hip JRF and body mass. Stansfield & Nicol [102] used a user built muscle model consisting of 47 muscles and found that normal patients had greater hip JRFs than their THR counterparts. Meanwhile, Crownshield et al. [74] computed JRFs using the minimisation of maximum muscle stress criterion using a 30 muscle model. They found that the magnitude of JRF in a group of normal patients was correlated to gait velocity. Much of the literature focuses on pathological gait or the sensitivity of computational models to variables such as kinematics, joint centre position and muscle properties. There is very little in the analysis of normal healthy human gait.

A moment describes the rotary actions of a force whilst a joint moment describes the rotary action of a joint [103]. Moments are produced internally during gait to counteract the external forces that would otherwise cause the body to collapse. The calculation of moments at a joint are a product of the inertial properties of the segment and the angular acceleration as seen in Equation 6 where M represents joint moment, I the inertial properties and α the angular acceleration. Moments can be calculated using kinematic and GRF data. Muscles produce moments of force across joints

during the gait cycle and inverse dynamics can be used to determine whether these muscles are either in the extensor or flexor groups and the magnitude of the rotational force produced.

$$\sum M_z = I\alpha \quad (6)$$

Moments have had their relationship with demographic and anthropometric measurements studied. Typically joint moment changes have been linked to variations in joint kinematics [104]. Lelas et al. [73] found that moments at the knee during certain phases of the gait cycle shared a linear relationship to gait velocity. Likewise, Goldberg et al. [105] and Alcock et al. [72] found that peak joint moments increased with increasing levels of gait velocity. Similar results were found by Winter et al. [106] and Crownshield et al. [74]. Goldberg et al. [105] also found a stronger quadratic link between peak knee extension and gait velocity, with peak hip and knee flexion moments being less sensitive. Lathrop et al. [107] demonstrated that there was no significant association between walking speed and the magnitude of asymmetry between limbs. These studies indicate that many of the changes in gait including walking slower caused by pathology may have a significant effect on the moments generated at joints.

Gender has also been analysed with conflicting results. Lathrop et al. [107] found that there existed no differences in joint moment symmetry levels between genders. Boyer et al. [64] found no significant differences existed at the knee in terms of sagittal and frontal plane moments but did however find that females had greater hip extension, adduction and internal rotation joint moments whilst men had greater hip abduction joint moments. These results are of particular interest when analysing THR patients, where more and more younger active males are undergoing surgery together with the traditional older patient. The differences in gender are also important when studying LLI patients, where females are considered more likely to be symptomatic [7].

The study by Seung-Uk et al. [80] was able to conclude that no significant differences existed between normal and obese individuals in terms of sagittal plane joint moments whereas Browning et al. [75] discovered that obese individuals produce greater knee adduction moment which increased with walking speed. Similarly, Harding et al. [108] showed obesity levels had an effect on knee adduction, flexion and rotation moments during gait. Devita et al. [78] found that there were no differences in terms of knee moments when comparing obese individuals to healthy controls when speed was controlled. Browning et al. [75] found that hip moments did not change significantly with varying levels of velocity.

The results of McMillan et al. [81] found that knee flexion moments were significantly lower in obese patients during initial heel strike and late stance phase, whilst subjects who were obese also had significantly lower hip extension moments at heel strike together with significantly higher hip flexion moments during late stance. McMillan et al. also found that obese individuals exhibited significantly lower hip and knee abduction moments relative to controls, which conflicts with the results of Browning et al. [75]. These results do not show a definitive link between body mass and joint moments and thus do not provide any information on whether THR patients, who are commonly overweight, will have their body mass directly effect the magnitude of joint moments.

Other studies which have analysed joint moments have found that variability in knee and hip moments decreased with cadence [106] and peak knee extension and rotational moments were correlated to stride length [109]. Comparing symmetry between limbs in terms of moments has shown either high symmetry exists across all joints [110, 111] or that there is knee adduction moment asymmetry [112]. Schache et al. [113, 114] found that the joint moment was highly susceptible to the reference frame used in its measurement (distal, proximal, laboratory). with the differences particularly prevalent in the transverse plane and pathological gait. Alcock et al. [72] found older patients to have a reduced amount of ankle plantarflexion whilst Crownshield et al. [74] found a negative correlation between peak moment and age. The literature demonstrates high variability between normal patients and hence the greater potential for errors in moment calculation. It would be expected that due to greater non-uniformity seen in THR patients, there is greater potential for error in their results. All kinetic results thus must be closely evaluated before conclusions can be drawn.

2.1.7 Temporal-Spatial Parameters

Alcock et al. [72] showed that changes in velocity were the principal cause in temporal-spatial parameter variations between groups and individuals. Investigations which have ignored age when analysing the velocity of individuals have observed that men walk at a velocity between 1.18 - 1.51 m/s [115–117] whilst women walk at around 1.10 - 1.12 m/s [117, 118]. Hollman et al. [115] however were able to show that when gait speed was normalised for height, differences between genders in terms of gait velocity disappeared. Their conclusions indicated that velocity was a function of height and leg length whereas gender was a confounding variable due to the disproportionate

anthropometric measurements between men and women. A more recent study by Bruening et al. [119] however demonstrated that on average women walked slightly faster than men despite being 14cm shorter. The differences may have been due to the recruitment of physically stronger female military personal. Boyer et al. [64] observed no link between velocity and gender.

In terms of age, older people have generally been shown to walk slower than younger people [60, 68, 109, 115, 120–122]. Women over the age of 60 have demonstrated velocities between 0.89 m/s - 1.28 m/s [64, 72, 117, 121, 123] whilst younger women shown less variation with velocities between 1.11 m/s - 1.39 m/s [82, 84, 119, 121, 124–126]. Likewise, men over 60 demonstrate a smaller velocity between 1.16 m/s - 1.36 m/s [64, 68, 84, 115, 117, 121–123]. Younger men show a range between 1.19 m/s - 1.45 m/s [82, 119, 121–124, 127, 128]. The smallest values in the range for younger males (1.19 m/s) and females (1.11 m/s) as found in the literature were from a study conducted by Cho et al. [82] on Korean adults. This may be related to the smaller body proportions of people from the Far-East when compared to Europe and America which is believed to impact on gait temporal-spatial parameters.

Despite studies consistently demonstrating older individuals having a smaller gait velocity than younger subjects, Blanke & Hageman [129] found no significant difference between older and younger men and suggested any differences between the two in similar studies were due to population size and methodology. Normative studies usually report greater velocities than population based studies due to the latter including patients who may have underlying pathological conditions which will be more prevalent in older individuals [115]. It has been suggested that obese individuals walk slower than non-obese individuals in order to decrease joint loading [75, 76, 78, 79]. The systematic review by Browning et al. [130] confirms this to be a loss of approximately 0.2 m/s on average, whilst Sanford et al, [101] found there to be no difference. Alcock et al. [72] suggested a linear relationship exists between velocity and age with there being an approximate 1.2% decrease in velocity per year over a 5 year period for elderly patients whilst Himan et al. [121] interpreted the link as a cubic function. Bendall et al. [131] argued that the decrease in velocity with age is linked to multiple variables such as height, calf muscle strength, physical activity levels and general health.

Stride length refers to the distance traversed by two successive placements of the same foot during regular gait. Authors differ in their analysis of stride length with some reporting relative values, for instance in relation to height or leg length, whilst others reporting absolute values.

Alexander [132] suggested that Equation 7 could be used as a more unbiased method in comparing stride length:

$$\text{Relative Stride Length} = \frac{\text{Stride Length}}{\text{Leg Length}} \quad (7)$$

Cho et al. [82] demonstrated that leg length was statistically not significant in terms of temporal-spatial differences between groups and instead suggested other anatomical and habitual factors as the underlying cause. On the other hand, Kerrigan et al [84] showed the importance of normalising stride length for height where absolute stride length was greater for men but relative stride length in relation to height was greater for women. Hollman et al. [115] found gender differences to exist in stride length both before and after normalisation for height, showing that height was not a significant factor.

Men in general have a greater stride length than women for all ages [82, 84, 133]. Studies which evaluated the stride length of younger men found that they walked within a range of 1.26m-1.56m [69, 82, 84, 116, 119, 124, 128, 133, 134] whilst younger women walked with a stride length of 1.16m-1.43m [82, 84, 119, 124, 125, 128, 133, 134]. Kerrigan et al. [84] found differences between the genders to be statistically significant. Comparison between older and younger women have concluded that younger women have longer stride length than older women [135–137]. Hollman et al. [115] observed both older men and older women to gradually decrease stride length in 5 year intervals from the age of 70 with on average men undertaking a 1.39m stride length and women 1.23m.

The analysis of stride length in relation to age has drawn conflicting conclusions with it being greater in younger individuals [68, 116, 120] to there being no statistically significant difference [129, 138]. These differences may however be simply down to study design with Devita & Hortobagyi demonstrating that when matched for velocity values, there is no difference between the groups. Crownshield et al. [74] found that a non-linear relationship existed between stride length and velocity. Browning & Kram [75] demonstrated that stride length did not differ significantly between obese patients when velocity was controlled, indicating that velocity may be the factor which causes the discrepancies between stride lengths. Blanke & Hageman [129] matched the elderly and normal groups in terms of leg length due to its perceived effect on stride length and found that there were no statistically significant differences between the groups. Cho et al. [82] however argued this could

potentially be an invalid assumption. Kirtley et al. [109] found that there existed a negative linear relationship between stride length and age.

The percentage of time spent in the stance and swing phases of the gait cycle are known to be effected by velocity, leading to differences between older and younger individuals when measured.. Blanke et al. [129] observed that younger men spent 57.6% of the gait cycle in stance and 42.4% in swing phase. These values differ for those of a young women who Jimenez et al. [125] demonstrated spent 60.9% in stance 39% in swing. Kadaba et al. [124] found that men spent slightly longer in stance (61%) than women (60.7%). Both older men and older women over the age of 60 show an increased stance phase time with men averaging between 59% - 74% [115, 139, 140] and women 61.2% - 69% [115, 139]. Swing phase time is decreased in older men to between 35.8% - 38.9% [129, 139]. Comparisons between younger and older women however show similar swing time durations with the former staying in swing for 39% [125] of the gait cycle and the latter 38% - 39% [115, 139]. Obese individuals walk in a similar manner to elderly subjects with an increase in stance and increase in swing phase proportions of the gait cycle. Differences in stance and swing phase times may reflect differences in gait velocity, with a faster walking speed correlating to a decrease in stance phase time and an increase in swing phase time [141].

2.2 Total Hip Replacement Patients

2.2.1 Etiology

A hip replacement is a relatively common procedure in the UK with over 91,000 operations carried out in 2014 and 100,000 in 2015 [142]. Patient satisfaction levels are high with over 90% of patients satisfied postoperatively [3]. This type of surgery can be performed as a total replacement or a hemi (half) replacement. A THR, also known as Total Hip Arthroplasty (THA), is a surgical procedure where the whole of the hip joint is replaced by an artificial implant. Surgical intervention is normally required when patients complain of excessive hip pain or show signs and symptoms of arthritis, with the aim of the procedure to restore hip range of motion and alleviate pain.

There are generally three components to the hip replacement implant in THR; the acetabular cup, the liner and the femoral component. There can however be additional components depending on the implant type. The Acetabular cup is placed into the acetabulum in a process which requires surgical removal of cartilage and bone. A liner is placed inside the cup which is typically made of polyethylene or ceramic. The femoral component fits into the femur which has bone removed from it during surgery so that it is able to accept the stem which is attached to the femoral head. This can be seen in Figure 11

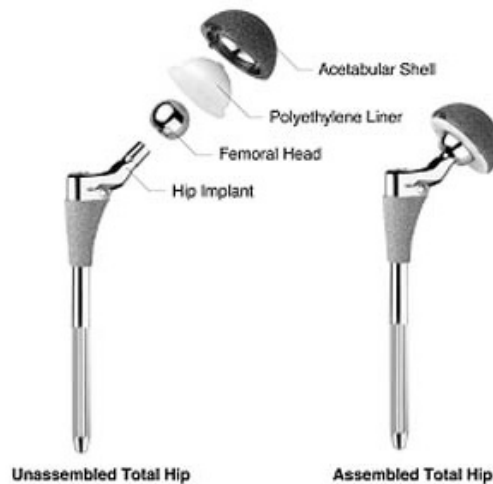


Figure 11: Total Hip Replacement Components [143]

2.2.2 Gait

The kinematics, kinetics and temporal-spatial parameters during gait can give an indication to the success of THR and may aid in predicting long term outcome. This had led there to be an

extensive body of literature in the analysis of gait following THR with studies focusing on varying areas of interest. These include comparing gait following THR against effects post-surgery alone [144–155], implant type and alignment [153, 154, 156–161], methods of arthroplasty [162–169], age [170], gender [171–173], preoperative levels [160, 171, 174–178, 178–187], normal healthy levels [102, 161, 164, 170, 171, 173, 174, 178, 180, 188–199], contralateral joint mechanics [194, 199–202], environmental factors [203] and surgical approach [172, 200, 204–215].

Studies have differed in not only the comparisons made, but in many other factors. For instance, the follow up time has varied between 6-120 months and the number of THR patients studied has ranged between 2-13. Patient average age has varied between 44-74 [216]. Almost all studies analysed THR patient gait at self-selected speeds, with Mocket et al & Illyes [58] being one of the few exceptions. Studies also differed in the surgical approach taken, although this was not an independent variable in most studies. Likewise most investigations do not match THR patients to controls in terms of age, gender, BMI or height. Each of these variables can confound results.

2.2.3 Gait Kinematics

The study by Perron et al. [171] which analysed the effects of THR on women is one of only two studies looking at kinematics from the perspective of demographics. It was found that compared to controls, women had a 59% drop in peak hip extension levels and a 63% increase in anterior pelvic tilt at toe off. This was coupled with a decrease in hip rotation RoM. At heel strike, there was a 25% decrease in peak knee flexion. For the ankle, there was a 26% increase in dorsiflexion half-way between mid-stance and toe off. Tateuchi et al. [173] found that significant differences existed between maximum hip extension angle and pelvic rotation between women post-THR and a control group also consisting of women.

Authors have attempted to find a link between kinematics and the type of hip implant used. Olsson [153] found that maximum VGRF and gait velocity could be used to distinguish between the cemented Charnley and non-cemented HP Garches implants. Meanwhile, Gotze et al. [156] found that a customised implant produced a smaller decrease in hip sagittal plane RoM compared to controls (11.4%) and compared to a conventional stem group (17.4%). This may have been linked to implant design, with a better positioned implant with a more favourable design (e.g. a larger head allowing greater RoM) allowing patients to take greater strides.

A study by Tsai et al. [159] found that the amount of hip internal rotation was directly linked to cup anteversion, cup medial-lateral translation, cup inferior-superior translation and hip anteversion. Comparisons in terms of varus-vargus angulation of the hip joint were made by Hodge et al. [161]. Results indicated that the valgus group had a greater RoM which was similar to that of control subjects. The varus group demonstrated a greater reduction in peak hip extension angle together with greater asymmetry compared to the non-operated side.

Another area of interest is that of the type of THR undertaken and the corresponding effects on kinematics. Bach et al. [164] compared Robodoc, a robotic surgical system which assists surgeons in correctly placing the implant, to conventional THR methods. The results showed that the patients who had undergone Robodoc surgery demonstrated a reduction in hip flexion compared to a healthy control group and at a similar level to the conventional THR method. There were no significant differences between the operated groups in the frontal plane with regards to hip kinematics. Bennet et al. [167] compared the minimally invasive and traditional THR methods at 2 days and 6 weeks postoperatively. No significant differences were found in terms of joint kinematics. A study by Andersson et al. [168] aimed to understand whether early weight bearing activities following THR had an influence on kinematics in the first 24 weeks. Once again no significant differences were found between the early weight bearing and late weight bearing THR groups. The type of THR appears to have little effect on kinematics.

An aligned area to that of arthroplasty technique is that of surgical approach, in which comparisons are made to the location of the incision during THR. Two studies by Queen et al. [204, 209] found no differences in kinematics from 6 weeks to 1 year following THR between the anterolateral¹, posterolateral and direct lateral² approaches. On the other hand, Holnapy et al. [207] found that differences did exist in terms of the posterolateral approach showing that postoperative gait was more similar to that of controls, with the exception of pelvic rotation. Kiss & Illyes [208] compared the direct lateral and anterolateral approaches and found significant differences in hip kinematics at 3, 6 and 12 months post-surgery. A similar study by Mayr et al. [215] found that patients who had undergone the direct lateral approach had greater improvements in gait after 12 weeks than those who had undergone the anterolateral approach. Significant differences between the anterolateral and posterolateral groups were found by Lugade et al. [211], with the former showing a smaller hip

¹Involves the detachment of one third of the Gluteus Medius to gain access to the hip joint. The muscle is subsequently reattached

²Is where the surgeon makes a curvilinear split through the anterior portion of the Gluteus Medius in order to gain access to the anterior face of the hip joint

RoM. Figure 12 demonstrates three different surgical incision approaches.

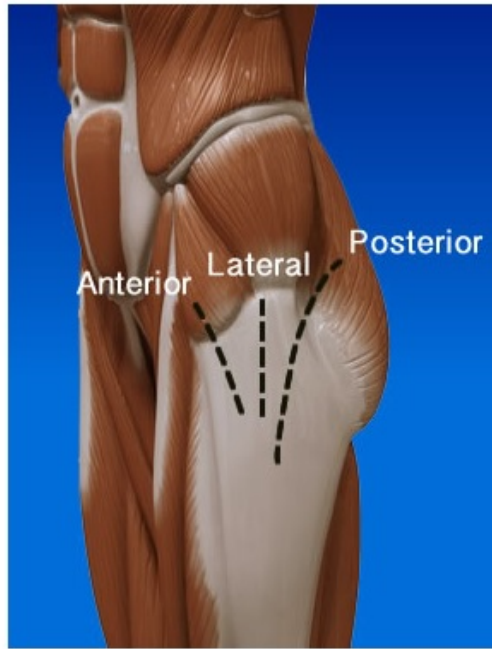


Figure 12: A schematic showing the anterior, lateral and posterior incision sites for a THR [217]

Rathod et al. [205] compared the direct anterior approach to the posterolateral approach and found significant differences between the methods 6 months post-surgery in terms of hip internal-external rotation. Jolles et al [212], who also compared the direct anterior approach to the posterolateral, similarly found differences with the posterolateral patients showing greater internal rotation. This was hypothesised to be linked to the release and repair of the external rotators during posterolateral approach surgery. Whatling et al [200] also compared the posterolateral approach to the direct lateral approach, with the latter showing a smaller RoM at the hip and pelvis. It is clear from the literature that in the majority of cases the type of surgical approach has a large impact on clinical patient outcomes.

Kharma et al. [201] found that contralateral hip and knee biomechanics remain unchanged following THR. Tsai et al. [202] however found significantly higher hip internal rotation during the stance phase and greater hip adduction during the swing phase on the non-operated side. The increase in internal rotation levels was also seen by Hakkinen [175]. Similar RoM values were found for hip motion in all three planes, with the operated side showing on average more variability. Horstmann et al. [180] found that the contralateral hip and knee showed a smaller RoM compared to controls, which was still however greater than that of the operated side. Whatling [200] compared gait symmetry between the operated and non-operated sides using different surgical approaches.

They concluded that the use of the posterolateral approach over the direct lateral approach led to greater symmetry in terms of RoM at the hip but less symmetry at the pelvis in terms of tilt.

The two most common types of gait analysis with regards to THR are comparisons to preoperative measurements or to normal healthy controls. With regards to the former, Wykman et al. [150] found that there were no significant differences in preoperative and postoperative gait following THR. Other studies found an increase in hip flexion RoM coupled with an increase in peak hip extension [178–181, 187, 204, 208, 209]. Studies however differ with some finding an increase in hip frontal plane motion [187, 205, 208], whilst others observing no change to preoperative levels [179, 205], demonstrating the high inter-patient variability and difficulty in assessing the success of surgical procedures. Hip rotation RoM has been observed to increase following surgery [179, 187, 205, 208] or remain the same [205]. Improvements in pelvic motion [178, 181], knee flexion [178] and ankle dorsiflexion [178] have been seen postoperatively.

Most kinematic results have compared postoperative THR gait to a control group of healthy normal individuals. A majority of studies [154, 156, 164, 178–181, 197, 204, 208, 210, 213] show that post-THR, gait kinematics improve to a certain extent but are never able to reach the level of normal healthy individuals. This is through showing greater asymmetry between limbs and a smaller RoM for all planes of motion at every joint. To the authors knowledge, the investigations by Tatateuchi et al. [192] and Casartelli et al. [188] are the only published works where the kinematics post-surgery are equivalent to controls. The amount of hip flexion and extension are often both greatly reduced, with the literature review by Ewen et al. [218] finding a cross study RoM for THR patients of between 23.2° - 40.8° , with controls having values between 31.3° - 51.8° . Reductions have also been seen in the frontal and transverse planes of hip motion [164, 213] together with smaller peak ankle dorsiflexion angles [195]. Post-THR kinematics at the pelvis and the knee have been found to be similar to controls [195] or different to controls [197, 207]. As THR patients show high variability and that there are many factors which can impact kinematics, it is not surprising to find results from different studies which conflict with each other.

2.2.4 Gait Kinetics

The kinetic outputs of gait following THR have been investigated. VGRFs have been shown to decrease on the operated side following THR and the characteristic double peaks to occur at different stages during the gait cycle [149, 189, 191]. Olsson [153] found the magnitude of the peak VGRFs

could be used to distinguish between the type of hip implant that had been used. There however appear to be no significant differences between the non-operated side and controls [189, 191]. Surgical approach does not significantly impact the magnitude of GRFs [163], although Leutche et al. [162] did find that the minimally invasive THR method produced results more similar to controls between 8 - 14 weeks post-surgery.

JRFs have previously been computed using computational rigid body mechanics or through experimental results from specially designed implants which can calculate in-vivo forces. With regards to the latter, the study by Bergmann et al. [148], is considered the gold standard and is what comparisons are generally made against. This study analysed the gait of 4 instrumented hip prosthesis in 4 patients at varying speeds. These results for the four patients can be seen in Figure 13 together with the hip contact forces predicted for the operated side of THR patients using AnyBody by Li et al. [199].

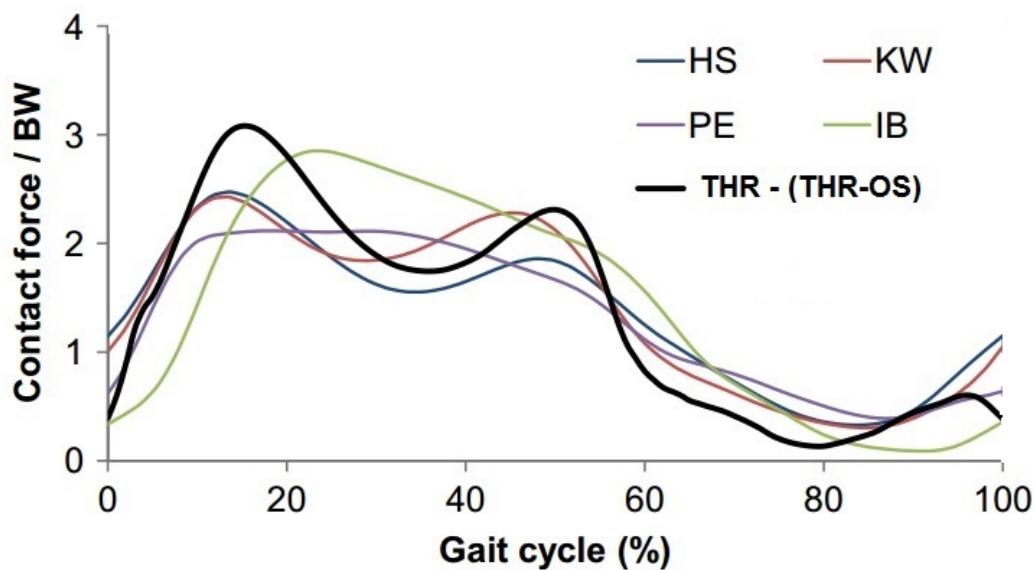


Figure 13: The black line denotes the average THR force computed by Li et al. whilst all other lines denote individual patient results during gait at a self-selected speed by Bergmann et al. [199]

Bergmann et al. found that during level walking, intra-individual differences between patients were small, whilst the inter-individual differences were significantly larger. Peak hip contact forces during gait were found to be on average $2.47\text{N/kg} \pm 0.26$. Due to the variability shown and that the analysed patients had their gait measured at various times following THR (between 11 and 31 months), the results do not give an accurate representation for a particular period of time after surgery. An earlier study by Bergmann et al. [219] investigated JRFs in two atypical THR patients.

They found that JRFs increased with gait velocity. Meanwhile, van den Bogert et al. [146] found that the average peak JRF following THR using an instrumented prosthesis for a group of 9 patients was $2.5\text{N/kg}\pm 0.3$.

Brand et al. [147] studied the gait of two THR patients from both the experimental in-vivo and computational perspectives. A disadvantage was however that the experimental gait analysis results were produced 3 months prior to the gait analysed for the computational dynamics. For the in-vivo results, they found JRFs peaked at around $2.5\text{-}3.5\text{N/kg}$. The accuracy of the results is questionable due to one of the two patients used in the study having the instrumental implant used as a part of revision surgery. Davy et al. [145] found similar results with the peak hip JRF being between $2.6\text{-}2.8\text{N/kg}$. Schwachmeyer et al. [155] observed median joint forces of 2.66N/kg in their analysis of 6 patients with instrumented hip prostheses. These studies often however do not mention if patients have issues on the non-operated side or other musculoskeletal problems, making comparisons inconclusive.

As with the in-vivo results, computational results are highly dependent on kinematics, temporal-spatial parameters and most importantly the model used for inverse dynamics. There is however sparse literature dealing with hip JRFs following THR. Li et al. [199] compared a cohort of THR patients against controls and found that normal patients exhibited greater force during gait whilst there was not a significant difference in force between the operated and non-operated hips. This computation was undertaken via the use of AnyBody (Aalborg, Denmark) which comprises of 70 muscles with a lower extremity model of 18DoF. AnyBody has been validated in terms of its computation of JRFs against that of Bergmann et al. [148] by Manders et al. [220].

As joint moments are computed as a product of the joint moment arm and JRF, they are also impacted by factors which effect forces such as kinematics and walking speed. As the position of the joint centre post-surgery can vary considerably, the moment arm calculation can show some significant differences between patients. This leads to high variability in joint moment results. Peterson et al. [157] found that peak abductor moment at the hip showed greater improvement with the use of the Mallory-head Exeter prosthesis compared to a resurfacing implant 12 weeks post-surgery. It was suggested that this was due to the Mallory-head Exeter prosthesis requiring a less invasive surgical procedure. Abductor moments however show a trend to decrease following THR compared to healthy controls [165, 166, 171, 179, 181, 195, 196, 198, 214, 215], despite statistical

significance not always being achieved. Some studies found that no changes were present in terms hip extension moment following THR [165, 179, 213] whilst others found a reduction [166, 198, 215].

Hodge et al. [161] found that their varus stem group produced hip flexion moments significantly greater than controls, whilst the valgus group produced similar results to that of controls. Perron et al. [171] observed a decrease in peak external rotation moment during mid-stance, a 25% decrease in peak knee extension moment at weight acceptance and a 25% decrease in ankle eversion moment during toe-off for women following THR. Other studies have also found a loss in peak knee extension moment [196].

Comparing moments between the operated and non-operated sides, Miki et al. [178] found that there existed asymmetry in terms of hip extension and abductor moments preoperatively. These differences also existed postoperatively at various points in the gait cycle. Abductor moment was however found to recover on the operated side to non-operated levels 6 months following surgery. In addition, Miki et al. found that peak hip extension moments were inversely related to gait velocity. Foucher et al. [201] were able to conclude from their study that there existed significant differences in peak hip abductor and internal rotation moment between the non-operated side and the controls. These changes did not improve during a follow up study after 1 year. Tateuchi et al, [192] is the only study which found no statistically significant differences were detected. It is clear that there is not a single factor which is important when determining joint moments but a multiplicity of many different factors. This can make it difficult to confidently state conclusions.

2.2.5 Temporal-Spatial Parameters

Temporal-spatial parameters of THR patients have been analysed both preoperatively and postoperatively. Generally THR patients have been found to walk slower than healthy controls [172, 194, 195, 198, 199, 221], although there have been investigations which found no difference [197, 210]. THR patients have also been found to walk faster following surgery [152, 163, 184, 196]. Across studies, the average gait velocity for THR patients preoperatively is between 0.91m/s-1.21m/s [196, 205] and postoperatively is between 0.707m/s-1.36m/s [157, 163, 196, 200, 205, 210, 218]. Bennet et al. [169] in their study which analysed immediate postoperative gait achieved smaller average values between 0.27m/s-0.29m/s.

Meneghini et al. [163] found that gait velocity increased postoperatively regardless of the surgical

approach used with Leutche et al. [162] discovering that velocity was more similar to that of controls if the minimally invasive procedure had been used. Patients who have undergone the posterolateral surgical approach have been found to walk faster [163, 200] and slower [205] than patients who have undergone the direct lateral approach. Olsson et al. [153] discovered that postoperative gait velocity could be used to distinguish between the type of implant used during surgery. Velocity has also been described as the cause of the differences between healthy cohorts and THR patients, with speed matched results demonstrating equal gait parameters between the two [193].

Stride length has been reported to be smaller for THR patients relative to controls [102, 161, 171, 194, 195, 198, 210, 221] or not statistically different [161, 166, 192]. A smaller stride length is expected due to the commonly seen smaller RoM in the hip sagittal plane. Mayr et al. [215] found that 12 weeks post-surgery, patients who had undergone the direct lateral surgical approach had significantly increased their stride length whilst those who had undergone the anterolateral approach had not. This demonstrates that the removal and repair of muscles using a particular technique potentially weakens the abductor muscles more and limits the patients ability to improve their gait pattern post-surgery. Stride length may however have been associated with leg length which could have confounded some of the results observed.

Results between patient groups are often compared through the comparison of stance and swing phase times. Kyriazis & Rigas [154] observed a decrease in stance phase time following THR compared to preoperative levels. It was found by Queen et al. [204, 209] that surgical approach had no effect on the stance phase time whilst Deshmukh et al. [206] found that there was. Stance time is longer in healthy controls [189, 191] and greater post-surgery [189]. Swing time has been found to not be significantly effected by surgical approach by Queen et al. [204, 209] but was found to have increased in the study by Bhargava et al. [189].

2.3 Leg Length Inequality Patients

2.3.1 Etiology

Anisomelia of the legs, better known as a leg length inequality, is the condition where paired leg length is noticeably different as can be seen in Figure 14 [222]. Naturally occurring LLI is surprisingly common, with Woerman & Binder-Maclead [223] reporting 70% of otherwise healthy individuals having a LLI, with approximately 23% having a difference of 10mm or more [224]. Guichet et al. [225] reported that despite these large numbers, only 1 in every 1000 individuals would require medical treatment to overcome symptoms associated with LLI through the use of a shoe lift.

A difference in leg length can be due to asymmetries at the hip caused by different femoral offsets, at the knee due to different knee heights [226] or at the ankle. Of these individuals, there are a proportion who are symptomatic and another who are asymptomatic. The magnitude of what constitutes a symptomatic LLI has been heavily discussed in the literature with varying cut-off levels suggested. In terms of patient subjective feedback, differences ranging from 5mm - 60mm have been reported to be the amount of discrepancy to cause symptoms such as lower back pain. Objective analysis measuring significant changes in biomechanics suggest a range from 3.2mm - 49mm [227]. A consensus exists in the literature that generally anything below 10mm is acceptable. A significant difference in leg length can lead to the development of nerve palsy, limp, osteoarthritis in the shorter limb, spinal deficiencies, instability and the need for surgery [9].

Although there is a high success rate for THR with 100,000 operations undertaken in 2015 alone [142], some patients complain of having a LLI postoperatively. A symptomatic LLI patient can be defined as a individual who post-THR perceives a change in leg length which they are troubled by to such an extent that they require revision surgery. LLI following THR can be split into two distinct etiological categories; those with an anatomical LLI due to the shortening of bone and those with a functional LLI such as muscle shortening as a result of a contracture. Anatomical LLI, also known as a true LLI, can be subdivided further into types 1 and 2 [11]. A type 1 anatomical LLI is caused by the component itself such as the stem being too long, the cup being placed too low or incomplete stem insertion into the femur whilst type II is due to the mal-positioning of component including excessive amounts of antversion or retroversion of the acetabular cup [7]. A type I anatomical LLI increases soft tissue tension around the joint and reduces instability [11]. This leads to a compromise having to be made between stability and patient satisfaction, with a greater increase in leg length leading to a more stable joint. Approximately 10% of all patients following THR are symptomatic

for an anatomical LLI [6], with a typical patient seen in Figure 14.

Patients who undergo bilateral THR are more likely to be symptomatic for an LLI due to having undergone the surgical procedure twice. Alfaro-Adrian et al. [228] found that 9% of operated hips were bilateral. With the relatively large number of THRs in the UK annually and with studies demonstrating on average greater differences in leg length for bilateral over unilateral patients [229], careful preoperative/intra-operative planning is required to ensure minimal patient dissatisfaction when both hip joints are replaced.

Functional LLI, also known as apparent LLI, occurs due to tightening of muscle or bone leading to an adduction or abduction contracture on the perceived longer side [7]. Other common causes include knee hyper-extension, supination or pronation of one foot relative to the other and lumbar scoliosis caused by pelvic obliquity [222].



Figure 14: The typical stance adopted by an individual with an LLI with the longer leg flexed to accommodate its change in length

[11]

Patients are more able to tolerate a shortening of leg length than lengthening [230]; this is thought to be related to soft tissues that may be stretched if lengthened. A post-THR follow-up study undertaken by Konyves & Bannister [227] revealed that 60% of patients who had undergone

THR had acquired an increase in leg length on the operated side, with 32% having a decrease and equality only achieved in 8% of patients. Whitehouse et al. [231] found that 90% of patients had a longer leg postoperatively with just 8% having their leg shortened. Most of the changes in leg length were very small in magnitude with only 21% exceeding 10mm, which is the level suggested by Beard et al. [232] for functional outcomes to worsen. The relatively large number of patients who are symptomatic has led LLI to become one of the most common causes of orthopaedic malpractice claims [17, 18], with it contributing to almost 5% of all medical errors [233].

2.3.2 Risk Factors, Clinical Symptoms and Treatment

McWilliams et al. [7] identified several risk factors which could potentially increase the possibility of a patient becoming symptomatic for a LLI. These can be broadly split into three categories of pre-existing factors, preoperative techniques and postoperative techniques. An atypical anatomy such as poor bone stock or a narrow femoral canal potentially can lead to difficulties in inserting the artificial stem into the femur [7]. This can be further complicated by individuals with high BMI levels. Shorter individuals with smaller pelvises will have any leg lengthening contribute more to their overall height which will produce a greater amount of pelvic tilt [234, 235]. Due to this, females are more likely than males to be symptomatic for a LLI.

Individuals with low physiological thresholds are also at greater risk as they may not be able to withstand the increased demands that the LLI puts onto their gait [7]. Surgeons are required to make joint stability their priority during surgery over equalisation of leg length, with only 70% of procedures making leg length equalisation a goal [236]. Ineffective communication between clinician and patient can lead to unrealistic postoperative expectations and hence increase the likelihood of being symptomatic. This notion however contradicts the findings of White & Dougall [237] and Whitehouse et al. [231] who observed no statistical relationship between LLI magnitude and patient satisfaction.

Planning prior to the operative procedure in terms of component usage and surgical technique form an essential relationship to the postoperative outcome. Preoperative templating refers partly to the position from which to measure the level of femoral neck resectioning during surgery and the type of implant to be used [238]. In a series of 110 primary hip replacement cases, Knight & Atwater [236] found that acetabular cup size was correctly predicted in 62% of cases and the size

of cementless stems was only correctly predicted 42% of the time.

Konyves & Bannister [227] found that 82% of postoperative increases in leg length were linked to stem position with there being no association between LLI and acetabular centre of rotation. In addition, they also found that the type of femoral component used had a statistically significant effect postoperatively with the CPT components usage leading to fewer leg length differences compared to Exeter, C stem, Charnley and the IPS. Further still, Konyves & Bannister [227] demonstrated for their cohort of patients that the posterior surgical approach produced on average a smaller magnitude of LLI (1.2mm) compared to the lateral approach (6 mm). Statistical testing was not performed to determine the significance of this result. Another study by Nam et al. [239] found no statistically significant difference between a posterolateral and anteriorolateral surgical approaches in terms of the magnitude of postoperative LLI.

Intra-operatively, there are many factors which can dictate whether a patient will be symptomatic for an LLI. Having the patient positioned in the supine position provides the surgeon with a clear view of the acetabulum and reduces the possibility of improper component positioning [9]. The position of the legs can still be a potential source of error with as little as 5° - 10° abduction or adduction leading to a 8mm - 17mm change in clinically measured leg length [240]. It also makes intraoperative measurement between the anterior superior iliac spine and the medial malleolus easier. Surgical technique may also have an influence on postoperative result with Williamson & Reckling [241] observing that fewer patients had an LLI if the greater trochanter was removed during surgery; trochanteric osteotomy is however now rarely practiced in modern hip arthroplasty surgery.

The symptoms associated with LLI following THR vary according to a variety of factors. Symptoms can arise immediately postoperatively or can occur at a later stage [7]. Small inequalities which are under 10mm are usually well tolerated by patients and go unnoticed. In general, those individuals involved in more demanding activities are more likely to be symptomatic compared to less active individuals regardless of the magnitude of the leg length difference [222]. If symptoms do arise, physiotherapy is often used successfully as a treatment. Nerve palsy and neurogenic pain can occur with any degree of leg lengthening but may resolve if leg equalisation is achieved following revision surgery [242].

Inequalities greater than 20mm usually lead to greater patient dissatisfaction through back pain

and gait abnormalities, with the latter leading to increased muscle activity, heart rate and oxygen consumption levels [243, 244]. Edwards et al. [245] found that patients with a peroneal palsy had an average LLI of 27 mm whilst those with a sciatic nerve palsy had an average of 44 mm. Nerve injuries are more common in woman due to the vulnerable sciatic nerve being in closer proximity to the surgical site [7, 246]. Changes in gait often accompany an LLI with limping and fatigue being commonly observed [7]. Symptoms can also arise at other joints on the operated sided limb and also on the non-operated side limb.

A LLI has been associated with implant dislocation, aseptic loosening [247] and stress fractures [222]. Swaminathan et al. [248] demonstrated that an increased load is placed on the shorter leg when static whilst Krakovitis [249] found that the weight bearing area of the femoral head reduced by 5% with a 10mm increase in leg length. Visuri et al. [247] suggested that a postoperative LLI is the most important variable in predisposing patients to aseptic loosening following a hip replacement. Friberg [250] reported that 46% of individuals with an LLI between 10mm - 14mm had stress fractures and 66% of those with an LLI between 15mm - 20mm had stress fractures. This is potentially a consequence of edge loading, which occurs due to poor positioning of the hip component [251]. Gofman & Trueman [252] suggest that an elongated leg may be a predisposing factor for the development of osteoarthritis at the hip and the knee. Golightly et al. [253] found that subjects symptomatic for an LLI were more likely to have knee symptoms (26.1%) than those without (17.7%).

2.3.3 Radiographic Measurement of LLI

There are many techniques utilised today to measure LLI including imaging (CT, MRI, Ultrasound, plain radiography, computed radiography and digital radiography [254]), via the use of a clinical tape measure and visual inspection [255]. Clinicians are often required to choose the most appropriate technique to use and take into account factors such as cost, magnification, accuracy and safety. Visual inspection is usually avoided due to not being an objective measure but has been shown to produce high levels of inter-examiner agreement when determining whether a significant amount of LLI exists [255].

A review of the literature by McWilliams et al. [256] found 4 different radiography techniques used to measure leg length. The most popular was the method which creates a reference line between the inferior portions of the two teardrop landmarks before creating an inter teardrop

line, with leg length measured as the perpendicular distance between this line and the centre of the lesser trochanter. A second commonly used method was that of measuring the perpendicular distance between the inter-ischial line and the centre of the lesser trochanter. These methods are more commonly referred to as the Woolson and Williamson methods respectively, which can both be seen in Figure 15. The other common radiography methods found were the use of mercury and a scanogram.

McWilliams et al. [256] provide the only thorough analysis of the reliability of the Woolson and Williamson methods, which they compared to the McWilliams method. McWilliams found that the methods of Woolson and Williamson were comparable to their own method for inter-reader and intra-reader reliability of measurements taken from the same radiograph, even when taken on different occasions. The method as used by McWilliams has the additional advantage of being able to distinguish a LLI caused by cup position and a LLI caused by stem position. The Williamson method has been found to be more reproducible in other studies than that of Woolson, despite errors as large as 5mm being common [257]

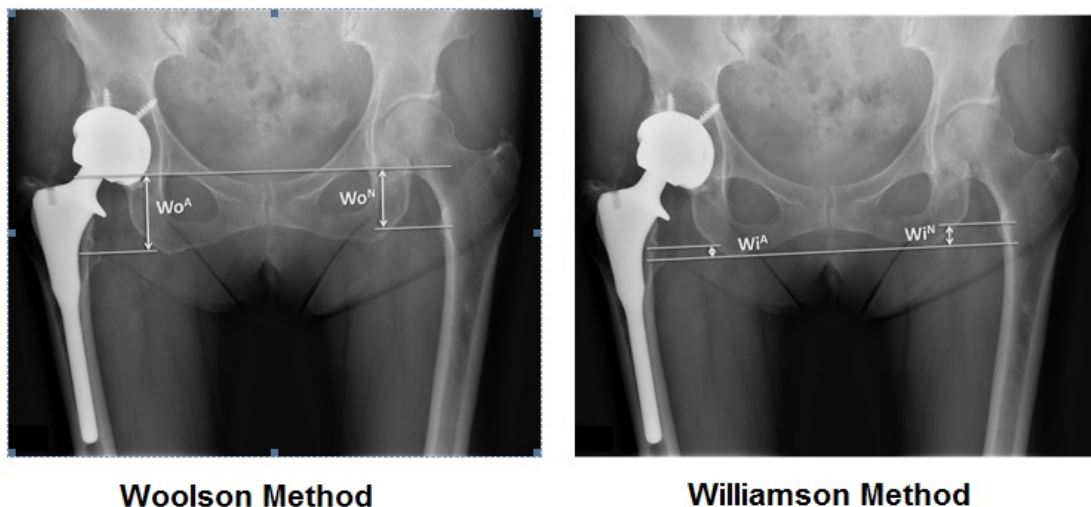


Figure 15: Two of the commonly used leg length measuring techniques on radiographs [7]

2.3.4 Hip Joint Centre

There are many methods used in the literature to determine the position of the HJC (Hip Joint Centre) which make use of anatomical landmarks on patient radiographs such as those of Fessy et al. [258], John & Fisher [259] and Ranawat et al. [260]. These methods however rely on the quality and magnification of the x-rays used with the methods of John & Fisher and Ranawat et

al. requiring the pelvic height, calculated using the superior pelvic rim, which is not always visible. Many of these techniques also utilise anatomical landmarks such as Kohlers line. These may provide an accurate representation of HJC but may cause issues in that some anatomical landmarks become less visible following surgery. This has been shown by Robb et al. [261] who were able to identify the teardrop on both sides of the hip on 93% of occasions on normal healthy people whilst Albinana et al. [262] only identified it on 16% of post-THR patients. The true physiological hip centre is calculated by placing a circle around the femoral head and then drawing two perpendicular lines producing a quadrant in the circle [263].

2.3.5 Gait Kinematics

To the authors knowledge, the studies by Budenberg et al. [264] and Li et al. [221] are the only publications to analyse dynamic motion of patients symptomatic for an LLI following THR. They found that during gait, LLI patients walked with a reduction in hip flexion-extension and abduction-adduction RoM and an increase in internal-external rotation RoM. In theory, most of the THR patients studied in the literature have a certain amount of LLI due to it being relatively common, with study subjects potentially being a mixture of symptomatic and asymptomatic individuals. Much of the literature in terms of kinematics focuses on naturally occurring LLI, paediatric LLI and artificially induced LLI. These studies may not necessarily accurately depict the anatomical changes which occur for a structural LLI where the discrepancy is at the bone. Some of these results may however help in understanding why patients who have an LLI post-THR are symptomatic.

The compensatory mechanisms used by subjects during gait can occur at the trunk, pelvis, hip, knee and ankle. The joints on both the longer and shorter side of the leg can be affected. These occur to shorten the longer leg and increase the length of the shorter leg. Most authors agree with the types of compensatory mechanisms used by subjects with a natural LLI. Kaufman et al. [265] stated that mechanisms to shorten the longer leg include increasing pelvic obliquity, hip abduction, knee extension during mid-stance and vaulting over the longer leg. For shortening the longer leg, a subject potentially increases hip and knee flexion, dorsiflexes the ankle and increases pelvic tilt [265]. Gurney et al [244] corroborate this where they found that an artificial LLI led to increased hip flexion, knee flexion, and abduction of the longer leg. In addition, they observed that 5% of the subjects demonstrated hip hiking through lumbar side flexion during swing phase on the longer leg. Gurney et al. found a total of 10 compensatory strategies used with 18% of subjects showing no changes in gait regardless of the magnitude of the LLI.

A significant study in the analysis of gait for individuals with LLI was that of Walsh et al. [235], who observed the same compensatory mechanisms as discussed previously when simulating LLI with the addition of ankle pronation on the shorter side. They also found that the ankle was very sensitive to kinematic changes for any level of LLI whilst knee kinematic changes became more significant at greater LLI magnitudes. Walsh et al. were able to demonstrate that with increasing levels of LLI between 10mm - 50 mm, the amount of pelvic obliquity, hip flexion and knee flexion showed a corresponding increase at heel strike on the longer side. The increasing levels of flexion at the knee and the hip would have been to provide adequate foot clearance for the leg to move from the stance phase into the swing phase. No significant changes in dynamic motion were found in the frontal or transverse planes.

Another area of analysis is that of statics. Similar compensatory mechanisms as shown in dynamics occur with pelvic obliquity, flexing of the hip and the knee on the longer leg and plantarflexing the ankle on the shorter leg [222]. Walsh et al. [235] found that during standing, simulated levels of LLI caused an increase in knee flexion from 20mm upwards whilst pelvic obliquity was at its greatest at a magnitude of around 30mm. Vink et al. [266] and Cummings et al. [267] similarly found a linear increase in pelvic tilt with artificial leg length with the former specifying a peak value of 11° at 50mm.

2.3.6 Gait Kinetics

The results of Li et al. [221] are currently the only available with regards to kinetics of symptomatic LLI patients post-THR. They found that on average LLI patients had smaller JRFs at heel strike and toe off but greater JRFs at mid-stance when compared to asymptomatic THR patients. Similar results were also found for the VGRF. Peak moments were found to be smaller in the LLI patients.

The study by Brand & Yack [268] is the only published work to predict JRFs at the hip for simulated LLI magnitudes ranging from 23mm - 70mm. Forces were calculated via inverse dynamics using GRFs, segment kinematics and segment inertial properties as an input. The use of a 35mm lift led to a 6% decrease in the force of the second peak on the longer side whilst a 65 mm lift led to a 14% decrease. On the shorter side for the same lift an increase in the first peaks force was seen. A general trend found that increasing shoe lift led to a decrease in the force on the longer side joint.

White et al. [269] compared structural LLI patients to healthy normals and to those with a simulated LLI and found that the latter showed greater force transmission through the shorter leg. During every phase of the gait cycle, both the structural LLI group and the simulated LLI group had greater force transmission through the shorter leg, apart from toe off where greater transmission occurred through the longer side. Schuit et al. [270] examined 18 adult volunteers with a structural LLI and found minimal difference in VGRF between the short (782N) and long limb (780N).

2.3.7 Temporal-Spatial Parameters

A very small number of studies have commented on the temporal-spatial parameter data obtained following gait analysis of subjects with a natural or induced LLI. Once again, to the authors knowledge, Li et al. [221] are the only study to have reported on temporal-spatial parameters for symptomatic LLI patients post-THR. Their results found that relative to asymptomatic THR patients, individuals symptomatic for a LLI had a reduced gait velocity ($\approx . 0.90\text{m/s}$) and a shorter stride length. A study by Zhang et al. [271] on asymptomatic LLI patients following THR found a longer leg length was linked to a smaller walking velocity. Non-THR LLI subjects have also been studied in the literature, with velocity being unaffected by leg length [272]. Smaller discrepancies in leg length may be more difficult to compensate for with a motor response such as walking slower due to them not being detected by the subject.

2.4 Computational Modelling of Gait

2.4.1 The Conventional Gait Model

Rigid body models are defined through the placement of markers on a subjects body. The Conventional Gait Model (CGM) was developed by Kadaba et al. [124] and Davis et al. [273]. The model describes the marker set, the calculations used to estimate the position and orientation of the body segments and the conventions used to describe kinetic and kinematic joint outputs. Use of these models began over 20 years ago when motion capture technology was still in early development and became popular due to the advantage of reducing the number of markers and hence the complexity of the algorithms used to calculate kinematics.

The CGM has many derivatives and can go under many different names including Helen Hayes, Newington and the Vicon PiG model. These types of models are hierarchical in that more proximal markers influence the position of distal joint centres which causes the propagation of errors down the kinematic chain. Commonly only the three rotational DoF are assessed during clinical analysis, however removing the translational DoF can lead to errors in results [274].

The International Society of Biomechanics (ISB) has proposed a general reporting standard on how hip kinematics should be measured and published during motion analyses [275]. This is based upon anatomical landmarks [276] and can be seen in Figure 16. The use of the ISB proposal can however be challenging as some anatomical locations, such as those at the knee and ankle, are medially placed and so can be obscured by the opposing limb. For this reason, the popularity of the CGM has not decreased with all of its derivatives such as Helen Hayes and the Vicon PiG model still commonly used.

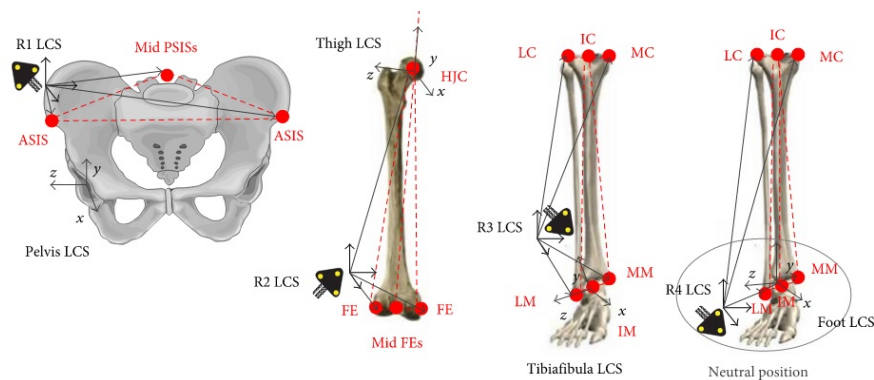


Figure 16: ISB recommended joint coordinate axes [275]

2.4.2 Hip Joint Centre Estimation

The estimation of the HJC is important for the CGM and all its derivatives including PiG. Different methods are often used including predictive [273, 277–287] and functional, where the latter can be sub-divided into transformation techniques [288–292] and sphere fitting techniques [293–299]. These methods are tested for their accuracy against a "Gold Standard" imaging methods such as x-rays, MRI (Magnetic Resonance Imaging), CT (Computed Tomography) and ultrasound. The predictive methods makes use of regression equations which have previously been derived from cadaver measurements. The HJC in the CGM is estimated using regression equations, with those of Bell [277–279], Davis [273] and Harrington [280] being the most popular.

The accuracy of the predictive method is highly sensitive to marker placements and anthropometric measurements [299]. In addition, most studies have looked at normal healthy individuals, whilst very few have analysed THR patients. Leardini et al. [300] have shown that the equations by Bell and Davis are not accurate representations of the HJC even for healthy individuals. Many of the studies which have been undertaken to compare HJC regression methods have supported their own technique as being the most accurate. This may be due to bias where it was known beforehand that a particular method would be better suited to the type of measurement being made or Gold Standard being used.

A systematic review by Kainz et al. [301] found that the Harrington hip regression equation produced the smallest average error across studies of between 14mm - 17mm relative to Gold Standard techniques. Anderson et al. [302] found that the Harrington method outperformed the methods proposed by Bell and Davis. A study undertaken by Harrington et al. [280] found that similar levels of error persisted regardless of the type of group being measured by their own regression equation together with those of OrthoTrak, Bell and Davis.

Bell et al. [279] compared their own regression technique to that of Andriacchi et al. [281] and Tylkowski et al. [282] in children and found that their method was superior. Kirkwood et al. [303] compared the regression equations of Bell, Andriacchi and Seidel et al. [287] in normal healthy people. The method of Andriacchi was found to be the most accurate with respect to the x-ray Gold Standard. McGibbon et al. [304] found that the Bell regression equation produced the most accurate results when compared to the methods of Seidef, Andriacchi and Tylkowski where the Gold Standard was a cadaver. Via the use of ultrasound as a comparison, Peter et al. [305] found that

the regression equation of Harrington outperformed that of Bell where the measured group were children with Cerebral Palsy.

Sangeux et al. [306] were able to conclude from their study that the Harrington method outperforms the method as proposed by Davis. A study on cadavers by Seidel et al. [287] found that their method was more accurate than that of Bell. Weinhandl [284] found that their Greater Trochanter method was more accurate than that of Bell when the Gold Standard was a functional method. It is clear that there are a variety of opinions in the literature regarding which is the most accurate regression equation and care must be taken in selecting the most appropriate for the subject group being analysed.

Conventional Gait Model Vs 6DoF

An alternative model called CAST (Calibrated Anatomical System Technique) or the 6DoF model, is now becoming more popular after Benedetti et al.'s [307] first application. The 6DoF model is based upon the use of cluster markers placed on the thigh and shank together with markers being placed in the medial sides of the knee and ankle. Each of these marker clusters consists of three or four non-collinear markers attached onto a rigid base [276]. Using these clusters of markers, the amount of marker artefact is reduced compared to markers placed directly onto the skin [308]. Figure 17 illustrates the CAST model.

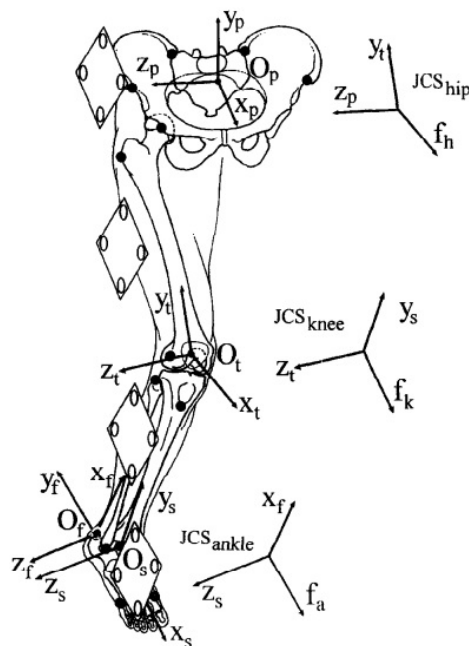


Figure 17: The CAST model as originally defined by Benedetti et al. [307]

The CAST marker system avoids the problems associated with the CGM through segments not sharing markers together with joint centres and axes rotations being defined by the medial and lateral markers at that particular joint. For instance, the AJC is defined to lay half-way between the lateral and medial ankle markers. The orientation of the joint axes are also defined at the joint, with the medial-lateral axis passing through the medial and lateral joint markers, the superior-inferior axis from distal to proximal joint centre and the anterior-posterior being a cross-product of both.

Basset et al. [309] showed that both the PiG and CAST marker sets produce comparable joint angles in the sagittal plane whilst differing significantly more in the frontal and transverse planes. This occurred due to the high probability of mid-thigh and mid-shank marker misplacement in addition to the errors associated with the absence of medial markers in the PiG setup [309]. Buczek et al. [310] computed slightly different results when comparing PiG to CAST, with a total of 6 variables statistically different in the sagittal plane and 4 in the transverse plane. No differences were present in the frontal plane. Thigh marker offset has been observed to be up 42mm [311] from its desired position leading to a shift in the joint axes [312]. Baker et al. [313] have demonstrated how thigh marker offset can effect the measurement of hip rotation. The misplacement of markers can also have an effect on the location of joint centres as determined by regression equations, leading to errors in kinetic and kinematic results [38]. Human error can also be a cause for error through the misidentification of joint centres and other anatomical features due to lack of experience or poor judgement [47].

Zuk & Pezowicz [276] found good agreement between a general CGM marker system and CAST, with the greatest similitude in results being in the sagittal plane and the smallest in the transverse. The greatest inter-trial variability was seen at the pelvis and the knee for both marker systems. Overall however there were no significant differences in the repeatability of either marker set. Likewise, Collins et al. [314] found comparable performance levels between the two protocols in their assessment using a treadmill. Knee frontal plane angles in the CGM however showed evidence of cross talk and hip rotation angles were vastly different between the marker sets. Several other studies have also found that the CGM produces inferior results in the transverse plane [315, 316] or generally has a more variable kinematic and kinetic output [317].

Ferrari et al. [318] compared 5 marker protocols on two healthy subjects and one patient with a knee prosthesis using an in-house marker set which used markers positions from both CAST and

CGM, with PiG representing the CGM. Comparisons were made in terms of kinematics and kinetics. Intra-protocol variability was high for each marker system protocol. The greatest consistency between protocols was found in the sagittal plane of the hip and the least in the non-sagittal planes of the knee and ankle. Knee abduction-adduction for the patient showed the greatest amount of variability in PiG. PiG was hence seen as inferior in its measurement of abnormal knee motion, caused by a knee prosthesis, in the frontal plane. Stronger correlations were found for kinetic variables in terms of joint moments, with ankle dorsi-plantar flexor moments particularly well correlated between CAST and the PiG.

2.4.3 Soft Tissue Artefact

Soft tissue artefact (STA) can have a large impact on kinematic results [33, 289, 307, 319, 320]. This is as during motion the movement of muscle over bone violates the assumptions of rigid body dynamics. Errors produced can be as large as the joints RoM. Marker displacement caused by STA in the literature ranges from 4.4mm - 27mm [321, 322] for the thigh and between 2.5mm - 15.3mm [321–323] for the shank. The absence of a definition for certain landmarks can lead to slight differences in marker placement between studies, which may have caused many of the differences observed in the literature [323, 324]. These difficulties are amplified when placing markers in high fat density areas where it can become hard to detect specific anatomic locations [47]. This poses a particular issue in determining joint centres due to the large amount of tissue surrounding their anatomy and therefore can have a significant impact on the calculation of kinematics and kinetics [290, 304]. It is hoped that in the future direct imaging of the tissues using MRI or fluoroscopy will reduce the effects of STA.

2.5 Rigid Body Modelling

Inverse Dynamics and Optimisation Techniques

The underlying principle behind muscle modelling is the calculation of forces and moments. Both are most often computed through either the use of forward or inverse dynamics. Forward dynamics is the use internal forces/moments to calculate motions whereas inverse dynamics uses kinematics motions and external forces (GRF and inertial) to compute internal forces/moments. The use of inverse dynamics is more common in the gait analysis community due to its greater computational speed and stability compared to forward dynamics [325]. This is in addition to the complexity in formulation of forward dynamics models together with the difficulty in estimating certain input parameters such as muscle properties. The disadvantages of the inverse dynamics technique include that it is unable to determine individual muscle contributions without further optimisation steps and is restricted to the analysis of experimental results only.

There are a number of assumptions that inverse dynamics makes including that the joints are frictionless, that segment masses are concentrated at the centre of mass and that there are no co-contractions of agonist and antagonist muscles [326]. These assumptions can however lead to errors during inverse dynamics. For instance, a preoperative THR patient may have arthritis at the joint which could invalidate the assumption of a frictionless joint. The mass also may not be concentrated at the centre of mass and may be distributed more on one side of the body, such as in a LLI patient where a subject may lean over the operated side.

Inverse dynamics calculations are undertaken via the use of a rigid body model. Each body is used to represent a particular segment of the human body. By Newton's Third Law, each force has an equal and opposite reaction force. This allows the computation of moments and forces at any joint using inverse dynamics. The inverse dynamics algorithm begins at the foot and follows a recursive process in computing moments and forces firstly at the ankle joint, followed by the knee joint before terminating at the hip joint.

The accurate modelling of the structures and functions of muscles are important in inverse dynamics calculations during gait. This is of particular importance in the analysis of THR patients as it can aid in gaining a greater understanding of post-surgery complications in the rehabilitative process. The greatest problems in muscle modelling arise through muscle redundancy and unknown cost functions, which can include minimisation of muscle stress or activity. In terms of the former,

this occurs due to the number of muscles in the human body exceeding the required amount to balance an external force. This leads to the number of muscles exceeding the models degree of freedom [327]. As a consequence, the system will consist of overdetermined equilibrium conditions implying an infinite number of solutions [328].

When undertaking an inverse dynamics calculation, a set of equilibrium equations can be defined as in Equation 8. Here the vector F represents the unknown muscle and joint forces, C is the required coefficient matrix and r is representative of the external and inertial forces [328].

$$CF = r \quad (8)$$

If F contains more elements than there are equations (i.e. $F > r$), Equation 8 is indeterminate and has infinitely many solutions. If $F < r$, a solution cannot be found exactly and only approximations can be made [329]. If $F = r$, only one analytical solution exists. For Equation 8 to be determinate, there must be as many muscles as there are DoF at the joint. This is however not the case in the human body [325].

Physiologically, the problem of an overdetermined muscle system is solved by the central nervous system (CNS) which selects a set of muscles that will be involved in the motion being undertaken [325]. This is more problematic following THR where muscle attachment points are changed, leading to the CNS to select a different optimal muscle recruitment pattern. The combinations chosen by the CNS in terms of muscle activation patterns are very similar between individuals, indicating that there is an optimal muscle selection criterion based on either energy expenditure, the effort required, muscle fatigue or a combination of all [330].

Optimisation theory is a method used post inverse dynamics to determine individual muscle contributions from net joint moments. Techniques which are used to determine muscle forces include minimisation of the maximum muscle force output and minimising energy. It is believed that optimisation theory is able to depict the force sharing which occurs in-vivo in its most simplistic form. Static optimisation is able to resolve net joint moments into individual muscle moments and forces at each instant in time. It is commonly used [328] perhaps due to the lower computational cost compared to other dynamic optimisation techniques [331], although both give comparable results [332]. Critics of static optimisation argue that its non-time dependent nature prevents the incorporation of physiological muscle such as stretching of a muscle unit in one time instant effecting

another instant [330, 331, 333].

Dynamic optimisation overcomes these issues as it is time dependant and can analyse data with the initial and/or final values only [330]; there are however limitations in that a large number of data parameters is required which is often infeasible. Furthermore, dynamic optimisation being time dependent is computationally expensive which has led to very few studies using it over static optimisation. Anderson & Pandy [331] showed that the solutions with regards to muscle force for both static and dynamic calculations were practically the same, with the dynamic solution requiring 1000 times more computational time. Dynamic optimisation could in some cases be preferable to static when coupled with forward dynamics in being able to predict novel movements using muscle activations as an input. This would be ideal for LLI patients who would have patient specific gait cycles caused by variations in the abductor muscle strengths following surgery. Furthermore, the dynamic optimisation would be ideal when combined with forward dynamics in addressing the force re-distribution of muscles following THR.

Optimisation theory is in general preferred to the reduction method first postulated by Paul [100] in 1976 which aims to convert an indeterminate into a determinate problem [334]. The reduction method reduces the number of design variables by grouping similar muscles together. Another technique, first documented by Pierrynowski & Morrison [335] and called the addition method, poses to add constraints until the number of degrees of freedom is equal to the number of muscles; this method however suffers from making invalid assumptions about muscle activation patterns [336]. The purpose of the optimisation technique is to minimise the objective function which depicts the in-vivo CNS [336]. This minimisation can include parameters such as maximum muscle strength and metabolic energy consumed [337]. A linear programming equation using these can then be set up as shown, where G represents the objective function:

$$\begin{aligned} \text{Minimise} \quad & G(f^m) \\ \text{Subject to} \quad & cf=r \\ & f_i^m \geq 0 \\ & i = 1 \dots n^m \end{aligned}$$

2.5.1 Muscle Recruitment

The simplest type of muscle recruitment and objective function is linear where two muscles share a load [338]. The use of linear objective functions has however received significant criticism as studies

such as Hardt [339] and Pedersen et al. [340] have shown for complex musculoskeletal systems too few muscles are recruited that do not correspond well to EMG (Electromyograph) data. Linear muscle recruitment shows no muscle synergy as the strongest muscle does all the work making it physiologically unrealistic [341]. The use of non-linear approaches has been discussed as being advantageous in this respect as it can predict the activation of muscle agonists without the need for an upper bound on the muscle force [342]. Linear optimisations' use today is mainly due to efficiency and ease of use [343]. Equation 9 is of a typical linear muscle recruitment function where f_i is the force generated in muscle i and N_i is the maximum force capacity of muscle i [344].

$$G = \frac{f_1}{N_1} + \frac{f_2}{N_2} \quad (9)$$

The second type of muscle recruitment and objective function is quadratic where large terms in the summation are penalised, allowing for a greater distribution of the load between several muscles [341]. The quadratic function also works to reduce the recruitment of muscles with very small moment arms [345]. This method in addition allows for the control of computational cost which is linked to the square of the quantity of unknowns [346]. One method of reducing the number of unknowns is through assuming muscles in the same heteronymous group produce the same amount of activity once stimulated [346]. However, this method is less stable, more expensive and takes greater computational time to process when compared to linear recruitment [347]. Both linear and quadratic optimisation are subjected to errors through the sensitivity of muscle forces to model parameters [348] and the use of different parameters in literature [349]. Despite this, a study by Modense et al. [350] has shown that quadratic muscle recruitment is the most accurate when modelling the lower limb relative to other recruitment techniques. The quadratic recruitment technique is shown in Equation 10, with the variables having been defined previously:

$$G = \sum_{i=1} \left(\frac{f_i}{N_i} \right)^2 \quad (10)$$

In general, the higher the order of the objective function the greater the synergy between muscles [351]. By replacing the value of 2 in the quadratic objective function with any value $p > 2$, will convert the quadratic equation into a polynomial objective function. In software programs such as AnyBody, $p \geq 5$ does not converge to a solution; this may be as higher values lead to numerical instability due to the rapid contraction and relaxation of muscles [351]. The most popular value in the literature for p is 3 which was shown by Crownshield et al. [352] to be the most reliable during

gait. Values of p greater than 3 cause greater synergy up until 100 which as shown by Challis et al [353] leads to physiologically unrealistic results such as all muscles sharing an even load. Modense et al. [350] have shown that lower powers of the objective function value for p coincide more closely to the hip JRF results for THR patients as produced by Bergmann [148]. A polynomial muscle recruitment equation can be seen below.

$$G = \sum_{i=1} \left(\frac{f_i}{N_i} \right)^p \quad (11)$$

Theoretically, as $p \rightarrow \infty$, muscle recruitment would move towards a min/max formulation which can be seen as a muscle fatigue criterion [351]. In this situation, all the muscles which can possibly work together to counteract the load do so making the relative load of any recruited muscle as small as possible [354]. This type of muscle recruitment is known as the min/max criterion which is a minimisation of the maximum muscle activity [355]. The min/max criterion is formulated as follows:

$$G(f^M) = \max \frac{(f_i)^M}{N_i}$$

for $i = 1, \dots, n^M$

2.5.2 Muscle Geometry

There are two schools of thought when it comes to muscle geometry. The first, basing itself on the work by A.V. Hill, model muscles as contractile elements coupled with elastic elements [356]. The second, following in the footsteps of A.F Huxley, attempt to model the microscopic phenomena in muscle contraction leading to the construction of differential equations [356]. The most basic of muscle geometry assumes "via points" where muscle passes between two points in a straight line [357, 358], which can be seen in Figure 18. A literature review however shows that variations exist between studies in terms of the quantity of via-points used to model a particular muscle. These most likely occur due to the difficulties in measuring muscle path geometry in-vivo [359]. An example of this is the Gluteus Maximus which has been modelled using 1 line (Thelen et al. [360]), 2 lines (Kepple et al. [361]) and 3 lines (Scheys et al.[362]). The use of lines to model muscles does come with its disadvantages however as it limits the amount of complexity that can be modelled and also assumes that all the fibres in the muscle have an equivalent moment arm [363]. For the Gluteus Maximus, it may also be inappropriate to model via a series of lines due to it having broad attachment sites [363]. This can be overcome by splitting the muscle up into smaller segments, such as in the AnyBody system, and then using multiple line segments to represent the attachments.

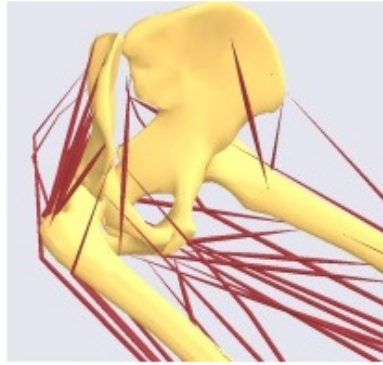


Figure 18: Lines used to represent muscles in AnyBody
[364]

There exist differences between the muscle anatomy of both males and females. This can cause difficulties with models taking into account the physiology of both genders or producing a model specific to one gender. Difficulties also arise in modelling THR patients due to the changes in muscular geometry following surgery. This includes changes in anatomy which could impact modelling in terms of via points, muscle strength and mass. The specific case of modelling LLI can also be problematic due to the modelling of muscles not in their natural state but having been made taut during the operating procedure. As a knock on effect, this can cause changes in other parameters which determine the behaviour of the muscle which may lead to poor reliability of the results.

In terms of determining muscle force, variables such as fibre length and angle of pennation are important in producing models which simulate physiological conditions [365]. Fibre length is important due to it being proportional to muscle velocity. Reduction in fibre length, such as following THR, could therefore have a large impact on muscle parameters and must be modelled correctly. The mass of the muscle is also another important factor which must be taken into consideration. As muscle mass increases, PCSA (Physiological Cross Sectional Area) increases non-linearly [366]. It is vital for any muscle model to incorporate a realistic PCSA due to it being proportional to the muscle force. As individuals differ in their muscle mass and hence PCSA, even in those who share similar height and weight, it is not possible to produce an ideal model which can be used for all subjects. For this reason there are many simple models which assume a constant muscle strength. The more complicated models allow more detailed modelling and account for the stiffness of passive structures.

2.5.3 Sensitivity

Computational software now allows for the development of complex musculoskeletal models in order for parameters such as force generating capacity, muscle moment arm lengths and muscle tendon lengths to be used to predict the outcome following treatment. The current trend in computational modelling is for the use of subject specific models which use imaging data such as MRI. Through this models can be built which closely match those of the desired patient by for example having the correct muscle attachment points. This however can be very time consuming and can be irrelevant due to its application being limited to single subjects whilst not being applicable to the general population. Furthermore, a study by Carbone et al. [367] showed that small errors in the origin or insertion points of the muscle can have a significant impact on muscle force predictions. The choice of origin and insertion of the fibre is not a trivial task [357]. This can be of particular importance in modelling pathological conditions or surgery such as THR where the insertion and via points could have been either changed or had their corresponding muscle fibre removed.

Sensitivity studies such as those carried out by Schutte et al. [368] have shown that variations in muscle geometry due to factors such as age, sex, pathology and weight amongst others can affect the output of computational studies [369]. Scheys et al. [370] stated that the scaling of models can lead to errors through poor marker placement and the assignment of incorrect coordinate systems. Despite the sensitivity studies which have been carried out showing the factors which can affect the performance of a model, the lack of coordinated effort between research groups has led to some of the results in the literature to be questioned [357]. These include if the underlying mathematical assumptions are valid due to the lack of rigorous testing. Furthermore, the large number of constraints that a comprehensive model of a musculoskeletal system would require would not guarantee a solution; thus many models use simplified constraints in order to obtain results which can vary between studies [357].

Delp et al. [371] have shown a relationship to exist between subject specific anatomy and the moment generating capacity of muscles in the hip. The neck-shaft angle and neck length have been shown by Lenaerts et al [372] to share a relationship to forces and moments. An increase in neck-shaft angle was established to lead to an increase in muscular activity in many of the abductor muscles whilst the opposite occurred with an increase in neck length. The wrapping points of muscle fibres in a model have been illustrated to share a relationship with JRFs [373]. Other studies demonstrated that the position of the HJC [374] and orientation of the joint axes can effect

both kinematics and kinetics [375, 376]. Lenaerts et al. showed that the anterior placement of the HJC led to a significant drop in the peak flexion-extension moments [372].

2.5.4 Model Comparison

One of the first rigid body models developed which incorporated muscles was by Chadwick et al. [377]. This model was however unrealistic and its application was limited [378]. Over the past twenty years two distinct categories of software packages have been used for the simulation of human biomechanics. These packages are engineering software (e.g. MATLAB, ANSYS, ADAMS, SD/FAST) and musculoskeletal packages (SIMM, Visual 3D, AnyBody, Lifemodeller) [379, 380]. None of these packages are however open-source, preventing the manipulation by users of the underlying code to suit the needs of the model [379]. Difficulties also arise when research groups utilise different packages which may differ in their underlying mathematical code. Furthermore, during the inverse dynamics simulation, many groups employ differing notations including vectors, Euler angles and matrices which can make comparisons at times difficult [381].

The current two most popular musculoskeletal packages are Opensim and AnyBody which both have their advantages and disadvantages. The former is open source allowing users to modify the code and tailor it to their needs whilst AnyBody does not have this capability. Furthermore, Opensim has a very large international community with users spanning over 30 countries and contributing to an online database where models can be shared. AnyBody also has a similar database which is however smaller. Both Opensim and AnyBody differ in their capabilities with the latter only able to carry out inverse dynamics simulations whilst the former can in addition carry out forward dynamics.

A typical musculoskeletal model has inputs of bone surface geometry, a joint kinematics description, a muscle path description and muscle architecture [358]. Bone surface geometry can either be obtained from cadavers or live subjects using imaging techniques or through using previous study data. This process can however be very time consuming and varies between systems using different cadavers. Muscle geometry can be customised via segmentation using MRI [382].

The hip joint has been modelled as three hinges [383] and as a spherical joint [369, 372, 384]. Difficulties arise in the modelling of joints as they do not perform the simple rotations about fixed axes as simulated by many computer systems [359]. It is also very rare for a model to incorporate

a detailed ligament anatomy with Cleather et al. [385] being one of the very few. There are also differences in the number of muscles modelled such as 26 [369], 43 [386], 86 [372] and 163 [387]. This raises the question of how many muscles are required to accurately depict physiological conditions in both healthy and diseased joints. A smaller number of muscles can be used to convert an indeterminate system to a determinate one which may simplify the solution but reduce the validity of the study [357].

2.6 Biotribology

Tribology is the study of lubrication, wear and friction whilst the area involving medical devices is called biotribology. The success and longevity of joint replacements forms a subset of this area.

2.6.1 Archard Equation

Equation 12 is of the Archard equation, which is used to predict the volume of wear based upon the concept of surface asperity contact. K represents the wear constant, L the applied load and S the sliding distance of the hip bearing. The Archard equation assumes that the volume of wear is not dependent on the contact area, is time independent and also that the surface roughness of the articulating surfaces has no effect on wear [388]. It also does not take into account the effects of cross shear. Advances in the field have however allowed for the inclusion of contact area [389, 390] and cross shear [391] dependent parameters into more complex wear models. The equation shows that an increase in load at the hip joint or an increase in the sliding distance, leads to an increase in the volume of wear. Pin-on-plate testing has been undertaken in attempting to determine values for K [392]. This is despite it being found that the value of K is often not a constant and is a function of contact pressure [389].

$$\text{Wear Volume} = KLS \quad (12)$$

The sliding distance is computed to be the amount of movement that the femoral head undergoes relative to the acetabular cup over the course of the gait cycle. This can be calculated by selecting a single loci or multiple loci on the femoral head and summing up the total change in their position/s over the course of the gait cycle. Equation 13, as defined by Bennet et al. [393], can be used to compute the sliding distance in all three directions (x-anterior/posterior, y-medial/lateral and z-superior-inferior) for a gait cycle of k gait instants.

$$\sum_{n=1}^k [\sqrt{(x_{i+1} - x_i)^2 + (y_{i+1} - y_i)^2 + (z_{i+1} - z_i)^2}] \quad (13)$$

A greater sliding distance is achieved by taking longer strides. A longer stride leads to greater movement in the anterior-posterior direction of the femoral head relative to the acetabular cup and hence increase the sliding distance. An increased sliding distance, and hence wear rate, is also seen when using a larger femoral head due to the increase in head circumference. All of the above rules apply to UHMWPE implants

2.6.2 Hertz Contact Theory

The contact area of two spheres (e.g. the femoral head and acetabular cup) occurs in theory at a single point. In reality, the contact between the two curved surfaces is over a small area due to the elastic deformation of the surfaces [394]. The classical Hertz's theory of contact is centred around non-adhesive contact and makes a number of assumptions. These are:

- The surfaces in contact are conforming and continuous
- The contact area is frictionless
- The surfaces show both linear and elastic properties
- Any strains in the contact area are small

The Hertz contact theory can be used to compute the contact area between the femoral head and the acetabular cup using the Equations 14 to 17. A number of variables including the instantaneous resultant joint force (F), the radii of the femoral head (D_1) and cup (D_2) together with each components Youngs Modulus (β_1/β_2) and Poissons Ratio (γ_1/γ_2).

The relative radius between the femoral head and acetabular cup, D^* is computed using Equation 14, whilst the relative Youngs Modulus, β^* is found using Equation 15. From these values, the contact radius and contact area can be calculated using Equations 16 and 17. Using the contact area, only those points which are in contact between the cup and the femoral head are used. Figure 19 illustrates the contact area between the femoral head and acetabular cup.

$$D^* = \frac{D_1 D_2}{D_2 - D_1} \quad (14)$$

$$\beta^* = \frac{\beta_1 \beta_2}{\beta_1(1 - \gamma_1^2) + \beta_2(1 - \gamma_2^2)} \quad (15)$$

$$\text{Contact Radius} = C = \left(\frac{3F_i D^*}{4\beta^*}\right)^{1/3} \quad (16)$$

$$\text{Contact Area} = A = C_i^2 \pi \quad (17)$$

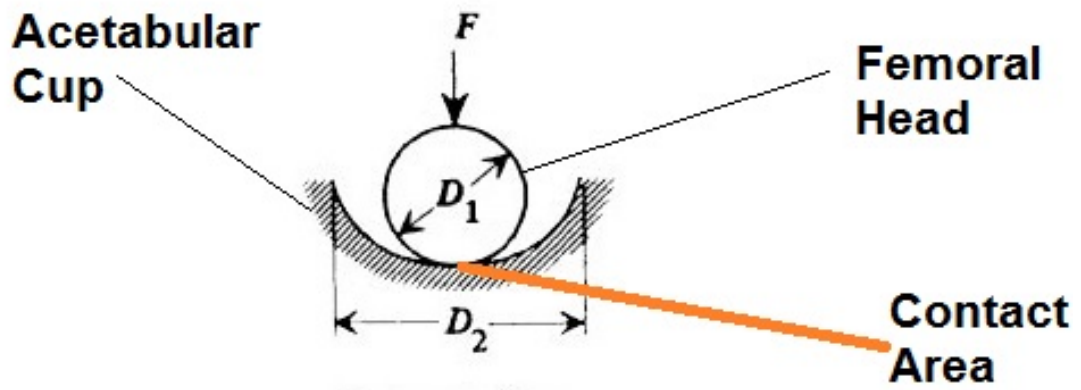


Figure 19: An illustration of the contact area between the femoral head and acetabular cup. The contact area will change overtime with the varying levels of joint force. [395]

2.6.3 Cross Shear

Since the 1960's, UHMWPE has been used successfully as a bearing material in THR [396]. Studies have concluded that conditions such as osteolysis arise due to UHMWPE debris [397]. The polyethylene particles released into the tissues can cause aseptic loosening and the eventual resorption of bone due to the inflammatory response of macrophages [398]. The volume of wear produced shares a relationship to dynamic joint loads and sliding distance [399]. Cross shear is the frictional work produced in the transverse direction to the Principal Molecular Orientation (PMO) i.e. the direction of orientation of the UHMWPE fibres [391]. Polymer molecules PMO is aligned to be in the same direction of the primary motion (hip flexion-extension). The cross shear ratio is thus defined as in Equation 18, which is the general form of the equation. A more detailed calculation and equation is defined by Kang [391].

$$\text{Cross shear ratio} = \frac{\text{Frictional work perpendicular to the PMO}}{\text{Total frictional work}} \quad (18)$$

Unidirectional motion of the femoral head relative to the UHMWPE cup in the direction of the PMO would in theory produce the least amount of wear through a smaller cross shear ratio. Research has found that multidirectional motion of loci on the femoral head can lead to an increase in the amount of wear debris produced. Molecules orientated in one direction lead to a collective hardening of the UHMWPE component leading to a reduction in wear, whilst this does not occur for molecules orientated in multiple directions. Unidirectional motion has been found to overtime lead to wear up to 300% smaller than multidirectional motion [400, 401]. Multidirectional motion wear testing on UHMWPE implants has produced wear rates similar to those seen clinically [198]. This has led to the development of cross linked fibres, which makes UHMWPE more isotropic [396].

Galvin et al. [402] found that despite cross linked UHMWPE showing a reduced wear rate, this was dependent on the condition of counter-surfaces and the amount of multidirectional motion. Similarly, serum concentration levels have been found to lead to reduced wear.

2.6.4 Contact Surface Motion Paths

Motion paths, also known as slide tracks and wear paths, are used to view the path taken by selected loci on the femoral head over the course of the gait cycle. The shapes of the paths produced can be used to predict wear rates. The number of paths produced on the femoral head is determined by the number of loci which are initially selected. Commonly, 20 points are selected following the method of Ramamurti et al. [403]. Motion paths are produced and analysed both computationally and using hip simulators.

The location of the Ramamurti points are defined relative to the femoral head equator, which passes through the centre of the Great Circle. The Great Circle, as seen in Figure 20 is the region of intersection between a sphere and a plane which passes through the centre of the sphere. For the Ramamurti points, the sphere is the femoral head. The Great Circle is oriented such that it is perpendicular to the long axes of the femoral head and neck of the hip implant.

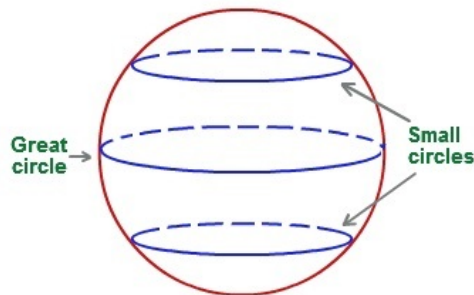


Figure 20: The Great Circle illustrated together with two smaller circles which cannot be classified as Great Circles

[403]

The first 10 points are equally spaced on the semicircle which passes through the most superior point of the equator, the most inferior point of the equator and the apex of the femoral head. The second set of 10 points are equally spaced on the semicircle which passes through the most anterior point of the equator, the most posterior point of the equator and the apex of the femoral head. The Ramamurti points can be seen in Figure 21.

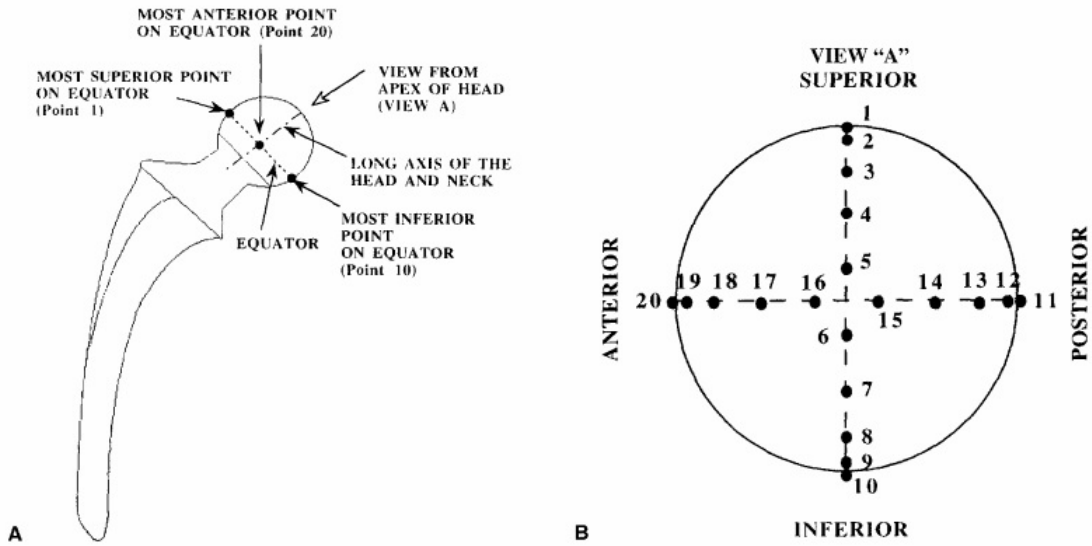


Figure 21: Image (A) shows where the Ramamurti points are located relative to the shape of the femur whilst (B) shows how the points are located with respect to each other on the femoral head viewed from directly above the apex of the femoral head

[403]

Determining the position of the loci at each time interval is undertaken through the use of a rotation matrix. There are however 6 cardan angle sequences which can be applied to determine the new position of a loci at each time interval. These are through applying the 3 motions (flexion-extension, abduction-adduction, internal-external rotation) in different orders. Equation 19 is of a rotation matrix which applies the x axes first, followed by the y and concludes with the z axis. The joint angle values can be substituted into Equation 19 and multiplied by the position vector of the loci at gait instant n , allowing for the computation of the position vector at gait instant $n+1$. Studies have however shown that the choice of cardan angle sequence has little effect on the results [404].

$$\mathbf{P}_\alpha = \begin{pmatrix} \cos(y)\cos(z) & -\cos(y)\sin(z) & \sin(y) \\ \sin(x)\sin(y)\cos(z) + \cos(x)\sin(z) & -\sin(x)\sin(y)\sin(z) + \cos(x)\cos(z) & -\sin(x)\cos(y) \\ -\cos(x)\sin(y)\cos(z) + \sin(x)\sin(z) & \cos(x)\sin(y)\sin(z) + \sin(x)\cos(y) & \cos(x)\cos(y) \end{pmatrix} \quad (19)$$

Figure 22 shows typical motion paths produced on the femoral head both computationally (a) and using a hip simulator (b). Commonly, the individual motion paths show quasi-elliptical, tear drop or figures of 8 in terms of their shape. These shapes were reported by Bennet et al. [405] in their study on THR patients and by Budenberg et al. [264] in their study on both normal and LLI

patients.

Motions in the human body do not occur in a particular sequence but occur simultaneously, with cardan angles simply used as a mechanism to analyse data. The current recommended method by the ISB (International Standards of Biomechanics) is XYZ, with flexion-extension being followed by abduction-adduction and finally internal-external rotation. This sequence is recommended due to the notion that the first rotation (flexion-extension) is where the greatest amount of angular displacement occurs [406], whilst it has also been shown to be the most appropriate in activities with large flexion-extension through the smallest planar cross talk relative to other sequences [407].

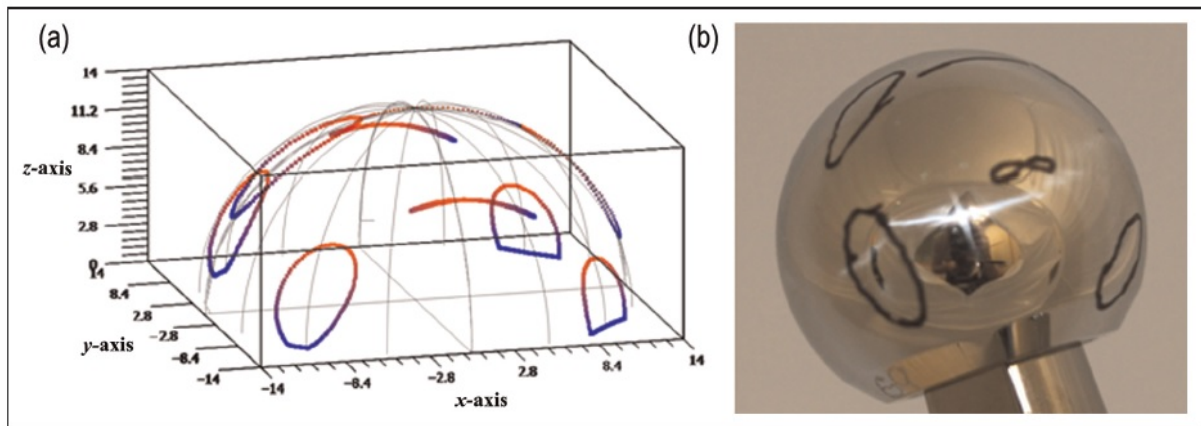


Figure 22: Image (a) shows motion paths over the femoral head produced computationally (b) shows motion paths as produced by a hip simulator when a method is used to track the loci during the gait cycle

[264]

2.6.5 Aspect Ratios

One technique used in attempting to estimate wear rates through simulating the effects of cross shear is via the computation of the aspect ratio. This is typically undertaken by calculating the ratio of the length to the breadth of each motion path. These are then averaged to produce an average aspect ratio across the gait cycle over the head and cup. The number of individual aspect ratios calculated depends on the number of loci initially selected to produce motion paths. Figure 23 illustrates how the aspect ratio is calculated. Theoretically, the closer the aspect ratio is to 1 (i.e. an equal length and breadth), the greater the amount of multidirectional motion and the greater the volume of wear. A positive correlation has been found with the inverse of the aspect ratio and the volume of wear debris [393].

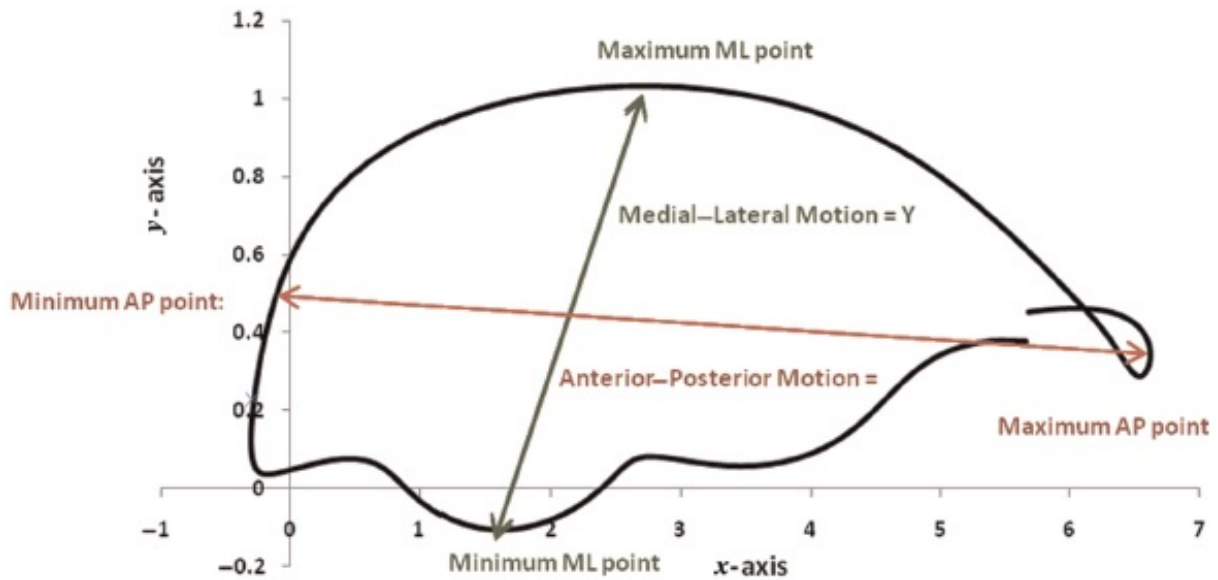


Figure 23: A typical image of the aspect ratio. This image shows a 2D representation of a 3D motion path

[264]

The aspect ratio has been computed in THR patients. Davy et al. used 20 points and computed the aspect ratio to range between 2.08 and 5.36, with results averaging 3.33 [408]. Bennet et al. [198] found an average aspect ratio of 3.97 for 159 THR patients (ranging between 2.13-10.86). An age matched normal group had a slightly smaller average aspect ratio of 3.71 (ranging between 2.83-5.32). Just 13% of these patients had an aspect ratio of greater than 5.5. They also found a poor correlation between age and the aspect ratio, which was an unexpected result due to older patients commonly showing a loss of hip RoM. Budenberg et al. [264] used an in-house program to compute motion paths over 20 Ramamurti points for both normal and LLI patients. Results indicated that LLI patients averaged an aspect ratio of 1.7 (ranging between 0.16-7.87) whilst those in the normal group averaged 1.8 (ranging between 0.29-6.75). The results of different studies are however difficult to compare due to patient variability and the methods used, with the results for Bennet et al. and Budenberg et al. using a different order of cardan angle rotations.

2.6.6 Lubrication

Fluid film lubrication occurs when two surfaces are not in contact and are separated by a lubricant [409]. This can be fully described by fluid entrainment and squeeze film. Entrainment occurs when fluid is dragged into the contact area through the relative motion of two articulating surfaces [410]. This can be seen in Figure 24.

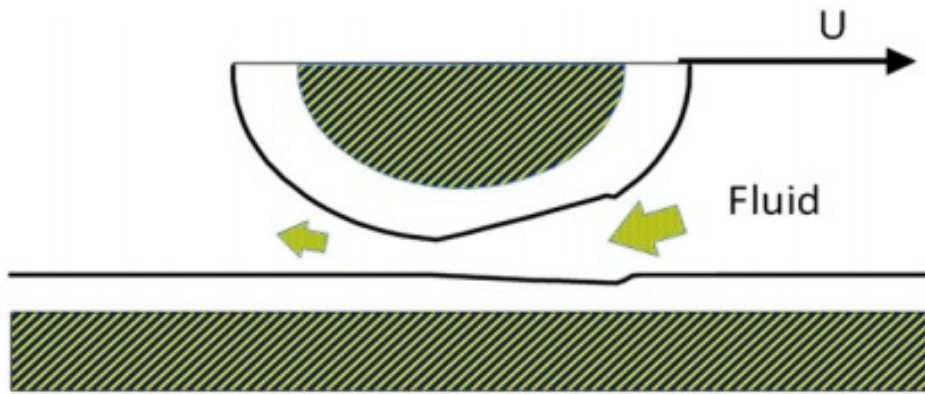


Figure 24: A schematic demonstrating fluid entrainment and the dragging of fluid into the contact area between the surfaces

[410]

Equation 20, also known as the Hamrock & Dowson equation [23], computes fluid thickness which requires a number of constants and variables that need to be defined. Here R represents the equivalent radius of the bearing, the viscosity of the lubricant is defined by η , ω represents load, E' the material stiffness and μ the sliding velocity. The Hamrock & Dowson equation is not ideal as it assumes a constant sliding velocity and is time independent.

$$\text{Film} = 2.789R \left(\frac{\mu\eta}{E'R} \right)^{0.65} \left(\frac{\omega'}{E'R^2} \right)^{-0.21} \quad (20)$$

The lubrication thickness is proportional to the Sommerfeld number, which is a product of the relative velocity of the articulating surfaces divided by the load and the viscosity of the lubricant [410]. Squeeze film lubrication occurs where two surfaces which are initially separated rapidly move towards each other, with fluid being squeezed in between. Squeeze film lubrication can be measured using the Higginson [411] equation as seen in Equation 21. Here dt represents the time step.

$$\text{Film} = 2.86R \left(\frac{\omega}{E'R^2} \right)^{0.167} \left(\frac{dtE'}{\eta} \right)^{-0.5} \quad (21)$$

It is accepted that a friction coefficient below 0.01 is unlikely to create frictional forces which damage the articulating surfaces [412]. However a combination of physical activity such as walking that creates a load on the hip joint and an elevated friction coefficient can lead to surface shearing of the prostheses which could increase wear and reduce stability. For the coefficient to stay substantially below 0.01, a combination of lubricating mechanisms must be used due to the effect differences in activity levels have on the hip joint. During gait, fluid film lubrication is generated which reduces contact stresses, contact pressure and the hydrostatic pressure of the fluid film thus increasing

the stability of the joint [412]. This coupled with low loading of the joint will increase the life of the implant by reducing the force of friction. Fluid film lubrication maintains fluid thickness and prevents friction that leads to wear from occurring between the surfaces during cyclic loading.

The relationship between lubrication, friction and wear can be demonstrated through the Stribeck curve where the λ ratio determines the lubrication regime present. The λ ratio is defined by Stewart [410] as "the ratio of the predicted minimum film thickness to the combined surface roughness of the articulating surfaces". Equation 22 is of the λ ratio, where h_{min} is the minimum fluid thickness and R is the composite sum of cup and femoral head roughness [22]. The thicker the fluid film between the acetabular cup and femoral head, the less contact there is between asperities and hence a decrease in friction and wear. Figure 25 is of the Stribeck curve.

$$\lambda = \frac{h_{min}}{R} \quad (22)$$

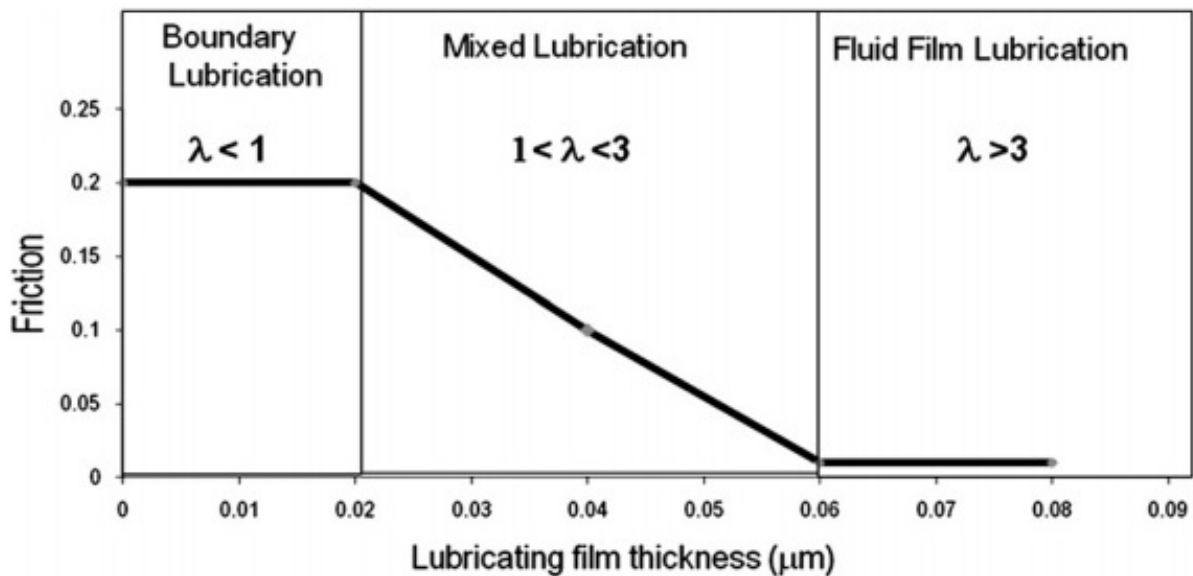


Figure 25: The Stribeck curve
[410]

2.7 Summary of Literature

The aim of this study as defined in the *Introduction* is:

Aim: To understand why certain patients following a Total Hip Replacement are symptomatic for a Leg Length Inequality whilst others remain asymptomatic

The literature review was undertaken to explore, understand and critique the literature so that the study objectives, also defined in the *Introduction*, could be tailored to meet the aim. A variety of different areas were covered including gait analysis, rigid body dynamics and tribology. A number of the key findings are listed and briefly discussed below:

The gait of THR patients has been studied extensively

The analysis of gait has been extensive for both healthy and THR patients. The analysis of gait kinematics has been thorough with joint angles often being reported for the pelvis, hip, knee and ankle. Other areas of study have included temporal-spatial parameters, joint moments and JRFs. Due to the increasing number of THR procedures being undertaken per annum globally, the gait of patients both preoperatively and postoperatively has been examined such that it exceeds the number of studies for normal individuals. Studies have also been more specific, focussing on particular variables such as implant type, gender or surgical technique. More recent advances in the field have focussed on increasing the complexity of musculoskeletal models and hence their accuracy in predicting hip JRFs and muscle moments through the use of subject specific modelling.

Joint angles, moments and forces are sensitive to anthropometric, demographic and temporal-spatial parameters

It was often reported in the literature that joint angles, moments and forces were effected by variables such as leg length, gender and walking velocity. There was also evidence of links between anthropometrics, demographics and temporal-spatial parameters such as males having greater walking velocity whilst hip abduction-adduction RoM was linked to femoral offset. Some of the more significant findings included that peak joint angles, moments and forces were linked to reduced walking velocity and increasing age, together with stride length being a function of both leg length and height. Differences in post-operative gait for THR patients was also found to be linked to the surgical approach, implant type and the environment.

Normal and THR patients differ in their gait characteristics

THR patients display different gait characteristics to controls through showing a loss in gait symmetry and reductions in joint RoM. A loss of gait velocity is common, with corresponding reductions in peak joint moments, VGRFs and hip JRFs. Postoperatively, THR patients improve in their gait characteristics overtime, but are never able to reach the levels of healthy individuals.

The measurement of gait is prone to error

The number of and type of errors present in the analysis of human gait are numerous, effecting both healthy and operated patients. Of these there are errors in anthropometric measurements, protocol errors and computational modelling. Anthropometric measurement errors include under or overestimating clinical measures such as the knee width. Errors in the gait analysis protocol include the movement of the skin with respect to the underlying bone that the marker is placed upon (Soft Tissue Artefact), marker misplacement and errors in force plate and camera calibration, amongst many others. Computational modelling errors however appeared to be the greatest concern, with the selection of optimisation technique, muscle recruitment criterion, errors in joint centre definitions, orientations of segments and the selection of cardan angle sequence being particularly challenging issues.

LLI is a considerable problem due to the number of symptomatic patients

A study by Wylde et al. [6] found that around 10% of THR patients were symptomatic for an anatomic LLI. If it is taken into consideration that in 2015 alone, 100,000 individuals underwent a THR, around 10,000 people would have been symptomatic for an LLI. As the number of THR procedures per annum increases due to an ageing population, these numbers will likewise increase.

There is not a consensus on what level of LLI is the threshold for patients to become symptomatic

There is a consensus in the literature that a discrepancy in leg length of up to 10mm is acceptable. There does not however exist a consensus on what the minimum threshold level for being unacceptable is. This is due to the different leg length difference values found in the literature across studies and the impact of subjectivity in patients being symptomatic.

Analysis of the gait, anthropometrics and wear rates of Symptomatic LLI patients in the literature is virtually non-existent

The present review of the literature has found very little on the gait of patients who are symptomatic for an LLI following THR. There have been no studies which have analysed the effect of being symptomatic for an LLI on the kinematics at the pelvis, knee and ankle. Only a single study has been previously undertaken on hip motion, hip JRFs and VGRFs of symptomatic LLI patients following THR, by Li et al. [199]. This study however used a limited set of patients, with there being patients with an anatomical LLI, a functional LLI caused by muscle shortening and individuals with secondary conditions all being included in the same dataset. Likewise, a thorough analysis of clinical measurements such as the inter-hip distance have as of yet not been undertaken.

Segment optimisation and inverse kinematics are two main techniques used to compute kinematics from motion capture data

Segment optimisation is where markers which are attached to a rigid body segment are used in tracking the motion of the segment and in computing the pose and position at each time frame. This method assumes that all markers move along together with the segments to which they are attached to and that their positions in relation to the segment coordinate system do not change. Inverse kinematics also attempts to provide the position and orientation of all segments at each time interval. This is however undertaken through a process of least squares where the residuals between the model marker positions and the experimental marker positions are minimised. Joints are explicitly defined, whereas in segment optimisation all joints are treated independently, allowing inverse kinematics to limit motion between segments such as the abduction-adduction movement of the knee joint.

There is some uncertainty with regards to how muscles distribute load over the hip joint

It is not known for certain how the CNS selects which muscles to utilise for a particular load. In-vivo studies have shown that the sharing of loads spans across multiple muscles, with the distribution of loads often being computed using a polynomial muscle criterion. Which muscles are selected and how much force is produced are computed using a variety of methods including minimisation of the maximum muscle force and minimisation of metabolic cost.

The longevity of a hip joint implant is dependent on a variety of implant and patient specific factors

Cross shear, joint loads, sliding distance and activity levels were all found to effect the longevity

of a hip implant. This was together with walking velocity, with an increase in walking speed leading to greater fluid film lubrication during entrainment. Other factors which were implant specific included the amount of cross linking of the acetabular cup and the size of the femoral head, with a larger femoral head leading to greater sliding distances.

2.8 Study Objectives

Four study objectives were defined in the *Introduction* in order to answer the study aim. Using the summary of the literature, the objectives are listed below together with a brief description of the techniques which were utilised and the reasoning behind any analysis.

Objective 1 - Understand whether differences exist in both anthropometric measurements and demographics between Symptomatic LLI and asymptomatic Happy THR patients

This study objective aids in understanding whether differences between the Symptomatic LLI patients and Happy THR patients are purely down to anthropometrics (e.g. height, femoral offset, cup angle) or demographics (e.g. age). This will investigate the missing areas in the current literature which are not currently addressed thoroughly using the most accurate clinical measurement techniques available. Demographic data was compared through clinical notes whilst anthropometric measurements of patients were made using a clinical measurements software package.

Objective 2 Examine whether LLI patients show a characteristic gait pattern in their kinematic, kinetic and temporal-spatial results together with comparing them to asymptomatic Happy THR and Normal patients

The 2nd objective would help to understand the role that differences in kinematics, kinetics and temporal-spatial parameters between patient groups may have on determining whether a patient is symptomatic for an LLI. Joint angles, hip JRFs and VGRFs were studied together with many temporal-spatial parameters. This analysis was undertaken using the PiG marker set on Visual3D. The data itself was obtained prior to the present study.

Objective 3 - Compute how error using the PiG model may have effected the variability seen in the clinical gait analysis results

To be able to make informed conclusions, there must be confidence in the results. The PiG protocol, as demonstrated in the literature, is one of the most commonly used marker sets in

measuring human gait. The literature review demonstrated that PiG is susceptible to errors in both the standing and dynamic trials; there is still however much scope for further scrutiny. A thorough sensitivity analysis of both the standing and dynamic trials was undertaken in analysing the impacts of marker misplacement, the choice of HJC regression equation, joint width error measurement and a comparison against the CAST marker set. This was undertaken in Visual3D using data obtained prior to the present study and with data acquired for specific sensitivity studies.

Objective 4 - Analyse how differences in kinematics, kinetics and temporal-spatial parameters effect the Symptomatic LLI, Happy THR and Normal groups in terms of predicted wear rates and lubrication thickness

The literature found that currently there does not exist an in depth analysis of factors which could influence the wear rates of LLI patients. This investigation aimed to analyse the clinical data obtained prior to the study in terms of cross shear ratios, aspect ratios, motion paths and lubrication regimes in order to determine the potential impact on hip joint prosthesis.

3 Generic Methods - Implementing PiG in Visual3D and AnyBody

3.0.1 Plug-in-Gait

Background

PiG is the commercial name used by Vicon in their application of the CGM. The marker set has historically been one of the most common methods utilised in the clinical environment for gait analysis due to its relative ease of use and rapid implementation. This is through the relatively small number of markers used and the absence of medially based markers. The absence of medial markers however does lead to difficulties in the estimation of the KJC and AJC where the position is effectively defined through the accuracy of the clinician in measuring joint width. Anthropometric measurements including leg length, body mass, height, knee width and ankle width are used in the definition of body segments. The model is built using a total of 16 markers placed on the pelvis, hip, knee and the foot as shown in Figure 26.

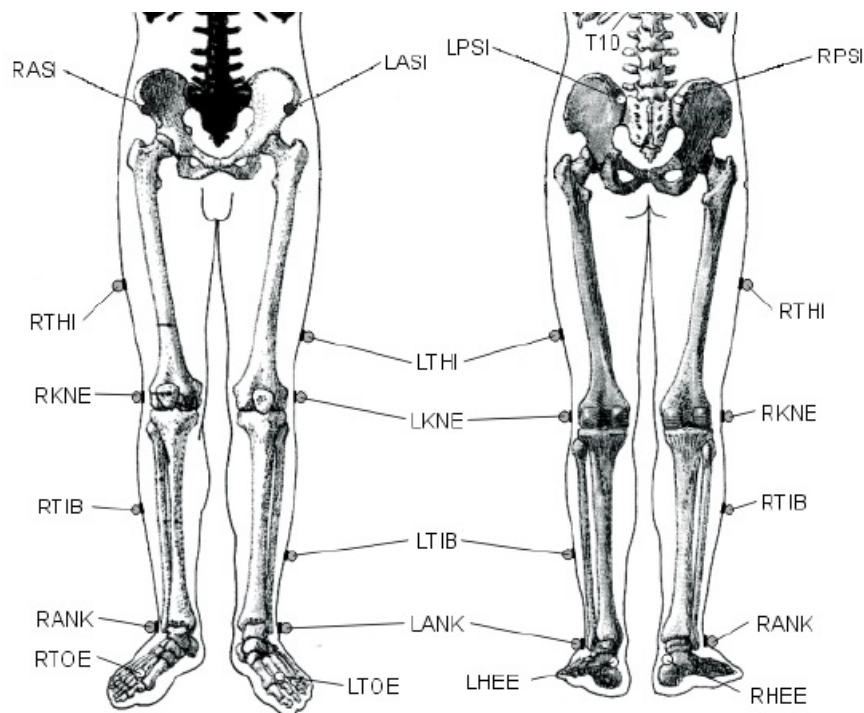


Figure 26: The Plug-in-Gait marker set with the marker names which are conventionally used. The left image gives the front view of the marker positions whilst the right image the back view.
[413]

The pelvis is defined through bony landmarks which are easily identifiable. Two markers are placed on the anterior superior iliac spine on the right and left hand sides (RASIS & LASIS) whilst two markers are placed on the right and left sides of the posterior superior iliac spine (RPSIS &

LPSIS). The PSIS markers are placed on the S2 vertebra which is indicated by the level of the skin dimples. Misplacement of any of these markers would create artefact in the pelvis angle [414].

The thigh segment has two markers placed on it. The first of these, called LTHI/RTHI (Left Thigh & Right Thigh), are placed at a lateral position on the thighs just below the swing of the hand. The RKNE/LKNE (Right Knee & Left Knee) markers are placed on the lateral epicondyles of the knees which are found through establishing the point at which the lower leg appears to rotate. Similar to the thigh segment, the shank segment also has two markers. The RTIB/LTIB (Right Tibia & Left Tibia) markers are placed on the lateral aspects of each shank at around a third of the way down the segment whilst the RANK/LANK (Right Ankle & Left Ankle) markers are placed on the lateral ankle. On the foot there are markers on the 2nd metatarsal RTOE/LTOE (Right Toe & Left Toe) and at the heel RHEE/LHEE (Right Heel & Left Heel). Clinical gait analysis requires that a segment is defined via the use of 3 or more markers, which leads to virtual joint centre markers needing to be created during the processing of captured gait data for the hip, knee and ankle (HJC, KJC & AJC).

Defining Joint Centres

The PiG marker protocol is designed in a way which allows markers to be shared between segments, such as the KJC which is shared between the thigh and the shank. This means that errors produced in the proximal segment can be passed onto the distal segment which can be amplified down the kinematic chain. For instance, inaccurate measurement of leg length or ASIS distance due to poor marker placement can have an effect on the position of the HJC. The KJC is defined to lie on the plane formed by the HJC, lateral thigh marker and lateral knee marker and thus errors in any of these in terms of placement, or computation with regards to the HJC, will introduce error in calculating the position of the KJC.

When calculations for the position of the AJC are undertaken, a total of 9 markers would have had a direct influence on computing its location. Thus the position of the AJC is potentially the most unreliable in PiG which has led to authors attempting to find alternative solutions [415]. The exact positions of the KJC and AJC are defined to be a clinically measured width (knee width or ankle width) from the lateral knee or lateral ankle marker. Computation of the KJC and AJC are illustrated in Figure 27.

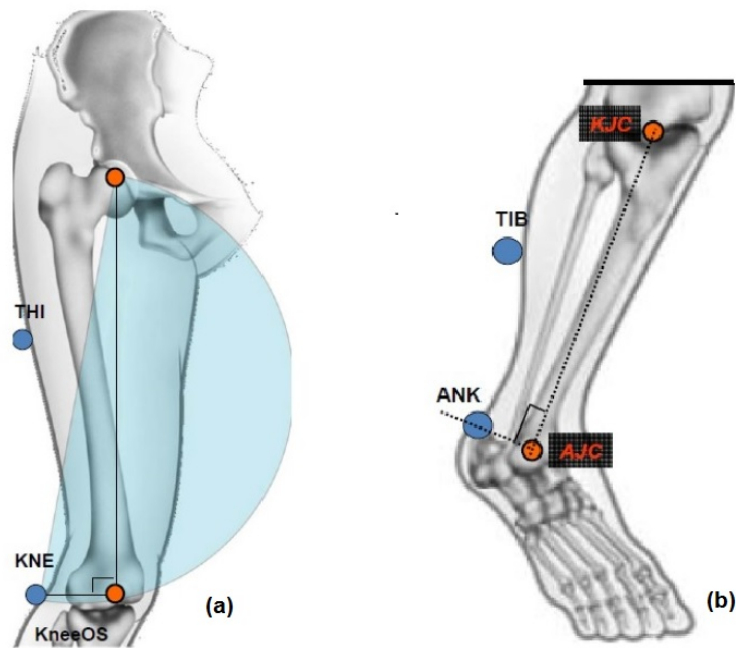


Figure 27: (a) - The KJC is computed using the HJC, lateral thigh marker and lateral knee marker plane together with the knee width via the chord function. (b) - The AJC is computed using the KJC, lateral shank marker and lateral ankle marker plane together with the ankle width via the chord function.

[43]

To avoid errors caused by the misplacement of the lateral thigh marker and thus to reduce the amount of error down the kinematic chain, a Knee Alignment Device (KAD) is often used to aid in determining the orientation of the knee joint axes [416]. This can be seen in Figure 28.



Figure 28: A patient with a KAD. A virtual knee marker is assumed to exist equidistant from the 3 markers on the device. The direction formed by the line passing through the virtual knee marker and the knee wand marker(both circles) is the knee flexion-extension axis

[417]

The position of the lateral segment markers (the lateral thigh (LTHI/RTHI) and the lateral shank (LTIB/RTIB) markers) play a large role in defining the orientation of the segment axes. This is through their effect on determining the anterior-posterior position of the distal joint centre in the plane produced for their computation. A lateral segment marker which is placed too anterior on the thigh leads to a more posterior distal joint centre and vice versa. This can be seen in Figure 29.

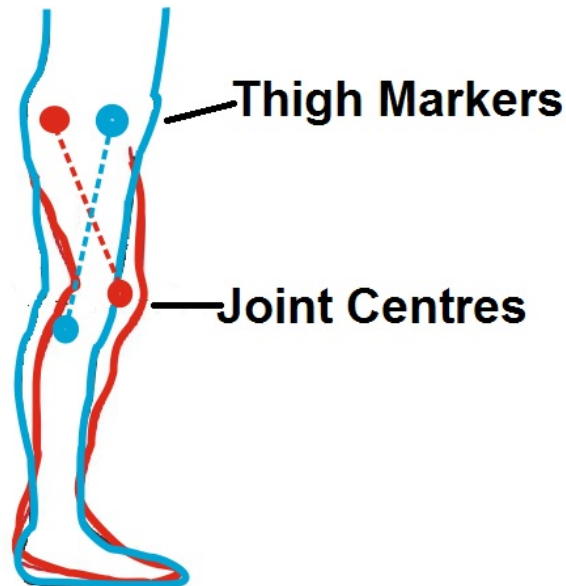


Figure 29: The effects of thigh marker positioning on the KJC. A more anterior thigh marker leads to a more posterior KJC whilst a more posterior thigh marker leads to a more anterior KJC. The same could be said for the relationship between the lateral shank marker and the AJC.

The HJC-KJC-Lateral Knee Marker and KJC-AJC-Lateral Ankle Marker angles must be 90° , as illustrated in Figure 27. This often means that the KJC and/or AJC will be offset in the superior-inferior or medial-lateral directions in addition to moving in the anterior-posterior direction. Schematics in Figures 30 and 31 attempt to explain this.

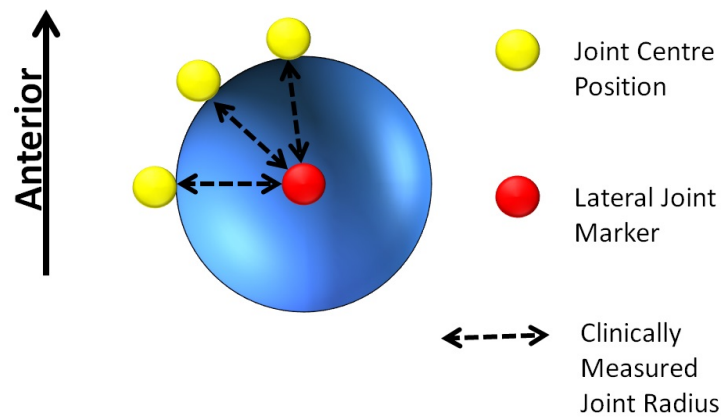


Figure 30: Schematic representing the potential positions of the KJC/AJC in the knee/ankle joint as viewed from above the joint. The edges of the sphere represent all the positions that the KJC/AJC can take through the joint width measurement. The effects of the plane which is used to compute the distal joint centre can be seen, with a joint centre which is more anterior also moving laterally due to the clinically measured joint width.

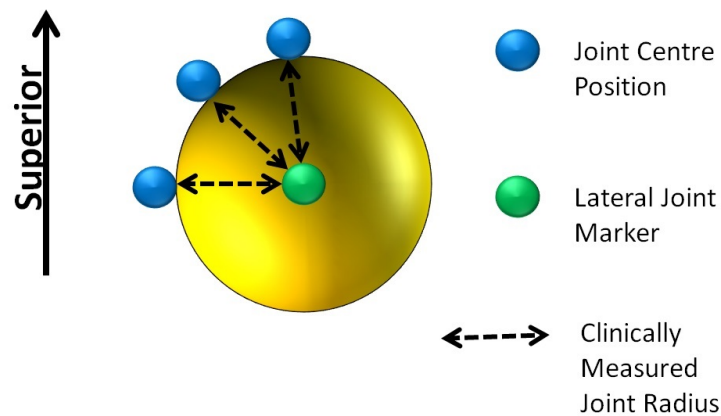


Figure 31: Schematic representing the potential positions of the KJC/AJC in the knee/ankle joint as viewed from the front of the joint. The edges of the sphere represent all the positions that the KJC/AJC can take through the joint width measurement. The effects of the plane which is used to compute the distal joint centre can be seen, with a joint centre which is more anterior also moving either superior or inferior due to the clinically measured joint width.

Axes Orientations

The lateral segment markers also have a role in determining the orientation of segment axes through their definition of the distal joint centre positions. If a computed distal joint centre is more anterior than the lateral joint marker (the lateral knee (LKNE/RKNE) marker or the lateral ankle marker (LANK/RANK)), this leads to external rotation of the segment whilst if the distal joint centre is more posterior than the lateral segment marker this leads to internal rotation. The schematic in Figure 32 attempts to explain this.

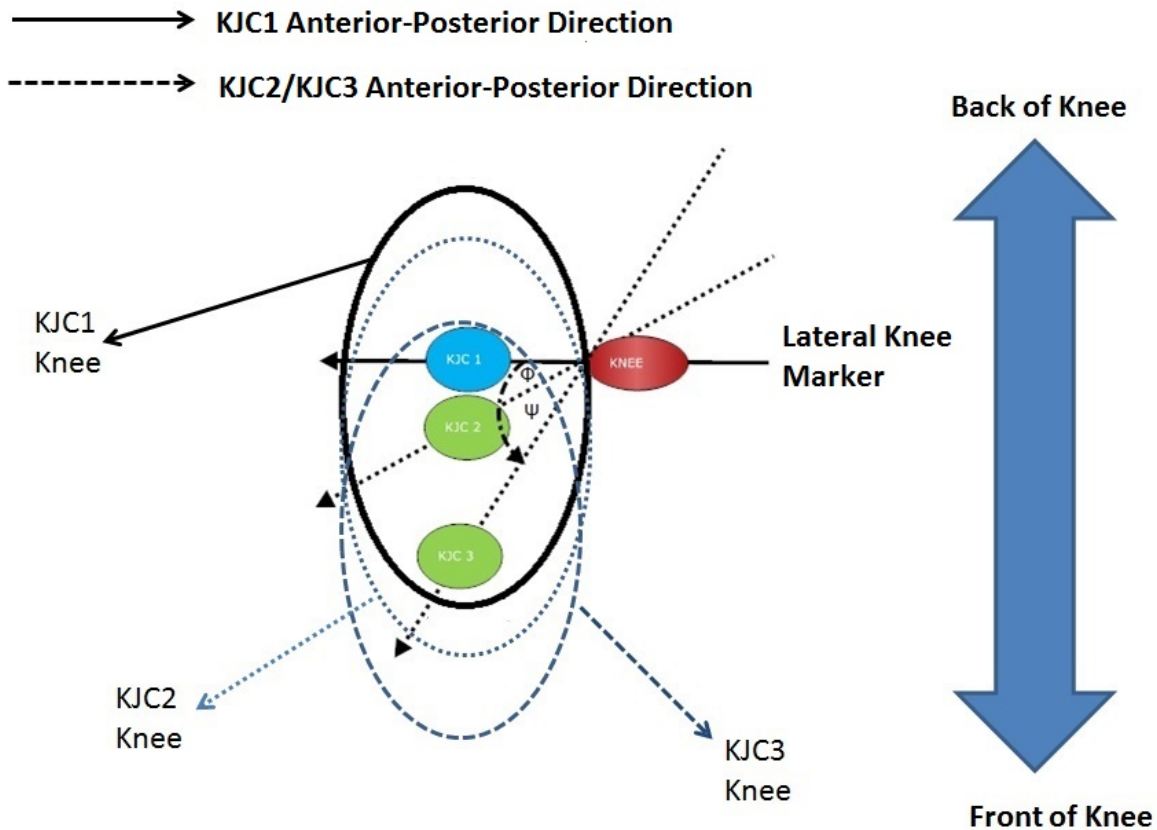


Figure 32: The symbols Φ and Ψ represent angles formed between the lateral knee marker and different KJC's, which is equivalent to the rotation of the thigh. As can be seen, a more anterior KJC leads to a greater angle between the KJC and lateral knee marker (measured between the anterior-posterior directions), causing external rotation of the thigh. The same could be said of the lateral shank marker and AJCs positions.

A common consequence of axes misorientation due to placing a lateral segment marker either too anterior or posterior is cross talk between axes. This is where a particular motion is measured incorrectly as another motion. Examples include abduction being measured as adduction and flexion being measured as abduction. This can be seen in Figure 33. Misorientation of a segment axes can also be effected by the other markers on a segment and also the anthropometric measurements; however in most cases their effects are very small.

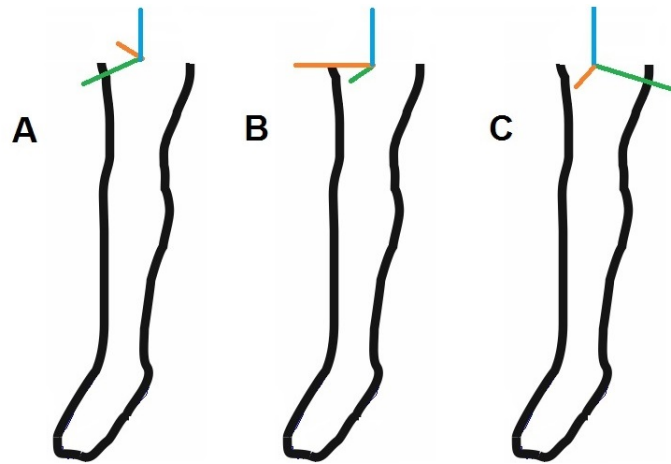


Figure 33: The leg in the diagram is assumed to be a left leg. (A) represents an internally rotated thigh due to anterior positioning of the lateral thigh marker, (C) represents a externally rotated thigh due to posterior placement of the lateral thigh marker, (B) represents a natural joint axes orientation. The red axes represents flexion-extension, with an anterior rotation of the axes being flexion and a posterior rotation being extension. The green axes represents abduction-adduction, with a medial rotation of the axes being adduction and a lateral rotation being abduction. The blue axes represents internal-external rotation. Changes in the orientation of the axes redefine where each motion is measured from and hence leads to cross-talk between axes.

Joint Centre Offset

A joint centre offset can occur in any of the three planes of motion and can effect both kinematic and kinetic results, without altering the axes of orientation. An example can be seen in Figure 34 in terms of the abduction-adduction of the thigh. An overestimation in the measurement of the knee joint width can lead to the KJC being too medial. A KJC which is too medial leads to an adduction offset at the distal portion of the thigh and an abduction offset at the proximal end during the initial standing trial. This would lead to there being an offset in the hip and knee abduction-adduction results, with results for the hip showing greater abduction and those for the knee greater adduction. Similar effects are also produced with the anterior-posterior movement of the joint centre.

Joint moments can also be effected. Taking the example once again of the knee and its medial-lateral position, a knee width which is overestimated will lead to a more medial KJC, and thus increase the amount of knee abduction moment. The vice versa would also be true for knee adduction moment. However, hip abduction-adduction moment on this occasion would not be effected as the positions of proximal joint centres are unaffected by distal changes.

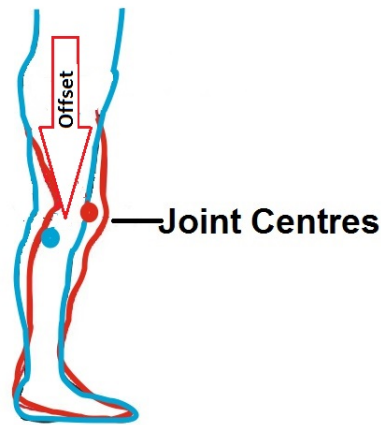


Figure 34: The effects of joint centre offset on kinematics and kinetics. A more medial KJC in the standing trial leads to an adduction offset at the distal portion of the thigh and an abduction offset at the proximal portion.

Foot Rotation

Rotation of the foot differs to that of the thigh and shank due to the segment being orientated at approximately 90° relative to the shank. Unlike the other segments, the position of the AJC has a significant effect on determining the medial-lateral tilt and rotation of the foot. This is explained and illustrated in greater detail in Figure 35.

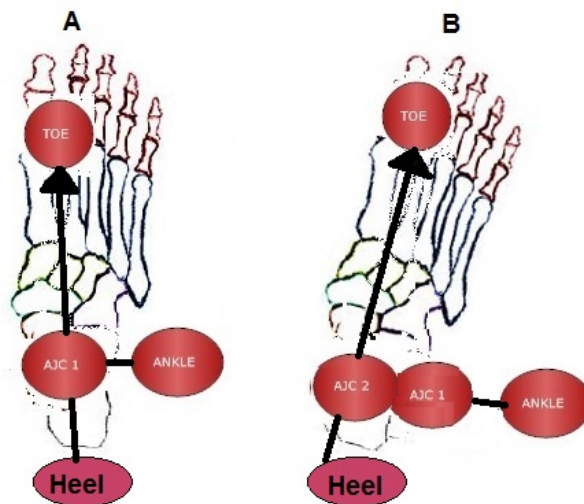


Figure 35: A top view of the foot, with ankle, toe and AJC markers. The foot is defined from the AJC/AJC2 to the toe marker. An AJC positioned more medial, lateral, anterior or posterior to the original position will alter the amount of foot rotation. A more medial AJC, such as AJC2 in schematic B relative to AJC1, leads to greater external rotation whilst a more lateral AJC would lead to a more internally rotated foot. Likewise, a more anterior or posterior AJC is also likely to lead to errors in rotation but is itself dependent on the amount of medial or lateral error. For instance in schematic (A), an error in only the anterior or posterior directions will have no effect as the AJC and toe marker are parallel. If they were not parallel, an anterior or posterior offset would cause a change in foot rotation. Changes in the position of the AJC/AJC2 also effect the foots relationship with the heel marker, which defines the foot medial-lateral tilt.

3.0.2 Visual3D

Visual3D (Germantown, MD, USA) is a 3D biomechanics analysis tool used to quantify motion as captured by a 3D motion capture system with users ranging from universities to commercial organisations. It is able to process data captured with any motion capture system as long as the C3D file format and real time streaming are used. Applications include rehabilitation, neuroscience, robotics, sports, orthopaedics and many more.

Segment Optimisation

Visual3D has two methods which can be used to determine the position and orientation of a segment. These are segment optimisation and inverse kinematics. Segment optimisation is where markers attached to a rigid segment are used to track the motion of the segment and calculate the pose and position at each data frame. This method assumes that all markers move along with the body segments to which they are attached and that their position in relation to the segment coordinate system remains unchanged. Provided that there is a minimum of three non-collinear markers placed on a segment, Visual3D will have enough information to determine a pose. A weakness of the PiG model is that there are only two markers attached to each segment. The 3rd marker which is used is the virtual marker either produced through regression equations (HJC) or through proximal marker positions and joint.

The segment coordinate system is setup via the use of the non-collinear markers whilst the laboratory coordinate system is defined during the calibration of the static trial. The latter is assumed to remain constant in analysis. The position and orientation of the segment coordinate system relative to the laboratory coordinate system can be used to completely describe motion of each segment through the use of a least squares approach. To illustrate this, assume a point \mathbf{A} is located in the segment coordinate system. The location of the point in the laboratory coordinate system (\mathbf{P}) is given by:

$$\mathbf{P} = \mathbf{T} \mathbf{A} + \mathbf{O} \quad (23)$$

where \mathbf{T} is the rotation matrix from the segment coordinate system to the laboratory coordinate system and (\mathbf{O}) is the translation between coordinate systems. Also vice-versa is possible with the location of a point in the laboratory coordinate system used to find a point in the segment coordinate system through Equation 24.

$$\mathbf{A} = \mathbf{T}^{-1}[\mathbf{P} - \mathbf{O}] \quad (24)$$

In reality, placement of markers onto a rigid body is not perfect and hence errors will be introduced into the analysis. An example of this would be at the thigh where markers placed at the lateral side of the knee and the greater trochanter exhibit high levels of STA whilst markers on the middle portion of the thigh are prone to be knocked off during walking. Hence, for each target marker an error term is introduced:

$$\epsilon = \mathbf{P} - (\mathbf{T} \mathbf{A} + \mathbf{O}) \quad (25)$$

During motion of the rigid body, a new transformation matrix \mathbf{T} and translation vector \mathbf{O} are computed at every instant provided that \mathbf{A} can be measured in the segment coordinate system and \mathbf{P} can be measured in the laboratory coordinate system using Equation 26. Here m represents the total number of markers on the rigid body segment. Minimising the sum of the squares of Equation 26 with respect to the orthonormal constraint as defined in Equation 27.

$$\sum_{i=1}^m ((\mathbf{P}_i - \mathbf{T} \mathbf{A}_i) - \mathbf{O}) \quad (26)$$

$$\mathbf{T}^{-1} \mathbf{T} = \mathbf{T}^T - \mathbf{I} = 0 \quad (27)$$

Visual3D solves this minimisation problem based on the method of Spoor & Veldpaus through the use of lagrangian multipliers.

$$g(\mathbf{T}) = \mathbf{T}^T \mathbf{T} - \mathbf{I} = 0 \quad (28)$$

Body Modelling

The start of the analysis process requires a static trial to be loaded to the main Visual3D interface. Subsequently dynamic motion trials can be linked to the static trial. In Visual3D landmarks are defined as virtual marker positions which in the case of the PiG model are the HJC, KJC and AJC for both limbs. Segments used in the production of the PiG model were the pelvis, left thigh, right thigh, left shank, right shank, left foot, right foot and the laboratory. A fully built Visual3D model can be seen in Figure 36.

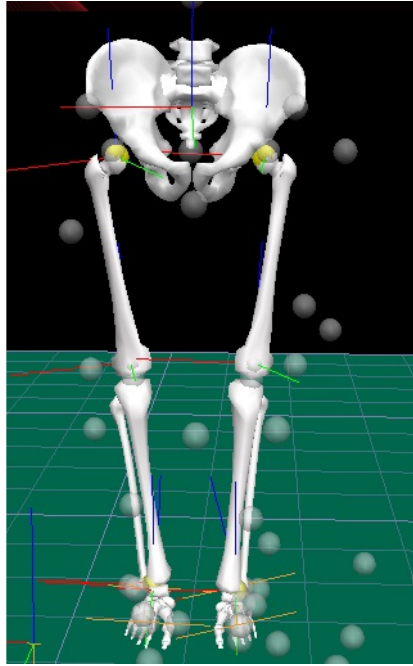


Figure 36: A static trial in Visual3D with segment definitions of the pelvis, thigh, shank and foot

Creation of the Pelvis Segment and Hip Joint Centres

The first segment created is that of the pelvis due to PiG following a hierarchal structure. Visual3D allows the creation of three different pelvises which differ in the location and number of markers used during motion capture. For the use of PiG, the pelvis defined by Davis et al. [273] is used where the segment is situated between the ASIS and PSIS markers. All of these markers are also used for tracking the pelvis during gait. This can be seen in Figure 37.

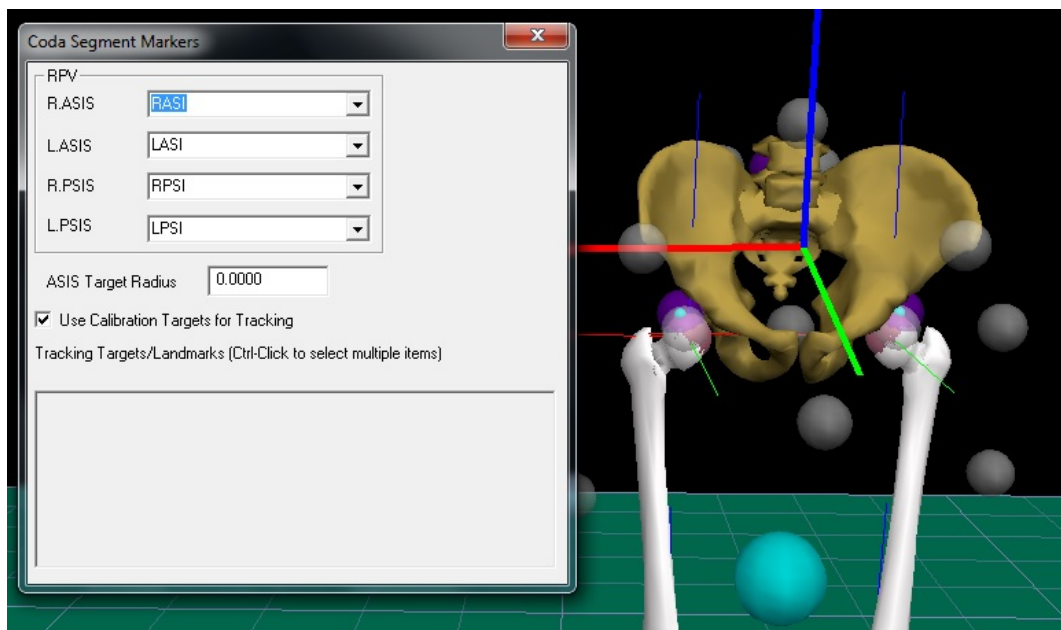


Figure 37: The Davis pelvis as defined in Visual3D

A virtual marker is defined at the mid-point of the posterior markers called the SACR marker. The plane of the pelvis is therefore defined as a triangle existing between the two ASIS markers and the SACR marker which can be visualised in Figure 38. The x direction is defined to exist between the origin and the right ASIS marker where the origin is defined as the mid-point of the ASIS markers. The z-axis is perpendicular to the x-y plane and the y-axis is a cross product of the x and z axes. The origin of the pelvis can be computed using Equation 29.

$$\overrightarrow{\text{Origin}} = \frac{\overrightarrow{\text{RASI}} + \overrightarrow{\text{LASI}}}{2} \quad (29)$$

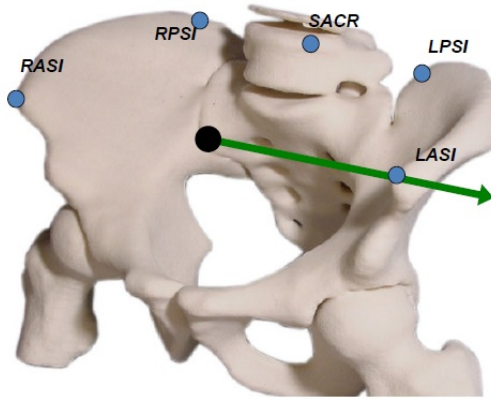


Figure 38: A schematic of a pelvis with the pelvic marker placements and the origin as defined as half way between RASI and LASI

[43]

Calculation of the HJC is often carried out using a regression equation which utilises anthropometric measurements. Bell's equation, as seen in Equations 30 and 31, uses as an input the ASIS distance in its calculation of the position vector of the HJC. Harrington produced a regression equation which is used commonly as seen in Equations 32 and 33. This equation uses the ASIS distance together with clinical leg length measurement from the ASIS to the medial malleoli. The definitions of ASIS distance and pelvic depth are illustrated in Figure 39.

$$\overrightarrow{\text{RHJC}} = (0.36 * \text{ASIS Distance}, -0.19 * \text{ASIS Distance}, -0.3 * \text{ASIS Distance}) \quad (30)$$

$$\overrightarrow{\text{LHJC}} = (-0.36 * \text{ASIS Distance}, -0.19 * \text{ASIS Distance}, -0.3 * \text{ASIS Distance}) \quad (31)$$

$$\overrightarrow{\text{RHJC}} = (0.33 * \text{ASIS Distance} + 0.0073, -0.24 * \text{Pelvic Depth} - 0.0099, -0.30 * \text{ASIS Distance} - 0.0109) \quad (32)$$

$$\overrightarrow{\text{LHJC}} = (-0.33 * \text{ASIS Distance} - 0.0073, -0.24 * \text{Pelvic Depth} - 0.0099, -0.30 * \text{ASIS Distance} - 0.0109) \quad (33)$$

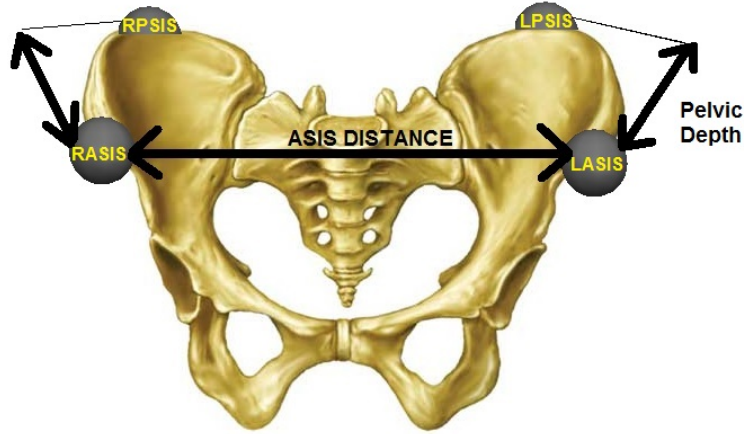


Figure 39: Measurements of ASIS distance are taken as the medial-lateral distance of the centre of the RASIS (Right Anterior Superior Iliac Spine) marker and the centre of the LASIS (Left Anterior Superior Iliac Spine) marker. Pelvic depth is computed as the average distance between the RASIS and RPSIS (Right Posterior Superior Iliac Spine) markers and the LASIS and LPSIS (Left Posterior Superior Iliac Spine) markers

[419]

A third often used HJC regression model is that of Davis et al. [273] which is listed in Equations 34 and 35. These Equations require the use of leg length and marker radius data obtained from the laboratory and pre-defined values for many of the angles and constants, which can be seen from Equations 36 - 42. Figure 40 demonstrates the derivation of this equation as undertaken by Davis et al. via a schematic.

$$\begin{aligned} \overrightarrow{\text{RHJC}} = & (-S(C \sin(\theta) - 0.5 * \text{ASIS distance}), (-\alpha - R_{\text{marker}})\cos(\beta) + C \cos(\theta) \sin(\beta), \\ & (-X_{\text{dis}} - R_{\text{marker}})\sin(\beta) - C * \cos(\theta) \cos(\beta)) \quad (34) \end{aligned}$$

$$\begin{aligned} \overrightarrow{\text{LHJC}} = & (S(C \sin(\theta) - 0.5 * \text{ASIS distance}), (-\alpha - R_{\text{marker}})\cos(\beta) + C \cos(\theta) \sin(\beta), \\ & (-X_{\text{dis}} - R_{\text{marker}})\sin(\beta) - C * \cos(\theta) \cos(\beta)) \quad (35) \end{aligned}$$

A cadaver study determined that:

$$C = 0.115 * \text{Leg Length} - 0.0153(\text{in meters}) \quad (36)$$

$$\theta = \frac{28.4\pi}{180} \quad (37)$$

$$\beta = \frac{18.0\pi}{180} \quad (38)$$

$$\alpha = \text{ASIS to ASIS distance, measured during clinical exam in meters} \quad (39)$$

$$X_{dis} = 0.1288 * \text{Leg Length} - 0.04856 \quad (40)$$

$$R_{marker} = \text{marker Radius in meters} \quad (41)$$

$$S = +1 \text{ for the right side and } -1 \text{ for the left side} \quad (42)$$

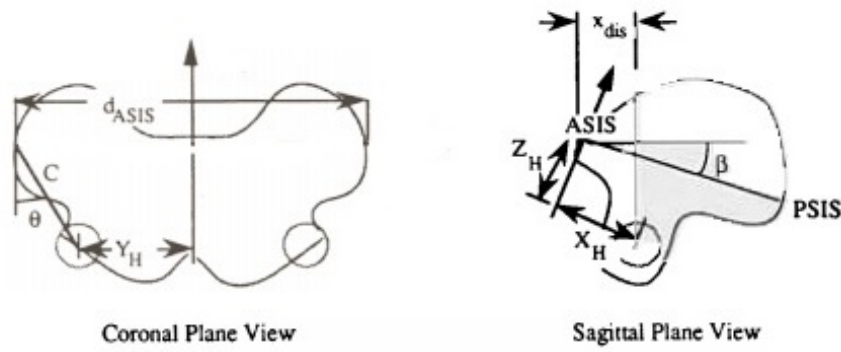


Figure 40: Schematic demonstrating the anthropometric measurements used by Davis in formulating their HJC equation

Creation of the Thigh Segment

Following the creation of the pelvis segment, the thigh segments are created. The proximal end of the thigh is defined to be the position of the HJC whilst the distal end is defined as the lateral knee marker. The radius of the proximal end (femoral offset), is defined via Equation 43.

$$\text{Femoral Offset} = \frac{\text{Inter Hip Joint Centre Distance}}{2} \quad (43)$$

The rotation of the thigh and the femoral axis at the HJCs is defined by the lateral thigh markers. The long axis (z-axis) is defined vertically with respect to the laboratory origin, the x-axis (abduction-adduction) as being perpendicular to the plane formed by the lateral thigh marker,

lateral knee marker and HJC whilst the y-axis (flexion-extension) as a cross product of the x and z axes. A thigh marker placed too anterior leads to higher internal rotation and a too posterior placement leads to excessive external rotation. Motions are tracked through the lateral thigh, lateral knee and HJC markers. Creation of the segment in Visual3D can be seen in Figure 41.

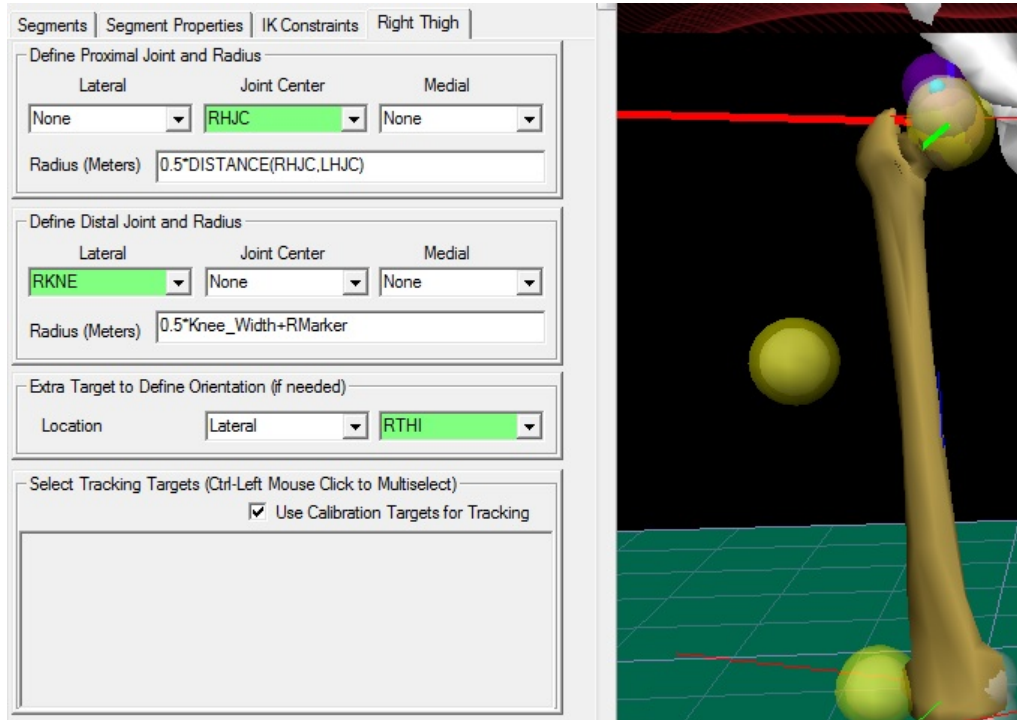


Figure 41: The creation of the thigh segment, with the RTHI and RKNE markers coloured yellow.

Creation of the Shank Segment

The KJC forms the proximal end of the shank. It is calculated via the chord function using the HJC, lateral thigh marker and lateral knee marker. This is described in Figure 27 on page 71 of the *Generic Methods*. The medial-lateral position of the KJC and the radius of the proximal end of the shank is defined via Equation 44 whilst the distal radius, which is also the ankle width, is defined via Equation 45. The KJC together with the lateral shank and lateral ankle markers are tracked during gait to compute shank kinematics and kinetics.

$$\text{Knee Radius} = \frac{\text{Knee Width} + \text{Marker Radius}}{2} \quad (44)$$

$$\text{Ankle Radius} = \frac{\text{Ankle Width} + \text{Marker Radius}}{2} \quad (45)$$

The long axis (z-axis) of the shank is defined vertically from the KJC to the HJC, the x-axis (abduction-adduction) as being perpendicular to the plane formed by the lateral shank marker,

lateral ankle marker and KJC whilst the y-axis (flexion-extension) as a cross product of the x and z axes. Creation of the segment in Visual3D can be seen in Figure 42.

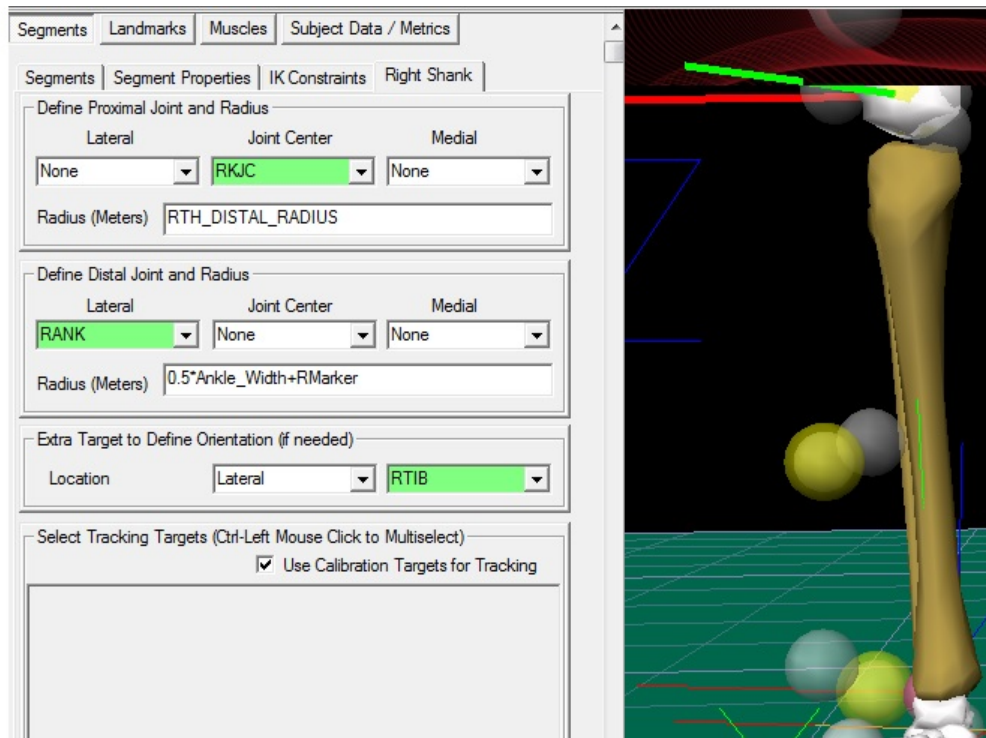


Figure 42: The creation of the shank segment, with the lateral shank and lateral ankle markers coloured yellow.

Creation of the Foot Segment

The AJC forms the proximal end of the foot. It is calculated via the chord function using the KJC, lateral shank marker and lateral ankle marker. This is described in Figure 27 on page 71 of the *Generic Methods*. The lateral shank marker determines the anterior-posterior position of the AJC whilst the ankle radius as computed in Equation 45 is used to define the medial lateral position of the joint centre relative to the lateral ankle marker.

Similar to what was seen at the knee, the long axis (z-axis) of the foot is defined to exist between the AJC and the KJC, whilst the x-axis (dorsiflexion-plantarflexion) is formed perpendicular to the plane of the lateral shank marker, lateral ankle marker and the KJC. Once again, the x-axis (eversion-inversion) is formed by the cross product of the x and z unit vectors.. The foot is however rotated at approximately 90° degrees relative to the shank. This causes a phase difference in the orientation of the axes of 90°. The creation of the foot in Visual3D can be seen in Figure 43.

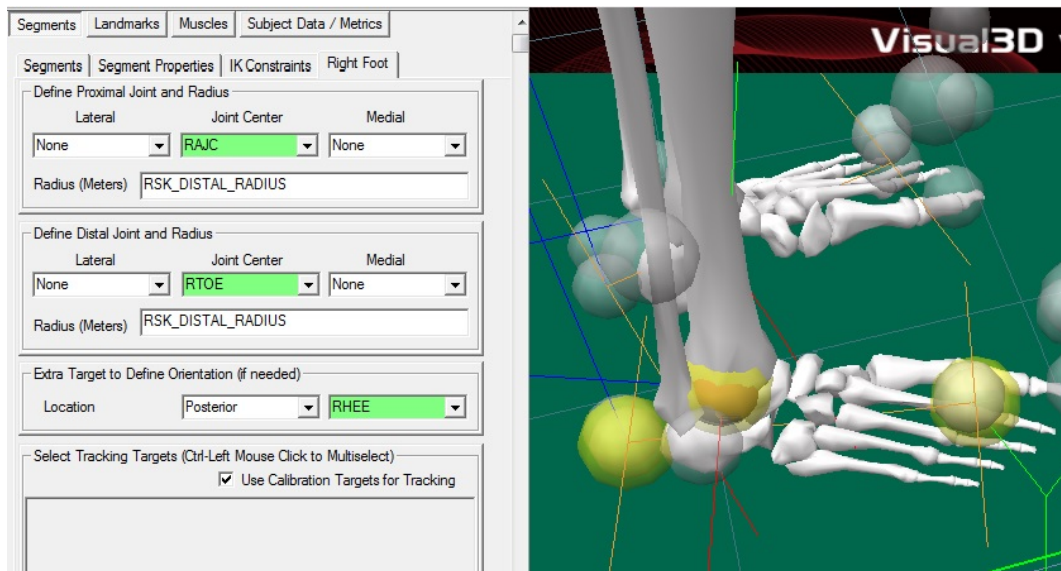


Figure 43: The creation of the foot segment, with the ankle centre, heel and toe markers coloured yellow.

3.0.3 AnyBody

Background

AnyBody (AnyBody Technology, Aalborg, Denmark) is a software program used to simulate human body mechanics. Motion capture data can be imported to drive the default model and forces can be calculated using the 1000+ muscle elements. Alternatively, subject specific models can be built to fit population data or certain individuals. AnyBody is a software program where users contribute to the enhancement of the models through submission of various biomechanical models based on the AnyBody system with regards to various activities. This has led to the development of a model repository, a collection of free validated models which are downloadable and can be utilised by subscribers to the AnyBody software.

Inverse Kinematics

The inverse kinematics process in AnyBody attempts to provide the position and orientation of all segments at each time interval. This is done through a process of least squares where the residuals between the model marker positions and the experimental marker positions are minimised. Each marker adds constraints to the segment, with a total of three per marker. Some markers can be better placed than others, with those generally on bony landmarks such as the lateral epicondyle of the knee being best placed and those on the muscular region of the thigh the most likely to be misplaced.

Figure 44 shows the experimental markers (red) and the model markers (blue). The experimental markers differ with some of them having red arrows whilst others having green. Those with green arrows indicate the direction that that specific marker can be optimised. Red arrows show that the particular markers position will not be optimised. Not all markers can be optimised as this may lead to kinematic failure. Generally, enough markers must be fixed to be able to equal the models degrees of freedom. Some markers also need to be fixed to ensure that segment lengths and joint axes can be appropriately defined. For instance, if all the pelvic markers were optimised then any arbitrary tilt of the pelvis could produce a feasible solution [420].

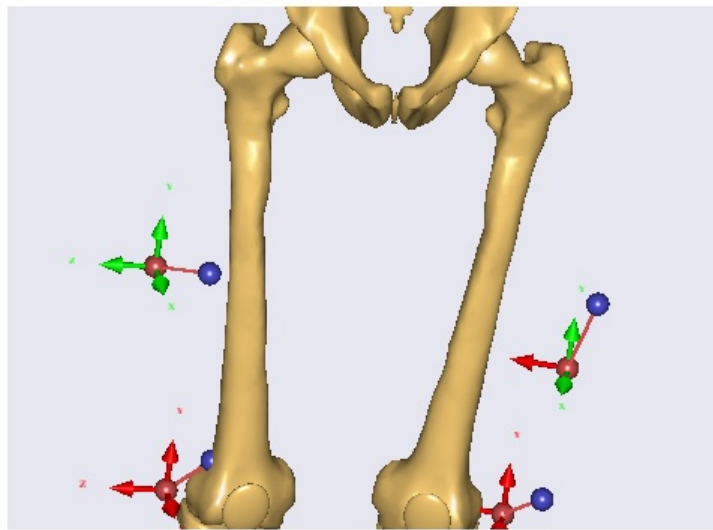


Figure 44: Model marker and experimental marker positions in the loaded AnyBody model

An initial guess is made of coordinates of the segments q^0 and parameters in the model p^0 . The initial guess of the segment coordinates does not have a bearing on the kinematic outcome of the results. This is undertaken by specifying the angles of the pelvis, hip, knee and foot together with the segment lengths. This is repeated until the virtual markers from the model approximately line up with the recorded markers from the .C3D file. If this does not occur and kinematic analysis fails at the initial guess, another initial guess must be made by the user. This is usually in terms of segment length with the angles of the segments remaining the same. If the kinematic analysis fails at another point in the analysis due to exceeding the error bounds of the model, either the error bound can be decreased or the frame numbers used in the model decreased to exclude where the error occurred. To ensure the accuracy of the model and to prevent errors being propagated, the decreasing of error bounds is not usually encouraged.

During kinematic analysis, AnyBody defines two sets of equations which must be solved:

$$\psi(q(t), d, t) \tag{46}$$

$$\phi(q(t), d, t) \tag{47}$$

where Equation 46 is with regards to marker constraints such as differences between the model and experimental marker positions whilst Equation 47 is with regards to joint constraints. The optimisation process aims to find an optimal solution at each time frame with the minimal difference between the model and experimental markers with respect to the joint constraints. Following analysis, kinematic results can be extracted from AnyBody. The optimised parameters such as the joint angles are then saved into a temporary file which are used in the kinetic analysis.

Inverse Dynamics

During kinetic analysis, a number of items must be specified which will directly impact the results following inverse dynamics. These are all with regards to muscle properties. In principle, AnyBody uses three muscle modelling types:

- AnyMuscleModel
- AnyMuscleModel2ELin
- AnyMuscleModel3E

The first of these, AnyMuscleModel, is a very simple muscle model which has a single input of muscle isometric strength. These strength values are taken from cadaver studies. They are however unsuitable in modelling THR due to not depicting the muscle morphology after surgery. Another of the available muscle types is AnyMuscleModel2ELin. The advantage of using this muscle type over AnyMuscleModel is that the muscle strength is assumed to be proportional to current length and contraction velocity.

When using the AnyMuscleModel2ELin model, Anybody assumes that the tendon is linearly elastic and contains two elements which include the muscle (contractile element) and serial elastic elements (tendon). The justification for the use of elastic properties is that muscles have an innate passive elastic capacity. The drawback of using this model is that the force can be reduced to zero even if the muscle is significantly stretched whilst in reality the passive elasticity will always provide

a force. It would also be difficult to use this model when analysing THR due to the loss of elastic capacity in some of the muscles which have been either been shortened or damaged during surgery.

The final type of muscle model used by Anybody is AnyMuscleModel3E which is a full on Hills Model. The name is due to the three components of the model: a contractile element representing the active muscle fibres, a serial-elastic element which represents tendon elasticity and a parallel elastic element representing the passive stiffness of muscle fibres. The AnyMuscleModel3E model works by firstly recruiting the muscles and then computing the tendon elongation. Subsequently, it calculates the influence of tendon elongation on muscle strength and corrects the muscle activity. The solution provided is however only an approximation because in theory a change in muscle strength may alter the force distribution which is not reproduced in the Anybody system. Instead all corrections are local.

Generally when setting up an equilibrium equation for the musculoskeletal system it is of the following form:

$$Cf = r \quad (48)$$

where f is a vector of muscle and JRFs, r is another vector which represents external and inertia forces whilst c is a matrix of equation coefficients. Despite this being a linear system which would at first glance appear trivial to solve, difficulties arise due to two reasons. The first of these is that muscles can only pull and not push which implies that the only solutions available are positive or zero in sign with regards to muscle force. The second reason is with respect to muscle redundancy where the muscular system has more muscles than required to balance and external forces. In-vivo, the CNS instantaneously chooses a set of muscles which are optimum for the task. This can be formulated as:

$$\begin{aligned} \text{Minimise} \quad & G(f^m) \\ \text{Subject to} \quad & cf=r \\ & f_i^m \geq 0 \\ & i = 1 \dots n^m \end{aligned}$$

AnyBody can be used as a tool to guess the type of function that G is. It can estimate this function G as linear, quadratic or polynomial which have all been discussed previously. Linear muscle recruitment, despite being unrealistic, is included in the AnyBody modelling software for

completeness and when required can be used to determine the strongest muscles in a given complex system. Use of the quadratic muscle recruitment criterion also poses problems when used in the Anybody system due to the results at times not being physiological, although Modense et al. [350] would challenge this.

To overcome the problems posed by these methods, the min-max formulation for muscle recruitment is commonly selected. This recruitment criterion ensures that the maximum output for all the muscles which are able to contract for a specified pose is minimised. Loads are thus not placed on a small number of muscles and are instead distributed between many of the muscles in the close vicinity. This is similar to what is thought to occur physiologically [325].

3.0.4 Statistics

Bartlett's test was used to find whether the variances of compared measurements in each group were equal. Normality was tested for prior to analysis using the Anderson-Darling test. If normality was found, the one-way ANOVA test was used in SPSS at the 5% significance level together with the Tukey post-hoc. If normality was not found for analysis with more than one group, the non-parametric Kruskal-Wallis one-way ANOVA was used in SPSS at the 5% significance level. All statistics were reported to 2 significant figures. 95% confidence intervals were also calculated using Equation 49 where μ is the average, σ the standard deviation and n the number of variables.

$$\text{C.I} = \frac{\mu \pm 1.96\sigma}{\sqrt{n}} \quad (49)$$

4 Anthropometrics & Demographics

4.1 Aims & Objectives

The aim of this study was to understand the differences in anthropometric measurements made clinically and demographic factors between between symptomatic LLI patients and asymptomatic individuals following a THR, which for this study were labelled as Happy THR patients. Variables studied included the femoral offset, leg length difference, inter-hip distance and cup inclination angle in terms of anthropometrics together with height, age and with BMI for demographics.

4.2 Methodology

4.2.1 Initial Clinical Method

By LMBRU (Leeds Musculoskeletal Biomedical Research Unit) Staff

Ethical approval was obtained prior to the start of the study from the Leeds West National Health Service Ethics Committee Ref: 09/H1307/63³. The ethical opinion includes provision for future use of the data for related purposes such as computational modelling. Data was anonymised before being used for analysis.

The investigation involved a rigorous selection of patients who had undergone THR for a period greater than a year and were either "happy" or were symptomatic for a leg length difference. The exclusion criteria for the patients in the symptomatic leg length difference and Happy THR groups are listed below. Inclusion into each group was undertaken prior to the commencement of the present study, where LLI patients were initially screened and operated on at other hospitals across Leeds before being referred to Chapel Allerton Hospital (Leeds, UK) due to it being a specialist joint replacement hospital. All patients in the Happy THR group had a postoperative Oxford Hip Score⁴ above 35 indicating little or no discomfort. Oxford Hip Scores for the LLI group ranged from 5-48.

All patients who were symptomatic only perceived a difference in leg length post-THR, with differences being at the hip joint. The surgical procedure did not effect the lengths of the shank or the height of the ankle joint. Each of the LLI patients had been implanted with an UHMWPE prosthesis. A control group of Normal healthy subjects was recruited from a clinical list of healthy

³See *Appendix II* for approval form, participant information sheet samples and consent form samples on pages 341-350

⁴The Oxford Hip Score is a qualitative assessment of daily function in THR patients consisting of 12 questions. Each question has a score from 0-4, with 0=severe pain and 4=no pain [421]

volunteers who each demonstrated the maximum Oxford Hip Score of 48 for both the hip and the knee. The exclusion criteria for this group is also listed below.

All patients had unilateral hip replacements. In total 14 Happy THR patients (Age 64 ± 11.2) and 26 Symptomatic LLI patients (Age 59.8 ± 9.6) were recruited together with a cohort of 38 Normal healthy individuals (Age 45 ± 12.6)⁵. These groups were not matched for age or gender. Happy THR patients were asked to volunteer for the analysis together with the Normal healthy volunteers at Chapel Allerton Hospital in Leeds. These patients underwent clinical gait analysis at Chapel Allerton Hospital.

Exclusion Criteria for LLI Patients

- Not undergone unilateral THR
- Had undergone any other joint replacement procedure e.g resurfacing at the hip, knee or ankle
- Did not complain of perceiving a difference in leg length post-THR
- Not been referred for revision surgery
- Had congenital differences in leg length or differences caused by non-THR surgery which caused clinical symptoms
- Had pre-existing musculoskeletal problems which would be expected to effect gait
- Had other health issues which would be expected to effect gait

Exclusion Criteria for Happy Patients

- Not undergone unilateral THR
- Had undergone any other joint replacement procedure e.g resurfacing at the hip, knee or ankle
- Complained of perceiving a difference in leg length post-THR only, with no complaints prior to surgery
- Had pre-existing musculoskeletal problems which would be expected to effect gait
- Had other health issues which would be expected to effect gait

⁵See pages 339-340 in *Appendix I* for patient lists

Exclusion Criteria for Normal Controls

- Had undergone any type of joint replacement surgery
- Had health issues which would be expected to effect gait

4.2.2 Non-Clinical Method

(By Author)

The initial 26 Symptomatic LLI patients recruited for clinical gait analysis were screened post-analysis for secondary conditions. This led to the subsequent removal of 8 patients with additional underlying pathologies. This information was provided through medical notes taken during clinical analysis. Additional patients were removed from the LLI and Happy THR groups due to radiographs being unavailable. Overall, the radiographs of 13 LLI and 11 Happy THR patients were analysed. No anthropometric results were produced for the Normal group due to these patients not having undergone radiographic analysis. All radiographs used were of patients who had given informed consent for the images to be used in research.

4.2.3 Clinical Method

(By author and Bobin Varghese)

Measurements were made using a clinical software package called PACS (Picture Archiving and Communication System). This system stores patient radiograph data and allows design tools to be utilised for measurements. Once anthropometric measurements were made on individual radiographs, the values were multiplied by a magnification value. This was as the radiograph images were stored on a standardised scale, with measurements not depicting actual anthropometrics. The real measurement values were found by measuring the width of the calibration ball on each radiograph as seen in Figure 45 and comparing it to its actual known width of 2.5cm. The ratio produced was defined as the magnification value. All PACS measurements were then multiplied by this ratio value to find the true measurement.



Figure 45: A radiograph of a LLI patient with the calibration ball labelled.

Hip Joint Centre

Four measurements were made using PACS; leg length, femoral offset, inter-hip distance and cup inclination angle. The most important landmark to identify in these measurements was the HJC. Traditionally, there exist many methods to measure the precise location of the HJC which all rely on the correct identification of landmarks such as the teardrop. The quality of the x-rays however included patients which did not have the anterior-superior iliac spine or the teardrop visible, thus making it not possible to utilise many of the methods used in literature⁶ such as those of Fessy et al. [258], John & Fisher [259], Pierchon et al. [422] and Ranawat et al. [423].

The true physiological hip centre is calculated by placing a circle around the femoral head and then drawing two perpendicular lines producing a quadrant in the circle [263]. This method has previously been used in the literature [263, 424–426]. The centre of this quadrant is the HJC. Due to the difficulties in using the traditional methods in measuring hip centre on a radiograph, it was decided to use this method of drawing a circle over the femoral head. This can be seen in Figure 46. A horizontal line from the most medial to the most lateral portion of the circle and a vertical line from the most superior to the most inferior portions of the circle were also drawn. The intersection of these lines was determined to be the HJC.

⁶Details of these methods are given in the *Generic Methods*

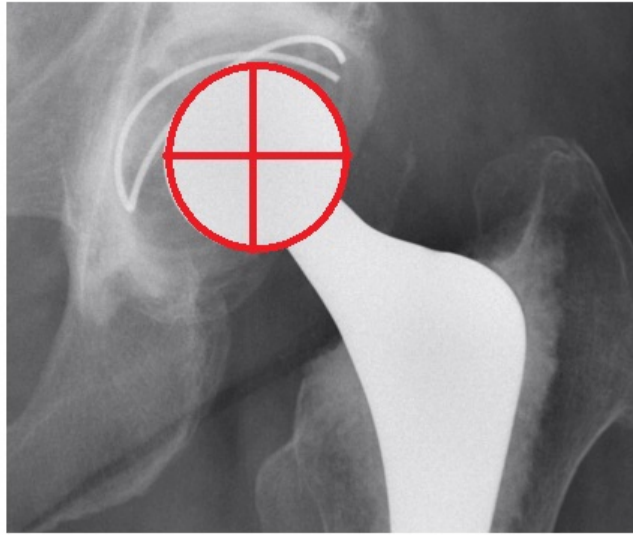


Figure 46: Derivation of the HJC through the use of bisecting lines over the femoral head of the hip implant. The horizontal line crosses from the most medial to the most lateral portion of the femoral head whilst the vertical line crosses from the most superior to the most inferior. Image analysis undertaken for this illustration in Coreldraw and represents what occurred in PACS

Inter-Hip Distance

Inter-hip distance was measured as the horizontal length between the left and right HJCs. Figure 47 demonstrates this measurement.

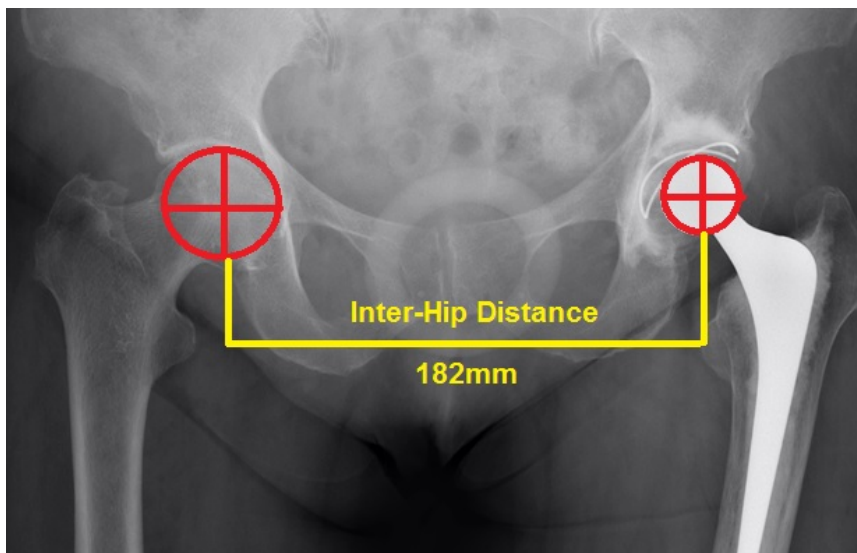


Figure 47: Calculation of inter-hip distance on a radiograph using Coreldraw, representative of PACS.

Femoral Offset

An increase in leg length is often produced by the artificial implant having a greater femoral offset than the natural hip joint. Measurements were made by computing the perpendicular distance from the HJC to the line passing through the long axis of the femur. This can be seen in Figure 48.

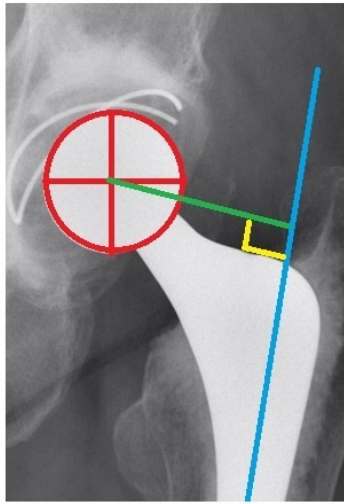


Figure 48: Calculation of femoral offset on a radiograph. The HJC position was computed first, with a line then drawn from the HJC to the line passing through the long axis of the femur, meeting at a right angle. In this Figure, the green line denotes the femoral offset.

Cup Inclination Angle

The cup inclination angle is the elevation of the acetabular cup relative to a reference line. For this study, the method of Pluot et al. [427] was used with the ischial tuberosity used as the reference line which was subtended by a line connecting the inferior and superior aspects of the acetabular cup. The angle formed was defined as the cup inclination angle. Figure 49 demonstrates this measurement.

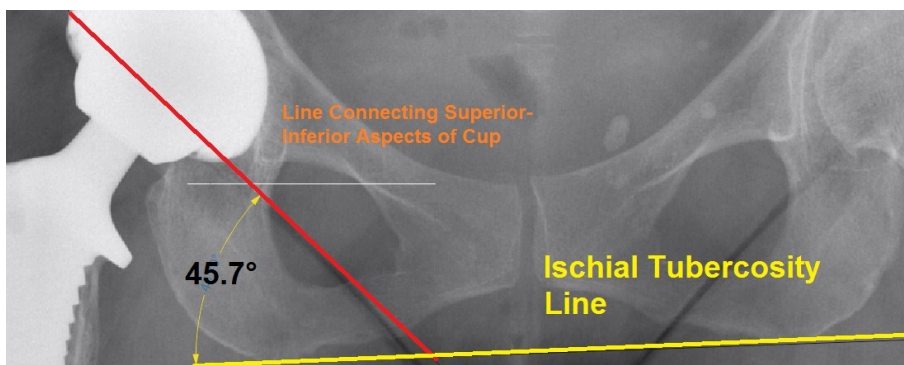


Figure 49: Calculation of cup inclination angle on a radiograph using CorelDraw, representing how measurements were undertaken in PACS.

Leg Length

The calculation of leg length followed the methodology as defined by McWilliams et al. [256], as seen in Figure 50. Calculation of leg length differences was achieved by firstly drawing a line which connected the HJCs of the two femoral heads. Parallel lines were then drawn at the most inferior

point of the teardrop and at the lesser trochanter on both sides of the hip. The vertical length between the line joining the HJC and the teardrop was measured on both sides of the hip. Any difference between the two was due to differences in cup height on the operated side. The vertical length between the inferior portion of the teardrop and the lesser trochanter was also measured on both hips. Any difference in length between the two was due to differences in stem length on the operated side. The overall LLI was found by summing the differences between cup height and stem length.

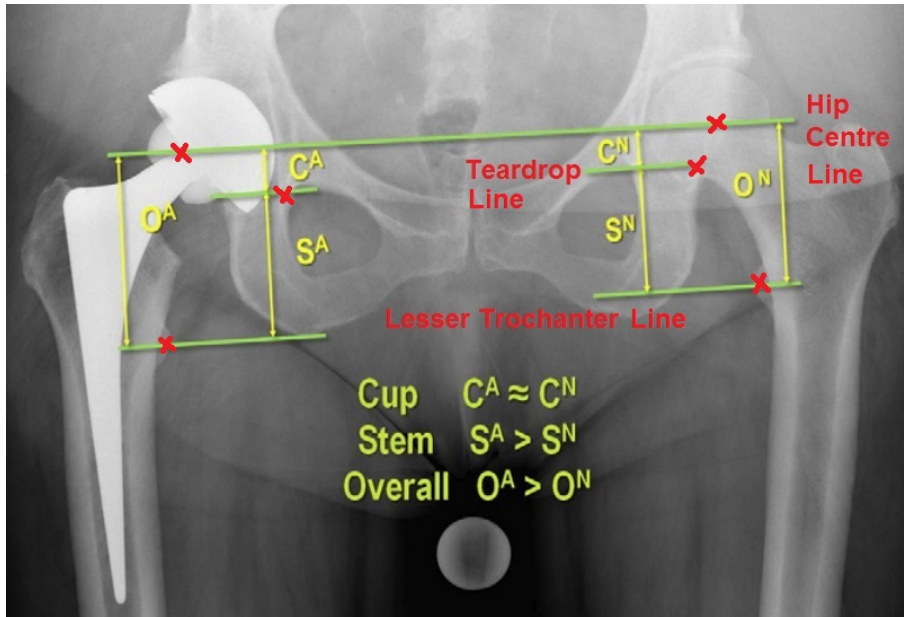


Figure 50: Calculation of leg length using the McWilliams method on a radiograph. C^A and S^A represent artificial cup and stem length respectively with C^N and S^N representing the natural cup and stem length. O^A and O^N represent the overall length found through the addition of the C^A and S^A and C^N and S^N measurements.

Figure adapted from McWilliams et al. [11]

Demographics

Demographic measurements included age, height and BMI. As these measurements did not require radiographs, all of the Symptomatic LLI (13) and Happy THR (14) patients could be included. BMI was measured using Equation 50.

$$\text{BMI} = \frac{\text{Weight}(\text{kg})}{\text{Height}(\text{m})^2} \quad (50)$$

4.3 Results - Anthropometrics

4.3.1 Femoral Offset

Femoral offset has been reported in various studies to range from 39.3mm to 47.1 mm following THR [165, 428–431]. For the Symptomatic LLI group on the operated side there was an average femoral offset of $41.8\text{mm} \pm 4.19\text{mm}$ whilst on the non-operated side it was computed as $41.3\text{mm} \pm 6.57\text{mm}$. For the asymptomatic Happy THR group, on the operated side an average of $47.1\text{mm} \pm 7.47\text{mm}$ was computed with the non-operated side having a femoral offset on average $42.3\text{mm} \pm 5.56\text{mm}$ long. Using a one-way ANOVA, it was found there were no statistically significant differences between the groups ($p > 0.05$).

Despite there being no differences between the groups in the results, a general trend was seen with the LLI patients having on average an approximately 13% smaller femoral offset. McGrory et al. [429] found that a greater femoral offset was linked to greater muscle abductor strength. Other studies have demonstrated that a greater femoral offset is linked to increased stability [428, 429, 432]. In addition, a larger femoral offset has been linked to an increase in RoM, a drop in the amount of abductor force and abductor moment arm length required during gait [429]. These factors may have been the underlying reason why the LLI patients were symptomatic and the Happy THR patients were asymptomatic.

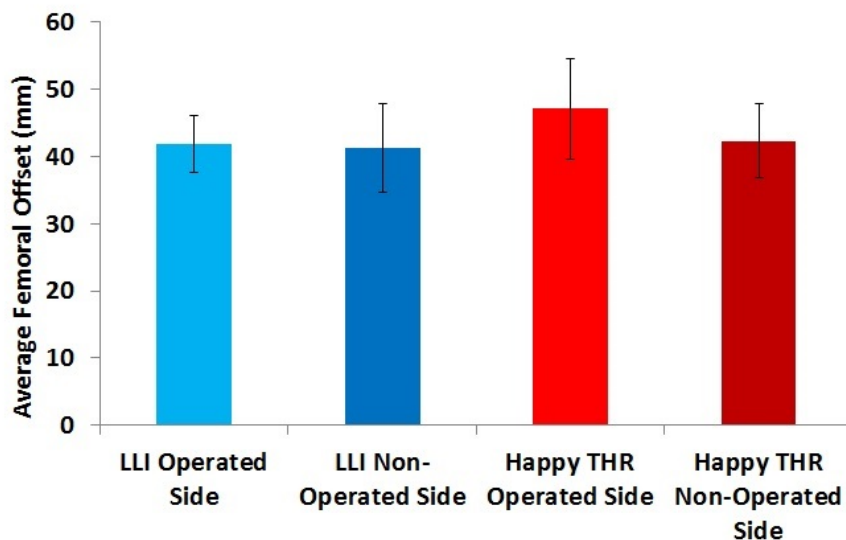


Figure 51: Average femoral offset compared between the LLI and Happy THR groups together with standard errors.

4.3.2 Inter-Hip Centre Distance

There were no statistically significant difference found in terms of inter-hip distance between the LLI ($176\text{mm}\pm 8.83\text{mm}$) and Happy THR ($184.8\text{mm}\pm 21.7\text{mm}$) groups using the t- test ($p>0.05$), which can be seen in Figure 52. Results were in the same range as found for a healthy individual (169mm) by Charlton et al. [433].

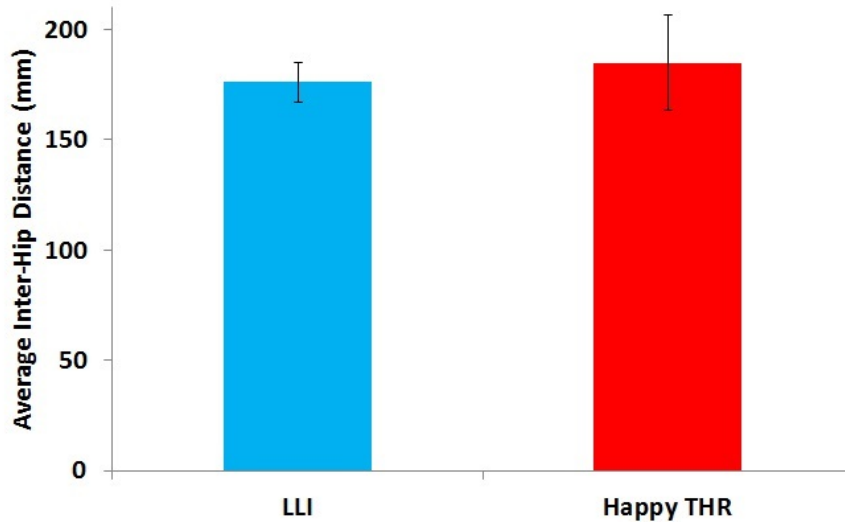


Figure 52: Average inter HJC distance compared between the LLI and Happy THR groups together with standard errors

4.3.3 Cup Inclination Angle

For the LLI group, the operated side cup had an inclination angle of $41.9^\circ\pm 13.7^\circ$ with the operated side of the Happy THR group having an angle of $45.5^\circ\pm 4.66^\circ$. Results for the non-operated sides revealed natural anatomical cup inclination angles of $54^\circ\pm 4.64^\circ$ and $50.3^\circ\pm 6.27^\circ$ for the LLI and Happy THR groups respectively. Results for both the operated ($p>0.05$) and non-operated sides ($p>0.05$) were found to be statistically not significant using the t-test at the 5% significance level. Results can be seen graphically in Figure 53.

Unlike the current results, Pennington et al. [434] found using the same method significant differences in cup inclination angle between the operated 45.4° and non-operated sides 43.5° of Happy THR patients which were statistically significant. Their study was however taken on a significantly larger patient cohort. Similar results were found by Bennet [405] with THR patients demonstrating average cup inclination angles 44.4° on the operated side.

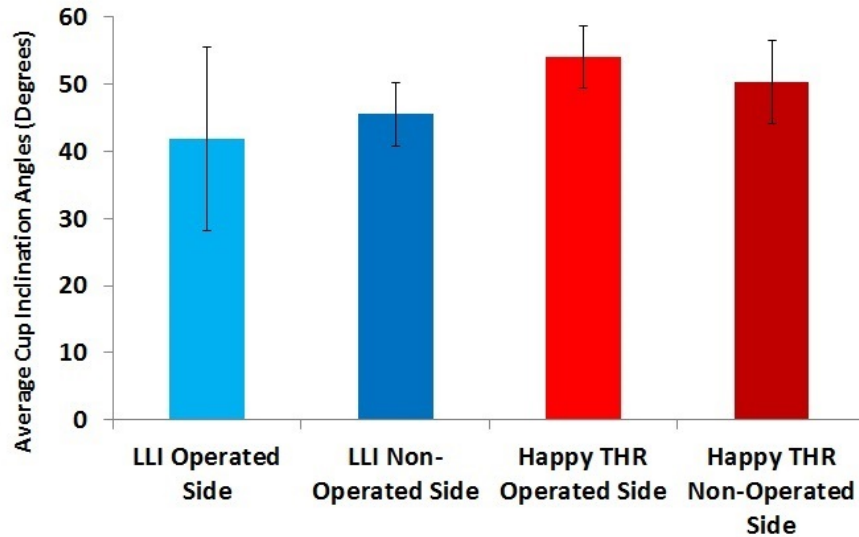


Figure 53: Average cup inclination angles compared between the LLI and Happy THR groups together with standard errors

4.3.4 Leg Length Difference

Out of the LLI patients, 13 (100%) had a longer operated leg whilst for the asymptomatic THR group 5 (50%) had a longer operated leg. Ranawat et al. [230] demonstrated that LLI patients were more able to tolerate shortening of a leg more than a lengthening. This could potentially be due to the stretching of the soft tissues around the hip when lengthening of the leg occurs.

If those patients with shortening of the operated limb are removed from the Happy THR group, the remaining patients had on average the operated side $5.30\text{mm} \pm 4.64\text{mm}$ longer than the non-operated side. Those patients with a decrease in leg length had on average the operated side $-4.68\text{mm} \pm 3.16\text{mm}$ shorter than the non-operated side. An ANOVA comparing the lengthened and shortened Happy THR patients to the LLI group produced statistically significant results ($p < 0.01$), with a Tukey demonstrating the difference were between the shortened side and the other two groups. Figure 54 illustrates this. This analysis has shown that when lengthening of the leg does occur following THR, the magnitude of leg length does not effect whether an individual is symptomatic or not.

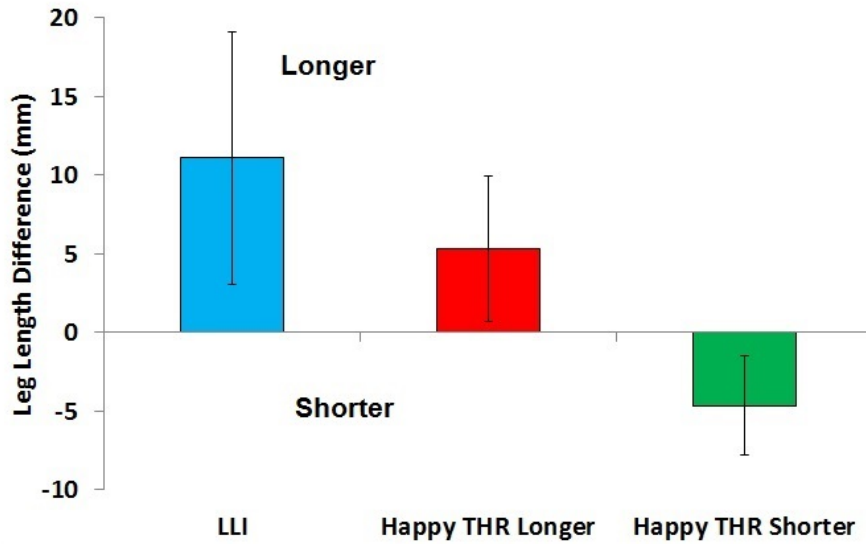


Figure 54: Comparison of the leg length differences of the LLI group to the Happy THR group, where the latter is split into results with an increase in operated leg length and a decrease. Standard errors are included.

Figure 55 illustrates that the differences in leg length were greater at the stem for both the Happy THR and LLI patients, with the differences in stem length being 64% greater in the Symptomatic LLI group. The one-way ANOVA found no statistically significant differences in terms of stem length difference between both groups ($p > 0.05$). Likewise, a Kruskal-Wallis test found no significant difference between the LLI and Happy THR groups in terms of cup height ($p > 0.05$).

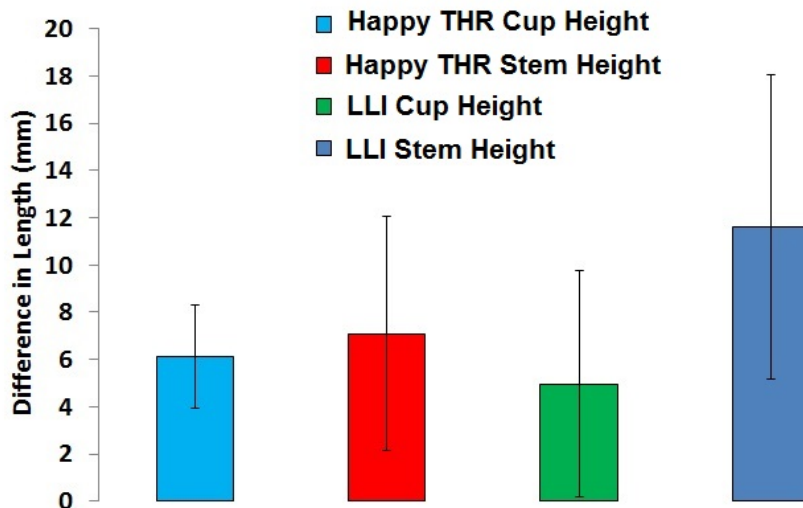


Figure 55: Average absolute differences in cup height and stem length between the operated and non-operated sides of each group. Standard errors are included.

4.4 Results - Demographics

Table 2 shows results for both the LLI and Happy THR patient groups in terms of demographics. Results between the groups in terms of BMI and age were similar. Significant differences were however present in terms of height, with the average Happy THR patient being 6% taller than the average LLI patient. Full results can be found in Appendix I on pages 339 - 340.

Table 2: Demographics for the LLI and Happy THR groups with average results and standard errors together with t-test results

	LLI	Happy THR	T-test
BMI	29.4±4.04	29.6±6.08	p>0.05
Height(m)	1.61±0.07	1.70±0.10	p<0.01
Age (years)	61.3±10.4	64.3±11.2	p>0.05

4.5 Discussion

4.5.1 Leg Length Difference

Theoretically speaking, a greater leg length difference is more likely to lead to clinical symptoms. Figure 56 demonstrates the amount of pelvic obliquity (medial-lateral tilt) seen when leg lengths are equal (A) and when the operated side leg is longer (B). A positive pelvic obliquity here is defined as the superior direction tilt of the pelvis on the longer operated side. A greater superior pelvic obliquity would be a direct consequence of an increased leg length. Patients with the longest leg length differences were therefore more likely to have increased levels of pelvic obliquity and thus more likely to suffer from symptoms such as lumbar scoliosis [222].

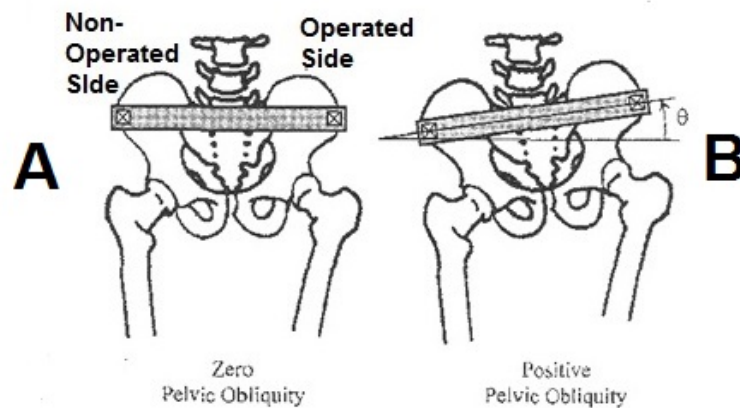


Figure 56: Pelvic obliquity levels when there is zero obliquity (A) and when there is positive obliquity (B) with the operated side lifted upwards.

Figure 57 shows how, from using geometry alone, pelvic obliquity increases linearly with leg length difference as a function of the inter-hip distance. Obliquity angles were computed using basic trigonometry for known leg length differences and inter-hip distances. It was found that the smaller the inter-hip distance, the greater the impact of the leg length difference on pelvic obliquity and hence potentially clinical outcomes. Similar conclusions are drawn in the literature [234, 235].

Results from Figure 57 also illustrate that the relationship between leg length difference and the computed static pelvic obliquity angle is clustered around two regions. These regions are $<5\text{mm}$ and between $10\text{-}15\text{mm}$. The average height of the patients with a LLI $<5\text{mm}$ was 1.63m whilst the remaining patients averaged 1.66m . The average inter-hip distance of the patients with a LLI $<5\text{mm}$ was 180mm whilst the remaining patients also averaged 180mm . Neither height ($p>0.05$) nor inter-hip distance ($p>0.05$) was found to statistically differ between these subgroups.

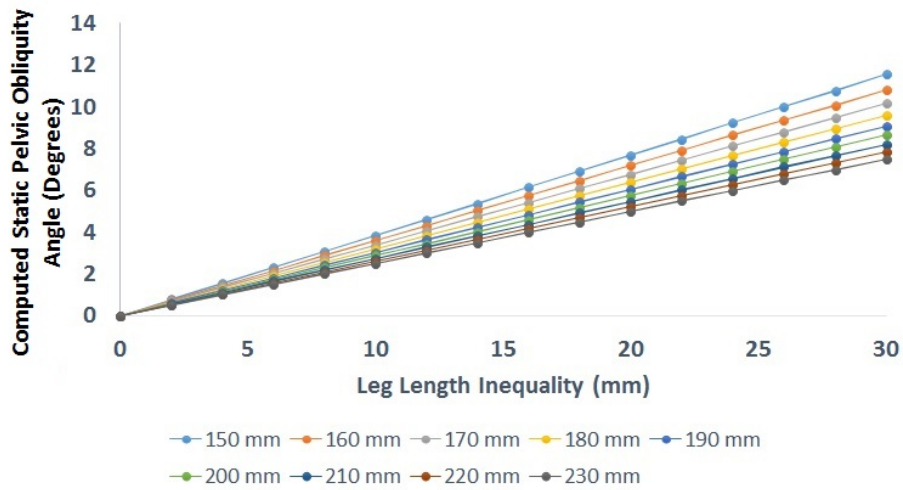


Figure 57: The effect that varying the leg length difference has on pelvic obliquity angle as a function of inter-hip distance

Figure 58 demonstrates how this linear relationship in Figure 57 is linked to the anthropometric results as seen for the LLI and Happy THR patients. Smaller static pelvic obliquity angles were computed for the Happy THR group, which would have been linked to the smaller leg length differences. It appeared that a leg length difference of $>13\text{mm}$ or a pelvic obliquity $>5^\circ$ was sufficient for a patient to be symptomatic for an LLI following THR. This follows closely the 10mm threshold commonly suggested in literature as the minimum amount of discrepancy required for clinical symptoms to develop. Using the SRCC, there was however no link detected between the dynamic peak superior pelvic obliquity during a normalised gait cycle and the magnitude of leg

length (SRCC =0.06). Patients compensated for having a difference in leg length using a variety of methods at the pelvis.

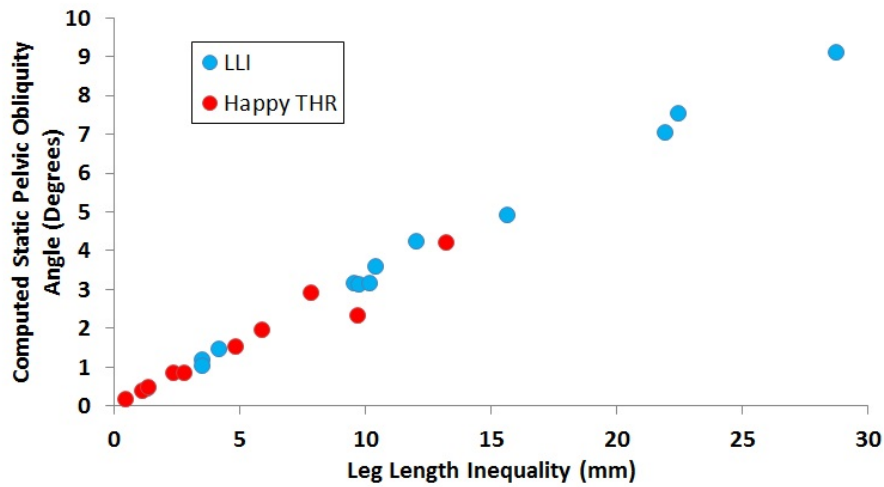


Figure 58: The effect that varying leg length differences have on pelvic obliquity angle for both the LLI and Happy THR groups

4.5.2 Height

With regards to height, it was found that taller individuals were more likely to be in the "Happy" THR group than the LLI group. Results also indicated that there was no significant difference in terms of femoral offset between the groups. This was surprising as it would be expected that the taller Happy THR group would have greater average femoral offsets [436]. The LLI patients thus may have been symptomatic due to having hip prosthesis which were larger than required.

Differences between the heights of patients in the Happy THR and LLI groups may simply have been due to bias in the results with the THR group having a higher proportion of males. The Happy THR group had 10 males (1.75 metres \pm 0.08) whilst the LLI group had 3 (1.69 metres \pm 0.06). The Happy THR also had 4 females (1.59 metres \pm 0.05) with the LLI group having 10 (1.58 metres \pm 0.04). Results for height may also reflect that individuals who are taller are able to accommodate small changes in leg length during gait using their greater height. This could be through methods such as greater pelvic rotation and knee flexion, which are commonly used compensatory mechanisms of individuals with a LLI [222].

4.6 Conclusion

Disadvantages in comparing radiographic anthropometric results to one another include the potential errors in measurement techniques together with the masking of true measurements caused by diseases such as osteoarthritis. Nevertheless, this study is the first to measure the anthropometric properties and demographics of symptomatic LLI patients following THR and compare them to asymptomatic THR patients. Results showed that femoral offset, so often linked to changes in leg length following surgery, did not significantly differ between the groups. It was however suggested that this was potentially due to the LLI patients having implants used which were larger than required and thus causing patients to become symptomatic. No statistical significance was detected for the inter-hip distance, cup inclination angle, magnitude of leg length where the operated side had been lengthened, age, and BMI. Height was found to differ between the groups which may have been linked to their being more males in the Happy THR group or that taller individuals were more likely to tolerate changes in leg length.

5 Kinematics & Temporal-Spatial Parameters

5.1 Aims & Objectives

The aim of this study was to understand the differences in kinematic variables and temporal-spatial parameters between symptomatic LLI patients and asymptomatic individuals following a THR, which for this study were labelled as Happy THR patients. Comparisons were also to be made against a Normal group in order to study how operated patients differ to their healthy counterparts. Variables studied included the differences when looking at joint angles from the perspective of the whole gait cycle, when standing and at particular gait events. The purpose of this analysis was to understand the changes in gait biomechanics which occur with LLI and to postulate how they may effect clinical outcomes.

5.2 Methodology

5.2.1 Initial Clinical Method

By LMBRU (Leeds Musculoskeletal Biomedical Research Unit) Staff

A description of the patient cohort used together with the recruitment method is described in the *Anthropometrics & Demographics* chapter on page 90. Each patient underwent clinical gait analysis in a gait laboratory (Chapel Allerton Hospital, Leeds, UK) using an eight-camera Vicon MX motion analysis system (Oxford Metrics, Oxford, England) with the PiG marker set used⁷. Cameras captured at a rate of 150 Hz with a 2 megapixel resolution. A working volume of 10 x 11 x 2.5 m was computed as giving less than 0.2 mm in camera error during the calibration of the laboratory. A L-shaped frame with markers attached was placed in the centre of the capture volume, with the frame being visible to all the cameras. A T-shaped calibration wand which has markers attached was then waved so that all positions in the desired volume were captured by the camera. Calibration is only valid for the camera configuration it was undertaken for. For this reason, every patient had the data capture area calibrated before gait analysis. Two Bertec force plates (Bertec Corp, Worthington, OH) were used with each capturing force data at 1000 Hz.

Markers were placed on the lateral sides of the thigh, knee, shank and ankle together with markers on the foot and the pelvis. Altogether, four markers defined the pelvis segment, two markers defined the thigh segment, two the shank segment and two the foot. Leg lengths were measured using a block placed under the shorter limb which levelled the pelvis and hence allowed

⁷See Figure 26 on page 69 in the *Generic Methods*

measurement of length between the anterior superior iliac spine and the medial ankle for both limbs via a tape measure. Knee and ankle width were measured using a caliper with an error of ± 1 mm.

A standing trial was followed subsequently by at least 2 walking trials along a 5 metre walkway. The laboratory was setup such that the patients walked in the direction of the y-axis, whilst the z-axis was defined as being the vertical and the x-axis the medial-lateral axis. In the Vicon motion analysis system, markers were labelled for each trial, filtering of data occurred and the size of the trials was trimmed by removing frame numbers at the beginning or at the end of the trial. Data was provided in a C3D file format which contained marker positions with respect to time together with GRF and force platform data.

5.2.2 Non-Clinical Method

(By Author)

The initial 26 Symptomatic LLI patients recruited for clinical gait analysis were screened for secondary conditions which led to the subsequent removal of patients with additional underlying pathologies. This information was provided through medical notes taken during clinical analysis and included patients with conditions such as having a TKR in addition to a THR. In total, 8 patients were removed from the Symptomatic LLI group using this method. An additional 5 patients were removed due to reasons including being asymptomatic, having poor contact with the force plate and having some data files either missing or being duplicates of other patients.

A further 3 patients were removed from the Happy THR and Normal groups respectively from the original cohort due to data quality issues. These ranged from the data files for gait being too small which prevented data for consecutive heel strikes from being extracted, marker dropouts and marker mislabelling which could potentially lead to non-representative joint motion curves being produced. In total, 13 patients in the Symptomatic LLI group, 11 patients in the Happy THR group and 35 Normal healthy people had their gait analysed for this study.

All motion and standing trials for the condensed groups were then imported into Visual3D where a body model was built as defined on pages 77- 85 in the *Generic Methods*. The model assumed that each segment had 6DoF and that there were no explicit joint definitions with the Davis HJC regression equation used to define the position of the HJC in the pelvic reference frame. Markers in the PiG model were used both for defining segment endpoints/axes orientations together with

tracking motion. Results were produced by measuring the angle of one segment (motion segment) with respect to another (reference segment). This is further detailed in Table 3. Joint motions were computed using a cardan angle sequence of xyz where x was flexion-extension, y abduction-adduction and z rotation. Flexion, abduction and internal rotation were defined as being positive whilst extension, adduction and external rotation were defined as being negative.

Table 3: Table showing segment motions in 6DOF Visual3D model. X measured anterior (flexion)-posterior (extension) motion, Y medial (adduction)-lateral (abduction) motion and Z rotation

Motion Segment	Reference Segment	Motion Type	Axis
Operated Side Pelvis	Laboratory	Obliquity	Y
Operated Side Pelvis	Laboratory	Rotation	Z
Right Thigh	Pelvis	Right Hip Flexion-Extension	X
Left Thigh	Pelvis	Left Hip Flexion-Extension	X
Right Thigh	Pelvis	Right Hip Abduction-Adduction	Y
Left Thigh	Pelvis	Left Hip Abduction-Adduction	Y
Right Shank	Right Thigh	Right Knee Flexion-Extension	X
Left Shank	Left Thigh	Left Knee Flexion-Extension	X
Right Foot	Right Shank	Right Ankle Dorsi-Plantar Flexion	X
Left Foot	Left Shank	Left Ankle Dorsi-Plantar Flexion	X

A review by Gurney [222] demonstrated that LLI patients compensate in certain planes of motion at particular joints including showing changes in pelvic obliquity and rotation, hip flexion-extension and abduction-adduction, knee flexion-extension together with ankle dorsi-plantar flexion. For this reason, only these planes of motion were analysed in order to produce a more focused analysis.

Gait Events

A comparison was made across the groups in terms of three gait events; initial heel strike, mid-stance and toe off. These gait events were defined prior to analysis via the use of the force vector on the force plate. The frame number of the gait cycle data which corresponded with the first occurrence of the force vector was defined as initial heel strike whereas the frame number which corresponded with the final occurrence of the force vector was defined as toe off. Mid-stance was defined to exist exactly half-way between heel strike and toe off. Figure 59 shows the points in the gait cycle which were selected as heel strike and toe off. All joint angle data was extracted from Visual3D after restricting gait cycle kinematics between heel strike and toe off, thus allowing identification of values which correspond to each of the gait events.

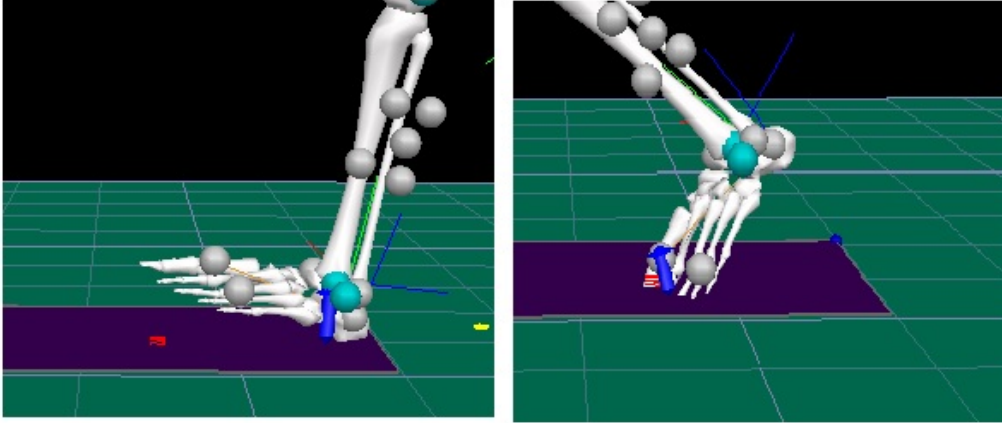


Figure 59: The image on the left shows the identification of heel strike on the force plate with the initial force vector produced. The image on the right shows the identification of toe off with the terminal force vector produced.

Gait Cycle Comparison

Results were compared for all 6 of the previously mentioned joint motions and temporal- spatial parameters (velocity, stride length, stance time, swing time, cycle time) between consecutive heel strikes of the same foot. This was from heel strike onto the force plate to heel strike off the force plate. All results were normalised to 100 percentiles. Comparisons were made across the groups in terms of maximum angles, minimum angles and RoMs. Normalised raw results were also represented graphically and were further analysed using tables. With regards to the tables, these depicted the average results for the raw graph results e.g. for every LLI patient, the peak hip flexion angle is selected and an average value is produced using all the values for the whole group. This was undertaken on the raw results as the peak values may occur at different points in the gait cycle.

Symmetry Index

A symmetry index, produced by Robinson et al. [437] and defined in Equation 51, was then used to determine the level of asymmetry between the two limbs of each patient in terms of temporal-spatial-parameters. This technique was chosen as it allows a reference to be made against the average result. X_L and X_R represented the parameter being studied on the left and right legs respectively. A perfect symmetry would give a value of 0%.

$$SI = \frac{X_L - X_R}{(X_L + X_R)^{\frac{1}{2}}} \times 100\% \quad (51)$$

Standing Angles

Standing joint angles were measured during the initial calibration standing trials. The standing trial was limited to the first 10 frames in order to minimise motion artefact. A single standing angle value was extracted from the analysis which was the average value for that particular motion being studied in the first 10 frames. This was undertaken for the pelvis, hip, knee and ankle.

5.3 Results - Dynamic Joint & Segment Angles

5.3.1 Pelvic Obliquity

Pelvic obliquity has previously been defined in Figure 56 on page 101 in the *Anthropometrics and Demographics* chapter. Figure 60 illustrates the average pelvic obliquity, or superior-inferior tilt, for all three groups whilst Figure 61 shows the raw results. As the pelvis is treated as a single segment in Visual3D by having a single coordinate system lying half-way between the ASIS markers, there is only a single curve for each group instead of a curve for the left and right limbs. The peak superior pelvic obliquity for the Happy THR and the Symptomatic LLI group were 70% and 134% less respectively than a Normal healthy person.

Statistically significant differences were found between all groups in terms of gait cycle maximum angle ($p < 0.01$) and minimum angle ($p < 0.02$) when using the raw results. This is further demonstrated in Table 4. Differences existed between the LLI and Happy THR patients to that of the Normal cohort for the maximum angle and between the Symptomatic LLI and Normal groups in terms of the minimum angle, as demonstrated with a post-hoc Tukey test.

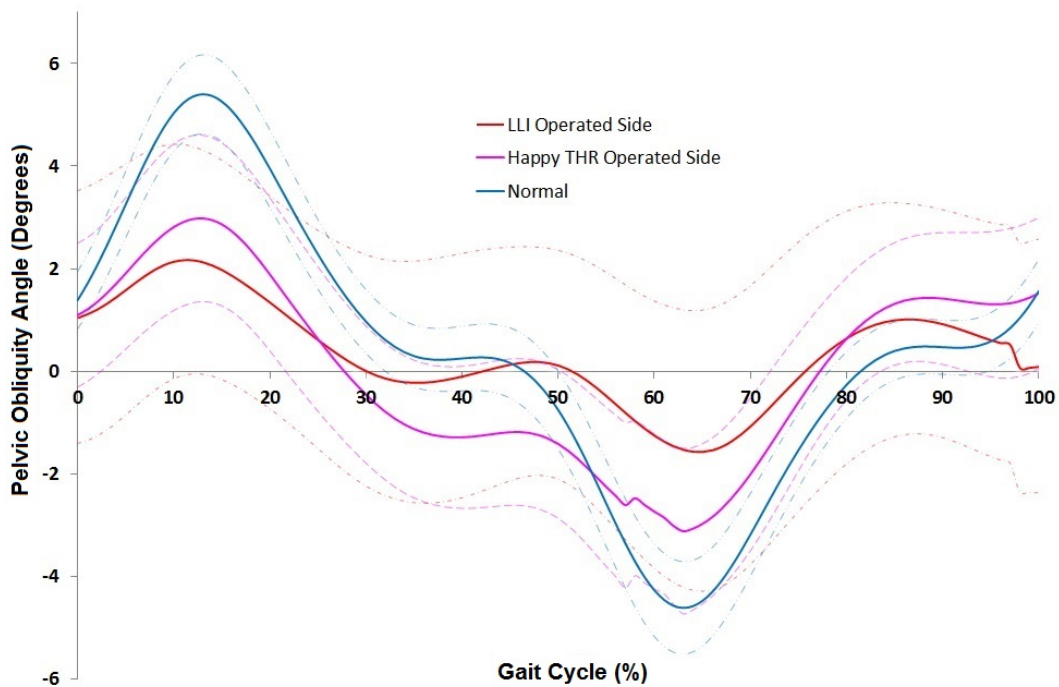


Figure 60: Average pelvic operated side superior obliquity (+) & inferior obliquity (-) angles together with 95% confidence intervals over a normalised gait cycle between consecutive heel strikes of the same foot. The dashed lines represent the associated confidence intervals for each sample.

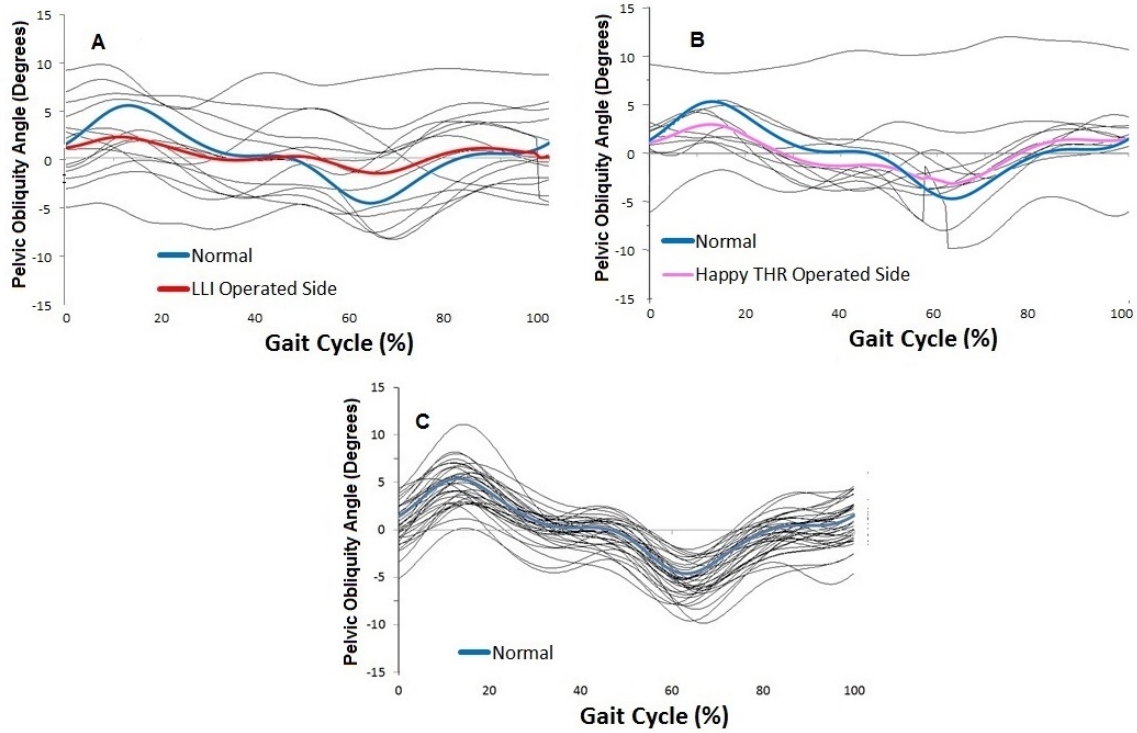


Figure 61: Raw pelvic operated side superior(+) and inferior(-) obliquity angle results for all three groups over a normalised gait cycle between consecutive heel strikes of the same foot. (A) Operated side LLI patients (B) Operated side Happy THR patients (C) Normal Healthy Patients. The blue curve in each graph is the same and represents the average pelvic obliquity for the Normal group

Table 4: Maximum angle, minimum angle and RoM in terms of averaged results for the raw pelvic operated side superior(+) and inferior obliquity(-) for all patients in each group. * and † represent statistical significance. Comparisons are made in columns. All values are in degrees.

	Maximum	Minimum	RoM
Normal	5.08 *†	-4.30 *	9.38
Symptomatic LLI Operated Side	2.17 †	-1.55 *	3.72
Happy THR Operated Side	2.98 *	-3.12	6.10

5.3.2 Pelvic Rotation

The schematic in Figure 62 demonstrates how pelvic rotation during this study was computed.

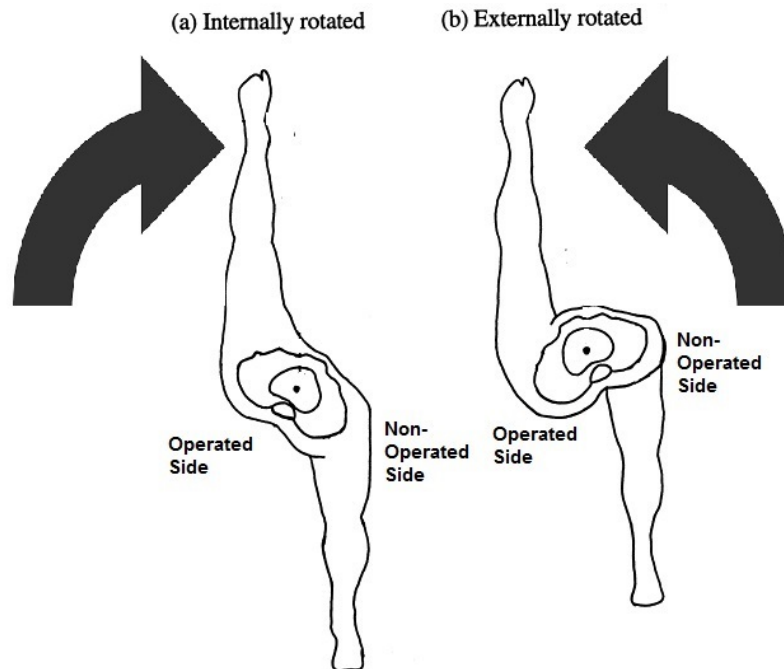


Figure 62: Schematic demonstrating the physical characteristics of pelvic internal-external rotation. Positive internal rotation (a) was taken to be the anterior rotation of the operated sided pelvis whilst external rotation (b) was posterior rotation of the operated sided pelvis [438].

Results for pelvic rotation showed that the Symptomatic LLI group and Happy THR group demonstrated a similar shaped curve to that of the Normal cohort despite both having a reduced rotation angle. All curves had wide confidence intervals demonstrating the large variability within each group. These results are illustrated in Figure 63. Raw results are illustrated in Figure 64. The decrease in RoM is further quantified in Table 5 with the maximum of the Symptomatic LLI group showing a 50% reduction in pelvic rotation relative to the Normal cohort. Significant differences were found between the groups in terms of maximum angle ($p < 0.03$) and minimum angle ($p < 0.03$). A post-hoc Tukey test revealed that these differences existed between the Normal and Symptomatic LLI patient groups. An outlier existed in the Symptomatic LLI group with one particular patient demonstrating increased internal pelvic rotation

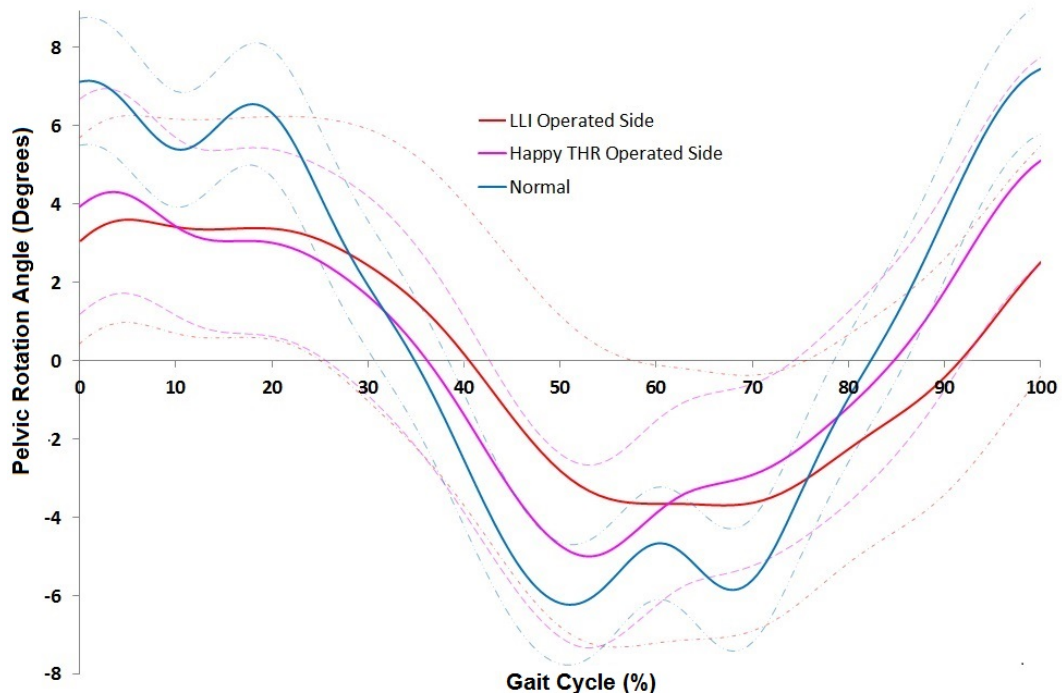


Figure 63: Average pelvis operated side anterior rotation (+) & posterior rotation (-) angles together with 95% confidence intervals over a normalised gait cycle between consecutive heel strikes of the same foot. The dashed lines represent the associated confidence intervals for each sample.

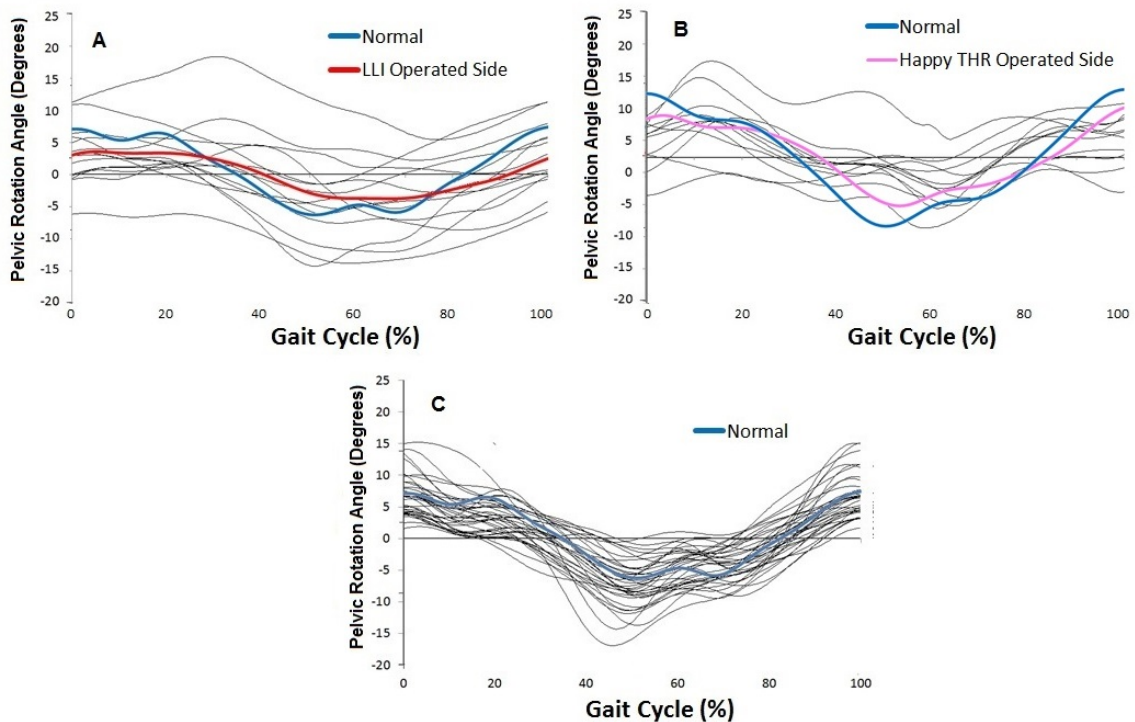


Figure 64: Raw operated side anterior rotation (+) & posterior rotation (-) angle results for all three groups over a normalised gait cycle between consecutive heel strikes of the same foot. (A) Operated side LLI patients (B) Operated side Happy THR patients (C) Normal healthy patients. The blue curve in each graph is the same and represents the average pelvic rotation for the Normal group

Table 5: Maximum angle, minimum angle and RoM in terms of averaged results for the raw pelvic operated side internal(+) and external(-) rotation for all patients in each group. * represents statistical significance for Maximum and Minimum Values. Comparisons are made in columns. All values are in degrees.

	Maximum	Minimum	RoM
Normal	7.46 *	-6.23 *	13.7
Symptomatic LLI Operated Side	3.62 *	-3.7 *	7.72
Happy THR Operated Side	6.10	-3.80	9.89

5.3.3 Hip Flexion-Extension

The schematic in Figure 65 demonstrates how hip flexion-extension was measured during this study.

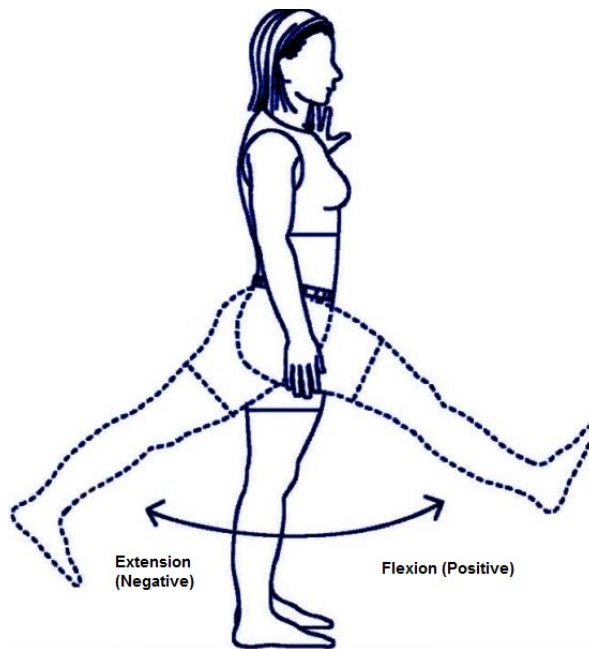


Figure 65: Schematic demonstrating the physical characteristics of hip flexion-extension. Anterior movement of the thigh relative to the pelvis was referred to as hip flexion whilst posterior movement of the thigh relative to the pelvis was referred to as hip extension.

[439].

Results from Figure 66 show that all groups had similar amounts of peak hip flexion angle at initial and terminal heel strikes. However, the amount of hip motion between mid-stance and the end of stance phase differed between the groups with the LLI patients showing reduced extension on the operated side. The Normal group extended their hip to around 10° which was greater than the non-operated side of the Happy THR group (5°) and the non-operated side of the LLI group (4°).

Raw data results can be seen in Figure 67. Table 6 shows that relative to operated side of the Symptomatic LLI patients, the Normal healthy patients had 44% greater hip flexion-extension

RoM, 2% smaller maximum flexion angle and a 280% greater maximum extension angle. Results were more similar between Normal and Happy THR patients. The LLI group had the smallest RoM. No statistically significant differences were found between any of the operated/non-operated limbs together with the Normal cohort for the maximum flexion angle ($p > 0.05$). A statistically significant difference was however found with regards to the minimum angle, or the maximum extension angle, with $p < 0.01$. This difference was shown to exist between the operated side of the LLI group relative to all others.

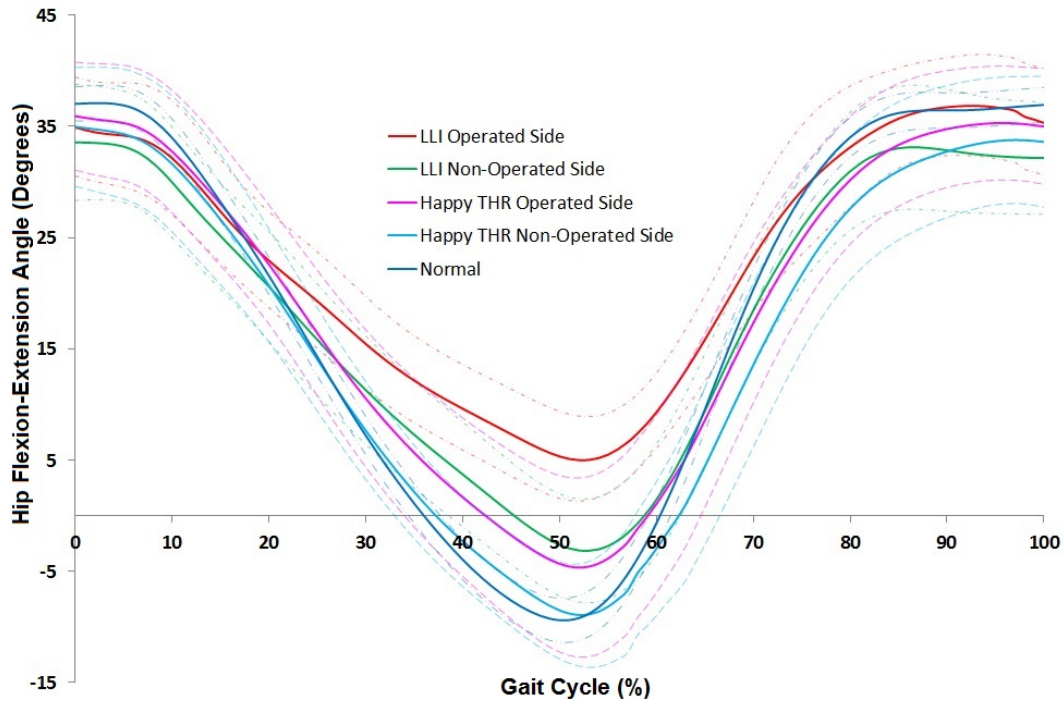


Figure 66: Average hip flexion (+) extension (-) angles together with 95% confidence intervals over a normalised gait cycle between consecutive heel strikes of the same foot. The dashed lines represent the associated confidence intervals for each sample.

Table 6: Maximum angle, minimum angle and RoM in terms of averaged results for the raw hip flexion (+)-extension (-) angle compared between hips for all patients in each group. *, †, ▷ and ◊ represent statistical significance for Maximum and Minimum Values. Comparisons are made in columns. All values are in degrees.

	Maximum	Minimum	RoM
Normal	36.1 [◊]	-9.29 [*]	45.4
Symptomatic LLI Operated Side	36.9	5.13 ^{*†▷◊}	31.6
Symptomatic LLI Non-Operated Side	33.6	-3.16 [†]	36.0
Happy THR Operated Side	35.9	-4.67 [▷]	40.6
Happy THR Non-Operated Side	35.0	-8.94 [◊]	43.9

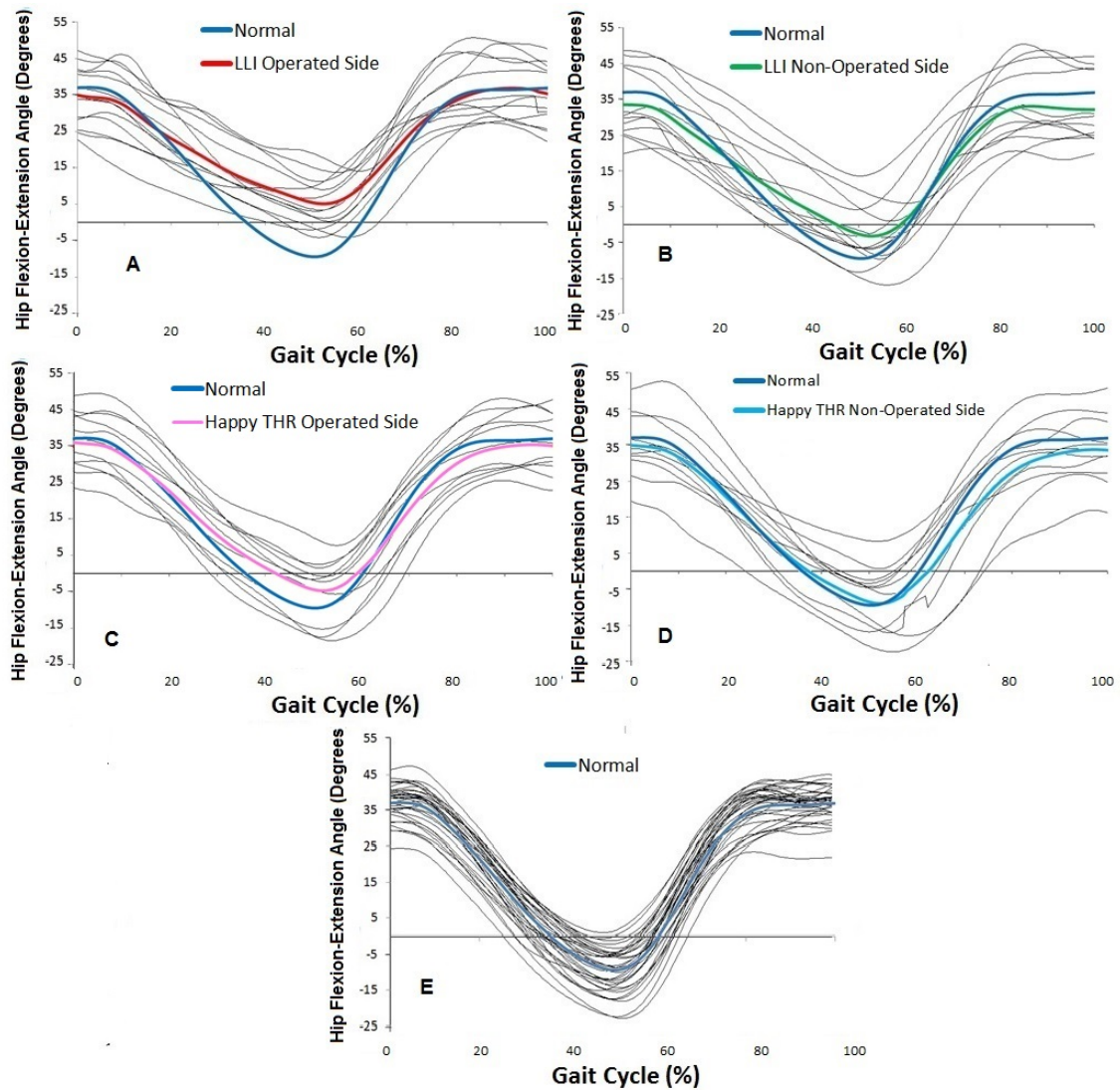


Figure 67: Raw hip flexion (+)-extension (-) angle results for all three groups over a normalised gait cycle between consecutive heel strikes of the same foot. (A) Operated side LLI patients (B) Non-operated side LLI patients, (C) Operated side Happy THR patients (D) Non-operated side Happy THR patients (E) Normal healthy patients. The blue curve in each graph is the same and represents the average hip flexion-extension for the Normal group

5.3.4 Hip Abduction-Adduction

The schematic in Figure 68 demonstrates how hip abduction-adduction was measured during this study.

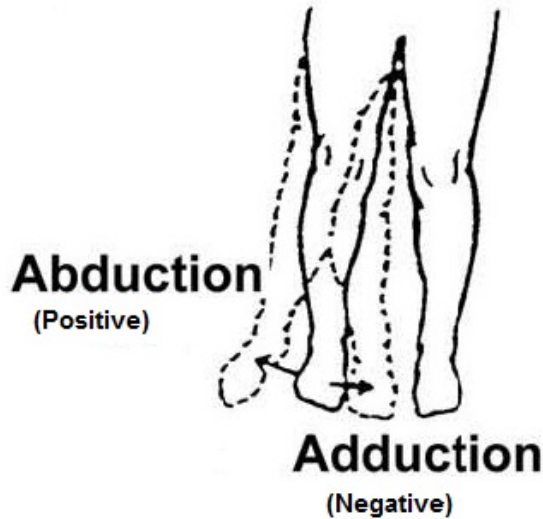


Figure 68: Schematic demonstrating the physical characteristics of hip abduction-adduction. The lateral movement of the thigh with respect to the pelvis away from the mid-line of the body was referred to as hip abduction. The medial movement of the thigh with respect to the pelvis towards the mid-line of the body was referred to as hip adduction.

[440]

Figure 69 demonstrates that differences existed between the groups in terms of hip abduction-adduction. Relative to the Normal group, the Happy THR and Symptomatic LLI group both showed a loss of hip adduction which was particularly prevalent in the latter with a reduction of 50% in peak angle. The operated side of LLI patients showed very little hip adduction, whilst the Happy THR group lost $\approx 4^\circ$ of adduction compared to Normal patients.

Raw results can be seen in Figure 70. Table 7 demonstrates that the LLI patients had the smallest RoM in the abduction-adduction plane. No statistically significant differences were found in terms of peak hip abduction angle ($p > 0.05$). Significant differences were however found with regards to the maximum amount of adduction ($p < 0.01$). A post-hoc Tukey test demonstrated that this significance was between the Normal individuals and both the operated and non-operated sides of the LLI and Happy THR groups.

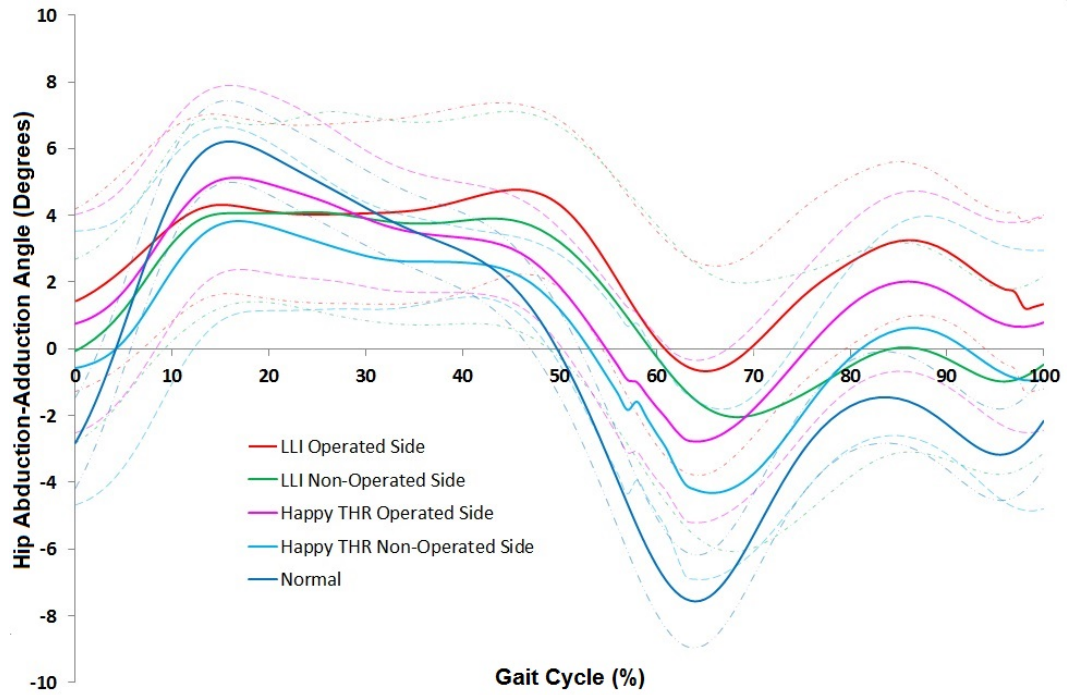


Figure 69: Average hip abduction (+) adduction (-) angles together with 95% confidence intervals over a normalised gait cycle between consecutive heel strikes of the same foot. The dashed lines represent the associated confidence intervals for each sample.

Table 7: Maximum angle, minimum angle and RoM in terms of averaged results for the raw hip abduction (+)-adduction (-) angles compared between hips for all patients in each group. *, †, ▷ and ◊ represent statistical significance for Maximum and Minimum Values. Comparisons are made in columns. All values are in degrees.

	Maximum	Minimum	RoM
Normal	6.20	-7.07 ^{*†▷◊}	13.3
Symptomatic LLI Operated Side	4.78	-0.63 [*]	5.41
Symptomatic LLI Non-Operated Side	4.10	-2.05 [†]	6.14
Happy THR Operated Side	5.13	-2.78 [▷]	7.91
Happy THR Non-Operated Side	3.83	-4.32 [◊]	8.15

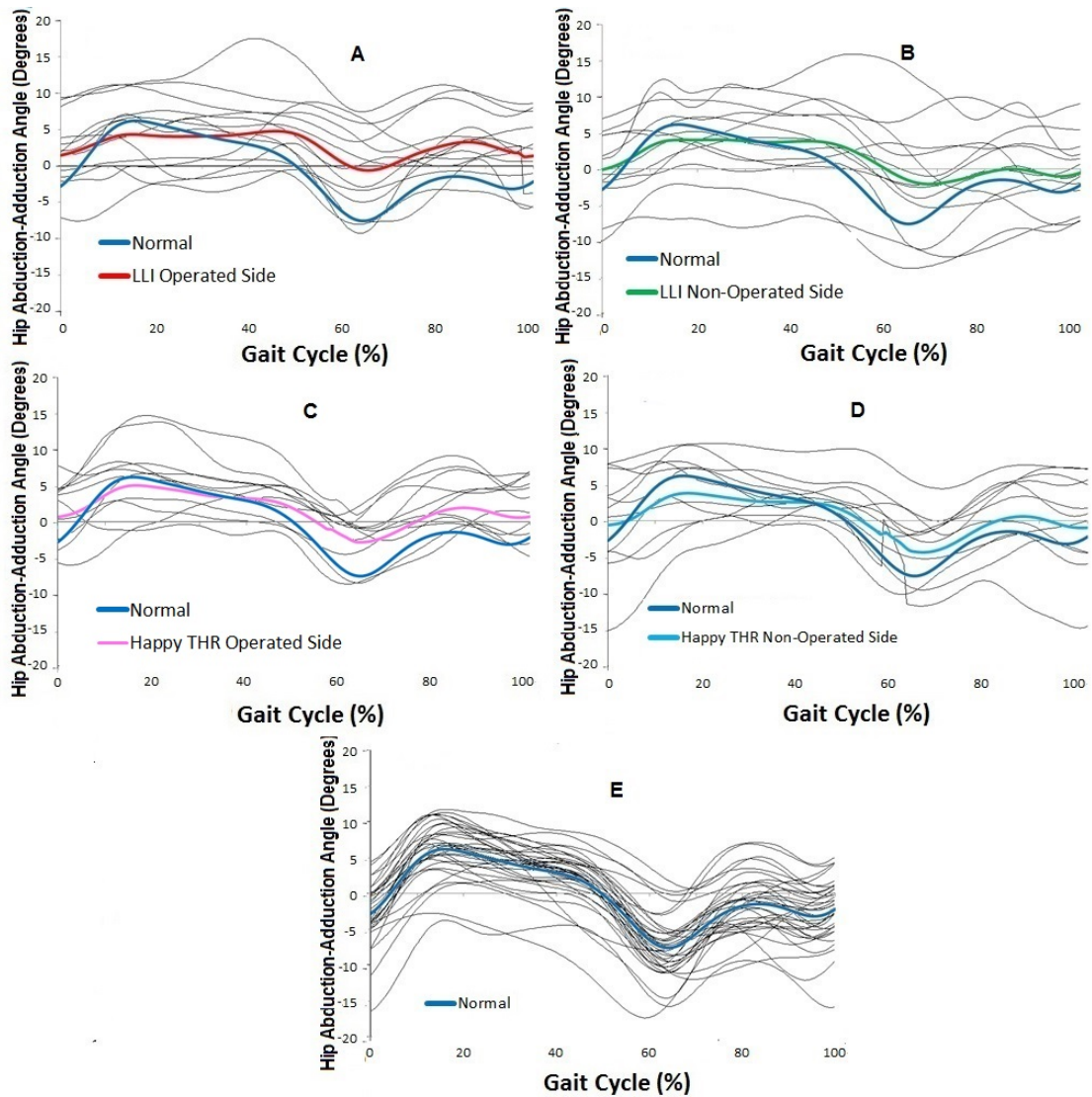


Figure 70: Raw hip abduction (+)-adduction (-) angle results for all three groups over a normalised gait cycle between consecutive heel strikes of the same foot. (A) Operated side LLI patients (B) Non-operated side LLI patients, (C) Operated side Happy THR patients (D) Non-operated side Happy THR patients (E) Normal healthy patients. The blue curve in each graph is the same and represents the average hip abduction-adduction for the Normal group

5.3.5 Knee Flexion-Extension

The schematic in Figure 71 demonstrates how knee flexion-extension was measured during this study.

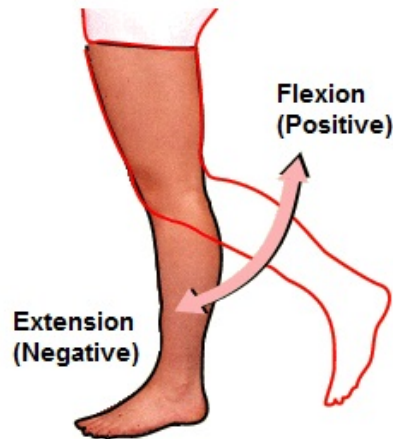


Figure 71: Schematic demonstrating the physical characteristics of knee flexion-extension. The posterior movement of the shank relative to the thigh is referred to as flexion and the anterior movement of the shank relative to the thigh is referred to as extension.

[441].

Average knee flexion-extension is compared between the groups in Figure 72. The Happy THR group shared a common curve shape to that of the Normal cohort with the only significant difference appearing during the swing phase with there being 5° - 10° reduction in peak flexion. Both knees of the LLI patient showed reduced flexion in the stance and swing phases of gait, with there being on average a 16% drop on the operated and 22% drop on the non-operated sides relative to the Normal group. Both knees of the LLI patients on average flexed to a smaller angle than that of Happy THR patients. Confidence intervals remained narrow for all groups showing that there was little variability between patients within each group.

Raw results can be seen in Figure 73. Table 8 quantifies the raw results and also complements the results of Figures 73 by showing that Happy THR patients had a knee flexion-extension range of motion which was approximately 3° - 5° less than that of Normal individuals on both the operated and non-operated sides. The LLI patients demonstrated a similar RoM to that of the Happy THR group on the operated side, however, the non-operated side on average had a RoM of $\approx 40^{\circ}$ less than the the Normal group and $\approx 10^{\circ}$ less than the Happy THR group. Statistically significant differences were found in terms of the maximum knee flexion angle ($p < 0.01$) with a Tukey test revealing that the difference existed between the Normal group and the non-operated side of the Symptomatic LLI group. Similarly, a statistically significant difference was found for the minimum

knee flexion angle during gait ($p < 0.04$), which a Tukey test found to exist between the operated and non-operated sides of the Symptomatic LLI group.

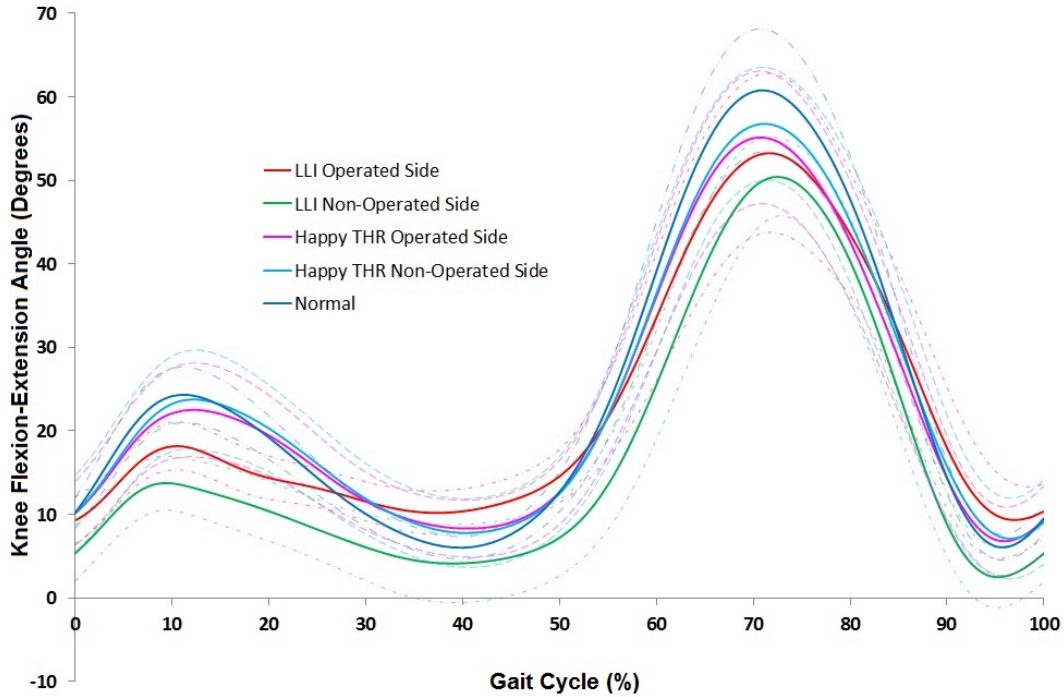


Figure 72: Average knee (+) extension (-) angles together with 95% confidence intervals over a normalised gait cycle between consecutive heel strikes of the same foot, The dashed lines represent the associated confidence intervals for each sample.

Table 8: Maximum angle, minimum angle and RoM in terms of averaged results for the raw knee flexion (+)-extension (-) angles compared between knees for all patients in each group. * and † represent statistical significance for Maximum and Minimum Values. Comparisons are made in columns. All values are in degrees.

	Maximum	Minimum	RoM
Normal	61.6 *	5.23	66.8
Symptomatic LLI Operated Side	53.3	9.31 †	62.6
Symptomatic LLI Non-Operated Side	50.4 *	2.49 †	52.9
Happy THR Operated Side	55.1	6.78	61.9
Happy THR Non-Operated Side	56.8	7.14	63.9

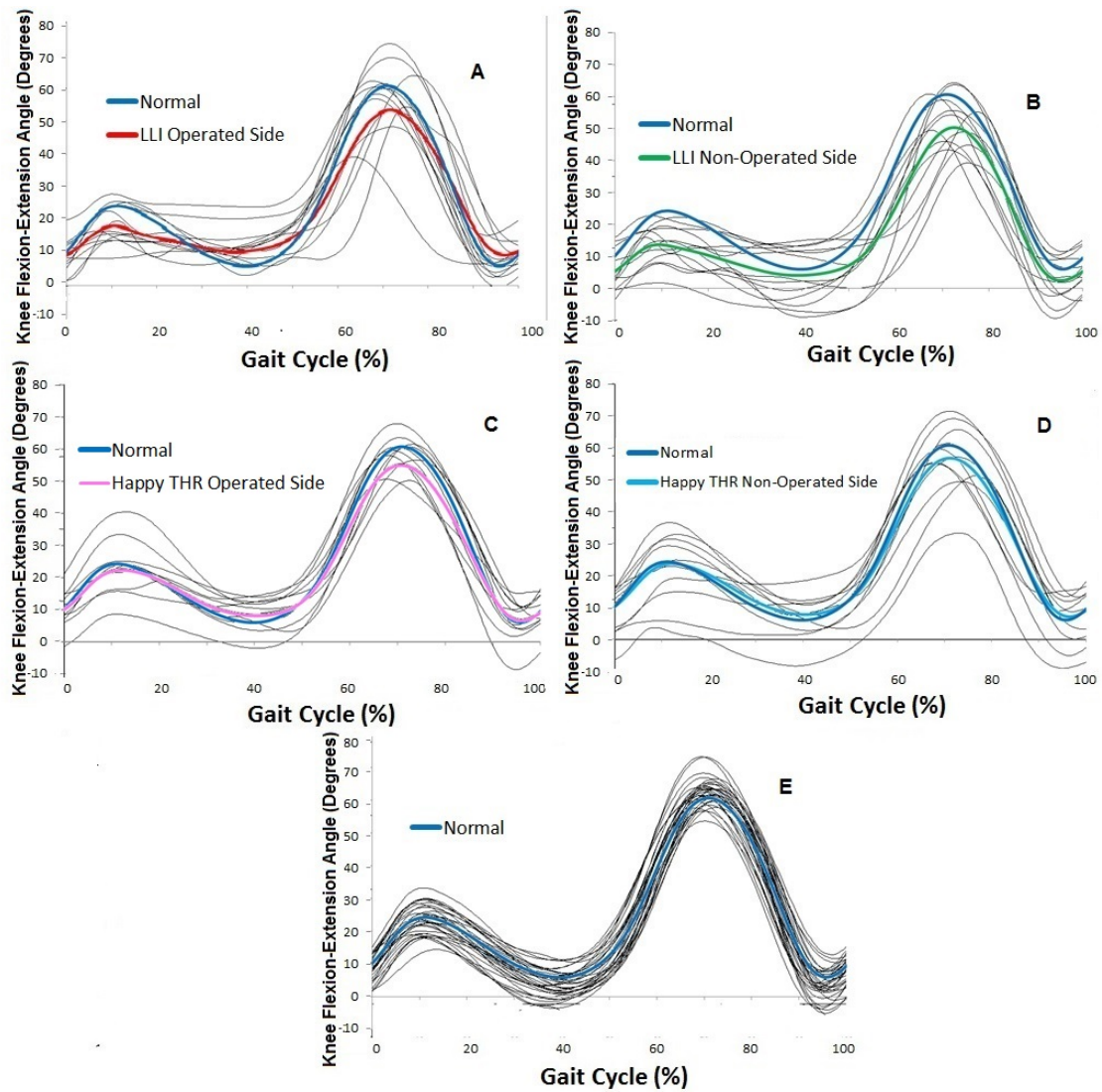


Figure 73: Raw knee flexion (+)-extension (-) angle results for all three groups over a normalised gait cycle between consecutive heel strikes of the same foot. (A) Operated side LLI patients (B) Non-operated side LLI patients, (C) Operated side Happy THR patients (D) Non-operated side Happy THR patients (E) Normal healthy patients. The blue curve in each graph is the same and represents the average knee flexion-extension for the Normal group

5.3.6 Ankle Dorsi-Plantar Flexion

The schematic in Figure 74 demonstrates how ankle dorsi-plantar flexion was measured during this study.

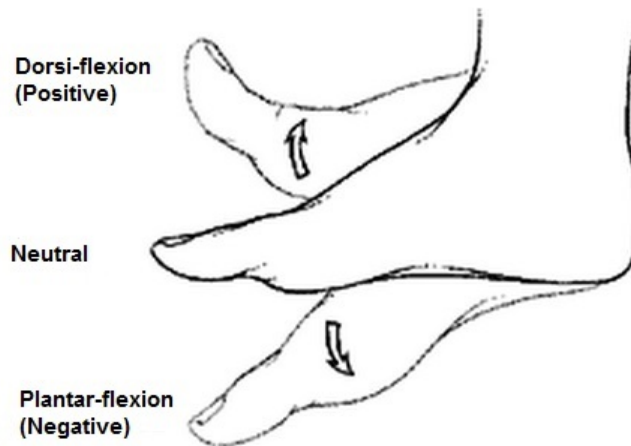


Figure 74: Schematic demonstrating the physical characteristics of ankle dorsi-plantar flexion. The pointing of the toes upwards towards the shank is classed as dorsiflexion and the pointing downwards away from the shank is referred to as plantarflexion

[442].

Figure 75 refers to the averaged results for each group in terms of ankle dorsi-plantar flexion during gait. A high degree of symmetry was shown by the Happy THR group whilst there were large differences between the operated and non-operated sides for the Symptomatic LLI group. Wide confidence intervals existed for all groups indicating a degree of uncertainty in the results. Both operated groups however maintained the same general shape as for the Normal patients.

Table 9 analyses numerically the results of the raw results in Figure 76. The average RoM of both limbs for the Happy THR group demonstrated a high degree of symmetry. This was not however the case for the LLI group where the RoM in the shorter leg was reduced by 4° . In addition, both the Symptomatic LLI and Happy THR groups demonstrated a loss of peak ankle plantar-flexion relative to the Normal cohort. The ankle of the operated sided leg in the LLI group and both ankles of the Happy THR group on average also showed greater dorsiflexion than the average Normal healthy patient, with the LLI patients showing a 29% increase. Statistically significant results were found in terms of peak dorsiflexion angle with $p < 0.01$. A Tukey test found that these differences existed between the non-operated side of the Symptomatic LLI group and all other groups. Similarly, a statistically significant difference was found with regards to the peak

plantarflexion angle of $p < 0.03$. Using the Tukey test it was found that these differences existed between the Normal cohort of patients and the operated side of the Symptomatic LLI group.

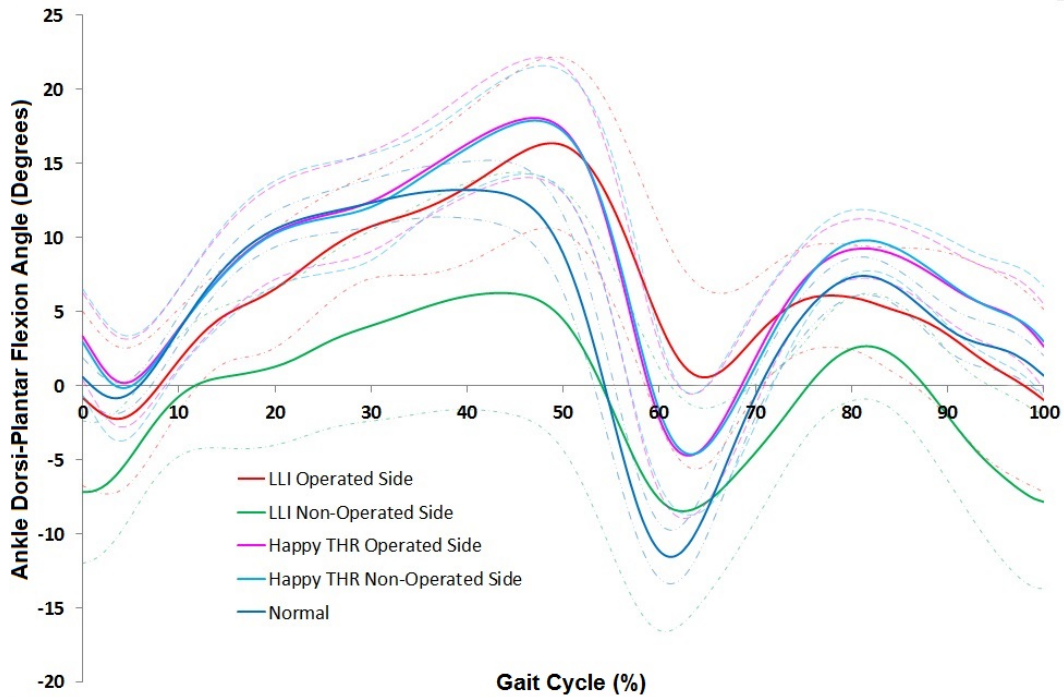


Figure 75: Average ankle dorsiflexion (+) plantarflexion (-) angles together with 95% confidence intervals over a normalised gait cycle between consecutive heel strikes of the same foot. The dashed lines represent the associated confidence intervals for each sample.

Table 9: Maximum angle, minimum angle and RoM in terms of averaged results for the raw ankle dorsi(+)-plantar(-) flexion angles compared between ankles for all patients in each group. *, †, ▷ and ◊ represent statistical significance for Maximum and Minimum Values. All values are in degrees.

	Maximum	Minimum	RoM
Normal	12.7*	-10.7*	23.4
Symptomatic LLI Operated Side	16.4†	-2.25*	18.7
Symptomatic LLI Non-Operated Side	6.25,*†▷◊	-8.46	14.7
Happy THR Operated Side	18.1▷	-4.72	22.8
Happy THR Non-Operated Side	17.9◊	-4.62	22.5

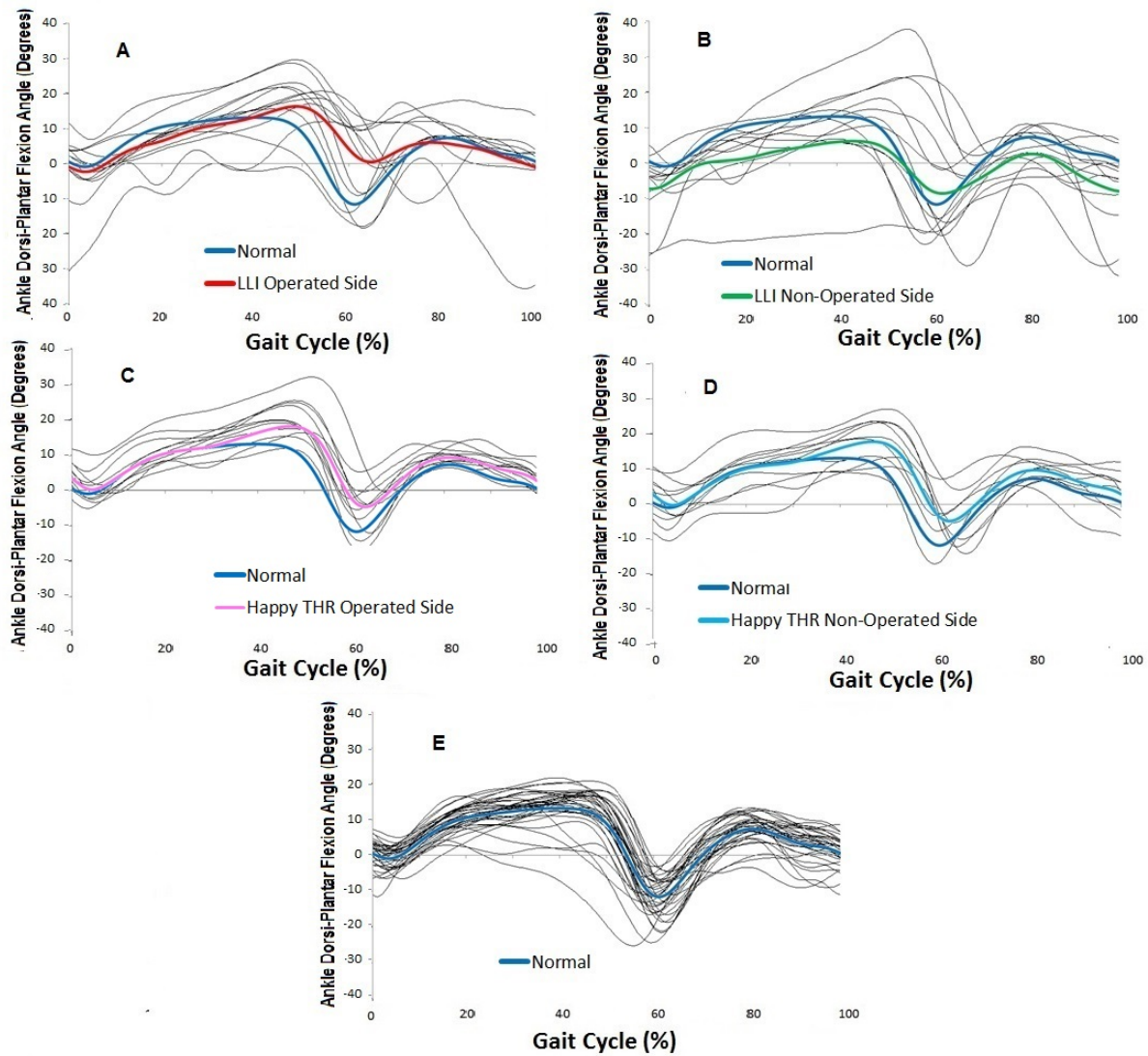


Figure 76: Raw ankle dorsi (+)-plantar (-) flexion angle results for all three groups over a normalised gait cycle between consecutive heel strikes of the same foot. (A) Operated side LLI patients (B) Non-operated side LLI patients, (C) Operated side Happy THR patients (D) Non-operated side Happy THR patients (E) Normal healthy patients. The blue curve in each graph is the same and represents the average ankle dorsi-plantar flexion for the Normal group

5.4 Results - Gait Events

5.4.1 Heel Strike

Figure 77 illustrates the average joint angle results for the specified motions at heel strike. No statistically significant differences were found in terms of hip flexion-extension ($p>0.05$), hip abduction-adduction ($p>0.05$), knee flexion-extension ($p>0.05$), pelvic superior-inferior obliquity ($p>0.05$) and pelvic internal external rotation ($p>0.05$). A statistically significant difference was however found in terms of ankle dorsi-plantar flexion angle ($p<0.01$). A Tukey test demonstrated that these differences occurred between the non-operated side of the LLI group and all other groups.

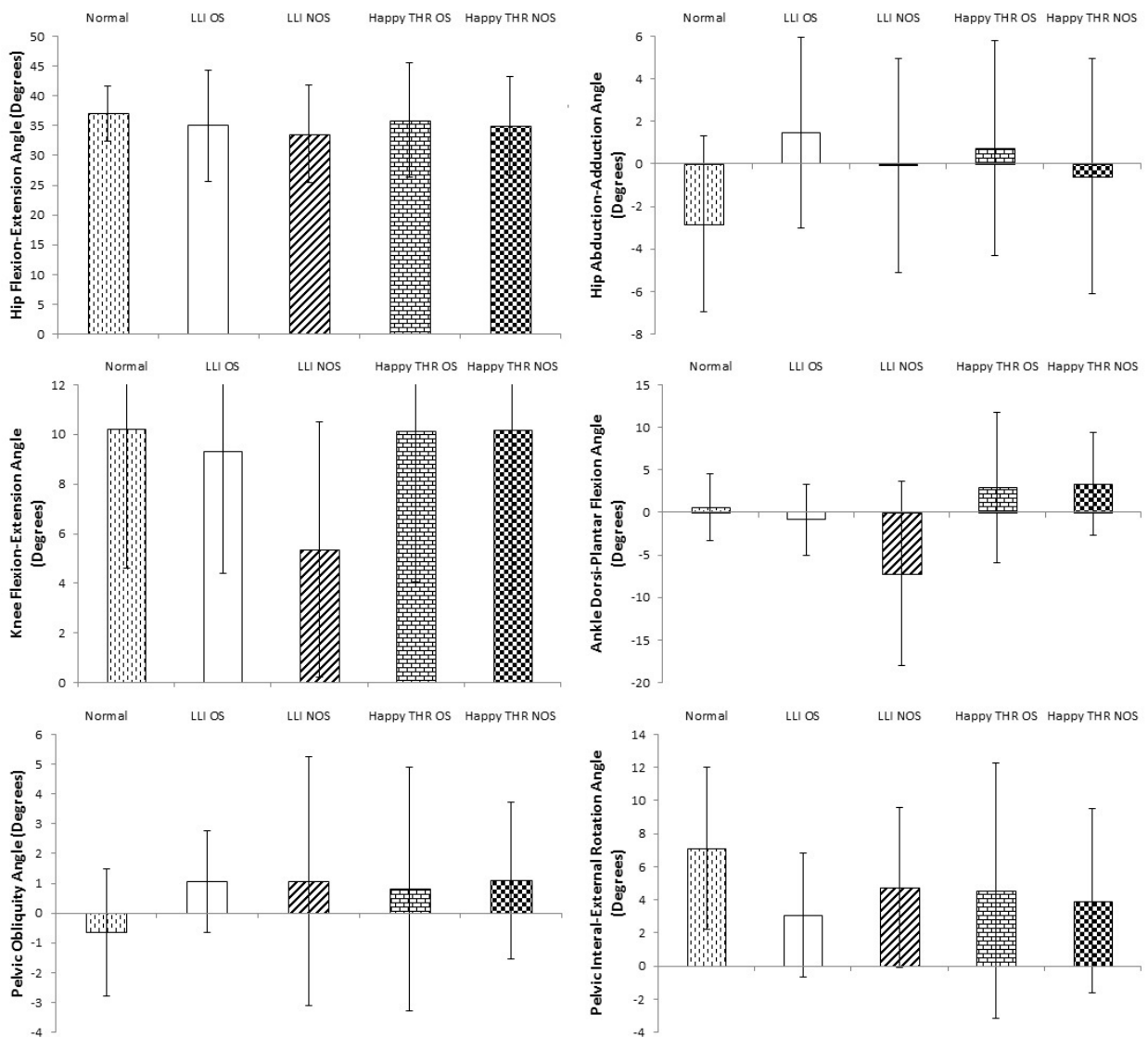


Figure 77: Average heel strike joint angles together with standard errors for the operated (LLI OS) and non-operated (LLI NOS) sides of the Symptomatic LLI group, the operated (Happy THR OS) and non-operated (Happy THR NOS) sides of the Happy THR group together with the results of the Normal patient group

5.4.2 Mid-Stance

Statistically significant results were found to exist at ankle dorsi-plantarflexion ($p < 0.01$) during mid-stance with a Tukey post-hoc test demonstrating that this difference was between the non-operated side of the LLI group to all other groups. Statistical significance was also detected to exist between the non-operated side of the LLI group compared to all other groups in terms of knee flexion angle ($p < 0.02$). Differences in terms of hip flexion-extension ($p > 0.05$), hip abduction-adduction ($p > 0.05$), pelvic superior-inferior obliquity ($p > 0.05$) and pelvic internal-external rotation ($p > 0.05$) were found to not have statistical significance. Results can be seen in Figure 78.

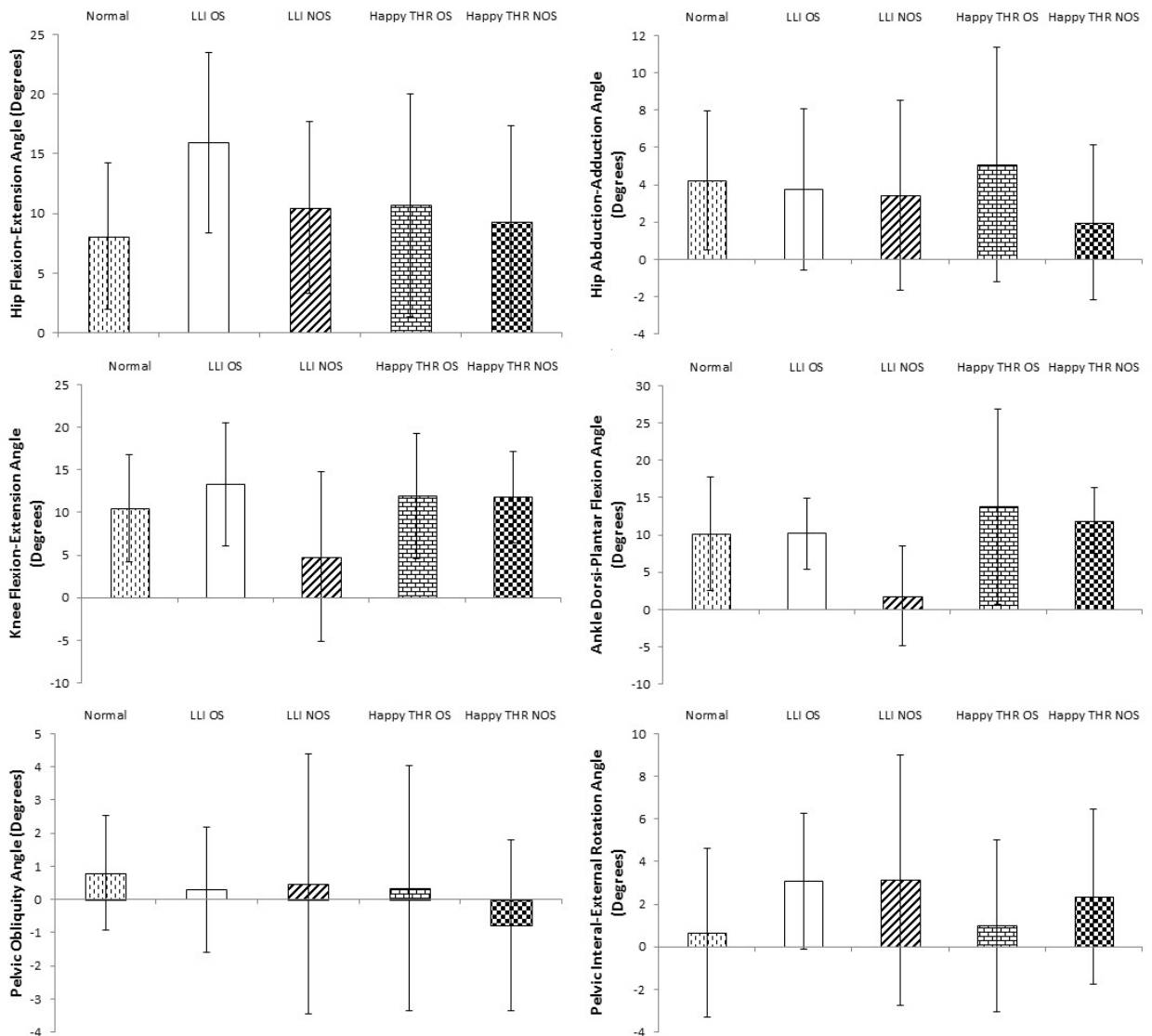


Figure 78: Average mid-stance joint angles together with standard errors for the operated (LLI OS) and non-operated (LLI NOS) sides of the Symptomatic LLI group, the operated (Happy THR OS) and non-operated (Happy THR NOS) sides of the Happy THR group together with the results of the Normal patient group

5.4.3 Toe Off

Toe off results are illustrated in Figure 79. Statistically significant differences were found for hip flexion-extension ($p < 0.01$), abduction-adduction ($p < 0.02$), knee flexion-extension ($p < 0.02$), ankle dorsi-plantar flexion ($p < 0.01$) and pelvic obliquity ($p < 0.01$). For hip flexion-extension differences were between the operated side of the LLI group and all others, for hip abduction-adduction between the Normal patients and the non-operated/operated sides of the LLI group together with the operated side of the Happy THR group and at the knee/ankle between the operated and non-operated sides of the LLI patients. Differences for pelvic obliquity occurred between the Normal group and the LLI/Happy THR groups. No trends could be detected in terms of pelvic rotation ($p > 0.05$).

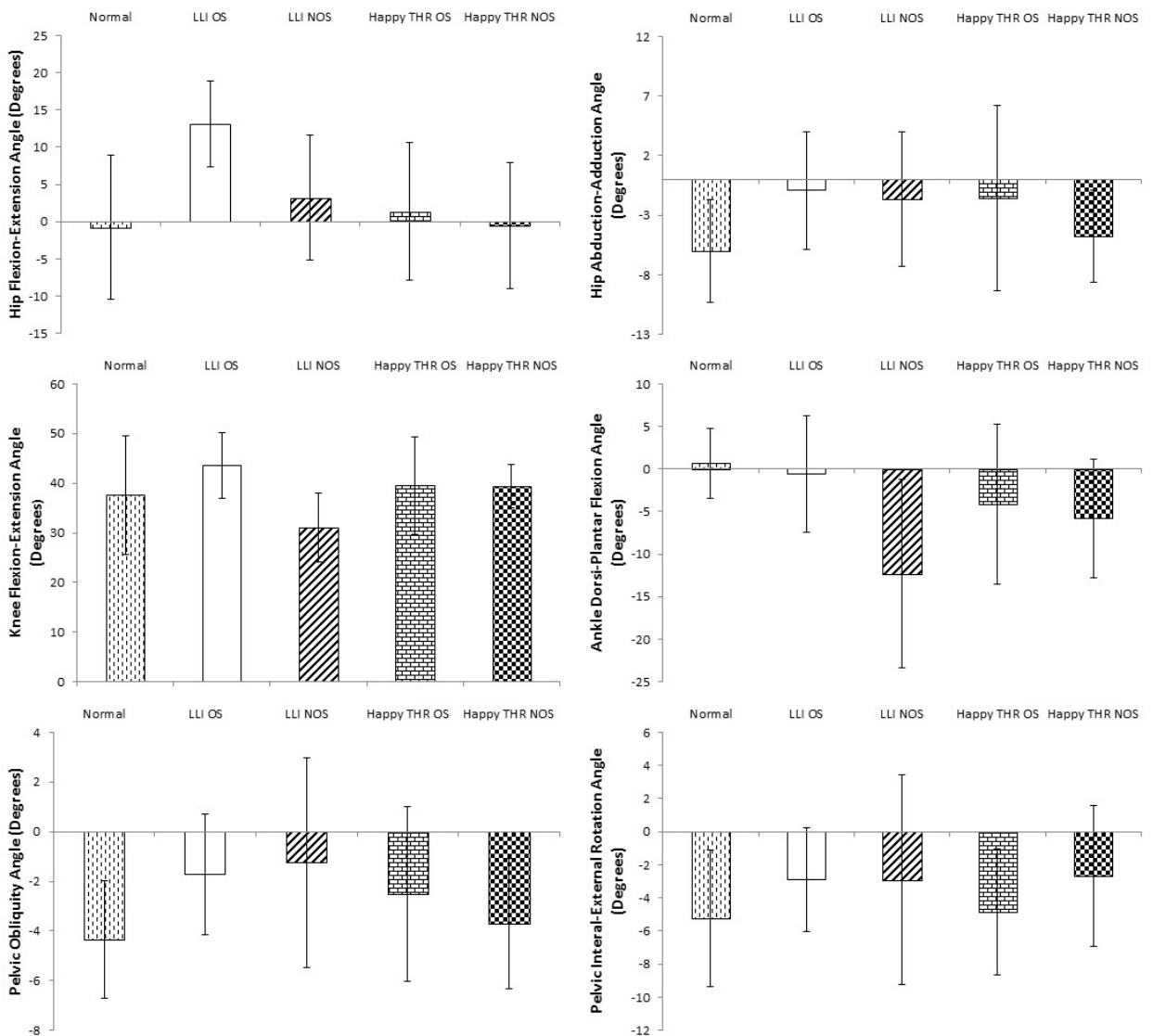


Figure 79: Average toe off joint angles together with standard errors for the operated (LLI OS) and non-operated (LLI NOS) sides of the Symptomatic LLI group, the operated (Happy THR OS) and non-operated (Happy THR NOS) sides of the Happy THR group together with the results of the Normal patient group

5.5 Results - Standing Joint Angles

Figure 80 demonstrates standing joint angle results. The average standing hip flexion angle of 14.8° for the operated side of the Symptomatic LLI group was double that of an average Normal individual (7.82°). Hip flexion angle differences were statistically significant between the groups using the ANOVA ($p < 0.03$). A Tukey test found the difference to exist between the operated side of the LLI group and to every limb in all other groups. With regards to hip abduction-adduction and pelvic rotation, comparisons between groups were not statistically significant ($p > 0.05$). Pelvic obliquity was found to be significant ($p < 0.01$), however, with a difference of just under 2° between the groups this was not considered meaningful.

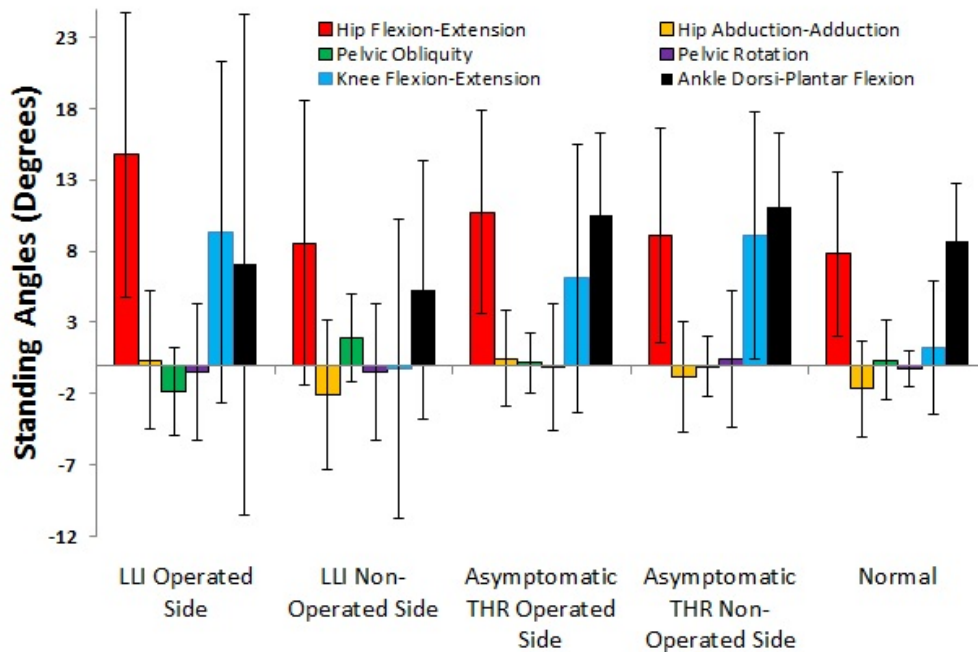


Figure 80: Standing joint angles together with standard errors

Standing knee flexion-extension was also found using a Tukey post-hoc test to be significantly greater (9.3°) on the operated side of Symptomatic LLI patients compared to the non-operated side (-0.26°) and Normal patients (1.22°) ($p < 0.01$). There was a total loss of knee flexion on the non-operated side of the LLI group with extension instead being shown. The non-operated side of the Happy THR group demonstrated a similar standing knee angle to the operated side of the Symptomatic LLI group at 9.3° . The operated side of the Happy THR group also remained flexed at the knee at 6.1° . The Normal group demonstrated a small amount of knee flexion when standing.

5.6 Results - Temporal-Spatial Parameters

5.6.1 Raw Results

Table 10 lists the temporal-spatial parameters obtained from the analysis of all three patient groups. LLI patients walked 29% slower than the Happy THR patients which in themselves walked 23% slower than the Normal group ($p < 0.01$). Normal healthy people were also found to have a shorter cycle time of 15% and 9% relative to the operated sides of both the LLI and Happy THR groups. Symptomatic LLI patients demonstrated significantly ($p < 0.01$) shorter stride length compared to THR and Normals on both the operated (9% & 43%) and non-operated sides (13% & 46%). Stance phase time was found to show statistical significance between all groups ($p < 0.01$), with the general trend being that LLI patients had 21% and 6% longer stance times on the operated side relative to Normal patients and the operated side of the Happy THR group. There were no statistically significant differences in terms of swing phase time on the operated ($p > 0.05$) and non-operated sides ($p > 0.05$). Results could reflect the differences in the average age of patients in each group.

Table 10: Temporal-spatial data for all patient groups with * and † used to represent statistically significant differences at the 5% significance level across columns

Parameter	Normal	LLI	Happy THR
Stance Time Operated Side (s)	0.57±0.05*	0.69±0.10*	0.65±0.05*
Stance Time Non-Operated Side (s)	0.57±0.05*	0.72±0.13*	0.64±0.06*
Swing Time Operated Side (s)	0.41±0.03	0.43±0.09	0.42±0.04
Swing Time Non-Operated Side (s)	0.41±0.03	0.42±0.04	0.42±0.09
Walking Speed (m/s)	1.49±0.16*	0.94±0.24*	1.21±0.19*
Cycle Time Operated Side (s)	0.98±0.06†	1.13±0.17*	1.07±0.08†
Cycle Time Non-Operated Side (s)	0.98±0.06†	1.14±0.16*	1.07±0.09†
Stride Length Operated Side (m)	1.46±0.23*	1.02±0.20*	1.34±0.17*
Stride Length Non-Operated Side (m)	1.46±0.23*	1.00±0.18*	1.29±0.21*

Stride length measurement is often normalised to either height or leg length due to the disproportionate effect of size. The stride length data in Table 10 was not normalised. In Table 11 the results were normalised to height due to the leg length varying between limbs. It was found that when normalising for height, there were no significant differences between the operated sides against each other and the Normal group ($p > 0.05$). Statistical differences however remained between the non-operated sides and the Normal group ($p < 0.01$), with a Tukey post-hoc demonstrating that the differences existed between all three groups.

Table 11: Temporal-spatial parameters for all patient groups with * and † used to represent statistically significant differences at the 5% significance level across columns

Parameter	Normal	LLI	Happy THR
Normalised Stride Length Operated Side	0.86±0.06	0.62±0.12	0.79±0.07
Normalised Stride Length Non-Operated Side	0.86±0.06*	0.63±0.12*	0.75±0.09*

5.6.2 Temporal-Spatial Symmetry

Table 12 lists the results produced when looking at temporal-spatial symmetry between limbs across each group. This was undertaken using Equation 53. It was found using the one-way ANOVA that significant differences existed during both the stance phase and the swing phase ($p < 0.01$). A Tukey post-hoc test revealed that these differences were between the Symptomatic LLI group relative to the Happy THR and Normal cohorts. Likewise, cycle time was found to significantly differ between the groups ($p < 0.01$) with a Tukey test finding that once again these differences were between the Symptomatic LLI group relative to the Happy THR and Normal healthy subjects. Statistically significant differences were also found in terms of stride length ($p < 0.03$), with a Tukey test revealing that the difference was between the Symptomatic LLI and Happy THR groups.

Table 12: Temporal-spatial parameter symmetry index values for all patient groups with * and † used to represent statistically significant differences at the 5% significance level across columns. Results rounded to nearest integer

Parameter	Normal	LLI	Happy THR
Stance Phase Time (s)	5±5*	15±16*†	5±4†
Swing Phase Time (s)	3.±4.*	12±13*†	3±2†
Cycle Time Time (s)	8±7*	25±22*†	9±9†
Stride Length (m)	17±13	33±33*	16±15*

5.7 Discussion

5.7.1 Dynamic Joint & Segment Angles

Most kinematic results in the literature have compared the postoperative THR gait to a control group of healthy normal individuals. The majority of studies [154, 156, 164, 178–181, 197, 204, 208, 210, 213] show that post-THR, gait kinematics such as joint RoM and temporal-spatial parameters including velocity improve to a certain extent, but are never able to reach the level of normal healthy individuals. Improvements are slow with changes in gait characteristics having been observed 10 years post-surgery [179]. To the authors knowledge, the investigations by Tatateuchi et al. [192] and Casartelli et al. [188] are the only published works where the kinematics post-surgery are equivalent to controls. The Happy THR and Symptomatic LLI groups were all recruited for clinical

gait analysis at a minimum one year postoperatively. The variability produced in the dynamic joint angles, gait symmetry index, standing angles and temporal-spatial results thus may be reflective of patients at different stages of the recovery time line. This study assumed all patients were at the same level of recovery, (all were analysed 12 months post-surgery) with the results suggesting that a difference in leg length leads to gait abnormalities.

Comparing to Literature

To assess the validity of the data produced during this study, a comparison was made against the results of Bovi et al. [443] (2011) in their article *A multiple-task gait analysis approach: kinematic, kinetic and EMG reference data for healthy young and adult subjects*. Their study comprised of a total of 40 individuals, with 20 subjects being classed as young (age 10.8 ± 3.2) and 20 as adults (age 43.1 ± 15.4). For the purpose of this study, the adult population was used as it more closely resembles the patient populations used in this study. As Bovi et al. only used normal healthy individuals, the comparison against Bovi et al. was against the Normal controls.

Figure 81 shows that there was very little difference in terms of pelvic obliquity angle over the course of the gait cycle between the results of the Normal group and Bovi, with motion curves almost perfectly aligning. Pelvic rotation results in Figure 81 show considerable differences between the Normal group and Bovi et al. results. The Normal group had a greater RoM with larger amounts of both internal and external rotation occurring. These differences may however have been down to the large variability within each group, with Bovi et al. having an average gait cycle standard deviation of 4.61° computed and the Normal group a standard deviation of 4.81° .

Results were very similar in terms of hip flexion-extension, with the greatest differences occurring towards the beginning and end of the gait cycle. The Normal patient group however showed less variability in terms of average gait cycle standard deviation (5.34°) than Bovi et al. (8.44°). Hip abduction-adduction was found to be similar between the two groups. Greater variability was however found in the results of Bovi with an average gait cycle standard deviation of 4.41° compared to 3.86° in the Normal group. Knee flexion-extension joint angles and standard deviations were similar between Bovi et al. (4.29°) and Normal patients (5.33°). The Normal patient group demonstrated greater flexion during the stance phase and a smaller peak knee flexion during swing. The results of Bovi et al. showed a complete loss of ankle dorsiflexion and a similar gait cycle standard deviation (4.76°) relative to the Normal group (3.89°), potentially due to different ankle

axes orientation. The literature more closely resembles Normal group results [444–446].

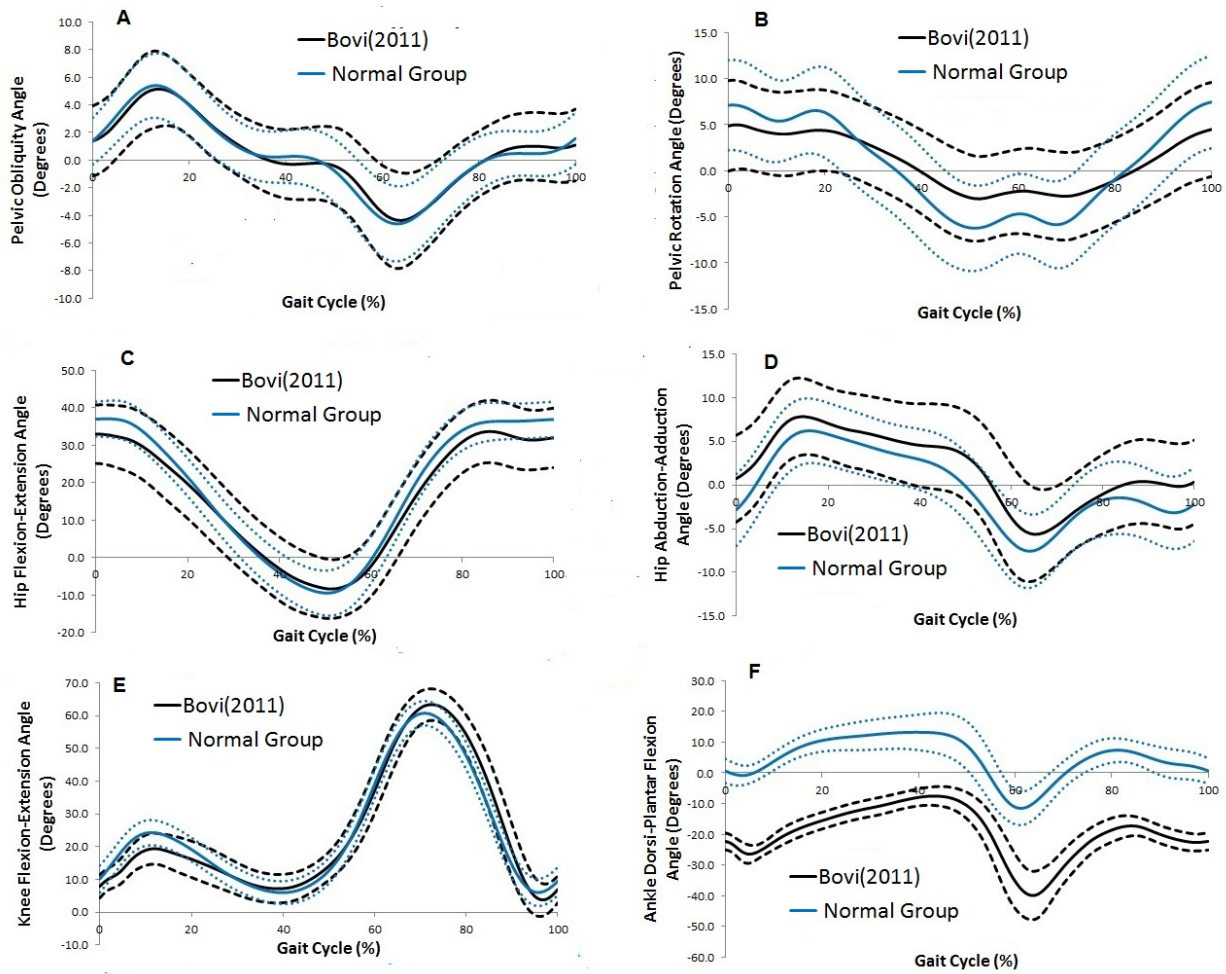


Figure 81: Average pelvic superior (+) - inferior obliquity (-) (A), pelvic anterior (+) - posterior (-) rotation (B), hip flexion (+) - extension (-) (C), hip abduction (+) - adduction (-) (D), knee flexion (+) - extension (-) (E) and ankle dorsi (+)-plantar (-) flexion (F) angle comparison between the Normal patient results to that of Bovi et al. over consecutive heel strikes normalised to 100 percentiles. Error intervals of ± 1 standard deviation are also plotted for each group.

Overall, the results produced in terms of the Normal group can be used in confidence in that they represent the average healthy patient. As the LLI and Happy THR patient data was collected via the same techniques, it can be assumed that this data was also accurate.

Pelvic Obliquity

Results demonstrated that Symptomatic LLI patients and Happy THR patients differed in terms of pelvic obliquity relative to each other and to the Normal healthy patients. Illyes et al. [447] studied pelvic motion following THR and made comparisons to controls but differed in the results of their study with the operated patients demonstrating an increase in superior pelvic obliquity. This has also been demonstrated to occur in non-THR LLI patients [222]. Figure 61 however

demonstrated that LLI patients differed in the type of pelvic obliquity shown, with some remaining in superior obliquity on the operated side throughout the gait cycle whilst others remained in inferior pelvic obliquity. Patients did not exhibit the oscillating pattern from superior obliquity to inferior and finally back to superior as seen in Normal patients.

From Figure 61 it can be seen that the LLI patients compensated following THR via the use of two different mechanism. The LLI patients exhibiting increased superior pelvic obliquity were showing characteristics of Trendelenburg gait, a pathological gait pattern which occurs when the weakened abductors on the operated side of the pelvis allow the pelvis to exhibit inferior obliquity on the opposing side. This occurred during the stance phase to decrease the workload of the weakened abductor muscles thus allowing for a less energy demanding gait pattern. In the swing phases these patients undertook hip hiking, where the pelvis was lifted superiorly to aid in foot clearance and advance the swing leg forwards [47]. Gurney [222] states that on the longer side an increase in inferior pelvic obliquity can be used as a method to increase the length of the shorter limb, which is what the second group of LLI patients appear to be doing. The Happy THR group produced results which were more similar to those of Normal patients in terms of pelvic angle over the gait cycle, despite one patient showing excessive superior obliquity and another excessive inferior obliquity.

Pelvic Rotation

Pelvic rotation demonstrated a loss in RoM for both the Happy THR and LLI groups relative to the Normal cohort. Statistically significant differences were only found between the Symptomatic LLI and Happy THR groups in terms of maximum rotation angle. Illyes et al. found that THR patients exhibited greater maximum pelvic rotation and an overall greater RoM, which goes against the results in the present study. The same conclusion was drawn by Kiss et al. [208] when using the direct-lateral surgical approach, with results being more similar to controls when using the antero-lateral approach. Lenaerts et al. [181] found a decrease in pelvic rotation for THR patients, which is more consistent with the results of the present study. The literature indicates that variables such as surgical technique effect pelvic rotation, which may reflect the differences seen between the results in this study and those seen in previous studies.

Hip Flexion-Extension

A statistically significant loss of hip extension occurred on the operated side of the Symptomatic LLI patients relative to all other groups. Loss of hip extension has been observed in many other

studies analysing gait following THR [157, 159, 178–181, 187, 202, 204, 208, 209, 448]. A reduction in peak hip extension has previously been associated with hip flexion contractures [65, 171] and a reduction in abductor muscle strength [71]. It is quite possible that the LLI patients were showing a significant loss of extension due to muscle weakness around the hip joint. Hip contractures have been suggested by Perron et al. [171] and Bennet et al. [198] to lead to a slower gait velocity and thus limit the amount of hip extension seen. This does not however agree the results obtained for the Symptomatic LLI group, where a SRCC did not detect a relationship between the maximum hip extension angle for each patient and gait velocity (SRCC =0.52<0.56). Likewise, no significant link was found between minimum hip flexion-extension angle and the magnitude of LLI (SRCC =0.16<0.56) or femoral offset (SRCC =0.15<0.56). The loss of hip extension may thus be a characteristic typical of LLI patients which is independent of velocity and leg length, but may be linked to a variable not analysed in the present study such as muscle strength

The review cross study by Ewen et al. [218] found RoM for THR patients between 23.2° - 40.8° with controls having values between 31.3° - 51.8°. Results from Table 6 demonstrate that the patients used in this study lie on average within these ranges. Crownshield et al. [74] found that the RoM in the sagittal plane of the hip shared a linear relationship to velocity, with the reduction in the Happy THR and LLI patient hip RoM most likely being due to a slower walking speed (Table 12). A SRCC found a positive correlation between operated side LLI patient velocity and hip sagittal plane RoM (SRCC =0.63>0.56).

Figure 82 compares hip flexion-extension on the operated sides of the Symptomatic LLI and Happy THR groups to that of Pospischill et al. [449], who analysed the gait of 40 THR patients with half having undergone MIS (Minimally Invasive Surgery) and the other half a standard THR. Gait was also analysed for the patients preoperatively. The results produced by Pospischill et al. demonstrated significant changes in RoM postoperatively. At the 10 day postoperative stage both the MIS and standard THR technique patients displayed a loss of extension compared to preoperative levels but were able to produce results similar to that of normal healthy individuals at the 3 month period. Comparing results showed that the Symptomatic LLI patients had hip extension levels which were very similar to the amount seen preoperatively. The Happy THR patients, who had been operated on at a minimum of a year before clinical gait analysis, demonstrated similar results to the MIS and standard Technique groups at 3 months with the exception of having greater RoM. Using these results, it can be postulated that LLI patients may become symptomatic following

THR due to their gait remaining at preoperative levels.

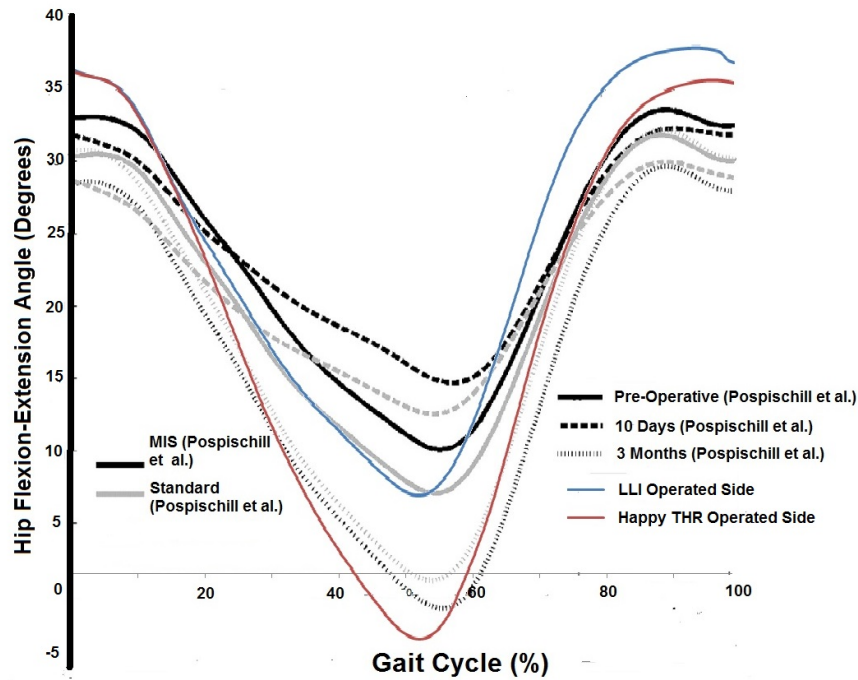


Figure 82: Comparing the results of Pospischill et al. to the experimental results of the operated sides of the Symptomatic LLI and Happy THR groups in terms of hip flexion-extension over a normalised gait cycle between consecutive heel strikes of the same foot . Pospischill et al. have results for both MIS (Minimally Invasive Surgery) THR and standard THR at 10 days and 3 months post-surgery together with the preoperative results.

Figure adapted from Pospischill et al. [449]

Hip Abduction-Adduction

Results demonstrated that there was large variability between the groups in terms of hip abduction-adduction. An increase in hip abduction was seen on average in the swing phase on the operated sides of both the Symptomatic LLI and Happy THR groups, which is a characteristic of hip circumduction occurring during gait. Circumduction at the hip is where excessive hip abduction occurs as the leg swings forward. Abducting of the hip leads to the lateral movement of the swing leg in an arc shape which increases leg clearance from the ground and is a common indicator of leg length difference [133]. This mechanism was potentially used to move the swing leg forward rather than hip flexion-extension due to the loss of extension on the operated side hip. The amount of hip abduction however did not correlate with the magnitude of leg length difference ($SRCC = 0.25 < 0.56$).

As stated previously, this study is unique in analysing the gait of patients symptomatic for a LLI following THR which means that there are no current publications which can be compared to as a

gold standard. In this manner, the conclusion drawn of the LLI patients showing circumduction are the first of their kind. However, the mechanism of circumduction has been found to be a common compensatory mechanism for individuals with a naturally occurring LLI [222]. A decrease in THR patient abduction-adduction RoM has been found by Bennet et al. [198] and Lenaerts et al. [181] which was also demonstrated within the present results.

Knee Flexion-Extension

Results demonstrated that LLI patients showed reduced knee flexion relative to Normal and Happy THR patients. Significant differences were present between the non-operated side and the operated side of the LLI patients in terms of minimum angle and between the non-operated side and the Normal patients with regards to maximum angle. Significant differences in knee angle were found at toe off between the operated and non-operated sides of the Symptomatic LLI group, with the operated side showing 17% greater peak knee flexion. This was potentially due to the greater foot clearance required in order to move the longer operated side leg forwards.

The kinematics of the knee are reported less often than those of the hip by studies in literature of gait following THR. Perron et al. [171] in their study on women post-THR found a decrease in peak knee flexion during mid-stance, which can also be seen on the non-operated side of the LLI group. Mont et al. [165] in a study of 58 THR patients found that knee flexion was not significantly altered following THR in terms of minimum joint angle and RoM relative to controls, which complements the present results where no statistically significant differences were found between the Happy THR and Normal groups. Other studies have different opinions with Agnosti et al. [197] finding an increase in peak knee flexion angle 12 months postoperatively and Bennet et al. [198] observing a decrease in knee RoM on the operated side. Horstmann et al. [180] found that there was a decrease in RoM of the non-operated sided knee relative to controls, which was also seen in the present study.

The review by Gurney [222] found that knee flexion often increased on the longer side during gait in patients with an LLI, which goes against the results observed in this study where on average a decrease was seen. A SRCC found that a strong positive correlation existed ($SRCC = 0.80 > 0.56$) between peak knee flexion angle during the gait cycle and gait velocity which may explain the reduction in peak flexion. The non-operated sides of both the Symptomatic LLI and Happy THR groups showed an increase in knee extension. No link was found between the magnitude of leg length and maximum knee extension angle ($SRCC = 0.11 < 0.56$). A significant link was found

however found between maximum knee extension and velocity, with slower patients showing more extension (SRCC = -0.76 < -0.56).

Ankle Dorsi-Plantar Flexion

Comparisons in terms of ankle dorsi-plantar flexion demonstrated that there was large variability between the groups. Normal patients produced the most consistent results with the smallest standard deviation. An increase in ankle dorsiflexion on the operated side and an increase in plantarflexion on the non-operated side was seen on average in both the LLI and Happy THR groups. . Statistical differences were observed during various gait events. This may have however been due to the large outliers present, especially for the LLI group.

Comparing the present results to the literature shows that due to the variability shown across studies, it is not possible to state with certainty why the results produced increased dorsiflexion on the operated side and increased plantarflexion on the non-operated side. However, a SRCC test found statistically significant positive correlation (SRCC = 0.65 > 0.56) between peak dorsiflexion angle and the magnitude of leg length on the operated side of LLI patients, indicating that dorsiflexion could be a mechanism used to compensate for a difference in leg length. The results for the ankle however should be taken with caution due to the hierarchical nature of the PiG marker system where the AJC position and hence the position of the joint axis is determined by a total of 10 proximal markers (4 pelvis, 3 thigh, 3 shank) and two clinical joint width measurements at the knee and the ankle⁸.

As with the results at the knee, there are fewer literature articles which detail the kinematics of the ankle following THR than the hip. Of those that do exist, many only make a passing reference and do not go into reasons why the particular results are being obtained. Mont et al. [165] in a study analysing 58 THR patients found that ankle dorsiflexion following THR was at similar levels to that of healthy controls. Similarly, Lenaets et al. [181] also found there to be no significant differences between the dorsiflexion shown post-THR relative to healthy controls.

On the other hand, the study by Perron et al. [171] on gait of women following THR found a 26% increase in dorsiflexion in the period between mid-stance and toe off 6-18 months following surgery, similar to what was found in this study. Beaulieu et al. [195] however found a decrease in

⁸See pages 69- 75 and 80- 82 in the *Generic Methods* for more information

ankle dorsiflexion on the operated side following THR. Bennet et al. [198] found that only elderly THR patients had a loss in peak ankle dorsiflexion, whilst younger individuals maintained similar results to that of controls. This conclusion was also drawn by Bach et al. [164] with loss of muscle function together with a reduced walking speed given as the most likely justifications. Lenaets et al. [181] also found no significant changes in ankle dorsi-plantar flexion on the non-operated side. The variability in study conclusions shows the non-uniform nature of THR patients following gait and is an area which requires more research.

5.7.2 Temporal-Spatial Parameters

The Symptomatic LLI group showed reduced values for gait velocity and stride length compared to the other groups and greater values for cycle time, stance phase time, swing phase time, and stride length. The average velocity for Happy THR patients (1.21 m/s) fell within the range as found in literature of between 0.707m/s-1.36m/s [157, 163, 196, 200, 205, 210, 218]. Gait velocity at 0.94 m/s for the LLI group was significantly smaller than the results for the Happy THR group and fell into the lower regions of the range reported for THR patients in the literature. Zhang et al. [271] observed that a greater leg length difference was linked to a smaller walking velocity, with the LLI patients on average having a greater difference than their Happy THR counterparts. The Normal patient group had a velocity (1.49 m/s) which ranged at the top end of what is found in the literature, with the largest comfortable walking speed found being 1.51 m/s [115–117]. Velocity was shown to share a strong linear relationship with hip flexion-extension RoM and maximum knee flexion angle.

The results for swing phase time had no statistical significance detected, indicating that differences between the groups may have been due to natural variation. Stride length was found to be significantly different between all groups on the non-operated side independent of height. This may indicate that smaller stride lengths on the non-operated side are a commonly used mechanism in THR patients to compensate for abnormalities on the operated side, such as in a vaulting gait pattern. In a vaulting gait cycle, the longer leg demonstrates excessive hip and knee flexion together with moving the heel higher off the ground to provide adequate foot clearance. As a consequence, the shorter leg often displays compensatory mechanism to increase the leg length. Winter [106] stated that a decrease in step length is often due to a reduction in contralateral hip and knee extension. A SRCC however found no link between stride length and hip flexion (SRCC =-0.50>-0.56)

or knee flexion (SRCC =-0.14>-0.56) on the operated side of LLI patients. This was perhaps due to the large inter-patient variability in the LLI group

Greater temporal-spatial asymmetry was found in the Symptomatic LLI group compared to the other patient groups. In particular, Symptomatic LLI patients showed greater asymmetry in stance phase time, swing phase time and cycle time compared to the differences found in the Normal and Happy THR patients. This indicates that individuals may be asymptomatic following THR due to showing consistent gait parameters between the two limbs, similar to the levels in healthy individuals. Guedes et al. [170] however did find that a group of 23 THR patients had a statistically greater asymmetry in terms of stance phase time relative to controls.

5.7.3 Standing Joint Angles

When static, the Happy THR and Normal group showed a symmetrical static gait posture in terms of both hip and knee flexion-extension. The LLI group however stood with a flexed longer leg, and had the greatest hip and knee flexion on the operated side as a means of compensating for the increase in leg length, with the results for both angles being statistically significant. A strong positive correlation was found between hip flexion-extension and knee flexion-extension standing angles on the operated side (SRCC =0.83>0.56).

The LLI non-operated side was the only limb on average to show knee extension, perhaps as a method used to increase leg length. No correlation was found between the operated and non-operated sided knees (SRCC =0.16<0.56) or the operated sided hip and the non-operated sided knee (SRCC =0.26<0.56) with regards to extension. Weak correlation was found between the magnitude of leg length and hip flexion on the operated side (SRCC =0.28<0.56), operated side knee flexion (SRCC =0.08<0.56) and non-operated side knee extension (SRCC =0.30<0.56). Walsh et al. [235] found that during standing, simulated levels of LLI caused an increase in knee flexion on the longer side as a method to compensate and maintain balance, which it appears the patients in the Symptomatic LLI group were doing.

5.7.4 Errors in Results

All experimental results are subject to error. The errors in the PiG model are linked to poor marker placement, the choice of HJC regression equation and inaccurate clinical anthropometric

measurements. These can effect joint centre positions and segment rotations leading to offsets in joint angle results together with cross talk occurring between segment axes. This is particularly problematic in obese patients as recruited for this study where landmarks on the body are more difficult to locate⁹.

5.8 Conclusion

This is the first report undertaking an analysis of gait compensatory mechanisms for patients symptomatic for a LLI following THR. Patients with a LLI on average demonstrated significantly reduced peak hip extension and knee flexion angles together with greater hip abduction and ankle dorsiflexion angles relative to Happy THR and Normal patients. It was found that LLI patients on the operated side characteristically develop a loss of hip extension. A Trendelenburg gait together with circumduction of the swing leg were also commonly seen in the LLI patients.

There was generally greater asymmetry in motion of the LLI patients, compared to the Normal or Happy THR patients with many of the compensatory mechanisms occurring during toe off. LLI patients showed significantly reduced walking speeds and associated reductions in stride length. Conclusions drawn from the results however must be taken with caution due to the small number of patients used, the high sensitivity of the PiG marker set to errors in marker placement and anthropometric measurements together with the absence of preoperative gait data as a comparison.

⁹See pages 70- 75 and 80- 82 in the *Generic Methods* for more information

6 Kinetics

6.1 Aims & Objectives

The aim of this chapter was to compare and contrast a group of symptomatic LLI patients to that of asymptomatic THR and Normal control groups in terms of VGRFs, resultant JRFs and moments. This was to establish whether LLI patients produce different forces and moments during gait at particular gait events, in terms of peak forces/moments and to study if they showed greater gait asymmetry.

6.2 Methodology

6.2.1 Initial Clinical Method

A description of the patient cohort used together with the recruitment method is described in the *Anthropometrics & Demographics* chapter on page 90 whilst the clinical gait analysis method is detailed in the *Kinematics & Temporal-Spatial Parameters* chapter on page 105.

6.2.2 Non-Clinical Method

(By Author)

The same method in selecting patient data was used as in the *Kinematics & Temporal-Spatial Parameters* chapter on page 106. One additional patient in the Happy THR and Normal groups respectfully had their JRF results removed due to being very large outliers which effected the averages of the results, giving a total of 10 Happy THR and 34 Normal patients together with 13 Symptomatic LLI patients. These outliers were caused by marker drop out.

AnyBody is a multi-body dynamics system which is able to compute JRFs and joint moments via inverse dynamics, a procedure where the external moments which can be derived from the VGRFs and kinematics. Only the VGRF was selected for analysis and not the medial-lateral/anterior-posterior forces due to the vertical forces producing the largest and most meaningful results. The musculoskeletal model in the AnyBody repository is based upon the anthropometric measurements produced by the University of Twente and has been previously validated by Forster et al. [336] and Manders et al. [220].

The model consisted of 11 segments including the talus, foot, shank, patella and thigh on both sides together with the pelvis. Scaling was used to accurately depict joint positions and segment

lengths for each subject. Due to the redundancy of the human body, more muscles are available than are required. Hence an optimisation method is used in AnyBody to mimic the CNS. Equation 52 shows how hip joint and muscle forces are computed in AnyBody where f is a vector of muscle and JRFs, r is another vector which represents external and inertia forces whilst c is a matrix of equation coefficients.

$$Cf = r \quad (52)$$

The method selected for this study was that of minimising the maximum muscle force, allowing for a realistic amount of load sharing to occur. To achieve this, constraints were applied to Equation 52 which prevented muscles from becoming overloaded and promoted the sharing of load¹⁰. Resultant JRFs, VGRFs and moments (hip flexion-extension, hip abduction-adduction, knee flexion-extension, ankle dorsi-plantar flexion) were extracted from AnyBody for two trials of every patient from heel strike onto the force plate to heel strike off the force plate. One trial was with respect to right foot contact onto the force plate whilst the other was with respect to left foot contact. Data was normalised to 100 percentiles. To offset variations in weight between the patient groups, all results were normalised for bodyweight.

Table 13 shows how each of the joint moments and the joint reaction force were measured. The selected moments were in the same planes as the motions were in the kinematic analysis. VGRFs and JRFs were measured in newton's per kg whilst moments were measured in newton metres per kg (N-m/kg). See pages 85 - 89 in the *Generic Methods* for further details on the procedures used to compute forces and moments in AnyBody.

Table 13: Table showing how moments and forces were measured in AnyBody

Local Segment	Reference Segment	Measurement
Right Thigh	Pelvis	Right Hip Joint Reaction Force
Left Thigh	Pelvis	Left Hip Joint Reaction Force
Right Thigh	Pelvis	Right Hip Flexion-Extension Moment
Left Thigh	Pelvis	Left Hip Flexion-Extension Moment
Right Thigh	Pelvis	Right Hip Abduction-Adduction Moment
Left Thigh	Pelvis	Left Hip Abduction-Adduction Moment
Right Shank	Right Thigh	Right Knee Flexion-Extension Moment
Left Shank	Left Thigh	Left Knee Flexion-Extension Moment
Right Foot	Right Shank	Right Ankle Dorsi-Plantar Flexion Moment
Left Foot	Left Shank	Left Ankle Dorsi-Plantar Flexion Moment

¹⁰See pages 47- 50 in the *Literature Review* for information

Averages & Raw Data Analysis

Averages for VGRFs, JRFs and moments during the course of the gait cycle were produced for each patient group, with the Happy THR and LLI groups having an operated and non-operated side average and the Normal group a left and right side average. When comparisons were required during certain points in analysis to a single Normal patient average, the left side of the Normal group was used. Averages together with standard deviations for each of the variables studied were computed in Excel. Raw data was also analysed as a whole, with the standard deviation of the average results at each percentile of the gait cycle being calculated, averaged and compared.

Force/Moment Maximum-Minimum

Once the data had been normalised, the maximum and minimum force and moment results were identified for each patient and comparisons made. For VGRFs and JRFs, comparisons were made across groups and between groups for the 1st and 2nd peaks of the gait cycle together with the troughs.

Gait Symmetry Index

A symmetry index, produced by Robinson et al. [437] and defined in Equation 53, was used to determine the level of asymmetry between the two limbs of each patient. This technique was chosen as it allows a reference to be made against the average result. X_L and X_R represented the average of the parameter being analysed on the left and right legs respectively. A perfect symmetry would give a value of 0%. The SI was rounded to the nearest integer value. Gait symmetry was analysed for VGRFs, JRFs and moments.

$$SI = \frac{X_L - X_R}{(X_L + X_R)^{\frac{1}{2}}} \times 100\% \quad (53)$$

Gait Events

A comparison was also made across the groups in terms of three gait events; initial heel strike, mid-stance and toe off. The frame number of the gait cycle data which corresponded with the first occurrence of the force vector was defined as initial heel strike whereas the frame number which corresponded with the final occurrence of the force vector was defined as toe off. Mid-stance was defined to exist exactly half-way between heel strike and toe off. These coincided with the gait instants as defined for kinematics in the *Kinematics & Temporal-Spatial Parameters* chapter, as seen in Figure 59 on 108.

6.3 Results - Ground Reaction Force

Figure 83 illustrates results for the patients groups in terms of VGRF. Normal healthy individuals demonstrated an average VGRF over the stance phase of $0.77 \text{ N/kg} \pm 0.35$, with Happy THR patients having an average stance phase value of $0.68 \text{ N/kg} \pm 0.36$ for the operated side and $0.75 \text{ N/kg} \pm 0.33$ on the non-operated side. The Symptomatic LLI group showed an average VGRF of $0.63 \text{ N/kg} \pm 0.33$ on the operated side and $0.66 \text{ N/kg} \pm 0.36$ on the non-operated side. Statistical significance was not detected between these results using the one-way ANOVA ($p > 0.05$).

The operated and non-operated sides of the Happy THR group produced almost identical average force curves. The double peak shape of the curve was maintained for the Happy THR patients for both the operated and non-operated sides. Wider confidence intervals relative to the Normal group were however seen. The LLI group overall showed a reduction in the amount of average force relative to the other groups at all points in the gait cycle, excluding at the trough (between $\approx 25\% - 40\%$) where they showed greater force. LLI patients also had peaks which were less distinguishable, with the non-operated side showing slightly greater amounts of force on average.

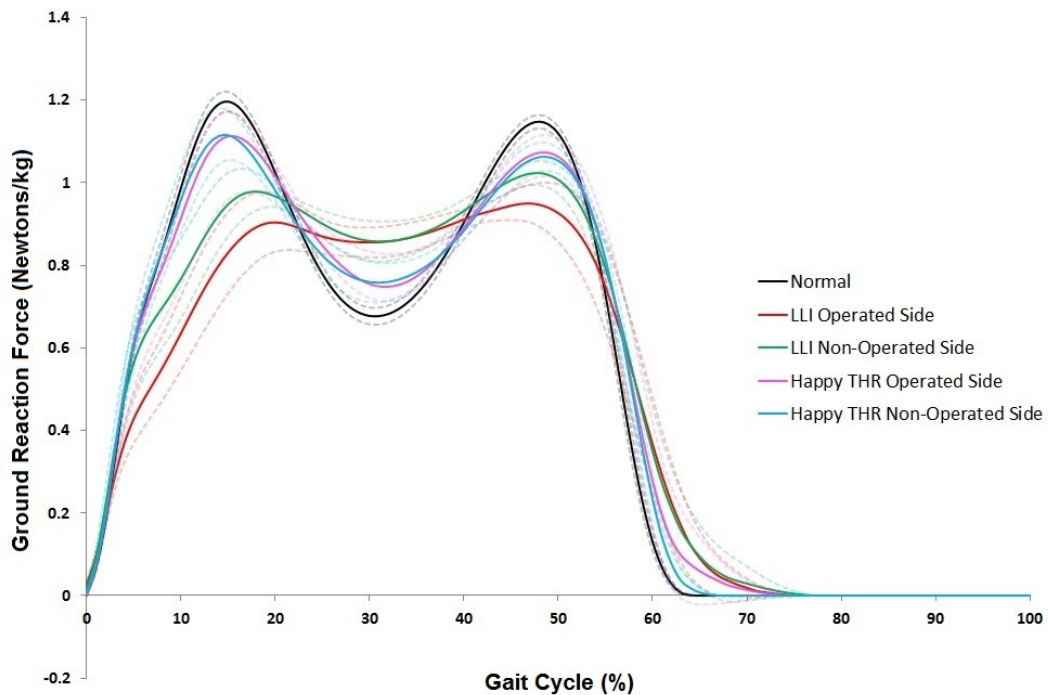


Figure 83: Comparing VGRF between the operated and non-operated sides of the LLI and THR groups to that of the average Normal healthy individuals together with 95% confidence intervals over a normalised gait cycle between consecutive heel strikes of the same foot. Results have been normalised for bodyweight.

Figure 84 shows the average VGRF, normalised for bodyweight, at the two peaks of the VGRF curve together with the trough which occurs between them. The Normal group had the largest average 1st peak (1.20 N/kg±0.09). The operated side of the Happy THR group (1.15 N/kg±0.12) and non-operated side (1.13 N/kg±0.12) showed smaller average 1st peak values. The LLI group had on average a 20% reduction relative to the Normal group (1.00 N/kg±0.08) on the operated side and on average a 14% reduction to the Normal group on the non-operated side (1.05 N/kg±0.08). Statistically significant differences were found between the Normal group and the operated (p<0.01) and non-operated (p<0.01) sides of the Symptomatic LLI group. A significant difference was also found between the operated sides of the LLI patients to the operated (p<0.01) and non-operated (p<0.01) sides of the Happy THR patients.

At the 2nd peak greater differences were observed between the groups. Once again the Normal group on average had the greatest 2nd peak (1.15 N/kg±0.08). For the Happy THR group the operated side (1.09 N/kg±0.09) had a 2% greater average peak force value than the non-operated side (1.07 N/kg±0.07). This was also the case for the operated (1.00 N/kg±0.05) and non-operated sides (1.04 N/kg±0.06) of the Symptomatic LLI group, with there being a 4% difference. Statistically significant differences were found between the Normal group and the operated (p<0.01) and non-operated (p<0.01) sides of the Symptomatic LLI group together with the non-operated side of the Happy THR patients (p<0.02). A significant difference was also found between the operated sides of the LLI and Happy THR patients (p<0.04).

The troughs which occurred between the 1st and 2nd peaks, were found on average to be at their smallest in the Normal group (0.67 N/kg±0.09). Greater average trough force was found on the operated (0.73 N/kg±0.08) and non-operated (0.75 N/kg±0.09) sides of the Happy THR group. This was however small in comparison to the peak trough forces on the operated (0.85 N/kg±0.08) and non-operated (0.84 N/kg±0.10) sides of the Symptomatic LLI group. Significant differences were found between the Normal patients and the operated (p<0.01) and non-operated (p<0.01) sides of the LLI patients. In addition, significant differences were found between the operated (p<0.02) and non-operated sides (p<0.04) of the LLI patients and the operated side of Happy THR subjects.

Comparisons were also made between the average results of the 1st and 2nd peaks within each group. A statistically significant difference was found between the 1st and 2nd peaks in the Normal

group ($p < 0.03$), with the 1st peak exceeding the 2nd in magnitude. No significant differences were however found between the two peaks in the LLI patients on the operated and non-operated sides ($p > 0.05$). Likewise, no statistically significant differences were found in the Happy THR group between the 1st and 2nd peaks on the operated and non-operated sides ($p > 0.05$).

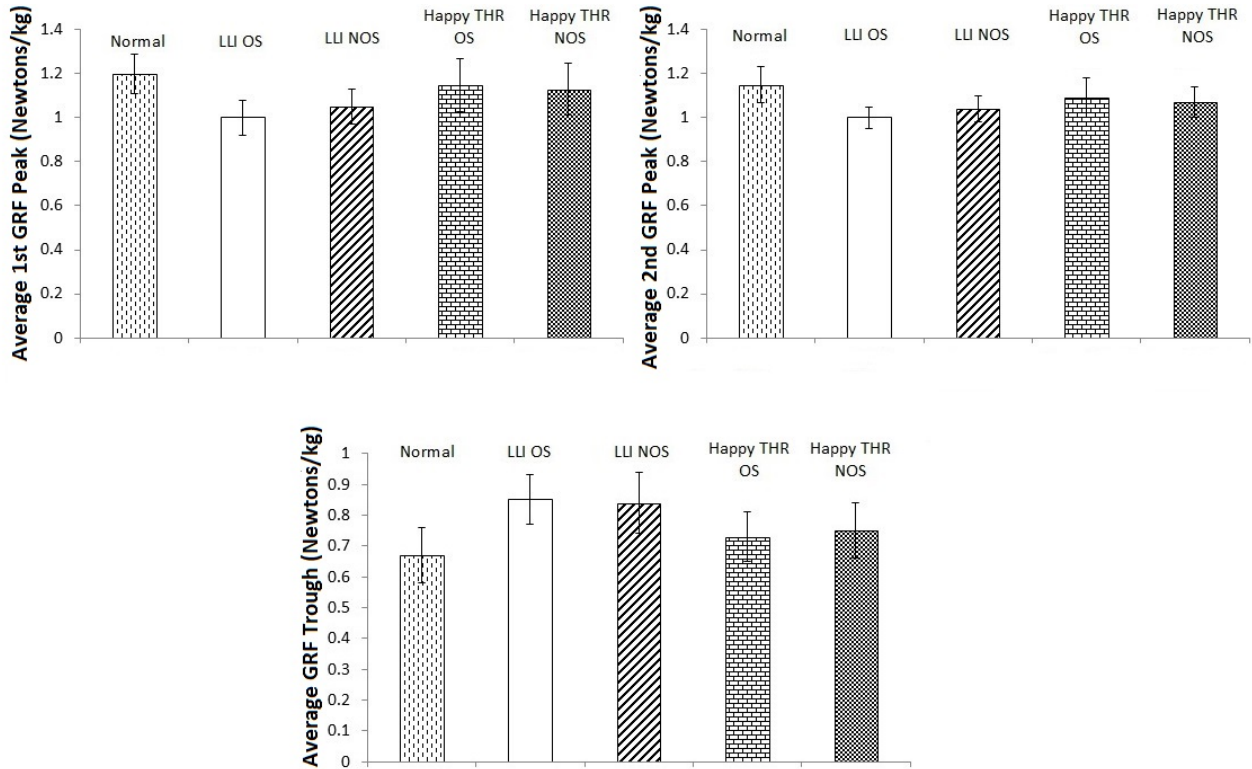


Figure 84: Average VGRF 1st peak, 2nd peak and trough for Normal, LLI Operated Side (LLI OS), LLI Non-Operated Side (LLI NOS), Happy THR Operated Side (Happy THR OS) and the Happy THR Non-Operated Side (Happy THR NOS) groups together with standard errors.

Figure 85 demonstrates the symmetry index of VGRFs at 4 instants during the stance phase of the gait cycle. At the 0% instant of the gait cycle, a test statistic of $p < 0.01$ was found using the one-way ANOVA, with the Tukey post-hoc finding differences between the LLI and Normal groups. At 20%, significant differences were also found between the LLI group and Normals ($p < 0.03$) together with the LLI group and Happy THR patients ($p < 0.02$).

At 40%, significant differences were found between Happy THR patients and LLI patients ($p < 0.01$) together with Happy THR patients and Normal healthy individuals ($p < 0.01$). Significant differences were also found at 60% ($p < 0.01$), between the Happy THR and Normal groups. Overall, the greatest gait symmetry was observed in the Normal healthy patients and the least in the Symptomatic LLI patients.

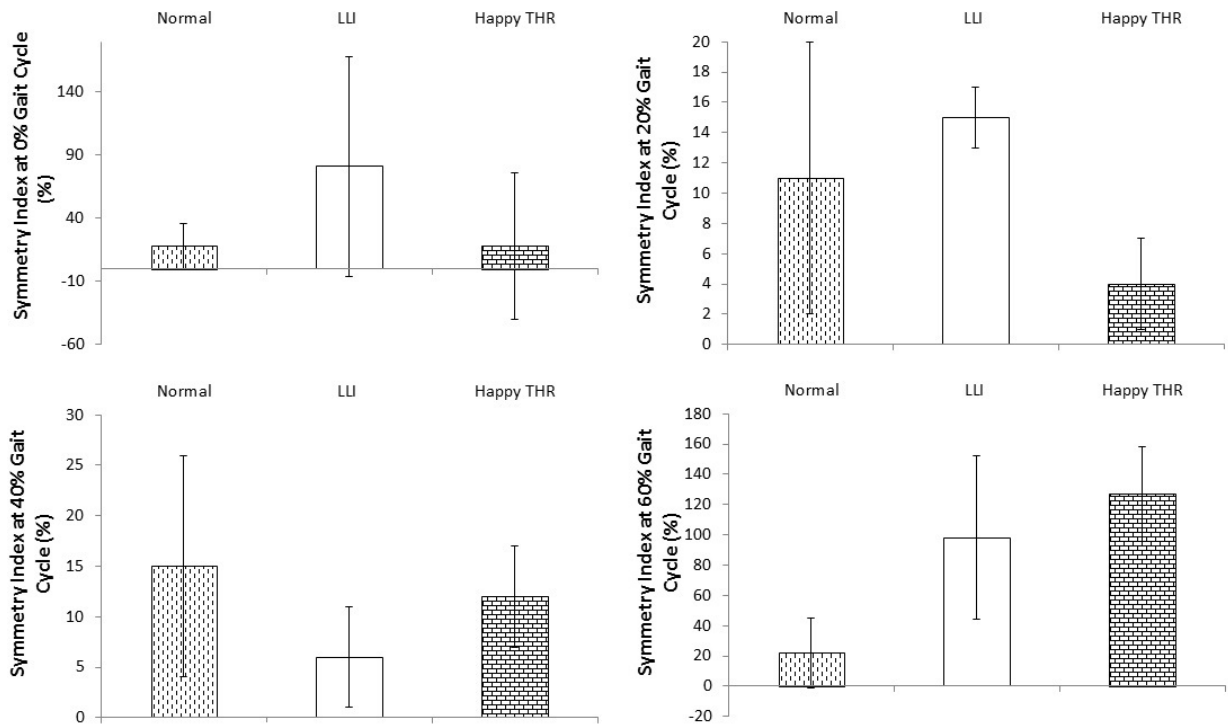


Figure 85: VGRF Symmetry Index results following normalisation for bodyweight for all patient groups at 0%, 20%, 40% and 60% gait intervals together with standard errors.

Figure 86 demonstrates the VGRF normalised for body weight at mid-stance. A one-way ANOVA test using SPSS found statistically significance between the groups ($p < 0.01$). Further analysis using a Tukey post-hoc revealed that these differences were between Normal patients and all other groups.

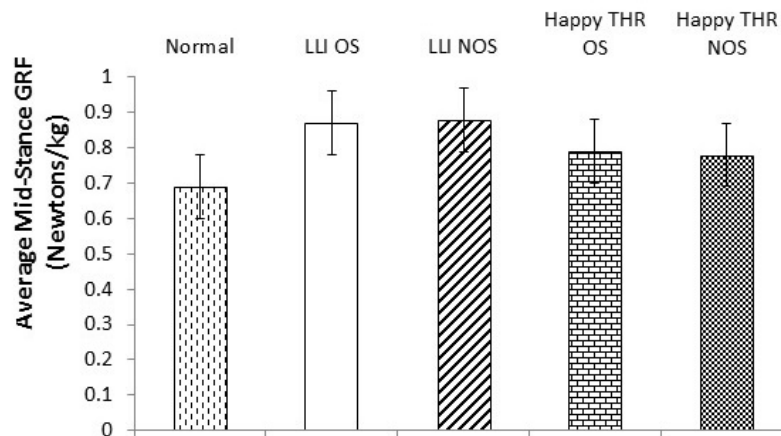


Figure 86: VGRF results following normalisation for bodyweight for all patient groups at mid-stance for Normal, LLI Operated Side (LLI OS), LLI Non-Operated Side (LLI NOS), Happy THR Operated Side (Happy THR OS) and the Happy THR Non-Operated Side (Happy THR NOS) groups together with standard errors.

Figure 87 illustrates the raw data which was used in this analysis. There was an outlier on the operated side of the LLI group, which did not show the characteristic VGRF curve shape. The op-

erated side of the Symptomatic LLI group showed less variability (Standard Deviation =0.40N/kg) compared to the non-operated side (Standard Deviation =0.46N/kg). Greater variability was found in the Happy THR group on both the operated side (Standard Deviation=0.46N/kg) and non-operated sides (Standard Deviation=0.44N/kg). Normal individuals demonstrated similar levels of variability (Standard Deviation=0.46N/KG).

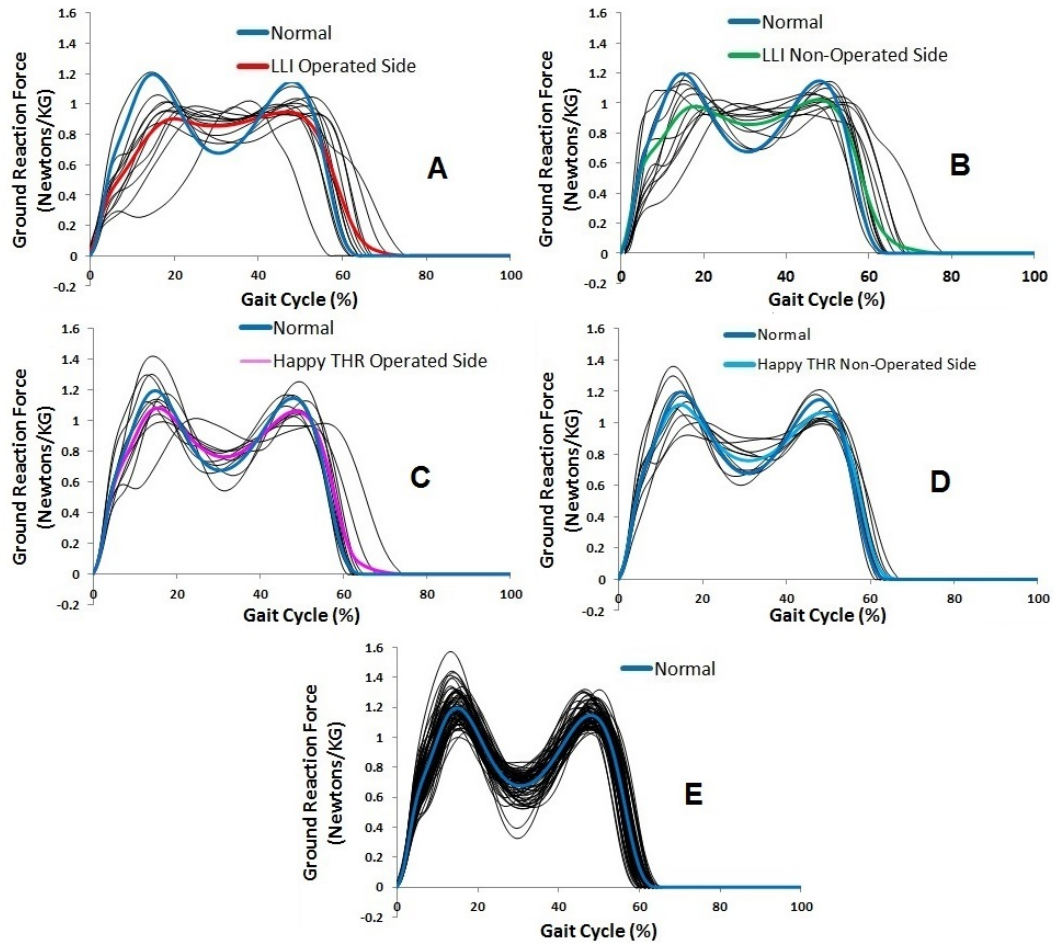


Figure 87: Raw VGRF results for all three groups over a normalised gait cycle between consecutive heel strikes of the same foot. (A) Operated side LLI patients (B) Non-operated side LLI patients, (C) Operated side Happy THR patients (D) Non-operated side Happy THR patients (E) Normal Healthy Patients. Average lines are added to each graph for the particular group being studied together with the average Normal patient result. Results have been normalised for bodyweight.

6.4 Results - Hip Joint Reaction Force

Figure 88 demonstrates results for the patients groups in terms of JRF. Normal healthy individuals produced a double peaked force curve with an average JRF over the stance phase when normalised for bodyweight of $2.14 \text{ N/kg} \pm 0.84$. For Happy THR patients, smaller levels of JRF were present relative to the Normal group with an average stance phase value of $1.74 \text{ N/kg} \pm 0.83$ for the operated side and $2.00 \text{ N/kg} \pm 0.74$ on the non-operated side. The Symptomatic LLI group showed an average JRF of $1.56 \text{ N/kg} \pm 0.71$ on the operated side and $1.75 \text{ N/kg} \pm 0.86$ on the non-operated side. A statistically significant difference was detected between the averages of the Normal ($p < 0.01$) and non-operated side of the Happy THR patients ($p < 0.01$) relative to all others.

The shapes of the JRF curves were very similar to those of VGRFs. The operated and non-operated sides of the Happy THR group, as with VGRFs, produced almost identical average force curves. The LLI group overall showed a reduction in the amount of average force relative to the other groups at all points of the gait cycle excluding the trough at around mid-stance. LLI patients also had peaks which were less distinguishable relative to the Happy THR and Normal groups, with the non-operated sides generally showing slightly greater amounts of force on average.

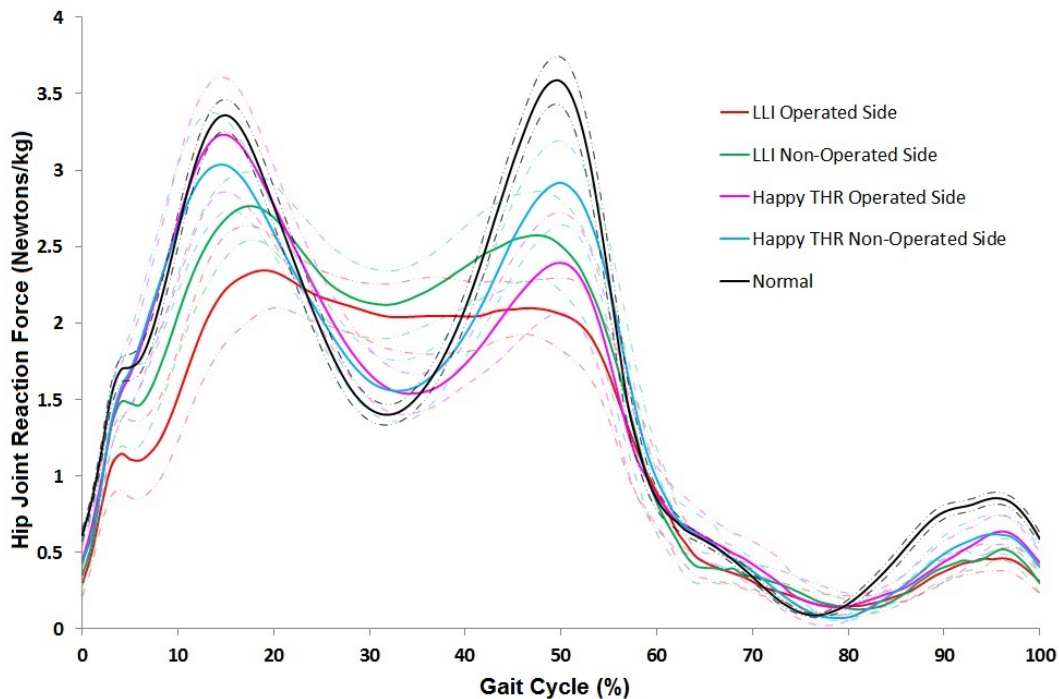


Figure 88: Comparing hip JRFs between the operated and non-operated sides of the LLI and THR groups to that of the average Normal healthy individuals together with 95% confidence intervals over a normalised gait cycle between consecutive heel strikes of the same foot. Results have been normalised for bodyweight.

Figure 89 shows the average JRF, normalised for bodyweight, at the two peaks of the JRF curve together with the trough which occurs between them. The Normal group had the largest average 1st peak (3.29 N/kg±0.46). The operated side of the Happy THR group (3.17 N/kg±0.36) and non-operated side (3.12 N/kg±0.63) showed smaller average 1st peak values. The LLI group differed, with the non-operated side showing a similar average peak value (3.18 N/kg±0.43) to both sides of the Happy THR group and the operated side showing a substantial reduction (2.64 N/kg±0.57). A significant difference was detected between the operated side of the LLI group against Normal patients (p<0.01).

At the 2nd peak greater differences were observed between the groups. Once again the Normal group on average had the greatest 2nd peak (3.69 N/kg±0.67). The Happy THR group on the operated side (2.46 N/kg±0.62) had a smaller average peak force relative to the non-operated side (2.95 N/kg±0.56). This was also the case for the operated (2.35 N/kg±0.51) and non-operated sides (2.65 N/kg±0.69) of the Symptomatic LLI group. Statistically significant differences were detected between the Normal patients and the operated (p<0.01) and non-operated (p<0.01) sides of the LLI group and operated (p<0.01) and non-operated (p<0.01) sides of the Happy THR group.

The troughs which occurred between the 1st and 2nd peaks were found to have the smallest average peak force in the Normal group (1.35 N/kg±0.29). Greater average trough force was found on the operated (1.47 N/kg±0.17) and non-operated (1.54 N/kg±0.38) sides of the Happy THR group. This was however smaller in comparison to the peak trough forces on the operated (1.80 N/kg±0.42) and non-operated (1.92 N/kg±0.41) sides of the Symptomatic LLI group. Significant differences were found between the Normal patients against the operated (p<0.01) and non-operated (p<0.01) sides of the LLI group together with the operated side of the Happy THR group against the non-operated side of the LLI group (p<0.02).

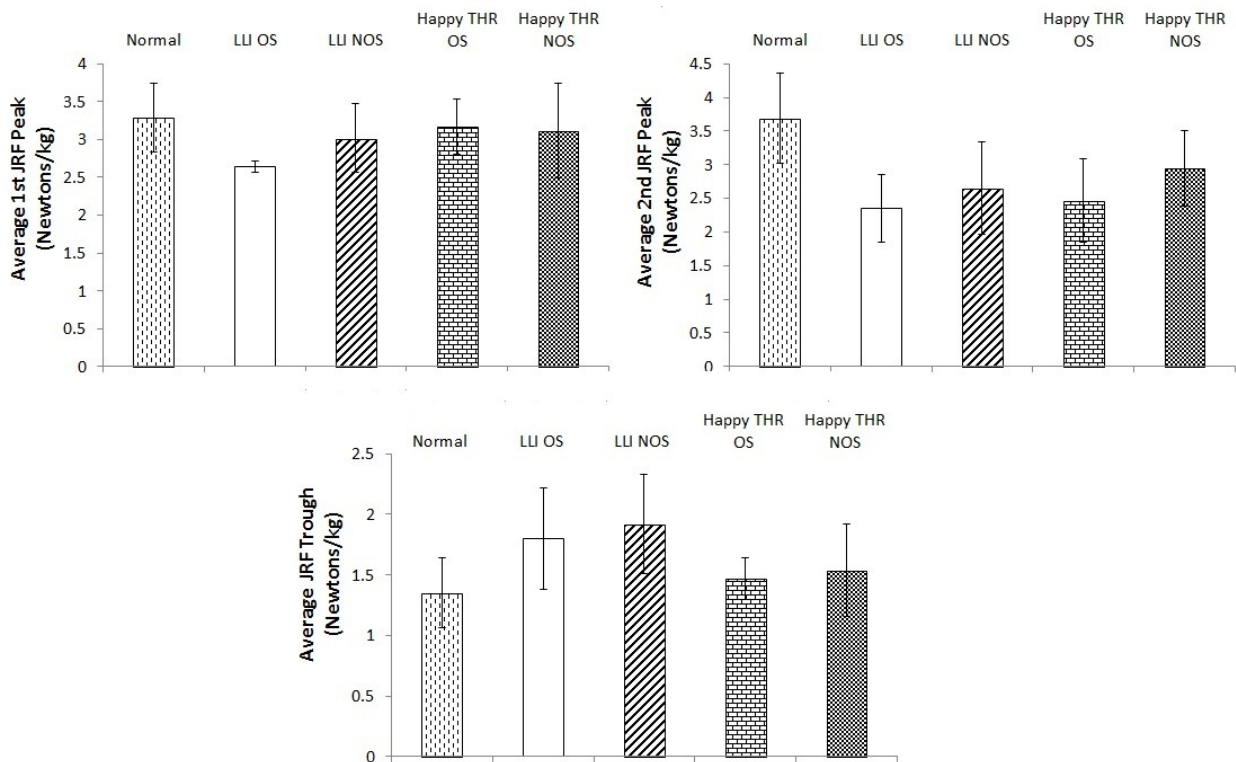


Figure 89: Average hip JRF 1st peak, 2nd peak and trough for Normal, LLI Operated Side (LLI OS), LLI Non-Operated Side (LLI NOS), Happy THR Operated Side (Happy THR OS) and the Happy THR Non-Operated Side (Happy THR NOS) groups together with standard errors

Figure 90 shows the symmetry index values in terms of JRF for all three groups using Equation 53. Statistical significance was detected at 0% (heel strike) of the gait cycle using the ANOVA, with the Tukey test clarifying that the differences were between the LLI patients against the Normal ($p < 0.01$) and Happy THR groups ($p < 0.01$). Likewise, a significant difference was detected at 20% between the LLI group against the Normal ($p < 0.01$) and Happy THR groups ($p < 0.05$).

At 40%, differences were detected via the ANOVA ($p < 0.01$) and were found by the Tukey to exist between the LLI patients relative to the Happy THR ($p < 0.02$) and Normal ($p < 0.01$) patients. The 60% interval was found to have statistically significant differences between the Normal and LLI group ($p < 0.01$). Overall, the greatest gait asymmetry was observed in the Symptomatic LLI patients, who also showed the greatest variability in results.

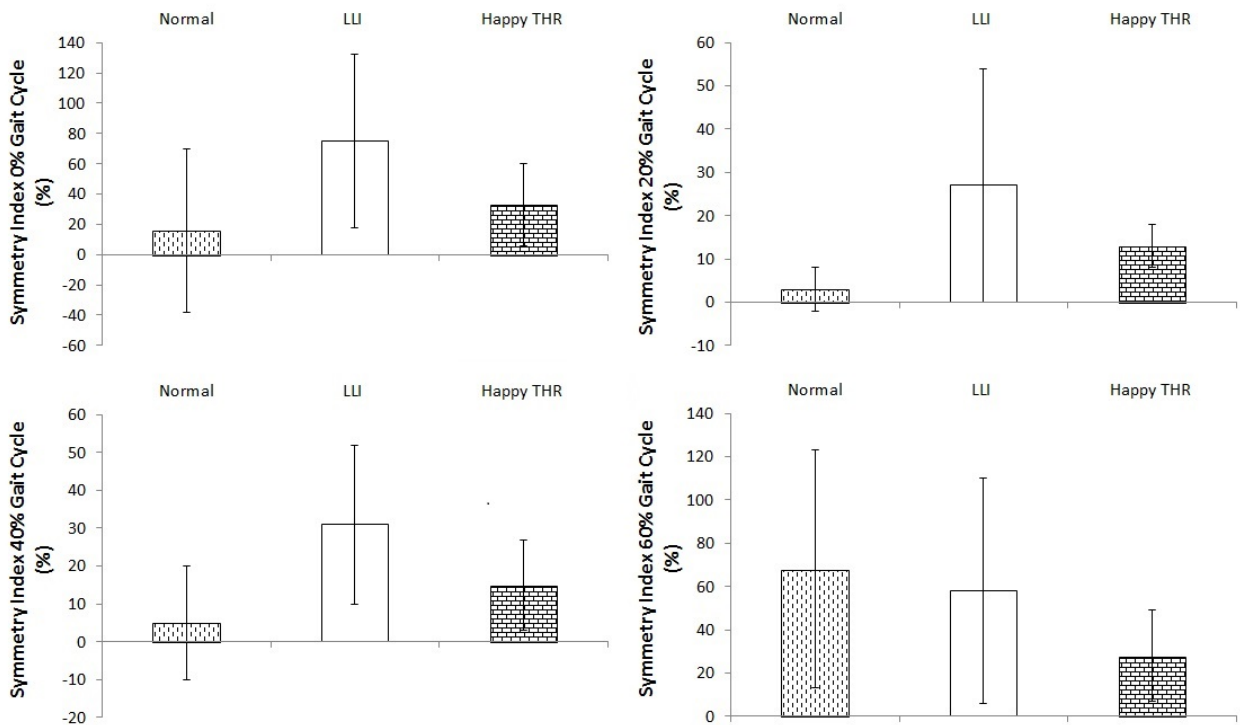


Figure 90: Hip JRF symmetry index results following normalisation for bodyweight for all patient groups at 0%, 20%, 40% and 60% gait intervals together with standard errors

Figure 91 shows the average hip JRF normalised for body weight for each group at heel strike, mid-stance and toe off. The Normal group produced the greatest amount of hip force at heel strike ($0.61 \text{ N/kg} \pm 0.17$) with the least being produced by the operated side of the LLI patients ($0.31 \text{ N/kg} \pm 0.23$). A one-way ANOVA at the 5% significance level found a p-value of <0.01 . A Tukey post-hoc test demonstrated that these differences were between the Normal group and both the operated and non-operated sides of the LLI patients.

Results at mid-stance differed more than heel strike, with the greatest average force occurring on the non-operated side of the LLI patients ($2.11 \text{ N/kg} \pm 0.52$) and the smallest in the Normals ($1.41 \text{ N/kg} \pm 0.30$). The greatest variability was in the LLI group. A one-way ANOVA test at the 5% significance level demonstrated statistically significant differences between the groups ($p < 0.01$). A Tukey test revealed that these differences existed between the Normal group and both the operated and non-operated sides of the LLI group.

At toe off the greatest average hip JRF across the groups occurred in Normal patients ($0.65 \text{ N/kg} \pm 0.17$) and the smallest in the non-operated side of the LLI patients ($0.34 \text{ N/kg} \pm 0.18$). The greatest standard deviation and hence variability was in the Happy THR group (0.23 N/kg). A

one-way ANOVA test found a statistically significant result existed between the groups ($p < 0.02$). A Tukey post-hoc determined that this difference was between the Normal group and both the operated and non-operated sides of the LLI group.

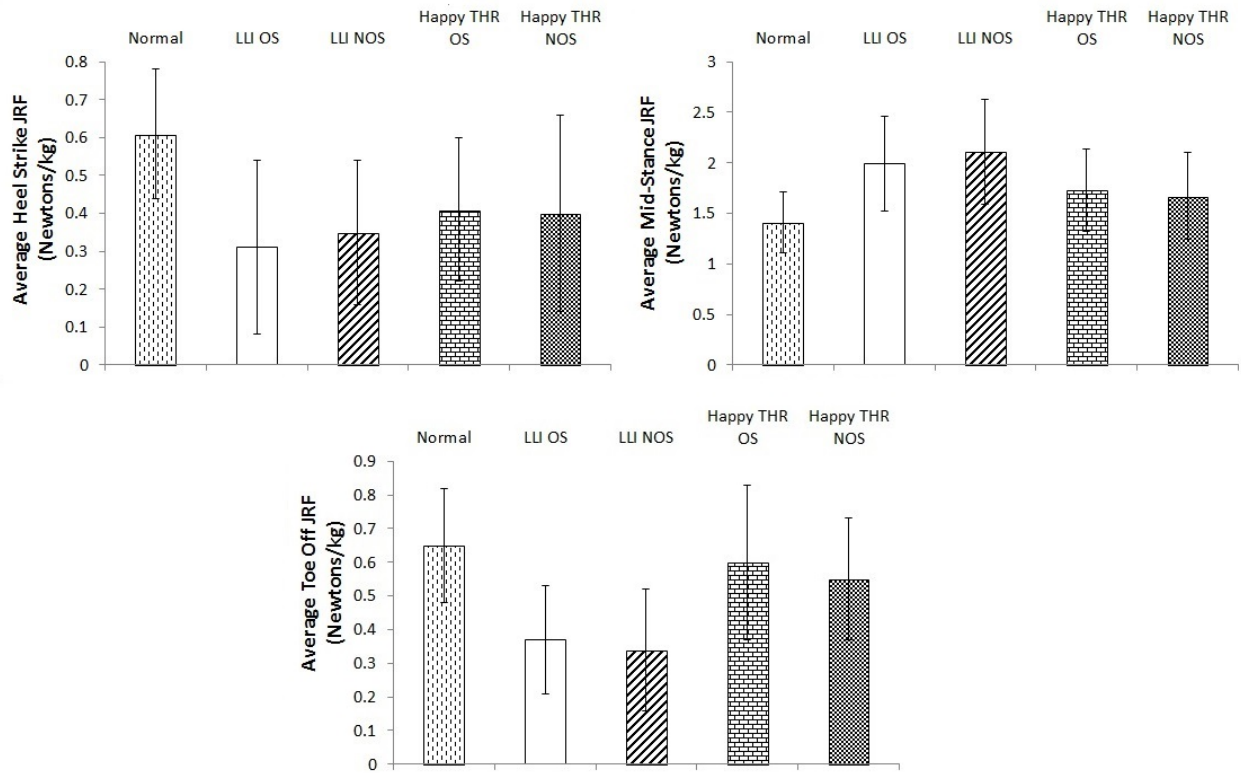


Figure 91: Hip JRF results following normalisation for bodyweight for all patient groups at heel strike, mid-stance and toe off for Normal, LLI Operated Side (LLI OS), LLI Non-Operated Side (LLI NOS), Happy THR Operated Side (Happy THR OS) and the Happy THR Non-Operated Side (Happy THR NOS) groups together with standard errors

Figure 92 illustrates the raw data for both limbs for the operated groups together with those of Normal patients. The LLI and Happy THR group, as with VGRFs, demonstrated smaller JRFs and greater variability in results relative to Normal controls. The operated side of the LLI group showed slightly less variability in terms of average gait cycle standard deviation (0.43 N/kg) than the non-operated side (0.44 N/kg). Smaller variability was present in the Normal patients (0.36 N/kg) and both on the operated (0.38 N/kg) and non-operated (0.34 N/kg) sides of the Happy THR group.

Within the raw results there were some outliers. This is particularly seen in (A) in Figure 92, where two LLI patients showed a complete loss of the characteristic hip JRF curve shape, with only a single peak being present. In addition, (C) and (D) have a Happy THR patient with excessive JRF at the 1st peak. Likewise, there were 3 patients in the Normal group who demonstrated excessive

JRF at the 2nd peak.

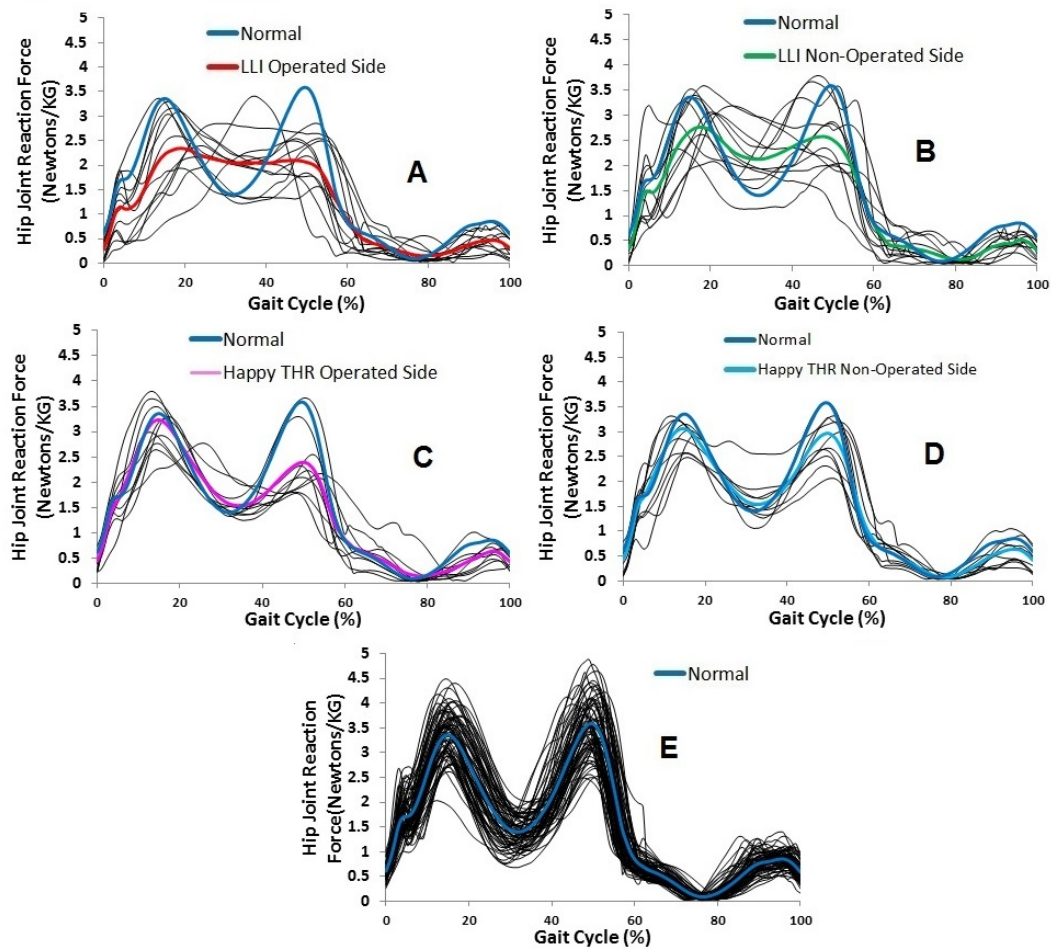


Figure 92: Raw hip JRF results for all three groups over a normalised gait cycle between consecutive heel strikes of the same foot. (A) Operated side LLI patients (B) Non-operated side LLI patients, (C) Operated side Happy THR patients (D) Non-operated side Happy THR patients (E) Normal healthy patients. Average lines are added to each graph for the particular group being studied together with the average Normal patient result. Results have been normalised for bodyweight.

6.5 Results - Joint Moments

6.5.1 Hip Flexion-Extension

Figure 93 shows the average hip flexion-extension joint moments during gait when comparing all three clinical groups. Normal patients demonstrated 37% greater average peak flexion (-) moment than the operated side of the Happy THR group which in itself showed 42% greater flexion moment than the operated side of the Symptomatic LLI group. The non-operated sides for Happy THR and LLI groups showed 10% and 30% greater peak hip flexion moment compared to their corresponding operated sides respectively. Confidence intervals were widest for the Symptomatic LLI group. Swing phase results were similar across groups.

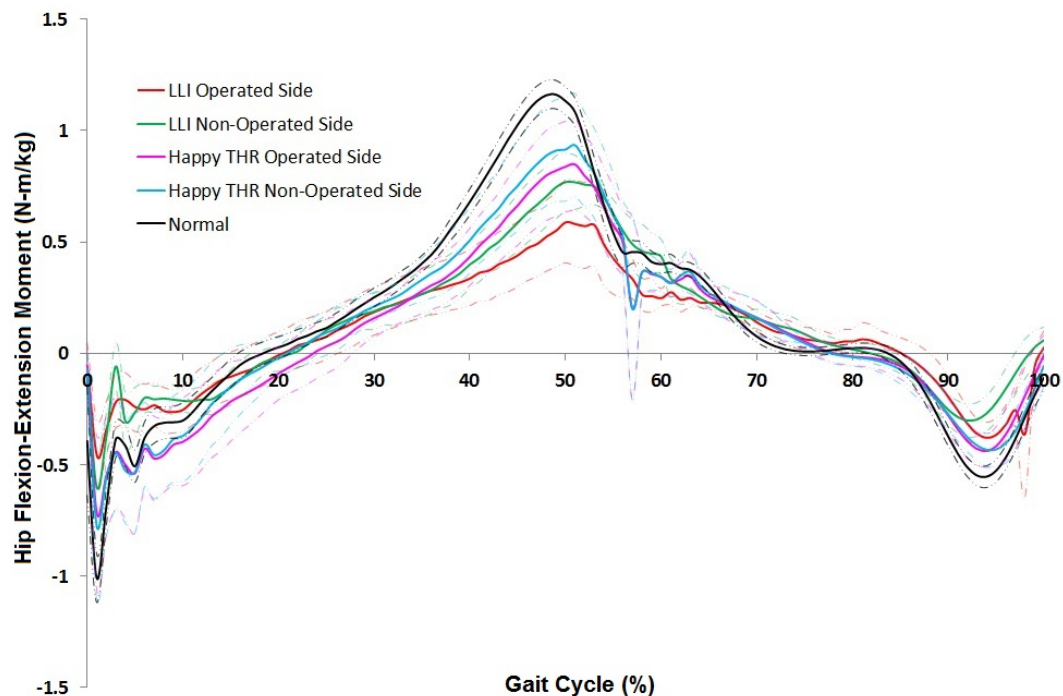


Figure 93: Average hip flexion (+)-extension (-) moments during gait for all patient groups together with 95% confidence intervals over a normalised gait cycle between consecutive heel strikes of the same foot. Results have been normalised for bodyweight.

Figure 94 shows a comparison of the raw results in terms of maximum hip flexion and extension moments. Raw results are shown in Figure Figure 95. Maximum flexion moment was found to differ between the Normal healthy individuals and all other groups ($p < 0.01$) using the one-way ANOVA and Tukey post-hoc. For maximum extension moment, a significant difference was found between the Normal group and the operated side of the LLI patients ($p < 0.01$). There were however many outliers, especially in the LLI patients.

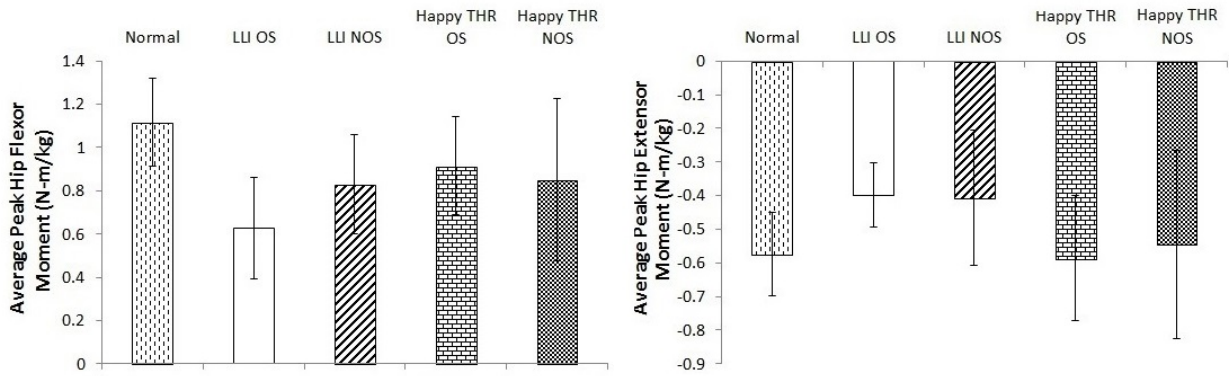


Figure 94: Peak hip flexion (+)-extension (-) moments in terms of averaged raw results between consecutive heel strikes of the same foot over a normalised gait cycle for all patients in each group. Results have been adjusted for bodyweight. Standard errors are included.

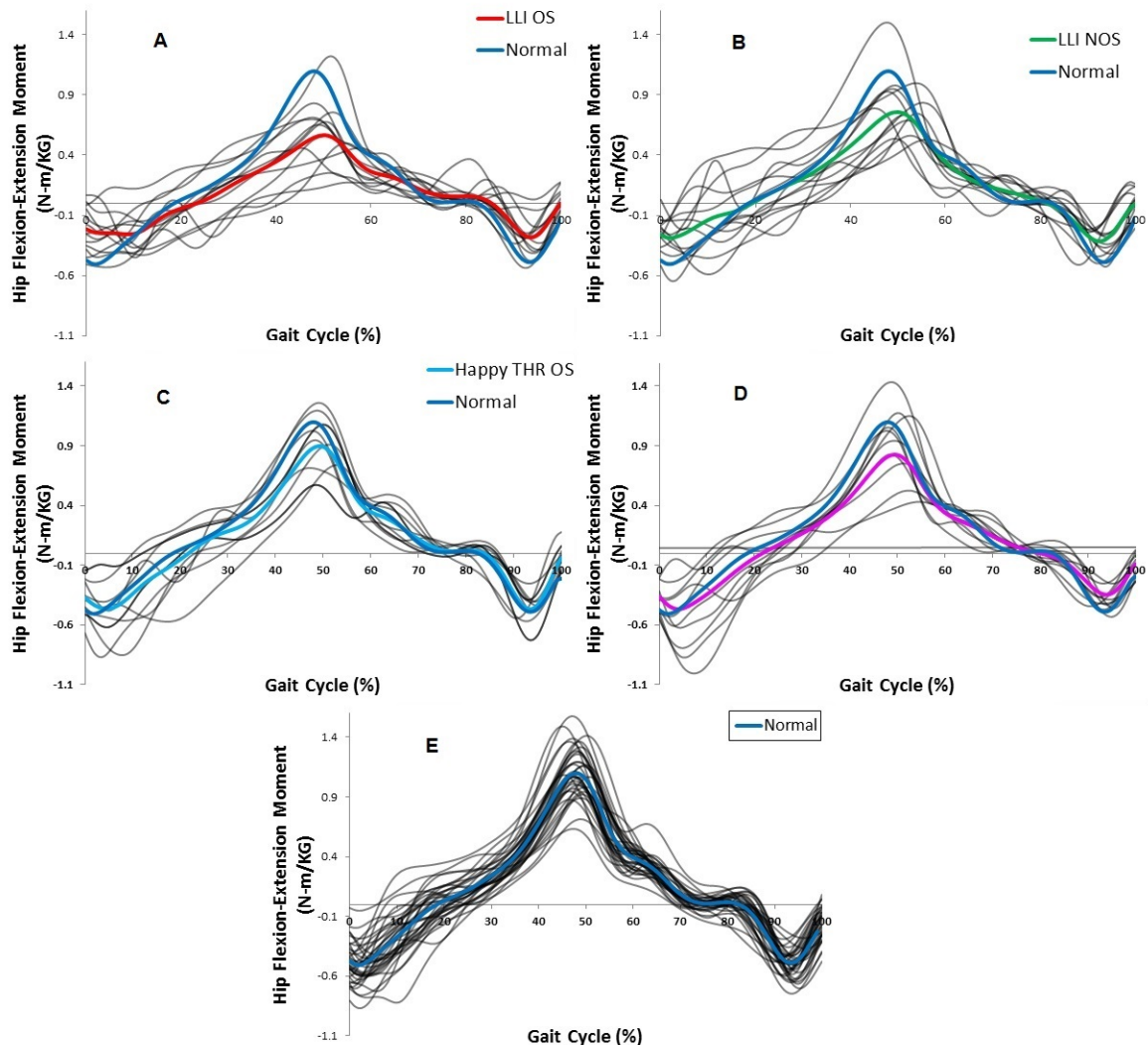


Figure 95: Raw hip flexion (+)-extension (-) moment results for all three groups over a normalised gait cycle between consecutive heel strikes of the same foot. (A) Operated side LLI patients (B) Non-Operated side LLI patients (C) Operated side Happy THR patients (D) Non-Operated side Happy THR patients (E) Normal Healthy Patients. Average lines are added to each graph for the particular group being studied together with the average Normal patient result. Results have been normalised for bodyweight.

6.5.2 Hip Abduction-Adduction

Figure 96 shows the average hip abduction-adduction joint moments during gait. The Normal group produced a smaller second hip abduction curve peak relative to the other groups, with it being 31% smaller than that of the non-operated side LLI patient average. Both the operated and non-operated averages for the Happy THR group showed a characteristic double peak shape which was not visible for the average operated side LLI results. Normal patients demonstrated greater adduction moment relative to all other groups, with the LLI operated side showing reduction by a factor of 5.

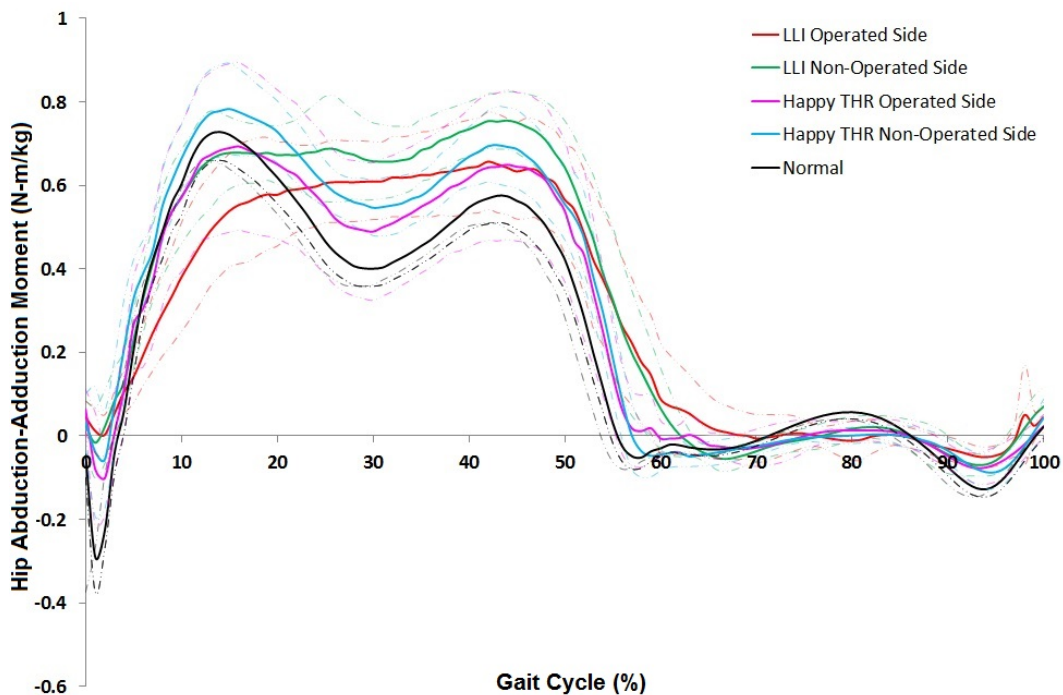


Figure 96: Hip abduction (+)-adduction (-) moments during gait for all patient groups together with 95% confidence intervals over a normalised gait cycle between consecutive heel strikes of the same foot. Results have been normalised for bodyweight.

Figure 97 shows a comparison of the results in terms of maximum raw hip abduction and adduction moments, which can be seen in Figure 98. No statistically significant differences were detected using the one-way ANOVA in terms of maximum hip abduction moment ($p > 0.05$). A statistically significant difference was however detected for maximum hip adduction moment ($p < 0.01$), with a Tukey test determining that this was between the Normal group and all other groups.

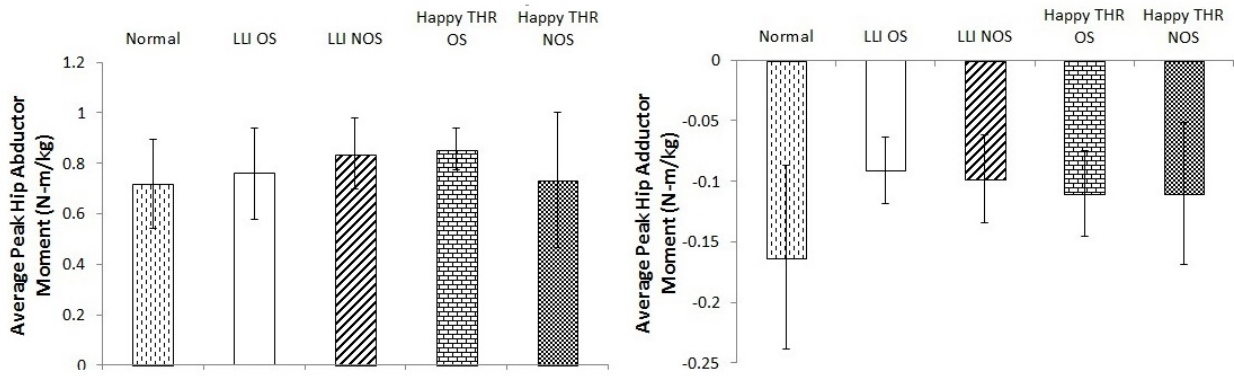


Figure 97: Peak hip abduction (+) - adduction (-) moments in terms of averaged raw results between consecutive heel strikes of the same foot over a normalised gait cycle for all patients in each group. Results have been adjusted for bodyweight. Standard errors are included.

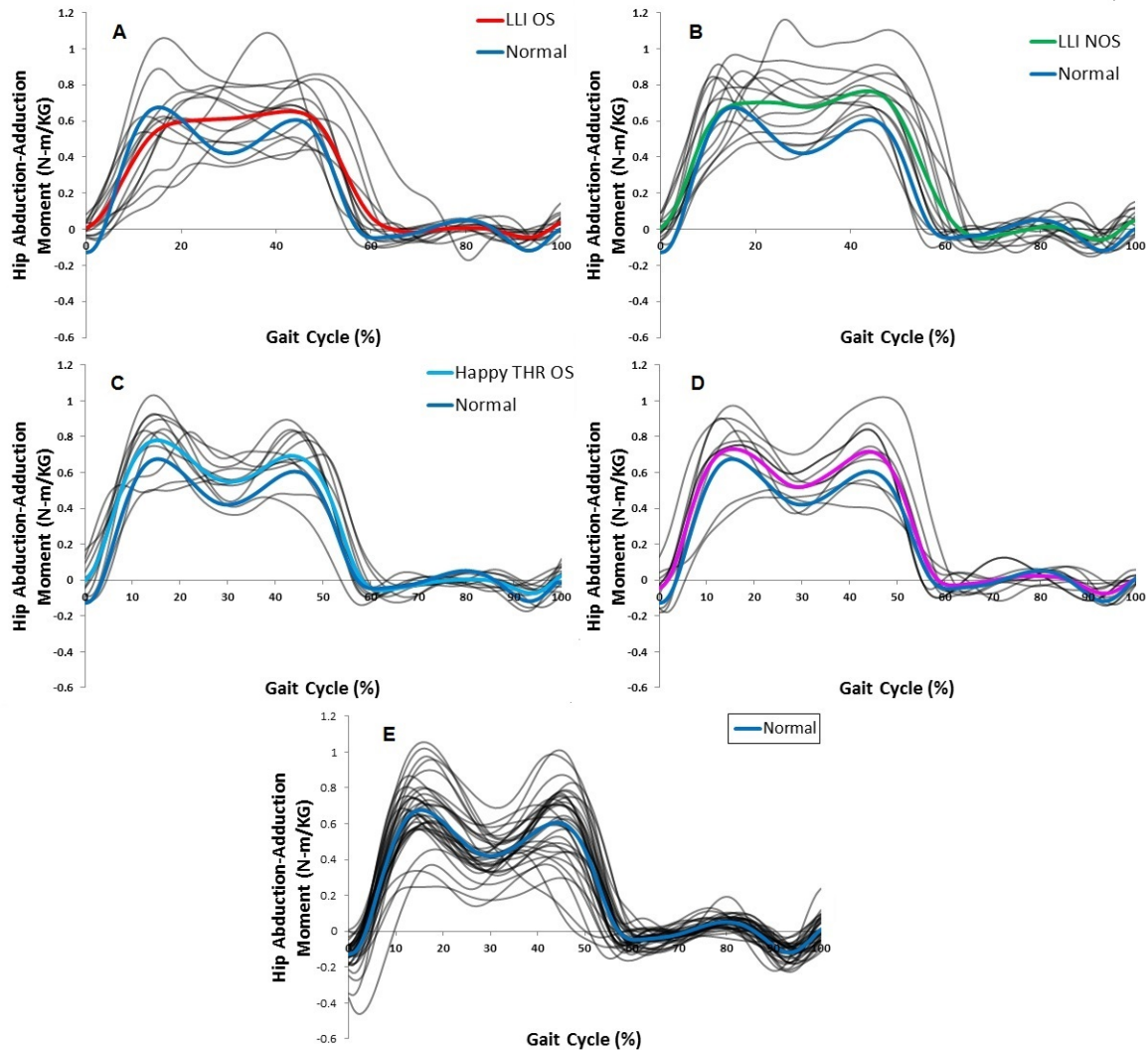


Figure 98: Raw hip abduction (+)-adduction (-) moment results for all three groups over a normalised gait cycle between consecutive heel strikes of the same foot. (A) Operated side LLI patients (B) Non-Operated side LLI patients (C) Operated side Happy THR patients (D) Non-Operated side Happy THR patients (E) Normal Healthy Patients. Average lines are added to each graph for the particular group being studied together with the average Normal patient result. Results have been normalised for bodyweight.

6.5.3 Knee Flexion-Extension

Figure 99 shows the average knee flexion-extension joint moments during gait. A general trend can be seen with the Normal and Happy THR groups showing very similar curve shapes with comparable moment levels. The Symptomatic LLI group however differed in that it showed a reduced extension moment during the stance phase, with an average peak extensor magnitude 119% less than that of Normal patients. Similar results were also present for the maximum knee flexion moment, with the LLI group on average producing a 57% decrease relative to the Normal cohort. Wide confidence intervals were computed, with the largest being for the operated side of the Symptomatic LLI group (0.2 N-m/kg).

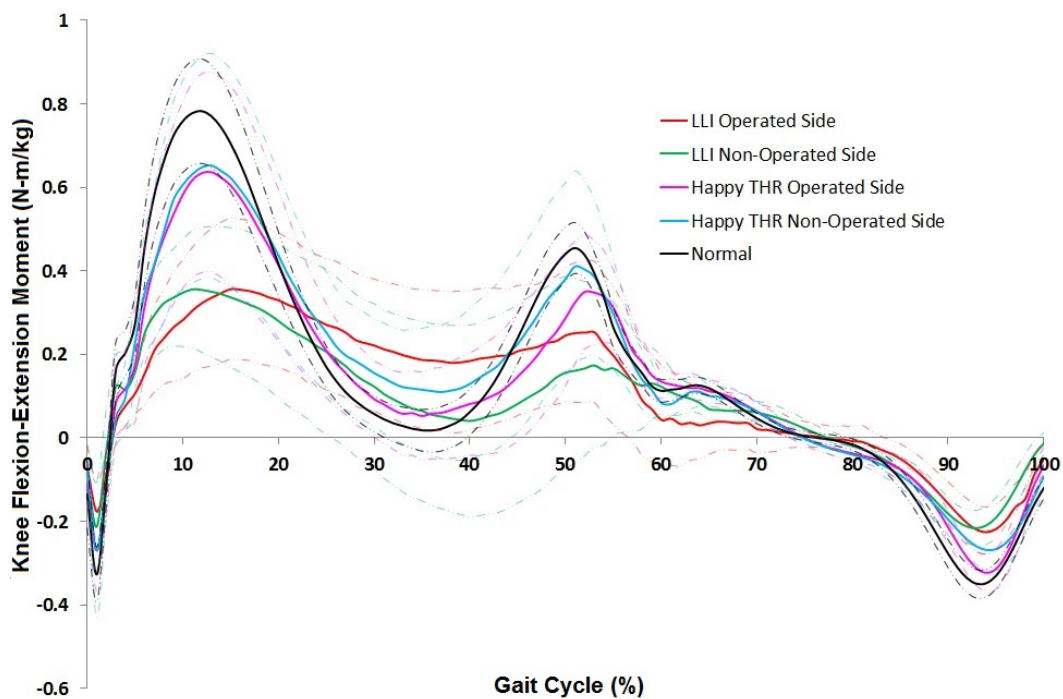


Figure 99: Knee flexion (-)-extension (+) moment during gait for all patient groups together with 95% confidence intervals over a normalised gait cycle between consecutive heel strikes of the same foot. Results have been normalised for bodyweight.

Raw results are seen in Figure 101, with Figure 100 comparing maximum knee flexion-extension moments. Statistically significant differences were found to exist between the Normal and Happy THR groups against the operated ($p < 0.01$) and non-operated sides ($p < 0.01$) of the LLI group with regards to maximum knee extension moment. A statistically significant difference was also detected for maximum knee flexion moment. Significant differences were found between the Happy THR non-operated side and the operated ($p < 0.01$) and non-operated sides ($p < 0.01$) of the LLI group. Significant differences were also found between the Normal group against the Happy THR operated side ($p < 0.02$), LLI operated side ($p < 0.01$) and LLI non-operated side ($p < 0.01$).

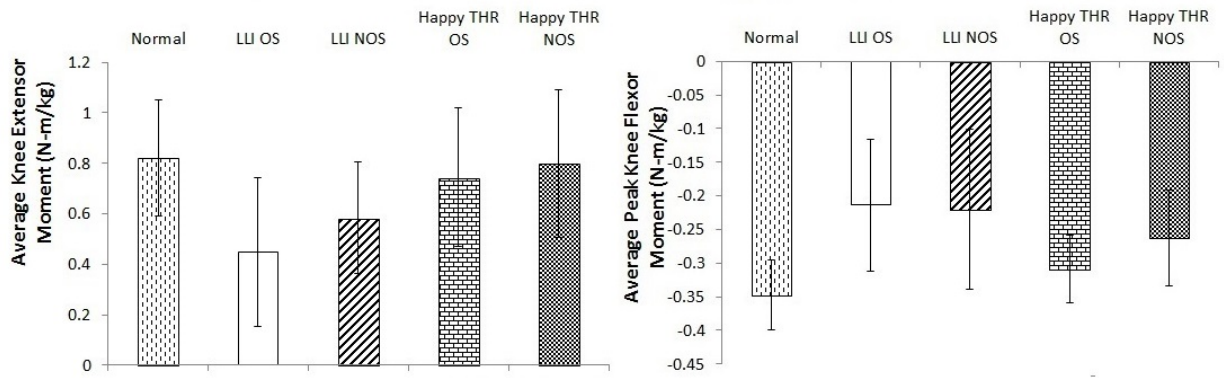


Figure 100: Peak knee flexion-extension moments in terms of averaged raw results between consecutive heel strikes of the same foot over a normalised gait cycle for all patients in each group. Results have been adjusted for bodyweight. Standard errors are included.

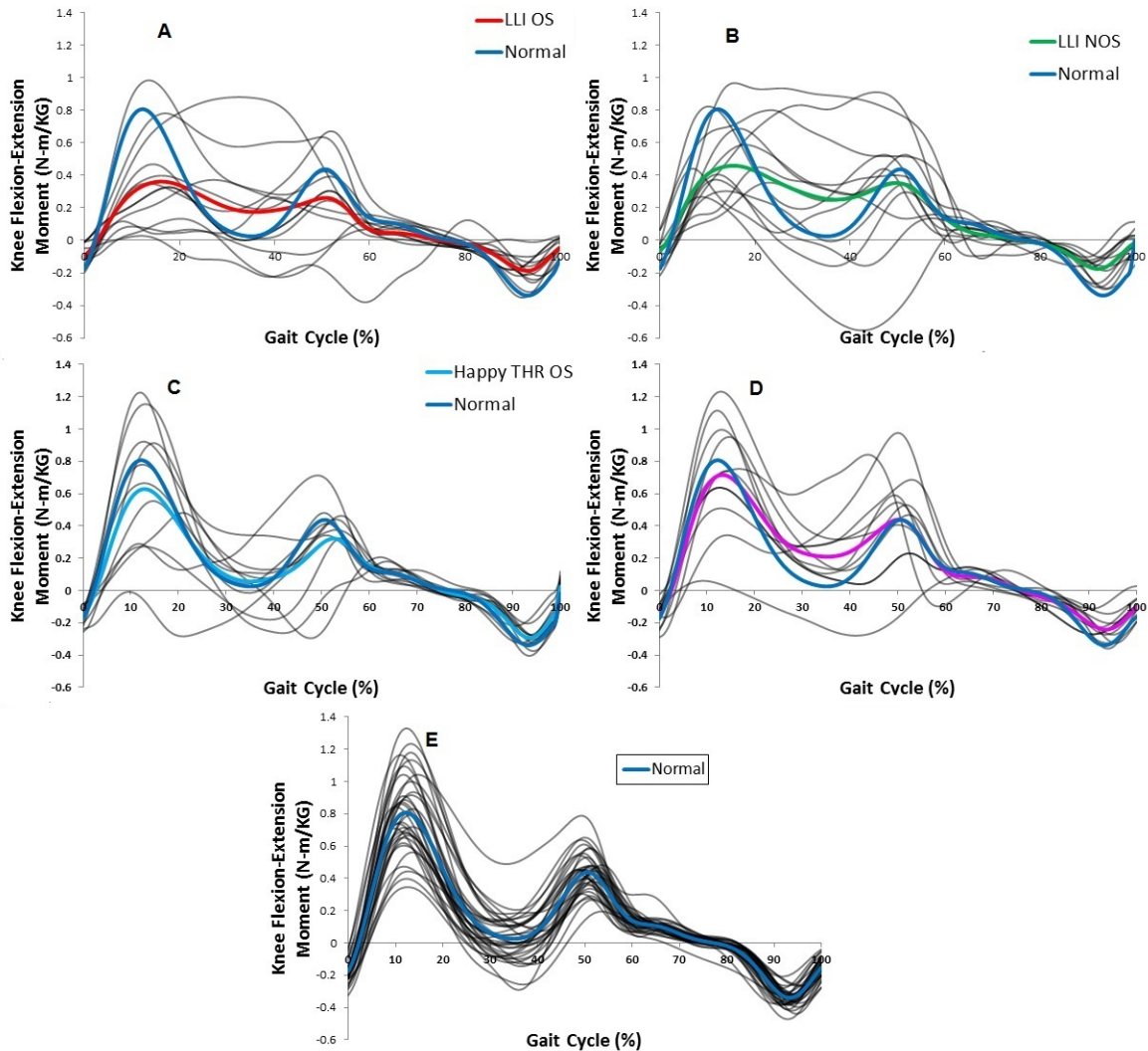


Figure 101: Raw knee flexion (-)-extension (+) moment results for all three groups over a normalised gait cycle between consecutive heel strikes of the same foot. (A) Operated side LLI patients (B) Non-Operated side LLI patients (C) Operated side Happy THR patients (D) Non-Operated side Happy THR patients (E) Normal Healthy Patients. Average lines are added to each graph for the particular group being studied together with the average Normal patient result. Results have been normalised for bodyweight.

6.5.4 Ankle Dorsi-Plantar Flexion

Figure 102 shows ankle dorsi-plantarflexion joint moments during gait. A general trend can be seen with the non-operated side of the Happy THR and Normal groups demonstrating the greatest ankle plantarflexion moment, followed by the operated side of the Happy THR patients. The non-operated side of the LLI group, unlike that of the Happy THR patients, was significantly influenced leading to a 34% reduction in plantarflexion moment relative to that of Normal healthy individuals.

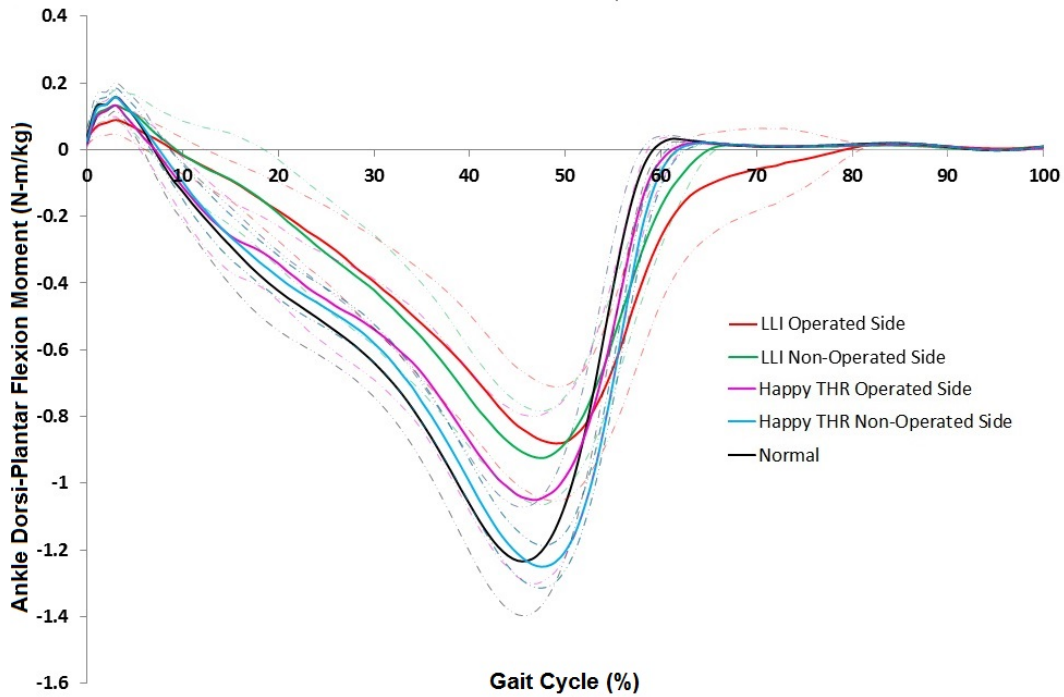


Figure 102: Ankle dorsi (+)-plantar (-) flexion moments during gait for all patient groups together with 95% confidence intervals over a normalised gait cycle between consecutive heel strikes of the same foot. Results have been normalised for bodyweight.

Figure 103 shows a comparison of the raw results in terms of maximum ankle dorsi-plantarflexion moments, with Figure 104 illustrating the raw curves. Statistically significant differences were found with regards to maximum average ankle dorsiflexion moment ($p < 0.01$) using the one-way ANOVA. A Tukey post-hoc revealed that the differences were between the operated side of the LLI group and all other groups. Maximum average ankle plantarflexion moment was found to significantly differ between the Normal group and the operated ($p < 0.01$) and non-operated sides ($p < 0.01$) of the LLI patients.

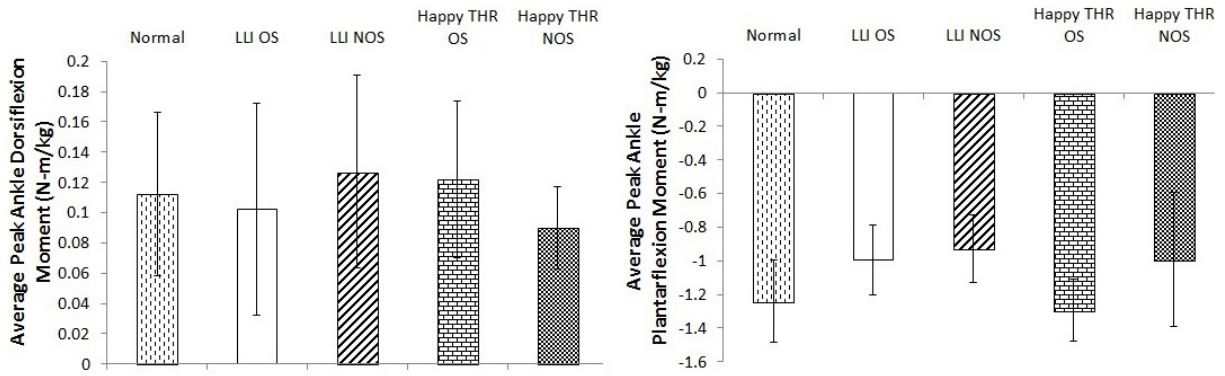


Figure 103: Peak ankle dorsi (+)-plantar (-) flexion moments in terms of averaged raw results between consecutive heel strikes of the same foot over a normalised gait cycle for all patients in each group. Results have been adjusted for bodyweight. Standard errors are included.

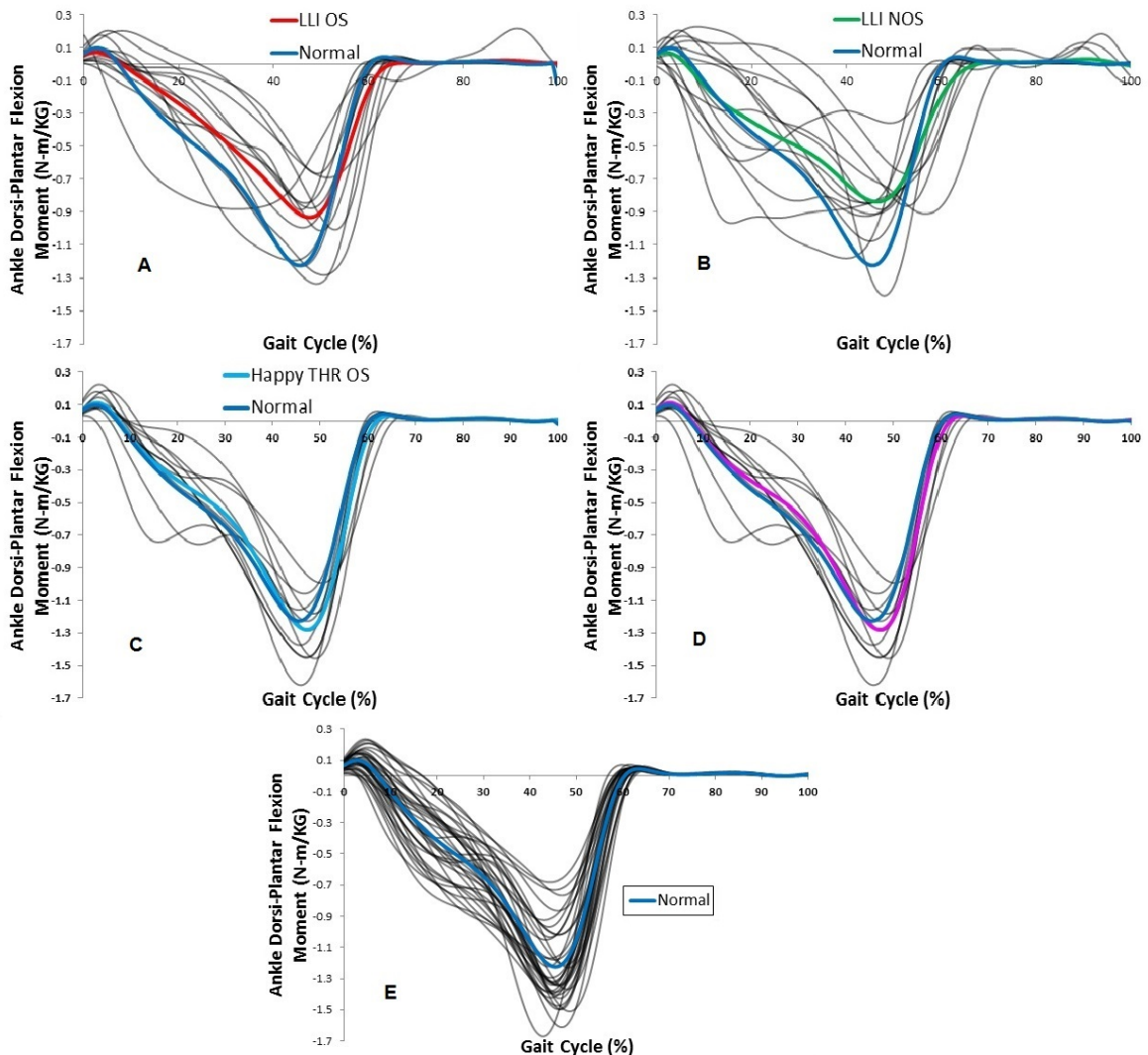


Figure 104: Raw ankle dorsi (+)-plantar (-) flexion moment results for all three groups over a normalised gait cycle between consecutive heel strikes of the same foot. (A) Operated side LLI patients (B) Non-Operated side LLI patients (C) Operated side Happy THR patients (D) Non-Operated side Happy THR patients (E) Normal Healthy. Average lines are added to each graph for the particular group being studied together with the average Normal patient result. Results have been normalised for bodyweight.

6.6 Results - Gait Events (Moments)

6.6.1 Heel Strike

No statistically significant differences were detected for joint moments using the one-way ANOVA in terms of hip flexion-extension ($p > 0.05$), hip abduction-adduction ($p < 0.06$), knee flexion-extension ($p > 0.05$) or ankle dorsi-plantarflexion ($p > 0.05$). Results can be seen in Figure 105.

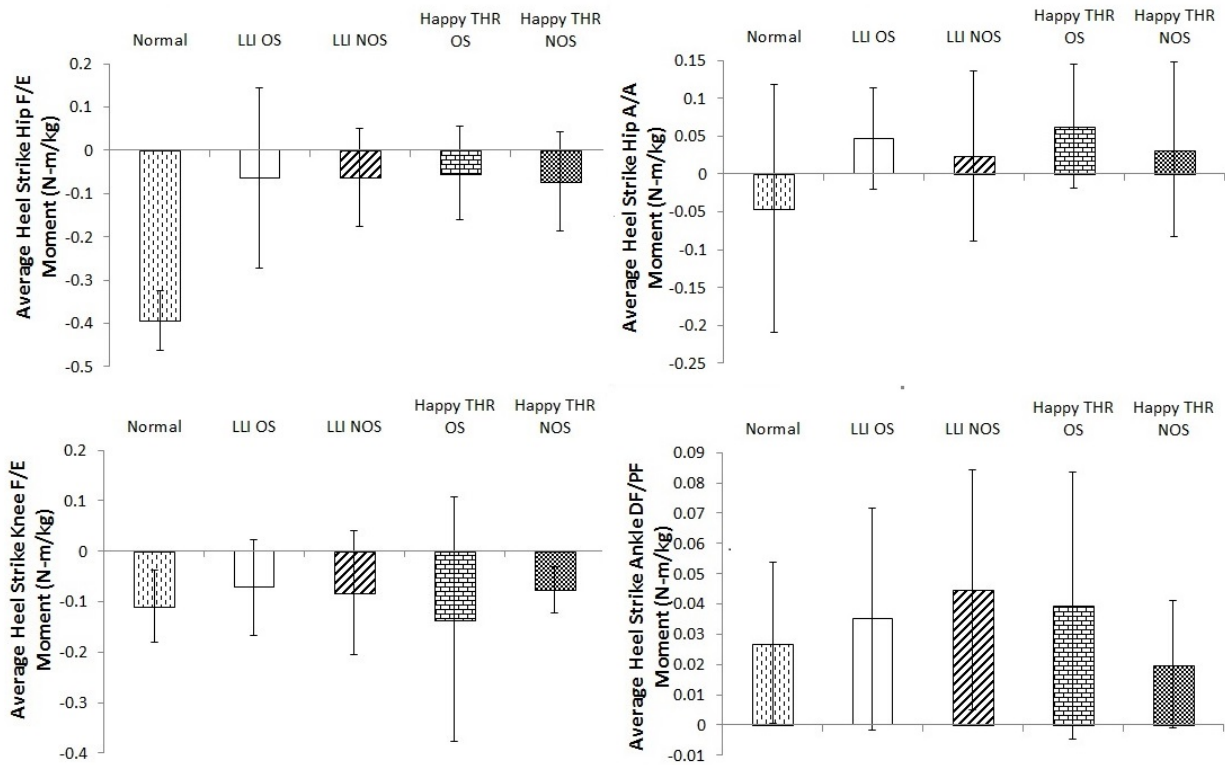


Figure 105: Average heel strike joint moments with standard errors for the Normal, Happy THR and Symptomatic LLI groups. Results have been normalised for bodyweight.

6.6.2 Mid-Stance

No statistically significant differences were detected for joint moments using the one-way ANOVA in terms of hip flexion-extension ($p > 0.05$), hip abduction-adduction ($p > 0.05$) or knee flexion-extension ($p > 0.05$). A statistically significant result was however found for ankle dorsi-plantar flexion ($p < 0.03$) for the operated side of the Happy THR group against the operated side of the Symptomatic LLI group and Normal healthy people. Results can be seen in Figure 106.

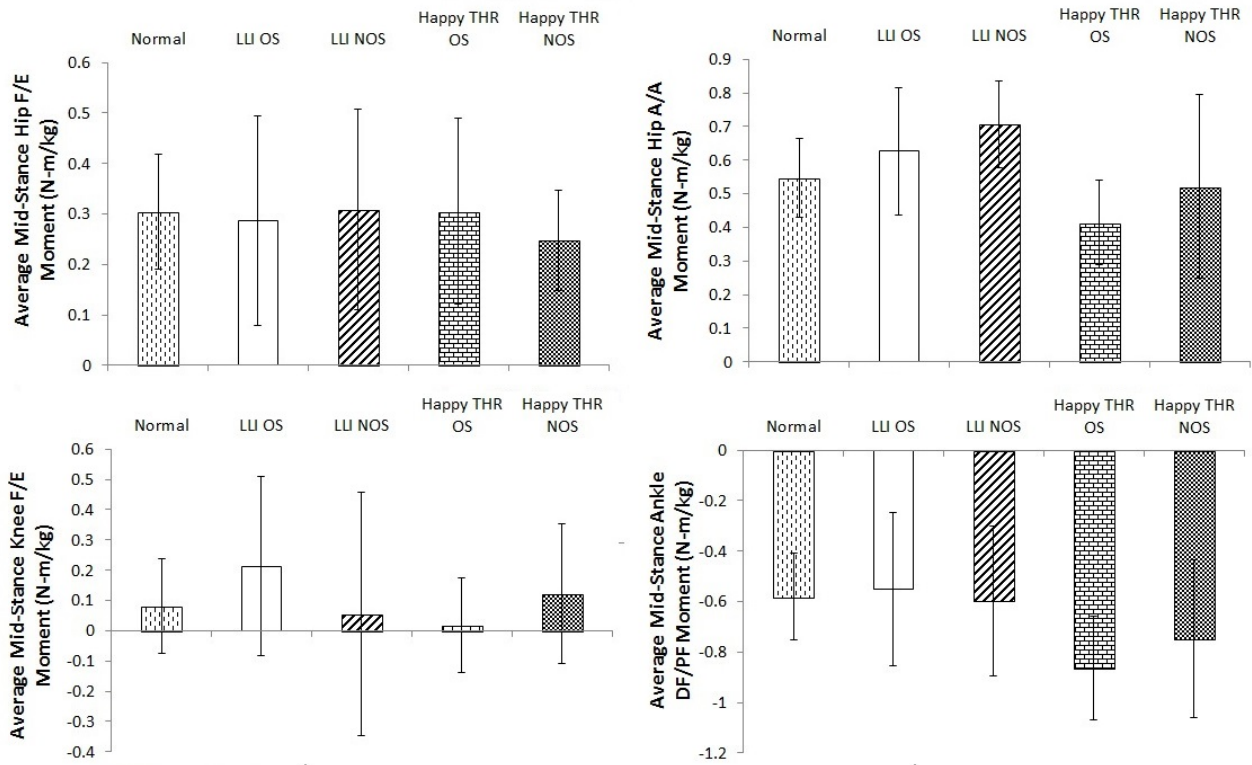


Figure 106: Average mid-stance joint moments with standard errors for the Normal, Happy THR and Symptomatic LLI groups. Results have been normalised for bodyweight.

6.6.3 Toe Off

Statistically significant differences were detected for moments in terms of hip flexion-extension ($p < 0.01$), hip abduction-adduction ($p < 0.01$) and knee flexion-extension ($p < 0.01$). Differences occurred between the Normal group and all other groups. No statistically significant differences were detected at toe off in terms of ankle dorsi-plantar flexion ($p > 0.05$). Results can be seen in Figure 107.

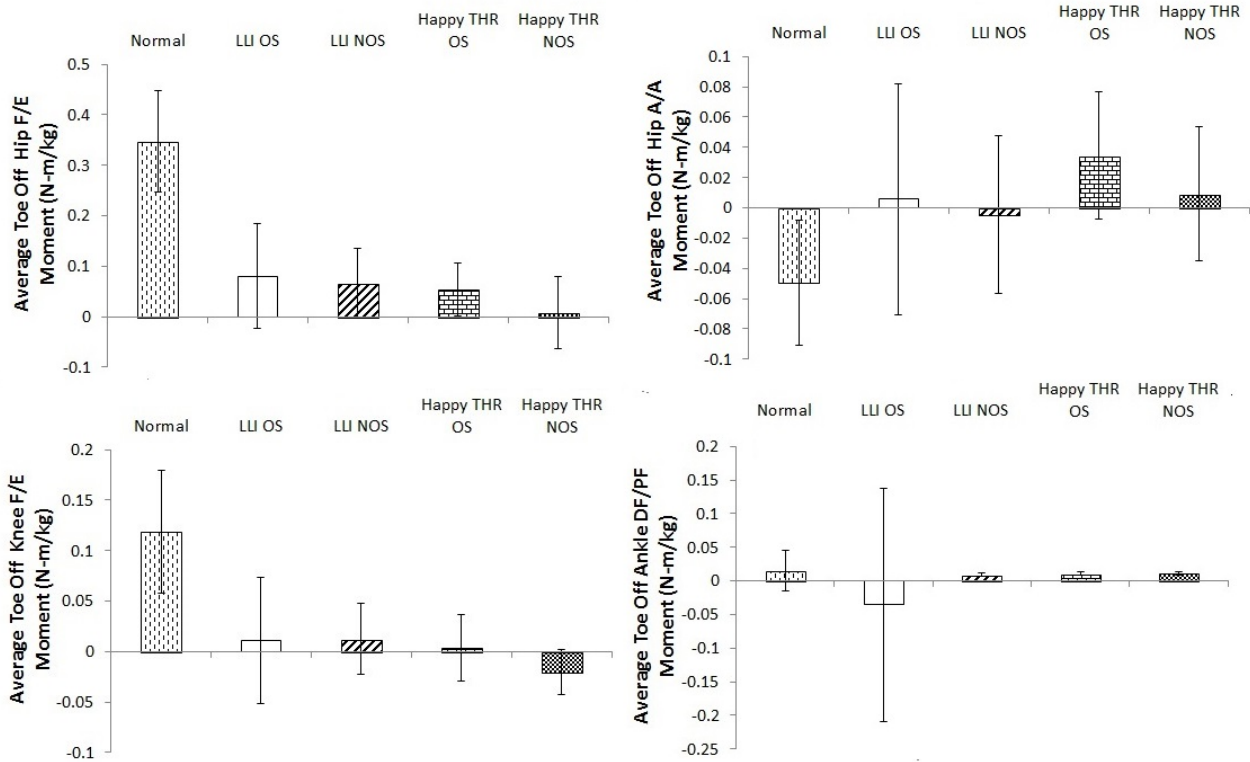


Figure 107: Average toe off joint moments with standard errors for the Normal, Happy THR and Symptomatic LLI groups. Results have been normalised for bodyweight.

6.7 Discussion

As with kinematics, kinetic results in literature for patients following THR vary due to a variety of factors. One of the major variables is patient recovery time, with individuals over the course of time recovering in terms of their kinetic output to similar levels as Normal patients. Improvements are slow with changes in gait occurring from 10 days to 10 years post-surgery [179]. For instance, Lugade et al. [211] found that when measuring a cohort of THR patients VGRFs at both 6 weeks and 16 weeks postoperatively, greater symmetry was shown at the latter measurement. Likewise, Meneghini et al. [163] found that surgical technique influenced the amount of VGRF seen post-surgery. Results in terms of joint moments have generally been more consistent, with the literature review by Kolk et al. [216] concluding that nearly all studies agree on findings for hip joint moments in both the sagittal and frontal planes.

The Happy THR and Symptomatic LLI groups were all recruited for clinical gait analysis at a minimum one year postoperatively. The variability produced in the VGRFs, JRFs, joint moments and in the gait symmetry index thus may be reflective of patients at different stages of the recovery time line. However the analysis completed in this study assumes all patients were at the same level of recovery and the results suggest that LLI causes characteristic gait abnormalities.

6.7.1 Comparing to Literature I

To assess the validity of the data produced during this study, a comparison was made against the results of Bovi et al. [443]. As Bovi et al.¹¹ only used normal healthy individuals, our comparison against Bovi et al. was against our Normal controls.

Figure 108 compares kinetic results between the Normal patient group and that of Bovi et al. For VGRFs (**A**), curves differ in shape with the 2nd peak of the results produced by Bovi exceeding the magnitude of the 1st peak, opposite to what occurred in the Normal group. The Normal patient group showed greater force at the 1st peak (1.2 N/kg±0.09) than Bovi (1.08 N/kg±0.08), which was found to be statistically significant using the one-way ANOVA (p<0.01). Results were almost identical at the 2nd of the two peaks between the Normal group (1.15 N/kg±0.08) and Bovi et al. (1.15 N/kg±0.08), where no statistical significance was found (p>0.05).

With regards to hip flexion-extension moments (**B**), both cohorts match up closely; there were however discrepancies present at initial heel strike and towards the end of the swing phase, where the Normal group showed increased hip flexion moment. In addition, the Normal group showed a greater peak flexion moment. Comparing peak flexion moments between the groups, a one-way ANOVA detected a statistically significant difference (p<0.01) between the results of the Normal (1.16 N-m/kg±0.19) group and Bovi (0.74 N-m/kg±0.22). The results of Bovi et al. also had wider confidence intervals indicating a greater variability in the subject cohort.

It can also be seen that the Normal group exhibited some hip adduction moment (**C**) at heel strike whilst this is absent in the results as produced by Bovi. In addition, the 1st and 2nd hip abduction peaks for Bovi et al. exceeded those of the Normal patients. A significant difference (p<0.02) was found at the 1st peak between the Normal group (0.72 N-m/kg±0.20) and the results of Bovi (0.80 N-m/kg±0.16). A significant difference (p<0.01) was also found at the 2nd peak between the Normal group (0.58 N-m/kg±0.19) and the results of Bovi (0.82 N-m/kg±0.20).

Likewise, Figure 108 depicts the results of both the average Normal patient and that of Bovi with regards to knee flexion-extension moment (**D**). The main differences between the curves was at the beginning and ending of the gait cycle together with the two peaks. Normal patients also showed greater peak knee extension moment at the 1st (0.78 N-m/kg±0.38) and 2nd (0.45 N-m/kg±0.18)

¹¹Further details of the study by Bovi et al. are given in the *Kinematics & Temporal-Spatial Parameters* chapter on page 132

peaks in and around the mid-stance period relative to the 1st ($0.42 \text{ N-m/kg} \pm 0.19$) and 2nd ($0.22 \text{ N-m/kg} \pm 0.10$) peaks as shown by Bovi, which were both found to be statistically significant ($p < 0.01$). Results also indicated that the Normal group demonstrated smaller peak plantarflexion moment (**E**) ($-1.23 \text{ N-m/kg} \pm 0.28$) than the cohort used by Bovi ($-1.32 \text{ N-m/kg} \pm 0.12$). This was found to be not statistically significant at the 5% level using the one-way ANOVA ($p > 0.05$). The variability in the Normal group was larger.

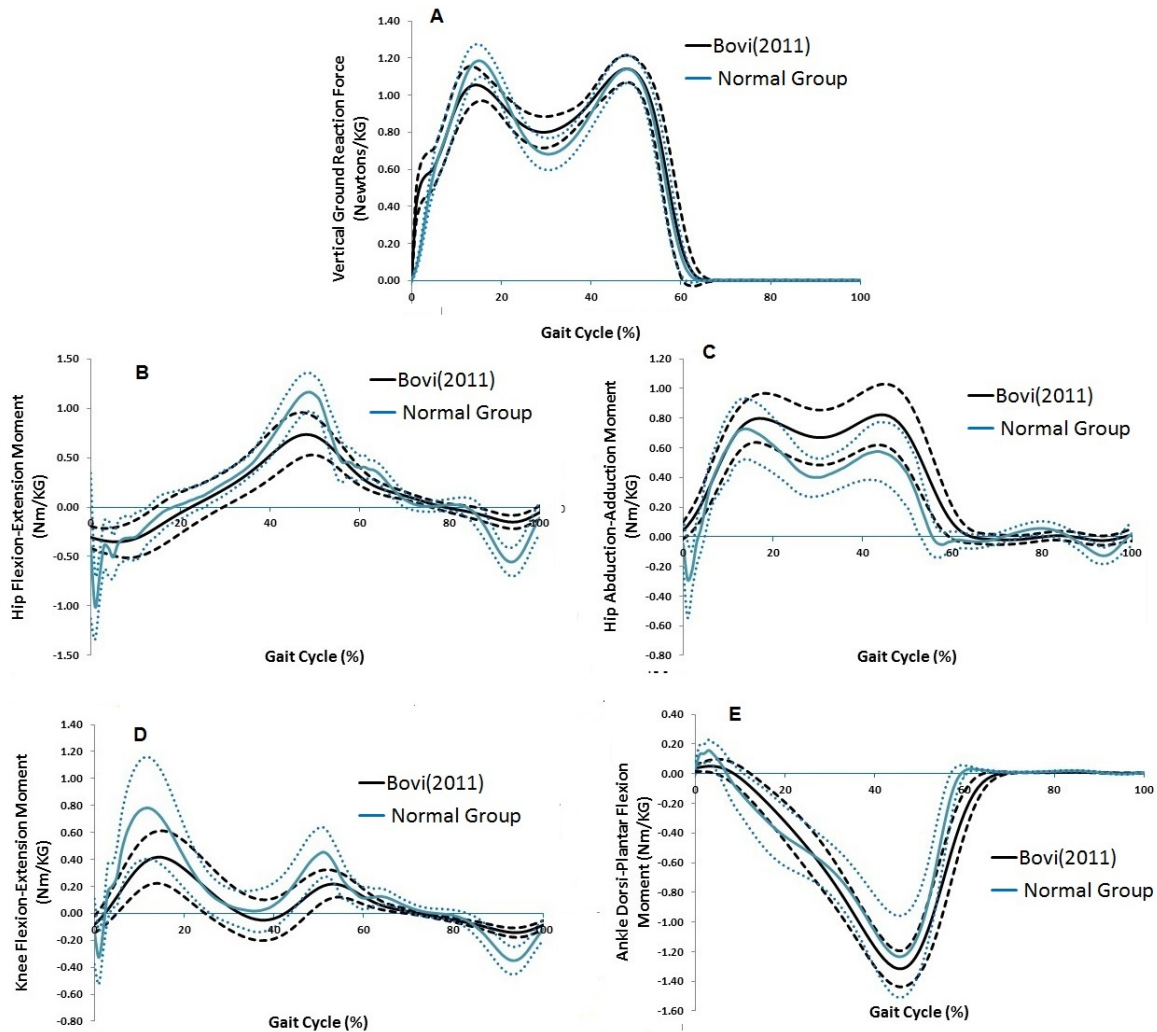


Figure 108: Average VGRFs (A), hip flexion (+) - extension (-) moments (B), hip abduction (+) - adduction (-) moments (C), knee flexion (+) - extension (-) moments (D) and ankle dorsi (+)-plantar (-) flexion moments (E) comparison between the Normal patient results to that of Bovi et al. over consecutive heel strikes normalised to 100 percentiles. Error intervals of ± 1 standard deviation are also plotted for each group. Results are normalised for bodyweight

Overall, the present results for the Normal group showed similarity relative to Bovi with regards to shape of moment curves, with there however being some significant differences at various gait instances. These differences can potentially be due to a number of reasons which are highlighted by Bovi et al. including differences in gait velocity (Normal 1.49m/s, Bovi 1.22m/s, statistically

significant using ANOVA at 5% significance level), study design together with the use of different marker systems. The Normal group made use of the PiG model and had inverse dynamics calculations undertaken using the AnyBody software. Bovi used the Leardini marker set together with EMG's to measure muscle activations and hence forces, which contributed to moment calculations.

6.7.2 Comparing to Literature II

The PhD thesis by J.P Paul titled *Forces at the human hip joint*, remains one of the few studies which has analysed JRF for normal healthy individuals. For this reason, the Normal group was compared to the results of Paul in Figure 109. Comparing the results showed that Paul and the Normal group shared similar gait characteristics in terms of JRF curve shape, with it being apparent that Paul's curve would be almost identical to the Normal curve if it was shifted slightly to the left.

Results for the Normal group and Paul demonstrated a greater 2nd peak than 1st. The 1st peak produced an average JRF value of 3.22 N/kg \pm 0.05 for Normal patients and 3.00 N/kg for the results produced by Paul. The 2nd peak produced an average JRF value of 3.62N/kg \pm 0.13 for Normal patients and 4.29 N/kg for the results produced by Paul. Statistical testing could not be undertaken as no standard deviation data was available for the data produced by Paul.

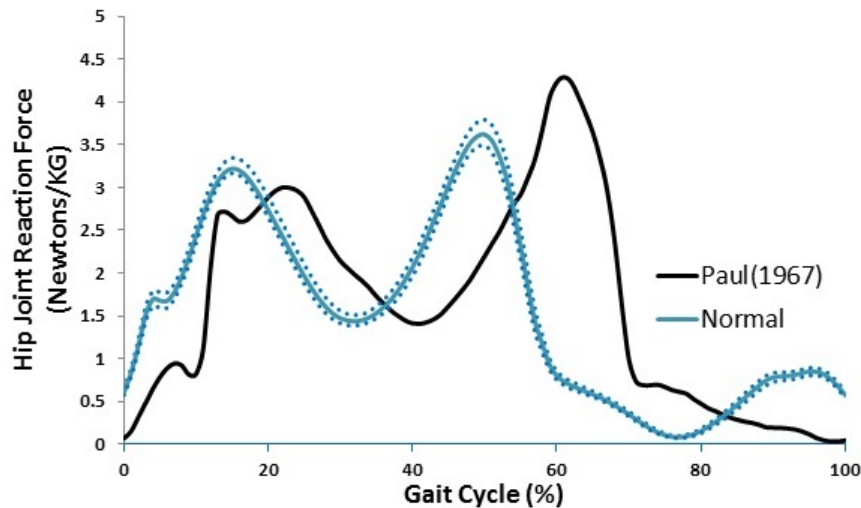


Figure 109: Resultant Hip JRF during gait for the average Normal group patient against Paul (1967) together with ± 1 standard error intervals over a normalised gait cycle between consecutive heel strikes of the same foot for the former. Results were normalised for bodyweight.

The greater detail in AnyBody with regards to muscle architecture and simulation of more

accurate muscle recruitment techniques¹² makes the results as produced from an inverse dynamics perspective more reliable than those of Paul. The inverse dynamics process used by Paul grouped muscles together in computing their JRFs and excluded certain smaller muscles (e.g. Quadratus Femoris, Gemellus Inferior) due to their small volume. Paul also assumed a linear muscle recruitment model with a maximum of two muscles recruited at any time instant for a given load. Errors in kinematics would have been amplified in both models during inverse dynamics when calculating variables such as segment acceleration through double differentiation of the initial displacement equations. There would have also been other errors in the marker placement motion capture process. Therefore it is difficult to establish which results are more accurate and reliable. For the remainder of this discussion, comparisons will be made against the Normal group and it will be assumed that these results are correct.

6.7.3 Vertical Ground Reaction Force

On average LLI patients showed smaller VGRFs relative to Happy THR patients who themselves showed smaller forces than Normal individuals. In addition, the average LLI patient lost the characteristic double peak VGRF curve shape, which was maintained by Normal and Happy THR patients. This however led to the LLI patients having greater VGRF during mid-stance relative to the other groups.

Many studies have been undertaken in analysing the variabilities between individuals with regards to VGRFs. The differences in patient results as seen in the present study could be due to walking speed [75], with LLI patients walking the slowest and having the smallest peak VGRFs. Alternatively, the results could be linked to diminished energy levels [99], with the LLI patients using a asymmetric and inefficient gait. Results in the present study however do conflict with previous studies which found that no differences existed between the non-operated side and a control group [189, 191]. Statistically significant differences were found between the Normal group and the non-operated sides of the Symptomatic LLI and Happy THR groups in terms of peak VGRF, gait symmetry and at mid-stance. Differences were potentially present due to some of the studies in the literature having patients who had completed a prescribed rehabilitation protocol, whilst the patients used in the Happy THR and Symptomatic LLI group had not done so.

To test whether the present results coincide with the conclusions formed by various studies in

¹²See page 48 in the *Literature Review for further information*

the literature, VGRF was compared to velocity in Figure 110. A general trend existed with the 1st peak in the VGRF curve and gait velocity (**A**), with an increase in velocity leading to greater peak force. A SRCC detected statistical significance at the 5% level ($0.77 > 0.26$). A more detailed analysis however revealed that Normal patients alone gave a smaller value (SRCC = $0.59 > 0.31$, statistically significant) together with LLI patients on both the operated (SRCC = $-0.08 > -0.56$, statistically not significant) and the non-operated (SRCC = $0.44 < 0.56$, statistically not significant) sides. The results appear to be highly skewed due to the Happy THR group, where the operated (SRCC = $0.88 > 0.62$, statistically significant) and non-operated (SRCC = $0.82 > 0.62$, statistically significant) sides produced strong correlation.

For the average 2nd peak VGRF (**B**), the SRCC found that a general trend existed (SRCC = $0.70 > 0.26$, statistically significant). Analysing the results individually, the greatest SRCCs were found by the non-operated sides of the THR (SRCC = $0.63 > 0.62$, statistically significant) and LLI (SRCC = $0.69 > 0.56$, statistically significant) patients. Weaker correlation was found in Normal (SRCC = $0.44 > 0.31$, statistically significant) and the operated sides of the Happy THR (SRCC = $0.31 < 0.62$, not statistically significant) and LLI (SRCC = $0.05 < 0.56$, not statistically significant) groups.

With regards to the magnitude of the average VGRF trough found between the two peaks (**C**), a strong overall correlation was found (SRCC = $-0.88 < -0.26$, statistically significant). When analysing results individually, strong correlation was present in the Normal (SRCC = $-0.81 < -0.26$, statistically significant), Happy THR operated (SRCC = $-0.87 < -0.56$, statistically significant) and non-operated (SRCC = $-0.87 < -0.56$, statistically significant) sides together with the LLI operated (SRCC = $-0.92 < -0.62$, statistically significant) and non-operated (SRCC = $-0.70 < -0.62$, statistically significant) sides.

It is clear that velocity had a large impact on the magnitude of peaks and trough in terms of VGRFs. The strongest gradient was for the trough (C) which was closely followed by the gradient for the 1st peak. The 2nd peak showed the smallest gradient. All results however show that the relationship between VGRF and gait velocity was linear.

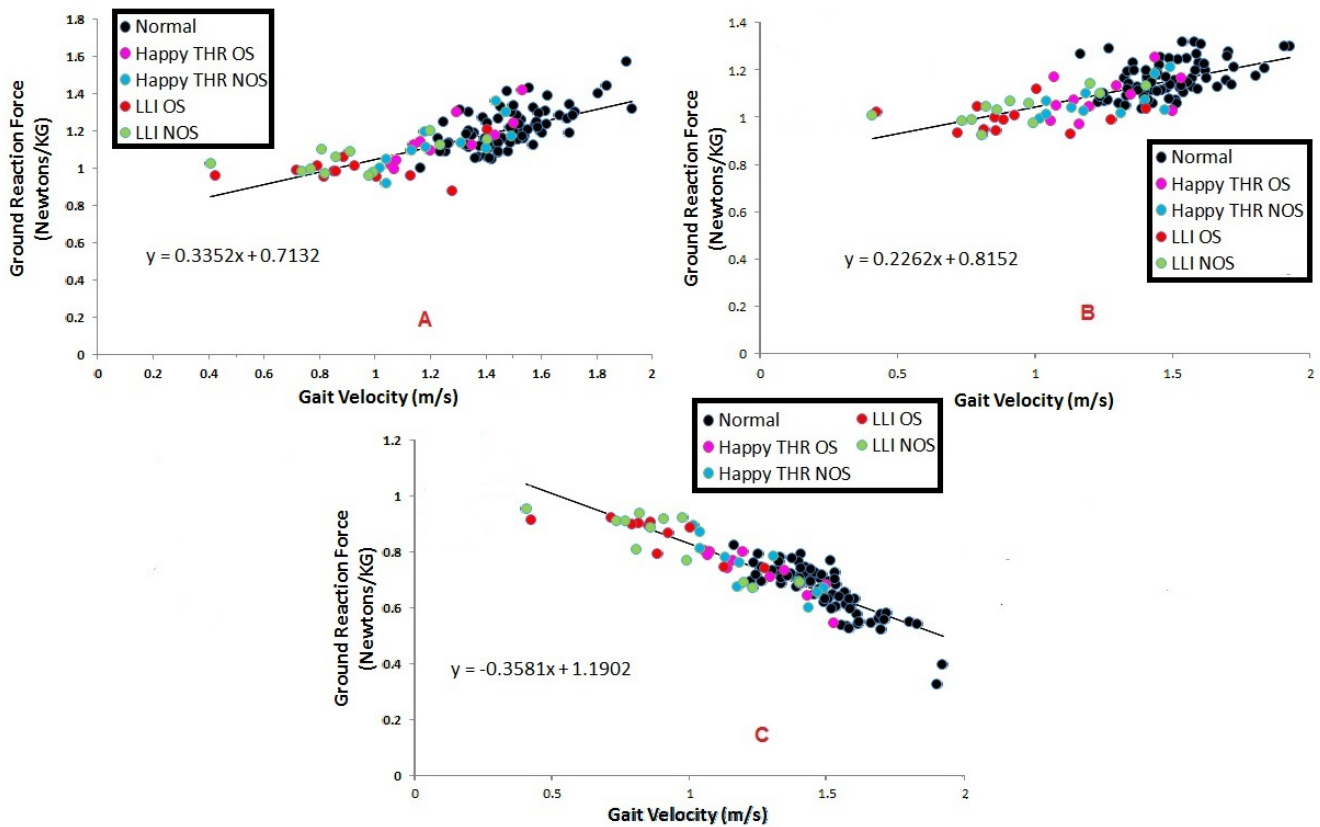


Figure 110: Normalised VGRF gait cycle results at the 1st peak (A), 2nd peak (B) and trough (C) between consecutive heel strikes of the same foot for all clinically measured data together with lines of best fit.

No significant links were found in terms of the operated side of the LLI group between the 1st peak and magnitude of LLI (SRCC = 0.02 < 0.56, statistically not significant), height (SRCC = -0.27 > -0.56, statistically not significant) or age (SRCC = 0.18 < 0.56, statistically not significant). Likewise on the non-operated side, age (SRCC = -0.38 > -0.56, statistically not significant) and height (SRCC = 0.01 < 0.56, statistically not significant) did not have an effect.

For the 2nd of the two peaks, no significant links were found for the operated side of the LLI patients with age (SRCC = 0.18 < 0.56, statistically not significant), height (SRCC = -0.47 > -0.56, statistically not significant) or LLI magnitude (SRCC = -0.25 > -0.56, statistically not significant). Likewise for the non-operated side, no significant correlations could be found with respect to LLI magnitude (SRCC = 0.17 < 0.56, statistically not significant) or height (SRCC = -0.04 > -0.56, statistically not significant). A significant link was however found with age (SRCC = -0.87 < -0.56, statistically significant) i.e. the smaller the 2nd of the two peaks, the older the individual. This was potentially due to the loss of muscle strength overtime in older patients, leading to the smaller force exerted during push off during the stance phase.

6.7.4 Hip Joint Reaction Force

On average LLI patients demonstrated smaller hip JRFs relative to Happy THR patients who themselves showed smaller forces than Normal individuals. The average LLI patient lost the characteristic double peak JRF curve shape, which was maintained by Normal and Happy THR patients, similar to what occurred in terms of VGRF. The non-operated sides showed greater JRF than their operated counterparts. Gait asymmetry was also greatest in the Symptomatic LLI group.

Bergmann et al. [148] found that during level walking the intra-individual differences between patients were small whilst the inter-individual differences were much larger. Peak hip JRFs during gait were found to be on average $2.47\text{N/kg} \pm 0.26$. This was found to be statistically smaller than the Happy THR operated side ($3.17\text{N/kg} \pm 0.36$, $p < 0.01$) but not to the operated side of the LLI patients ($2.64\text{N/kg} \pm 0.57$, $p > 0.05$) using the one-way ANOVA at the 5% significance level. Due to the variability shown and that the analysed patients had their gait measured at various times following THR (between 11 and 31 months), the results do not provide accurate results for a particular period in time.

An earlier study by Bergmann et al. [219] investigated hip JRFs in two atypical THR patients. They found that forces increased with gait velocity. Meanwhile, van den Bogert et al. [146] found that the average peak JRF following THR using an instrumented prosthesis for a group of 9 patients was $2.5\text{N/kg} \pm 0.3$, which was once again statistically smaller than the Happy THR operated side ($p < 0.01$) but no different to the operated side of the Symptomatic LLI patients ($p > 0.05$). Compared to the literature, the patients in the Happy THR group exhibited greater JRFs. This may however be due to these patients being "Happy" through having a gait similar to healthy individuals and thus making them more satisfied following surgery, whilst those studied in the literature are often symptomatic.

Using all the patient data collectively in Figure 111, it was found that there was a weak link between the 1st JRF peak (**A**) and gait velocity (SRCC = $0.46 > 0.26$, statistically significant). No link could be found individually for the Normal (SRCC = $0.15 < 0.32$, statistically not significant), Happy THR non-operated (SRCC = $0.5 < 0.62$, statistically not significant) side together with the operated (SRCC = $0.38 < 0.62$, statistically not significant) and non-operated (SRCC = $-0.06 > -0.56$, statistically not significant) sides of the LLI group. A moderate correlation was however found for the operated side of the Happy THR patients (SRCC = $0.77 > 0.62$, statistically significant). It can

be concluded that gait velocity shared a weak monotonic relationship with the magnitude of the 1st JRF peak.

A correlation was found between gait velocity and the 2nd peak (**B**) (SRCC =0.57>0.26, statistically significant). No link could be found individually for the Normal group (SRCC =0.28<0.32, statistically not significant), Happy THR operated side (SRCC =0.34<0.56, statistically not significant), Happy THR non-operated side (SRCC =0.24<0.62, statistically not significant) or the non-operated side of the LLI patients (SRCC =-0.41>-0.56, statistically not significant). Statistically significant results were however found for the operated side of the LLI group (SRCC =-0.59<-0.56, statistically significant). Overall it can be concluded that there was a weak monotonic relationship between the magnitude of the 2nd peak for the operated side of LLI patients and gait velocity.

A weak negative correlation was found between gait velocity and the JRF trough (**C**) between the 1st and 2nd peaks. Individually, weak relationships were found in the Normal (SRCC =-0.51<-0.32, statistically significant), Happy THR operated side (SRCC =-0.44<0.62, statistically not significant), LLI operated side (SRCC =-0.55>-0.56, statistically not significant) and LLI non-operated side (SRCC =0.28<0.56, statistically not significant). Strong correlation was found for the non-operated side of the Happy THR group (SRCC =-0.72<-0.62, statistically significant). Overall it can be concluded that there was a weak monotonic link between the magnitude of the trough and gait velocity.

For the operated side of the Symptomatic LLI group, the 1st JRF peak was not found to be correlated with pelvic width (SRCC =0.08<0.26, statistically not significant), magnitude of LLI (SRCC =0.41<0.56, statistically not significant), height (SRCC =-0.01<-0.56, statistically not significant) and femoral offset (SRCC =0.45<0.56, statistically not significant). Likewise for the 2nd hip JRF peak, no significant differences were found with respect to pelvic width (SRCC =0.39<0.56, statistically not significant), the magnitude of LLI (SRCC =-0.16>-0.56, statistically not significant), height (SRCC =0.08<0.56, statistically not significant) or femoral offset (SRCC =0.52<0.56, statistically not significant). For completeness the trough was also compared to anthropometric measurements with the same results occurring. No correlation was found between the trough and femoral offset (SRCC =0.47<0.56, statistically not significant), pelvic width (SRCC =-0.18>-0.56, statistically not significant), LLI magnitude (SRCC =-0.23<0.56, statistically not significant) or height (SRCC =0.25<0.56, statistically not significant).

Figure 111 also illustrates the results for the 1st peak, 2nd peak and trough in terms of the line of best fit for hip JRFs without distinguishing between groups. Results indicated that the smallest gradient was for the trough (C), closely followed by the gradient for the 1st peak (A). The 2nd peak showed the steepest gradient (B). These gradients exceeded those found for VGRFs, demonstrating that an increase in velocity had a greater impact on JRFs than VGRFs, although VGRFs had a stronger monotonic relationship, according to the SRCC, to gait velocity. Much variability was shown for all three gait instants with their being patients walking at opposite ends of the speed spectrum still producing similar levels of hip JRF. Results suggest agreement with Hashimoto et al. and Bergmann et al. [219, 450] who found that hip JRF increased with walking velocity.

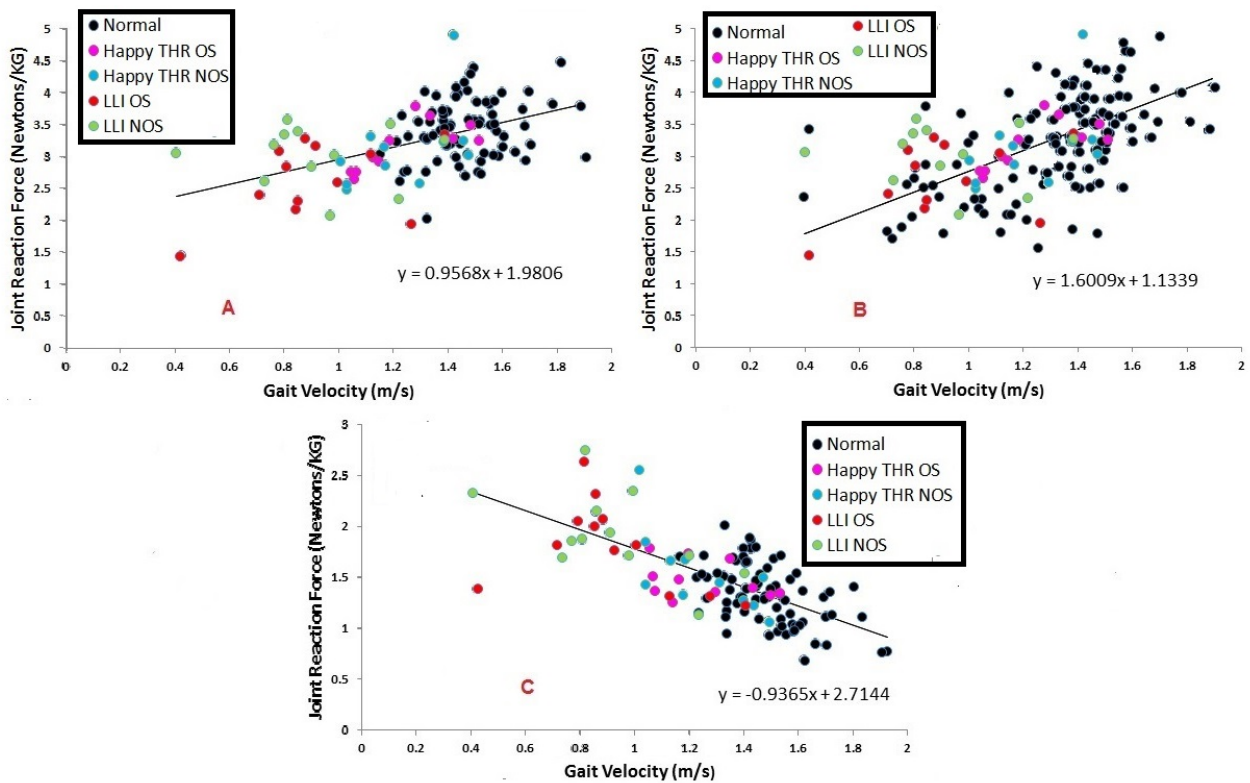


Figure 111: Normalised hip JRF results at the 1st peak (A), 2nd peak (B) and trough (C) between consecutive heel strikes of the same foot for all clinically measured data together with lines of best fit.

6.7.5 Joint Moments

Hip Flexion-Extension Moment

Results indicated that generally Symptomatic LLI and Happy THR patients showed a loss of peak hip flexion moment relative to Normal individuals together with a reduced average flexion moment value at toe off. These results also agree with many other studies [166, 198, 215] which

have shown a reduction in extensor moment following THR.

Previous studies have also suggested that peak moments share a relationship with gait velocity [72, 74, 105, 106]. A correlation was found between these variables which was significant at the 5% level (SRCC =0.46>0.26). When analysing the results individually however, no correlation was found for the Normal group (SRCC =0.04<0.255), the operated side of Happy THR patients (SRCC =-0.14<0.62) or the non-operated side of Happy THR patients (SRCC =0.20<0.62). A significant link was however found on both the operated side (SRCC =0.60>0.56, statistically significant) and non-operated side of the LLI patients (SRCC =0.61>0.56 statistically significant). Overall it appears that there was a significant link between walking velocity and peak flexion moment for LLI patients.

Hip Abduction-Adduction Moment

No significant differences were found in terms of peak abduction moment, although for the Symptomatic LLI group there was the loss of the characteristic double peak shape, similar to what occurred for the VGRFs and hip JRFs. Differences were present however at toe off, with the Normal group showing statistically greater adduction moment than the other groups. The present study did not find significant differences between the non-operated sides of the LLI and Happy THR groups against the Normal group, whereas Foucher et al. [201] found that significant differences existed between THR patients and controls. Likewise, both the Happy THR and Symptomatic LLI patients did not show a decrease in peak abductor moment despite this being commonly seen post-THR [165, 166, 171, 179, 181, 195, 196, 198, 214, 215], although statistical significance is not always detected.

A significant link could not be found with velocity for the LLI operated side (SRCC =0.4<0.56) and non-operated side (SRCC =0.31<0.56) when compared to peak abductor moment. Likewise, no links were found with Normal patients (SRCC =0.03<0.36) or Happy THR operated side (SRCC =-0.05<0.36). A significant correlation was however found with the Happy THR non-operated side (SRCC =0.48<0.36). The significant result however may have no clinical significance as patients who were walking faster in the Normal group and those walking slower in the LLI group showed no link to peak abduction moment.

No statistical differences could be found across the groups in terms of age (SRCC =0.23<0.26)

or height (SRCC =0.08<0.26). Comparisons were made for the LLI group with regards to anthropometric parameters. No significant relationships were found between peak abductor moment and femoral offset (SRCC =-0.23>-0.56), magnitude of LLI (SRCC =-0.33>-0.56) or pelvic width (SRCC =-0.19>-0.56). As no trends could be detected, the differences between the groups may have been due to natural variation or errors in the measurement of gait.

Knee Flexion-Extension Moment

Results found that LLI patients had significantly reduced peak knee flexion and peak extension moments. Results also differed significantly at toe off. Peak extension moment was reduced in the Happy THR patients relative to the Normal group, although statistical significance was not found. The results in the present study match those seen in the literature, with reductions in peak knee extensor moment commonly seen post-THR [171, 196].

Combining all of the knee extension data together across groups and comparing against gait velocity found no statistical significance (SRCC =0.18<0.26). Individually, statistical significance was found for the operated side of the LLI patients (SRCC =0.71>0.56, statistically significant). No significance was found for the Normal (SRCC =-0.2>-0.34, statistically not significant), LLI non-operated side (SRCC =-0.17>0.56, statistically not significant), Happy THR operated side (SRCC =0.26<0.62, statistically not significant) or Happy THR non-operated side (SRCC =0.56<0.62, statistically not significant).

Stride length was found not to have a significant link to peak knee extension levels (SRCC =0.16<0.26), as was height (SRCC =0.14<0.26) or age (SRCC =-0.17>-0.26).. No statistical differences were detected between the operated side of the LLI patient and the magnitude of LLI (SRCC =0.22<0.23), femoral offset (SRCC =-0.18>-0.23) or pelvic width (SRCC =-0.15>-0.23).

Ankle Dorsi-Plantar Flexion Moment

Results found statistically significant differences existed between the Symptomatic LLI group and Normal individuals with respect to both peak dorsiflexion and peak plantarflexion angles, with there also being differences in joint moments during mid-stance. Ankle moments following THR are not commonly discussed in the literature. Studies have however shown that a loss in peak plantarflexion moment is associated with being older [72] and obese [81], which were characteristics of both the Happy THR and Symptomatic LLI groups.

As with the previous results, the hierarchical nature of the maximum plantar flexion moment from the Normal group having the largest to the LLI group having the smallest matches up with the pattern shown for temporal-spatial parameters such as velocity and stride length. This thus makes it possible that the results were due to the LLI and Happy THR patients walking slower with smaller stride lengths relative to their Normal counterparts.

Overall a significant link was found between velocity and maximum ankle plantarflexion moment (SRCC =0.34>0.26). Analysing the results individually, no significant differences were found with regards to Normal patients (SRCC =0.05<0.34), on the operated side of LLI patients (SRCC =0.16<0.56, statistically not significant), on the operated side of the Happy THR group (SRCC =0.20<0.62, statistically not significant) and the non-operated side of the Happy THR non-operated side (SRCC =0.48<0.62, statistically not significant). Significance was however found on the non-operated side of the LLI patients (SRCC =0.57>0.56, statistically significant). Taking into consideration all of the results, it can be concluded that peak ankle plantarflexion moment had a weak correlation with gait velocity.

6.7.6 Errors in Results

All experimental results are subject to error. The errors in the PiG model are linked to poor marker placement, the choice of HJC regression equation and inaccurate clinical anthropometric measurements. These can effect joint centre positions and segment rotations leading to offsets in joint angle results together with cross talk occurring between segment axes. This is particularly problematic in obese patients as recruited for this study where landmarks on the body are more difficult to locate¹³.

6.8 Conclusion

This is the first report undertaking an analysis of gait compensatory mechanisms for patients with LLI following THR. Patients with LLI following THR on average demonstrated significantly smaller hip JRFs and VGRFs relative to Normal and asymptomatic individuals. There were no characteristic gait patterns found specific to all LLI patients; data variability was higher in this cohort

¹³See pages 70- 75 and 80- 82 in the *Generic Methods* for more information

than in Happy THR patients. Differences in terms of forces and moments shared a link to walking velocity, although this was inconclusive. Overall, the differences between the three clinical groups appear to be significant and may indicate variability between asymptomatic THR and symptomatic LLI patients in implant success rates and hence patient satisfaction levels. Conclusions drawn from the results however must be taken with caution due to the small number of patients used, errors in marker placement, errors in anthropometric measurements and the absence of preoperative gait data as a comparison.

7 Critiquing Clinical Results

7.1 Rationale

This study has analysed the kinematics in the *Kinematics & Temporal-Spatial Parameters* chapter (pages 105-141) and kinetics in the *Kinetics* chapter (pages 142-179) of three patient groups; Symptomatic LLI, a "Happy" group of asymptomatic THR patients together with a Normal healthy control group. Visual inspection of body segment rotations during the standing trial revealed that many patients in each group had segments which were rotated excessively to what would be considered the norm. This occurred due to the method used in determining segment rotations in the PiG marker system¹⁴, together with markers being placed by the clinician purposely at slightly different positions in order for the right and left leg to be differentiated. Figures 112-114 demonstrate for a particular LLI patient how misplacement of segment markers led to excessive rotation of joint axes.

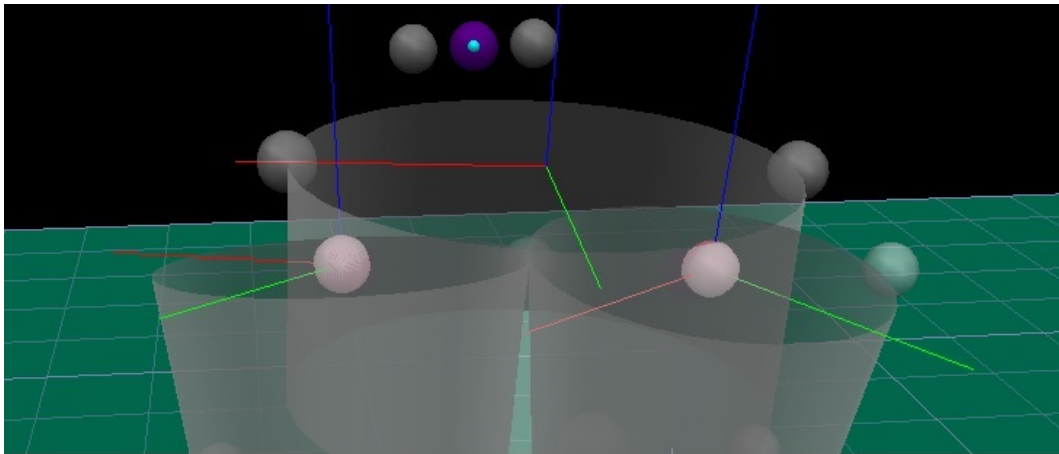


Figure 112: Image from Visual3D demonstrating excessive hip axes rotation due to poor lateral thigh marker positioning on both the left and right sides. The centre axes are of the pelvis whilst the axes on the left and right hand sides represent the hip. The green axis (anterior-posterior) represents abduction-adduction, the red axis (medial-lateral) flexion-extension and the blue internal-external rotation. It would be expected that the anterior-posterior axis in a subject is rotated such that it generally faces the direction that the individual is standing. This was not the case for this particular patient for either hip, with there instead being excessive external rotation.

¹⁴See Figures 27-33 on pages 71- 75 of the *Generic Methods* for more information on how PiG works

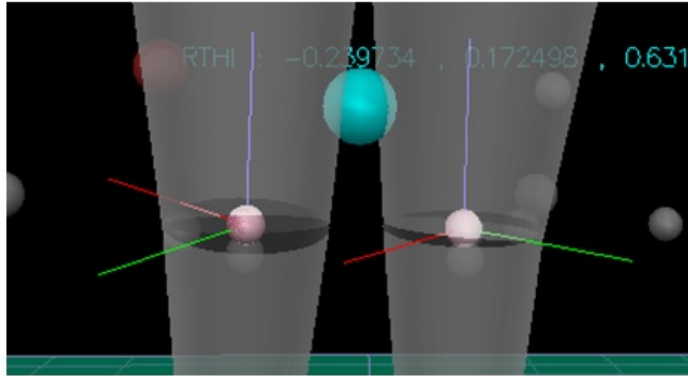


Figure 113: Image from Visual3D demonstrating excessive knee axes external rotation on both the left and right sides due to poor lateral shank marker positioning. Typically, the axes would be rotated such that the green axis (anterior-posterior) is facing in the same direction as the subject is standing. At both of the knees shown, the green axis was excessively externally rotated indicating that the lateral shank marker which defines the rotation of the axes was placed too posterior.

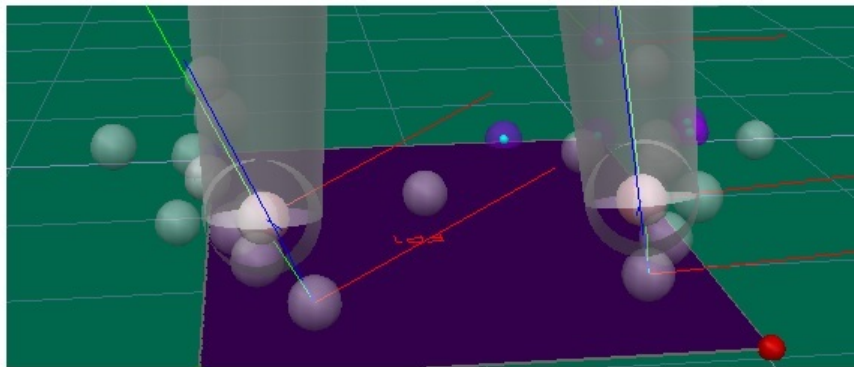


Figure 114: Image from Visual3D demonstrating both an excessively rotated foot (left) and a correctly rotated foot (right). The foot in Visual3D was defined to exist between the toe marker and the AJC with the medial-lateral rotation of the joint axes, defined at the AJC, being dependent on the position of the heel marker relative to the foot. A heel marker which is incorrectly placed leads to there being either an inversion or eversion offset in the results.

7.2 Aims & Objectives

Difficulties in measuring anatomical positions and placing markers in patient groups with high BMIs such as the Symptomatic LLI (29.4 BMI \pm 4.04) and Happy THR (29.6 BMI \pm 6.08) are common. The rotation of the joint axes at the thigh and shank is controlled by the positioning of a single marker, the lateral thigh marker for the thigh and the lateral shank marker for the shank. The aim of this study was to scrutinise the motion capture data captured clinically with regards to the variability in joint axes rotation through comparison against a set of Pilot data. From this it could be deduced whether the orientation of the axes fell into the error range as expected when subjectively placing markers on a segment and also what effect that they had on kinematic and kinetic results.

7.3 Methodology

7.3.1 Subject

A group of 8 student subjects (Age 24 ± 2.6 , 6 female 2 male) with an average BMI of 22.1 ± 2.5 and average LLI of 2.91 ± 2.20 (measured using a tape measure from the ASIS to the medial ankle) were recruited following ethical approval for gait analysis at the University of Leeds¹⁵. Subjects were selected based on them having no physical deformities of the lower limbs together with having a BMI level of under 25. This was to ensure that the STA, which may have effected the results in the clinical groups, was minimised. A 13 camera Qualisys (California, USA) motion capture system was used with students being marked up following the PiG marker set as described on pages 69- 70 of the *Generic Methods*. Calibration of the system was undertaken by the method as described on page 105

7.3.2 Gait Analysis

Markers were placed with extra care in order to reduce error. This included the exposure of the thigh and shank which allowed placement of markers directly onto muscle. Calibration of the data capture region was undertaken prior to analysis with a standard deviation of 0.87cm. Motion capture data for when the subjects were standing still with their arms outstretched was captured for a period of 7 seconds. All subjects undertook 3 trials before markers were labelled, file frame numbers truncated, data interpolated and exported from Qualisys. Following each standing trial, markers were all removed and then replaced 3 times so averages could be produced for each subject.

7.3.3 Body Model

The exported C3D files were imported into Visual3D where a rigid body model was built, with segments defined at the pelvis, thigh, shank and foot together with the use of anthropometric measurements. The standing trial in Visual3D was defined to exist for only 10 frames and an average position over these frames was taken to be the standing value. Definition of segments and axes rotations followed the method described on pages 77- 85 of the *Generic Methods*. The Davis HJC regression equation [273] was used and computed via a combination of marker positioning and anthropometric measurements taken prior to motion capture¹⁶ for a definition of Davis' HJC regression equation together with Equations 36-42 for definition of the variables used on pages 81- 82 of the *Generic Methods*.

¹⁵Ethical approval, participant forms and consent forms found from page 351 in the *Appendix III*

¹⁶See Equations 34-35

The rotation of the pelvis, thigh, shank and foot was measured relative to the laboratory coordinate system using the right hand rule. Figure 115 illustrates a subject standing trial together with both segment and laboratory axes labelled. The laboratory coordinate system had been pre-defined during calibration and remained the same for every individual trial analysed. Rotation of the segment towards the mid-line of the body was defined as positive rotation (internal rotation) whilst that away from the mid-line of the body was referred to as negative rotation (external rotation). Results were then averaged for each patient over their three trials before a global average was produced for all subjects.

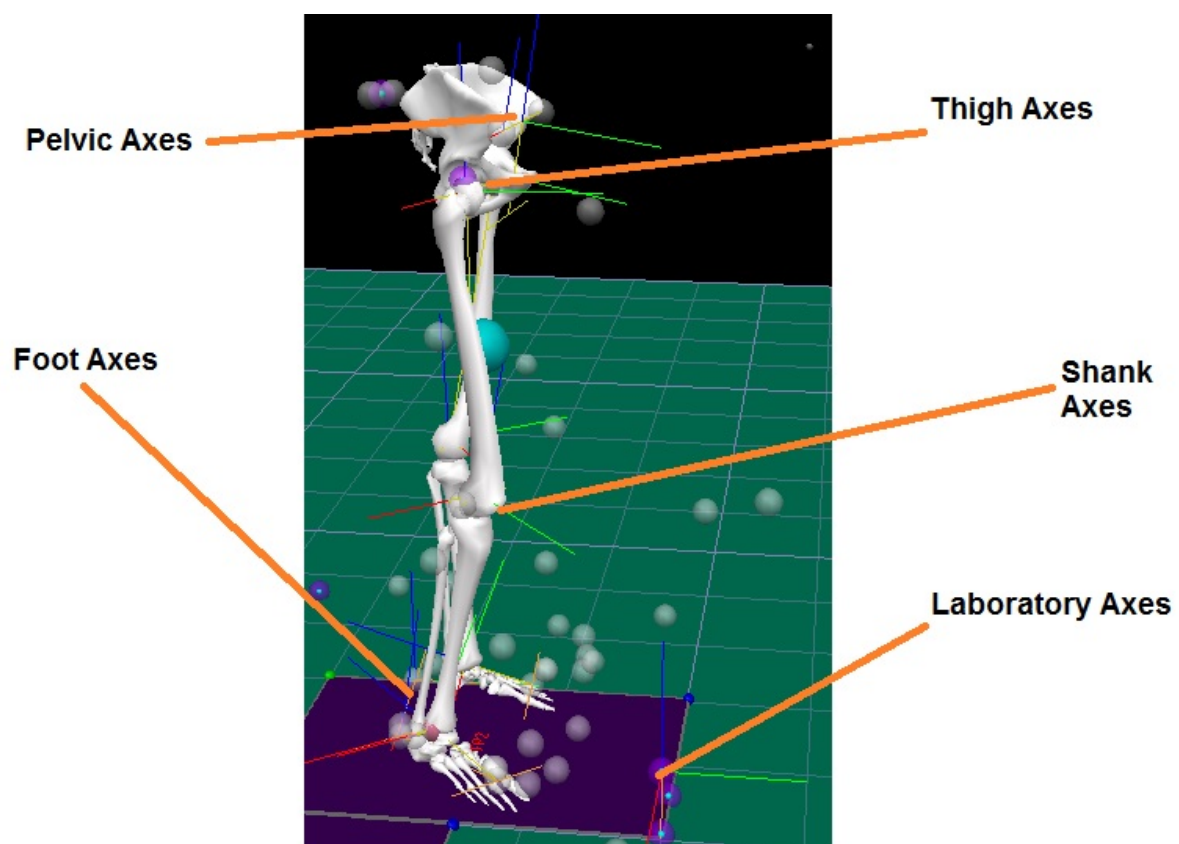


Figure 115: Image from Visual3D demonstrating the pose of a single subject volunteer during the standing trial. Segment axes were measured against the laboratory axes in terms of computing segment rotation.

Standing segment angles using the same model were also computed for the Symptomatic LLI, Happy THR and Normal groups. Each clinical group had a single standing file produced during their analysis at hospital. Out of the original patient groups, the same method was used as on page 106 of the *Kinematics & Temporal-Spatial Parameters* chapter to condense the numbers in each group to 13 Symptomatic LLI, 11 Happy THR and 35 Normal patients. The standing segment angle results were then compared to the Pilot group.

7.4 Results - Standing Segment Angles

Results comparing segment rotations between groups can be seen in Figure 116, with negative (-) results depicting external rotation and positive (+) results internal rotation. Pelvic rotation was very similar between the groups and had narrow error bars. No statistically significant differences were detected using the one-way ANOVA at the 5% significance level ($p > 0.05$). The clinical groups had the thigh externally rotated with the greatest on the non-operated leg of the Happy THR group ($-12.5^\circ \pm 10.9^\circ$) and the least in the Normal group ($-6.82^\circ \pm 10.3^\circ$). The Pilot group however showed on average internal rotation of the thigh 5.28° , although no statistical significance was detected ($p > 0.05$).

At the shank the angle of the segment with respect to the laboratory was larger for the clinical groups than that of the thigh with values ranging between -24.9° and -32.6° , with the greatest angle occurring on the non-operated side of the Happy THR group and the smallest in the operated side. The Pilot data produced an average segment angle of $-6.60^\circ \pm 26.9^\circ$. A one-way ANOVA found statistical significance between the groups ($p < 0.01$), with a Tukey post-hoc test demonstrating that these differences were between the Pilot data and all other groups. Statistical significance was not found between the clinical and Pilot data ($p < 0.08$) with regards to foot rotation. The greatest amount of foot rotation was in the Pilot group ($-18.8^\circ \pm 9.08^\circ$) and the least for the non-operated side of the Symptomatic LLI patients ($-7.88^\circ \pm 5.34^\circ$).

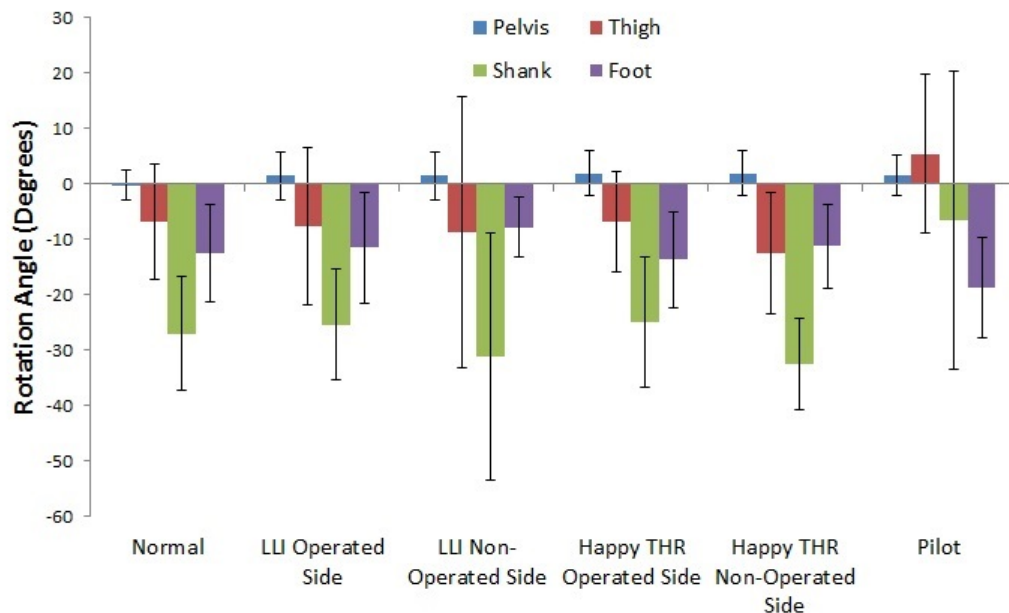


Figure 116: Segment rotations of the pelvis, thigh, shank and foot for all clinical groups together with Pilot data. Positive (+) angles depict internal rotation and negative (-) angles depict external rotation. Standard errors are included.

7.5 Methodology II

7.5.1 Subject

All 35 Normal patients from the *Kinematics & Temporal-Spatial Parameters* chapter were used.

7.5.2 Gait Analysis

Standing angles and peak joint angle/moment results were obtained from the *Kinematics & Temporal-Spatial Parameters* chapter for every Normal patient. See page 105 or the method. Motion capture data for when the subjects were standing still with their arms outstretched was captured for a period of 7 seconds. All subjects had 2 standing trial results.

7.5.3 Body Model

See page 182 in this chapter.

7.6 Results - Effect on Kinematics & Kinetics

Joint Angles

Figure 117 is with regards to the effects of the initial standing trial average thigh rotation with respect to the laboratory to maximum joint angles. A significant link was found between the rotation of the thigh and maximum hip flexion angle (SRCC =0.35>0.34), showing that the greater the internal rotation of the thigh the greater the maximum gait cycle hip flexion. This was due to some hip abduction-adduction being measured as hip flexion. No such links were however found for the maximum hip extension angle (SRCC =0.09<0.34), maximum abduction angle (SRCC =-0.19>-0.34) or maximum adduction angle (SRCC =-0.16>-0.34). Likewise, no statistically significant links were also found for maximum knee flexion (SRCC =-0.02>-0.34), maximum knee extension (SRCC =0.03<0.34), maximum ankle dorsiflexion (SRCC =0.04<0.34) or maximum ankle plantar-flexion (SRCC =0.03<0.34) angles.

Results for hip flexion-extension RoM (SRCC =0.19<0.34), hip abduction-adduction (SRCC =0.01<0.34), knee flexion-extension (SRCC =-0.09>-0.34) and ankle dorsi-plantar flexion (SRCC =-0.02>-0.34) all showed that there was no significant link between standing thigh angle and joint RoM. These results are illustrated in Figure 118.

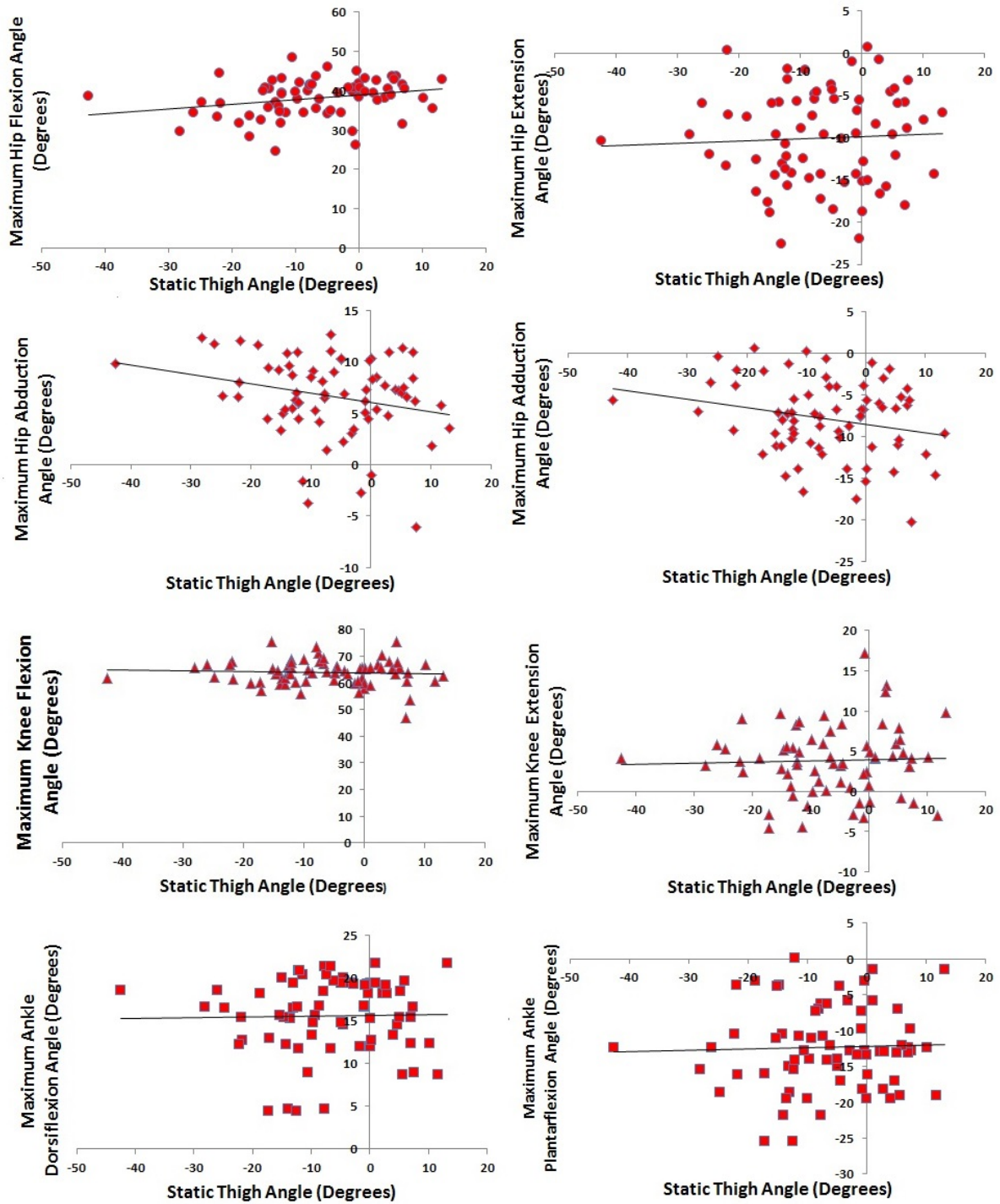


Figure 117: The effect of varying initial thigh standing angles when measured against the laboratory axes to maximum hip flexion- extension, hip abduction-adduction, knee flexion-extension and ankle dorsi-plantar flexion joint angles.

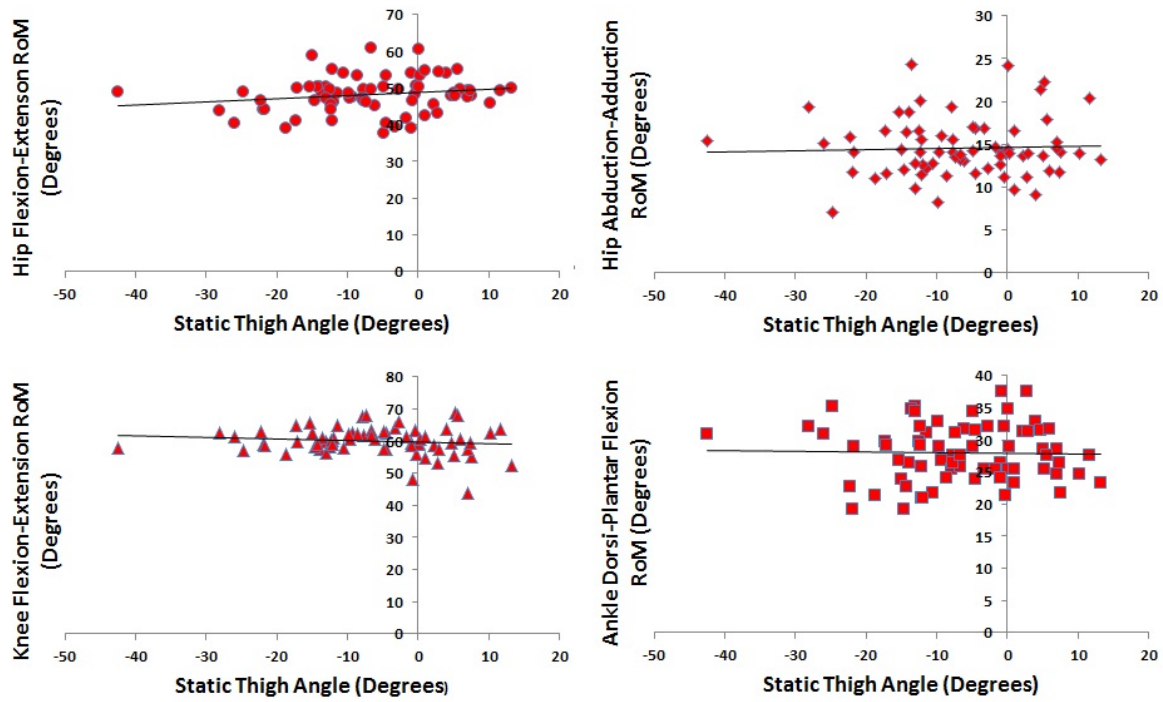


Figure 118: The effect of varying initial thigh standing angles when measured against the laboratory axes to hip flexion-extension, abduction-adduction, knee flexion-extension and ankle dorsi-plantarflexion RoM.

Figure 119 is with regards to the effects of the initial standing trial average shank rotation with respect to the laboratory against maximum hip flexion-extension, hip abduction-adduction, knee flexion-extension and ankle dorsi-plantar flexion joint angles. No significant links were found for the maximum hip flexion ($SRCC = 0.15 < 0.34$), extension ($SRCC = 0.05 < 0.34$), abduction ($SRCC = -0.03 > -0.34$) or adduction ($SRCC = -0.07 > -0.34$) angle. This was expected as shank rotation has no effect on the thigh which is used to compute hip kinematic results. Likewise, no statistically significant relationships were found between the average shank rotation and maximum knee flexion ($SRCC = 0.27 < 0.34$), knee extension ($SRCC = 0.18 < 0.34$), ankle dorsiflexion ($SRCC = -0.02 > 0.34$) or ankle plantarflexion ($SRCC = 0.01 < 0.34$) angle.

Results for hip flexion-extension ($SRCC = 0.07 < 0.34$), hip abduction-adduction ($SRCC = -0.01 > -0.34$), knee flexion-extension ($SRCC = 0.09 < 0.34$) and ankle dorsi-plantar flexion ($SRCC = -0.01 > -0.34$) all showed that there was no significant link between standing shank angle and joint RoM. These results are illustrated in Figure 120.

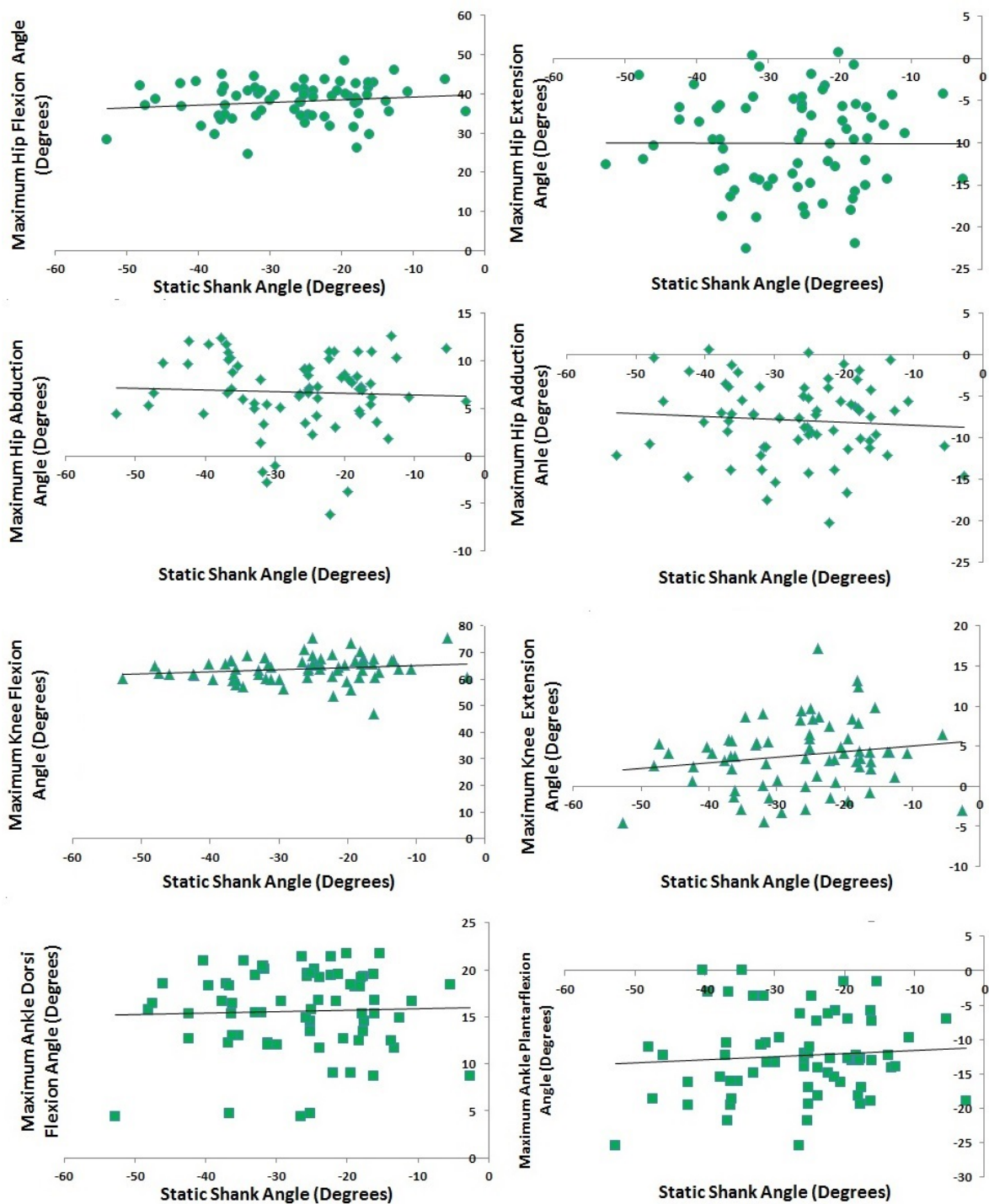


Figure 119: The effect of varying initial shank standing angles when measured against the laboratory axes to maximum hip flexion-extension, hip abduction-adduction, knee flexion-extension and ankle dorsi-plantarflexion joint angles.

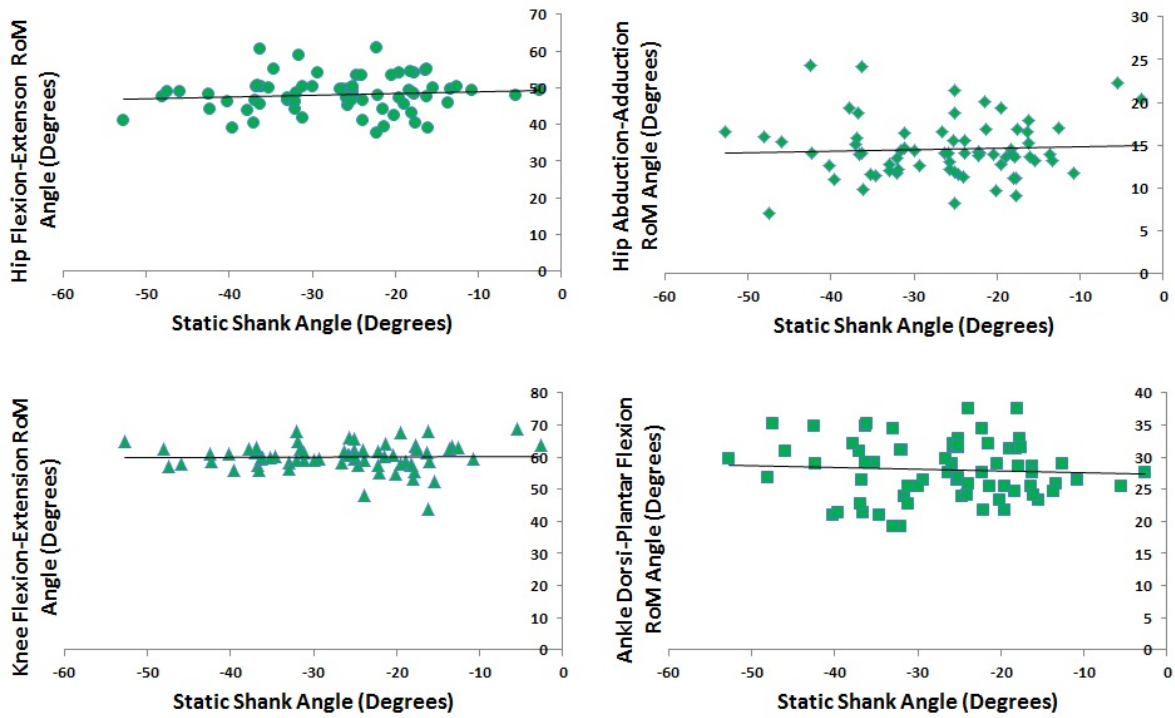


Figure 120: The effect of varying initial shank standing angles when measured against the laboratory axes to hip flexion-extension, abduction-adduction, knee flexion-extension and ankle dorsi-plantarflexion RoM.

Figure 121 is with regards to the effects of the initial standing trial average foot rotation with respect to the laboratory to hip flexion-extension, hip abduction-adduction, knee flexion-extension and ankle dorsi-plantar joint angle maximums. No significant links were found for the maximum hip flexion (SRCC = -0.2 > 0.34), extension (SRCC = -0.14 > 0.34), abduction (SRCC = -0.11 > -0.34) or adduction (SRCC = -0.01 > -0.34) angle. This was expected however as the rotation of the foot has no bearing on hip kinematics. Likewise, no statistically significant relationships were found between the average foot rotation and maximum knee flexion (SRCC = 0.00 < 0.34), knee extension (SRCC = -0.08 > 0.34), ankle dorsiflexion (SRCC = 0.12 < 0.34) or ankle plantarflexion (SRCC = 0.14 < 0.34) angle. Foot rotation also has no effect on knee kinematics.

Results for hip flexion-extension RoM (SRCC = 0.01 < 0.34), hip abduction-adduction (SRCC = -0.08 > -0.34), knee flexion-extension (SRCC = 0.07 < 0.34) and ankle dorsi-plantar flexion (SRCC = -0.07 > -0.34) all showed that there was no significant link between standing foot angle and joint RoM. This was expected as the rotation of the foot has no bearing on hip and knee kinematics. Results are illustrated in Figure 122.

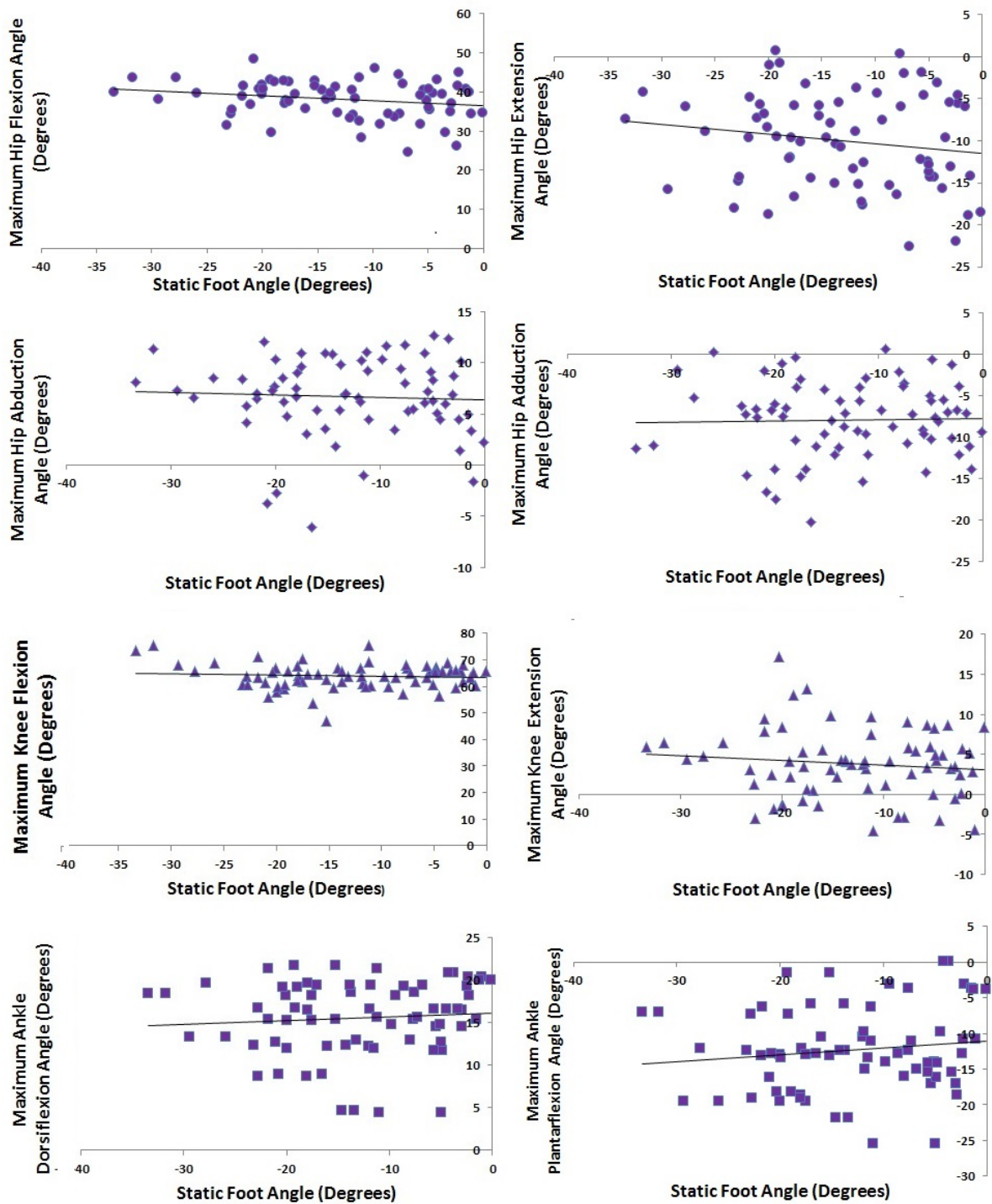


Figure 121: The effect of varying initial foot standing angles when measured against the laboratory axes to maximum hip flexion- extension, hip abduction-adduction, knee flexion-extension and ankle dorsi-plantar flexion joint angles.

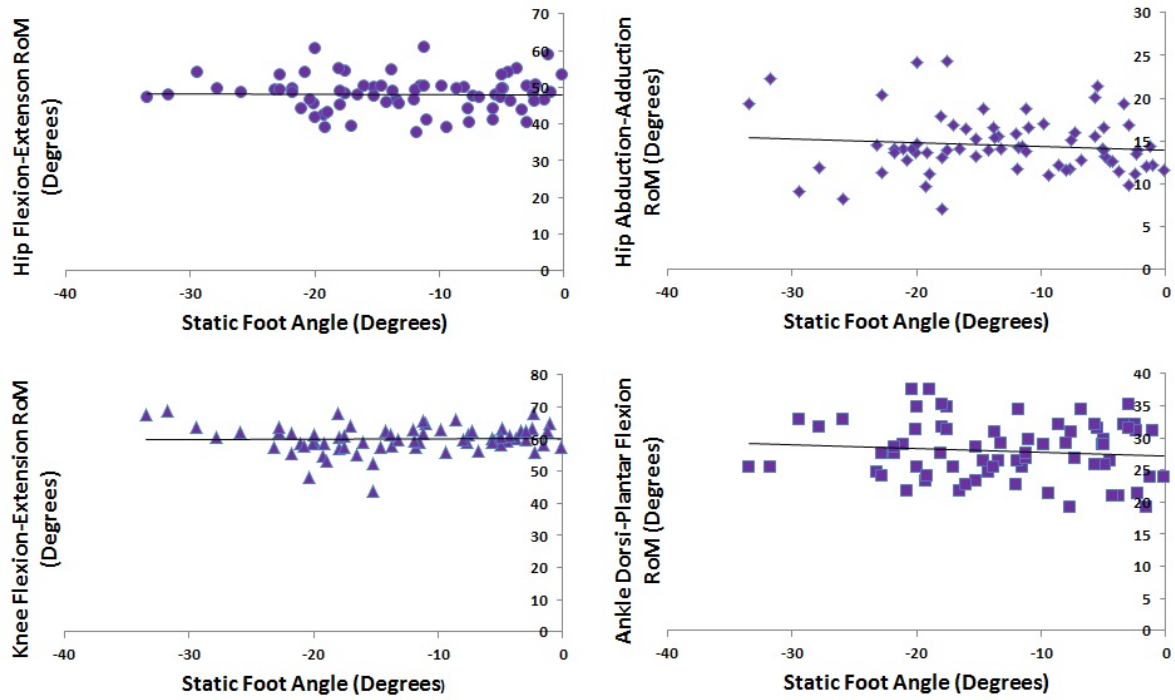


Figure 122: The effect of varying initial foot standing angles when measured against the laboratory axes to hip flexion-extension, abduction-adduction, knee flexion-extension and ankle dorsiflexion-plantarflexion RoM.

Joint Moments

Figure 123 is with regards to the effects of the initial standing trial average thigh rotation with respect to the laboratory against hip flexion-extension, hip abduction-adduction, knee flexion-extension and ankle dorsi-plantar flexion moment maximums. No significant links were found for the maximum hip flexion ($SRCC = -0.08 > 0.34$), extension ($SRCC = 0.05 < 0.34$), abduction ($SRCC = -0.16 > -0.34$) or adduction ($SRCC = 0.13 < 0.34$) moment. Thus it can be concluded that the rotation of the thigh axis has no bearing on hip moments. Likewise, no significant links were found for the maximum knee flexion ($SRCC = 0.08 < 0.34$), knee extension ($SRCC = -0.03 > -0.34$), ankle dorsiflexion ($SRCC = -0.02 > -0.34$) or ankle plantarflexion ($SRCC = 0.08 < 0.34$) moment. It can therefore also be concluded that the rotation of the thigh axis has no bearing on knee and ankle moments in the sagittal plane.

Results for hip flexion-extension RoM ($SRCC = -0.12 > -0.34$), hip abduction-adduction ($SRCC = -0.22 > -0.34$), knee flexion-extension ($SRCC = 0.07 < 0.34$) and ankle dorsi-plantar flexion ($SRCC = 0.05 < 0.34$) all showed that there was no significant link between standing thigh angle and moment range. These results are illustrated in Figure 124.

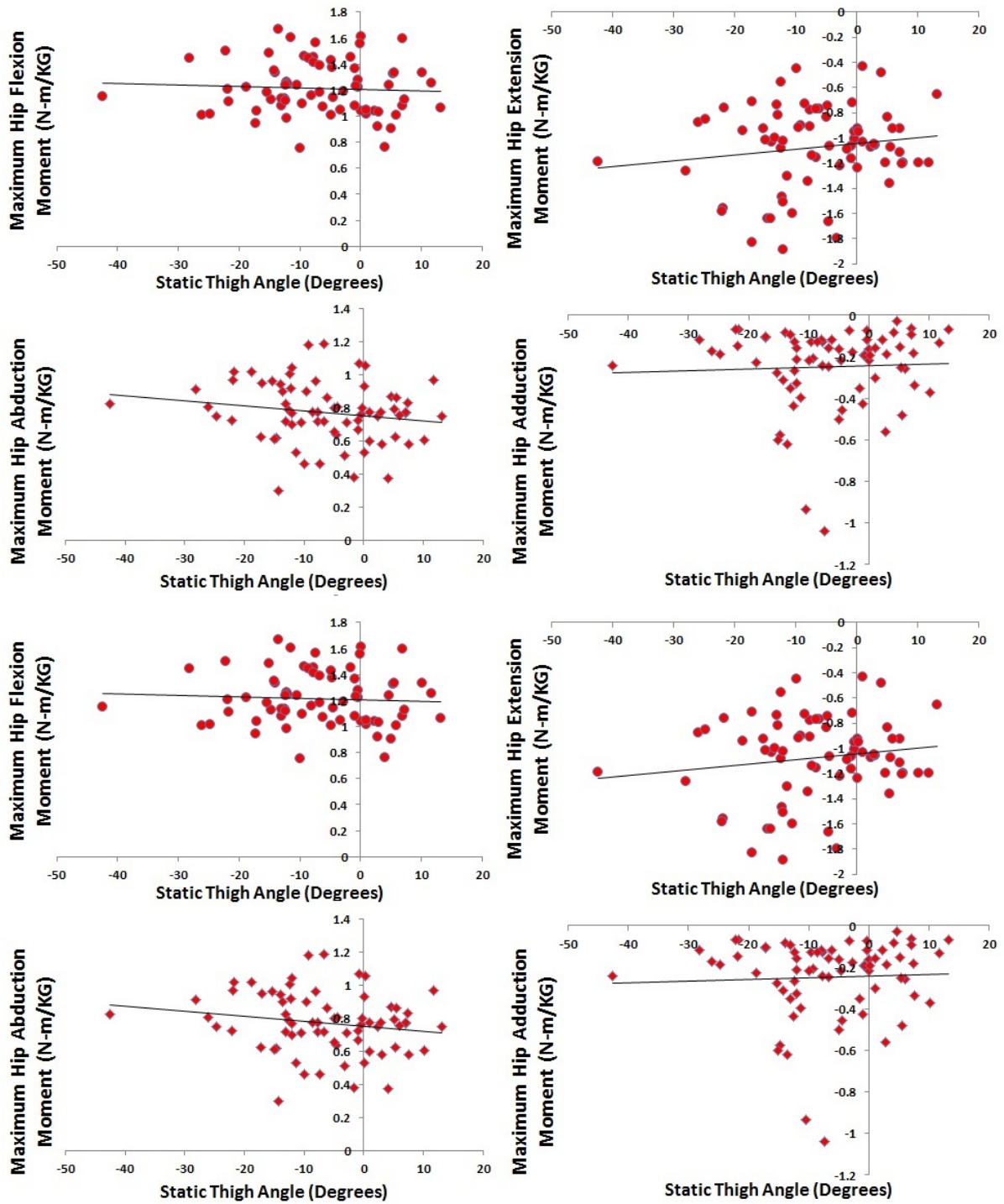


Figure 123: The effect of varying initial thigh standing angles when measured against the laboratory axes to maximum hip flexion-extension, hip abduction-adduction, knee flexion-extension and ankle dorsi-plantar flexion moments.

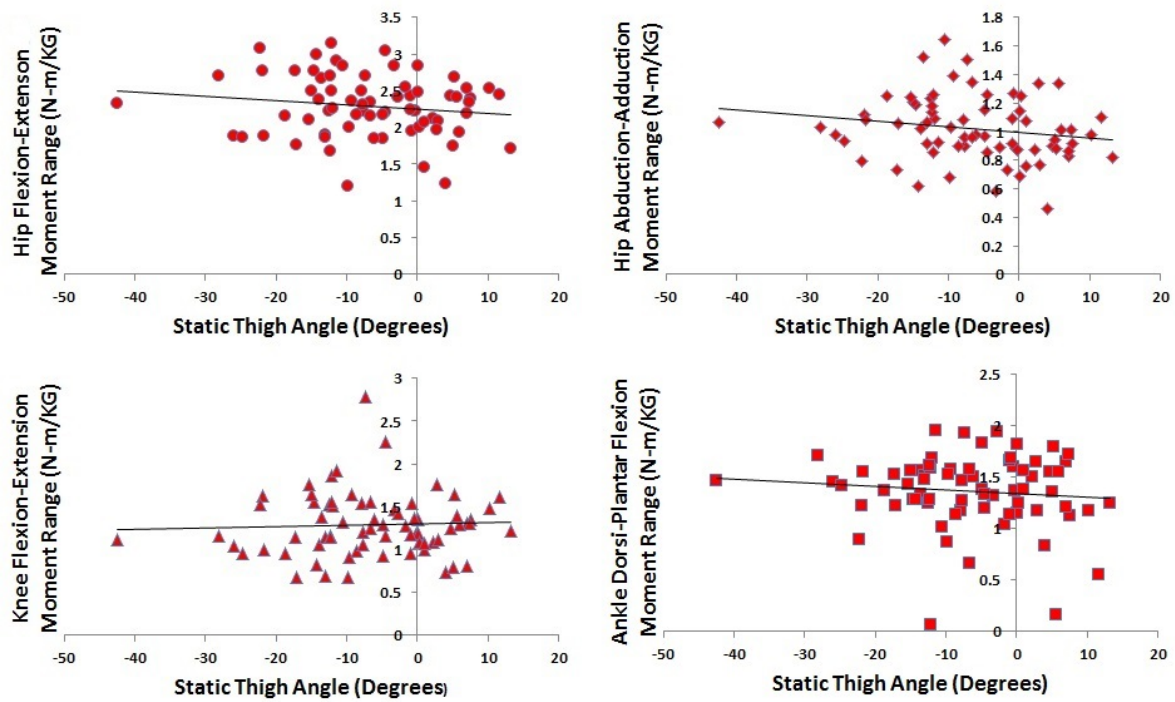


Figure 124: The effect of varying initial thigh standing angles when measured against the laboratory axes to range of moment in terms of hip flexion-extension, hip abduction-adduction, knee flexion-extension and ankle dorsi-plantar flexion.

Figure 125 is with regards to the effects of the initial standing trial average shank rotation with respect to the laboratory against hip flexion-extension, hip abduction-adduction, knee flexion-extension and ankle dorsi-plantarflexion moment maximums. No significant links were however found for the maximum hip flexion ($SRCC = -0.20 > -0.34$), extension ($SRCC = -0.02 > -0.34$), abduction ($SRCC = -0.06 > -0.34$) or adduction ($SRCC = -0.02 > -0.34$) moment. Thus it can be concluded that the rotation of the shank axis has no bearing on hip maximum moments. Likewise, no significant links were found for the maximum knee flexion ($SRCC = 0.04 < 0.34$), knee extension ($SRCC = -0.14 > -0.34$), ankle dorsiflexion ($SRCC = -0.01 > -0.34$) or ankle plantarflexion ($SRCC = 0.16 < 0.34$) moment. It can therefore be concluded that the rotation of the shank axis has no bearing on knee and ankle moments in the sagittal plane.

Results for hip flexion-extension ($SRCC = 0.25 < 0.34$), hip abduction-adduction ($SRCC = 0.44 > 0.34$), knee flexion-extension ($SRCC = 0.20 < 0.34$) and ankle dorsi-plantar flexion ($SRCC = 0.20 < 0.34$) moment range all showed that there was no significant link between standing foot angle and joint moment range. These results are illustrated in Figure 126.

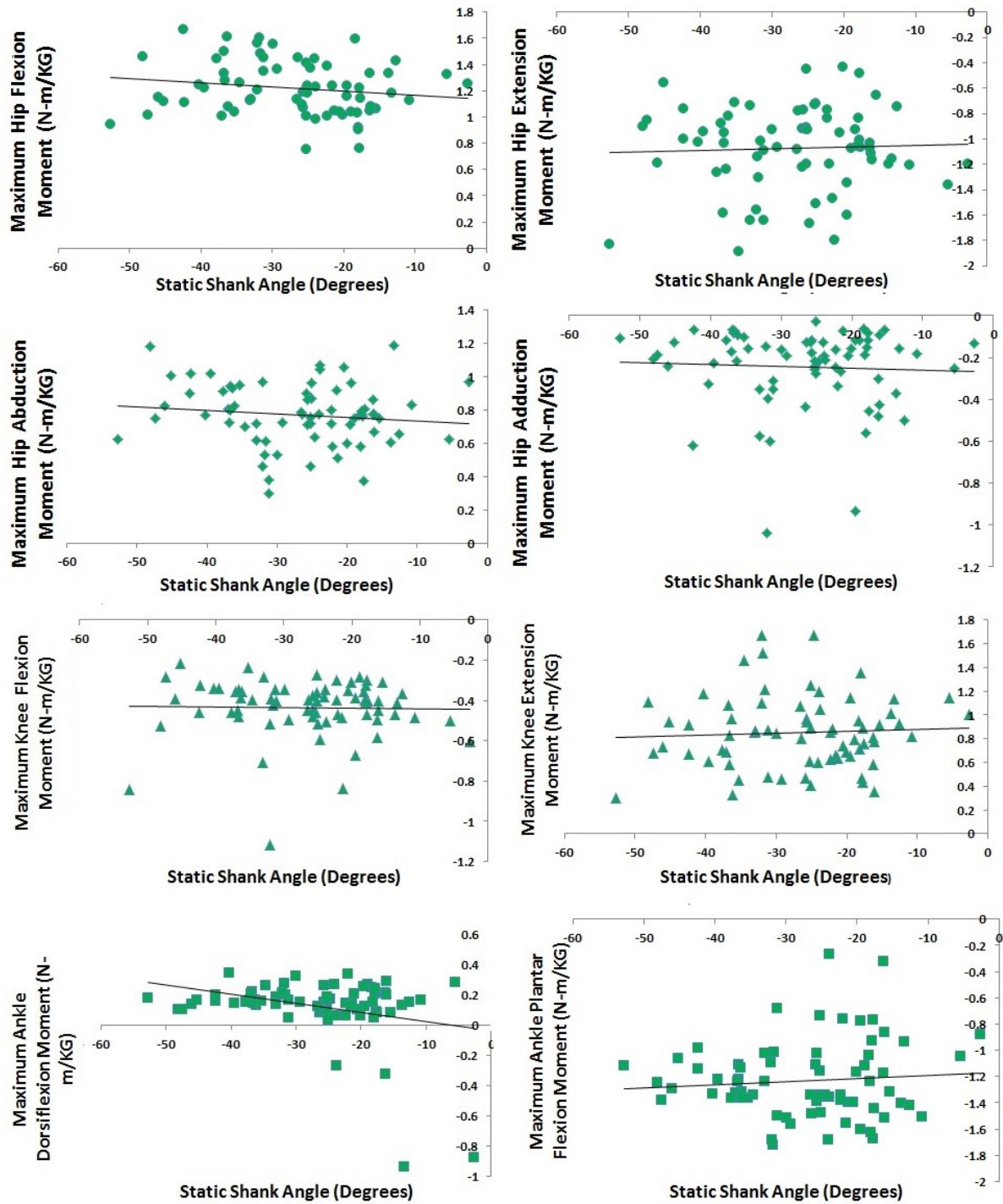


Figure 125: The effect of varying initial shank standing angles when measured against the laboratory axes to maximum hip flexion-extension, abduction-adduction, knee flexion-extension and ankle dorsi-plantarflexion moments.

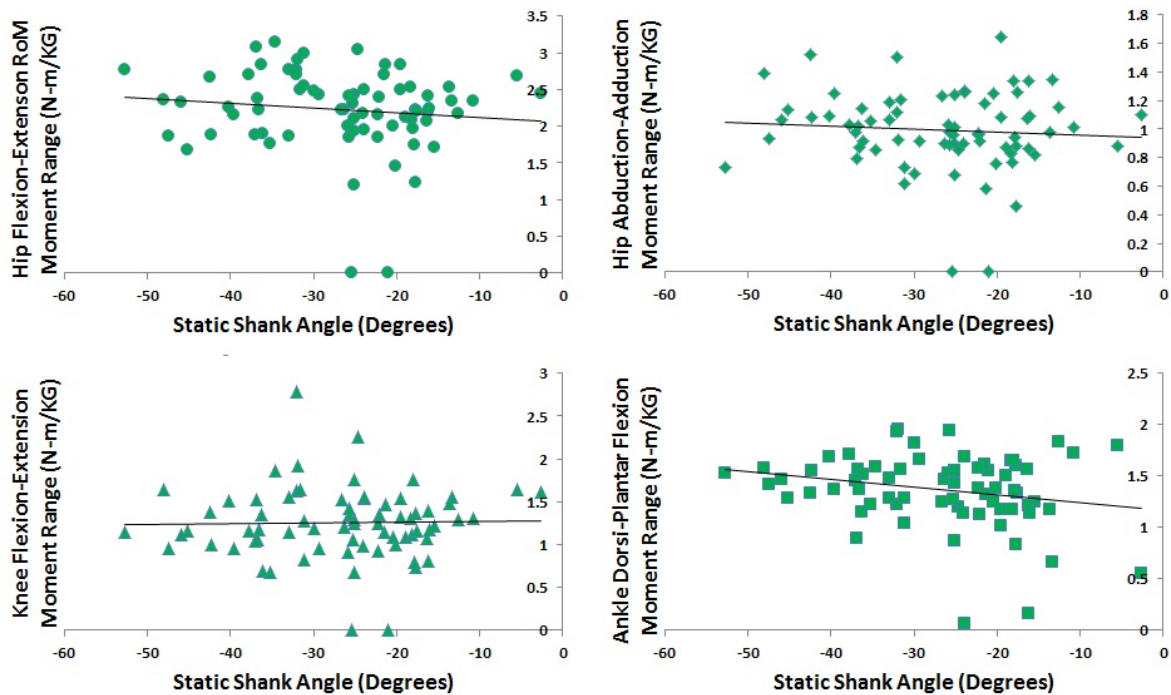


Figure 126: The effect of varying initial shank standing angles when measured against the laboratory axes to range of moment in terms of hip flexion-extension, hip abduction-adduction, knee flexion-extension and ankle dorsi-plantar flexion.

Figure 127 is with regards to the effects of the initial standing trial average foot rotation with respect to the laboratory against hip flexion-extension, hip abduction-adduction, knee flexion-extension and ankle dorsi-plantarflexion moment maximums. No significant links were found for the maximum hip flexion ($SRCC = 0.19 < 0.34$), extension ($SRCC = 0.25 < 0.34$), abduction ($SRCC = 0.26 > 0.34$) or adduction ($SRCC = -0.21 > -0.34$) moments. Thus it can be concluded that the rotation of the foot axis has no bearing on hip maximum moments. Likewise, no significant links were found for the maximum knee flexion ($SRCC = 0.19 < 0.34$), knee extension ($SRCC = -0.21 > -0.34$), ankle dorsiflexion ($SRCC = -0.25 > -0.34$) or ankle plantarflexion ($SRCC = -0.26 > -0.34$) moments. It can therefore also be concluded that the rotation of the foot axis has no bearing on knee and ankle moments in the sagittal plane.

Results for hip flexion-extension ($SRCC = 0.25 < 0.34$), hip abduction-adduction ($SRCC = 0.24 > 0.34$), knee flexion-extension ($SRCC = 0.20 < 0.34$) and ankle dorsi-plantar flexion ($SRCC = 0.20 < 0.34$) moment range all showed that there was no significant link between standing foot angle and joint moment range. These results are illustrated in Figure 128.

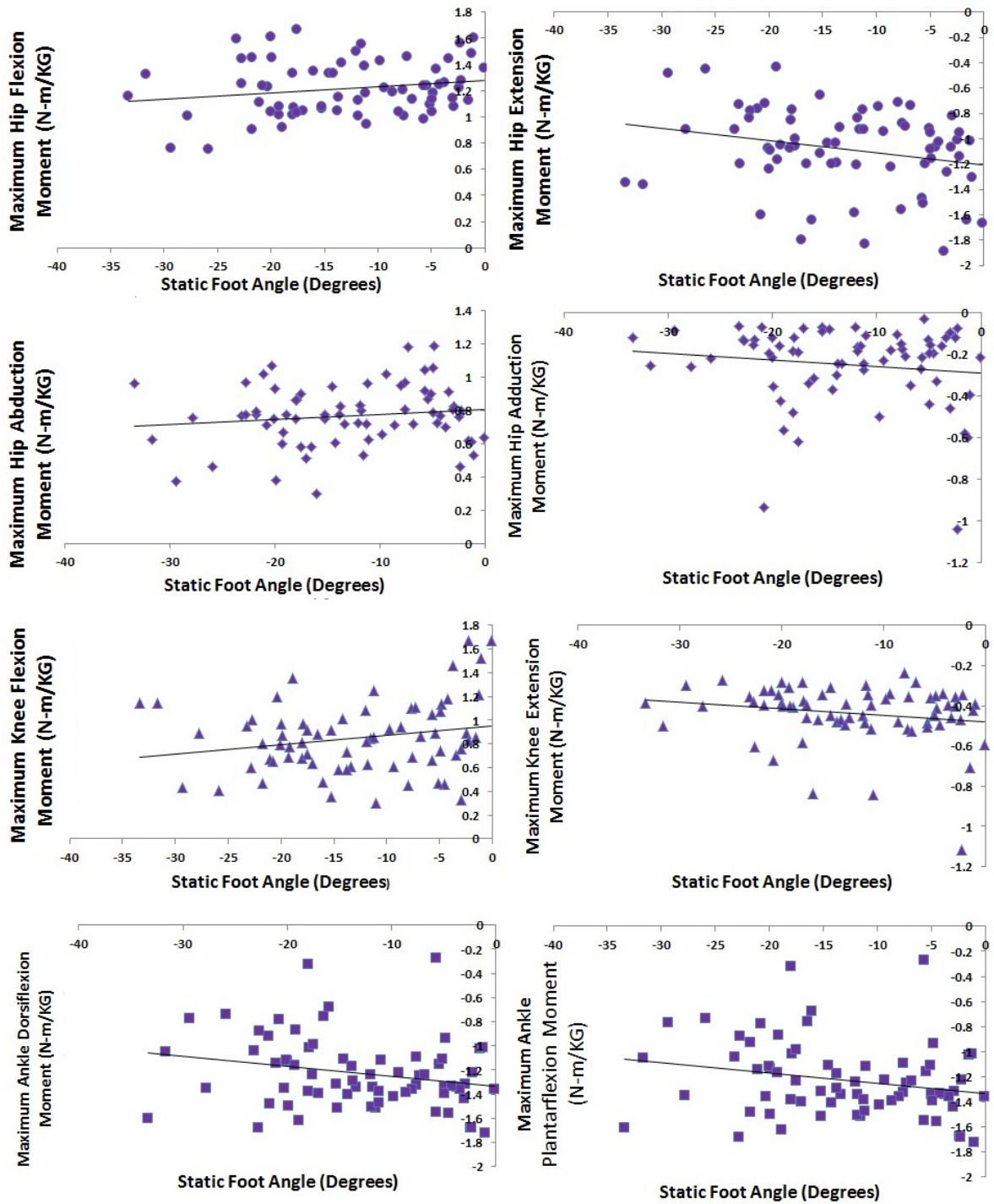


Figure 127: The effect of varying initial foot standing angles when measured against the laboratory axes to maximum hip flexion-extension, hip abduction-adduction, knee flexion-extension and ankle dorsi-plantar flexion moments.

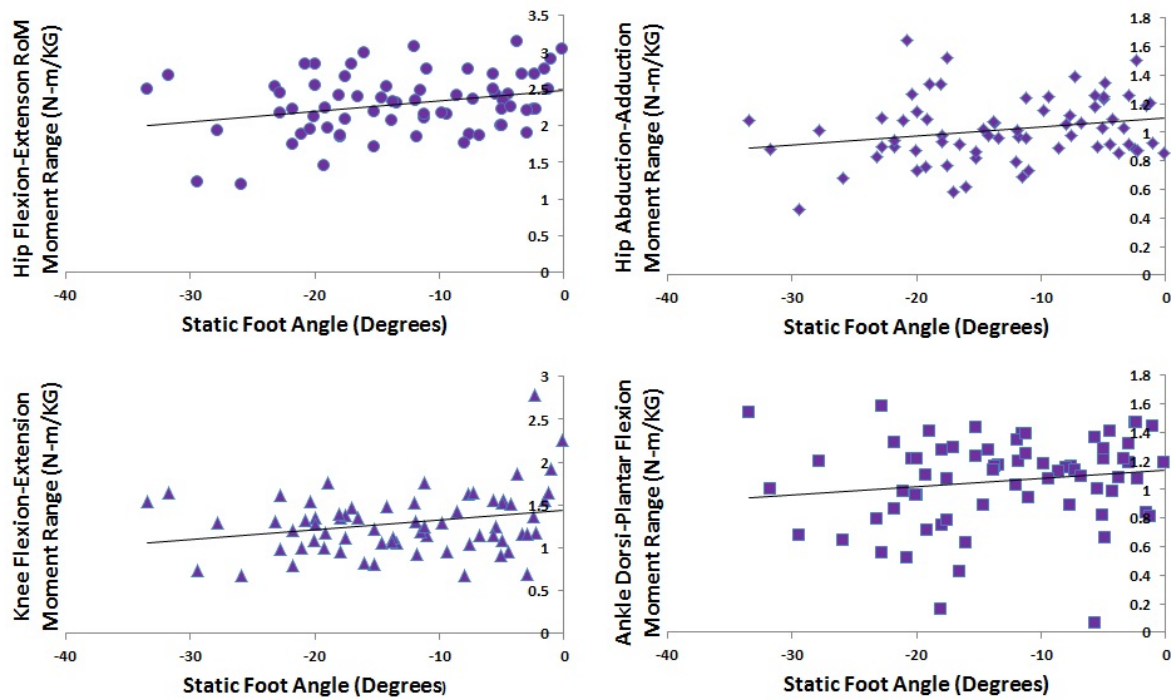


Figure 128: The effect of varying initial foot standing angles when measured against the laboratory axes to maximum knee flexion-extension and ankle dorsi-plantarflexion moments

7.7 Discussion

To the authors knowledge, this is the first study to have been undertaken which has compared standing segment angles between patient groups. Due to the novelty of the present research, it makes comparisons to published literature for verification difficult. The trends shown in the results demonstrate that excessive external rotation of segments was more common than excessive internal rotation. This indicates that for the clinical patient measurements, placing the lateral segment markers posterior was more common than placing them anterior. The present results found that there were no statistically significant differences between the clinical groups and also when compared to the Pilot cohort at the pelvis, thigh and foot. General trends were seen, with the Pilot group demonstrating internal rotation of the thigh, conflicting with what was found in the clinical data. Significant differences were however found at the shank.

As the foot is naturally externally rotated between 5° - 15° with respect to the shank [42], results should reflect the foot having a greater rotation angle with respect to the laboratory than the shank. For all the clinical groups we however have the external rotation of the shank being greater than

that of the foot. This was not the case for the Pilot test cohort where foot rotation with respect to the laboratory was greater than the angle made by the shank, although large standard error values were present. As the foot angles were not too dissimilar between the clinical groups, it can be concluded that the shank angles in the Symptomatic LLI, Normal and Happy THR groups were unreliable. The Pilot data produced results more in line with what would be expected. As the anterior-posterior position of the lateral shank marker dictates the rotation of the shank axis (more anterior leads to greater internal rotation and more posterior leads to greater external rotation), the patient groups appear to have had their shank markers placed too posterior. The large standard errors present show that inter-patient variability may be a result of the difficulties in the positioning of the lateral shank marker.

Overall weak correlations were found for the Normal group between kinematics and kinetics when compared to the rotation of a segment. It thus may be concluded that segment rotations have negligible impact on maximum and minimum joint angles, joint moments, ranges of motions/moments and resultant hip JRFs. The comparisons made between individual patients may not have been accurate representations due to the differing values for measured parameters for each individual. For instance, a group of patients listed in terms of ascending thigh internal rotation angle may not show a corresponding increase in hip flexion angle due to different walking speeds, with slower patients showing less peak flexion. However the results of this study provide confidence in the clinical patient kinematic and kinetic results, with it being determined that errors in segment rotation caused by poor marker placement would have a minimal effect.

7.8 Conclusion

The initial aim of this investigation was to determine whether the differences observed between patient groups were due to poor marker placement, which may have been evident in terms of segment rotations. A general trend was found at the thigh with excessive external rotation in the clinical groups together with the shank showing statistically greater external rotation in the clinical groups relative to a Pilot group. From the perspective of dynamics, a poor correlation was found between amount of internal/external rotation of a segment and joint/moment ranges together with maximum angles/moments forces. A more internally rotated thigh led to a greater peak hip flexion angle. As only a small number of parameters were significantly effected, it was difficult to draw a conclusion linking the reliability of the results to poor marker placement. Other factors such as

gait velocity and stride length may have had a greater contribution to the kinematic and kinetic variability seen than marker misplacement alone. This gives confidence that the PiG marker set used in the current study was of suitable reliability to compare clinical groups.

8 A Critique of PiG - I

8.1 Aims & Objectives

The aim of this study was to compare and contrast how the choice of HJC regression equation and errors in anthropometric measurements (knee and ankle joint width) effects joint centre positions, standing angles, dynamic angles and moments at the hip, knee and ankle. These results were important in determining the accuracy of the clinical data and in determining the amount of error that could potentially be produced through either conscious selection (HJC regression equations) and measurement error (joint widths).

8.2 Methodology

8.2.1 Subject

Analysis was undertaken in Visual3D on a typical male LLI patient from the cohort selected at random, with a BMI of 28.1 and LLI of 40mm. The LLI patient had been implanted with an UHMWPE prosthesis and was suffering from symptoms serious enough to warrant revision surgery¹⁷. The patient also had clinical knee and ankle width measurements made using a caliper for both the left and right sides, averaging 110mm for the knee and 70mm for the ankle.

8.2.2 Gait Analysis

As with all the data obtained from clinical analysis, the patient was subject to the PiG model with a total of 16 markers present on the lower extremity which included the pelvis, two thighs, two shank bones and two feet¹⁸. One standing trial was used together with 5 dynamic motion trials. Joint angles and moments were measured over a single gait cycle beginning at heel strike onto the force plate and ending with heel strike off the force plate of the same foot.

8.2.3 Body Model

The body model as defined on pages 77 - 85 in the *Generic Methods* was used. Hip motion was measured between the thigh and the pelvis, knee motion was measured between the shank and the

¹⁷See page 90 in the *Anthropometrics & Demographics* chapter for further information

¹⁸See pages 69- 70 of the *Generic Methods* for more information

thigh and ankle motion was measured between the foot and the shank. Moments were computed via inverse dynamics.

8.2.4 Hip Joint Centre

The impact that the choice of HJC regression equation had on distal joint centre position together with joint angles and joint moments was analysed. Due to the absence of a marker on the greater trochanter, PiG does not allow the user to define the HJC location to be a measured distance (femoral offset) from a known landmark. The Davis, Harrington and Bell HJC regression equations were used and compared in the present study. The definition, derivation and application of each equation into Visual3D are discussed on pages 80 - 82 in the *Generic Methods*. All joint centre position measurements were taken against the laboratory coordinate system.

8.2.5 Joint Radius

In Visual3D and the PiG model, the knee and ankle width is taken as an input to calculate the joint width together with marker diameter. These equations can be seen in Equations 54 and 55. In the analysis of the LLI patients, a marker diameter of 14mm was used.

$$\text{KJC} = \frac{(\text{Marker Diameter} + \text{Knee Width})}{2} \quad (54)$$

$$\text{AJC} = \frac{(\text{Marker Diameter} + \text{Ankle Width})}{2} \quad (55)$$

For the analysis of the knee, an initial knee width was taken of 110mm which was increased in 5mm intervals up until 135mm, giving a range of 25mm. An initial ankle joint width of 70mm was selected which was increased in 5mm increments to that of 95mm. Each analysis was undertaken independently, with the use of a 110mm knee width when analysing the ankle width sensitivity and a 70mm ankle width when analysing knee width sensitivity. Changes in both joint angles and joint centres were measured.

8.3 Results - Hip Centre Regression Equation - Standing Trial

Figure 129 demonstrates that the choice of HJC regression equation did have an impact on the orientation of segments, however this was minimal and not clinically significant. The greatest difference at the thigh (0.51°), shank (0.50°) and foot (0.27°) were between the equations of Davis and Harrington.

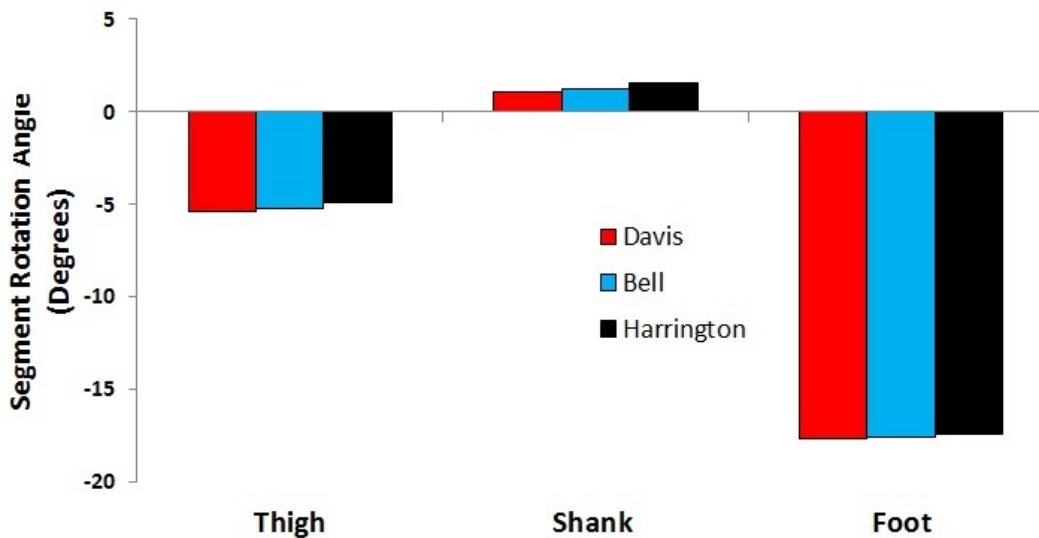


Figure 129: The effect of different HJC regression equations on orientation of thigh, shank and foot segments.

Figure 130 demonstrates that there were differences in the position of all the joint centres in the model as a direct result of the choice of HJC regression equation. The greatest similarity in results was between Davis and Bell whilst the largest differences were between Harrington and Davis. The greatest differences between the methods in terms of joints were seen at the hip which was followed by the knee and then the ankle. At the hip the largest displacement occurred in the anterior-posterior direction, with there being large differences between the equations of Harrington and Davis (27.1mm) together with Bell and Harrington (20.1mm). Smaller differences were present in the medial-lateral and inferior-superior directions. The choice of HJC had a large effect at the knee, with the greatest difference once again occurring between the regression equations of Harrington and Davis (9.75mm) in the anterior-posterior direction. This was also the case for the ankle, with Harrington and Davis producing the greatest difference in the anterior-posterior directions (2.92mm).

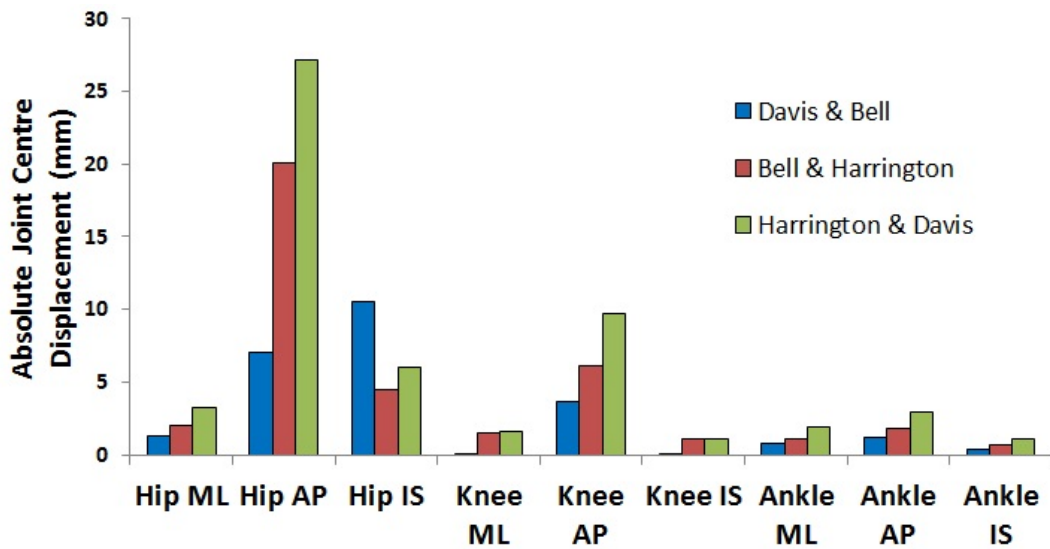


Figure 130: The effect of different HJC regression equations on the positions of the HJC, KJC and AJC.

8.4 Results - Hip Centre Regression Equation - Dynamic Trial

8.4.1 Hip

Figure 131 demonstrates how the HJC regression equations impacted hip joint angles and moments. There was little difference in terms of hip flexion-extension angle (**A**) between the Davis, Bell and Harrington HJC regression equations. Table 14 further demonstrates this, with the average gait cycle joint angle being <5% different between the groups. The results using the HJC regression equation as developed by Davis for abduction-adduction angle (**C**) yielded reduced large differences of around 20% when compared to that of Bell and Harrington, whilst the Bell and Harrington HJCs themselves had little difference (3.66%). Differences can be linked to Figure 130. The Harrington equation was more similar to that of Bell than to that of Davis in terms of medial-lateral position of the HJC. The Harrington and Bell equations would have had, according to Figure 131, more medial HJC positions relative to that of Davis. This more medial HJC would have led to an abduction offset at the thigh and hence at the HJC axis (i.e. that the definition of what abduction and adduction were would have changed).

Hip rotation (**C**) is measured between the rotation of the thigh and the pelvis. As the pelvis is not modified in any way, the changes seen are directly due to the thigh. The HJC has an effect in

computing the position of the KJC¹⁹, which is used to compute the rotation of the thigh²⁰. Due to the Harrington HJC regression equation producing the most different HJC position, whilst those of Bell and Davis were more similar, the present results show more similarity in the rotation curves between Davis and Bell. The greater internal rotation of the Harrington HJC equation was due to a more anterior KJC relative to the lateral knee marker, when compared to the KJCs of Davis and Bell. The more anterior KJC marker led to external rotation of the thigh, causing there to be rotation offset where some external rotation was measured an internal rotation and results to be measured as greater internal rotation angles.

Joint moments also differed. This was particularly during the stance phase, where the results for the Harrington HJC produced more flexion moment than the other two methods. Table 14 further illustrates this where the results of Harrington were more than 10% different to those of Bell and Davis, whilst the results of Davis and Bell were more similar through only showing a 1.18% difference. Figure 130 on page 203 showed that the Harrington HJC regression equation had the greatest differences relative to those of Bell and Davis in the anterior-posterior direction. Differences during the stance phase occurred due to the Harrington regression equation producing a HJC which was more posterior, thus leading to a flexion offset during analysis and a change in moment arm. Very little differences existed in terms of moments for both abduction-adduction (**D**) and internal-external rotation (**E**).

Table 14: Percentage difference between the average hip flexion (+)-extension (-) angles (**FE**) and moments (**FE**), abduction (+) adduction (-) angles (**AA**) and moments (**AA**), internal (+) external rotation (-) angles (**IER**) and moments (**IER**) for the Davis, Harrington and Bell HJC regression equations over 5 normalised gait cycle trials between consecutive heel strikes of the same foot

Regression Equation / Variable	Davis & Bell	Davis & Harrington	Bell & Harrington
Hip FE Angle	1.20%	2.73%	3.87%
Hip FE Moment	1.18%	12.2%	11.1%
Hip AA Angle	22.1%	19.2%	3.66%
Hip AA Moment	8.71%	7.65%	1.16%
Hip IER Angle	191 %	528%	673%
Hip IER Moment	7.86 %	6.99%	1.42%

¹⁹See Figures 27 and 29 on pages 71- 72 in the *Generic Methods*

²⁰See Figure 32 on page 74 in the *Generic Methods*

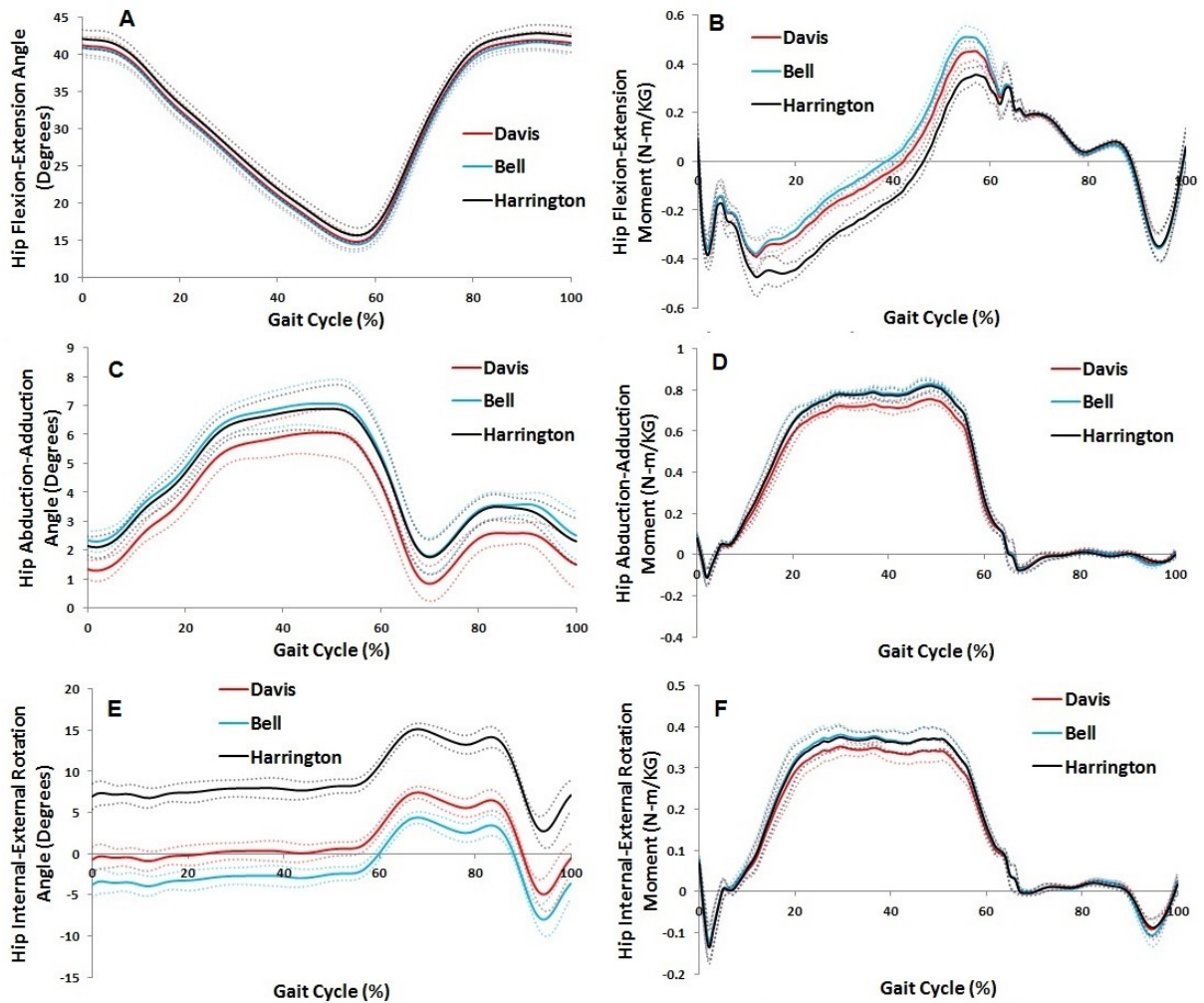


Figure 131: Average hip flexion (+)-extension (-) angles (A) and moments (B), abduction (+) adduction (-) angles (C) and moments (D), internal (+) external rotation (-) angles (E) and moments (F) for the Davis, Harrington and Bell HJC regression equations over 5 normalised gait cycle trials between consecutive heel strikes of the same foot

8.4.2 Knee

Figure 132 demonstrates that there did not exist any significant differences between the methods of Davis, Bell and Harrington in terms of knee flexion-extension angle, with Table 15 showing that the greatest average joint angle difference was less than 5%. Much larger differences were evident in terms of abduction-adduction, with the results of Davis and Harrington being more similar during the stance phase whilst those of Bell exhibited less adduction. During the swing phase there were significant differences between the groups with the average results of Harrington showing at its peak 15° more adduction than that of Bell. Table 15 shows that the biggest difference was between the results of Bell and Harrington (45.8%).

Figure 132 also shows that the choice of HJC regression equation had a significant impact on

knee rotation. The results for knee rotation for Davis and Bell were very similar; however those for Harrington were vastly different and showed greater external rotation. These can once again be put down to the differences in initial HJC position and the knock on effects in computing the KJC and the orientation of the shank axes. This can be seen from Table 15 where the results comparing Harrington were greater than those comparing Davis and Bell.

Significant difference in terms of knee flexion-extension moment between the Davis, Bell and Harrington HJC regression equations. The greatest difference appeared to be between the results of Bell and Harrington which was especially evident between 10%-20% of the gait cycle. These results reflect the differences in position of HJC when using the Bell, Davis and Harrington Equations as seen in Figure 130 on page 203 o. The Harrington HJC had the greatest peak knee flexion moment, which was due to it having the most anterior KJC.

Differences existed for a number of reasons. The first being that the selected HJC regression equation effected the position of the KJC, which is tracked during gait and used to compute kinematics. The second reason was the differences in axes orientations for the selected HJC regression equations. The lateral shank marker determines the amount of shank rotation. As knee abduction-adduction is measured in the frontal plane between the thigh and the shank, changes at the thigh in terms of rotation of the segment axes would also have effected the obtained results ²¹. As the Harrington HJCs position was the most different, it would have effected the position of the KJC so that its position differed significantly to those of Davis and Bell. This would have then led to large variability in the rotation of the shank axes. The greater amplitude of the adduction curve shows that there may also have been some cross talk between axes. There was very little impact on knee abduction-adduction and rotation moments.

²¹See Figure 33 on page 75 in the *Generic Methods*

Table 15: Percentage difference between the average knee flexion (+)-extension (-) angles (**FE**) and flexion (-)-extension (+) moments (**FE**), abduction (+) adduction (-) angles (**AA**) and moments (**AA**), internal (+) external rotation (-) angles (**IER**) and moments (**IER**) for the Davis, Harrington and Bell HJC regression equations over 5 normalised gait cycle trials between consecutive heel strikes of the same foot

Regression Equation / Variable	Davis & Bell	Davis & Harrington	Bell & Harrington
Knee FE Angle	0.63%	4.05%	4.65%
Knee FE Moment	1.91%	39.4%	38.2%
Knee AA Angle	29.9%	22.7%	45.8%
Knee AA Moment	0.58%	3.78%	4.38%
Knee IER Angle	3.46 %	8.96%	12.1%
Knee IER Moment	3.68 %	2.01%	1.59%

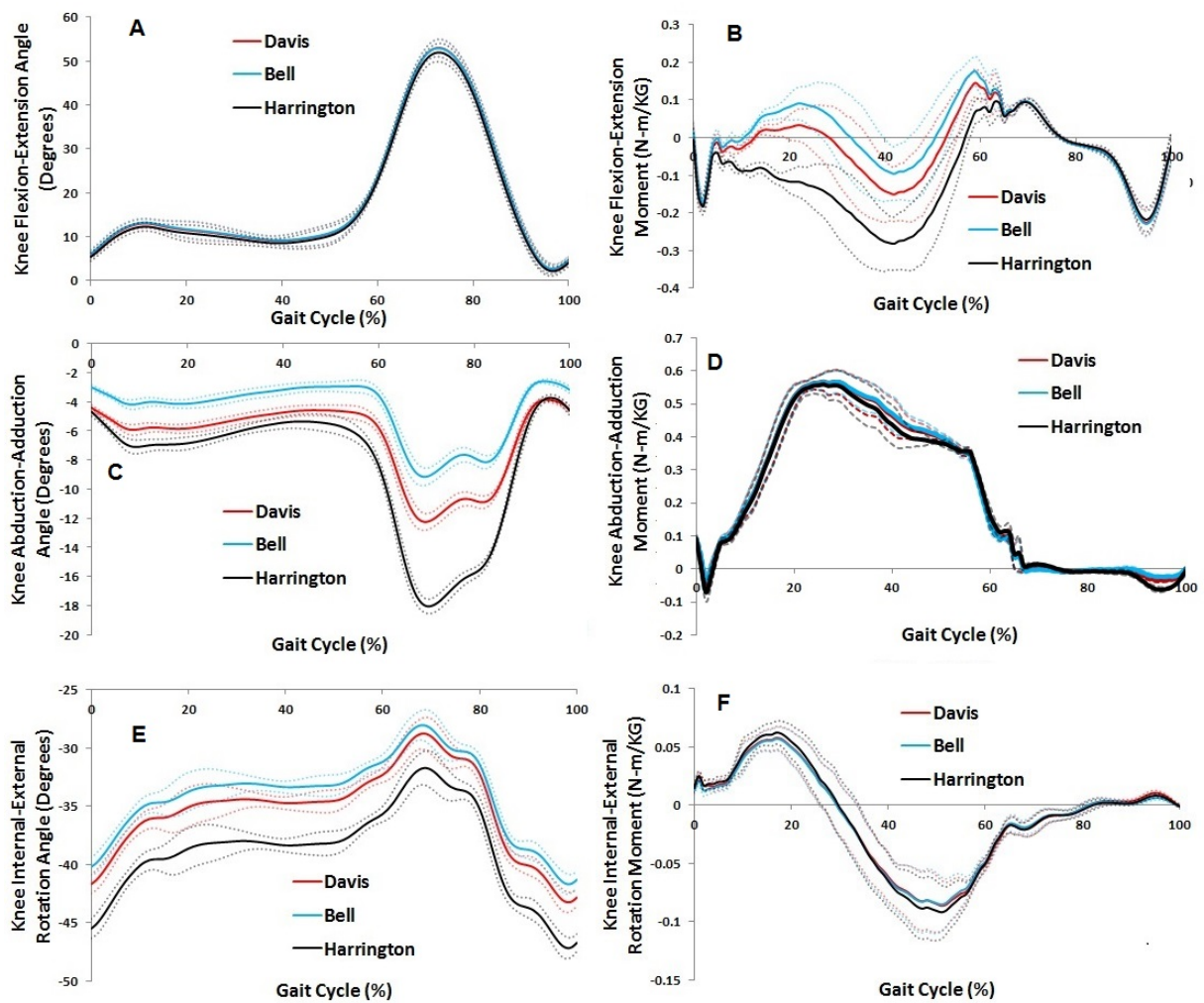


Figure 132: Average knee flexion (+)-extension (-) angles (**A**) and flexion (-)-extension (+) moments (**B**), abduction (+) adduction (-) angles (**C**) and moments (**D**), internal (+) external rotation (-) angles (**E**) and moments (**F**) for the Davis, Harrington and Bell HJC regression equations over 5 normalised gait cycle trials between consecutive heel strikes of the same foot

8.4.3 Ankle

Figure 133 and Table 16 shows that the choice of HJC regression equation had very little effect on ankle dorsi-planar flexion angle. This is a reflection on Figure 130, where the choice of HJC regression equation had very little effect on the position of the AJC in the anterior-posterior direction. Significant differences however existed between the HJC regression equations in terms of their effects on ankle inversion-eversion angle. The choice of the Bell regression equation lead to the greatest amount of inversion. The use of the Davis equation produced a curve which was very similar to that of Bell. Results with the Harrington hip were very different however, with the angle curve appearing to have been offset by over 5° . This can be further illustrated in Table 16 where the Harrington HJC equation produced the greatest percentage differences of over 100%.

The changes in terms of AJC position were minimal when selecting a HJC. The choice of HJC regression equation has a very minimal effect on the medial-lateral positions of both KJCs and AJCs. This is as the medial-lateral position is determined by the clinically measured knee and ankle widths. Instead, the differences seen in terms of ankle eversion-inversion were due to variations between the models in the orientations of the axes at the shank, with eversion-inversion being computed using the shank frontal plane. As was seen in the results for hip abduction-adduction, the choice of regression equation impacted the joint angles produced. This then had a knock on effect at the knee in terms of computing knee abduction-adduction. This same effect was also seen at the foot.

The choice of HJC regression equation had an effect on ankle internal-external rotation angle. The results of Bell and Davis were more similar whilst that of Harrington were more different. This is further evidenced by Table 16 where the results of Harrington produced the greatest percentage difference. These differences were due to the changes at the shank in terms of axes orientation, with rotation being measured with both the shank and foot axes. Very little changes were found to occur in terms of ankle joint moments.

Table 16: Percentage difference between the average ankle dorsiflexion (+)-plantarflexion (-) angles (**FE**) and moments (**FE**), eversion (+) inversion (-) angles (**EI**) and moments (**EI**), internal (+) external rotation (-) angles (**IER**) and moments (**IER**) for the Davis, Harrington and Bell HJC regression equations over 5 normalised gait cycle trials between consecutive heel strikes of the same foot

Regression Equation / Variable	Davis & Bell	Davis & Harrington	Bell & Harrington
Ankle DPF Angle	0.23%	0.63%	0.85%
Ankle DPF Moment	1.06%	3.03%	4.06%
Ankle E/I Angle	18.4%	126%	167%
Ankle E/I Moment	0.93%	4.40%	5.29%
Ankle IER Angle	7.17 %	12.5%	18.7%
Ankle IER Moment	.256 %	5.93%	6.45%

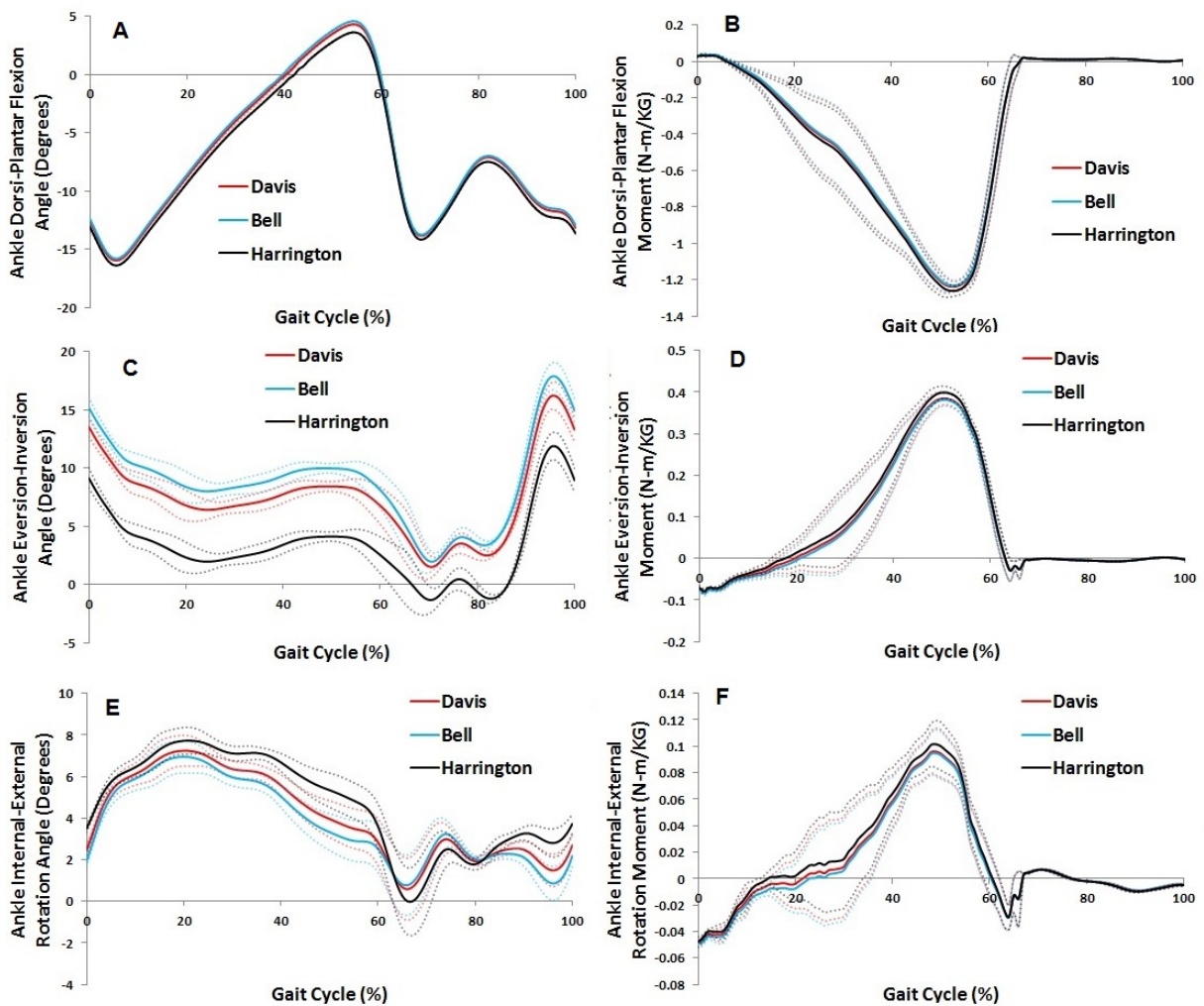


Figure 133: Average ankle dorsiflexion (+)-plantarflexion (-) angles (**A**) and moments (**B**), eversion (+) inversion (-) angles (**C**) and moments (**D**), internal (+) external rotation (-) angles (**E**) and moments (**F**) for the Davis, Harrington and Bell HJC regression equations over 5 normalised gait cycle trials between consecutive heel strikes of the same foot

8.5 Discussion I

To the authors knowledge, this is the first study to have analysed standing angles, dynamic angles and joint centre displacements using the PiG model for varying HJC regression equations. Studies analysing the PiG model or one of its sister CGMs have previously looked at the marker placement sensitivity of dynamic motion with regards to kinematics [313, 451] and compared the PiG model to other marker models [276, 309, 310, 314–318]. From this perspective, the current study is unique in its analysis of the PiG model during the standing trial and the effects on the distal joints at the knee and the ankle. Due to this, comparisons against literature cannot be made directly as no such data exists. There are however studies in the literature which compare HJC prediction methods, namely those of Harrington, Davis and Bell [305, 306].

The greatest differences in the standing trial were between the results of Harrington and Davis, with the least being between Davis and Bell for all directions at every joint (excluding hip superior-inferior positioning). It is clear from these results that the Harrington HJC regression equation²² produces vastly different results to those of Bell²³ and Davis²⁴. The accuracy of the predictive method is highly sensitive to marker placements and anthropometric measurements [299]. In addition, most studies in the literature have looked at normal healthy individuals, whilst very few have analysed THR patients. Leardini et al. [300] have shown that the equations by Bell and Davis may not even be accurate representations of the HJC for healthy individuals.

Differences in the KJC and AJC positions were multi-factorial. The HJC position was directly effected by the choice of regression equation in all three directions; the distal joint centres changes were however due to an alteration in the location of the plane used in their calculation, which was caused by the transformation of the relationship shared by the proximal joint centre to the other segment markers. Changes at the distal joint centre were then passed onto the next distal joint centre using the same method. The greatest changes occurred for all joints in the anterior-posterior direction due to the lateral segment markers, which define the anterior-posterior position of distal joint centres, having had the relationship they share with the proximal joint centre and lateral joint marker (lateral knee/lateral ankle) on that segment altered.

There are very few publications which have dealt with the choice of HJC regression equation and

²²Equations 32 and 33 on page 80 in the *Generic Methods*

²³Equations 30 and 31 on page 80 in the *Generic Methods*

²⁴Equations 34 and 35 on page 81 in the *Generic Methods*

joint kinematics during gait. One such study to have addressed this was by Kiernan et al. [452]. They however used the Harrington method as a Gold Standard relative to the results produced by Bell, Davis and the Orthotrak system. This was undertaken on gait in children, which is a vastly different cohort compared to the Symptomatic LLI studied during this investigation. A study by Chohan et al. [453] on the effects of the HJC equation on kinematics in obese patients found that significant differences existed between the results of Bell and Davis in all planes. This however is once again not comparable to the LLI group which is very non-uniform in terms of both demographics and anthropometrics. Stagni et al. [454] found that no significant changes occurred at the hip in terms of flexion-extension when the HJC was moved $\pm 30\text{mm}$.

There have been many studies which have looked at joint moments during gait; however, very few have analysed the effects of varying the joint centre position on moments during gait. This study therefore is one of the few available and is unique in the clinical LLI group that has been studied. None of the studies in the literature have directly compared HJC regression methods to each other in terms of joint moments. Stagni et al. [454] found that that the amount of hip extension moment increased with an anterior placed HJC and decreased with a posterior placed HJC. Likewise, a lateral placement of the HJC led to an increase in abductor moment whilst a medial placement led to a decrease. This is also what occurred in the present study.

Figure 134 shows a tally of the percentage differences between two particular HJC regression equations across all joints at every plane for both joint angles and moments. Results demonstrated that the choice of HJC regression equation had a larger effect on joint angles than moments. The differences observed between the results of Bell and Davis were the smallest whilst those involving Harrington were larger. This would have been linked to the initial position of the Harrington HJC, which as shown previously had a position which differed considerably from that of Davis and Bell. Smaller changes were seen in terms of moments as the HJC has a decreasing effect down the kinematic chain leading to very small changes in AJC position and thus moments.

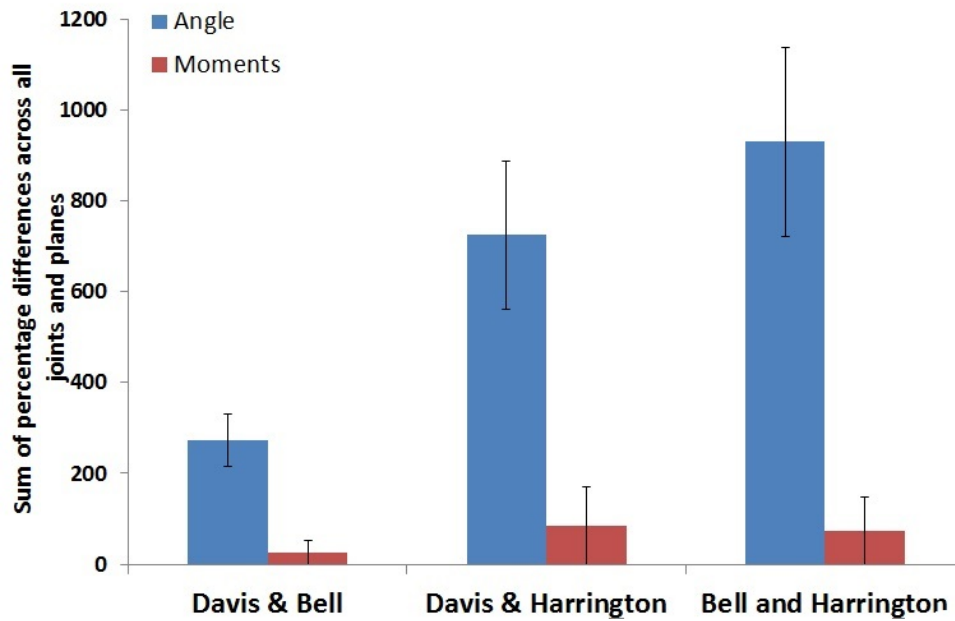


Figure 134: The sum of the percentage difference between the Bell, Davis and Harrington HJC calculation methods across all joints when analysing the average gait cycle joint angle and joint moment.

Figure 135 shows that the choice of HJC regression equation effected the hip kinematics the most and the knee the least. The hip was effected the most as the HJC forms a part of the thigh which is directly involved in hip kinematics. Despite there being some significant changes at the knee, they were smaller than at the ankle. This was largely due to the size of the segments. Variations in the HJC regression equation used would have effected the position of the KJC and AJC, with the former being part of the shank segment and the latter a part of the foot segment. The larger RoM of the shank segment would lead to there being smaller percentage changes in the position compared to the foot. This was the most likely reason for the differences observed.

The ankle motion was calculated using a potentially greater amount of erroneous data through the use of the KJC/AJC positions and axes rotation of both the shank and the foot. These all would have been effected by the choice of HJC, with the cumulative changes at the hip, knee and ankle being illustrated in terms of ankle motion. Results from Figure 135 also demonstrate that the choice of HJC regression equation effected results at the knee the greatest in terms of joints moments, although this was only slightly larger than the hip and the ankle.

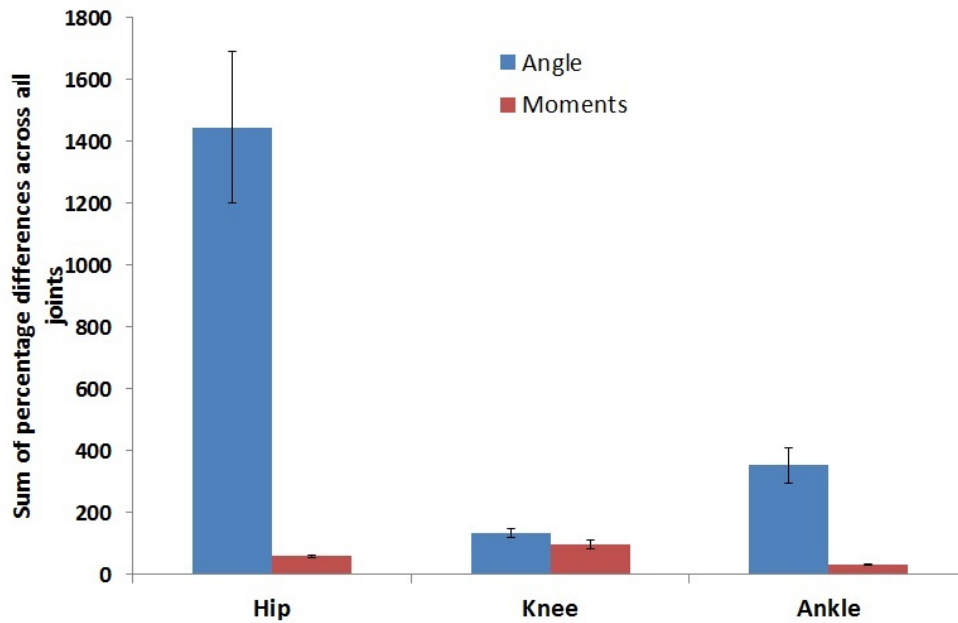


Figure 135: The sum of the percentage difference between the Bell, Davis and Harrington HJC calculation methods when comparing joints using the average gait cycle joint angle and joint moment. Hip results include hip flexion-extension, abduction-adduction and internal-external rotation. Knee results include knee flexion-extension, abduction-adduction and internal-external rotation whilst foot results include ankle dorsi-plantar flexion, ankle eversion-inversion and ankle internal-external rotation.

Figure 136 illustrates that the transverse plane was the most effected in terms of joint angles and the sagittal plane in terms of joint moments when analysing the use of different HJC equations. With regards to joint angles the transverse plane was expected to have the largest differences due to the different HJC/KJC/AJC positions altering the amount of segment rotation. With regards to moments, the sagittal plane had the greatest sum of changes due to the anterior-posterior position of the HJC/KJC/AJC being more effected than the other directions.

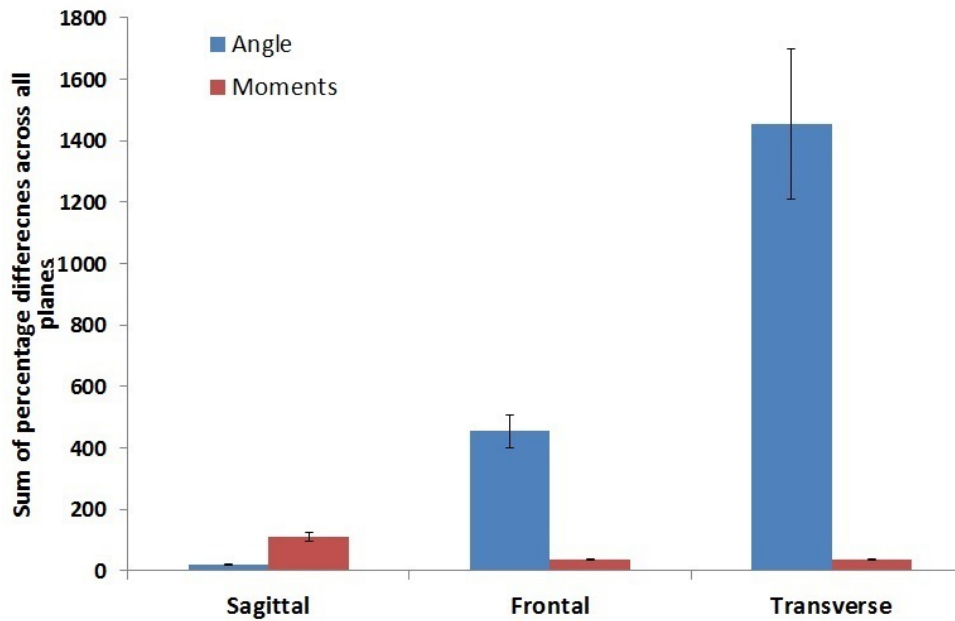


Figure 136: The sum of the percentage difference between the Bell, Davis and Harrington HJC calculation methods when comparing movement planes using the average gait cycle joint angle and joint moment. Sagittal results include hip flexion-extension, knee flexion-extension and ankle dorsiplantar flexion. Frontal results include hip abduction-adduction, knee abduction-adduction and ankle eversion-inversion. Transverse results include hip, knee and ankle rotation.

Many of the studies which have been taken to compare HJC regression methods have supported their own technique as being the most accurate. This may be due to bias where it was known beforehand that a particular method would be better suited to the type of measurement being made or Gold Standard (e.g. CT, MRI, Ultrasound) being used. A systematic review by Kainz et al. [301] found that the Harrington hip regression equation produced the smallest average error across studies of between 14mm-17mm relative to Gold Standard techniques. Other studies have come to similar conclusions [280, 302, 305, 306].

For the clinical study on Symptomatic LLI patients, the Davis HJC regression equation was used during the model building process. As the results in this study have shown together with those from the literature, the use of the Davis equation produces results which differ to those of Harrington, which has also been found to be more accurate. However with errors of up to 17mm present when using Harrington's equation, which makes up more than 60% of the difference between the Harrington and Davis HJC regression equations in the anterior-posterior direction of the hip (Figure 130), too much emphasis should not be put in deciding which equation to select due to measurement errors always being present.

Overall, results have indicated that the PiG model is sensitive in terms of hip kinematics and

kinetics to the choice of HJC regression equation. Most of the differences however appeared in the non-sagittal planes, whereas the clinical studies taken in the *Kinematics & Temporal Spatial Parameters* and *Kinetics* chapters used 6 different motions/moments, with only two being non-sagittal. Despite the choice of the Harrington HJC regression equation being shown in the present study and in the literature to significantly differ from both the Davis and Bell equations, this study found no benefit in its use when studying the planes of motion which typically THR patients compensate in.

8.6 Results - Knee Joint Radius Standing Trial

Figure 137 demonstrates that a 1mm change in joint width leads to a 0.5mm change in the medial-lateral position of the KJC using Equation 44, a gradient of $m = 0.5$. Figure 138 shows that greater changes occurred at the AJC in the anterior-posterior ($m = 0.06$) and medial-lateral directions ($m = 0.12$) than at the KJC ($m = 0.03, 0.04$). Results remained linear.

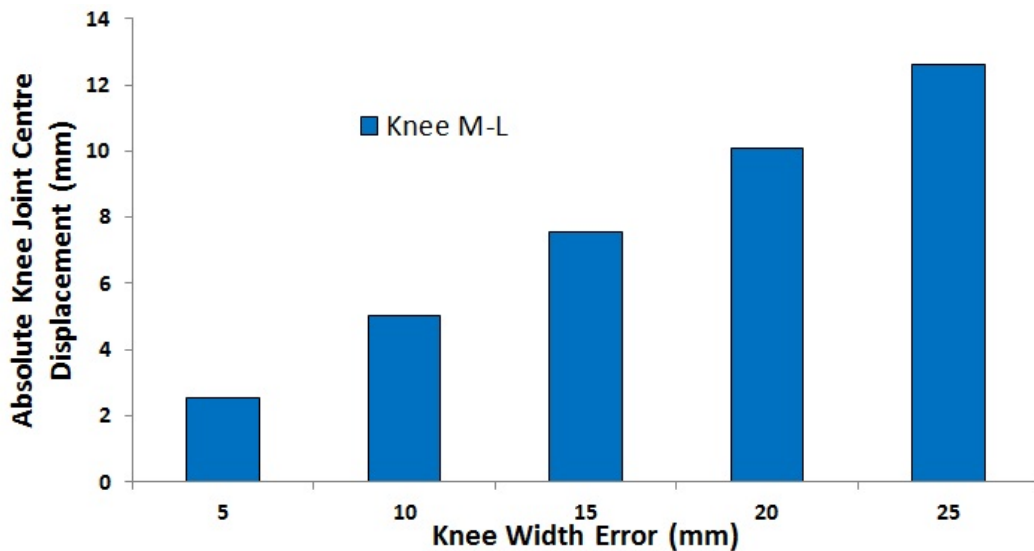


Figure 137: KJC medial-lateral displacement following increasing levels of knee width calculation error.

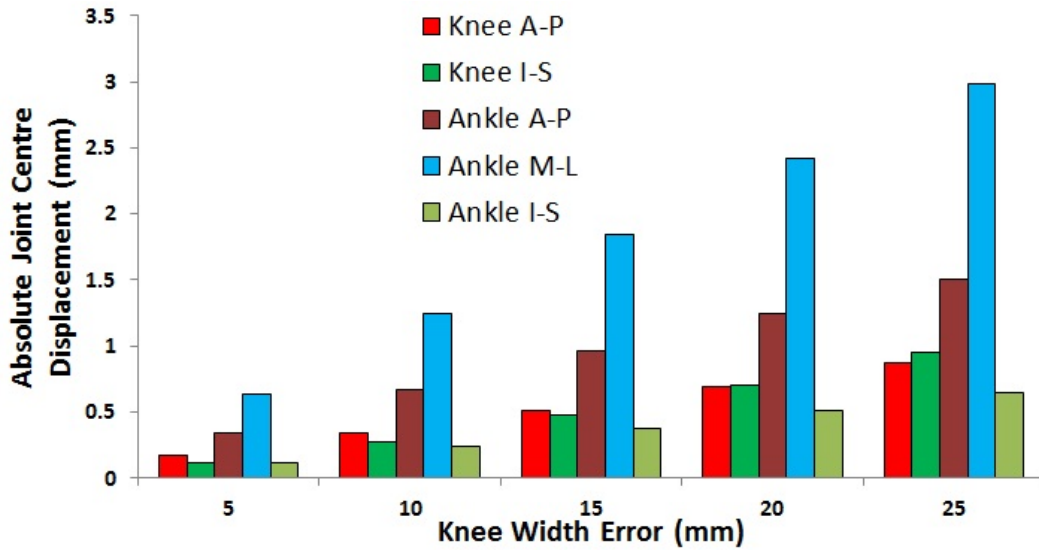


Figure 138: KJC and AJC displacement following increasing levels of knee width calculation error

The second analysis looked at the ankle and how errors in measurement of its width can lead to discrepancies in the location of the AJC. The HJC and KJC results were not included as they were unaffected by distal joint changes. Figure 144 shows the results which establish that increasing the level of ankle width error effects the medial-lateral position of the AJC the most ($m = 0.45$) and the inferior-superior the least ($m = 0.02$), with results remaining linear.

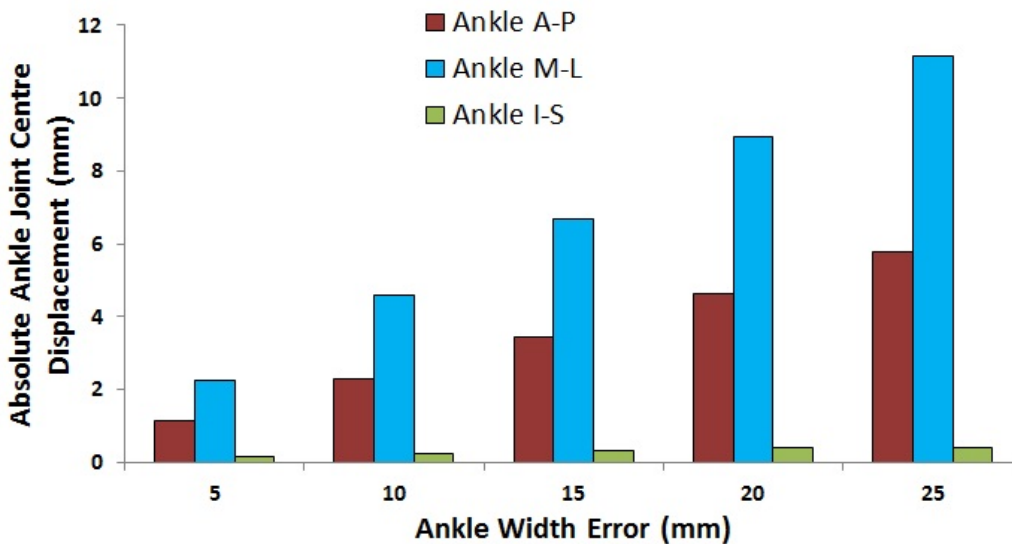


Figure 139: AJC displacement following increasing levels of ankle width calculation errors.

Results indicated that the joint width of the knee and ankle were sensitive to errors in measurement during clinical analysis. This could have a large impact on joint kinetics which rely on the accurate positioning of joint centres.

8.7 Results - Knee Joint Radius Dynamic Trial

8.7.1 Hip

There was virtually no effect of knee joint width error on hip joint moments, as can be seen in Table 17. This was due to the knee width not effecting the position of the HJC, with the minute changes seen being due to distal joint effects. Likewise, very little effect was seen in terms of joint angles in terms of hip flexion-extension and internal-external rotation.

The change in joint hip abduction-adduction angle caused by an error in knee width of $\pm 5\text{mm}$ exceeded the interval width for the original hip abduction-adduction confidence interval during the initial 40% of stance phase and the whole of the swing phase. An error of 10mm exceeded the confidence interval width for the whole of the gait cycle. This can be seen in Figure 140. Large percentage differences were found between the results in terms of average gait cycle angle, as displayed in Table 17. Differences were linked to the change in the abduction-adduction offset of the thigh, which is dictated by knee width.

Table 17: Percentage difference between the average hip flexion (+)-extension (-) angles (**FE**) and moments (**FE**), abduction (+) adduction (-) angles (**AA**) and moments (**AA**), internal (+) external rotation (-) angles (**IER**) and moments (**IER**) for varying knee width errors over 5 normalised gait cycle trials between consecutive heel strikes of the same foot

Joint Width Error / Variable	Original & 5mm	Original & 10mm	5mm & 10mm
Hip FE Angle	0.06%	0.09%	0.03%
Hip FE Moment	1.42%	2.85%	1.39%
Hip AA Angle	21.1%	24.1%	8.03%
Hip AA Moment	0.53%	1.09%	0.55%
Hip IER Angle	0.06 %	0.09%	0.03%
Hip IER Moment	0.44 %	0.90%	0.46%

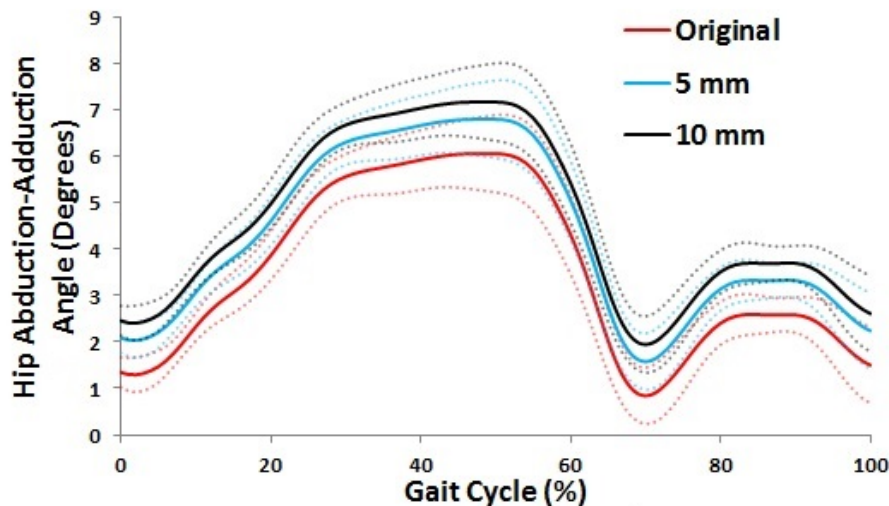


Figure 140: Average hip abduction (+)-adduction (-) angle at original knee width level and errors of 5mm and 10mm together with 95% confidence intervals for original knee width

8.7.2 Knee

The results for knee flexion-extension in Figure 141 and Table 18 demonstrate that an error in the measurement of knee width did not have a significant impact on knee flexion-extension angle. This was as errors in knee width have very little impact on the position of the KJC in the anterior-posterior direction or the orientation of the shank axes. However, a small knee joint width error of just 5mm led to a knee abduction-adduction angle curve which exceeded the 95% confidence interval width of the original measurement. Table 18 shows that these differences were significant, with a 5mm error leading to a change in average joint angle during the gait cycle of almost 20%. A change in knee width moves the medial-lateral position of the KJC, with the larger the knee width the more medial the KJC. The moving of the knee more medially leads to a change in how abduction-adduction is measured, with smaller adduction values being measured through there being an abduction offset²⁵. The change in KJC position also would have effected the orientation of the shank axes.

Results in Figure 141 also demonstrate that an error of 5mm led to a knee internal-external rotation angle which exceeded the 95% confidence interval of the original knee motion. Table 18 shows that this was achieved with small average percentage changes. All of the differences were due to changes in the orientation of the shank axes due to the new change in KJC positions. Knee flexion-extension and internal-external rotation moments remained largely unaffected by errors in knee joint width. Knee abduction-adduction moments were effected by approximately 5% for every 5mm error in knee width. A 10mm error in knee width also appeared for a short portion of mid-stance to exceed the 95% confidence interval for the original knee abduction-adduction moment. The changes in moment were linked to the movement of the KJC and the corresponding changes in joint moments and kinematics.

²⁵See Figure 33 on page 75 in the Generic Methods

Table 18: Percentage difference between the average knee flexion (+)-extension (-) angles (**FE**) and flexion (-)-extension (+) moments (**FE**), abduction (+) adduction (-) angles (**AA**) and moments (**AA**), internal (+) external rotation (-) angles (**IER**) and moments (**IER**) for varying knee width errors over 5 normalised gait cycle trials between consecutive heel strikes of the same foot

Joint Width Error / Variable	Original & 5mm	Original & 10mm	5mm & 10mm
Knee FE Angle	0.45%	0.65%	0.21%
Knee FE Moment	0.44%	0.87%	0.43%
Knee AA Angle	19.2%	40.6%	13.6%
Knee AA Moment	4.86%	10.8%	5.38%
Knee IER Angle	4.76%	7.52%	3.29%
Knee IER Moment	3.45 %	6.52%	3.96%

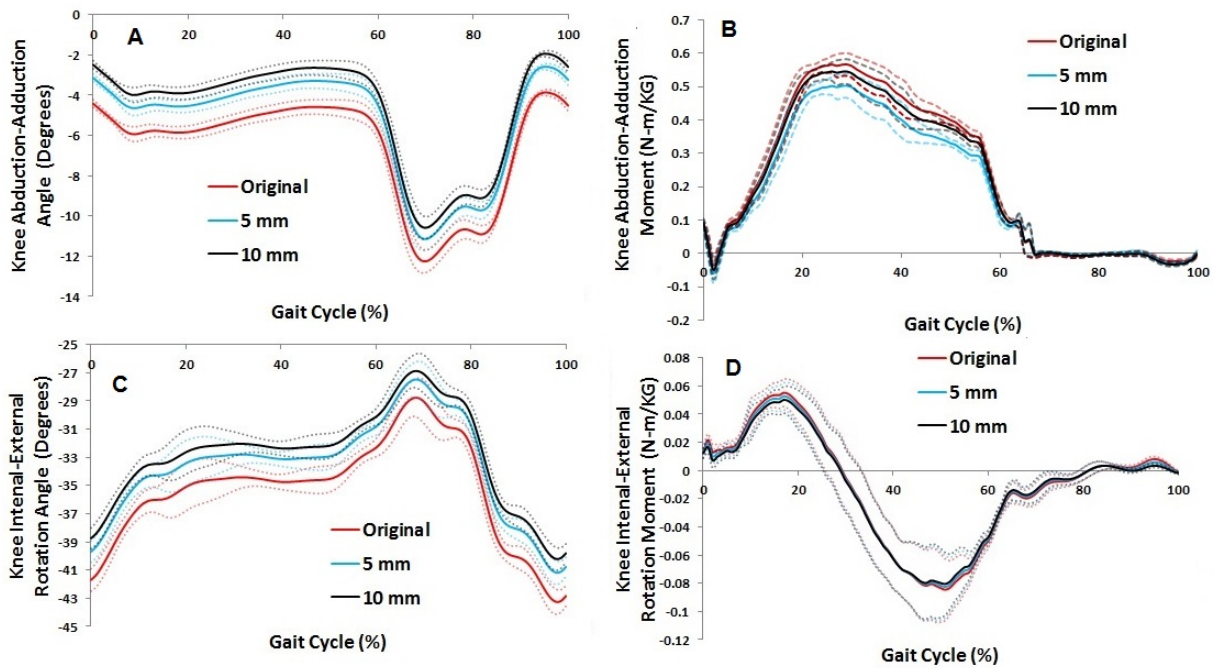


Figure 141: Average knee flexion (+)-extension (-) angles (**A**) and flexion (-)-extension (+) moments (**B**), abduction (+) adduction (-) angles (**C**) and moments (**D**), internal (+) external rotation (-) angles (**E**) and moments (**F**) for varying knee width errors over 5 normalised gait cycle trials between consecutive heel strikes of the same foot

8.7.3 Ankle

The effects for varying knee width on the ankle are shown in Figure 142 and Table 19. Results in terms of dorsi-plantar flexion were not significantly changed with errors in knee width measurement as illustrated in Table 19 and are thus not displayed in Figure 142. This was due to the AJC not being effected in the anterior-posterior direction by changes in knee width. Likewise, there were no significant changes in terms of ankle dorsi-plantar flexion, eversion-inversion or rotation moments due to the negligible effects on the position of the AJC by varying the knee width.

Results from Figure 142 and Table 19 illustrate that a 5mm error in knee width led to ankle eversion-inversion and rotation motion which exceeded the 95% confidence interval produced by the original motion. Large percentage differences existed when increasing the knee width error, which can be seen in Table 19. These differences occurred due to the knee width dictating the amount of abduction-adduction offset of the shank, which is used in the computation of ankle eversion-inversion. Internal-external rotation of the ankle was effected by errors in knee width measurement. Differences were due to the change in orientation of the shank axes.

Table 19: Percentage difference between the average ankle dorsiflexion (+)-plantarflexion (-) angles (**FE**) and moments (**FE**), eversion (+) inversion (-) angles (**EI**) and moments (**EI**), internal (+) external rotation (-) angles (**IER**) and moments (**IER**) for varying knee width errors over 5 normalised gait cycle trials between consecutive heel strikes of the same foot

Joint Width Error / Variable	Original & 5mm	Original & 10mm	5mm & 10mm
Ankle DPF Angle	0.08%	0.12%	0.03%
Ankle DPF Moment	0.26%	1.40%	1.65%
Ankle EI Angle	24.8%	57.2%	18.2%
Ankle EI Moment	0.64%	3.28%	3.90%
Ankle IER Angle	15.7%	32.0%	11.4%
Ankle IER Moment	1.67 %	8.14%	9.67%

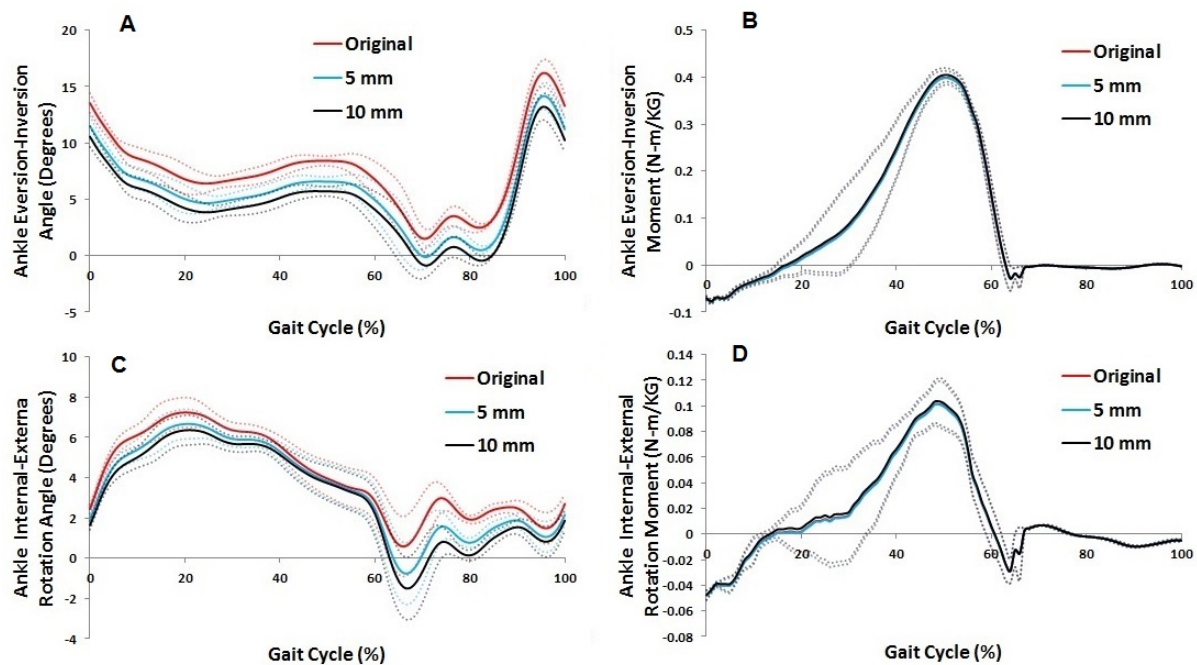


Figure 142: Average ankle dorsiflexion (+)-plantarflexion (-) angles (**A**) and moments (**B**), eversion (+) inversion (-) angles (**C**) and moments (**D**), internal (+) external rotation (-) angles (**E**) and moments (**F**) for varying knee width errors over 5 normalised gait cycle trials between consecutive heel strikes of the same foot

8.8 Discussion - II

A review of the literature found that there have been no previous studies which have analysed standing angles, dynamic angles or joint moments with regards to varying knee joint widths. This is the first study to do so. A sensitivity analysis of how errors in knee width effect joint kinematics potentially has never been studied previously due to the simplicity of the measurements that are made together with it being assumed that the use of a caliper with an error of $\pm 1\text{mm}$ produces reliable results. In terms of the latter this may be true for healthy individuals; however, during the analysis of clinically obese individuals, such as THR patients, the measurement of knee width is more difficult due to the high levels of soft tissue artefact around the joint.

In terms of standing angles, errors in measuring joint width were found to effect the medial-lateral positioning of the KJC and AJCs the greatest and the inferior-superior positioning the least. For dynamic trials, the analysis has shown that errors in knee width effect every joint and plane in terms of motions and moments but to varying extents. Figure 143 shows the sum of the percentage changes in terms of motion and moments overall together with at the joints and individual motion planes. For simplicity, the sum were taken for a 10mm error. Motion was effected by more than a factor of 4 greater than moments whilst in terms of joints the ankle was effected the most and the hip the least for both motions and moments.

Ankle joint angles were effected the most due to the change in the position of the KJC impacting the position of the AJC together with the changes in orientation of the shank and foot axes. As ankle kinematic results generally have a smaller RoM relative to the knee and hip, a greater impact was produced. Changes in joint moments were greatest at the knee due to the KJC having undergone the greatest displacement following the knee width error of 10mm. As changes in knee width determine the abduction-adduction of both the shank and the foot, the greatest changes in terms of planes occurred in the frontal plane.

Overall it can be seen that errors in knee width can effect kinematics and moments. These errors however tend to be concentrated in the frontal plane of the knee and the ankle. As these are not areas in which commonly LLI or THR patients compensate, any errors in knee width would not have significantly impacted either the kinematic or kinetic results in the clinical study.

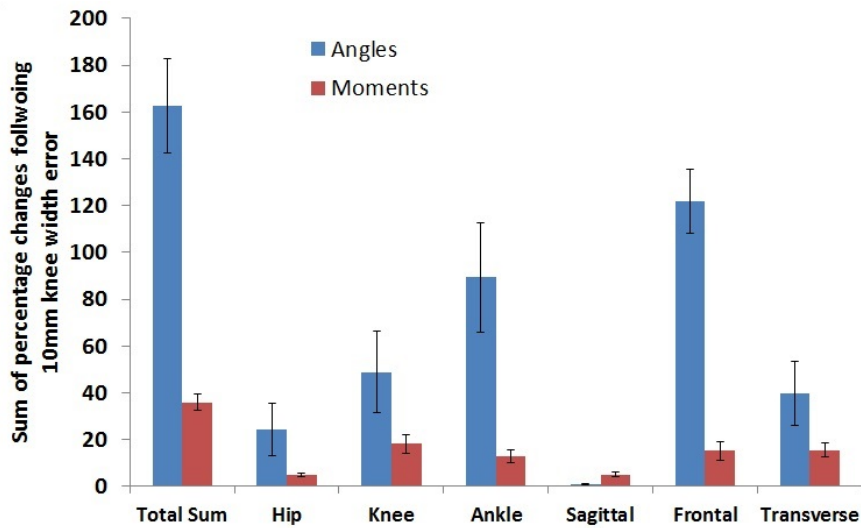


Figure 143: Sum of angles and moments across joints (hip, knee, ankle) and planes (sagittal, frontal, transverse) with regards to the average angle/moment change with a 10mm error in knee width during a normalised gait cycle between consecutive heel strikes of the same foot. Standard errors are also included.

8.9 Results - Ankle Joint Radius Standing Trial

The next analysis looked at the ankle and how errors in measurement of its width can lead to discrepancies in the location of the AJC. The HJC and KJC results were not included as they were unaffected by distal joint changes. Figure 144 shows the results which establish that increasing the level of ankle width error effects the medial-lateral position of the AJC the most ($m = 0.45$) and the inferior-superior the least ($m = 0.02$), with results remaining linear.

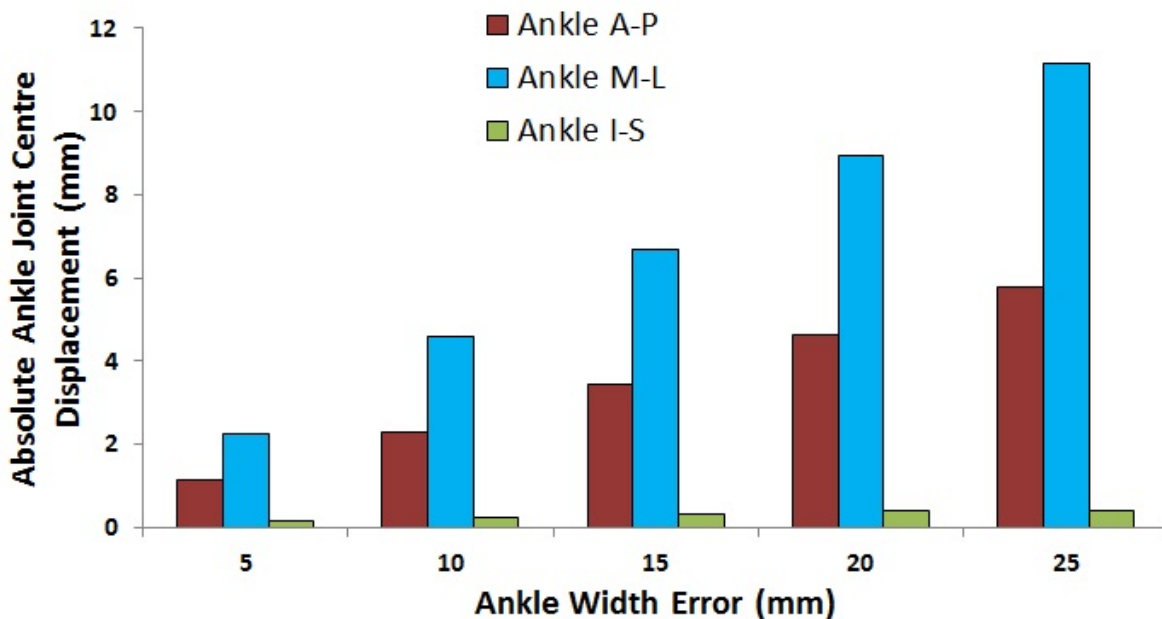


Figure 144: AJC displacement following increasing levels of ankle width calculation errors.

Results indicated that the joint width of the knee and ankle were sensitive to errors in measurement during clinical analysis. This could have a large impact on joint kinetics which rely on the accurate positioning of joint centres.

8.10 Results - Ankle Joint Radius Dynamic Trial

8.10.1 Hip & Knee

Due to the ankle joint being the most distal of all of the joints in PiG, changes in the position of the AJC have negligible impact on kinematics and kinetics at the hip and knee. For this reason, errors in ankle width measurement have very little effect at the proximal joints. Small changes were seen in terms of ankle dorsi-plantar flexion angle and moments due to the AJC not being effected significantly in the anterior-posterior direction. All results can be seen in Table 20.

Table 20: Percentage difference between the average hip/knee/ankle flexion (+)-extension (-) angles (**FE**) and moments (**FE**), abduction (+) adduction (-) angles (**AA**) and moments (**AA**), internal (+) external rotation (-) angles (**IER**) and moments (**IER**) for varying ankle width errors over 5 normalised gait cycle trials between consecutive heel strikes of the same foot

Joint Width Error / Variable	Original & 5mm	Original & 10mm	5mm & 10mm
Hip FE Angle	0%	0%	0%
Hip FE Moment	0.02%	0.06%	0.04%
Hip AA Angle	0%	0%	0%
Hip AA Moment	0.02%	0.06%	0.03%
Hip IER Angle	0 %	0%	0%
Hip IER Moment	0.22 %	0.44%	0.22%
Knee FE Angle	1.14%	2.34%	1.17%
Knee FE Moment	0.15%	0.33%	0.18%
Knee AA Angle	3.07%	5.78%	2.89%
Knee AA Moment	0.34%	0.68%	0.34%
Knee IER Angle	0.08 %	0.16%	0.08%
Knee IER Moment	0.99%	1.95%	0.98%
Ankle DPF Angle	0.06 %	0.11%	0.05%
Ankle DPF Moment	1.89%	3.93%	1.96%

8.10.2 Ankle

Figure 145 shows that measurement error in terms of ankle width can lead to changes in ankle eversion-inversion angle. A 5mm change led to a decrease in eversion and the joint angle to exceed the 95% confidence interval of the original ankle eversion-inversion results at certain portions in the graph. A 10mm error however led to a joint angle curve which exceeded the 95% confidence interval. Table 21 shows that on average, doubling the error in ankle measurement led to doubling of the percentage change in motion over the course of the gait cycle. Ankle eversion-inversion moment

was effected during the stance phase of the gait cycle. These differences are however insignificant as they do not exceed the 95% confidence intervals of the original results. Table 21 illustrates that these changes range from approximately 8%-11% over the course of the gait cycle.

Figure 145 also shows that measurement error in terms of ankle width can lead to changes in ankle internal-external rotation angle. A 5mm change led to an increase in internal rotation and the joint angle to exceed in the 95% confidence interval of the original ankle internal-external rotation results. At 10mm, even greater changes in ankle rotation relative to the original joint angle were seen. Table 21 lists the changes in joint angle over the course of the gait cycle. The variations in joint angles were due to how rotation is defined at the foot, as the angle formed between the long axis of the foot (between the AJC and toe marker) and the laboratory axes²⁶. Ankle internal-external rotation moment was effected during the stance phase of the gait cycle. These differences were however not found to be significant as they do not exceed the 95% confidence intervals of the original results. Large percentage differences were however seen in Table 21, which would have been due to the small ankle rotation moment values.

Table 21: Percentage difference between the average ankle eversion (+) inversion (-) angles (**IE**) and moments (**IE**) and internal (+) external rotation (-) angles (**IER**) and moments (**IER**) for varying ankle width errors over 5 normalised gait cycle trials between consecutive heel strikes of the same foot

Joint Width Error / Variable	Original & 5mm	Original & 10mm	5mm & 10mm
Ankle EI Angle	26.4%	110%	54.9%
Ankle EI Moment	10.8%	17.7%	8.79%
Ankle IER Angle	81.5%	61.6%	30.3%
Ankle IER Moment	25.1%	33.2%	16.5%

²⁶See Figure 35 on page 76 in the *Generic Methods* for further information

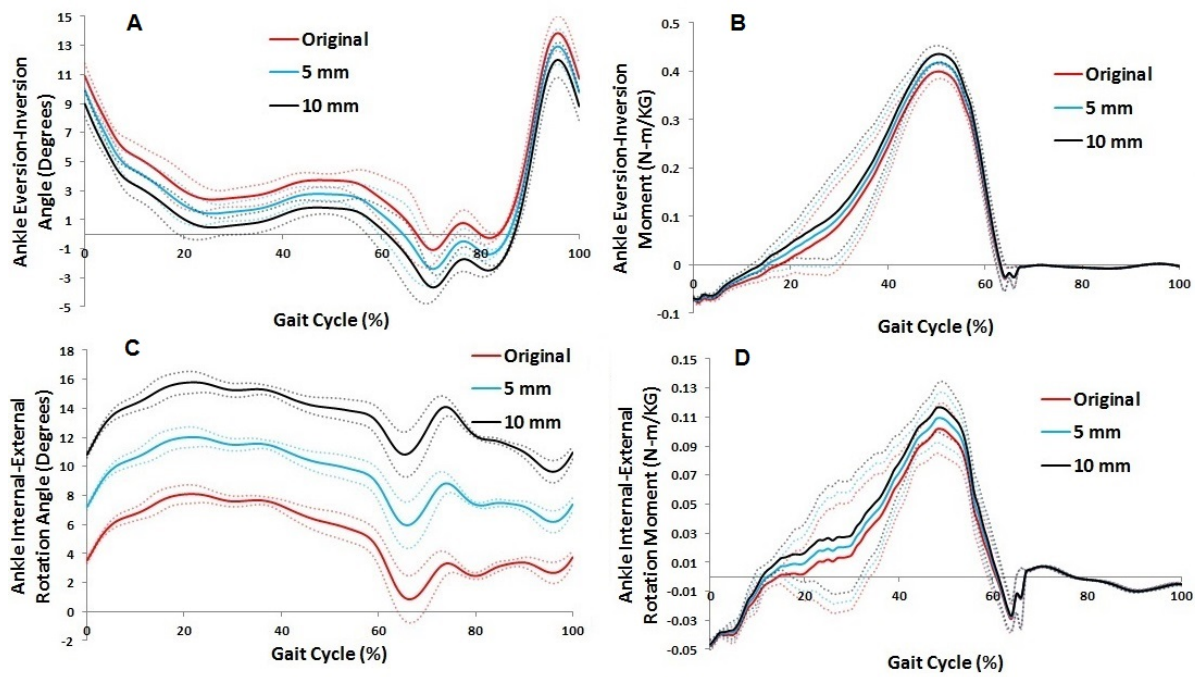


Figure 145: Average ankle eversion (+) inversion (-) angles (**A**) and moments (**B**) and internal (+) external rotation (-) angles (**C**) and moments (**D**) for varying ankle width errors over 5 normalised gait cycle trials between consecutive heel strikes of the same foot

8.11 Discussion - III

As with the results at the knee, this is the first study to determine the effects on joint angles and moments caused by errors in ankle width measurements. Standing trial analysis showed that errors in ankle width measurement effected the medial-lateral position of the AJC the most and the inferior-superior the least, as with what occurred for knee joint width errors. Results in terms of dynamic trials evidenced that errors in its measurement effect knee and ankle motion together with hip, knee and ankle moments during. Hip motion was however unaffected. This was as the ankle width alters the distal portion of the shank and does not effect the thigh or the pelvis, which are used together to compute hip motion. Hip moments were however effected slightly due to the computation of moments at a proximal joint requiring force data from the distal joint.

Figure 146 shows the cumulative percentage changes in motion and moments at each joint and every plane for a 10mm error in ankle width measurement. As can be seen, the greatest errors in terms of joint angles occurred at the ankle, with smaller errors being present at the knee and no error being propagated at the hip. Errors at the ankle were due to the change in position of the AJC leading to a rotation of the foot. This would change the relationship between the heel marker which defines the eversion-inversion axes orientation of the foot and the long axes of the

foot, defined between the toe marker and the AJC²⁷. Changes at the knee were smaller as errors in ankle width measurement lead to a change in the amount of abduction-adduction shown by the shank, but have negligible effect on knee flexion-extension and internal-external rotation.

In terms of planes the greatest changes occurred in the frontal plane with respect to motion and the transverse plane in terms of moments. With regards to motion, the ankle width had a direct effect on the amount of abduction-adduction of the shank segment, with the offset measured as knee abduction-adduction and ankle eversion-inversion in the frontal plane. The impact of changes in ankle width are not so significant in other planes. The greater change in moment in the transverse plane relative to the frontal plane was not meaningful due to the very small changes which occurred.

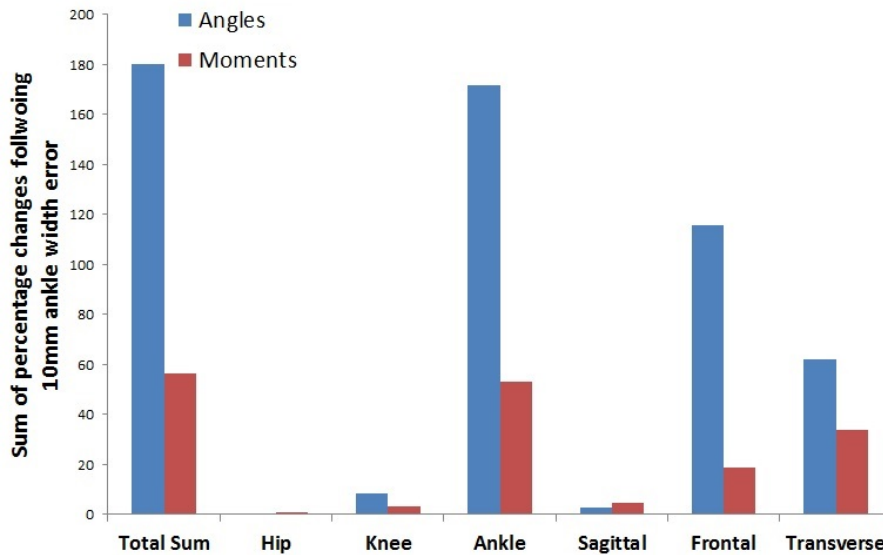


Figure 146: Sum of angles and moments across joints (hip, knee, ankle) and planes (sagittal, frontal, transverse) with regards to the average angle/moment change with a 10mm error in ankle width during a normalised gait cycle between consecutive heel strikes of the same foot. Standard errors are also included.

8.12 Conclusion

This is the first report undertaking an analysis of the standing trial in the PiG model with regards to HJC positions and joint centre positions. This study has analysed the effects of the choice of HJC regression equation and errors in joint width measurement on joint angles and moments during gait. The analyses of each parameter demonstrated that joint angle results were more sensitive than joint moment results. The ankle was the joint which was effected the most, with the choice of HJC, errors in knee width and errors in ankle width all effecting ankle joint angles and moments to varying

²⁷See Figure 35 on page 76 in the Generic Methods

extents. Due to the uncertainty of the position of the AJC in the PiG model, authors have attempted to compute its position via alternative methods [415]. However, the most critical measurement error was selecting the appropriate HJC regression equation, with the greatest percentage differences in average joint angles and moments being linked to the choice of equation.

With regards to the clinical data, it would appear that much of the results would have been unaffected by errors in HJC position or joint width due to the sagittal plane, which was studied at all the joints, having minimal changes. Errors in knee and ankle width were the most likely areas where discrepancies may have been introduced into the data due to the problematic nature of palpating bone on the knee and ankle. Both joints were likely to be covered in extensive amounts of fat tissue in the clinical THR groups. Hip abduction-adduction was however the least effected motion in the frontal plane. From these results, it can be stated with confidence that it was unlikely that either the choice of HJC regression equation or errors in joint width measurement caused significant changes to the clinical results. It is however recommended that for studies which are looking at frontal or transverse plane kinematics or kinetics, that the Harrington HJC regression equation is selected due to the evidence from the literature.

9 A Critique of PiG - II

9.1 Aims & Objectives

The aim of this study was to compare and contrast how the positioning of the lateral thigh and shank markers effected the kinematics and kinetics of all the joints in the PiG model with respect to the segment defining plane²⁸. The results produced were important in determining the accuracy of the clinical data, where there was great variability in the position of the lateral segment markers between patients.

9.2 Methodology

9.2.1 Subject

Analysis was undertaken on a typical male subject of weight 76KG, height 1.74 metres with no apparent LLI or any other medical conditions which could effect performance²⁹.

9.2.2 Gait Analysis

Gait analysis was undertaken at the School of Sports Science (University of Leeds) with a custom market set, which can be seen in Figure 147, whilst wearing a motion analysis velcro suit. A single calibration trial was captured along with 10 motion trials. Calibration of the system was undertaken by the method as described on page 105

This custom market set was a modified version of the classic PiG marker set. Additional markers were added to the left leg on the greater trochanter and medial aspects of the knee and ankle. A collection of markers was added along the lateral portions of the thigh and shank on the left leg. Markers of diameter 14mm were attached in 45mm inferior positioned increments from the greater trochanter all the way down to the lateral ankle marker. In total this lead to there being 8 lateral thigh markers and 8 lateral shank markers. Likewise, an additional 16 markers were placed one marker distance anterior to these original markers giving a total of 32 lateral markers on the thigh and shank.

²⁸See Figure 27 page 71 for a definitions of the segment defining planes for both the thigh and the shank

²⁹For more details, see the *Anthropometrics & Demographics* chapter on page 90



Figure 147: Custom marker set with two columns of lateral segment markers running from the greater trochanter to the lateral ankle markers.

9.2.3 Body Model

The body model as defined on pages 77 - 85 in the *Generic Methods* was used in Visual3D. Hip motion was measured between the thigh and the pelvis, knee motion was measured between the shank and the thigh and ankle motion was measured between the foot and the shank. Moments were computed via inverse dynamics.

9.2.4 Processing

Motions and moments for every plane were extracted from Visual3D together with the standard deviations between consecutive heel strikes of the left foot, the first of which was on the force plate and the second off the force plate. Only results for the left leg were used, as this was where the additional markers were placed. Data for all 10 trials was extracted multiple times, with the lateral thigh or lateral shank marker in the model being altered. Results for a particular variable for a particular joint were plotted on the same graph. To undertake this at the thigh, all 16 positions were selected one after another as the lateral segment marker and motions were extracted for all joints in all three planes. This was subsequently repeated at the shank. Comparisons were then

made in terms of motions and moments over the course of the gait cycle.

Results were categorised depending on the position of the lateral thigh/shank marker. Out of the 16 markers on each segment, the markers in the more anterior portion of the segment on the anterior row were defined as Anterior whilst those on the posterior row were defined as Posterior. Likewise, the 8 most proximal markers on the segment were labelled as Proximal and the 8 distal placed markers were labelled as Distal. This is illustrated in Figure 148. The results over all 10 trials for each selected thigh/shank marker were averaged. Every individual has a natural anatomical plane at both the thigh and the shank, which passes through the proximal and distal joint centres. The positions of the lateral segment markers effect the position and orientation of the plane produced in Visual3D which represents the natural plane. In theory, the position of the lateral segment marker should not effect the definition of the plane if it is correctly placed, hence any differences in the results between different marker placements are due to deviations from the true anatomical plane. All results were hence analysed in terms of deviation of the computed plane in Visual3D from the true anatomical plane passing through each segment.

Anterior Proximal
Posterior Proximal
Anterior Distal
Posterior Distal

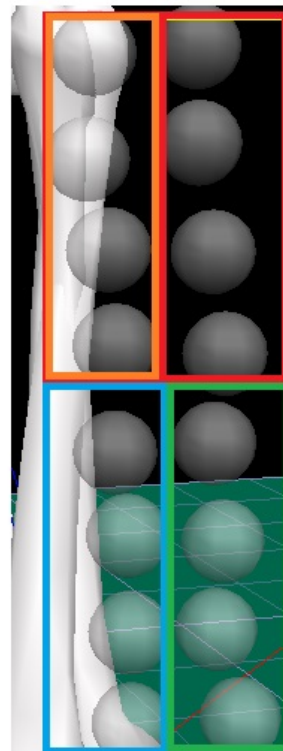


Figure 148: The definition of proximal, distal, anterior and posterior markers on the custom marker set. This image represents the thigh but the same method was applied to the shank

9.3 Results - Lateral Thigh Marker

9.3.1 Hip

Figure 149 shows results for the hip. Very little change was brought about by altering the segment defining plane in terms of joint moments (**B,D,F**), as the HJC position remained the same. The small differences which were seen were due to a combination of differences in distal joint centre position and differences in joint angles. A more internally rotated (anterior marker) thigh plane, relative to the true anatomical plane, was however found to effect both hip flexion-extension (**A**) and internal-external rotation (**E**). A more internally rotated plane lead to axes cross talk, with some flexion being measured as extension and some abduction measured as flexion. The vice-versa was true for a more externally rotated plane (posterior marker), with extension being measured as flexion³⁰. In terms of hip rotation, an internally rotated thigh plane lead to the internal rotation of the thigh whilst the external rotation of the plane lead to the external rotation of the thigh.

Hip abduction-adduction angle (**C**) showed little change when the segment plane was rotated either internally or externally relative to the true natural plane. Hip abduction-adduction in PiG is defined by the clinical joint width measurement, which is impacted by the segment plane by a minimal amount. Any differences observed were due to cross talk with the flexion-extension axes.

Results were amplified with more distal marker placement, with the segment plane becoming more internally/externally rotated and hence there being greater cross talk. This was due to the method based on which rotation is computed³¹, where effects are amplified due to the closer proximity of the lateral thigh and lateral knee markers, with errors in marker placement having a greater effect on the segment planes rotation. In theory, a marker placed more superior-inferior will have no effect on kinematics or kinetics if it is placed along the true anatomical plane of the thigh which is used to compute the KJC.

³⁰Cross talk between axes is demonstrated in Figure 33 on page 75 of the *Generic Methods*

³¹See Figure 27 on page 71 of the *Generic Methods*

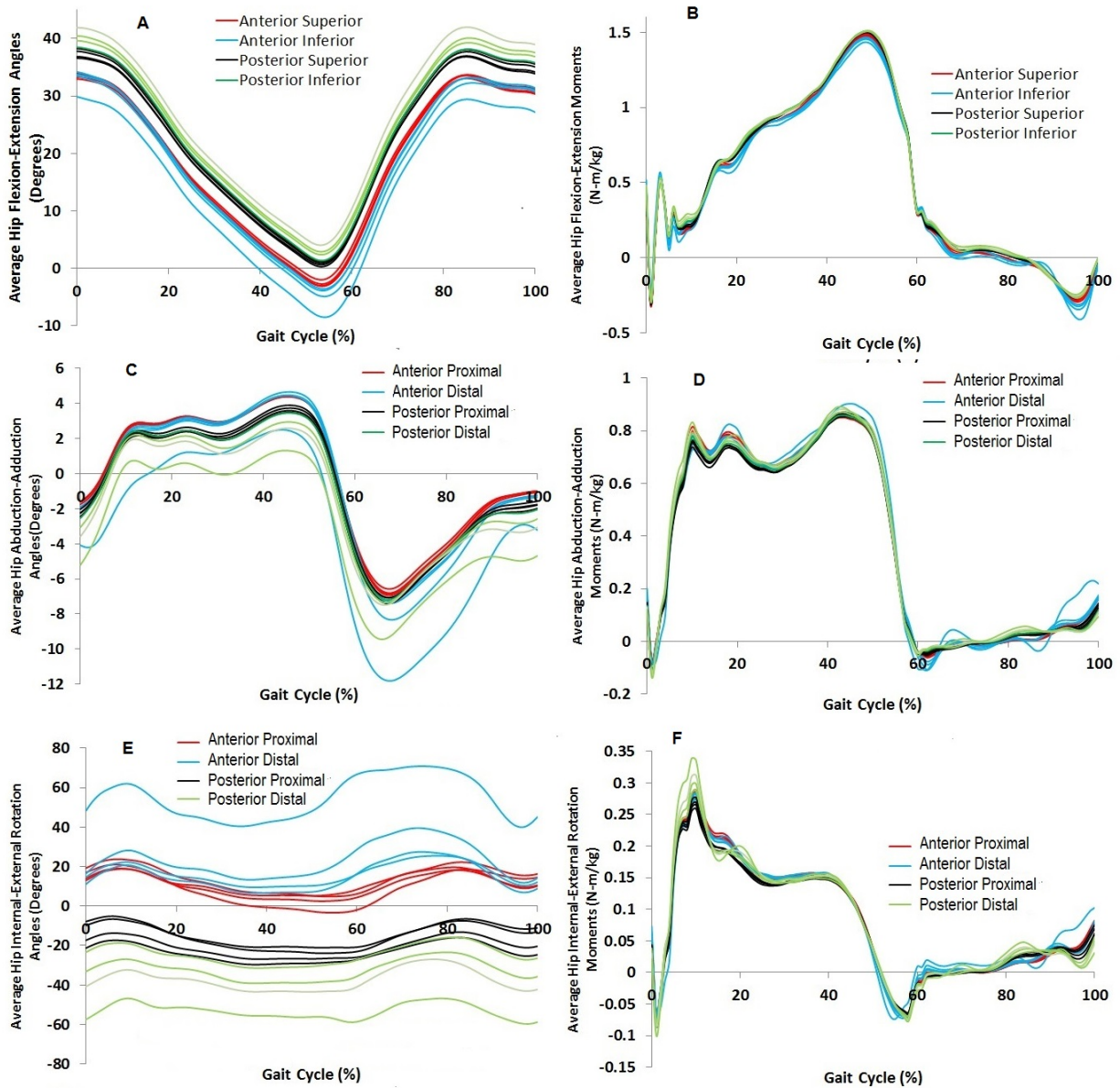


Figure 149: Average hip flexion (+)-extension (-) angles (A) and moments (B), abduction (+) adduction (-) angles (C) and moments (D), internal (+) external rotation (-) angles (E) and moments (F) for anterior-proximal, posterior-proximal, anterior-distal and posterior-distal positioned lateral thigh markers over 10 normalised gait cycle trials between consecutive heel strikes of the same foot

9.3.2 Knee

Figure 150 shows the effects of altering the thigh plane on knee joint angles and moments. As the KJC position is controlled by the thigh segment plane, any deviation from the true anatomical plane causes a shift in its position. A more internally rotated thigh plane (anterior markers) additionally leads to a more posterior KJC, through the movement of the distal portion of the plane posteriorly. The vice versa is also true for a more posteriorly rotated thigh plane (posterior markers), with an

anterior KJC produced³². These variations led to the results seen for both joint angles and moments in Figure 150.

It was found that on average, a thigh plane which is more posteriorly rotated and had a more anterior distal plane portion relative to the true anatomical plane led to an increase in peak knee flexion angle (**A**) whilst an anteriorly rotated plane with a more posterior distal plane portion led to a decrease in peak knee flexion. With regards to the plane with a more anterior distal portion and anterior KJC, this created a flexion offset where the knee flexion value increased by the offset angle value³³. The opposite was true for the plane with a more posterior distal portion of the thigh plane. Some knee abduction (**C**) could also be counted as flexion³⁴. The changes through cross talk of axes would however be minimal and would be outweighed by the effect of the position of the KJC changing.

A thigh segment plane which was more internally rotated than the true anatomic thigh plane led to some cross talk between hip abduction and adduction (Figure 149) i.e. adduction was measured as abduction. The effects at the knee in terms of abduction-adduction were however much greater. An external rotation of the thigh plane (posterior markers) led to abduction being measured whilst an internal rotation of the thigh plane (anterior markers) led to adduction being measured. Due to the differences seen in thigh plane rotation, the results appear to be reflections in the x-axis. For similar reasons, the variations in graph (**E**) in Figure 150 for knee rotation (**E**) were seen. More distally placed lateral thigh markers had a large impact on kinematics due to their proximity to the lateral knee marker in defining the plane, with errors in plane definition relative to the true anatomical thigh plane being amplified.

Unlike at the hip, knee moments were effected due to the position of the KJC being dependent the choice of lateral thigh marker. For the subject analysed, the VGRF vector remained posterior to the KJC throughout the stance phase. Hence a more posterior KJC caused by having a posterior distal thigh plane reduced the moment arm length whilst an anterior KJC increased the moment arm length. This led to the differences in magnitudes in terms of knee flexion-extension moment (**B**). In addition, a more posterior placement of the lateral thigh marker led to adduction moment whilst a more anterior placement led to abduction (**D**). This was due to the KJC moving either medially

³²See Figure 29 on page 72 of the *Generic Methods*

³³See Figure 34 on page 76 of the *Generic Methods*

³⁴Cross talk between axes is demonstrated in Figure 33 on page 75 of the *Generic Methods*

or laterally when the plane was formed to determine the KJC position. The posterior marker thigh plane produced the more variable results due to KJC being further away in the anterior direction and thus any changes produced in the medial-lateral position of the KJC leading to a larger effect. Changes were also seen in terms of rotation moments due to the KJC moving in the transverse plane (**E**).

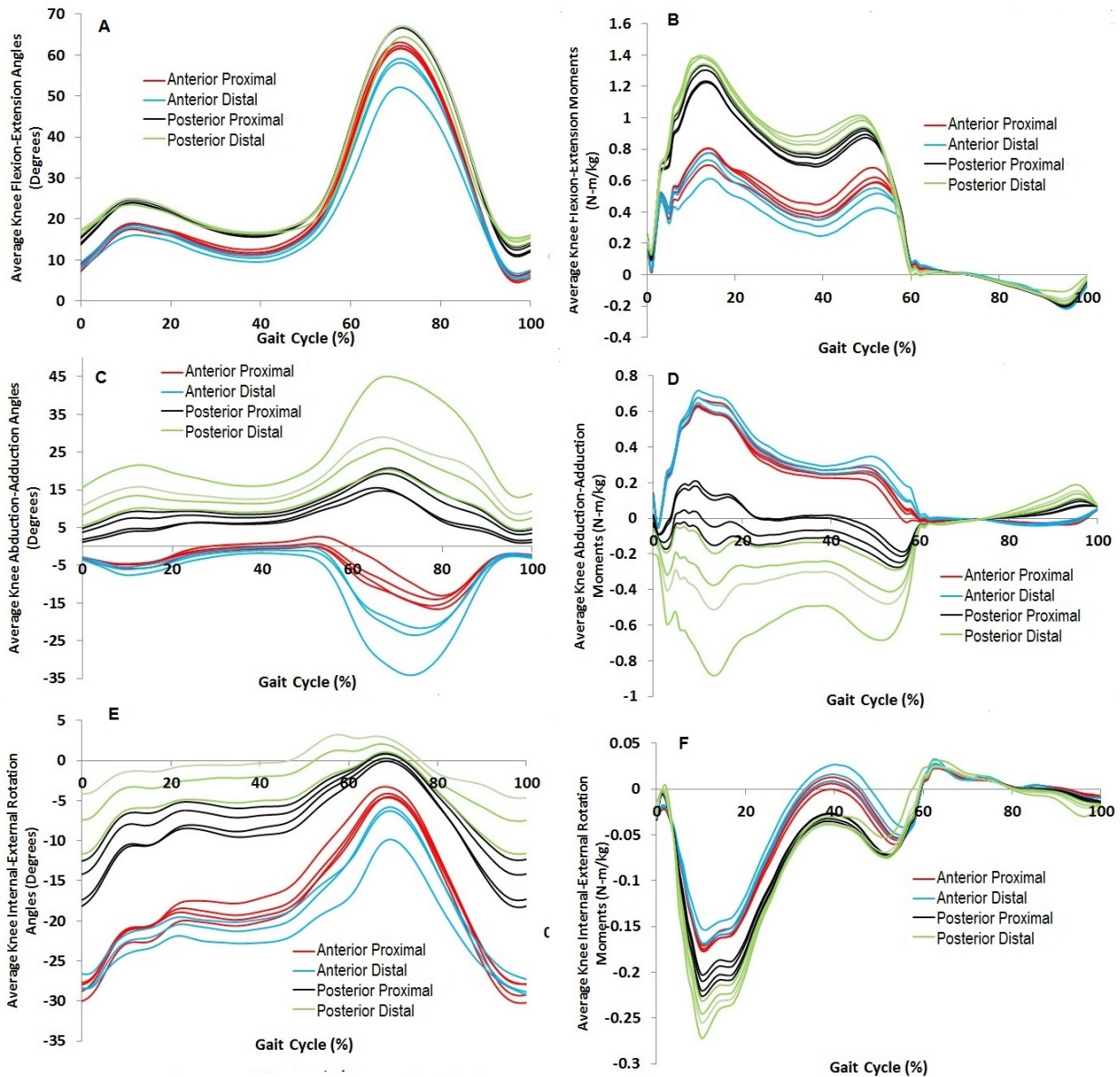


Figure 150: Average knee flexion (+)-extension (-) angles (**A**) and flexion (-)-extension (+) moments (**B**), abduction (+) adduction (-) angles (**C**) and moments (**D**), internal (+) external rotation (-) angles (**E**) and moments (**F**) for anterior-proximal, posterior-proximal, anterior-distal and posterior-distal positioned lateral thigh markers over 10 normalised gait cycle trials between consecutive heel strikes of the same foot

9.3.3 Ankle

Figure 151 illustrates results for the ankle. In PiG, the thigh and foot segments do not share any model markers, unlike the thigh and the shank which share the KJC. Hence any variability in results at the foot due to changes at the thigh are indirect and are due to changes at the shank, which themselves were caused by the thigh. The AJC was computed in a similar way to the KJC³⁵. A more anterior KJC caused by a thigh segment plane of which the distal portion is more anterior than the true anatomical plane (posterior thigh marker) leads to a more anterior KJC³⁶. A more anterior KJC would lead to the creation of a shank segment plane where the distal portion is more posterior than the true shank anatomical plane, leading to a posterior AJC.

Results as seen in graph (A) in Figure 151 reflect these variations, with a dorsiflexion offset being produced and the foot becoming longer so more motion is captured (the foot is defined between the AJC and toe marker). The vice-versa would be true for a more posterior KJC caused by a thigh segment plane of which the distal portion is more posterior than the true anatomical plane (anterior thigh marker). Differences in ankle eversion-inversion (C) and rotation (E) angles were due to a combination of medial-lateral movement of the AJC due to different definitions of the shank plane together with differences in shank and foot axes orientations. The eversion-inversion axis is defined by the relationship between the long axes of the foot (between the AJC and toe marker) against the position of the heel marker. A more anterior AJC led to a loss in the amount of motion measured, due to the smaller foot and hence closer proximity of the toe and AJC markers³⁷.

In terms of moments, the greatest ankle plantarflexion moment (B) were found in the thigh plane with the more anterior distal planes (posterior markers). A more anterior KJC causes the AJC to be more anterior. As the VGRF vector initially passes through the heel of the foot, a more anterior AJC would have a longer moment arm and thus a greater joint moment. Movement of the AJC in either the anterior or posterior direction also additionally leads to some medial-lateral movement of the AJC, which as (D) shows lead to VGRF to pass on opposite sides of the centre of the joint and lead to the change of sign in the results. There was also some movement in the transverse plane of the AJC, leading to changes in rotation moments. For both joint angles and joint moments, the more distal placed thigh markers caused the greater outlier results due to being in closer proximity to the lateral knee marker and thus impacting the position of the KJC more

³⁵See Figure 27 on page 71 of the *Generic Methods*

³⁶See Figure 32 on page 74 of the *Generic Methods*

³⁷See Figure 35 on page 76 of the *Generic Methods*

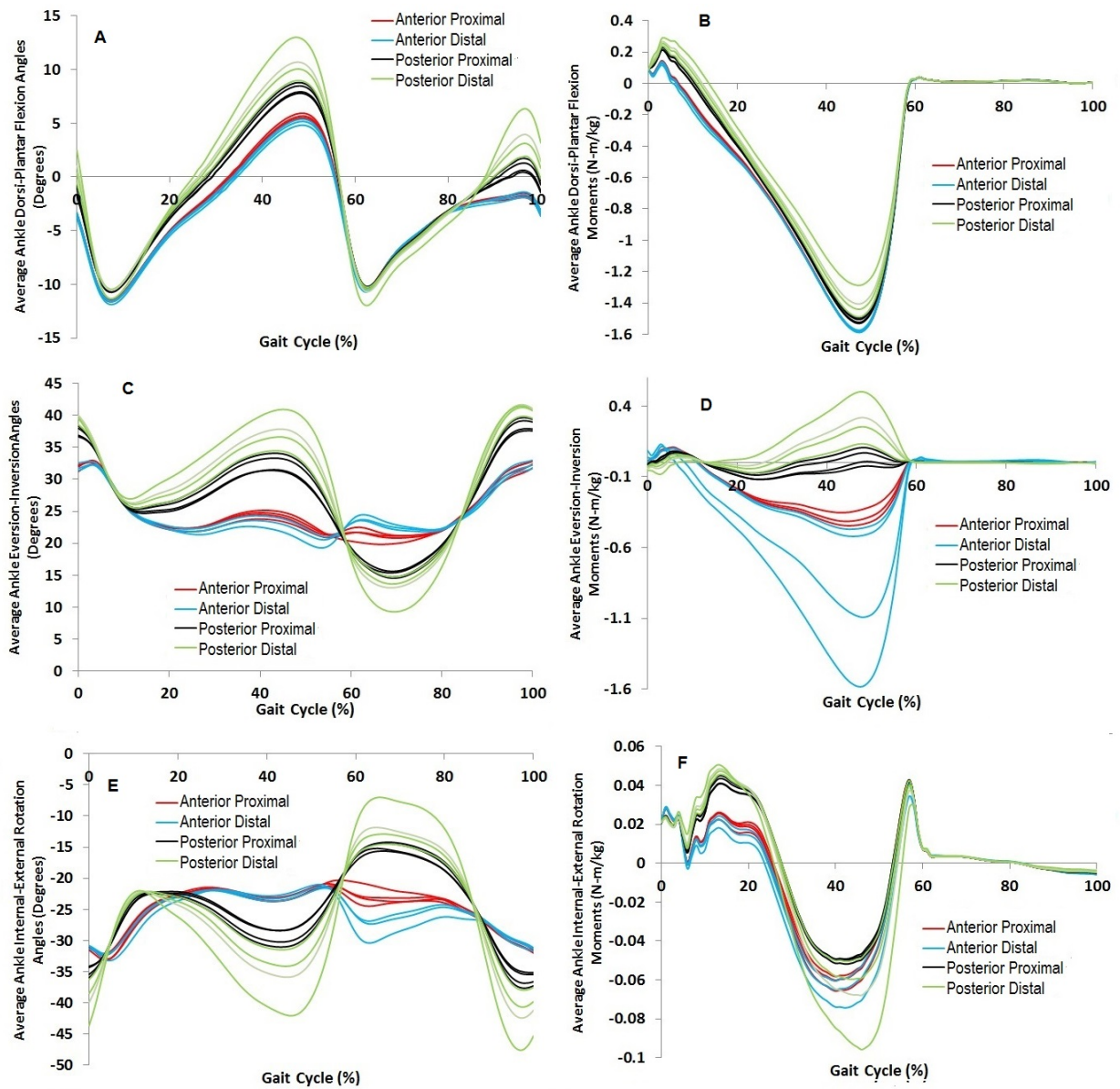


Figure 151: Average ankle dorsiflexion (+)-plantarflexion (-) angles (**A**) and moments (**B**), eversion (+) inversion (-) angles (**C**) and moments (**D**), internal (+) external rotation (-) angles (**E**) and moments (**F**) for anterior-proximal, posterior-proximal, anterior-distal and posterior-distal positioned lateral thigh markers over 10 normalised gait cycle trials between consecutive heel strikes of the same foot

greatly.

9.4 Results - Lateral Shank Marker

9.4.1 Hip

The hip is unaffected by the position of the lateral shank marker so was ignored for this particular study. The lateral shank marker has no effect on the hip in terms of altering the thigh segment plane. Negligible differences are produced in terms of joint moments.

9.4.2 Knee

Figure 152 shows results for the knee. The position of the lateral shank marker is not used to determine the position of the KJC, with all changes in terms of joint angles being due variations in the shank segment plane. Moments had negligible changes at the knee (graphs **(B)**, **(D)** and **(F)**). A more anterior lateral shank marker causes internal rotation of the shank plane³⁸. This leads to the flexion-extension axes rotating internally and thus the amount of measured flexion increasing **(A)**.

Greater internal rotation of the shank plane with respect to the true shank anatomical plane led to a loss of adduction whilst greater external rotation of the shank plane led to an increase in adduction **(C)**. The amount of abduction-adduction of a segment is controlled by the clinically measured knee width (or the ankle width for the foot). Internal rotation of the segment plane led to some adduction being counted as abduction. External rotation of the plane did not have as significant of an effect. This was as cross talk was minimal between abduction-adduction (as there was hardly any abduction). There was no cross talk between the flexion and extension axes. A more internally shank plane caused led to greater internal rotation of the knee with the opposite true for externally rotated planes **(E)**. Errors in the definition of the segment plane were amplified at the more distal regions of the shank due to markers being in closer proximity.

³⁸See Figure 32 on page 74 in the Generic Methods

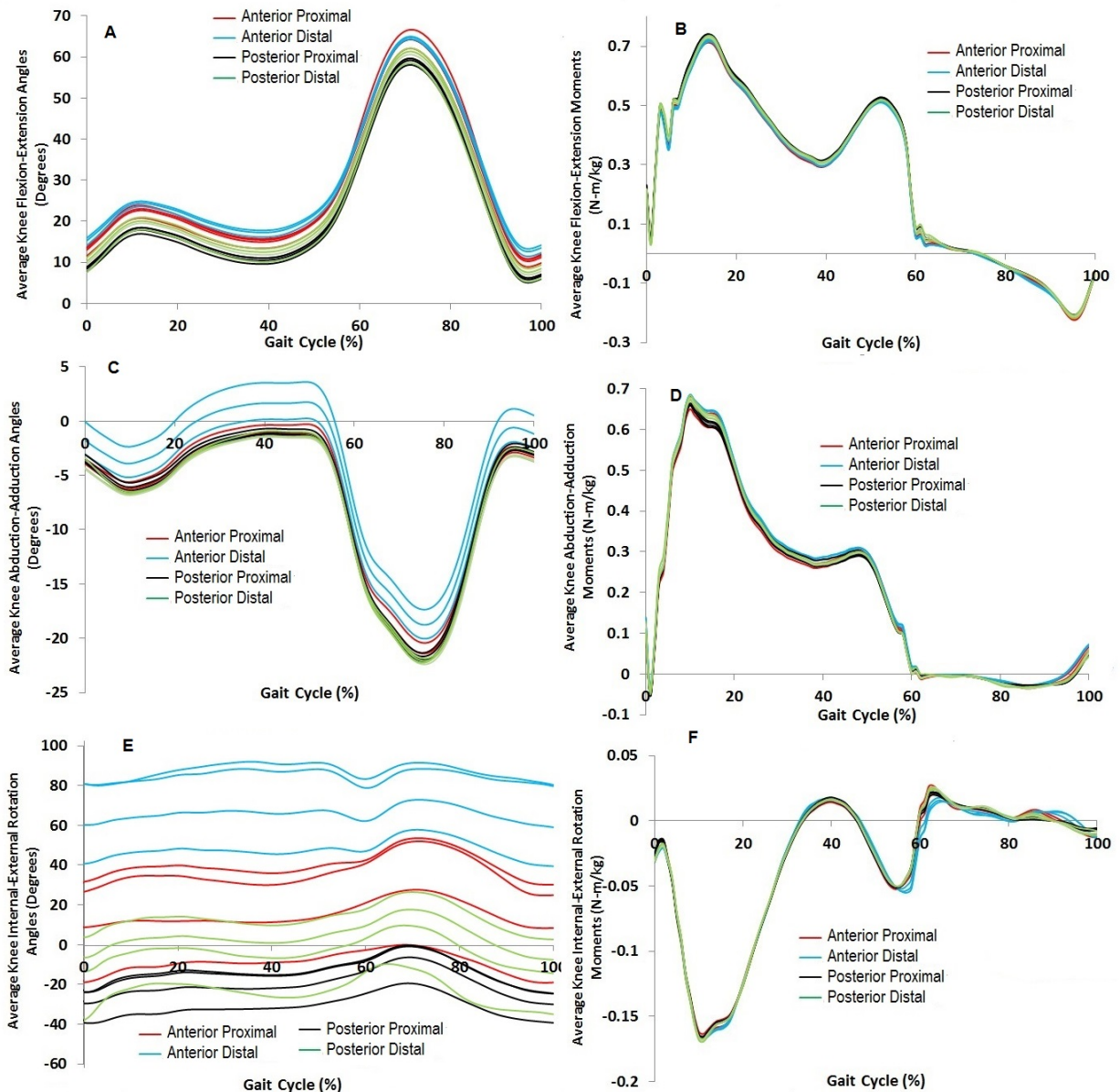


Figure 152: Average knee flexion (+)-extension (-) angles (**A**) and flexion (-)-extension (+) moments (**B**), abduction (+) adduction (-) angles (**C**) and moments (**D**), internal (+) external rotation (-) angles (**E**) and moments (**F**) for anterior-proximal, posterior-proximal, anterior-distal and posterior-distal positioned lateral shank markers over 10 normalised gait cycle trials between consecutive heel strikes of the same foot

9.4.3 Ankle

Results for the ankle can be seen in Figure 154. The results for the shank plane which was internally rotated were effected by Gimbal Lock for ankle dorsi-plantar flexion and rotation. Gimbal lock occurs when one of the axes becomes rotated at 90° , which leads to that particular axis overlapping with another axis and a loss of 1 degree of freedom occurring. In this particular example, the sagittal and transverse planes overlapped. A visual example of Gimbal lock is given in Figure 153. The heel marker determines the amount eversion-inversion tilt of the foot. An AJC which is too posterior,

caused by posterior distal portion of the shank plane, comes in close proximity to the heel marker. This eventually leads to the foot inverting close to 90° . This occurred at the more distal positions of the lateral shank marker, which had an amplified effect on the position of the AJC.

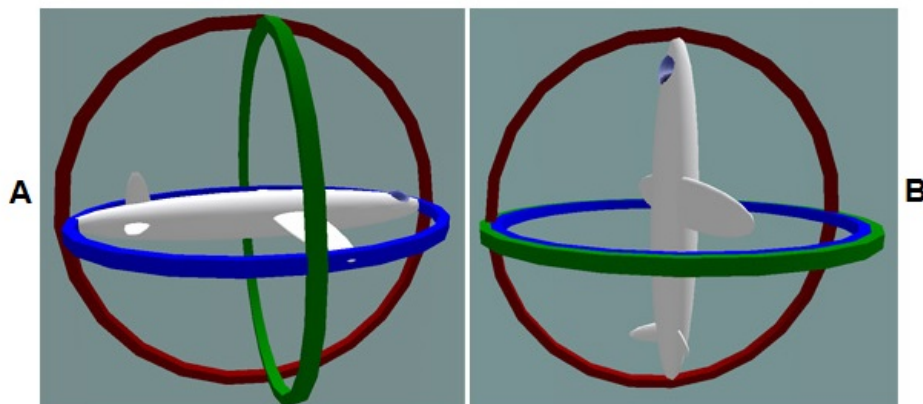


Figure 153: Demonstration of Gimbal Lock. In this example, the green circle represents the sagittal plane, the red circle the frontal plane and the blue the transverse plane. Image (A) is of a non-Gimbal locked axes whilst image (B) is of a Gimbal locked axes, where two gimbals have overlapped

In general, a more internally rotated shank plane led to a greater RoM, greater dorsiflexion angle and a loss in plantarflexion angle. This would be due to a plantarflexion offset in the results coupled with a change in the ankle joint axes orientation. Similar results were found in terms of eversion-inversion angle, with a more posterior AJC leading to a greater RoM. The results which did not have Gimbal Lock occur generally demonstrated external ankle rotation throughout the gait cycle.

Results showed that an internally rotated shank plane relative to the true anatomical plane led to greater dorsiflexion moments than an externally rotated shank plane. This was due to the posterior movement of the AJC, leading to the VGRF vector to pass anteriorly in relation to it. Greater internal rotation of the shank plane also led to an increase in ankle inversion moment³⁹. With the majority of moment results being that of inversion, it appears that the VGRF vector remained medial to the position of the AJC. The greater moments for the anterior placed lateral shank markers were due to different moment arm length. Very little differences were present in terms of ankle rotation moments.

³⁹See Figure 35 on page 76 of the *Generic Methods* for how the anterior-posterior position of the lateral shank marker can effect the medial-lateral position of the AJC

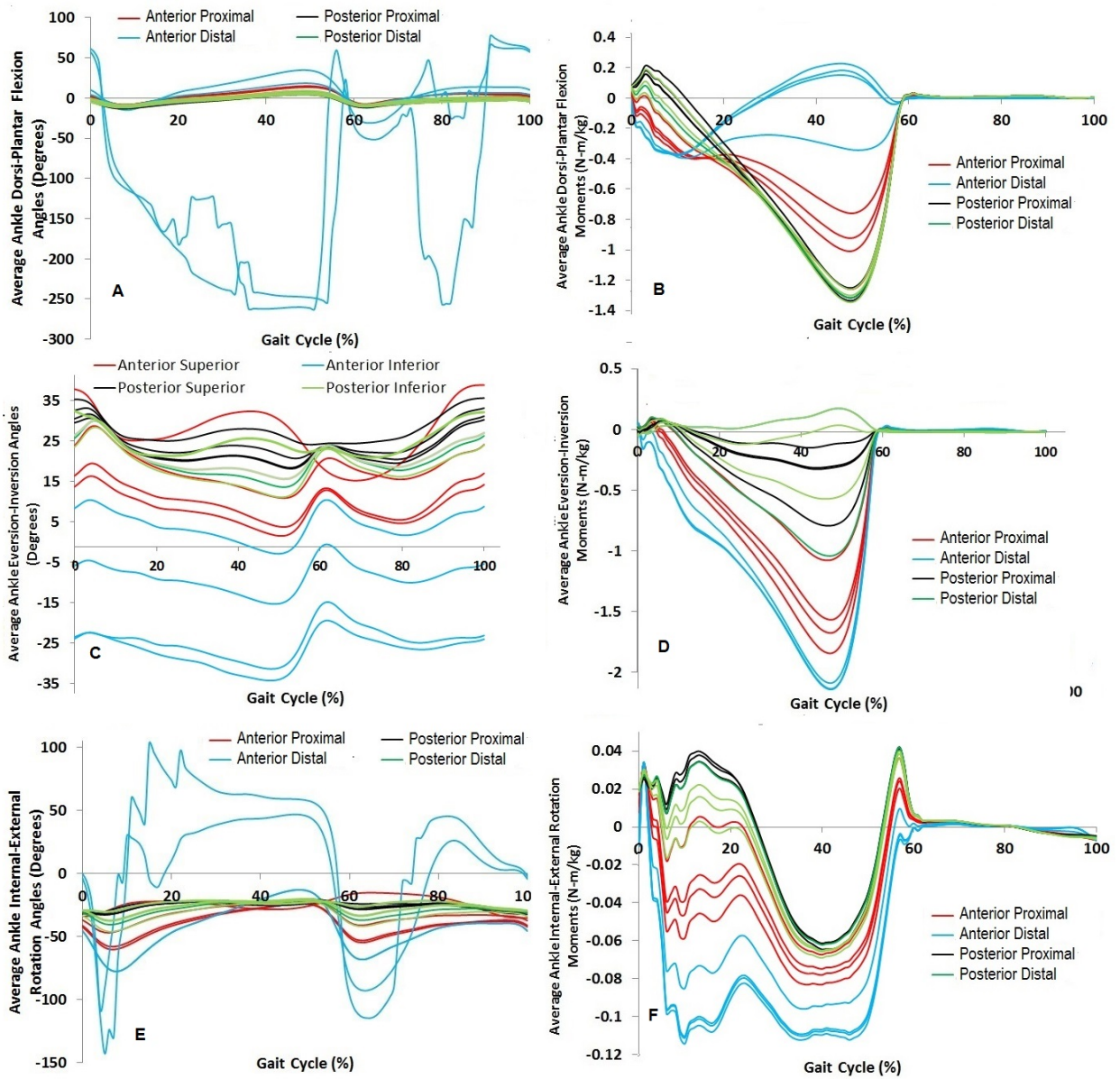


Figure 154: Average ankle dorsiflexion (+)-plantarflexion (-) angles (A) and moments (B), eversion (+) inversion (-) angles (C) and moments (D), internal (+) external rotation (-) angles (E) and moments (F) for anterior-proximal, posterior-proximal, anterior-distal and posterior-distal positioned lateral shank markers over 10 normalised gait cycle trials between consecutive heel strikes of the same foot

9.5 Discussion

This study is not the first to have analysed the effects of the lateral thigh/shank marker on the segment defined planes and hence kinematics/kinetics but is the first to use the undertaken methodology. Despite this, there has been research which has analysed the sensitivity of the PiG model against other marker systems which differ in their computation of segment rotation. Mahaffey [455] investigated the effects of adding or subtracting thigh marker offset in kinematic results post analysis. Basset et al. [309] found that kinematic results were highly sensitive using PiG relative to other marker sets such as CAST, particularly in the frontal and transverse planes. It was suggested that

the poor correlation of the PiG marker set to other markers sets in the transverse plane was linked to the lateral segment markers being involved in determining segment rotations. Several other studies have also found that PiG (or a very similar model) produces poor results in the transverse plane [315, 316] or has a more variable kinematic and kinetic output [317]

The present results have shown that the PiG model is sensitive to the orientation of the segment planes, as defined by marker positions, with there being large corresponding changes in the definition of the thigh and shank axes. Changes were greater in terms of joint angles. Every segment has a theoretical "natural" plane, along which the segment can be defined. If lateral segment markers are placed along this plane, then there will be no impact on the rotation of a segment and a substantial decrease on the effects on kinematics and kinetics. This plane is however almost impossible to define using the naked eye and can be erroneously calculated by computer systems, making the correct positioning of markers in models such as PiG pivotal. For the results of the present study, joint rotations differed between proximal-distal marker placements indicating that the markers were all not placed along the natural segment plane for the thigh and the shank.

General trends revealed that the greatest reliability in results was found in the proximal placement of the lateral thigh/shank marker, 50% or higher up on the segment. These markers even if not placed along the true thigh anatomical plane would exert a smaller effect on the rotation of the plane due to being further away from the lateral knee marker. The lateral knee marker and the distal joint centre together dictates the rotation of the segment planes. A more anteriorly rotated segment plane led to increasing internal rotation of a segment whilst a more posteriorly rotated plane led to increasing external rotation, which was expected. Many of the changes observed at the proximal segments were due to axes cross-talk and offsets caused by the displacement of the joint centre.

Markers placed at increasingly distal positions effected the planes produced at both the thigh (between the HJC, lateral thigh marker and lateral knee marker) and at the shank (between the KJC, lateral shank marker and lateral ankle marker) the most due to impacting the position of the plane the greatest, leading to the amplification of joint angle/moment results. In pathological gait patients with abnormalities at the hip, such as those with an LLI, the accurate placement of the thigh plane is essential in determining clinically meaningful kinematic results at the hip. When comparing the Anterior-Proximal and Posterior-Proximal markers to each other, on average the

4.5cm difference in marker position led to a 4.4° change in peak hip flexion angle, 0.73° in peak hip abduction and peak internal rotation of 31.3° . When however comparing the Anterior-Distal and Posterior-Distal markers to each other, on average a 4.5cm difference in marker position led to a 7.3° change in peak hip flexion angle, 1.44° in peak hip abduction and peak internal rotation of 68.2° . Similar trends were detected at the knee and ankle.

The orientation of the shank plane also had a large effect on both knee and ankle kinematics, with hip joint angles being unaffected. As with the thigh marker, the more distally placed lateral shank marker if placed such that the true anatomical shank plane was not correctly defined, lead to an amplification of error in results due to being closer to the AJC. The most intriguing of the results came with regards to ankle kinematics, with Gimbal Lock having occurred. From these results, it is suggested that the lateral shank marker be placed more towards the proximal end of shank and not near the distal end. Alternatively, medial markers should be added for the standing trial at both the knee and the ankle in order to aid the calculation of an accurate KJCs/AJCs and prevent any errors which lead to Gimbal Lock from occurring.

9.6 Conclusion

This study analysed the effects of the position of the lateral thigh and lateral shank markers on the orientations of the segment defining planes and as a consequence the effects on both joint angles and joint moments using a customised marker set. Overall results indicated that misorientation of the segment planes will have a significant impact on the output of results. Joint angles were particularly effected in the frontal and transverse planes due to the smaller RoM they possess relative to the sagittal plane. Differences in kinetics were generally minimal, with the greatest often being at the ankle. The shank marker was found to be more important than the thigh marker due to it having a very large effect on both the knee and the foot, of which the latter is significantly effected due to its smaller size. A particularly important observation from this study was the impact of placing the lateral segment marker too distal on a segment, with there being a corresponding amplification of effect in the more distal segments. In clinical studies patient factors have to be considered that thus limit the practical reliability of the data, however, by understanding gait sensitivity the critical aspects of the analysis can be focussed upon to optimise the results. For the clinical patient groups, errors could have been present due to marker misplacement.

10 A Comparison between PiG & CAST

10.1 Aims & Objectives

PiG and its parent CGM have often been compared to other motion capture marker systems such as CAST, as detailed in the *Literature Review*. However, all of these studies when comparing the PiG marker set to the CAST marker set make the erroneous selection of one of the markers on the thigh or shank cluster to act as the lateral thigh or lateral shank marker in the PiG model. This introduces bias into the results as in theory any one of the markers can be selected. Furthermore, these markers may not have been the position that a technician may have placed the lateral segment marker. To reduce the bias in the results by selecting one of these markers, a new method is proposed to increase the accuracy and reliability of the results obtained.

10.2 Methodology I

10.2.1 Subject

Following local ethical approval⁴⁰, a single male student volunteer with a height of 1.76 metres and mass of 77 Kg was recruited and undertook gait analysis at the School of Sports Science at the University of Leeds.

10.2.2 Gait Analysis

Altogether, 9 dynamic motion trials were analysed together with a single standing trial using the Qualisys motion capture system. Out of these trials, 8 trials were recorded with the individual walking at a comfortable speed whilst a single trial was recorded with them walking quickly. The comfortable walking speed results are labelled as "CAST" and "Plug-in-Gait" whilst the walking fast results are described as "CAST Fast" and "PiG Fast" in the results section. The individual walked over a force plate which was able to capture GRFs. Calibration of the system was undertaken by the method as described on page 105.

Both the PiG and CAST marker sets were placed on the subject simultaneously⁴¹. In total, 44 markers were placed on the individual with 4 at the pelvis, 6 on each thigh, 6 on each shank and 8 on each foot. All of the markers which are used in PiG also appear in CAST. One of the areas

⁴⁰Ethical approval, participant forms and consent forms found from page 351 in the *Appendix III*

⁴¹For further details on PiG, see pages 69 - 70 in the *Generic Methods*

where there is discrepancy is at the lateral portions of the thigh and shank, where in PiG a single marker is placed and in CAST a cluster of 4 markers is placed. To overcome this, an additional marker was placed in the middle of each cluster, as can be seen in Figure 155, to be used in the PiG model whilst the cluster markers would be used in the CAST. The pelvis was defined in the same way between the PiG and CAST models. There were differences between the definition of the thigh, shank and the foot.



Figure 155: The customised lateral segment (thigh and shank) markers used in this study. A marker was secured at the centre of each cluster and used to represent PiG, whilst the four remaining markers were used to represent CAST.

Both PiG⁴² and CAST⁴³ used the HJC as computed using the regression equation from Davis. The PiG model also used the lateral thigh marker to define the rotation of the thigh. This was ignored for the CAST model with rotation being defined using the position of both the lateral and medial knee markers relative to each other. In PiG, all the markers used to define the segment were also used in tracking the thigh. In the CAST model however, the four markers on the cluster were used for tracking. Under normal circumstances the HJC regression equation would not be used for CAST and rather the greater trochanter marker together with the femoral offset. As the femoral offset was however not measured clinically via the use of an x-ray, the use of the greater trochanter marker was ignored. The distal end of the thigh was defined as the lateral knee marker in PiG and the mid-point of the lateral knee and medial knee markers in CAST.

⁴²See pages 80 - 82 in the *Generic Methods*

⁴³See page 43 in the *Generic Methods*

The proximal end of the shank marker was defined using the model created KJC in PiG, whilst in CAST it was created using the midpoint of the lateral and medial knee markers. Furthermore, the distal end of the shank in PiG was defined at the lateral ankle marker whilst in the CAST model it was the midpoint of the lateral and medial ankle markers. These two markers also defined the rotation of the shank, whilst in PiG rotation was defined by the position of the lateral shank marker. All the markers used to define the shank were also used in tracking the segment for PiG whilst for the CAST model none of the markers used to define the segment were used. Instead, the four markers placed onto the shank as part of clusters were used for tracking.

The proximal end of the foot in PiG was defined using the AJC, which was computed using proximal markers and anthropometric measurements. The foot which was used for CAST was not the traditional definition. The proximal end was defined as the midpoint of the medial and lateral ankle markers. At the distal end of the foot, the CAST model defined the segment end point to be the midpoint of the markers placed on the 1st and 5th metatarsals. The distal end of the foot in PiG was defined by the toe marker on the 2nd metatarsal. Medial-lateral tilt (eversion-inversion) of the foot in PiG was defined by the heel marker whilst in CAST between the 1st and 5th metatarsals. All the markers used in the definition of the foot in PiG were used for tracking purposes. The CAST model however used the medial and lateral heel markers together with markers on the 1st and 5th proximal heads for tracking.

Both PiG and CAST were created in Visual3D. Joint angles and moments were extracted for the hip, knee and ankle in all three planes (sagittal, frontal, transverse) and normalised to 100 percentiles between consecutive heel strikes, of which the 1st occurred on the force plate and was identified as the first time frame of the force vector appearing. This was then used to help identify the corresponding heel strike off the force plate. The pelvis was ignored as both marker sets used the same configuration.

10.2.3 Body Model

The body model in Visual3D as defined on pages 77 - 85 in the *Generic Methods* was used for PiG. Likewise, the CAST model was built. Hip motion was measured between the thigh and the pelvis, knee motion was measured between the shank and the thigh and ankle motion was measured between the foot and the shank. Moments were computed via inverse dynamics.

10.3 Results

10.3.1 Hip

Figure 156 demonstrates that hip flexion-extension angles produced by the PiG marker set were offset showing greater flexion and a reduction in extension relative to CAST (**A**). On average the results for the PiG marker set did not go into extension (0.10°), whilst CAST had an average extension value of -4.16° . The CAST model however had a smaller average peak hip flexion value (31.0°) than PiG (34.4°). As the HJC positions between the models were the same, differences in the results were due to differences in axes rotation and the different markers used in tracking the segment. Differences in terms of peak hip flexion and extension angles were found to be statistically significant using the t-test at the 5% significance level ($p < 0.01$). Results for fast walking demonstrated increased hip flexion for both marker sets.

Hip abduction-adduction angles (**C**) did not vary considerably between the PiG and CAST marker sets. As the position of the HJC was the same between the models, differences were due to cross-talk between the flexion-extension and abduction-adduction axes of the thigh. PiG had smaller average peak hip adduction angle (-7.15°) than CAST (-7.30°), which was found not to be statistically significant ($p > 0.05$). The CAST model had a greater average peak hip abduction value (4.40°) than PiG (3.70°), with results being statistically significant ($p < 0.03$) using the t-test. Gait speed had very little effect.

Hip internal-external rotation angle (**E**) varied considerably between the PiG and CAST marker sets. CAST had greater average maximum hip rotation angle value (3.05°) than PiG (-16.8°). The PiG model had a greater average maximum external rotation value (-33.7°) than CAST (-11.5°). Both maximum and minimum were found to be statistically significant using the t-test at the 5% significance level ($p < 0.01$). The external rotation of the PiG results demonstrates posterior placement of the lateral thigh marker relative to the thigh long axis⁴⁴. The external rotation of the CAST results demonstrates that the lateral knee marker was placed more posterior than the medial knee marker. The effects of gait speed were similar between the groups.

Figure 156 on the other hand also demonstrates that hip moments did not vary significantly

⁴⁴See Figures 33 & 32 in the *Generic Methods*

between the PiG and CAST marker sets (**B**, **D** & **F**). This was expected however due to the HJC being the same between both CAST and PiG. No statistically significant differences were found in terms of moments ($p>0.05$), with the exception of average peak hip adduction moment ($p<0.05$). Despite this significant difference being found, from a clinical perspective it is not meaningful due to the small differences between the two marker sets. Moments were largely unaffected by walking speed, with there being little change when the subject walked quicker.

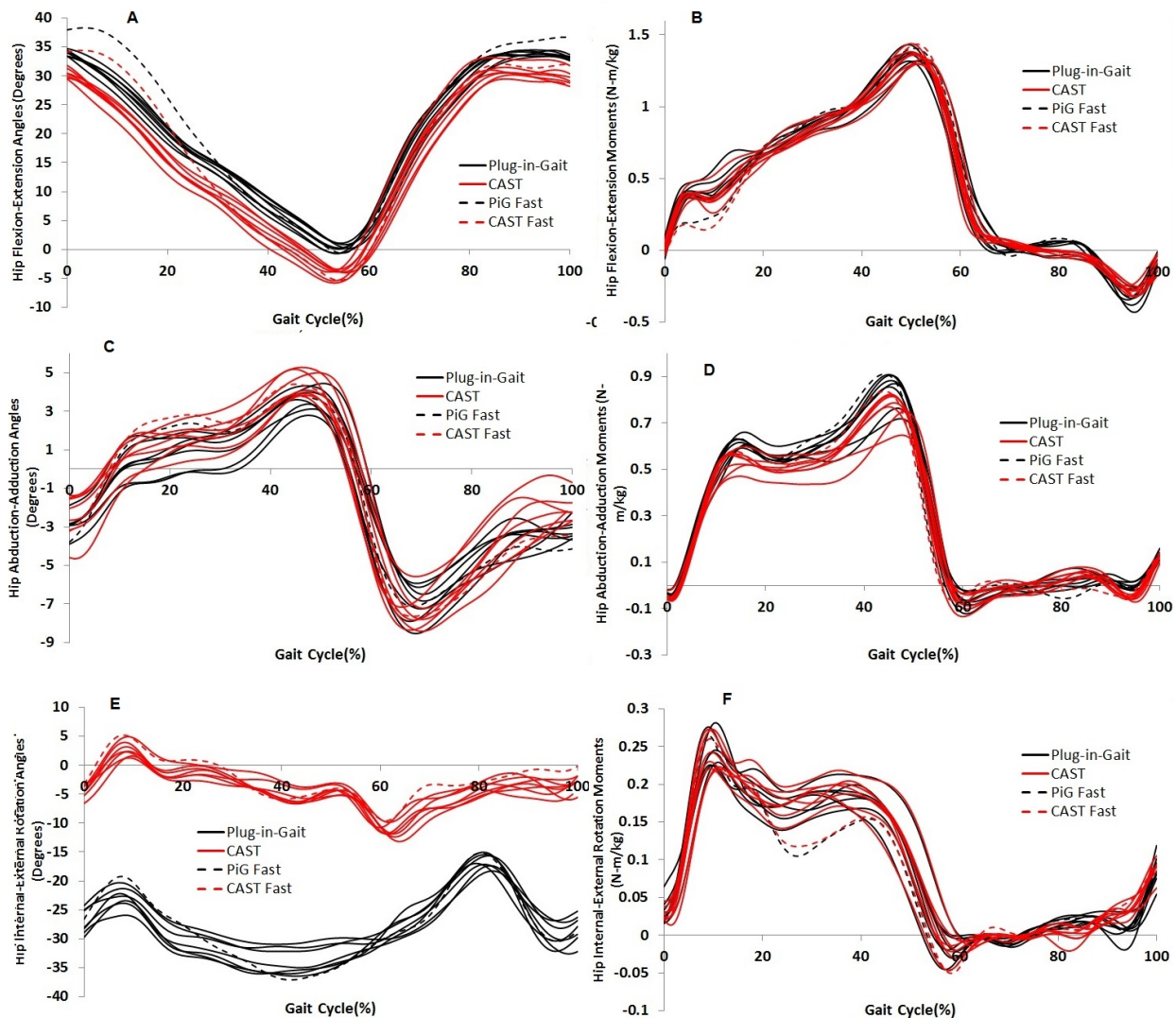


Figure 156: Average hip flexion (+)-extension (-) angles (**A**) and moments (**B**), abduction (+) adduction (-) angles (**C**) and moments (**D**), internal (+) external rotation (-) angles (**E**) and moments (**F**) for the PiG and CAST marker sets over 10 normalised gait cycle trials between consecutive heel strikes of the same foot

10.3.2 Knee

Figure 157 demonstrates that knee angles and moments varied considerably between the PiG and CAST marker sets. Differences would have arisen due to a combination of there being different

KJC positions for each model together with axes orientations. Results indicate that the KJC in PiG was more anterior than that in CAST, with some knee extension being measured as flexion⁴⁵. The relatively linear portion of the knee flexion-extension curve (**A**) during the stance phase shows that no knee flexion was taking place. This may have been due to walking speed, with the subject in this study having a relatively slow comfortable walking speed of 0.97m/s. The fast trials exhibited greater knee flexion during stance. CAST was more effected by speed with the fast trial being 6.62 standard deviations from the CAST mean whilst PiG was 5.73 standard deviations from the PiG mean. In terms of knee flexion-extension angle, CAST had a smaller average maximum knee flexion (58.8°) than PiG (63.7°). The PiG model had greater minimum gait cycle value (3.70°) than CAST (3.17°). Statistically significant results were found using the t-test at the 5% significance level with respect to the maximum ($p < 0.01$) and minimum angle ($p < 0.04$).

Knee abduction-adduction angles (**C**) varied considerably between the PiG and CAST marker sets. The motion with respect to the CAST model remained largely in abduction throughout the gait cycle whilst the results for PiG spent the majority of time in adduction. This would have been due to a number of differences, including the use of clinically measured joint widths to determine medial-lateral positions of the KJC in PiG, whereas in CAST this is computed as the mid-point between the medial and lateral knee markers. PiG had greater average maximum knee adduction (-19.5°) than CAST (-3.71°). The CAST model had a larger maximum value during the gait cycle value (2.55°) than PiG (-1.86°). All differences were found to be statistically significant using the t-test at the 5% significance level ($p < 0.01$). Knee abduction-adduction was greatly effected by gait speed for the PiG model and unaffected in the CAST model. Alterations in gait velocity have little impact on motion in the knee frontal plane. The large impact on the PiG model would have been linked directly to cross-talk between the flexion-extension and abduction-adduction axes, where flexion-extension is a variable commonly effected by speed.

Internal-external rotation angles for the knee (**E**) also varied significantly between the PiG and CAST marker sets. Results for CAST remained exclusively in external rotation whilst those for PiG remained mostly in internal rotation. This was once again due to the orientation of the shank axes. The orientation of the shank using CAST led to a shank more externally rotated than the thigh whilst using PiG led to a shank more internally rotated than the thigh. CAST had a smaller average maximum angle (-1.58°) than PiG (13.8°). The PiG model had a smaller maximum external

⁴⁵See Figure 32 in the *Generic Methods*

rotation angle during the gait cycle (-1.19°) than CAST (-9.69°). All differences were found to be statistically significant using the t-test at the 5% significance level ($p < 0.01$). Rotation angles were unaffected by gait velocity.

Figure 157 also demonstrates that knee flexion-extension moments (**B**) varied significantly between the PiG and CAST marker sets. PiG had a greater average peak knee extension moment (0.79 N-m/kg) than CAST (0.51 N-m/kg). PiG however had a smaller average peak knee flexion moment (-0.17 N-m/kg) than CAST (-0.19 N-m/kg). Statistically significant differences were found in terms of average peak knee extension ($p < 0.01$) and flexion moment ($p < 0.02$). Differences were due to the PiG model having a more anterior KJC and thus having a greater moment arm distance to the posterior VGRF vector.

Knee abduction-adduction moments (**D**) also varied significantly between the PiG and CAST marker sets. The greater variability seen in the PiG results may have been linked to the greater variation in joint angle results, with segment displacement used as a variable in the computation of joint moments. PiG had greater average peak knee adduction moment (-0.21 N-m/kg) than CAST (-0.04 N-m/kg). CAST however had a greater average peak knee abduction moment (0.36 N-m/kg) than PiG (0.15 N-m/kg). Statistically significant differences were found for the average peak knee abduction ($p < 0.01$) and adduction moments ($p < 0.01$) using the t-test at the 5% significance level. Knee abduction-adduction moment was effected by gait velocity in the PiG model but not for CAST. This would have been due to the kinematic changes observed in PiG.

Figure 157 demonstrates that knee internal-external rotation moments (**F**) also varied significantly between the PiG and CAST marker sets. PiG had greater average peak knee internal rotation moment (0.10 N-m/kg) than CAST (0.05 N-m/kg). CAST however had a greater average peak knee external rotation moment (-0.09 N-m/kg) than PiG (-0.04 N-m/kg). No statistically significant differences were found between the average peak knee internal rotation moments ($p > 0.05$). A statistically significant difference was however found in terms of external rotation moments ($p < 0.01$) using the t-test at the 5% significance level. Moments were unaffected by gait velocity.

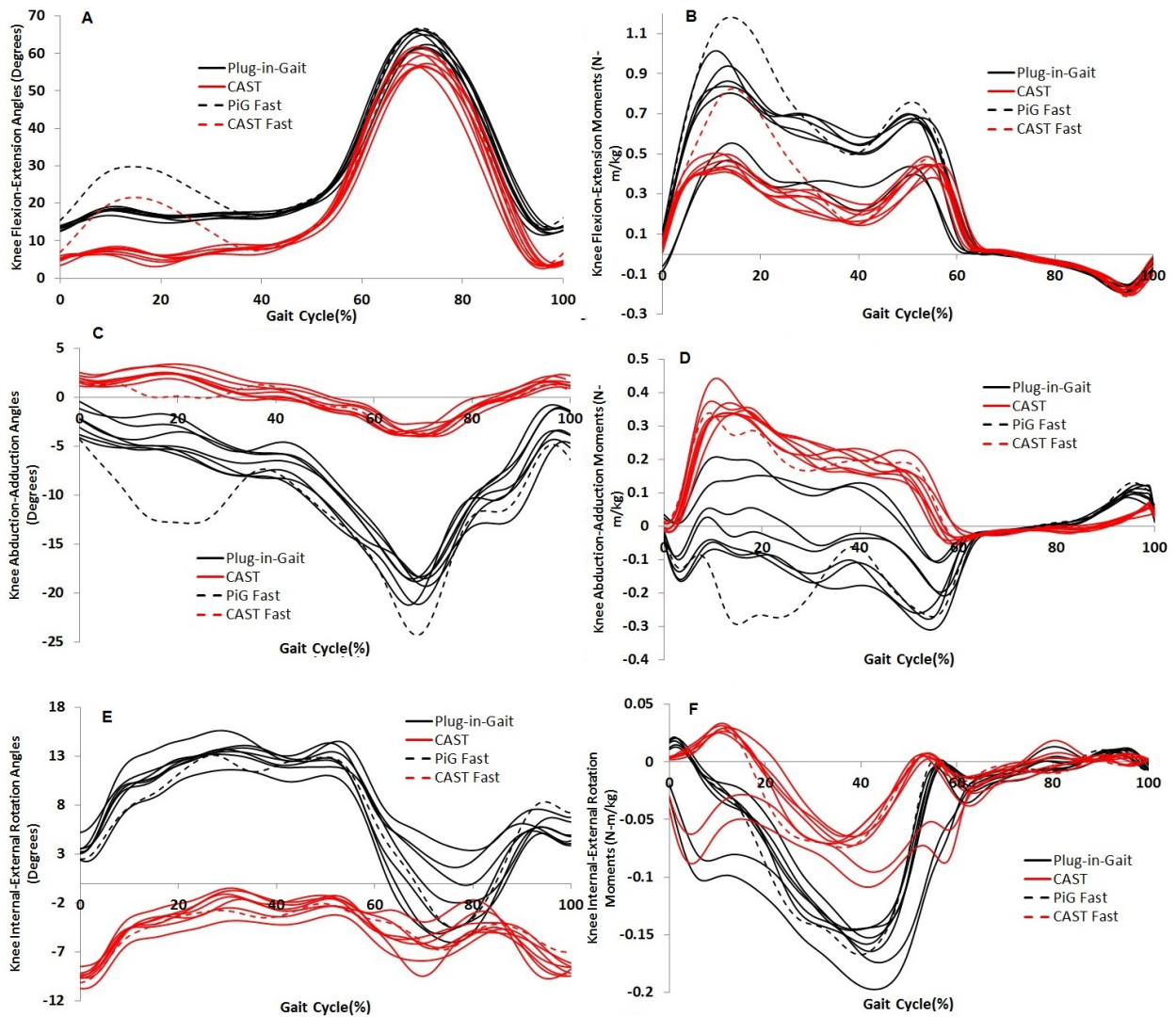


Figure 157: Average knee flexion (+)-extension (-) angles (**A**) and flexion (-)-extension (+) moments (**B**), abduction (+) adduction (-) angles (**C**) and moments (**D**), internal (+) external rotation (-) angles (**E**) and moments (**F**) for the PiG and CAST marker sets over 10 normalised gait cycle trials between consecutive heel strikes of the same foot

10.3.3 Ankle

Figure 158 demonstrates results for the ankle. Dorsi-plantar flexion angles (**A**) differed significantly between the PiG and CAST marker sets. The PiG marker set results remained in dorsiflexion for the majority of the gait cycle whilst the results for CAST remained in plantarflexion. Differences were not due to differences in the anterior-posterior position of the AJC (the positions of the AJC in both CAST and PiG appear to very similar, with little difference being seen in terms of ankle moments in Figure 158). Instead, the variability seen was likely due to the differences in the rotation of the ankle axes, caused by variations in the medial-lateral position of the AJC which

was computed using different techniques in PiG and CAST. CAST had a greater average maximum plantarflexion angle (-12.2°) than PiG (-3.18°). The PiG model had a greater average maximum dorsiflexion angle during the gait cycle (15.3°) than CAST (7.31°). Differences in terms of average peak dorsiflexion and plantarflexion were found to be statistically significant using the t-test at the 5% significance level ($p < 0.01$). The stance phase was effected by gait velocity, with there being an increase in dorsiflexion/loss of plantarflexion. This effect was slightly greater in CAST.

Ankle eversion-inversion angles (**C**) differed considerably between the PiG and CAST marker sets. Results using PiG demonstrated more ankle inversion than the results for CAST together with greater variability. This was due to how measurements are made in both CAST and PiG. The ankle calculation would have used the knee frontal plane results as a reference axes, which as shown previously were more consistent for CAST than PiG. In addition, different methods of computing the eversion offset are used by both methods⁴⁶. PiG had a smaller average maximum angle (-3.22°) than PiG (8.15°) and a larger minimum value during the gait cycle (-15.9°) than CAST (-4.01°). Maximum and minimum differences were found to be statistically significant using the t-test at the 5% significance level ($p < 0.01$). Ankle rotation angles (**E**) also differed considerably between the PiG and CAST marker sets. CAST had a smaller average maximum angle (-9.70°) than PiG (-11.5°). The PiG model had a greater maximum external rotation angle value during the gait cycle (-35.6°) than CAST (-17.4°). Statistically significant differences were found using the t-test at the 5% significance level in terms of maximum ($p < 0.02$) and minimum angle ($p < 0.01$).

Figure 158 also demonstrates that ankle dorsi-plantar flexion moments (**B**) did not vary significantly between the PiG and CAST marker sets. Overall, both marker sets had the same range of moment (1.74 N-m/kg). PiG had greater average peak ankle dorsiflexion moment (0.06 N-m/kg) than CAST (0.05 N-m/kg). Likewise, both had the same average peak dorsiflexion (0.07 N-m/kg) and plantarflexion (-1.67 N-m/kg) moments. In terms of rotation moments (**F**), both marker sets had the same average peak internal rotation moment (0.04 N-m/kg). PiG had a greater average maximum ankle external rotation moment (-0.12 N-m/kg) than CAST (-0.10 N-m/kg). No statistically significant differences were found in terms of peak ankle dorsi-plantar or internal-external rotation moments. ($p > 0.05$). Both were unaffected by gait velocity.

Ankle eversion-inversion moments (**D**) however did vary significantly between the PiG and

⁴⁶These are detailed on page 245

CAST marker sets. This would have been due to the different AJC positions and kinematics for each marker set result. Overall when comparisons were made, PiG had greater average maximum ankle eversion moment (0.31 N-m/kg) than CAST (0.10 N-m/kg). CAST had a greater average maximum ankle inversion moment (-0.05 N-m/kg) than PiG (0.00 N-m/kg). Statistically significant differences were found between the groups in terms of peak eversion ($p < 0.02$) and inversion moment ($p < 0.01$). Moments were unaffected by gait velocity and were predominantly external.

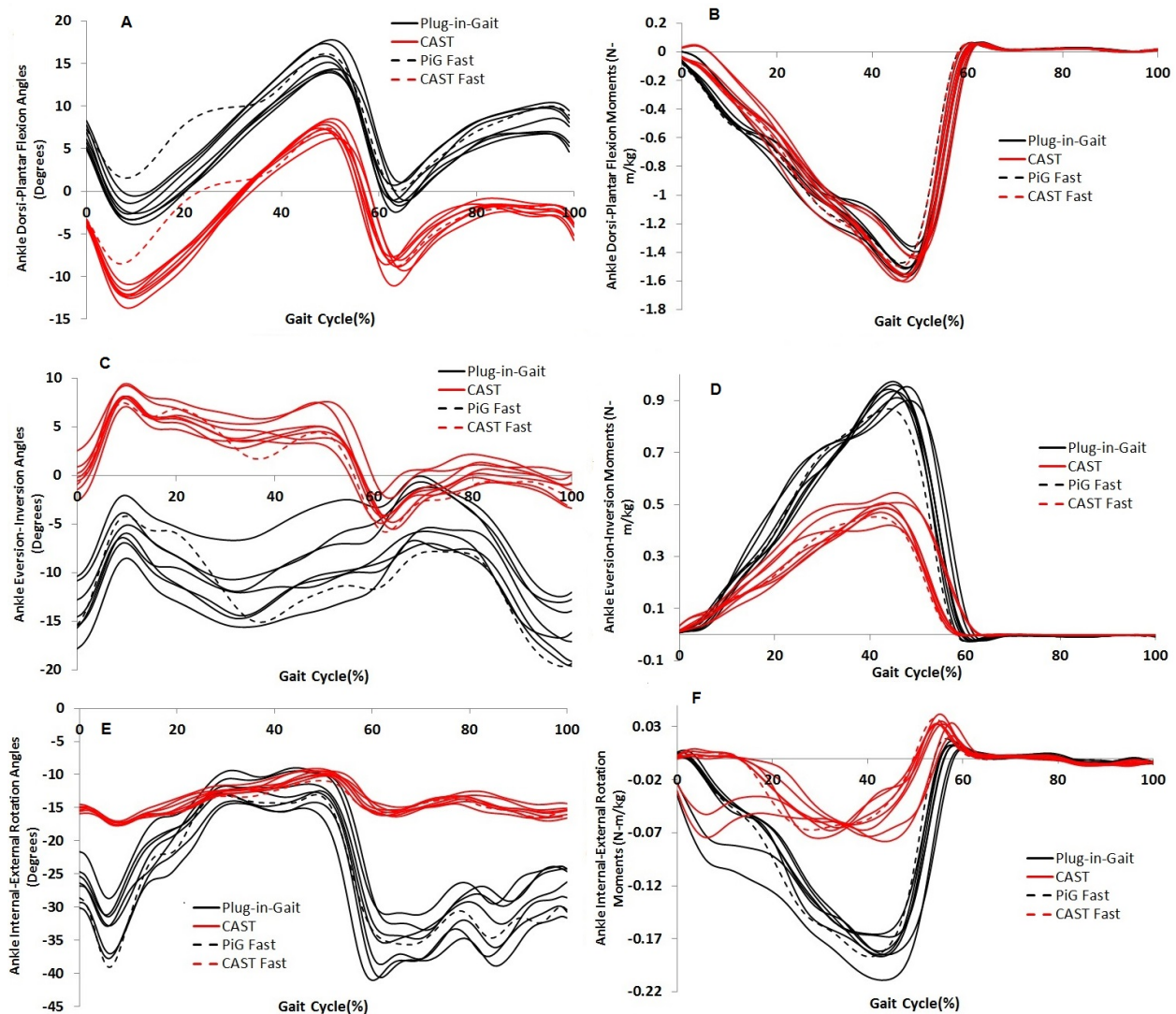


Figure 158: Average ankle dorsiflexion (+)-plantarflexion (-) angles (**A**) and moments (**B**), eversion (+) inversion (-) angles (**C**) and moments (**D**), internal (+) external rotation (-) angles (**E**) and moments (**F**) for the PiG and CAST marker sets over 10 normalised gait cycle trials between consecutive heel strikes of the same foot

10.4 Discussion I

Overall the results of this study correlate with what has been seen in the literature, with PiG showing more variability during gait relative to CAST and the greatest amount of variability being

in the transverse plane. Analysis found that the choice of marker set, whether that be PiG or CAST, impacts both joint angle and moment results. This was particularly the case for joint angles, with smaller changes being present in terms of joint moments. The interpretation of the results is however complicated when analysed together with the *A Critique of PiG - II* chapter, where the placement of the lateral segment marker and the definition of the segment plane in PiG had a very large impact on both joint angles and moments. Thus it may be that PiG is more similar or more dissimilar to CAST depending on the position of the lateral segment marker. The position of the marker cluster as used in CAST is less important as the markers are not used in defining joint centre positions or segment axes of rotation.

The clinical study undertaken in *Kinematics & Temporal Spatial Parameters* and *Kinetics* chapters used the PiG marker set for all three patient groups (Symptomatic LLI, Happy THR, Normal). The question then arises of how much of the differences observed between the joint angles and moments of the LLI patients when compared to the Normal patients was due to patient variability and how much was due to the choice of marker set. For the clinical groups, 6 motions were analysed with two at the pelvis (obliquity, anterior-posterior rotation), two at the hip (flexion-extension, abduction-adduction) together with one each at the knee (flexion-extension) and ankle (dorsi-plantar flexion). All these motions were selected due to them having previously been identified in literature to be planes of motion where compensatory mechanisms are used. The comparison between the Normal patients in this study to the results of Bovi found strong similarity between the results, indicating that the variability in marker placement was acceptable.

A comparison between the clinical results and the experimental results of this chapter can be seen in Table 22. Analysis demonstrated that the differences produced between the LLI and Normal patients in terms of peak hip flexion angle (0.20°) were smaller than the differences observed when comparing the PiG and CAST marker methods (3.4°). Similar results were also seen in terms of ankle dorsiflexion angle. The differences in peak knee flexion and hip abduction angle were however greater between the LLI and Normal patients. This suggests that the choice of marker set is important in producing reliable results. These results however do not indicate that either one of the PiG or CAST marker sets is superior to the other. Both marker sets are subject to error, of which not all can be removed.

Table 22: A comparison of the differences in peak joint angles between LLI/Normal patients and the differences between PiG and CAST

Motion	Difference (LLI & Normal patients)	Difference (PiG & CAST)
Hip Flexion	0.20°	3.4°
Hip Abduction	1.44°	0.7°
Knee Flexion	7.51°	4.9°
Ankle Dorsiflexion	3.19°	7.99°

10.5 Methodology II

AnyBody and AnyGait are two applications produced by AnyBody Technology in the analysis of gait. They however differ in how these use motion capture data. AnyBody does not follow the traditional method used by both Vicon and Visual3D in computing kinematics and kinetics using segment optimisation⁴⁷, but instead uses inverse kinematics. The experimental markers are matched to the model markers at each time point in a least square sense. The computation of results are optimised for various properties including segment lengths. Standing trials are not utilised and the models joint centres and axes orientations are based on scaling of the underlying model which depicts an average European male. The traditional AnyBody model follows the PiG marker protocol.

AnyGait is an alternative application produced by AnyBody Technology which follows the traditional 6DoF methodology utilised by Visual3D. Both the standing and dynamic trial are used and there is no optimisation of segments. There also are no model markers and hence the procedure of the least squares method is not used. Joint centres are calculated using the lateral and medial markers at the knee and the ankle, as in CAST, and not through scaling as with the AnyBody model. The AnyGait model can therefore be used to compute JRFs for the CAST marker set whilst the traditional AnyBody model can be used for PiG.

10.5.1 Subject

The same subject was used in *Method I* on page 243 were used.

10.5.2 Gait Analysis

Joint reaction forces were computed between consecutive heel strikes of the same foot from placement onto the force plate to the subsequent placement off the force plate. In total, 6 motion capture trials were used out of the 9 captured due to errors in the convergence of the inverse kinematics method.

⁴⁷See pages 77 - 78 in the *Generic Methods*

10.5.3 BodyModel

Analysis was undertaken in AnyBody (Version 5.2, AnyBody Technology, Aalborg, Denmark)⁴⁸. The Analysis was undertaken using the MoCapLowerExtremity model which represented PiG whilst the AnyGait model was used to represent CAST.

The 340 muscle lower body musculoskeletal model used in this study in AnyBody has been validated by Manders et al. [220] and Forster et al. [327]. The model used was composed of 11 segments (talus, foot, shank, patella and thigh for both legs together with the pelvis). The University of Twente [387] provided the anthropometric measurements from which inertial, joint centre and muscle parameters were derived from. A simple muscle model structure was selected for this study without force-velocity relationships which were found to have little effect on muscle and JRFs by Anderson & Pandy [331]. GRFs were applied to each foot where by the process of inverse dynamics JRFs were calculated. The problem of muscle redundancy (i.e. there being a greater number of muscles than degrees of freedom) was dealt with using polynomial muscle recruitment via minimising the maximum force for each muscle⁴⁹.

10.6 Results - Joint Reaction Forces

Figure 159 demonstrates the hip JRFs produced via the different AnyBody applications. As can be seen, the PiG model, as produced using MocapLowerExtremity, produced greater force than the AnyGait model during the 1st peak and 2nd gait cycle peaks, together with showing wider confidence intervals. For both curves, the 2nd peak exceeded the 1st. Multiple t-tests were undertaken at 10% gait intervals between the results of the MocapLowerExtremity and AnyGait model in order to establish whether significant differences existed. A statistically significant result at the 5% significance level was found at the 30% (p<0.03) instance of the gait cycle.

⁴⁸A thorough explanation of how AnyBody works, including on how joint angles and forces are computed is given in the *Generic Methods* on pages 85 - 89

⁴⁹See pages 48 - 50 in the *Literature Review*

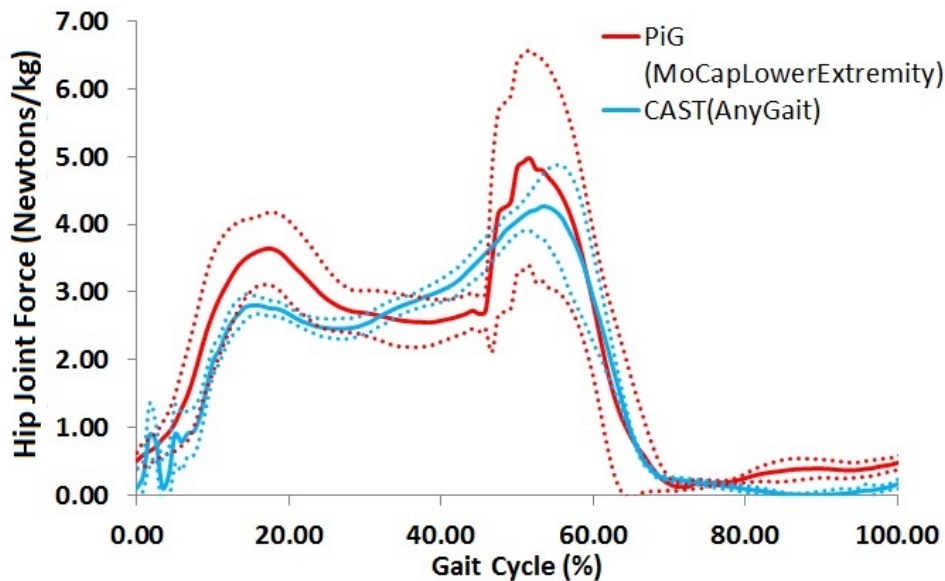


Figure 159: Hip joint forces comparing the PiG and CAST models between consecutive heel strikes of the same foot over a normalised gait cycle. Forces have been normalised for bodyweight. Results are plotted together with 95% confidence intervals

10.7 Discussion II

To date, this is the first study to have analysed hip JRFs during gait using two different marker sets. Results therefore provide a valuable insight into how variability in results can be attributed to the method of measurement in addition to natural patient variability. Previous studies have analysed patient groups as a whole using a variety of inverse dynamics techniques such as inverse kinematics and segment optimisation, or have used competitor rigid body dynamics software packages such as Opensim. This study has demonstrated that the choice of marker set and inverse dynamics method leads to significant changes in results.

The results for PiG produced a different JRF curve shape to CAST. Greater variability was shown in the results for PiG, with there being wider confidence intervals. Due to the optimisation procedure used in the inverse kinematics PiG model, optimisation took place in terms of marker positions and segment lengths prior to computation for every trial. The initial position of the model in terms of joint angles had to be modified so that the experimental markers lined up as closely as possible to the model markers. If this was not undertaken, kinematic failure was possible. As during each trial the subject walked slightly differently, the optimisation process was redone for every trial. This thus would have led to some of the variability seen between the results with the model being rescaled for every motion trial to have different joint centres. For the CAST AnyGait model, this was not the case, with the single standing trial determining joint centre positions whilst

the motion trials were used only for tracking.

These results bring into question the hip joint force results in *Kinetics* chapter i.e. how much of the differences seen between the LLI and Normal groups in terms of joint force were due to patient variability and how much was to do with the choice of marker system. Comparing the two groups, at the 1st joint force peak there was a difference of 0.65N/kg whilst at the 2nd peak there was a difference of 1.34N/kg. For the comparison between PiG and CAST, a difference of 0.7N/kg was found at the 1st joint force peak with there being a 0.72N/kg difference at the 2nd. As the differences in joint force produced by simply changing marker system were so large relative to the differences between patient groups, it shows that the choice of marker set can have a large effect on JRFs and therefore potentially on the interpretation of results from a clinical perspective.

The differences between the two applications in terms of results was also, apart from the marker sets being different, directly linked to how each of them operates. The standard AnyBody model uses a least squares approach, aiming to minimise the distance between the experimental and model markers from a global perspective. This is coupled with optimisation of measurements such as leg length, pelvic width and marker positions/weights. Thus, a misplaced marker at the thigh will lead to the least squares equation producing an erroneous global optimal position, with errors in the positions of the hip, knee and ankle centres. AnyGait works from an alternative standpoint in that there are no model markers for the experimental markers to be matched against. Likewise, there is no optimisation of segment lengths or marker positions. Instead, joint centres are calculated directly from the medial and lateral markers at the knee and ankle, with the centre being the mid-point of the two.

10.8 Conclusion

This study has demonstrated there exist substantial differences in terms of joint angles and hip JRFs between the uses of PiG and CAST. Differences were also apparent in terms of joint moments. This is the first study to have compared these models using the specified methods. PiG showed greater variability than CAST for joint angles. Overall the CAST model appeared to be superior to PiG with results showing less variability. However, the CAST marker model also potentially could produce erroneous results through limbs knocking contralateral markers and the misplacement of markers. It is recommended that for any future studies, extra care and precision be taken regardless

of the marker set used to ensure the minimisation of any errors. If CAST is being used, markers should be used which are large enough to be detected by the cameras whilst at the same time being small enough to avoid contralateral limb contact. For PiG, a KAD is recommended to ensure the correct position of the KJC.

11 Contact Surface Motion Paths

11.1 Aims & Objectives

The aim of this chapter was to analyse the effects of kinematics and kinetics on the durability of the hip implant in both LLI and Happy THR patients. This was undertaken through comparing the predicted amounts of wear between the groups using known wear equations, contact surface motion paths and lubrication equations. This would enable a greater understanding of the clinical impact of the different kinematic and kinetic results between patient groups.

11.2 Methodology

11.2.1 Clinical Method

A description of the patient cohort used together with the recruitment method is described in the *Anthropometrics & Demographics* chapter on page 90 whilst the clinical gait analysis method is detailed in the *Kinematics & Temporal-Spatial Parameters* chapter on page 105.

11.2.2 Non-Clinical Method

The same method in selecting patient data was used as in the *Kinematics & Temporal-Spatial Parameters* chapter on page 106.

Hertz Contact Area

Hertz contact theory is detailed on pages 56 - 57 in the *Literature Review*. The relative radius between the femoral head and acetabular cup, R^* was computed using Equation 56, whilst the relative Young's Modulus, β^* was found using Equation 57. From these values, the contact radius and contact area were calculated using Equations 58 and 59. Using the contact area, only those points which are in contact between the cup and the femoral head are used. For the particular analyses undertaken in this study, it was assumed that the cup was made from polyethylene and the head was metal. The head was assumed to have $R_1=14\text{mm}$, a Young's Modulus (β) $7.00\text{E}+08$ and Poisson's Ratio (γ) = 0.46. The cup was assumed to have $R_1=14.25\text{mm}$, a Young's Modulus (β) $2.10\text{E}+11$ and Poisson's Ratio (γ) = 0.3. These numerical values were taken from the literature [456].

$$R^* = \frac{R_1 R_2}{R_2 - R_1} \quad (56)$$

$$\beta^* = \frac{\beta_1\beta_2}{\beta_1(1 - \gamma_1^2) + \beta_2(1 - \gamma_2^2)} \quad (57)$$

$$\text{Contact Radius} = C = \left(\frac{3F_i R^*}{4\beta^*}\right)^{1/3} \quad (58)$$

$$\text{Contact Area} = A = C_i^2 \pi \quad (59)$$

Wear

Wear volume was estimated using Equation 60, known as the Archard Equation. Here W was the applied load, S the sliding distance and K a constant. This calculation assumed that the lubrication regime in each case is identical and not influenced by load, velocity or material.

$$\text{Wear} = KWS \quad (60)$$

Cross Shear

Cross shear theory is detailed on page 57 of the *Literature Review*. The amount of cross shear can be calculated using Equation 62, proposed by Kang et al. [391]. The numerator in Equation 62 represents Frictional work in the direction perpendicular to the PMO in the contact area whilst the denominator that of the total frictional work.

Kangs Equation assumes that a point P₀ on the femoral head moves to a point P₁ via sliding (anterior-posterior and medial-lateral motion) and rotation. In Equation 62, V_{total_y} and V_{total_x} represent the anterior-posterior and medial-lateral sliding velocities and σ_i represents the instantaneous stress during a point in the gait cycle, computed via Equation 61, where F_i is the instantaneous resultant force. Furthermore, Δt is the time step between each gait cycle point which for this study was 0.01. A full derivation is given by Kang.

$$\sigma_i = \frac{F_i}{A} \quad (61)$$

$$\frac{\sum_{i=1}^N \sigma_i \sin \alpha V_{total_y} \Delta t}{\sum_{i=1}^N \sigma_i \sqrt{(V_{total_x}^2 + V_{total_y}^2)} \Delta t} \quad (62)$$

Matlab

Contact surface motion paths are discussed on pages 58 - 60 of the *Literature Review*. For

this study, contact surface motion paths were computed using an in-house Matlab (MathWorks, Massachusetts, USA) code which had been previously validated numerically against the results of Barbour et al. [404]. The main purpose of the Matlab code was for the tracking of loci on the femoral head through the gait cycle and to display their movements graphically. This followed the technique used by Ramamurti et al. [403] through the use of 20 loci on the femoral head. This software allowed the radius of the acetabular cup, the inclination angle and the coverage angle to be defined. To ensure fairness across the groups, the cup radius was defined as 14mm, the inclination angle as 45° and the coverage angle as 180° .

The locations of these points was taken in reference to the femoral head equator, which passed through the centre of the Great Circle. The Great Circle is the region of intersection between a sphere and a plane which passes through the centre of the sphere. This circle was oriented such that it was perpendicular to the long axes of the femoral head and neck of the hip implant. The first 10 points were located equally spaced on the semicircle which passed through the most superior point of the equator, the most inferior point of the equator and the apex of the femoral head. The second set of 10 points were located equally spaced on the semicircle which passed through the most anterior point of the equator, the most posterior point of the equator and the apex of the femoral head. The Ramamurti points can be seen in Figure 160.

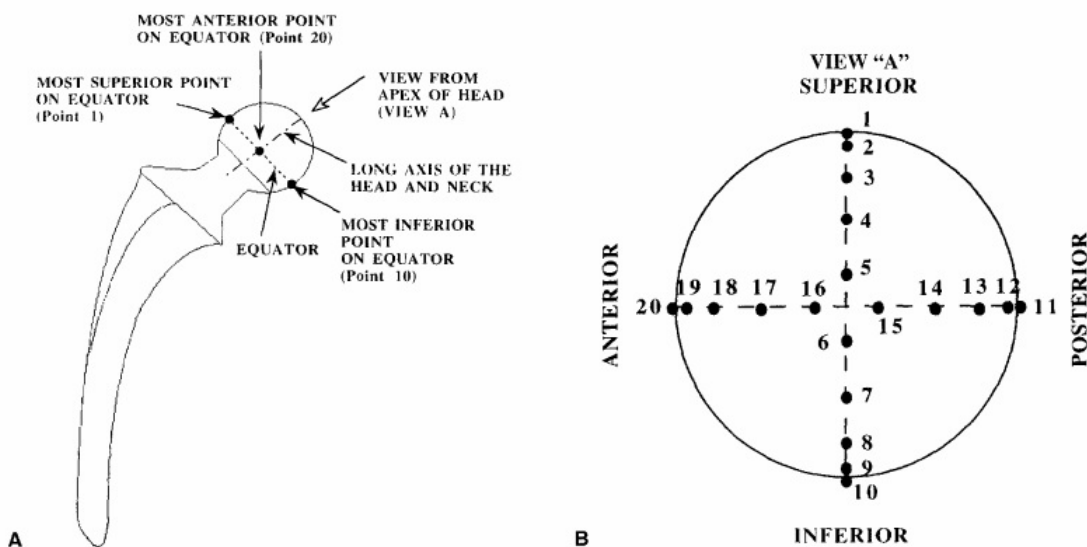


Figure 160: Image (A) shows where the Ramamurti points are located relative to the shape of the femur whilst (B) shows how the points are located with respect to each other on the femoral head viewed from directly above the apex of the femoral head

Gait data for each patient group which had been normalised to 100 percentiles was uploaded into the Matlab program. Only the hip data was used with an initial cardan angle sequence of XYZ, matching that as used in kinematics. A second cardan angle sequence of YZX was used as a comparison to Barbour et al. [404] and Budenberg et al.[264] . Hip flexion-extension was defined as X, abduction-adduction as Y and internal-external rotation as Z. The rotation matrix for XYZ rotation P_α can be seen in Equation 63 whilst that for YZX, P_β , can be seen in Equation 64. Each of these matrices were used to compute the position of a specific Ramamurti loci at each time instant.

$$\mathbf{P}_\alpha = \begin{pmatrix} \cos(y)\cos(z) & -\cos(y)\sin(z) & \sin(y) \\ \sin(x)\sin(y)\cos(z) + \cos(x)\sin(z) & -\sin(x)\sin(y)\sin(z) + \cos(x)\cos(z) & -\sin(x)\cos(y) \\ -\cos(x)\sin(y)\cos(z) + \sin(x)\sin(z) & \cos(x)\sin(y)\sin(z) + \sin(x)\cos(y) & \cos(x)\cos(y) \end{pmatrix} \quad (63)$$

$$\mathbf{P}_\beta = \begin{pmatrix} \cos(y)\cos(z) & \sin(y)\sin(x) - \cos(x)\cos(y)\sin(z) & \sin(z)\sin(x)\cos(y) + \sin(y)\cos(x) \\ \sin(z) & \cos(x)\cos(z) & -\cos(z)\sin(x) \\ -\cos(z)\sin(y) & \cos(x)\sin(y)\sin(z) + \sin(x)\cos(y) & \cos(x)\cos(y) - \sin(x)\sin(y)\sin(z) \end{pmatrix} \quad (64)$$

This led to the position of each loci on the femoral head, according to the XYZ cardan angle sequence, to be at first rotated in the X direction, followed by the Y and finally Z. The first computation using the initial position of the loci with respect to the equator, led to the loci moving from a point P_0 to a point P_1 . The procedure was then repeated until point P_{100} was reached. Code was built such that motions of the hip in all three directions could be taken as an input and the aspect ratio (relationship between length and width of motion paths) be calculated. An example of the output file produced demonstrating the movement of the loci can be seen in Figure 161.

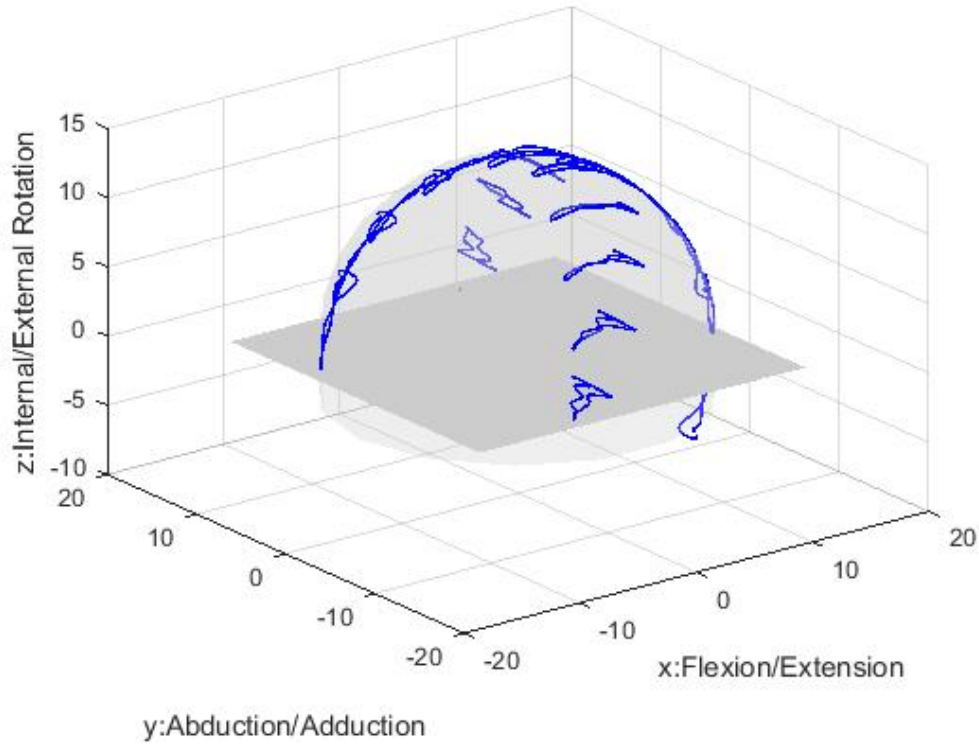


Figure 161: Motion paths produced by 20 loci on the femoral head computed via the in-house Matlab program

Aspect ratios are discussed on page 60 of the *Literature Review*. The Aspect Ratios for each Ramamurti point in the present study were found through an algorithm which was coded into Matlab. The algorithm was firstly able to compute the maximum anterior, posterior, medial and lateral positions of each motion path, where most was quantified as the greatest numerical distance away from the centre of the head (0,0,0). Following this, the magnitudes of the linear distances between the maximum anterior and posterior together with the maximum medial and lateral positions were found using Equation 65.

$$D_{1,2} = \sqrt{(x_2 - x_1)^2 + (y_2 - y_1)^2} \quad (65)$$

Following the calculations of $D_{1,2}$ the angles α_1 and α_2 , subtended by the maximum anterior and posterior or medial and lateral position coordinates respectively, were computed using Equation 66, with R being the radius of the cup.

$$\text{Sin}\left(\frac{\alpha_{1,2}}{2}\right) = \frac{D_{1,2}}{2R} \quad (66)$$

Once $\alpha_{1,2}$ had been found, the curved distances $L_{1,2}$ between the maximum anterior and pos-

terior together with the maximum medial and lateral positions were found using Equation 67

$$L_{1,2} = R\alpha \quad (67)$$

Using the $L_{1,2}$ values, the Aspect ratio calculation using Equation 68 can be completed. Figure 162 is a visual representation of how the aspect ratio can be calculated.

$$\frac{\text{Curved Maximum Anterior-Posterior Length Difference}}{\text{Curved Maximum Medial-Lateral Length Difference}} \quad (68)$$

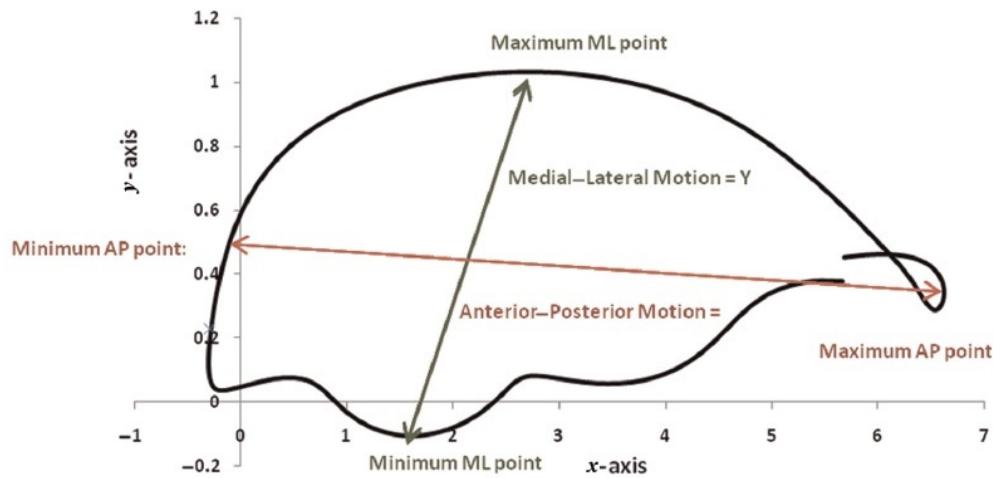


Figure 162: The calculation of the Aspect Ratio. The (x,y) coordinate values for the maximum and minimum anterior, posterior, medial and lateral points of each of the 20 motion paths were found. The Aspect Ratio was subsequently found using Equations 65-68. This image is from Budenberg et al. and is a 2D rendition of the 3D Aspect Ratio calculation.

[264]

Sliding distance was computed using Equation 69 which is adapted from Bennet et al. [393] who used 50 gait cycle points in contrast to the 100 used in this study. Following the method as proposed by Ramamurti et al. [403] with 20 loci, 100 gait cycle points were also used in this study. Here x_i , y_i and z_i represent the initial position of a loci on the femoral head at gait instant n whilst x_{i+1} , y_{i+1} and z_{i+1} represent the position at gait instant $n+1$. Summing of the displacements in each direction gave the sliding distance. Sliding speed was simply the sliding distance over time as can be seen in Equation 70

$$\sum_{n=1}^{99} [\sqrt{(x_{i+1} - x_i)^2 + (y_{i+1} - y_i)^2 + (z_{i+1} - z_i)^2}] \quad (69)$$

$$\text{Sliding Speed} = \frac{\text{Sliding Distance}}{\text{Cycle Time}} \quad (70)$$

Film Thickness

Lubrication theory is detailed on pages 61 - 63 in the *Generic Methods*. The theory of fluid film thickness can be described by fluid entrainment. Equation 71, also known as the Hamrock & Dowson equation, computes fluid entrainment which requires a number of constants and variables that need to be defined. Here R represents the equivalent radius of the bearing, the viscosity of the lubricant is defined by η , ω represents load, E' the material stiffness, μ the sliding velocity and finally t represents time.

For this analysis, the numerical values used followed those utilised by Dowson & Wright [23]. These were $\eta=2 \times 10^{-3}Ns/m^2$, $E'=10^7N/m^2$ and $R=1$ metre. The remaining values of ω and μ were taken from the clinical data, with ω being the average peak gait cycle joint force for each group and μ the sliding velocity. All values in Equation 71 were constants, except for the sliding velocity with the results for all 20 Ramamurti points used. This allowed there to be 20 results for Equation 71 in each group and allowed averages to be calculated.

$$\text{Film} = 2.789R\left(\frac{\mu\eta}{E'R}\right)^{0.65}\left(\frac{\omega'}{E'R^2}\right)^{-0.21} \quad (71)$$

11.3 Results - Wear

Table 23 shows the results using Equations 69 and 70. Results indicated that Normal patients on average (24.1mm) had the greatest sliding distance during gait and the operated side of LLI patients the smallest (17.5mm). Sliding velocity results showed that the Normal group had the largest sliding velocity (24.5mm/s). Likewise, the operated side of the LLI group had the smallest sliding velocity (15.5mm/s). A Kruskal-Wallis one way ANOVA found the differences to be statistically significant ($p<0.01$) for sliding distance together and sliding velocity ($p<0.01$) at the 5% significance level.

Table 23: Average sliding distances and velocities for each clinical group together with standard deviations

Group	Sliding Distance (mm)	Sliding Velocity (mm/s)
LLI Operated Side	17.5±2.74	15.5 ±2.43
LLI Non-Operated Side	20.3 ±2.98	17.8±2.60
Normal	24.1±4.19	24.5±4.23
Happy THR Operated Side	19.8±4.02	18.5±3.75
Happy THR Non-Operated Side	20.7±3.96	19.4±3.71

Figure 163 shows the sliding distances normalised for stride length. As can be seen, the LLI patients had the greatest average sliding distance over the 20 Ramamurti points. These results indicate that when Symptomatic LLI, Happy THR and Normal patients walk an equal distance,

the greatest sliding distance would occur in the LLI patients. This has implications in terms of wear, with the Archard Equation (Equation 60) being a function of load and sliding distance.

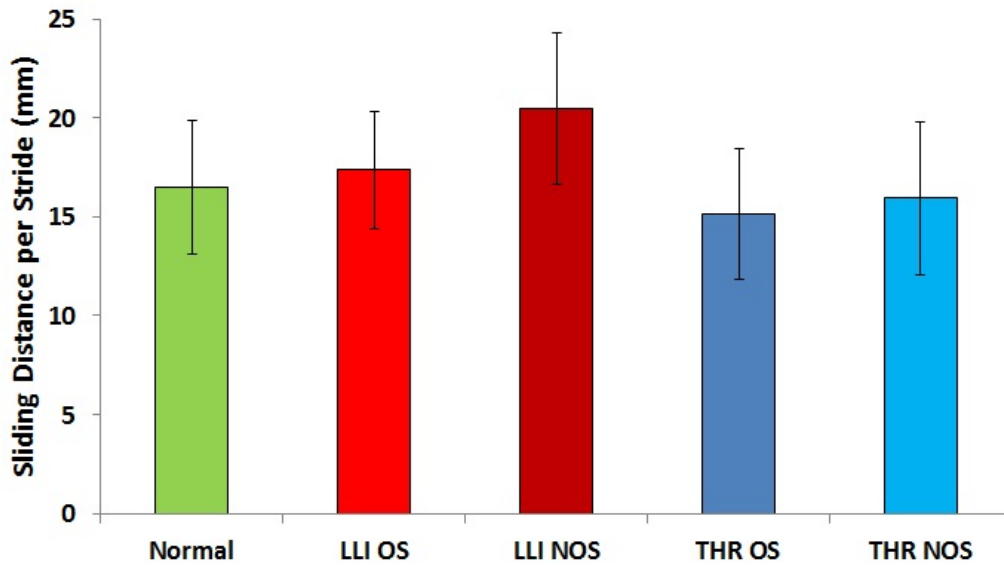


Figure 163: Average sliding distances for each of the clinical groups per stride length together with standard errors.

Figure 164 shows the results when computing the Kang cross shear over the Hertz Contact Area. All results plotted are the absolute values. The greatest cross shear was seen on the operated side of the Happy THR group (0.23 ± 0.08) with the smallest being on the operated side of the LLI group (0.01 ± 0.02). Large standard deviations were seen. The differences were found to be significant using the Kruskal-Wallis one-way ANOVA in SPSS at the 5% significance level ($p < 0.01$). The range of results together with the variability falls within the range as reported by Barnett [457].

Figure 165 shows the wear results as produced when using the Archard Equation (Equation 60). A value for the wear coefficient of $k = 1.5 \times 10^{-6} \text{mm}^3$ was selected which was an average taken from values found experimentally in the literature for metal on polyethylene implants [391, 458]. Peak JRFs for the average patient in each clinical group (Newton's) and sliding distances (mm) were also used. As the Normal patients do not have an in-vivo measured wear rate, for this study the Normal group represented the wear rate of a THR patient who walked exactly like a healthy individual. An assumption was made that LLI patients had the same wear rate as regular THR patients.

As the results produced were dimensionless, data was normalised to the results of the Normal group. Results indicated that the greatest amount of wear would occur in THR patients who walked like healthy individuals, followed by the Happy THR and with the LLI patients having the least

amount of wear. These results reflect that the Normal patients had the greatest hip load and sliding distance whilst the LLI patients had the least. From the perspective of the Archard Equation, it appeared that due to factors such as walking speed and hip load, which were smaller in both the LLI and Happy THR groups, Happy THR and LLI patients would have wear rates smaller than Normal individuals. If operated patients walked at the same velocity with the same amount of load as normal healthy individuals, they would according to the Archard Equation show an increased rate of wear.

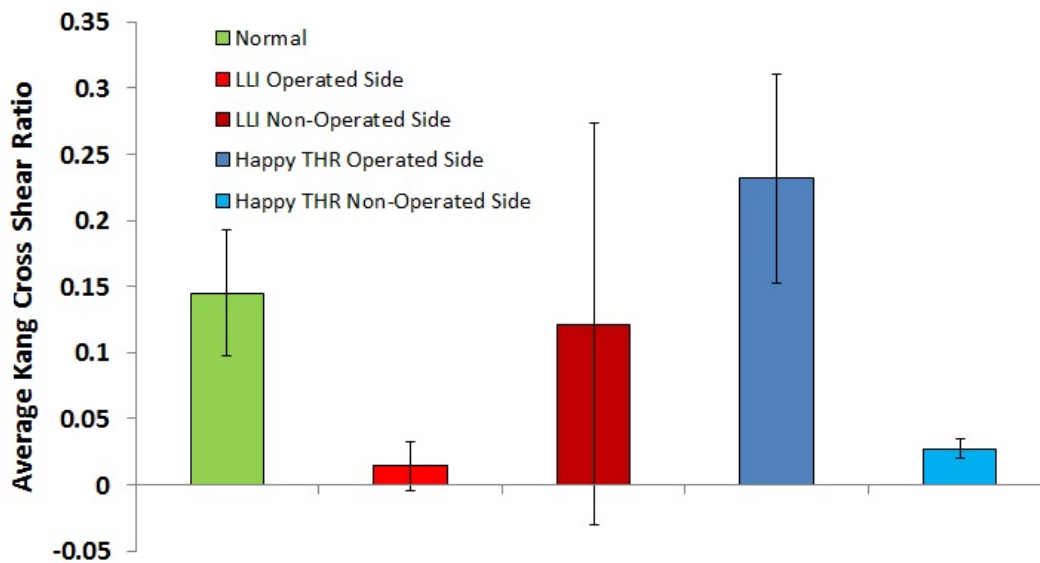


Figure 164: Average Kang cross shear ratio for each patient group together with standard errors over the Hertz Contact Area

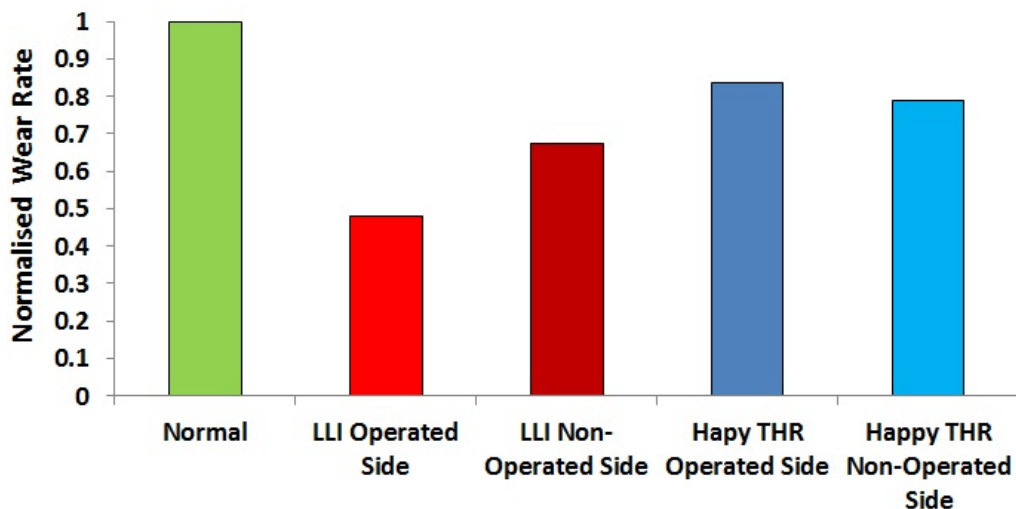


Figure 165: Normalised wear rate calculation for each group using the Archard Equation

11.4 Results - Motion Paths

Figures 166 and 167 illustrate the contact surface motion paths for all groups using the in-house Matlab program via the XYZ and YZX cardan angle sequences respectively. The motion paths had many differences in the size and shape of individual paths. Comparing the cardan angle sequences together, it was seen that the use of the YZX sequence produced motion paths which were more linear and therefore predict less wear.

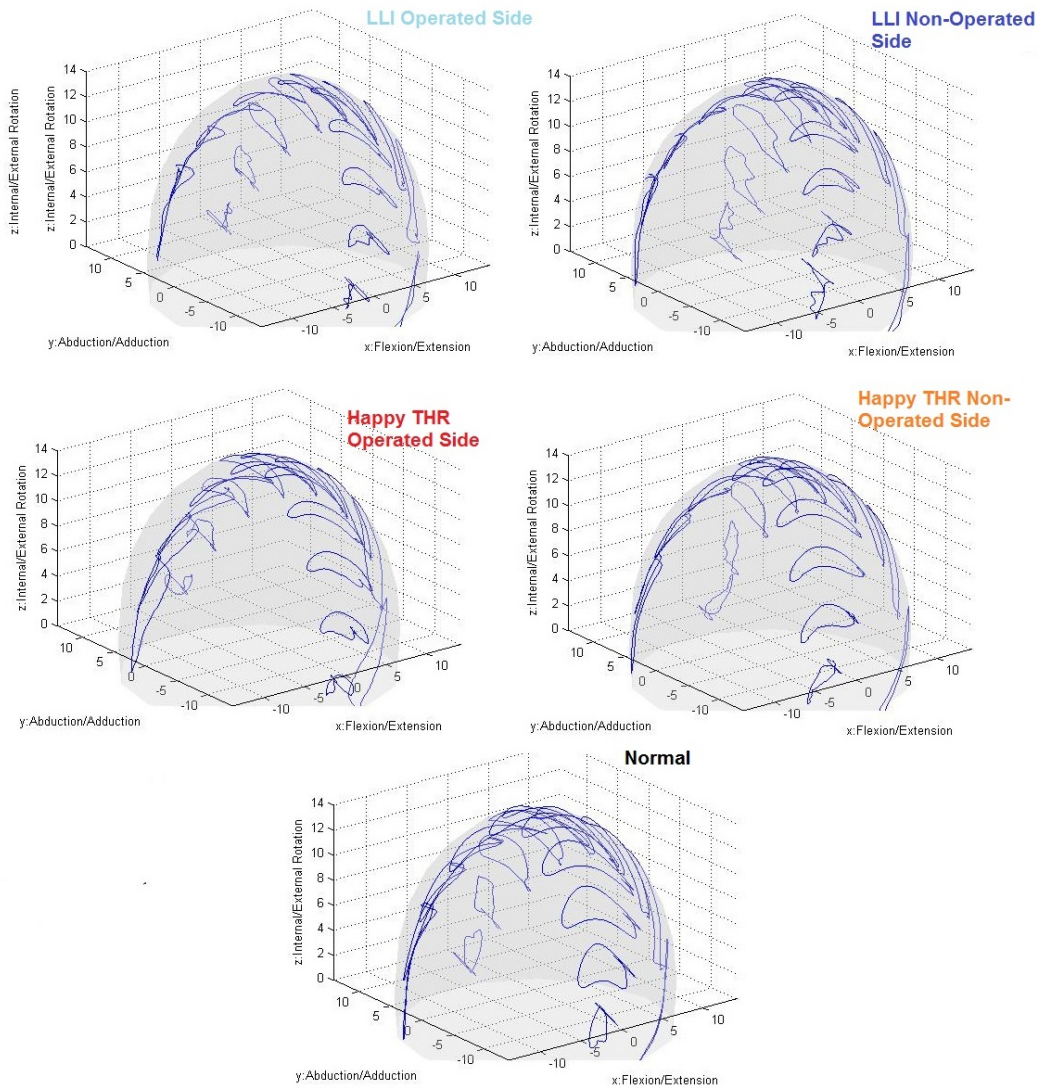


Figure 166: Contact surface motion paths as computed using an in-house Matlab code for all clinical groups at 20 Ramamurti points using the XYZ Cardan angle sequence

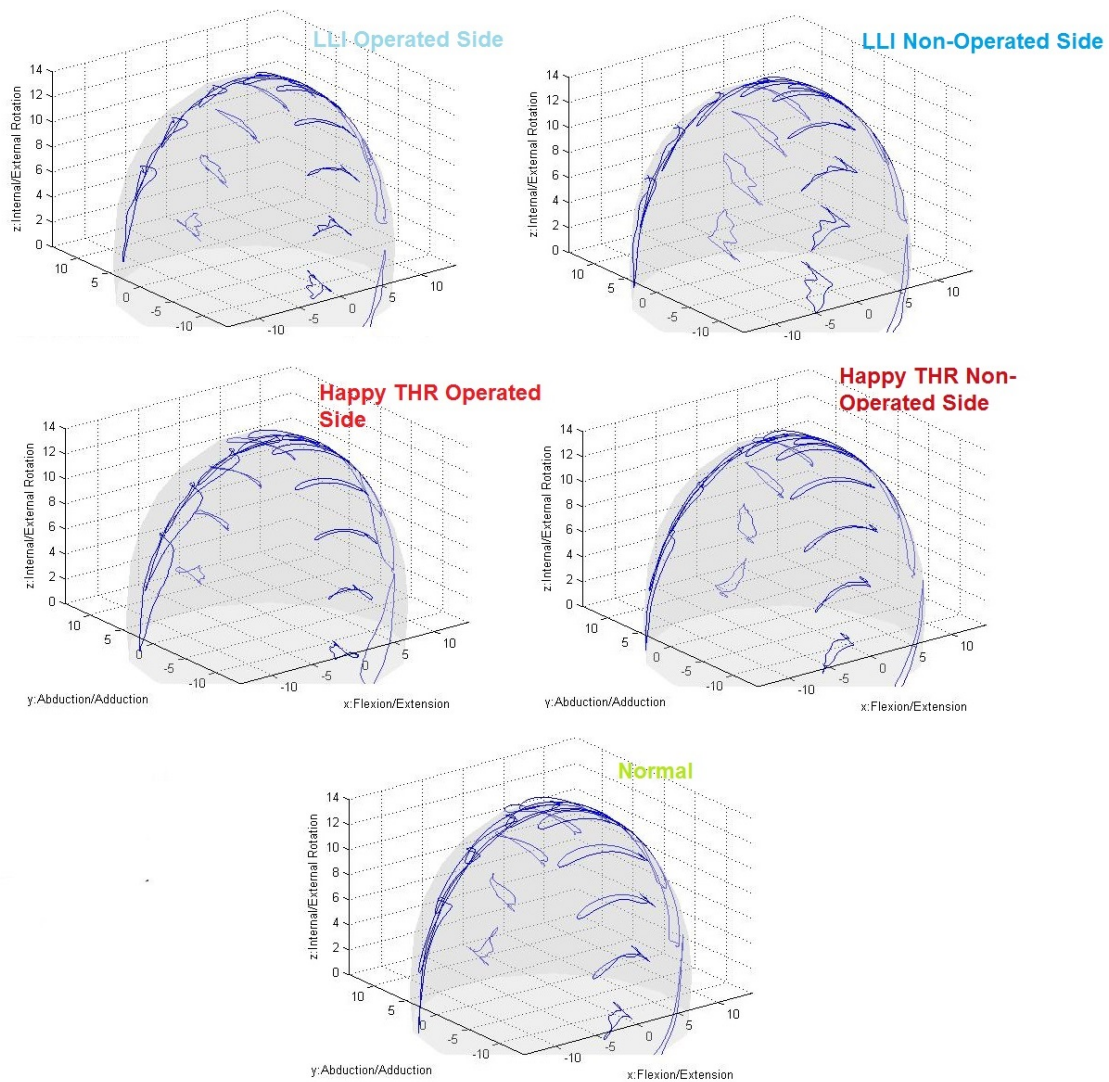


Figure 167: Contact surface motion paths as computed using an in-house Matlab code for all clinical groups at 20 Ramamurti points using the YZX Cardan angle sequence

The Normal group displayed a greater number of motion paths with either elliptical or quasi-elliptical shape for both cardan angle sequences, which is traditionally associated with multi-directional motion and increased cross shear. This was in contrast to the LLI patients who demonstrated the most linear motion paths. The Normal patient motion paths also appeared to be significantly larger. This corresponds well to the Normal patients having a greater RoM in the flexion-extension and abduction-adduction planes together with a greater sliding distance. These results are in direct conflict with those of Budenberg et al. [264], who found that LLI patients demonstrated motion paths which had more elliptical, quasi elliptical and figures of eight shapes using the YZX rotation matrix relative to healthy individuals.

Figure 168 shows the average aspect ratio over the 20 Ramamurti points for the average gait cycle for all the clinical groups. This was undertaken for both the XYZ and YZX cardan angle

sequences. The differences for both the XYZ and YZX sequences were found to be not significant using the one-way ANOVA in SPSS at the 5% significance level ($p > 0.05$).

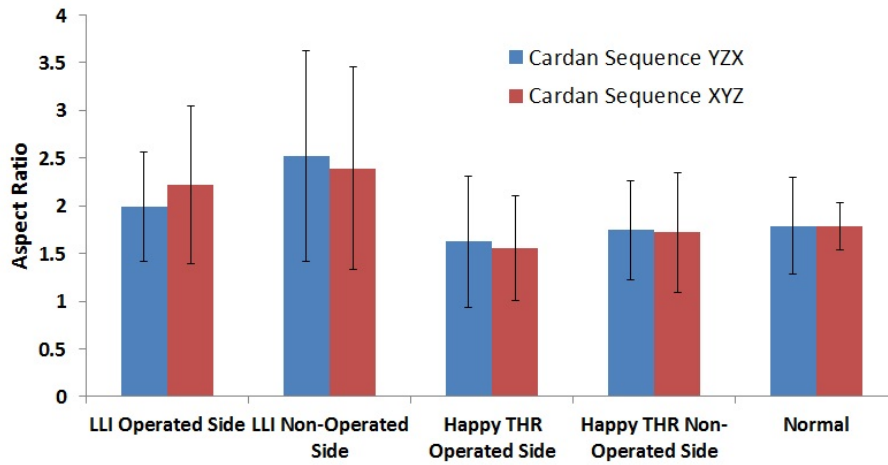


Figure 168: Calculated Aspect Ratios for each group together with standard errors for the XYZ and YZX cardan angle sequences

The *A Comparison between PiG & CAST* chapter (pages 243 - 258) established that the CAST and PiG marker sets differed in hip angle results. Figure 169 compares the motion paths of the same subject used in the chapter (see page 243) as measured using PiG and CAST over 20 Normalised Ramamurti points over 9 normalised gait cycle trials. The motion paths showed that PiG produced results with more elliptical and quasi-elliptical motion paths than that of CAST. This led to a larger average aspect ratio in PiG (1.83 ± 0.81) relative to CAST (1.68 ± 0.47). A Kruskal Wallis test found no statistically significant differences between the two marker sets ($p > 0.05$).

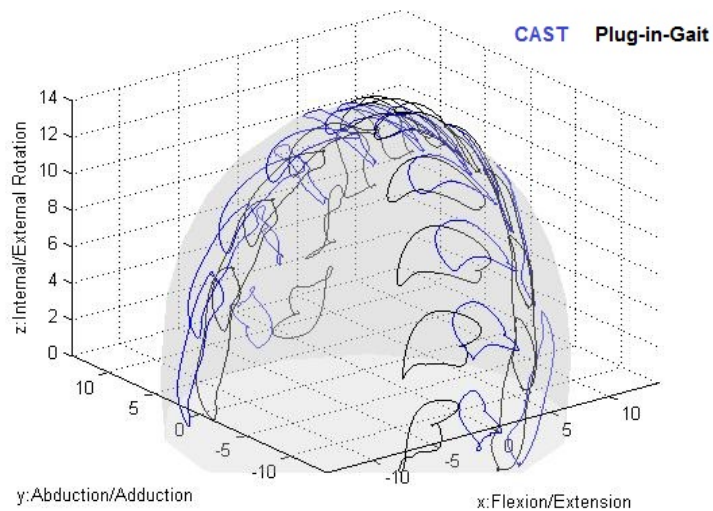


Figure 169: Comparing the motion paths on a 14mm femoral head between PiG and CAST when using the same motion trials. 20 Ramamurti points are used.

11.5 Results - Film Thickness

Figure 170 shows the total entraining lubrication fluid film thickness over the course of the gait cycle. As can be seen, the greatest amount of entraining lubrication occurred for the Normal healthy patients. Happy THR and LLI patients showed similar levels of fluid thickness. Using a Kruskal-Wallis one way ANOVA at the 5% significance level, statistical significance was found between the operated and non-operated sides of the LLI and Happy THR patients to the Normal group ($p < 0.01$). A smaller fluid thickness leads to less sacrificial wear and hence increased wear of the hip joint.



Figure 170: Average entraining lubrication fluid film thickness at peak hip JRFs over the course of the gait cycle using the Hamrock & Dowson Equations for entraining lubrication. Standard errors are also plotted.

11.6 Discussion

11.6.1 Sliding Distance/Sliding Velocity

Results from Table 23 showed that both Happy THR patients and their LLI counterparts on average had a shorter sliding distance over the course of the gait cycle relative to Normal individuals. This was expected due to the greater range of hip motion seen in the Normal group. The results found for sliding distances in the Happy THR group ($19.8\text{mm} \pm 4.02$) were larger than those found by Bennet et al. [393], which ranged between 10mm-18.1mm and Bennet et al. [459] who determined an average sliding distance of 19.2mm.

Another study by Bennet et al. [405] compared the sliding distances of a group of THR patients against healthy controls. On average, the 19 THR patients demonstrated sliding distances

of 18.1mm, with the healthy control group having a slightly smaller average (22.3mm) compared to the Normal cohort (24.1mm). The relative similarity in results between studies shows that in general THR patients show shorter sliding distances than healthy cohorts during the average gait cycle. The present study also found that when normalised for stride length, the LLI patients had the greatest sliding distance. This is important from a clinical perspective as it establishes that on average, if LLI patients are as active as Normal individuals, they would have increased wear rates and hence be at greater risk of implant failure.

Sliding distance and velocity are effected by the dimensions of the hip implant components. A greater femoral head radius leads to an increase in RoM, sliding distance and sliding velocity. For the present study the exact dimensions for the components were unknown, with a default level of 14mm radius used. This may however have effected the outcome of the estimation of wear, which relies on the sliding distance and velocity. The smaller sliding distances and velocities shown by the LLI and Happy THR group indicated that the hip implants used today wear at a sufficiently slow rate that should outlast the lifetime of an individual. Many of the patients who undergo THR are elderly and thus may walk slower due to weaknesses in muscles caused by advancing age. This may be a confounding factor in determining whether hip implant components are durable enough to last a patient a lifetime, with an increasing number of younger patients undergoing the THR procedure.

11.6.2 Cross Shear/Aspect Ratio

Calculations using the method proposed by Kang found that LLI patients on average showed less cross shear and more unidirectional motion relative to the other groups. This agrees with the study looking at aspect ratios which also came to the same conclusion. Barnett [457] also found that for the small number of LLI patients that were studied, a smaller cross shear ratio was computed relative to healthy controls.

Results indicated that there were no statistically significant differences between the groups with regards to aspect ratios. Budenberg et al. [264] analysed the same patient group with there being no patients removed as in the present study due to data quality or clinical issues. They reported a wide range of results for both LLI (0.16-7.87) and normal patients (0.29-6.75). No statistical testing was however taken comparing the LLI average (1.7) and the normal average (1.8).

Budenberg et al. used the YZX cardan angle sequence. Bennet et al. [460] used the same cardan

angle sequence but produced aspect ratios for both THR (3.97) and controls (3.71) which on average exceeded those seen in this study. The current recommended method by the ISB (International Standards of Biomechanics) is XYZ, with flexion-extension being followed by abduction-adduction and finally internal-external rotation. This sequence is recommended due the notion that the first rotation (flexion-extension) is where the greatest amount of angular displacement occurs [406], whilst it has also been shown to be the most appropriate in activities where large flexion-extension occurs through having the smallest planar cross talk [407]. This makes the present study the most accurate undertaken as of date due to using both the XYZ and YZX sequences, although significant differences were not found between the two. Overall, the results showed that patients in the Symptomatic LLI group were more likely to have hardening of the polyethylene fibres on the implant and thus have a reduced wear rate.

11.6.3 Lubrication

The final area of analysis was entrainment lubrication through the use of the Hamrock & Dowson equation. It was found that when using the peak gait cycle hip JRFs, the LLI patients showed similar fluid film thickness levels to Happy THR patients. The greatest thickness was found in the Normal group; however, in the computation of the results, constants were used such as the Poission's ratio which only apply to THR patients. Hence the results do not depict the results of a Normal healthy individual but of a patient who has undergone THR and is walking in a manner which similar to a healthy individual. From this perspective, the results show that if both LLI and Happy THR patients walked in a manner similar to that of healthy individuals instead of their most comfortable walking speed, fluid entrainment levels would increase and wear would decrease. With a reduced fluid film thickness there would be greater surface interaction and subsequently greater wear [461].

The fluid thickness level between the surfaces due to the mechanism of entraining has been linked to sliding velocity [410]. Those patients with the smaller sliding velocities demonstrated the smallest levels of entrainment. The Hamrock & Dowson equation is however limited in its use due to its time independent nature and is unable to model the changes which occur over time during the gait cycle [410]. To the authors knowledge, this is the first study which has analysed hip bearing lubrication in LLI patients.

11.7 Conclusion

This study has compared the LLI, Happy THR and Normal clinical patient groups in terms of tribology. Significant differences were found with LLI patients having shorter sliding distances, smaller sliding velocities and a reduced lubrication thickness relative to Normal healthy patients. These results, together with the unidirectional motion on the femoral head as computed using the cross shear ratio/aspect ratio for LLI patients, would lead to the reduction in the amount of wear. It was however also found that if LLI patients remain as active post-surgery as their healthy counterparts, an increase in sliding distance per stride would occur and lead to a greater wear rate. The differences between LLI and Happy THR patients in terms of entraining lubrication were minimal. Overall, results demonstrated that the success of the implant may be dependent on the activity levels of THR patients including the distance travelled and gait velocity.

12 Discussion

12.1 Background

The aim of this study was defined as:

To understand why certain patients following a Total Hip Replacement are symptomatic for a Leg Length Inequality whilst others remain asymptomatic

A review of the literature did not find a detailed analysis of the gait of patients who were symptomatic for an LLI post-THR. There also does not exist in the literature a comprehensive critique of PiG, the measurement tool for analysing gait in patients. For there to be a more focussed study, the aim was further split into smaller objectives. The remainder of this chapter will give a summary of the results obtained for each objective, together with the clinical implications of any results produced.

12.2 Objective 1

Understand whether differences exist in both anthropometric measurements and demographics between Symptomatic LLI and asymptomatic Happy THR patients

The first objective of this study was to analyse whether there were non-gait related features which distinguished the LLI patients from their Happy THR counterparts. Normal patients were excluded from this study due to radiographs not being available for the group. The anatomical LLI, which all LLI patients had in our study, was as a direct result of the placement of the artificial hip joint [11].

Height was found to be significantly different between the groups in the present study, with LLI patients being shorter as predicted. This may indicate that from a clinical perspective, taller individuals are more able to offset changes in leg length at their pelvis and minimise any disruption to gait. No statistically significant differences between the LLI and Happy THR patients were found in terms of femoral offset or leg length difference. Symptomatic LLI patients generally had a smaller femoral offset on the operated (41.8mm) and non-operated sides (41.3mm) relative to the Happy THR operated (47.1mm) and non-operated sides (42.3mm). A shorter femoral offset has been linked to increased joint instability, a reduction in abductor strength and a loss in RoM [429].

This loss of normal function may have contributed to the LLI patients being symptomatic, although the differences were not significant. Results may have however been confounded by the fact that a greater proportion of males were in the Happy THR group than the LLI group [462]. Nerve injuries are more common in woman due to the vulnerable sciatic nerve being in greater closer proximity to the surgical site [7, 246]. The present results agree with those of Dougall & White [237] who found that the magnitude of leg length had no impact on whether a patient was symptomatic. Welsh et al. [463] found that demographics were not linked to the magnitude of LLI, although they analysed a general population of LLI patients without having a more specific Symptomatic LLI group as in this study.

Likewise, there were no statistically significant differences detected between the LLI and Happy THR patients in terms of inter-hip distance, cup inclination angle, BMI or age. Inter-hip distances were larger for the Happy THR patients (184mm) than the LLI patients (176mm) and were in the same range as found by Charlton et al. [433]. This may also have been due to gender differences. The use of a trigonometric calculation found that those with smaller inter-hip distances may have been more likely to suffer from clinical symptoms due to a LLI. This may explain why there were more females than males in the LLI group. Unsurprisingly, age was not found to be a significant factor in distinguishing the results of the Symptomatic LLI and Happy THR groups. As THR is more common in older patients, the likelihood of the Symptomatic LLI and Happy THR patients having similar ages was high.

One of the more interesting outcomes of this objective was the finding that all of the Symptomatic LLI patients had a greater operated side leg length post-surgery. The Happy THR group had patients with either a shorter or longer operated side leg relative to the non-operated side. The literature often states that patients are more able to tolerate limb shortening than lengthening, with 10mm of lengthening often specified as the cut-off point when clinical symptoms appear, although this is disputed [464]. When shortening of the operated leg occurs, a LLI is still produced with the non-operated side being longer. As this is better tolerated by THR patients, being symptomatic with a longer operated side must be directly linked to the THR procedure. Increasing the length of the leg stretches the muscle tissue which may lead to pain and discomfort [465].

Study Limitations

Only 13 Symptomatic LLI and 11 Happy THR patients were available to analyse in terms of

radiographs. A greater number would have increased reliability. The small number of patients prevented a thorough analysis of the effects of gender, with the results suggesting that it may have impacted the study outcome. The measurements taken from radiographs are always subject to human error. Preoperative radiographs were unavailable, thus not allowing relative changes in leg length to be measured. This would have been a more reliable method in analysing Symptomatic LLI patients as some of them may have had a naturally occurring leg length difference, present in 70% of the population [223]. Leg lengths were assumed to be equal prior to surgery. Other areas where there was insufficient information was with the specifics of surgery. Beard et al. [232] found that the incidence of a LLI was reduced by using an epidural over other anaesthetic techniques.

Another study limitation was not being able to use a method from the literature in estimating the position of the HJC. This was of particular importance as the HJC was used in the calculation of all the anthropometric variables. Methods which have been proposed in the literature include those of Fessy et al [258], John & fisher [259] and Pierchon et al. [422]. These methods required the use of landmarks which were either not visible in some of the radiographs (e.g. superior pelvic rim) to techniques which were difficult to undertake due to poor quality radiographs (e.g. Koehlers line). The method used was to draw a circle over the femoral head, with the intersection of the lines passing through the most superior-inferior and medial-lateral portions of the circle being the position of the HJC [263, 424–426]. This method however may have been inaccurate due to the difficulty in locating the exact position of the femoral head in some radiographs.

12.3 Objective 2

Examine whether LLI patients show a characteristic gait pattern in their kinematic, kinetic and temporal-spatial results together with comparing them to asymptomatic Happy THR and Normal patients

The patient groups used had previously been analysed by Li et al. [199, 221, 466], Barnett et al. [457] and Budenberg et al. [264]; however this study used a refined dataset by removing patients with additional underlying pathologies such as a functional LLI (not caused by the implant but by muscle shortening) prior to analysis. The gait of patients with an LLI following THR has previously been studied [199, 221, 264, 457, 466], however this was the first such study to analyse the gait patterns of patients specifically symptomatic for a difference in leg length at the hip joint in terms of gait parameters at the pelvis, knee and ankle.

Results Summary

Results indicated that significant differences existed between Symptomatic LLI, Happy THR and Normal patients in terms of kinematics, kinetics and temporal-spatial parameters.

Standing Angles

LLI patients in their comfortable posture on average showed greater hip and knee flexion on the operated side whilst the knee on the non-operated side remained extended. These have previously been recognised as compensatory mechanisms in LLI patients to increase or decrease leg length [222]. Increased knee flexion on the longer side was also found by Walsh et al. [235] when simulating LLI. Happy THR patients showed more symmetry in their standing angles when comparing both legs, comparable to the levels as shown by Normal patients. The standing angle results were similar to the literature, however they were subject to error caused by poor marker placement. The standing angle differences between the groups were most likely due to patients compensating for a leg length difference, although differences in leg length between the two limbs were not found to be statistically significant. The Happy THR patients, on average being taller, were able to accommodate the change in leg length more easily and hence did not show the results as seen in the LLI patients. From a clinical perspective, it may be concluded that shorter patients with large leg length differences are most likely to show compensatory mechanisms in terms of standing angles.

Temporal-Spatial Parameters

LLI patients walked significantly slower (0.94 m/s) than Happy THR patients (1.21 m/s) who themselves walked significantly slower than Normal controls (1.49 m/s). The Happy THR velocity of 1.21 m/s was within the range often reported for healthy individuals [115–117]. Happy THR patients were walking at a speed that they were happy with as it was similar to their healthy peers. The LLI patients were walking at a comfortable speed, which uses the least amount of energy or causes the smallest amount of pain, rather than a happy speed which is similar to the range walked by healthy peers and also meets patient expectations of a return to normality post-THR. A study by Zhang et al. [271] found a longer leg length was linked to a smaller walking velocity. Non-THR LLI subjects have also been studied in the literature, with velocity being unaffected by leg length [272]. From these results it would appear that a combination of muscle weakness, the magnitude of leg length and confidence in walking postoperatively led to the LLI patients walking slower. The reduction in walking speed was an expected result, with patient who are happy naturally expected to walk at a greater speed than those who are symptomatic.

Statistically significant differences were also found between all three groups in terms of stance phase time and stride length on the operated side together with stride length on the non-operated side. Stride length for THR patients has been frequently shown in the literature to be smaller than that of Normal individuals [102, 161, 171, 194, 195, 198, 210, 221]. Further analysis found that LLI patients demonstrated the most asymmetry between the two limbs in terms of stance time, swing time and stride length. This may have been linked to a combination of the leg length discrepancy magnitude and height, with the smaller discrepancies between the limbs in the taller Happy THR group being more difficult to compensate for with a motor response due to them not being detected by the subject. A reduction in walking speed may have also been linked to muscle weakness with the potentially weaker muscles on the operated side hip of the LLI leading to a greater response by the patient in altering many of their walking parameters.

Kinematics

LLI patients demonstrated a loss of hip extension, greater circumduction in the swing phase, reduction in knee flexion during both stance and swing together with the increase in dorsiflexion of the ankle. Loss of hip extension in THR patients has also been found in the literature [171, 173] and has been linked to muscle weakness and a reduction in walking speed. Reduced levels of hip extension have also been observed preoperatively [449]. It was found that in terms of pelvic superior-inferior obliquity, the compensatory mechanisms used by the LLI patients could be split into two main mechanisms. One set of LLI patients were demonstrating Trendelenburg Gait (a pathological gait pattern which occurs when the weakened abductors on the operated side of the pelvis allow the pelvis to exhibit inferior obliquity on the opposing side) during stance and were hip hiking during swing, a method used to decrease the load on the already weakened abductors. The Trendelenburg gait would have been a direct consequence of the weakened abductors following THR, with the knock on effects of back pain and lumbar scoliosis often leading to significant amounts of pain [9]. As this was not seen for the Happy THR patients, it can be concluded that Trendelenburg gait was potentially a reason for some patients being symptomatic for an LLI.

The second type of mechanism was to show inferior obliquity throughout the gait cycle, a method commonly used to lengthen the shorter leg [222]. This was also not seen in the Happy THR group, implying that it may be another compensatory mechanism which may predispose being symptomatic. Most of the significant differences occurred at toe off due to patients exhibiting a

vaulting gait where they pivoted over the longer leg, allowing the shorter leg to swing over. Many of the kinematic changes across the joints can be linked to the reduced walking speed [73, 116, 118], with significant results found for peak knee flexion/extension and hip flexion-extension RoM. No positive correlation was found between the loss of hip extension on the operated side of the LLI patients and gait velocity, indicating that there may be another factor such as muscle weakness leading to the observed results. As this was a characteristic unique to the operated side of the Symptomatic LLI group, it was potentially another underlying cause for the LLI patients being symptomatic. Graf et al. [67] suggested that a loss of hip extension was characteristic of less active individuals, with muscles gradually weakening overtime. Muscle strength was however not a studied parameter, making its effects on kinematics inconclusive.

Kinetics

Kinetic results found that both VGRFs and JRFs were reduced in Happy THR and Symptomatic LLI patients relative to controls, with the latter showing the greatest asymmetry between limbs. Smaller VGRFs for THR patients have been reported in the literature [149]. The LLI patients also demonstrated the most asymmetry between limbs and between patients. Similar trends were found between the groups in terms of joint moments. Positive correlations were observed for peak JRFs and VGRFs against gait velocity, indicating that the reductions in peak forces and moments were influenced by walking slower. Thus an indirect link also existed between peak JRF/VGRF to the factor which was causing the Symptomatic LLI group patients to walk slower. As stated previously, potential reasons included the magnitude of leg length, weaker abductor muscles and confidence in their gait postoperatively. Clinically it would appear that the changes in kinetics, as with kinematics, in themselves did not determine whether a patient was symptomatic but were rather the effects of any anthropometric, physiological or psychological issues post-THR.

Study Limitations

Initially 26 Symptomatic LLI, 14 Happy THR and 38 Normal patients were analysed in terms of gait; however in all the groups patients were removed from the study due to reasons such as secondary pathological conditions and errors during gait measurement. This led to there only being 13 LLI, 11 Happy THR and 35 Normal patients. The literature varies with the number of operated patients in a random sample of publications ranging between 4-134 and controls between 4-25 [161, 166, 179, 194, 195, 198, 210].

Errors could have been present in the present results due to the small numbers of trials used to generate the average result for each patient. Each patient had as a minimum two motion trials in addition to the single standing trial. For this reason, two trials were used for every patient. However gait data is subject to both intrinsic (variability between trials e.g. different gait speeds) and extrinsic errors (measurement errors e.g. marker artefact) [467]. Maynard et al. [468] found that healthy individuals required on average 5 trials to reduce both errors types to an acceptable amount. Due to the greater variabilities shown in THR patient gait, the recommended number of trials ranges between 5-10 [467].

Qualitative studies were undertaken on all patients using the Oxford Hip Score⁵⁰ prior to the current study. Patients could not be contacted for further qualitative analysis due to their names having been anonymised. This was a disadvantage of the study as further questions could have been asked and more detailed responses obtained. The qualitative records also lacked information on variables which have been associated with postoperative LLI including the type of implant used [227], surgical technique [236, 241, 242] and patient activity levels [244].

The modelling of gait kinematics and joint moments in Visual3D may have also introduced errors into the results. The position and orientation of a segment can be determined using a variety of methods such as forward kinematics, inverse kinematics and segment optimisation (also known as 6DoF)⁵¹. One of the sources of error in our simulations would be due to the use of the segment optimisation model in Visual3D to compute joint angles and moments. This model incorrectly assumes that each segment has 6 variables which describe its position and orientation (3 translations and 3 rotations). For instance, the knee can be modelled as a hinge joint with a single DoF due to there being very little motion in the frontal and transverse planes.

Another potential source of error was the choice of the PiG model as the measurement system to determine joint angles, moments and forces. Results suggested that generally both kinematics and kinetics in PiG are highly dependent on marker position, the choice of HJC regression equation and clinical measurements. These may have introduced much of the variability seen in the results, although the greatest variability was found in the more extreme placements of the markers which was not undertaken in the clinical groups. Marker positioning in the clinical groups was however

⁵⁰The Oxford Hip Score is a qualitative assessment of daily function in THR patients consisting of 12 questions. Each question has a score from 0-4, with 4=no pain and 0=severe pain [421]

⁵¹For a detailed explanation of segment optimisation, please see pages 77 - 78 in the *Generic Methods*

not optimised, with markers placed more superior on the thigh or shank on the right leg and more inferior on the left in order to allow the clinician to be able to distinguish both legs from each other during data processing. This is illustrated in Figure 171.

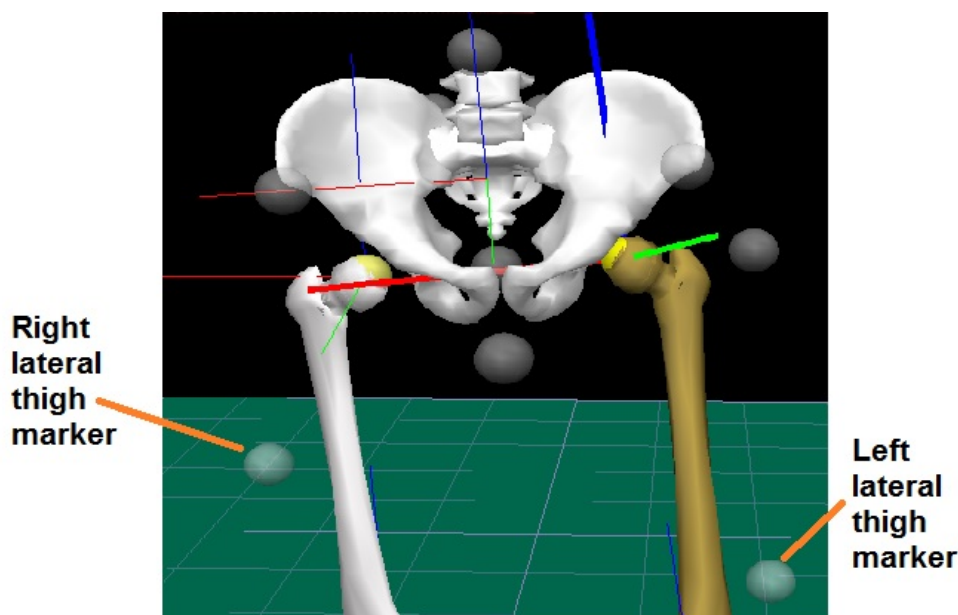


Figure 171: An image from Visual3D of an LLI patient with the lateral thigh markers on the left and right sides placed at different superior-inferior positions

Hip JRFs were computed in AnyBody (AnyBody Technology, Aalborg, Denmark)⁵². The calculation of JRFs in AnyBody at first required the recalculation of joint kinematics through the process of inverse kinematics, which differed to the 6DoF model used to calculate kinematics in Visual3D. The inverse dynamics method used to compute the JRFs was based upon the minimisation of a cost function in the rigid body model. This cost function is introduced due to the number of muscles crossing the joints being greater than the degrees of freedom, leading to a muscle redundancy problem. For this particular study, this cost function was specified as the minimisation of the maximum muscle force. This was based upon on assumptions of how the CNS works and is thus subject to error [325].

There are a number of assumptions that inverse dynamics makes including that the joints are frictionless, that segment masses are concentrated at the centre of mass and there are no co-contractions of agonist and antagonist muscles [326]. A preoperative THR patient may have arthritis at the joint which could invalidate the assumption of a frictionless joint. The mass also may not be concentrated at the centre of mass and may be distributed. Due to the complexity and time constraints

⁵²Details on how AnyBody works can be found on pages 85 - 89 in the *Generic Methods*

in building a subject specific patient muscle morphology, the average healthy persons default model in AnyBody was used. This model did not take into account the change in strength and location of muscles following THR or the general weakness in muscles due to atrophy which occurs with age, with most THR patients being over 60. No account was taken for differences in muscle morphology between genders.

Radiographs cannot indicate an accurate location of the HJC due to being only 2D. The method used in all of the studies in Visual3D was the Predictive Method, which utilises the positions of anatomical landmarks and equations which have been defined using cadaver studies. The measurements made on cadaveric specimens are often of healthy individuals and thus are not suitable for estimating the HJC position of THR patients. These methods also rely on the accuracy of the laboratory technician in correctly placing markers on bony landmarks which may have proven difficult in clinically obese THR patients. The Davis HJC [273] was selected and used due to it being the default technique used by Visual3D for PiG. The method as used by Harrington has been found to be superior to that of Davis [301, 302, 306]. Differences between HJC positions are however often small and unlikely to effect the conclusions draw from the present study.

12.4 Objective 3

Compute how error using the PiG model may have effected the variability seen in the clinical gait analysis results

The third objective of this study was to critique the Vicon PiG marker model used for motion capture during clinical analysis. The literature shows that the CGM, of which PiG is a derivative of, is very sensitive to the positioning of the lateral thigh and shank markers [315, 316] together with having a variable kinematic and kinetic output [317]. These studies were of particular importance as an often highlighted weakness of PiG is the hierarchical nature of the model where proximal changes can impact distal kinematics and kinetics, which has led to authors attempting to find alternative solutions [415].

Alternative marker systems such as CAST are commonly used today over PiG with literature showing that the results are not significantly different [276, 314] or that CAST is superior to PiG [310, 315–318]. Comparisons were made between PiG and CAST in terms accuracy and reliability using a novel method. The conclusions drawn would aid in assessing the reliability of the kinematic

and kinetic results obtained in the investigation. It was predicted that PiG would be very sensitive to marker placement, joint width measurement and the choice of HJC regression equation together with showing greater variability than CAST.

As expected, the positioning of the lateral segment markers effected both that particular segments rotation together with all distal segments in standing trials. Moving the lateral segment markers in the proximal-distal direction along the long axes of the thigh or shank had a greater impact on rotation, especially at the more distal segment regions. Errors in the proximal-distal positioning of the lateral thigh/shank markers had a large impact on both joint angles and moments. A marker misplaced by one marker distance (45mm) in the anterior-posterior direction was found to cause a 4.4° error in peak hip flexion, a 0.73° error in peak hip abduction and a 31.3° error in peak hip internal rotation. From a clinical perspective, these results indicated that PiG was prone to high levels of error if care was not taken during marker placement.

The choice of HJC regression equation (Bell, Davis or Harrington) was found to effect both joint angles and moments at all segments across all joints, with differences of $<5\%$ found for sagittal plane joint angles, up to 46% in frontal plane angles and $>200\%$ in the transverse plane. Differences in joint moments were generally a lot smaller, with the maximum difference between regression equations for any plane being $\approx 40\%$. Due to the hierarchical nature of PiG, the choice of the Davis HJC equation over those of Bell and Harrington would have impacted the results, with errors in the sagittal plane however only being less than 5% .

Errors of 10mm in joint width measurement in PiG were found to effect the hip the least and the ankle the most. Joint angles were more greatly effected than joint moments with moments only effected at the knee and ankle. The ankle was the most effected by clinical width measurements due to the impact of both the knee width and ankle width in determining the AJC position. Errors in knee width effected joint angles the most in the frontal plane of the knee ($\approx 41\%$) together with the frontal ($\approx 57\%$) and transverse (32%) planes of the ankle. Ankle width errors led to errors of $<6\%$ at the hip and knee in terms of moments, with larger errors of up to 110% being present at the ankle. These effects would have been amplified though many THR patients being clinically obese, making identification of landmarks and clinical width measurements difficult.

In the clinical patient study, the only frontal plane motion studied was that of hip abduction-

adduction whilst the only transverse plane motion was pelvic rotation. Pelvic kinematics are unaffected by joint width measures, whilst joint angles were effected by a clinically non-significant amount in terms of hip abduction-adduction. It can be concluded that errors from joint width measures were minimal in the patient gait analysis. Suggested improvements in the PiG model include the use of medial markers at the knee and ankle joints, which would then not require the need for clinical knee/ankle width measurements or multiple knee/ankle width measurements made and averages produced to increase reliability.

Substantial differences between the PiG and CAST marker sets were found in terms of joint angles, joint moments and JRFs. The greatest differences in results were found in the frontal and transverse planes, with there being a $> 20^\circ$ difference in terms of hip rotation. This agrees with the literature [309, 310, 315–318]. Greater similarity was found in the sagittal plane. PiG was found to show greater variability in results and larger standard deviations. Moments at the hip were largely unaffected by the choice of marker model due to the position of the HJC having been pre-defined using the Davis regression equation. Moments at the knee and ankle however were significantly effected with a PiG having a 55% greater peak knee extension moment and 140% smaller peak knee abduction moment than CAST. Hip JRFs were found to be greater using PiG together with showing wider 95% confidence intervals.

The selection of PiG over CAST would have effected the present results and potentially the conclusions drawn. The differences in peak hip flexion angle between PiG and CAST (3.4°) for a single patient exceeded the average difference between the LLI and Normal patients (0.7°), but were smaller in relation to the differences in minimum angle (14°). Comparing the two patient groups in terms of joint forces, at the 1st JRF peak there was a difference of 0.65N/kg whilst at the 2nd peak there was a difference of 1.34N/kg. For the comparison between PiG and CAST, a difference of 0.71N/kg was found at the 1st JRF peak with there being a 0.72N/kg difference at the 2nd. As the differences in kinematics/kinetics produced by simply changing marker system were so large relative to the differences between patient groups, it makes the selection of marker protocol used for gait analysis very important

Study Limitations

The same LLI patient was used for most of the sensitivity analyses with the use of only 5 trials, whereas for pathological gait between 5-10 trials have been recommended due to the potentially

large variability [467]. The accuracy of gait kinematics and kinetics was limited to the precision of the placement of markers on the pelvis, thigh, shank and foot. The comparison of PiG against CAST was also subject to errors. The first of these was that the lateral thigh/shank marker was not attached directly to the skin of the subject but only to the strapping of the cluster marker. Thus movement of the marker with respect to the strapping may have differed to what would have occurred had the marker been placed onto the skin. An additional error would have been introduced in the selection of marker cluster location. This would not have greatly effected the CAST results but as discussed previously, PiG is highly sensitive to the superior-inferior positioning of the lateral thigh/shank markers.

The inverse kinematics process in AnyBody attempts to provide the position and orientation of all segments at each time interval. This is undertaken through a process of least squares where the residuals between the model marker positions and the experimental marker positions are minimised. Each marker adds constraints to the segment, with a total of three per marker. On the other hand, the results of CAST used an application in AnyBody called AnyGait, which uses the segment optimisation method, also referred to as the 6DoF method. This model requires that all rigid bodies to be defined as independent, whilst the inverse kinematics approach requires explicit joint definitions. Due to the differences in the methods used to compute the JRF for both PiG and CAST, it remains unknown how much of the variability seen was due to the different marker systems and how much was due to the different techniques used to compute kinematics.

12.5 Objective 4

Analyse how differences in kinematics, kinetics and temporal-spatial parameters effect the Symptomatic LLI, Happy THR and Normal groups in terms of predicted wear rates and lubrication thickness

With there being no consensus in the literature with regards to how many patients following THR end up with an LLI, there is large scope for patients to develop clinical symptoms directly linked to leg length. The relatively large number of patients who are symptomatic has led LLI to become of one the most common causes of orthopaedic malpractice claims [17, 18] with it contributing to almost 5% of all medical errors [233]. For this reason, the impact of kinematics and kinematics on wear rates and lubrication regimes at the hip joint was studied. This included analysis through the use of the cross shear equation proposed by Kang et al. [391] and the fluid entrainment lubrication

equation developed by Hamrock and Dowson [23]. It was predicted that Symptomatic LLI patients would show the greatest predicted wear rates as a consequence of the greater variability in their motion (multidirectional motion).

Motion paths, describing the paths 20 selected points on the femoral head moved during an average gait cycle (Ramamurti et al. [403]), found that LLI patients had the most linear motion paths with there being very few quasielliptical motion paths. This led to a greater aspect ratio being found for the LLI patients. From a clinical perspective, this meant that more unidirectional motion was occurring between the UHMWPE acetabular cup and femoral head, leading to strain hardening [396]. This has been found to decrease the amount of wear [459]. Results from Kang's cross shear equation indicated that the smallest cross shear ratio was found on the operated side of the LLI patients, whilst larger ratios were found on the operated side of Happy THR patients and Normal patients. A smaller cross shear ratio also showed that LLI patients would experience less wear. Taking this perspective alone, it would indicate that LLI patients were less likely to have a hip failure and require revision surgery. However, analysis used gait data whilst other activities such as walking on stairs or running may lead to different amount of wear.

Other calculations found that the operated side of the LLI group had the smallest sliding distance and sliding velocity, whilst Normal patients had the greatest. This was however computed during a single stride. If the results were normalised for stride length, LLI patients had the greatest sliding distance. This would indicate greater wear according to both the Archard equation and Kang's cross shear equation and go against the conclusions of a reduced wear rate due to strain hardening of the UHMWPE cup. Lubricant levels in terms of entraining lubrication were found to be smaller in both the LLI and Happy THR patients relative to Normal patients, most likely due to a smaller walking velocity. Reduced fluid entrainment would additionally lead to greater surface interaction and greater wear. This indicated that if patients walk using similar gait characteristics to a Normal healthy individual, they could increase the level of fluid entrainment in the joint and potentially reduce the amount of wear that occurs; this may be an important clinical finding. The results from this section were unexpected as it was thought that LLI patients would show more multidirectional motion due to having to compensate for a leg length difference. However, this may have been counteracted by the reduction in the hip range of motion that these patients were walking with.

Study Limitations

Kang's cross shear ratio together with the aspect ratio also only give approximations for wear rates based on gait. It is possible that many of the THR patients undertake other activities such as walking up and down stairs or playing sports, which may increase the rate of wear of the hip implant. Bergmann et al. [148] reported a 23% increase in JRFs when walking upstairs relative to normal gait, which if incorporated into Kang equation would have impacted the results. The computation of many of the results was dependent on the input constants. These included material properties such as the Young's Modulus (β) and Poisson's Ratio (γ) together with the cup and femoral head radius. Joint angle and force data were also used as an input and hence the results were also dependent on their accuracy. Results were also dependent on the cardan angle sequence selected.

12.6 Concluding Remarks

To answer the initial project objective, we have evaluated different areas including anthropometrics, demographics, gait, marker systems and implant durability. Using all of these results, it is possible to give arguments in favour of why the patients in the LLI group were symptomatic. Listed below are four propositions together with the evidences for and against them being true.

12.6.1 Proposition 1

LLI patients were symptomatic directly due to having smaller body proportions

The evidence for this proposition includes that LLI patients were significantly shorter than Happy THR patients. This may however have been due to the greater proportion of females in the Symptomatic LLI patient group. If comparisons are made between two patients with an equal amount of leg length difference but with different heights, the leg length difference would make up a greater proportion of the overall height of the shorter individual. Hence this patient would be more likely to suffer from symptoms such as lumbar scoliosis. Patients with larger BMI's would be more likely to suffer from a difference in leg length due to being more difficult to operate on [7].

General trends were also found with LLI patients demonstrating larger leg length differences and shorter pelves, although differences were not statistically significant. Basic trigonometry showed that patients with these characteristics would have greater pelvic obliquity when standing and hence compensate more at the pelvis when walking. This can lead to pain and osteoarthritis in the hip and the knee on both the operated and non-operated sides, together with an increase in wear through edge loading [13, 244, 253, 469]. Females are often smaller in body proportions than males and are

more likely to suffer from sciatic nerve pain due to leg lengthening as the nerve is in closer proximity to the surgical site [470].

There are however counterarguments to body proportions being a factor linked to being symptomatic for an LLI. Variables such as femoral offset, BMI and inter-hip distance were not found to statistically differ between the LLI and Happy THR groups. In addition, studies have found that women are more likely to undergo THR, with the National Joint Registry (NJR) in 2012 finding that 60% of procedures were undertaken on women [1]. Thus it may not be surprising that one of the two clinical groups analysed had a greater proportion of females than males and hence smaller body proportions.

Overall, it can be seen that body proportions have an impact to a certain extent on determining whether patients are symptomatic for an LLI, with statistical significance found for height. General trends were also found for femoral offset and inter-hip distance, with LLI patients having smaller measured values than Happy THR. However, this implies that females are more likely to be symptomatic due to them more often being smaller than males. This, combined with the fact that females are more likely to suffer from surgical complications due to nerve pain, indicate that being female may share a stronger link to the Symptomatic LLI group than body proportion although all patients with smaller body proportions should be classified prior to surgery as being at a higher risk.

12.6.2 Proposition 2

LLI patients were symptomatic due to weakened abductor muscles and/or soft tissues

There are evidences linking being symptomatic for a LLI to abductor muscle weakness. Many of the LLI patients exhibited the Trendelenburg Gait pattern during walking which is a common symptom of weakened abductor muscles where the pelvis tilts downwards on the weakened side [471]. A loss of hip extension, as seen on the operated side of the LLI patients, has been linked to weaknesses in hip extensor muscles (Gluteus Maximus) [472], which are damaged during surgery. Extension levels remained closer to normal on the non-operated side. It thus is clear that the loss of extension on the operated side was linked to the operative procedure in terms of either being a consequence of muscle weakness or leg length. The latter cannot be true as the magnitudes of leg length differences between the two groups was found to not be significantly different.

All of the patients in the Symptomatic LLI group had an increase in leg length postoperatively via the use of a larger femoral offset, which requires increased soft tissue tension. Femoral offset results were not significantly different between the Symptomatic LLI and Happy THR patients. This was surprising as height was significantly greater for the Happy THR group, and has been found to strongly correlate to femur size [436]. It appears that the LLI patients on average had larger femoral offsets used than would be expected for their body size which potentially led to there not being statistical significance detected.

The present results do not indicate that any evidence existed against weakened muscle leading to a symptomatic LLI. Evidence however would be difficult to obtain as no direct testing on muscles was taken post-analysis in order to determine parameters such as muscle strength. In addition, there was no qualitative evidence indicating that the patients were complaining of muscle weakness or that they were troubled by changes in gait such as the Trendelenburg gait. A future study should attempt testing on muscle activity and strength levels via the use of an EMG/Biodex or an alternative measurement technique in order to see if there are significant differences between groups. A more thorough qualitative analysis should also be undertaken, with patients asked questions specifically related to their opinions on the effect of the operative procedure on the muscles around the hip.

Due to the lack of quantitative evidence analysing the functioning of the abductor muscles and the absence of qualitative information with regards to patient perspectives, it is difficult to conclusively say that the weakness of muscles around the hip joint was directly linked to patients being symptomatic for an LLI. However, results such as the majority of LLI patients showing a loss of hip extension on the operated side, a Trendelenburg gait and the impact of the selection of femoral offset on soft tissue laxity do indicate that the postoperative changes in muscles did share a relationship with whether a patient was symptomatic for an LLI.

12.6.3 Proposition 3

LLI patients were symptomatic due to abnormal gait characteristics

LLI patients walked significantly slower than Happy THR patients at potentially a "comfortable" speed, perhaps which causes less pain or uses less energy, rather than a natural or "happy" speed, defined as a speed which meets patients expectations post-THR and is within the range walked

by healthy peers. This may have led to the differences between the patient groups in terms of kinematics and kinetics. Patients in the LLI group also demonstrated greater hip flexion on the operated side and greater knee extension on the non-operated side when standing relative to Happy THR patients. They also showed knee extension on the non-operated side, which was not seen for the other groups. These are methods used to increase and decrease leg length respectively and may have made patients symptomatic due to there being an asymmetric stance.

During dynamic motion a vaulting gait was seen, with greater knee flexion at toe off for LLI patients relative to Normal patients on the operated side. On the non-operated side, a reduction in knee flexion was seen. LLI patients showed the greatest amount of asymmetry between limbs leading to an inefficient gait, which could have led to them being symptomatic [244]. Pospischill et al. [449] found that preoperatively patients showed a loss of hip extension on the operated side, as in the LLI group, which recovered overtime. It may be that the Symptomatic LLI group patients were symptomatic as they did not show an improvement in gait post-THR through maintaining the loss in hip extension.

Although there are certain evidences linking the LLI patients being symptomatic post-THR to an abnormal gait, changes in gait were most likely not the cause of patients being symptomatic but the effect. For instance, a reduced walking speed could be linked to other factors such as an asymmetric gait caused by one leg being longer than the other, muscle weakness or even a lack of confidence in walking ability. Differences in the standing angles were likely to share a relationship with the LLI/height ratio whilst the loss in hip extension during gait was potentially linked to the stretching of soft tissue around the hip during surgery or contractures/weaknesses in muscle developed preoperatively.

The only motion analysed in the present study was gait. It may be that patients found gait a more difficult activity but found other activities such as walking down the stairs easier. No detailed qualitative evidence was taken from the patients with regards to why they were symptomatic, including whether the asymmetry between the limbs or walking slower than they would prefer was problematic. Conclusions are therefore difficult to make. A future study should comprise of detailed qualitative results where patients are able to comment on how they are coping with daily activities following THR.

12.6.4 Proposition 4

LLI patients were symptomatic due to the increased rate of wear

The underlying reason for a patient being symptomatic may have been linked to the rate of wear. LLI patients had larger sliding distances per metre than Happy THR patients. These larger sliding distances per metre were found due to the LLI patients taking shorter strides. According to both the Archard wear equation and Kang's cross shear ratio, this would lead to greater wear over time. The resulting pain and stiffness at the joint may have led to patients becoming symptomatic.

There are however strong arguments against this proposition. Firstly, the impact of wear usually occurs in the longer term and is less likely to have short term effects, with some LLI patients being 1 year post-surgery. LLI patients had smaller resultant loads on average than Happy THR patients, which in theory would mean less wear. LLI patients also showed more unidirectional motion paths which leads to strain hardening on a polyethylene on metal cup and to a reduction in wear. This was demonstrated in the calculation of the aspect ratio and the motion paths of each loci on the femoral head. There was no qualitative evidence suggesting that patients complained about joint instability. There was also no information on patient activity levels following THR which would have influenced the amount of wear.

Overall it is difficult to make conclusions with regards to wear and being symptomatic for an LLI due to conflicting information together with the absence of certain information. Despite LLI patients showing greater sliding distances per metre, as these patients are symptomatic they are likely to walk shorter distances and hence according to both the Archard equation and Kang's Cross Shear equation there would be a reduction in the amount of wear. In addition, the present results show that the LLI patients had more unidirectional motion which supports the idea that they would have less wear than their Happy THR patients. The most conclusive amount of evidence for wear being a potential reason for being symptomatic would be if in-vitro wear testing comparing the relative motion between the head and the cup of both the Happy THR and LLI groups was undertaken. This could use specific input data such as the average motion paths produced by each patient group, gait cycle loads and the sliding velocity. A future study should address this.

12.7 Summary

The results of this investigation indicate that there is not a single factor which determines whether a patient is symptomatic for a LLI, with there being interactions between gait, wear and anthropometric measures. Our study has been limited in that additional factors which may have effected the results such as preoperative gait, preoperative anthropometrics, activity levels and additional qualitative information from a questionnaire are missing. In addition, due to the large number of statistical results in this study, the multiple hazard comparison applies making it increasingly likely that false positive results were obtained.

The most that we can conclude is that highly active females or males with small body proportions are most likely to be symptomatic for an LLI and should be identified prior to operative procedure as being high risk. A large majority of these patients also showed gait characteristics of muscle weakening, with the risk factor of being symptomatic increasing with more muscle invasive techniques or over-stretching of soft tissue through selecting a large femoral offset [465]. Gait characteristics are likely an effect of all the previously mentioned risk, rather than a cause in themselves.

12.8 Future Work

A future investigation which attempts to build upon this study should undertake the following:

1. Measure gait results both preoperatively and postoperatively using a larger data set. A larger dataset would give greater reliability in the results. Variables such as surgical technique, implant type and clinical experience should be compared as they have previously found to have an effect on determining whether a patient is symptomatic for an LLI [227, 236, 241, 242]. Variables such as height and BMI could be further analysed whilst it would also allow a thorough analysis on the effects of gender.
2. A more detailed form of qualitative assessment with questions probing the exact reasons for being symptomatic e.g. the time of symptom onset postoperatively.
3. Subject specific investigations on a greater range of activities e.g. stair climbing, to understand better the risks of LLI on the wear of the hip implant. Models could be built which closely match those of the desired patient by for example having the correct muscle attachment points. Carbone et al [367] showed that small errors in the insertion or via points of the muscle can have a significant impact on muscle force predictions. This can be of particular importance in

modelling pathological conditions or surgery such as THR where the insertion and via points could have been either changed or had their corresponding muscle fibre removed.

4. Investigate compensatory mechanisms of LLI patients using a less variable method such as CAST. The use of CAST was found to show less variability than PiG for angles, moments and forces.
5. Investigate the impact of a LLI on forces at the knee joint on both the operated and non-operated sides. As there are muscles which span both the hip and knee, JRFs at the knees could be effected and lead to osteoarthritis. For instance, the bicep femoris muscle at the hamstrings contributes to hip flexion and external rotation and likewise with the knee [28]. On the operated side, the distribution of load at the knee would change through the recruitment of different muscles.

13 Conclusion

This is the first study to undertake an analysis of gait, anthropometrics and wear rates for patients with a LLI following THR. The aim at the beginning of the study was:

To understand why certain patient following a Total Hip Replacement were symptomatic for a Leg Length Inequality whilst others remained asymptomatic

To answer this question, various studies were undertaken including comparing the gait of Symptomatic LLI patients to other patient groups, comparing anthropometric measures and demographics such as femoral offset and age, analysing the effect of gait kinematics and kinetics on wear together with a critique of the PiG marker system used to measure gait. Some of the more interesting results were that LLI patients showed a characteristic loss of hip extension on the operated side, variations in pelvic compensatory mechanisms although Trendelenburg gait was commonly seen, a reduction in walking speed, increased gait asymmetry, smaller body proportions and greater sliding distances per metre. From these results, four propositions were given stating that LLI patients were symptomatic potentially due to:

1. Having smaller body proportions
2. Weakened abductor muscles and/or soft tissues
3. Abnormal gait characteristics
4. Increased rate of wear

Overall, it was concluded that there was no definitive reason which could be pinpointed as being the reason why LLI patients were symptomatic. Evidence however did lean towards patients with smaller body proportions, weakened abductor muscles and an asymmetric gait being more likely to be symptomatic. There was however scope for error due to factors which were not controlled in this study such as not having preoperative data and the use of the PiG marker system, which was found to be very sensitive to marker positioning and the choice of regression equation in determining the position of the HJC. Nevertheless, this thesis has made some significant advances in the understanding of PiG and its important parameters for clinical application. The study provides a platform in attempting to identify those patients most at risk to developing a LLI, in determining errors in clinical measurement techniques and in specifying areas of future research which could be taken to build upon the current project.

14 References

- [1] “<http://www.njrcentre.org.uk/njrcentre/healthcareproviders/accessingthedata/statsonline/>,” Accessed June 2016.
- [2] H. Behrend, K. Giesinger, J. M. Giesinger, and M. S. Kuster, “The forgotten joint as the ultimate goal in joint arthroplasty: validation of a new patient-reported outcome measure,” *The Journal of arthroplasty*, vol. 27, no. 3, pp. 430–436, 2012.
- [3] R. E. Anakwe, P. J. Jenkins, and M. Moran, “Predicting dissatisfaction after total hip arthroplasty: a study of 850 patients,” *The Journal of arthroplasty*, vol. 26, no. 2, pp. 209–213, 2011.
- [4] A. Matsushita, Y. Nakashima, S. Jingushi, T. Yamamoto, A. Kuraoka, and Y. Iwamoto, “Effects of the femoral offset and the head size on the safe range of motion in total hip arthroplasty,” *The Journal of arthroplasty*, vol. 24, no. 4, pp. 646–651, 2009.
- [5] R. Blake and H. Ferguson, “Limb length discrepancies.,” *Journal of the American Podiatric Medical Association*, vol. 82, no. 1, pp. 33–38, 1992.
- [6] V. Wylde, S. Whitehouse, A. Taylor, G. Pattison, G. Bannister, and A. Blom, “Prevalence and functional impact of patient-perceived leg length discrepancy after hip replacement,” *International orthopaedics*, vol. 33, no. 4, pp. 905–909, 2009.
- [7] A. B. McWilliams, A. J. Grainger, P. J. O’Connor, A. C. Redmond, T. D. Stewart, and M. H. Stone, “A review of symptomatic leg length inequality following total hip arthroplasty.,” *Hip international: the journal of clinical and experimental research on hip pathology and therapy*, vol. 23, no. 1, pp. 6–14, 2012.
- [8] C. Clark, H. Huddleston, E. Schoch III, and B. Thomas, “Leg-length discrepancy after total hip arthroplasty,” *Journal of the American Academy of Orthopaedic Surgeons*, vol. 14, no. 1, pp. 38–45, 2006.
- [9] M. S. Austin, W. J. Hozack, P. F. Sharkey, and R. H. Rothman, “Stability and leg length equality in total hip arthroplasty,” *The Journal of arthroplasty*, vol. 18, no. 3, pp. 88–90, 2003.
- [10] Y. Golightly, K. Allen, C. Helmick, T. Schwartz, J. Renner, and J. Jordan, “Hazard of incident and progressive knee and hip radiographic osteoarthritis and chronic joint symptoms in individuals with and without limb length inequality,” *The Journal of Rheumatology*, vol. 37, no. 10, pp. 2133–2140, 2010.

-
- [11] A. McWilliams, T. D. Stewart, A. J. Grainger, P. J. OConnor, D. White, A. Redmond, and M. H. Stone, "Leg length inequality following total hip replacement," *Orthopaedics and Trauma*, vol. 25, no. 1, pp. 37–42, 2011.
- [12] A. White, "Study probes closed claim causes," *AAOS Bull*, pp. 26–27, 1994.
- [13] O. Friberg, "Clinical symptoms and biomechanics of lumbar spine and hip joint in leg length inequality," *Spine*, vol. 8, no. 6, pp. 643–651, 1983.
- [14] P. Gibson, T. Papaioannou, and J. Kenwright, "The influence on the spine of leg-length discrepancy after femoral fracture," *Journal of Bone and Joint Surgery-British Volume*, vol. 65, no. 5, p. 584, 1983.
- [15] K. Klein, I. Redler, and C. Lowman, "Asymmetries of growth in the pelvis and legs of children: a clinical and statistical study 1964-1967.," *The Journal of the American Osteopathic Association*, vol. 68, no. 2, p. 153, 1968.
- [16] W. Goldstein, A. Gordon, and J. Branson, "Leg length inequality in total hip arthroplasty," *Orthopedics*, vol. 28, no. 9, pp. S1037–S1040, 2005.
- [17] D. E. Attarian and T. P. Vail, "Medicolegal aspects of hip and knee arthroplasty," *Clinical orthopaedics and related research*, vol. 433, pp. 72–76, 2005.
- [18] A. Upadhyay, S. York, W. Macaulay, B. McGrory, J. Robbennolt, and B. S. Bal, "Medical malpractice in hip and knee arthroplasty," *The Journal of arthroplasty*, vol. 22, no. 6, pp. 2–7, 2007.
- [19] A. McWilliams, S. Douglas, A. Redmond, A. Grainger, P. OConnor, T. Stewart, and M. Stone, "Litigation after hip and knee replacement in the national health service," *Bone & Joint Journal*, vol. 95, no. 1, pp. 122–126, 2013.
- [20] D. W. Stoller, *Magnetic resonance imaging in orthopaedics and sports medicine*, vol. 1. Lippincott Williams & Wilkins, 2007.
- [21] W. R. Smith, B. H. Ziran, and S. J. Morgan, *Fractures of the pelvis and acetabulum*. CRC Press, 2013.
- [22] L. Mattei, F. Di Puccio, B. Piccigallo, and E. Ciulli, "Lubrication and wear modelling of artificial hip joints: A review," *Tribology International*, vol. 44, no. 5, pp. 532–549, 2011.

-
- [23] D. Dowson and V. Wright, *An introduction to the bio-mechanics of joints and joint replacement*. Wiley-Blackwell, 1981.
- [24] G. Baura, *Medical Device Technologies: A Systems Based Overview Using Engineering Standards*. Academic Press, 2011.
- [25] D. P. Byrne, K. J. Mulhall, and J. F. Baker, “Anatomy & biomechanics of the hip,” *Open Sports Medicine Journal*, vol. 4, no. 1, pp. 51–57, 2010.
- [26] P. K. Levangie and C. C. Norkin, *Joint structure and function: a comprehensive analysis*. FA Davis, 2011.
- [27] C. A. Myers, B. C. Register, P. Lertwanich, L. Ejnisman, W. W. Pennington, J. E. Giphart, R. F. LaPrade, and M. J. Philippon, “Role of the acetabular labrum and the iliofemoral ligament in hip stability an in vitro biplane fluoroscopy study,” *The American journal of sports medicine*, vol. 39, no. 1 suppl, pp. 85S–91S, 2011.
- [28] C. Milner, *Functional anatomy for sport and exercise: quick reference*. Routledge, 2008.
- [29] “<http://static1.squarespace.com/>,” December 2013.
- [30] <http://www.eng.mu.edu/wintersj/muscmod/nms-func-physiology/musc-lines-action.htm>.
- [31] J. P. Paul, *Forces at the human hip joint*. PhD thesis, University of Glasgow, 1967.
- [32] R. B. Martin, D. B. Burr, and N. A. Sharkey, *Skeletal tissue mechanics*. Springer, 1998.
- [33] C. Kirtley, *Clinical gait analysis: theory and practice*. Elsevier Health Sciences, 2006.
- [34] N. Shetty and S. Bendall, “(i) understanding the gait cycle, as it relates to the foot,” *Orthopaedics and Trauma*, vol. 25, no. 4, pp. 236–240, 2011.
- [35] D. J. Magee, *Orthopedic physical assessment*. Elsevier Health Sciences, 2013.
- [36] R. D. Tugui and D. Antonescu, “Cerebral palsy gait, clinical importance,” *Maedica*, vol. 8, no. 4, p. 388, 2013.
- [37] C. Kranz, “<http://www2.warwick.ac.uk/fac/sci/eng/meng/nongps/rnd/gait/>,” 2014.
- [38] D. H. Sutherland, “The evolution of clinical gait analysis part I: kinesiological emg,” *Gait & posture*, vol. 14, no. 1, pp. 61–70, 2001.

-
- [39] E. Ceseracciu, Z. Sawacha, S. Del Din, S. Ceccon, S. Corazza, and C. Cobelli, “Comparison of markerless and marker-based motion capture technologies through simultaneous data collection during gait,” *Gait & Posture*, vol. 30, pp. S14–S15, 2009.
- [40] L. Chiari, U. D. Croce, A. Leardini, and A. Cappozzo, “Human movement analysis using stereophotogrammetry: Part 2: Instrumental errors,” *Gait & posture*, vol. 21, no. 2, pp. 197–211, 2005.
- [41] J. Saboune and F. Charpillet, “Markerless human motion capture for gait analysis,” *arXiv preprint cs/0510063*, 2005.
- [42] “<http://www.idmil.org/mocap/plugin-gait+marker+placement.pdf>,” Accessed November 2015.
- [43] “<http://www.analisedemarcha.com/papers/manutencao/manuais/viconplug>,” Accessed January 2015.
- [44] “<http://web.archive.org/web/20080207010024/>,” Accessed September 2015 2015.
- [45] R. Morris and S. Lawson, “A review and evaluation of available gait analysis technologies, and their potential for the measurement of impact transmission,” *Newcastle University*, 2010.
- [46] “<http://umanitoba.ca/faculties/medicine/units/medrehab/images/ptforceplate>,” Accessed July 2012.
- [47] M. W. Whittle, *Gait analysis: an introduction*. 2003.
- [48] W. R. Taylor, R. M. Ehrig, G. N. Duda, H. Schell, P. Seebeck, and M. O. Heller, “On the influence of soft tissue coverage in the determination of bone kinematics using skin markers,” *Journal of Orthopaedic Research*, vol. 23, no. 4, pp. 726–734, 2005.
- [49] A. Peters, B. Galna, M. Sangeux, M. Morris, and R. Baker, “Quantification of soft tissue artifact in lower limb human motion analysis: a systematic review,” *Gait & posture*, vol. 31, no. 1, pp. 1–8, 2010.
- [50] K. Kaufman, “Future directions in gait analysis,” *J Rehabil Res Dev*, pp. 85–112, 1998.
- [51] A. Leardini, L. Chiari, U. Della Croce, and A. Cappozzo, “Human movement analysis using stereophotogrammetry: Part 3. soft tissue artifact assessment and compensation,” *Gait & posture*, vol. 21, no. 2, pp. 212–225, 2005.

-
- [52] D. Sutherland, "The evolution of clinical gait analysis: Part ii kinematics," *Gait & posture*, vol. 16, no. 2, pp. 159–179, 2002.
- [53] E. Oggero, G. Pagnacco, D. R. Morr, S. R. Simon, and N. Berme, "Probability of valid gait data acquisition using currently available force plates," *Biomedical sciences instrumentation*, vol. 34, pp. 392–397, 1998.
- [54] S. C. Wearing, S. R. Urry, and J. E. Smeathers, "The effect of visual targeting on ground reaction force and temporospatial parameters of gait," *Clinical biomechanics*, vol. 15, no. 8, pp. 583–591, 2000.
- [55] R. Riemer, E. T. Hsiao-Wecksler, and X. Zhang, "Uncertainties in inverse dynamics solutions: a comprehensive analysis and an application to gait," *Gait & posture*, vol. 27, no. 4, pp. 578–588, 2008.
- [56] D. A. Winter, *Biomechanics and motor control of human gait: normal, elderly and pathological*. 1991.
- [57] F. Dujardin, X. Roussignol, O. Mejjad, J. Weber, and J. Thomine, "Interindividual variations of the hip joint motion in normal gait," *Gait & Posture*, vol. 5, no. 3, pp. 246–250, 1997.
- [58] G. Möckel, C. Perka, G. Duda, *et al.*, "The influence of walking speed on kinetic and kinematic parameters in patients with osteoarthritis of the hip using a force-instrumented treadmill and standardised gait speeds," *Archives of orthopaedic and trauma surgery*, vol. 123, no. 6, pp. 278–282, 2003.
- [59] W. J. Hurd, T. L. Chmielewski, M. J. Axe, I. Davis, and L. Snyder-Mackler, "Differences in normal and perturbed walking kinematics between male and female athletes," *Clinical Biomechanics*, vol. 19, no. 5, pp. 465–472, 2004.
- [60] H. B. Menz, S. R. Lord, and R. C. Fitzpatrick, "Age-related differences in walking stability," *Age and ageing*, vol. 32, no. 2, pp. 137–142, 2003.
- [61] H. M. Clayton and H. C. Schamhardt, "Measurement techniques for gait analysis," *Equine locomotion*, pp. 55–76, 2001.
- [62] "<http://www.kungfuonline.com/perch/resources/bodyplanesw320h240.jpg>," Accessed October 2014.

-
- [63] I. Bouchrika and M. S. Nixon, “Exploratory factor analysis of gait recognition,” in *Automatic Face & Gesture Recognition, 2008. FG’08. 8th IEEE International Conference on*, pp. 1–6, IEEE, 2008.
- [64] K. A. Boyer, G. S. Beaupre, and T. P. Andriacchi, “Gender differences exist in the hip joint moments of healthy older walkers,” *Journal of biomechanics*, vol. 41, no. 16, pp. 3360–3365, 2008.
- [65] D. C. Kerrigan, L. W. Lee, J. J. Collins, P. O. Riley, and L. A. Lipsitz, “Reduced hip extension during walking: healthy elderly and fallers versus young adults,” *Archives of physical medicine and rehabilitation*, vol. 82, no. 1, pp. 26–30, 2001.
- [66] L. W. Lee, K. Zavarei, J. Evans, J. J. Lelas, P. O. Riley, and D. C. Kerrigan, “Reduced hip extension in the elderly: dynamic or postural?,” *Archives of physical medicine and rehabilitation*, vol. 86, no. 9, pp. 1851–1854, 2005.
- [67] A. Graf, J. O. Judge, S. Öunpuu, and D. G. Thelen, “The effect of walking speed on lower-extremity joint powers among elderly adults who exhibit low physical performance,” *Archives of physical medicine and rehabilitation*, vol. 86, no. 11, pp. 2177–2183, 2005.
- [68] K. M. Ostrosky, J. M. VanSwearingen, R. G. Burdett, and Z. Gee, “A comparison of gait characteristics in young and old subjects,” *Physical Therapy*, vol. 74, no. 7, pp. 637–644, 1994.
- [69] B. Pietraszewski, S. Winiarski, and S. Jaroszczuk, “Three-dimensional human gait pattern-reference data for normal men,” *Acta of Bioengineering and Biomechanics*, vol. 14, no. 3, pp. 9–16, 2012.
- [70] J. O. JudgeRoy, B. Davis, and S. Öunpuu, “Step length reductions in advanced age: the role of ankle and hip kinetics,” *The Journals of Gerontology Series A: Biological Sciences and Medical Sciences*, vol. 51, no. 6, pp. M303–M312, 1996.
- [71] J. Røislien, Ø. Skare, M. Gustavsen, N. L. Broch, L. Rennie, and A. Opheim, “Simultaneous estimation of effects of gender, age and walking speed on kinematic gait data,” *Gait & posture*, vol. 30, no. 4, pp. 441–445, 2009.
- [72] L. Alcock, N. Vanicek, and T. OBrien, “Alterations in gait speed and age do not fully explain the changes in gait mechanics associated with healthy older women,” *Gait & posture*, vol. 37, no. 4, pp. 586–592, 2013.

-
- [73] J. L. Lelas, G. J. Merriman, P. O. Riley, and D. C. Kerrigan, "Predicting peak kinematic and kinetic parameters from gait speed," *Gait & posture*, vol. 17, no. 2, pp. 106–112, 2003.
- [74] R. D. Crownshield, R. A. Brand, *et al.*, "The effects of walking velocity and age on hip kinematics and kinetics.," *Clinical Orthopaedics and Related Research*, vol. 132, pp. 140–144, 1978.
- [75] R. C. Browning and R. Kram, "Effects of obesity on the biomechanics of walking at different speeds," *Medicine and Science in Sports and Exercise*, vol. 39, no. 9, p. 1632, 2007.
- [76] P. P. Lai, A. K. Leung, A. N. Li, and M. Zhang, "Three-dimensional gait analysis of obese adults," *Clinical biomechanics*, vol. 23, pp. S2–S6, 2008.
- [77] L. Vismara, M. Romei, M. Galli, A. Montesano, G. Baccalaro, M. Crivellini, and G. Grugni, "Clinical implications of gait analysis in the rehabilitation of adult patients with prader-willi syndrome: a cross-sectional comparative study (prader-willi syndrome vs. matched obese patients and healthy subjects)," *Journal of neuroengineering and rehabilitation*, vol. 4, p. 14, 2007.
- [78] P. DeVita and T. Hortobágyi, "Obesity is not associated with increased knee joint torque and power during level walking," *Journal of biomechanics*, vol. 36, no. 9, pp. 1355–1362, 2003.
- [79] P. Spyropoulos, J. C. Pisciotta, K. N. Pavlou, M. Cairns, and S. R. Simon, "Biomechanical gait analysis in obese men.," *Archives of physical medicine and rehabilitation*, vol. 72, no. 13, pp. 1065–1070, 1991.
- [80] S.-u. Ko, S. Stenholm, and L. Ferrucci, "Characteristic gait patterns in older adults with obesity: results from the baltimore longitudinal study of aging," *Journal of biomechanics*, vol. 43, no. 6, pp. 1104–1110, 2010.
- [81] A. McMillan, A. Pulver, D. Collier, and D. Williams, "Sagittal and frontal plane joint mechanics throughout the stance phase of walking in adolescents who are obese," *Gait & posture*, vol. 32, no. 2, pp. 263–268, 2010.
- [82] S. Cho, J. Park, and O. Kwon, "Gender differences in three dimensional gait analysis data from 98 healthy korean adults," *Clinical biomechanics*, vol. 19, no. 2, pp. 145–152, 2004.
- [83] E. S. Chumanov, C. Wall-Scheffler, and B. C. Heiderscheit, "Gender differences in walking and running on level and inclined surfaces," *Clinical biomechanics*, vol. 23, no. 10, pp. 1260–1268, 2008.

-
- [84] D. C. Kerrigan, M. K. Todd, and U. D. Croce, "Gender differences in joint biomechanics during walking normative study in young adults," *American journal of physical medicine & rehabilitation*, vol. 77, no. 1, pp. 2–7, 1998.
- [85] R. Ferber, I. McClay Davis, and D. S. Williams Iii, "Gender differences in lower extremity mechanics during running," *Clinical Biomechanics*, vol. 18, no. 4, pp. 350–357, 2003.
- [86] J. A. DeLisa, *Gait analysis in the science of rehabilitation*, vol. 2. Diane Publishing, 1998.
- [87] G. Kamen, *Foundations of exercise science*. Lippincott Williams & Wilkins, 2001.
- [88] "<http://moon.ouhsc.edu/dthompso/gait/kinetics/grfbkgnd.htm>," Accessed December 2014 2014.
- [89] J. Watkins, *Fundamental Biomechanics of Sport and Exercise*. Routledge, 2014.
- [90] J. Perry, J. R. Davids, *et al.*, "Gait analysis: normal and pathological function.," *Journal of Pediatric Orthopaedics*, vol. 12, no. 6, p. 815, 1992.
- [91] B. Cigali, E. Ulucam, A. Yilmaz, and M. Cakiroglu, "Comparison of asymmetries in ground reaction force patterns between normal human gait and football players," *BIOLOGY OF SPORT*, vol. 21, no. 3, pp. 241–248, 2004.
- [92] E. C. Jansen, D. Vittas, S. Hellberg, and J. Hansen, "Normal gait of young and old men and women: ground reaction force measurement on a treadmill," *Acta Orthopaedica*, vol. 53, no. 2, pp. 193–196, 1982.
- [93] M.-C. Chiu and M.-J. Wang, "The effect of gait speed and gender on perceived exertion, muscle activity, joint motion of lower extremity, ground reaction force and heart rate during normal walking," *Gait & posture*, vol. 25, no. 3, pp. 385–392, 2007.
- [94] R. S. VanZant, T. G. McPoil, and M. W. Cornwall, "Symmetry of plantar pressures and vertical forces in healthy subjects during walking," *Journal of the American Podiatric Medical Association*, vol. 91, no. 7, pp. 337–342, 2001.
- [95] D. R. Burnett, N. H. Campbell-Kyureghyan, P. B. Cerrito, and P. M. Quesada, "Symmetry of ground reaction forces and muscle activity in asymptomatic subjects during walking, sit-to-stand, and stand-to-sit tasks," *Journal of Electromyography and Kinesiology*, vol. 21, no. 4, pp. 610–615, 2011.

-
- [96] M. Diop, A. Rahmani, A. Belli, V. Gautheron, A. Geysant, and J. Cottalorda, “Influence of speed variation and age on the asymmetry of ground reaction forces and stride parameters of normal gait in children,” *Journal of Pediatric Orthopaedics B*, vol. 13, no. 5, pp. 308–314, 2004.
- [97] T. Keller, A. Weisberger, J. Ray, S. Hasan, R. Shiavi, and D. Spengler, “Relationship between vertical ground reaction force and speed during walking, slow jogging, and running,” *Clinical Biomechanics*, vol. 11, no. 5, pp. 253–259, 1996.
- [98] J. Nilsson and A. Thorstensson, “Ground reaction forces at different speeds of human walking and running,” *Acta Physiologica Scandinavica*, vol. 136, no. 2, pp. 217–227, 1989.
- [99] D. P. LaRoche, E. D. Millett, and R. J. Kralian, “Low strength is related to diminished ground reaction forces and walking performance in older women,” *Gait & posture*, vol. 33, no. 4, pp. 668–672, 2011.
- [100] J. Paul, “Force actions transmitted by joints in the human body,” *Proceedings of the Royal Society of London. Series B. Biological Sciences*, vol. 192, no. 1107, pp. 163–172, 1976.
- [101] B. A. Sanford, J. L. Williams, A. R. Zucker-Levin, and W. M. Mihalko, “Hip, knee, and ankle joint forces in healthy weight, overweight, and obese individuals during walking,” in *Computational Biomechanics for Medicine*, pp. 101–111, Springer, 2014.
- [102] B. Stansfield and A. Nicol, “Hip joint contact forces in normal subjects and subjects with total hip prostheses: walking and stair and ramp negotiation,” *Clinical Biomechanics*, vol. 17, no. 2, pp. 130–139, 2002.
- [103] P. M. Arnos, *Age-related Changes in Gait: Influence of Upper-body Posture*. ProQuest, 2007.
- [104] M. M. Ardestani, M. Moazen, and Z. Jin, “Sensitivity analysis of human lower extremity joint moments due to changes in joint kinematics,” *Medical engineering & physics*, vol. 37, no. 2, pp. 165–174, 2015.
- [105] S. R. Goldberg and S. J. Stanhope, “Sensitivity of joint moments to changes in walking speed and body-weight-support are interdependent and vary across joints,” *Journal of biomechanics*, vol. 46, no. 6, pp. 1176–1183, 2013.
- [106] D. A. Winter, “Kinematic and kinetic patterns in human gait: variability and compensating effects,” *Human Movement Science*, vol. 3, no. 1, pp. 51–76, 1984.

-
- [107] R. L. Lathrop-Lambach, J. L. Asay, S. T. Jamison, X. Pan, L. C. Schmitt, K. Blazek, R. A. Siston, T. P. Andriacchi, and A. M. Chaudhari, “Evidence for joint moment asymmetry in healthy populations during gait,” *Gait & posture*, vol. 40, no. 4, pp. 526–531, 2014.
- [108] G. T. Harding, C. L. Hubley-Kozey, M. J. Dunbar, W. D. Stanish, and J. L. A. Wilson, “Body mass index affects knee joint mechanics during gait differently with and without moderate knee osteoarthritis,” *Osteoarthritis and Cartilage*, vol. 20, no. 11, pp. 1234–1242, 2012.
- [109] C. Kirtley, M. W. Whittle, and R. Jefferson, “Influence of walking speed on gait parameters,” *Journal of biomedical engineering*, vol. 7, no. 4, pp. 282–288, 1985.
- [110] A. J. Teichtahl, A. E. Wluka, M. E. Morris, S. R. Davis, and F. M. Cicuttini, “The associations between the dominant and nondominant peak external knee adductor moments during gait in healthy subjects: evidence for symmetry,” *Archives of physical medicine and rehabilitation*, vol. 90, no. 2, pp. 320–324, 2009.
- [111] H. Sadeghi, “Local or global asymmetry in gait of people without impairments,” *Gait & Posture*, vol. 17, no. 3, pp. 197–204, 2003.
- [112] B. D. Street and W. Gage, “The effects of an adopted narrow gait on the external adduction moment at the knee joint during level walking: Evidence of asymmetry,” *Human movement science*, vol. 32, no. 2, pp. 301–313, 2013.
- [113] A. G. Schache, R. Baker, and C. L. Vaughan, “Differences in lower limb transverse plane joint moments during gait when expressed in two alternative reference frames,” *Journal of biomechanics*, vol. 40, no. 1, pp. 9–19, 2007.
- [114] A. G. Schache and R. Baker, “On the expression of joint moments during gait,” *Gait & posture*, vol. 25, no. 3, pp. 440–452, 2007.
- [115] J. H. Hollman, E. M. McDade, and R. C. Petersen, “Normative spatiotemporal gait parameters in older adults,” *Gait & posture*, vol. 34, no. 1, pp. 111–118, 2011.
- [116] M. P. Murray, R. C. Kory, B. H. Clarkson, and S. Sepic, “Comparison of free and fast speed walking patterns of normal men,” *American Journal of Physical Medicine & Rehabilitation*, vol. 45, no. 1, pp. 8–24, 1966.
- [117] M. L. Callisaya, L. Blizzard, M. D. Schmidt, J. L. McGinley, and V. K. Srikanth, “Ageing and gait variability: a population-based study of older people,” *Age and ageing*, p. afp250, 2010.

-
- [118] T. Öberg, A. Karsznia, and K. Öberg, “Basic gait parameters: reference data for normal subjects, 10-79 years of age,” *Journal of rehabilitation research and development*, vol. 30, pp. 210–210, 1993.
- [119] D. A. Bruening, R. E. Frimenko, C. D. Goodyear, D. R. Bowden, and A. M. Fullenkamp, “Sex differences in whole body gait kinematics at preferred speeds,” *Gait & Posture*, 2014.
- [120] M. Samson, A. Crowe, P. De Vreede, J. Dessens, S. Duursma, and H. Verhaar, “Differences in gait parameters at a preferred walking speed in healthy subjects due to age, height and body weight,” *Aging Clinical and Experimental Research*, vol. 13, no. 1, pp. 16–21, 2001.
- [121] J. E. Himann, D. A. Cunningham, P. A. Rechnitzer, and D. H. Paterson, “Age-related changes in speed of walking,” *Medicine and science in sports and exercise*, vol. 20, no. 2, pp. 161–166, 1988.
- [122] J. Kavanagh, R. Barrett, and S. Morrison, “Upper body accelerations during walking in healthy young and elderly men,” *Gait & posture*, vol. 20, no. 3, pp. 291–298, 2004.
- [123] R. W. Bohannon, “Comfortable and maximum walking speed of adults aged 20-79 years: reference values and determinants,” *Age and ageing*, vol. 26, no. 1, pp. 15–19, 1997.
- [124] M. P. Kadaba, H. Ramakrishnan, M. Wootten, *et al.*, “Measurement of lower extremity kinematics during level walking,” *Journal of orthopaedic research*, vol. 8, no. 3, pp. 383–392, 1990.
- [125] J. M. H. Jiménez, V. A. A. García-Molina, J. M. P. Foulquie, M. D. Fernández, and V. M. S. Hermoso, “Spatial-temporal parameters of gait in women with fibromyalgia,” *Clinical rheumatology*, vol. 28, no. 5, pp. 595–598, 2009.
- [126] K.-A. Lai, C.-J. Lin, I. Jou, F.-C. Su, *et al.*, “Gait analysis after total hip arthroplasty with leg-length equalization in women with unilateral congenital complete dislocation of the hip—comparison with untreated patients,” *Journal of orthopaedic research*, vol. 19, no. 6, pp. 1147–1152, 2001.
- [127] A. Boonstra, V. Fidler, and W. Eisma, “Walking speed of normal subjects and amputees: aspects of validity of gait analysis,” *Prosthetics and Orthotics International*, vol. 17, no. 2, pp. 78–82, 1993.
- [128] L. E. Diamond, T. V. Wrigley, K. L. Bennell, R. S. Hinman, J. ODonnell, and P. W. Hodges, “Hip joint biomechanics during gait in people with and without symptomatic femoroacetabular impingement,” *Gait & Posture*, 2015.

-
- [129] D. J. Blanke and P. A. Hageman, "Comparison of gait of young men and elderly men," *Physical Therapy*, vol. 69, no. 2, pp. 144–148, 1989.
- [130] R. C. Browning, "Locomotion mechanics in obese adults and children," *Current Obesity Reports*, vol. 1, no. 3, pp. 152–159, 2012.
- [131] M. Bendall, E. Bassey, and M. Pearson, "Factors affecting walking speed of elderly people," *Age and Ageing*, vol. 18, no. 5, pp. 327–332, 1989.
- [132] R. Alexander, "Stride length and speed for adults, children, and fossil hominids," *American Journal of Physical Anthropology*, vol. 63, no. 1, pp. 23–27, 1984.
- [133] J. J. Callaghan, A. G. Rosenberg, and H. E. Rubash, *The adult hip*, vol. 1. Lippincott Williams & Wilkins, 2007.
- [134] E. Chao, R. Laughman, E. Schneider, and R. Stauffer, "Normative data of knee joint motion and ground reaction forces in adult level walking," *Journal of biomechanics*, vol. 16, no. 3, pp. 219–233, 1983.
- [135] P. A. Hageman and D. J. Blanke, "Comparison of gait of young women and elderly women," *Physical Therapy*, vol. 66, no. 9, pp. 1382–1387, 1986.
- [136] M. P. Murray, R. C. Kory, and S. B. Sepic, "Walking patterns of normal women.," *Archives of physical medicine and rehabilitation*, vol. 51, no. 11, p. 637, 1970.
- [137] F. Finley, K. Cody, and R. Finizie, "Locomotion patterns in elderly women.," *Archives of physical medicine and rehabilitation*, vol. 50, no. 3, p. 140, 1969.
- [138] A. Gabell and U. Nayak, "The effect of age on variability in gait," *Journal of Gerontology*, vol. 39, no. 6, pp. 662–666, 1984.
- [139] P. DeVita and T. Hortobagyi, "Age causes a redistribution of joint torques and powers during gait," *Journal of applied physiology*, vol. 88, no. 5, pp. 1804–1811, 2000.
- [140] A. Salarian, H. Russmann, F. J. Vingerhoets, C. Dehollaini, Y. Blanc, P. R. Burkhard, and K. Aminian, "Gait assessment in parkinson's disease: toward an ambulatory system for long-term monitoring," *Biomedical Engineering, IEEE Transactions on*, vol. 51, no. 8, pp. 1434–1443, 2004.
- [141] "<http://www.utdallas.edu/atec/midori/handouts/walkinggraphs.htm>," Accessed April 2016.

-
- [142] “<http://www.njrcentre.org.uk/njrcentre/healthcareproviders>,” Accessed January 2015.
- [143] “www.healthbase.com,” Accessed January 2015.
- [144] B. Stansfield, A. Nicol, J. Paul, I. Kelly, F. Graichen, and G. Bergmann, “Direct comparison of calculated hip joint contact forces with those measured using instrumented implants. an evaluation of a three-dimensional mathematical model of the lower limb,” *Journal of Biomechanics*, vol. 36, no. 7, pp. 929–936, 2003.
- [145] D. Davy, G. Kotzar, R. Brown, K. Heiple, V. Goldberg, J. Berilla, and A. Burstein, “Telemetric force measurements across the hip after total arthroplasty,” *The Journal of Bone & Joint Surgery*, vol. 70, no. 1, pp. 45–50, 1988.
- [146] A. J. van den Bogert, L. Read, and B. M. Nigg, “An analysis of hip joint loading during walking, running, and skiing,” *Medicine and science in sports and exercise*, vol. 31, no. 1, pp. 131–142, 1999.
- [147] R. A. Brand, D. R. Pedersen, D. T. Davy, G. M. Kotzar, K. G. Heiple, and V. M. Goldberg, “Comparison of hip force calculations and measurements in the same patient,” *The Journal of Arthroplasty*, vol. 9, no. 1, pp. 45–51, 1994.
- [148] G. Bergmann, G. Deuretzbacher, M. Heller, F. Graichen, A. Rohlmann, J. Strauss, and G. Duda, “Hip contact forces and gait patterns from routine activities,” *Journal of biomechanics*, vol. 34, no. 7, pp. 859–871, 2001.
- [149] K. C. Foucher, D. E. Hurwitz, and M. A. Wimmer, “Relative importance of gait vs. joint positioning on hip contact forces after total hip replacement,” *Journal of Orthopaedic Research*, vol. 27, no. 12, pp. 1576–1582, 2009.
- [150] A. Wykman and E. Olsson, “Walking ability after total hip replacement. a comparison of gait analysis in unilateral and bilateral cases,” *Journal of Bone & Joint Surgery, British Volume*, vol. 74, no. 1, pp. 53–56, 1992.
- [151] S. C. White and R. M. Lifeso, “Altering asymmetric limb loading after hip arthroplasty using real-time dynamic feedback when walking,” *Archives of physical medicine and rehabilitation*, vol. 86, no. 10, pp. 1958–1963, 2005.
- [152] C. Hodt-Billington, J. L. Helbostad, W. Vervaat, T. Rognsvåg, and R. Moe-Nilssen, “Changes in gait symmetry, gait velocity and self-reported function followings total hip replacement,” *Journal of rehabilitation medicine*, vol. 43, no. 9, pp. 787–793, 2011.

-
- [153] E. Olsson, "Gait analysis in hip and knee surgery.," *Scandinavian journal of rehabilitation medicine. Supplement*, vol. 15, pp. 1–55, 1985.
- [154] V. Kyriazis and C. Rigas, "Temporal gait analysis of hip osteoarthritic patients operated with cementless hip replacement," *Clinical Biomechanics*, vol. 17, no. 4, pp. 318–321, 2002.
- [155] V. Schwachmeyer, P. Damm, A. Bender, J. Dymke, F. Graichen, and G. Bergmann, "In vivo hip joint loading during post-operative physiotherapeutic exercises," 2013.
- [156] C. Götze, D. Rosenbaum, J. Hoedemaker, F. Bottner, and W. Steens, "Is there a need of custom-made prostheses for total hip arthroplasty? gait analysis, clinical and radiographic analysis of customized femoral components," *Archives of orthopaedic and trauma surgery*, vol. 129, no. 2, pp. 267–274, 2009.
- [157] M. K. Petersen, N. T. Andersen, P. Mogensen, M. Voight, and K. Søballe, "Gait analysis after total hip replacement with hip resurfacing implant or mallory-head exeter prosthesis: a randomised controlled trial," *International orthopaedics*, vol. 35, no. 5, pp. 667–674, 2011.
- [158] T.-Y. Tsai, J.-S. Li, S. Wang, D. Scarborough, and Y.-M. Kwon, "In-vivo 6 degrees-of-freedom kinematics of metal-on-polyethylene total hip arthroplasty during gait," *Journal of biomechanics*, vol. 47, no. 7, pp. 1572–1576, 2014.
- [159] T.-Y. Tsai, J.-S. Li, D. Dimitriou, and Y.-M. Kwon, "Does component alignment affect gait symmetry in unilateral total hip arthroplasty patients?," *Clinical Biomechanics*, vol. 30, no. 8, pp. 802–807, 2015.
- [160] M. Murray, D. R. Gore, B. J. Brewer, G. M. Gardner, and S. B. Sepic, "A comparison of the functional performance of patients with charnley and müller total hip replacement: A two-year follow-up of eighty-nine cases," *Acta Orthopaedica*, vol. 50, no. 5, pp. 563–569, 1979.
- [161] W. Hodge, T. Andriacchi, and J. Galante, "A relationship between stem orientation and function following total hip arthroplasty," *The Journal of arthroplasty*, vol. 6, no. 3, pp. 229–235, 1991.
- [162] S. Leuchte, A. Luchs, and D. Wohlrab, "[measurement of ground reaction forces after total hip arthroplasty using different surgical approaches]," *Zeitschrift für Orthopädie und ihre Grenzgebiete*, vol. 145, no. 1, pp. 74–80, 2006.

-
- [163] R. M. Meneghini, S. A. Smits, R. R. Swinford, and R. E. Bahamonde, “A randomized, prospective study of 3 minimally invasive surgical approaches in total hip arthroplasty: comprehensive gait analysis,” *The Journal of arthroplasty*, vol. 23, no. 6, pp. 68–73, 2008.
- [164] C. M. Bach, P. Winter, M. Nogler, G. Göbel, C. Wimmer, and M. Ogon, “No functional impairment after robodoc total hip arthroplasty,” *Acta Orthopaedica*, vol. 73, no. 4, pp. 386–391, 2002.
- [165] M. A. Mont, T. M. Seyler, P. S. Ragland, R. Starr, J. Erhart, and A. Bhave, “Gait analysis of patients with resurfacing hip arthroplasty compared with hip osteoarthritis and standard total hip arthroplasty,” *The Journal of arthroplasty*, vol. 22, no. 1, pp. 100–108, 2007.
- [166] J. Nantel, N. Termoz, P.-A. Vendittoli, M. Lavigne, and F. Prince, “Gait patterns after total hip arthroplasty and surface replacement arthroplasty,” *Archives of physical medicine and rehabilitation*, vol. 90, no. 3, pp. 463–469, 2009.
- [167] D. Bennett, L. Ogonda, D. Elliott, L. Humphreys, and D. Beverland, “Comparison of gait kinematics in patients receiving minimally invasive and traditional hip replacement surgery: a prospective blinded study,” *Gait & posture*, vol. 23, no. 3, pp. 374–382, 2006.
- [168] L. Andersson, A. Wesslau, H. Bodén, and N. Dalén, “Immediate or late weight bearing after uncemented total hip arthroplasty: a study of functional recovery,” *The Journal of arthroplasty*, vol. 16, no. 8, pp. 1063–1065, 2001.
- [169] D. Bennett, L. Ogonda, D. Elliott, L. Humphreys, M. Lawlor, and D. Beverland, “Comparison of immediate postoperative walking ability in patients receiving minimally invasive and standard-incision hip arthroplasty: a prospective blinded study,” *The Journal of arthroplasty*, vol. 22, no. 4, pp. 490–495, 2007.
- [170] R. C. Guedes, J. Dias, R. C. Dias, V. S. Borges, L. P. Lustosa, and N. Rosa, “Total hip arthroplasty in the elderly: impact on functional performance,” *Brazilian Journal of Physical Therapy*, vol. 15, no. 2, pp. 123–130, 2011.
- [171] M. Perron, F. Malouin, H. Moffet, and B. J. McFadyen, “Three-dimensional gait analysis in women with a total hip arthroplasty,” *Clinical Biomechanics*, vol. 15, no. 7, pp. 504–515, 2000.
- [172] D. R. Gore, M. P. Murray, S. B. Sepic, and G. M. Gardener, “Anterolateral compared to pos-

- terior approach in total hip arthroplasty: differences in component positioning, hip strength, and hip motion.,” *Clinical Orthopaedics and Related Research*, vol. 165, pp. 180–187, 1982.
- [173] H. Tateuchi, R. Tsukagoshi, Y. Fukumoto, H. Akiyama, K. So, Y. Kuroda, and N. Ichihashi, “Pelvic instability and trunk and hip muscle recruitment patterns in patients with total hip arthroplasty,” *Journal of Electromyography and Kinesiology*, vol. 23, no. 1, pp. 151–158, 2013.
- [174] M. Vissers, J. Bussmann, I. De Groot, J. Verhaar, and M. Reijman, “Walking and chair rising performed in the daily life situation before and after total hip arthroplasty,” *Osteoarthritis and Cartilage*, vol. 19, no. 9, pp. 1102–1107, 2011.
- [175] A. Häkkinen, H. Borg, H. Kautiainen, E. Anttila, K. Häkkinen, J. Ylinen, and I. Kiviranta, “Muscle strength and range of movement deficits 1 year after hip resurfacing surgery using posterior approach,” *Disability and rehabilitation*, vol. 32, no. 6, pp. 483–491, 2010.
- [176] K. Aminian, K. Rezakhanlou, E. De Andres, C. Fritsch, P.-F. Leyvraz, and P. Robert, “Temporal feature estimation during walking using miniature accelerometers: an analysis of gait improvement after hip arthroplasty,” *Medical & biological engineering & computing*, vol. 37, no. 6, pp. 686–691, 1999.
- [177] J. Wall, A. Ashburn, and L. Klenerman, “Gait analysis in the assessment of functional performance before and after total hip replacement,” *Journal of biomedical engineering*, vol. 3, no. 2, pp. 121–127, 1981.
- [178] H. Miki, N. Sugano, K. Hagio, T. Nishii, H. Kawakami, A. Kakimoto, N. Nakamura, and H. Yoshikawa, “Recovery of walking speed and symmetrical movement of the pelvis and lower extremity joints after unilateral tha,” *Journal of biomechanics*, vol. 37, no. 4, pp. 443–455, 2004.
- [179] K. C. Foucher, D. E. Hurwitz, and M. A. Wimmer, “Preoperative gait adaptations persist one year after surgery in clinically well-functioning total hip replacement patients,” *Journal of biomechanics*, vol. 40, no. 15, pp. 3432–3437, 2007.
- [180] T. Horstmann, R. Listringhaus, G.-B. Haase, S. Grau, and A. Mündermann, “Changes in gait patterns and muscle activity following total hip arthroplasty: A six-month follow-up,” *Clinical Biomechanics*, vol. 28, no. 7, pp. 762–769, 2013.
- [181] G. Lenaerts, M. Mulier, A. Spaepen, G. Van der Perre, and I. Jonkers, “Aberrant pelvis and

- hip kinematics impair hip loading before and after total hip replacement,” *Gait & posture*, vol. 30, no. 3, pp. 296–302, 2009.
- [182] M. Murray, D. R. Gore, B. J. Brewer, R. C. Zuege, and G. M. Gardener, “Comparison of functional performance after mckee-farrar, charnley, and muller total hip replacement: A six-month follow-up of one hundred sixty-five cases,” *Clinical orthopaedics and related research*, vol. 121, pp. 33–43, 1976.
- [183] M. Murray, B. J. Brewer, D. Gore, and R. Zuege, “Kinesiology after mckee-farrar total hip replacement. a two-year follow-up of one hundred cases,” *The Journal of Bone & Joint Surgery*, vol. 57, no. 3, pp. 337–342, 1975.
- [184] M. Brown, H. J. Hislop, R. L. Waters, and D. Porell, “Walking efficiency before and after total hip replacement,” *Physical therapy*, vol. 60, no. 10, pp. 1259–1263, 1980.
- [185] A. A. McBeath, M. S. Bahrke, and B. Balke, “Walking efficiency before and after total hip replacement as determined by oxygen consumption,” *The Journal of Bone & Joint Surgery*, vol. 62, no. 5, pp. 807–810, 1980.
- [186] W. T. Long, L. D. Dorr, B. Healy, and J. Perry, “Functional recovery of noncemented total hip arthroplasty,” *Clinical orthopaedics and related research*, vol. 288, pp. 73–77, 1993.
- [187] R. N. Stauffer, G. L. Smidt, and J. B. Wadsworth, “Clinical and biomechanical analysis of gait following charnley total hip replacement,” *Clinical orthopaedics and related research*, vol. 99, pp. 70–77, 1974.
- [188] N. C. Casartelli, J. F. Item-Glatthorn, M. Bizzini, M. Leunig, and N. A. Maffiuletti, “Differences in gait characteristics between total hip, knee, and ankle arthroplasty patients: a six-month postoperative comparison,” *BMC musculoskeletal disorders*, vol. 14, no. 1, p. 176, 2013.
- [189] P. Bhargava, P. Shrivastava, and S. Nagariya, “Assessment of changes in gait parameters and vertical ground reaction forces after total hip arthroplasty,” *Indian journal of orthopaedics*, vol. 41, no. 2, p. 158, 2007.
- [190] L. Sicard-Rosenbaum, K. E. Light, and A. L. Behrman, “Gait, lower extremity strength, and self-assessed mobility after hip arthroplasty,” *The Journals of Gerontology Series A: Biological Sciences and Medical Sciences*, vol. 57, no. 1, pp. M47–M51, 2002.

-
- [191] J. L. McCrory, S. C. White, and R. M. Lifeso, “Vertical ground reaction forces: objective measures of gait following hip arthroplasty,” *Gait & posture*, vol. 14, no. 2, pp. 104–109, 2001.
- [192] H. Tateuchi, R. Tsukagoshi, Y. Fukumoto, S. Oda, and N. Ichihashi, “Dynamic hip joint stiffness in individuals with total hip arthroplasty: relationships between hip impairments and dynamics of the other joints,” *Clinical biomechanics*, vol. 26, no. 6, pp. 598–604, 2011.
- [193] J. Goetz, J. Beckmann, B. Rath, S. Dullien, F. Koeck, and J. Grifka, “Gait kinematics of patients with total hip replacement (thr)influence of gait velocity on determining pathological findings,” *Gait & Posture*, vol. 30, pp. S65–S66, 2009.
- [194] J. Loizeau, P. Allard, M. Duhaime, and B. Landjerit, “Bilateral gait patterns in subjects fitted with a total hip prosthesis,” *Archives of physical medicine and rehabilitation*, vol. 76, no. 6, pp. 552–557, 1995.
- [195] M. L. Beaulieu, M. Lamontagne, and P. E. Beulé, “Lower limb biomechanics during gait do not return to normal following total hip arthroplasty,” *Gait & posture*, vol. 32, no. 2, pp. 269–273, 2010.
- [196] S.-L. Chiu, T.-W. Lu, and L.-S. Chou, “Altered inter-joint coordination during walking in patients with total hip arthroplasty,” *Gait & posture*, vol. 32, no. 4, pp. 656–660, 2010.
- [197] V. Agostini, D. Ganio, K. Facchin, L. Cane, S. M. Carneiro, and M. Knaflitz, “Gait parameters and muscle activation patterns at 3, 6 and 12 months after total hip arthroplasty,” *The Journal of arthroplasty*, vol. 29, no. 6, pp. 1265–1272, 2014.
- [198] D. Bennett, L. Humphreys, S. O'Brien, C. Kelly, J. Orr, and D. Beverland, “Gait kinematics of age-stratified hip replacement patientsa large scale, long-term follow-up study,” *Gait & posture*, vol. 28, no. 2, pp. 194–200, 2008.
- [199] J. Li, A. C. Redmond, Z. Jin, J. Fisher, M. H. Stone, and T. D. Stewart, “Hip contact forces in asymptomatic total hip replacement patients differ from normal healthy individuals: Implications for preclinical testing,” *Clinical Biomechanics*, vol. 29, no. 7, pp. 747–751, 2014.
- [200] G. M. Whatling, H. Dabke, C. A. Holt, L. Jones, J. Madete, P. Alderman, and P. Roberts, “Objective functional assessment of total hip arthroplasty following two common surgical approaches: the posterior and direct lateral approaches,” *Proceedings of the Institution of Mechanical Engineers, Part H: Journal of Engineering in Medicine*, vol. 222, no. 6, pp. 897–905, 2008.

-
- [201] K. C. Foucher and M. A. Wimmer, “Contralateral hip and knee gait biomechanics are unchanged by total hip replacement for unilateral hip osteoarthritis,” *Gait & posture*, vol. 35, no. 1, pp. 61–65, 2012.
- [202] T.-Y. Tsai, D. Dimitriou, J.-S. Li, K. W. Nam, G. Li, and Y.-M. Kwon, “Asymmetric hip kinematics during gait in patients with unilateral total hip arthroplasty: In vivo 3-dimensional motion analysis,” *Journal of Biomechanics*, 2015.
- [203] K. C. Foucher, L. E. Thorp, D. Orozco, M. Hildebrand, and M. A. Wimmer, “Differences in preferred walking speeds in a gait laboratory compared with the real world after total hip replacement,” *Archives of physical medicine and rehabilitation*, vol. 91, no. 9, pp. 1390–1395, 2010.
- [204] R. M. Queen, J. F. Schaeffer, R. J. Butler, C. C. Berasi, S. S. Kelley, D. E. Attarian, and M. P. Bolognesi, “Does surgical approach during total hip arthroplasty alter gait recovery during the first year following surgery?,” *The Journal of arthroplasty*, vol. 28, no. 9, pp. 1639–1643, 2013.
- [205] P. A. Rathod, K. F. Orishimo, I. J. Kremenec, A. J. Deshmukh, and J. A. Rodriguez, “Similar improvement in gait parameters following direct anterior & posterior approach total hip arthroplasty,” *The Journal of arthroplasty*, vol. 29, no. 6, pp. 1261–1264, 2014.
- [206] A. J. Deshmukh and J. A. Rodriguez, “Similar improvement in gait parameters following direct anterior & posterior approach total hip arthroplasty,” 2013.
- [207] G. Holnapy, Á. Illyés, and R. M. Kiss, “Impact of the method of exposure in total hip arthroplasty on the variability of gait in the first 6 months of the postoperative period,” *Journal of Electromyography and Kinesiology*, vol. 23, no. 4, pp. 966–976, 2013.
- [208] R. M. Kiss and Á. Illyés, “Comparison of gait parameters in patients following total hip arthroplasty with a direct-lateral or antero-lateral surgical approach,” *Human movement science*, vol. 31, no. 5, pp. 1302–1316, 2012.
- [209] R. M. Queen, R. J. Butler, T. S. Watters, S. S. Kelley, D. E. Attarian, and M. P. Bolognesi, “The effect of total hip arthroplasty surgical approach on postoperative gait mechanics,” *The Journal of arthroplasty*, vol. 26, no. 6, pp. 66–71, 2011.
- [210] M. S. Madsen, M. A. Ritter, H. H. Morris, J. B. Meding, M. E. Berend, P. M. Faris, and

- V. G. Vardaxis, "The effect of total hip arthroplasty surgical approach on gait," *Journal of Orthopaedic Research*, vol. 22, no. 1, pp. 44–50, 2004.
- [211] V. Lugade, A. Wu, B. Jewett, D. Collis, and L.-S. Chou, "Gait asymmetry following an anterior and anterolateral approach to total hip arthroplasty," *Clinical Biomechanics*, vol. 25, no. 7, pp. 675–680, 2010.
- [212] B. M. Jolles and E. R. Bogoch, "Posterior versus lateral surgical approach for total hip arthroplasty in adults with osteoarthritis," *The Cochrane Library*, 2006.
- [213] K. C. Foucher, M. A. Wimmer, K. C. Moio, M. Hildebrand, M. C. Berli, M. R. Walker, R. A. Berger, and J. O. Galante, "Time course and extent of functional recovery during the first postoperative year after minimally invasive total hip arthroplasty with two different surgical approaches: a randomized controlled trial," *Journal of biomechanics*, vol. 44, no. 3, pp. 372–378, 2011.
- [214] D. Varin, M. Lamontagne, and P. E. Beaulé, "Does the anterior approach for the hip provide closer-to-normal lower-limb motion?," *The Journal of arthroplasty*, vol. 28, no. 8, pp. 1401–1407, 2013.
- [215] E. Mayr, M. Nogler, M.-G. Benedetti, O. Kessler, A. Reinthaler, M. Krismer, and A. Leardini, "A prospective randomized assessment of earlier functional recovery in the patients treated by minimally invasive direct anterior approach: a gait analysis study," *Clinical Biomechanics*, vol. 24, no. 10, pp. 812–818, 2009.
- [216] S. Kolk, M. J. Minten, G. E. van Bon, W. H. Rijnen, A. C. Geurts, N. Verdonschot, and V. Weerdesteyn, "Gait and gait-related activities of daily living after total hip arthroplasty: A systematic review," *Clinical Biomechanics*, vol. 29, no. 6, pp. 705–718, 2014.
- [217] "<http://bonesmart.org/hip/hip-replacement-direct-anterior-approach/>," Accessed October 2015.
- [218] A. M. Ewen, S. Stewart, A. S. C. Gibson, S. N. Kashyap, and N. Caplan, "Post-operative gait analysis in total hip replacement patients: a review of current literature and meta-analysis," *Gait & posture*, vol. 36, no. 1, pp. 1–6, 2012.
- [219] G. Bergmann, F. Graichen, and A. Rohlmann, "Hip joint loading during walking and running, measured in two patients," *Journal of biomechanics*, vol. 26, no. 8, pp. 969–990, 1993.

-
- [220] C. Manders, A. New, and J. Rasmussen, "Validation of musculoskeletal gait simulation for use in investigation of total hip replacement," *Journal of Biomechanics*, vol. 41, p. S488, 2008.
- [221] J. Li, A. B. McWilliams, Z. Jin, J. Fisher, M. H. Stone, A. C. Redmond, and T. D. Stewart, "Unilateral total hip replacement patients with symptomatic leg length inequality have abnormal hip biomechanics during walking," *Clinical Biomechanics*, vol. 30, no. 5, pp. 513–519, 2015.
- [222] B. Gurney, "Leg length discrepancy," *Gait & posture*, vol. 15, no. 2, pp. 195–206, 2002.
- [223] A. L. Woerman and S. A. Binder-Macleod, "Leg length discrepancy assessment: Accuracy and precision in five clinical methods of evaluation*," *Journal of Orthopaedic & Sports Physical Therapy*, vol. 5, no. 5, pp. 230–239, 1984.
- [224] R. H. Gross, "Leg length discrepancy: how much is too much?," *Orthopedics*, vol. 1, no. 4, pp. 307–310, 1978.
- [225] J.-M. Guichet, J. M. Spivak, P. Trouilloud, and P. M. Grammont, "Lower limb-length discrepancy: an epidemiologic study," *Clinical orthopaedics and related research*, vol. 272, pp. 235–241, 1991.
- [226] L.-N. Veilleux, N. mi Dahan-Oliel, A. Pouliot-Laforte, A. Parent, M. Alotaibi, L. Ballaz, and R. Hamdy, "The effect of a knee-height asymmetry on gait patterns and physical parameters in two patients with a corrected leg-length discrepancy," *Gait & Posture*, vol. 49, p. 248, 2016.
- [227] A. Konyves and G. Bannister, "The importance of leg length discrepancy after total hip arthroplasty," *Journal of Bone & Joint Surgery, British Volume*, vol. 87, no. 2, pp. 155–157, 2005.
- [228] J. Alfaro-Adrian, F. Bayona, J. Rech, and D. Murray, "One-or two-stage bilateral total hip replacement," *The Journal of arthroplasty*, vol. 14, no. 4, pp. 439–445, 1999.
- [229] K. B. Turula, O. FRIBERG, T. S. LINDHOLM, K. TALLROTH, and E. VANKKA, "Leg length inequality after total hip arthroplasty.," *Clinical orthopaedics and related research*, vol. 202, pp. 163–168, 1986.
- [230] C. S. Ranawat, R. R. Rao, J. A. Rodriguez, and H. S. Bhende, "Correction of limb-length inequality during total hip arthroplasty," *The Journal of arthroplasty*, vol. 16, no. 6, pp. 715–720, 2001.

-
- [231] M. R. Whitehouse, N. S. Stefanovich-Lawbuary, L. R. Brunton, and A. W. Blom, "The impact of leg length discrepancy on patient satisfaction and functional outcome following total hip arthroplasty," *The Journal of arthroplasty*, vol. 28, no. 8, pp. 1408–1414, 2013.
- [232] D. Beard, J. Palan, J. Andrew, J. Nolan, and D. Murray, "Incidence and effect of leg length discrepancy following total hip arthroplasty," *Physiotherapy*, vol. 94, no. 2, pp. 91–96, 2008.
- [233] R. Thakral, A. J. Johnson, S. C. Specht, J. D. Conway, K. Issa, M. A. Mont, and J. E. Herzenberg, "Limb-length discrepancy after total hip arthroplasty: Novel treatment and proposed algorithm for care," *Orthopedics*, vol. 37, no. 2, pp. 101–106, 2014.
- [234] C. W. Hartman, B. J. Gilbert, and W. G. Paprosky, "Gender issues in total hip arthroplasty: Length, offset, and osteoporosis," in *Seminars in Arthroplasty*, vol. 20, pp. 62–65, Elsevier, 2009.
- [235] M. Walsh, P. Connolly, A. Jenkinson, and T. O'Brien, "Leg length discrepancy: an experimental study of compensatory changes in three dimensions using gait analysis," *Gait & posture*, vol. 12, no. 2, pp. 156–161, 2000.
- [236] J. L. Knight and R. D. Atwater, "Preoperative planning for total hip arthroplasty: quantitating its utility and precision," *The Journal of arthroplasty*, vol. 7, pp. 403–409, 1992.
- [237] T. White and T. Dougall, "Arthroplasty of the hip leg length is not important," *Journal of Bone & Joint Surgery, British Volume*, vol. 84, no. 3, pp. 335–338, 2002.
- [238] A. S. Desai, A. Dramis, and T. N. Board, "Leg length discrepancy after total hip arthroplasty: a review of literature," *Current reviews in musculoskeletal medicine*, vol. 6, no. 4, pp. 336–341, 2013.
- [239] D. Nam, P. K. Sculco, M. P. Abdel, M. M. Alexiades, M. P. Figgie, and D. J. Mayman, "Leg-length inequalities following total hip arthroplasty based on surgical technique," *Orthopedics*, vol. 36, no. 4, pp. e395–400, 2013.
- [240] V. K. Sarin, W. R. Pratt, and G. W. Bradley, "Accurate femur repositioning is critical during intraoperative total hip arthroplasty length and offset assessment," *The Journal of arthroplasty*, vol. 20, no. 7, pp. 887–891, 2005.
- [241] J. A. Williamson and F. W. Reckling, "Limb length discrepancy and related problems following total hip joint replacement," *Clinical orthopaedics and related research*, vol. 134, pp. 135–138, 1978.

-
- [242] J. Parvizi, P. F. Sharkey, G. A. Bissett, R. H. Rothman, and W. J. Hozack, "Surgical treatment of limb-length discrepancy following total hip arthroplasty," *The Journal of Bone & Joint Surgery*, vol. 85, no. 12, pp. 2310–2317, 2003.
- [243] M. G. Benedetti, F. Catani, E. Benedetti, L. Berti, A. Di Gioia, and S. Giannini, "To what extent does leg length discrepancy impair motor activity in patients after total hip arthroplasty?," *International orthopaedics*, vol. 34, no. 8, pp. 1115–1121, 2010.
- [244] B. Gurney, C. Mermier, R. Robergs, A. Gibson, and D. Rivero, "Effects of limb-length discrepancy on gait economy and lower-extremity muscle activity in older adults," *The Journal of Bone & Joint Surgery*, vol. 83, no. 6, pp. 907–915, 2001.
- [245] B. N. Edwards, H. S. Tullos, and P. C. Noble, "Contributory factors and etiology of sciatic nerve palsy in total hip arthroplasty," *Clinical orthopaedics and related research*, vol. 218, pp. 136–141, 1987.
- [246] T. P. Schmalzried, S. Noordin, and H. C. Amstutz, "Update on nerve palsy associated with total hip replacement," *Clinical orthopaedics and related research*, vol. 344, pp. 188–206, 1997.
- [247] T. Visuri, T. Lindholm, I. Antti-Poika, and M. Koskenvuo, "The role of overlength of the leg in aseptic loosening after total hip arthroplasty.," *Italian journal of orthopaedics and traumatology*, vol. 19, no. 1, pp. 107–111, 1992.
- [248] V. Swaminathan, M. Cartwright-Terry, J. Moorehead, A. Bowey, and S. Scott, "The effect of leg length discrepancy upon load distribution in the static phase (standing)," *Gait & posture*, vol. 40, no. 4, pp. 561–563, 2014.
- [249] P. Heidensohn, E. E. Hogue, J. D. Hohmann, D. Petersen, H. A. Riittimann, and Z. H. Wagner, "Leg length discrepancy the injured knee," 1977.
- [250] O. Friberg, "Leg length asymmetry in stress fractures. a clinical and radiological study.," *The Journal of sports medicine and physical fitness*, vol. 22, no. 4, pp. 485–488, 1982.
- [251] X. Hua, J. Li, Z. Jin, and J. Fisher, "The contact mechanics and occurrence of edge loading in modular metal-on-polyethylene total hip replacement during daily activities," *Medical engineering & physics*, vol. 38, no. 6, pp. 518–525, 2016.
- [252] J. Gofton and G. Trueman, "Studies in osteoarthritis of the hip: Part ii,* osteoarthritis of the hip and leg-length disparity," *Canadian Medical Association Journal*, vol. 104, no. 9, p. 791, 1971.

-
- [253] Y. Golightly, K. Allen, C. Helmick, J. Renner, and J. Jordan, "Symptoms of the knee and hip in individuals with and without limb length inequality," *Osteoarthritis and Cartilage*, vol. 17, no. 5, pp. 596–600, 2009.
- [254] S. Sabharwal and A. Kumar, "Methods for assessing leg length discrepancy," *Clinical orthopaedics and related research*, vol. 466, no. 12, pp. 2910–2922, 2008.
- [255] H. C. Woodfield, B. B. Gerstman, R. H. Olaisen, and D. F. Johnson, "Interexaminer reliability of supine leg checks for discriminating leg-length inequality," *Journal of manipulative and physiological therapeutics*, vol. 34, no. 4, pp. 239–246, 2011.
- [256] A. B. McWilliams, A. J. Grainger, P. J. O'Connor, A. C. Redmond, T. D. Stewart, and M. H. Stone, "Assessing reproducibility for radiographic measurement of leg length inequality after total hip replacement.," *Hip international: the journal of clinical and experimental research on hip pathology and therapy*, vol. 22, no. 5, pp. 539–544, 2011.
- [257] C. Heaver, J. St Mart, P. Nightingale, A. Sinha, and E. Davis, "Measuring leg length discrepancy using pelvic radiographs," in *Orthopaedic Proceedings*, vol. 94, pp. 178–178, Orthopaedic Proceedings, 2012.
- [258] M. Fessy, A. N'Diaye, J. Carret, and L. Fischer, "Locating the center of rotation of the hip," *Surgical and Radiologic Anatomy*, vol. 21, no. 4, pp. 247–250, 1999.
- [259] J. F. John and P. E. Fisher, "Radiographic determination of the anatomic hip joint center: a cadaver study," *Acta Orthopaedica*, vol. 65, no. 5, pp. 509–510, 1994.
- [260] C. S. Ranawat and J. Rodriguez, "Functional leg-length inequality following total hip arthroplasty," *The Journal of arthroplasty*, vol. 12, no. 4, pp. 359–364, 1997.
- [261] J. Robb, L. Rymaszewski, H. Bentley, and P. Donnan, "Reliability of the acetabular teardrop as a landmark," *Surgical and Radiologic Anatomy*, vol. 13, no. 3, pp. 181–185, 1991.
- [262] J. Albinana, J. Morcuende, and S. Weinstein, "The teardrop in congenital dislocation of the hip diagnosed late. a quantitative study," *J Bone Joint Surg Am*, vol. 78, no. 7, pp. 1048–55, 1996.
- [263] M. D. Schofer, T. Pressel, T. J. Heyse, J. Schmitt, and U. Boudriot, "Radiological determination of the anatomic hip centre from pelvic landmarks.," *Acta Orthopædica Belgica*, vol. 76, no. 4, p. 479, 2010.

-
- [264] S. Budenberg, A. Redmond, D. White, A. Grainger, P. OConnor, M. H. Stone, and T. D. Stewart, "Contact surface motion paths associated with leg length inequality following unilateral total hip replacement," *Proceedings of the Institution of Mechanical Engineers, Part H: Journal of Engineering in Medicine*, vol. 226, no. 12, pp. 968–974, 2012.
- [265] K. Kaufman, L. Miller, and D. Sutherland, "Gait asymmetry in patients with limb-length inequality," *Journal of Pediatric Orthopaedics*, vol. 16, no. 2, pp. 144–150, 1996.
- [266] P. Vink and H. Kamphuisen, "Leg length inequality, pelvic tilt and lumbar back muscle activity during standing," *Clinical Biomechanics*, vol. 4, no. 2, pp. 115–117, 1989.
- [267] G. Cummings, J. Scholz, and K. Barnes, "The effect of imposed leg length difference on pelvic bone symmetry," *Spine*, vol. 18, no. 3, pp. 368–373, 1993.
- [268] R. A. Brand and H. J. Yack, "Effects of leg length discrepancies on the forces at the hip joint," *Clinical orthopaedics and related research*, vol. 333, pp. 172–180, 1996.
- [269] S. C. White, L. A. Gilchrist, and B. E. Wilk, "Asymmetric limb loading with true or simulated leg-length differences," *Clinical orthopaedics and related research*, vol. 421, pp. 287–292, 2004.
- [270] D. Schuit, M. Adrian, and P. Pidcoe, "Effect of heel lifts on ground reaction force patterns in subjects with structural leg-length discrepancies," *Physical therapy*, vol. 69, no. 8, pp. 663–670, 1989.
- [271] Y. Zhang, W. He, T. Cheng, and X. Zhang, "Total hip arthroplasty: Leg length discrepancy affects functional outcomes and patients gait," *Cell biochemistry and biophysics*, vol. 72, no. 1, pp. 215–219, 2015.
- [272] R. A. Resende, R. N. Kirkwood, K. J. Deluzio, S. Cabral, and S. T. Fonseca, "Biomechanical strategies implemented to compensate for mild leg length discrepancy during gait," *Gait & Posture*, vol. 46, pp. 147–153, 2016.
- [273] R. B. Davis III, S. Ounpuu, D. Tyburski, and J. R. Gage, "A gait analysis data collection and reduction technique," *Human Movement Science*, vol. 10, no. 5, pp. 575–587, 1991.
- [274] A. Cereatti, V. Camomilla, G. Vannozzi, and A. Cappozzo, "Propagation of the hip joint centre location error to the estimate of femur vs pelvis orientation using a constrained or an unconstrained approach," *Journal of biomechanics*, vol. 40, no. 6, pp. 1228–1234, 2007.

-
- [275] G. Wu, S. Siegler, P. Allard, C. Kirtley, A. Leardini, D. Rosenbaum, M. Whittle, D. D DLima, L. Cristofolini, H. Witte, *et al.*, “Isb recommendation on definitions of joint coordinate system of various joints for the reporting of human joint motionpart i: ankle, hip, and spine,” *Journal of biomechanics*, vol. 35, no. 4, pp. 543–548, 2002.
- [276] M. Żuk and C. Pezowicz, “Kinematic analysis of a six-degrees-of-freedom model based on isb recommendation: A repeatability analysis and comparison with conventional gait model,” *Applied Bionics and Biomechanics*, vol. 2015, 2015.
- [277] A. L. Bell, R. A. Brand, and D. R. Pedersen, “Prediction of hip joint centre location from external landmarks,” *Human Movement Science*, vol. 8, no. 1, pp. 3–16, 1989.
- [278] A. L. Bell, R. A. Brand, and D. R. Pedersen, “Prediction of hip joint center location from external landmarks,” *Journal of Biomechanics*, vol. 20, no. 9, p. 913, 1987.
- [279] A. L. Bell, D. R. Pedersen, and R. A. Brand, “A comparison of the accuracy of several hip center location prediction methods,” *Journal of biomechanics*, vol. 23, no. 6, pp. 617–621, 1990.
- [280] M. Harrington, A. Zavatsky, S. Lawson, Z. Yuan, and T. Theologis, “Prediction of the hip joint centre in adults, children, and patients with cerebral palsy based on magnetic resonance imaging,” *Journal of biomechanics*, vol. 40, no. 3, pp. 595–602, 2007.
- [281] T. Andriacchi, G. Andersson, R. Fermier, D. Stern, and J. Galante, “A study of lower-limb mechanics during stair-climbing.,” *The Journal of Bone and Joint Surgery*, no. 62, pp. 749–57, 1980.
- [282] C. Tylkowski, S. Simon, and J. Mansour, “The frank stinchfield award paper. internal rotation gait in spastic cerebral palsy.,” *The hip*, p. 89, 1982.
- [283] K. M. Shea, M. W. Lenhoff, J. C. Otis, and S. I. Backus, “Validation of a method for location of the hip joint center,” *Gait & Posture*, vol. 5, no. 2, pp. 157–158, 1997.
- [284] J. T. Weinhandl and K. M. OConnor, “Assessment of a greater trochanter-based method of locating the hip joint center,” *Journal of biomechanics*, vol. 43, no. 13, pp. 2633–2636, 2010.
- [285] M. A. Hunt, T. B. Birmingham, T. R. Jenkyn, J. R. Giffin, and I. C. Jones, “Measures of frontal plane lower limb alignment obtained from static radiographs and dynamic gait analysis,” *Gait & posture*, vol. 27, no. 4, pp. 635–640, 2008.

-
- [286] J. L. Hicks and J. G. Richards, "Clinical applicability of using spherical fitting to find hip joint centers," *Gait & Posture*, vol. 22, no. 2, pp. 138–145, 2005.
- [287] G. K. Seidel, D. M. Marchinda, M. Dijkers, and R. W. Soutas-Little, "Hip joint center location from palpable bony landmarks: a cadaver study," *Journal of biomechanics*, vol. 28, no. 8, pp. 995–998, 1995.
- [288] S. S. H. U. Gamage and J. Lasenby, "New least squares solutions for estimating the average centre of rotation and the axis of rotation," *Journal of biomechanics*, vol. 35, no. 1, pp. 87–93, 2002.
- [289] T. F. Besier, D. L. Sturnieks, J. A. Alderson, and D. G. Lloyd, "Repeatability of gait data using a functional hip joint centre and a mean helical knee axis," *Journal of biomechanics*, vol. 36, no. 8, pp. 1159–1168, 2003.
- [290] S. J. Piazza, N. Okita, and P. R. Cavanagh, "Accuracy of the functional method of hip joint center location: effects of limited motion and varied implementation," *Journal of Biomechanics*, vol. 34, no. 7, pp. 967–973, 2001.
- [291] A. Cereatti, M. Donati, V. Camomilla, F. Margheritini, and A. Cappozzo, "Hip joint centre location: an ex vivo study," *Journal of Biomechanics*, vol. 42, no. 7, pp. 818–823, 2009.
- [292] K. Halvorsen, "Bias compensated least squares estimate of the center of rotation," *Journal of Biomechanics*, vol. 36, no. 7, pp. 999–1008, 2003.
- [293] S. J. Piazza, A. Erdemir, N. Okita, and P. R. Cavanagh, "Assessment of the functional method of hip joint center location subject to reduced range of hip motion," *Journal of Biomechanics*, vol. 37, no. 3, pp. 349–356, 2004.
- [294] R. A. Siston and S. L. Delp, "Evaluation of a new algorithm to determine the hip joint center," *Journal of Biomechanics*, vol. 39, no. 1, pp. 125–130, 2006.
- [295] F. Marin, H. Mannel, L. Claes, and L. Dürselen, "Accurate determination of a joint rotation center based on the minimal amplitude point method," *Computer Aided Surgery*, vol. 8, no. 1, pp. 30–34, 2003.
- [296] E. De Momi, N. Lopomo, P. Cerveri, S. Zaffagnini, M. R. Safran, and G. Ferrigno, "In-vitro experimental assessment of a new robust algorithm for hip joint centre estimation," *Journal of biomechanics*, vol. 42, no. 8, pp. 989–995, 2009.

-
- [297] T. Lu, "On the estimation of hip joint centre position in clinical gait analysis," *Biomedical Engineering Applications Basis Communications*, vol. 12, no. 2, pp. 89–95, 2000.
- [298] R. M. Ehrig, M. O. Heller, S. Kratzstein, G. N. Duda, A. Trepczynski, and W. R. Taylor, "The score residual: a quality index to assess the accuracy of joint estimations," *Journal of biomechanics*, vol. 44, no. 7, pp. 1400–1404, 2011.
- [299] M. H. Schwartz and A. Rozumalski, "A new method for estimating joint parameters from motion data," *Journal of biomechanics*, vol. 38, no. 1, pp. 107–116, 2005.
- [300] A. Leardini, A. Cappozzo, F. Catani, S. Toksvig-Larsen, A. Petitto, V. Sforza, G. Cassanelli, and S. Giannini, "Validation of a functional method for the estimation of hip joint centre location," *Journal of biomechanics*, vol. 32, no. 1, pp. 99–103, 1999.
- [301] H. Kainz, C. P. Carty, L. Modenese, R. N. Boyd, and D. G. Lloyd, "Estimation of the hip joint centre in human motion analysis: A systematic review," *Clinical Biomechanics*, vol. 30, no. 4, pp. 319–329, 2015.
- [302] M. S. Andersen, S. Mellon, G. Grammatopoulos, and H. S. Gill, "Evaluation of the accuracy of three popular regression equations for hip joint centre estimation using computerised tomography measurements for metal-on-metal hip resurfacing arthroplasty patients," *Gait & posture*, vol. 38, no. 4, pp. 1044–1047, 2013.
- [303] R. N. Kirkwood, E. G. Culham, and P. Costigan, "Radiographic and non-invasive determination of the hip joint center location: effect on hip joint moments," *Clinical Biomechanics*, vol. 14, no. 4, pp. 227–235, 1999.
- [304] C. McGibbon, P. Riley, and D. Krebs, "Comparison of hip center estimation using $i_{\bar{c}}$ in-vivo/ $i_{\bar{c}}$ and $i_{\bar{c}}$ ex-vivo/ $i_{\bar{c}}$ measurements from the same subject," *Clinical Biomechanics*, vol. 12, no. 7, pp. 491–495, 1997.
- [305] A. Peters, R. Baker, M. Morris, and M. Sangeux, "A comparison of hip joint centre localisation techniques with 3-dus for clinical gait analysis in children with cerebral palsy," *Gait & posture*, vol. 36, no. 2, pp. 282–286, 2012.
- [306] M. Sangeux, H. Pillet, and W. Skalli, "Which method of hip joint centre localisation should be used in gait analysis?," *Gait & posture*, vol. 40, no. 1, pp. 20–25, 2014.
- [307] M. Benedetti, F. Catani, A. Leardini, E. Pignotti, and S. Giannini, "Data management in gait analysis for clinical applications," *Clinical Biomechanics*, vol. 13, no. 3, pp. 204–215, 1998.

-
- [308] C. Angeloni, A. Cappozzo, F. Catani, and A. Leardini, “Quantification of relative displacement between bones and skin-and plate-mounted markers,” in *VIII Meeting on European Society of Biomechanics, Rome, Italy*, vol. 20, p. 279, 1992.
- [309] D. N. Bassett, G. Mantovani, M. Lamontagne, and G. Cerulli, “Variability of lower limbs kinematics influenced by marker set,” *Gait & Posture*, vol. 33, pp. S31–S32, 2011.
- [310] F. L. Buczek, M. J. Rainbow, K. M. Cooney, M. R. Walker, and J. O. Sanders, “Implications of using hierarchical and six degree-of-freedom models for normal gait analyses,” *Gait & posture*, vol. 31, no. 1, pp. 57–63, 2010.
- [311] “<https://gupea.ub.gu.se/bitstream/2077/22941/1/gupea2077229411.pdf>. 83,” Accessed July 2014.
- [312] J. Tan, *Advancing clinical gait analysis through technology and policy*. PhD thesis, Massachusetts Institute of Technology, 2009.
- [313] R. Baker, L. Finney, and J. Orr, “A new approach to determine the hip rotation profile from clinical gait analysis data,” *Human Movement Science*, vol. 18, no. 5, pp. 655–667, 1999.
- [314] T. D. Collins, S. N. Ghousayni, D. J. Ewins, and J. A. Kent, “A six degrees-of-freedom marker set for gait analysis: repeatability and comparison with a modified helen hayes set,” *Gait & posture*, vol. 30, no. 2, pp. 173–180, 2009.
- [315] F. L. Buczek, M. J. Rainbow, K. M. Cooney, M. R. Walker, and J. O. Sanders, “Comparing normal gait analyses using conventional and least-squares optimized tracking methods,” *International and Americal Societies of Biomechanics*, 2005.
- [316] A. Schmitz and D. G. Thelen, “Assessing performance of three types of biomechanical models applied to normal human gait,”
- [317] M. MuGhaffar, R. Abboud, and W. Wang, “A new lower limb model for motion analysis and its comparison with vicon plug-in-gait model,” *Gait & Posture*, vol. 36, p. S76, 2012.
- [318] A. Ferrari, M. G. Benedetti, E. Pavan, C. Frigo, D. Bettinelli, M. Rabuffetti, P. Crenna, and A. Leardini, “Quantitative comparison of five current protocols in gait analysis,” *Gait & posture*, vol. 28, no. 2, pp. 207–216, 2008.
- [319] R. Baker, “Gait analysis methods in rehabilitation [en línea],” *Journal of NeuroEngineering and Rehabilitation*.

-
- [320] K. Manal, I. McClay, S. Stanhope, J. Richards, and B. Galinat, “Comparison of surface mounted markers and attachment methods in estimating tibial rotations during walking: an in vivo study,” *Gait & posture*, vol. 11, no. 1, pp. 38–45, 2000.
- [321] A. Barré, B. M. Jolles, N. Theumann, and K. Aminian, “Soft tissue artifact distribution on lower limbs during treadmill gait: Influence of skin markers’ location on cluster design,” *Journal of biomechanics*, 2015.
- [322] M. S. Andersen, M. Damsgaard, J. Rasmussen, D. K. Ramsey, and D. L. Benoit, “A linear soft tissue artefact model for human movement analysis: proof of concept using in vivo data,” *Gait & posture*, vol. 35, no. 4, pp. 606–611, 2012.
- [323] T.-Y. Tsai, T.-W. Lu, M.-Y. Kuo, and H.-C. Hsu, “Quantification of three-dimensional movement of skin markers relative to the underlying bones during functional activities,” *Biomedical Engineering: Applications, Basis and Communications*, vol. 21, no. 03, pp. 223–232, 2009.
- [324] U. Della Croce, A. Leardini, L. Chiari, and A. Cappozzo, “Human movement analysis using stereophotogrammetry: Part 4: assessment of anatomical landmark misplacement and its effects on joint kinematics,” *Gait & posture*, vol. 21, no. 2, pp. 226–237, 2005.
- [325] J. Rasmussen, M. Damsgaard, and M. Voigt, “Muscle recruitment by the min/max criteria: a comparative numerical study,” *Journal of biomechanics*, vol. 34, no. 3, pp. 409–415, 2001.
- [326] C. Kirtley, “<http://www.clinicalgaitanalysis.com/teach-in/inverse-dynamics.html>,” Accessed September 2015.
- [327] E. Forster, U. Simon, P. Augat, and L. Claes, “Extension of a state-of-the-art optimization criterion to predict co-contraction,” *Journal of biomechanics*, vol. 37, no. 4, pp. 577–581, 2004.
- [328] S. Heintz, “Muscular forces from static optimization,” 2006.
- [329] V. C. Mow and R. Huiskes, *Basic orthopaedic biomechanics & mechano-biology*. Lippincott Williams & Wilkins, 2005.
- [330] B. I. Prilutsky and V. M. Zatsiorsky, “Optimization-based models of muscle coordination,” *Exercise and sport sciences reviews*, vol. 30, no. 1, p. 32, 2002.
- [331] F. C. Anderson and M. G. Pandy, “Static and dynamic optimization solutions for gait are practically equivalent,” *Journal of biomechanics*, vol. 34, no. 2, pp. 153–161, 2001.

-
- [332] F. C. Anderson and M. G. Pandy, "Individual muscle contributions to support in normal walking," *Gait & posture*, vol. 17, no. 2, pp. 159–169, 2003.
- [333] B. M. Nigg, B. R. MacIntosh, and J. Mester, *Biomechanics and biology of movement*. Human Kinetics, 2000.
- [334] B. Koopman, H. J. Grootenboer, and H. J. de Jongh, "An inverse dynamics model for the analysis, reconstruction and prediction of bipedal walking," *Journal of biomechanics*, vol. 28, no. 11, pp. 1369–1376, 1995.
- [335] M. R. Pierrynowski and J. B. Morrison, "Estimating the muscle forces generated in the human lower extremity when walking: a physiological solution," *Mathematical Biosciences*, vol. 75, no. 1, pp. 43–68, 1985.
- [336] E. Forster, *Predicting muscle forces in the human lower limb during locomotion*. VDI-Verlag, 2004.
- [337] T. A. Correa, K. M. Crossley, H. J. Kim, and M. G. Pandy, "Contributions of individual muscles to hip joint contact force in normal walking," *Journal of biomechanics*, vol. 43, no. 8, pp. 1618–1622, 2010.
- [338] "<http://www.anybodytech.com/fileadmin/anybody/docs/tutorials/>," Accessed July 2012.
- [339] D. E. Hardt, "Determining muscle forces in the leg during normal human walkingan application and evaluation of optimization methods," *Journal of Biomechanical Engineering*, vol. 100, no. 2, pp. 72–78, 1978.
- [340] D. Pedersen, R. Brand, C. Cheng, and J. Arora, "Direct comparison of muscle force predictions using linear and nonlinear programming," *Journal of Biomechanical Engineering*, vol. 109, no. 3, pp. 192–199, 1987.
- [341] "<http://www.anybodytech.com/index.php?id=926>," Accessed July 2012.
- [342] W. Herzog and P. Binding, "Cocontraction of pairs of antagonistic muscles: analytical solution for planar static nonlinear optimization approaches," *Mathematical biosciences*, vol. 118, no. 1, pp. 83–95, 1993.
- [343] M. Damsgaard, S. Christensen, and J. Rasmussen, "An efficient numerical algorithm for solving the muscle recruitment problem in inverse dynamics simulations," in *International Society of Biomechanics, XVIIIth Congress, July 8-13, 2001, Zurich, Switzerland*, 2001.

-
- [344] "<http://www.anybodytech.com/fileadmin/downloads/xjiang2011thesisnjit.pdf>," Accessed July 2012.
- [345] J. Rasmussen, M. de Zee, J. Dahl, and M. Damsgaard, "Salient properties of a combined minimum fatigue and quadratic muscle recruitment criterion,"
- [346] A. Murai, K. Kurosaki, K. Yamane, and Y. Nakamura, "Computationally fast estimation of muscle tension for realtime bio-feedback," in *Engineering in Medicine and Biology Society, 2009. EMBC 2009. Annual International Conference of the IEEE*, pp. 6546–6549, IEEE, 2009.
- [347] Y. Nakamura, K. Yamane, Y. Fujita, and I. Suzuki, "Somatosensory computation for man-machine interface from motion-capture data and musculoskeletal human model," *Robotics, IEEE Transactions on*, vol. 21, no. 1, pp. 58–66, 2005.
- [348] R. Raikova, "Prediction of individual muscle forces using lagrange multipliers methoda model of the upper human limb in the sagittal plane: I. theoretical considerations," *Computer Methods in Biomechanics and Biomedical Engineering*, vol. 3, no. 2, pp. 95–107, 2000.
- [349] R. Raikova and B. Prilutsky, "Sensitivity of predicted muscle forces to parameters of the optimization-based human leg model revealed by analytical and numerical analyses," *Journal of Biomechanics*, vol. 34, no. 10, pp. 1243–1255, 2001.
- [350] L. Modenese, A. Phillips, and A. Bull, "An open source lower limb model: Hip joint validation," *Journal of biomechanics*, vol. 44, no. 12, pp. 2185–2193, 2011.
- [351] "<http://www.anybodytech.com/index.php?id=927>," Accessed July 2012.
- [352] R. D. Crowninshield and R. A. Brand, "A physiologically based criterion of muscle force prediction in locomotion," *Journal of biomechanics*, vol. 14, no. 11, pp. 793–801, 1981.
- [353] J. Challis and D. Kerwin, "An analytical examination of muscle force estimations using optimization techniques," *Proceedings of the Institution of Mechanical Engineers, Part H: Journal of Engineering in Medicine*, vol. 207, no. 3, pp. 139–148, 1993.
- [354] "<http://www.anybodytech.com/index.php?id=928>," Accessed July 2012.
- [355] M. de Zee, S. Christensen, M. Damsgaard, and J. Rasmussen, "Anybody–musculo-skeletal modelling system based on inverse dynamics and beyond,"
- [356] "<http://www.anybodytech.com/684.0.html>," Accessed July 2012.

-
- [357] D. Cleather and A. Bull, “The development of lower limb musculoskeletal models with clinical relevance is dependent upon the fidelity of the mathematical description of the lower limb. part 1: equations of motion,” *Proceedings of the Institution of Mechanical Engineers, Part H: Journal of Engineering in Medicine*, vol. 226, no. 2, pp. 120–132, 2012.
- [358] S. Blemker, D. Asakawa, G. Gold, and S. Delp, “Image-based musculoskeletal modeling: Applications, advances, and future opportunities,” *Journal of magnetic resonance imaging*, vol. 25, no. 2, pp. 441–451, 2007.
- [359] M. A. Sherman, A. Seth, and S. L. Delp, “Simbody: multibody dynamics for biomedical research,” *Procedia Iutam*, vol. 2, pp. 241–261, 2011.
- [360] D. Thelen, F. Anderson, and S. Delp, “Generating dynamic simulations of movement using computed muscle control,” *Journal of Biomechanics*, vol. 36, no. 3, pp. 321–328, 2003.
- [361] T. Kepple, H. Sommer III, K. Siegel, and S. Stanhope, “A three-dimensional musculoskeletal database for the lower extremities,” *Journal of biomechanics*, vol. 31, no. 1, pp. 77–80, 1997.
- [362] L. Scheys, A. Van Campenhout, A. Spaepen, P. Suetens, and I. Jonkers, “Personalized mr-based musculoskeletal models compared to rescaled generic models in the presence of increased femoral anteversion: effect on hip moment arm lengths,” *Gait & posture*, vol. 28, no. 3, pp. 358–365, 2008.
- [363] S. S. Blemker, P. M. Pinsky, and S. L. Delp, “A 3d model of muscle reveals the causes of nonuniform strains in the biceps brachii,” *Journal of biomechanics*, vol. 38, no. 4, pp. 657–665, 2005.
- [364] “<http://www.anybodytech.com/fileadmin/anybody/docs/tutorials/>,” Accessed January 2013.
- [365] A. Agur, V. Ng-Thow-Hing, K. Ball, E. Fiume, and N. McKee, “Documentation and three-dimensional modelling of human soleus muscle architecture,” *Clinical Anatomy*, vol. 16, no. 4, pp. 285–293, 2003.
- [366] S. R. Ward, C. M. Eng, L. H. Smallwood, and R. L. Lieber, “Are current measurements of lower extremity muscle architecture accurate?,” *Clinical orthopaedics and related research*, vol. 467, no. 4, pp. 1074–1082, 2009.

-
- [367] V. Carbone, M. Van der Krogt, H. Koopman, and N. Verdonschot, “Sensitivity of subject-specific models to errors in musculo-skeletal geometry,” *Journal of biomechanics*, vol. 45, no. 14, pp. 2476–2480, 2012.
- [368] L. Schutte, S. Hayden, and J. Gage, “Lengths of hamstrings and psoas muscles during crouch gait: effects of femoral anteversion,” *Journal of orthopaedic research*, vol. 15, no. 4, pp. 615–621, 1997.
- [369] L. Scheys, K. Desloovere, P. Suetens, and I. Jonkers, “Level of subject-specific detail in musculoskeletal models affects hip moment arm length calculation during gait in pediatric subjects with increased femoral anteversion,” *Journal of biomechanics*, vol. 44, no. 7, pp. 1346–1353, 2011.
- [370] L. Scheys, K. Desloovere, A. Spaepen, P. Suetens, and I. Jonkers, “Calculating gait kinematics using mr-based kinematic models,” *Gait & posture*, vol. 33, no. 2, pp. 158–164, 2011.
- [371] S. Delp, A. Komattu, and R. Wixson, “Superior displacement of the hip in total joint replacement: Effects of prosthetic neck length, neck-stem angle, and anteversion angle on the moment-generating capacity of the muscles,” *Journal of orthopaedic research*, vol. 12, no. 6, pp. 860–870, 1994.
- [372] G. Lenaerts, F. De Groote, B. Demeulenaere, M. Mulier, G. Van der Perre, A. Spaepen, and I. Jonkers, “Subject-specific hip geometry affects predicted hip joint contact forces during gait,” *Journal of biomechanics*, vol. 41, no. 6, pp. 1243–1252, 2008.
- [373] N. Arjmand, A. Shirazi-Adl, and B. Bazrgari, “Wrapping of trunk thoracic extensor muscles influences muscle forces and spinal loads in lifting tasks,” *Clinical Biomechanics*, vol. 21, no. 7, pp. 668–675, 2006.
- [374] G. Lenaerts, W. Bartels, F. Gelaude, M. Mulier, A. Spaepen, G. Van der Perre, and I. Jonkers, “Subject-specific hip geometry and hip joint centre location affects calculated contact forces at the hip during gait,” *Journal of biomechanics*, vol. 42, no. 9, pp. 1246–1251, 2009.
- [375] J. Reinbolt, J. Schutte, B. Fregly, B. Koh, R. Haftka, A. George, and K. Mitchell, “Determination of patient-specific multi-joint kinematic models through two-level optimization,” *Journal of biomechanics*, vol. 38, no. 3, pp. 621–626, 2005.
- [376] S. Delp and W. Maloney, “Effects of hip center location on the moment-generating capacity of the muscles,” *Journal of biomechanics*, vol. 26, no. 4-5, pp. 485–499, 1993.

-
- [377] J. Chadwick, D. Haumann, and R. Parent, “Layered construction for deformable animated characters,” in *ACM Siggraph Computer Graphics*, vol. 23, pp. 243–252, ACM, 1989.
- [378] D. Lee, M. Glueck, A. Khan, E. Fiume, and K. Jackson, “A survey of modeling and simulation of skeletal muscle,” tech. rep., Citeseer, 2009.
- [379] M. Mansouri and J. Reinbolt, “A platform for dynamic simulation and control of movement based on opensim and matlab,” *Journal of biomechanics*, 2012.
- [380] M. Lund, M. de Zee, M. Andersen, and J. Rasmussen, “On validation of multibody musculoskeletal models,” *Proceedings of the Institution of Mechanical Engineers, Part H: Journal of Engineering in Medicine*, vol. 226, no. 2, pp. 82–94, 2012.
- [381] R. Dumas, E. Nicol, and L. Cheze, “Influence of the 3d inverse dynamic method on the joint forces and moments during gait,” *Journal of biomechanical engineering*, vol. 129, p. 786, 2007.
- [382] R. Zoroofi, T. Nishii, Y. Sato, N. Sugano, H. Yoshikawa, and S. Tamura, “Segmentation of avascular necrosis of the femoral head using 3-d mr images,” *Computerized medical imaging and graphics*, vol. 25, no. 6, pp. 511–521, 2001.
- [383] T. Pressel and M. Lengsfeld, “Functions of hip joint muscles,” *Medical engineering & physics*, vol. 20, no. 1, pp. 50–56, 1998.
- [384] R. Dumas, F. Moissenet, X. Gasparutto, and L. Cheze, “Influence of joint models on lower-limb musculo-tendon forces and three-dimensional joint reaction forces during gait,” *Proceedings of the Institution of Mechanical Engineers, Part H: Journal of Engineering in Medicine*, vol. 226, no. 2, pp. 146–160, 2012.
- [385] D. Cleather and A. Bull, “An optimization-based simultaneous approach to the determination of muscular, ligamentous, and joint contact forces provides insight into musculoligamentous interaction,” *Annals of biomedical engineering*, pp. 1–10, 2011.
- [386] I. Jonkers, N. Sauwen, G. Lenaerts, M. Mulier, G. Van der Perre, and S. Jaecques, “Relation between subject-specific hip joint loading, stress distribution in the proximal femur and bone mineral density changes after total hip replacement,” *Journal of biomechanics*, vol. 41, no. 16, pp. 3405–3413, 2008.
- [387] M. K. Horsman, H. Koopman, F. Van der Helm, L. P. Prosé, and H. Veeger, “Morphological muscle and joint parameters for musculoskeletal modelling of the lower extremity,” *Clinical biomechanics*, vol. 22, no. 2, pp. 239–247, 2007.

-
- [388] J. M. Thompson and M. K. Thompson, "A proposal for the calculation of wear," in *Proceedings Of The 2006 International Ansys Users Conference & Exhibition, Pittsburgh, Pa*, 2006.
- [389] F. Liu, A. Galvin, Z. Jin, and J. Fisher, "A new formulation for the prediction of polyethylene wear in artificial hip joints," *Proceedings of the Institution of Mechanical Engineers, Part H: Journal of Engineering in Medicine*, vol. 225, no. 1, pp. 16–24, 2011.
- [390] A. Abdelgaied, F. Liu, C. Brockett, L. Jennings, J. Fisher, and Z. Jin, "Computational wear prediction of artificial knee joints based on a new wear law and formulation," *Journal of biomechanics*, vol. 44, no. 6, pp. 1108–1116, 2011.
- [391] L. Kang, A. L. Galvin, T. D. Brown, Z. Jin, and J. Fisher, "Quantification of the effect of cross-shear on the wear of conventional and highly cross-linked uhmwpe," *Journal of biomechanics*, vol. 41, no. 2, pp. 340–346, 2008.
- [392] I. M. Hutchings, *Friction, lubrication and wear of artificial joints*. John Wiley & Sons, 2003.
- [393] D. Bennett, J. Orr, D. Beverland, and R. Baker, "The influence of shape and sliding distance of femoral head movement loci on the wear of acetabular cups in total hip arthroplasty," *Proceedings of the Institution of Mechanical Engineers, Part H: Journal of Engineering in Medicine*, vol. 216, no. 6, pp. 393–402, 2002.
- [394] "<http://fp.optics.arizona.edu/optomech/>," Accessed July 2016.
- [395] "<http://www.amesweb.info/hertziancontact/images/contactconfigurations.jpg>," Accessed July 2016.
- [396] A. Wang, "A unified theory of wear for ultra-high molecular weight polyethylene in multi-directional sliding," *Wear*, vol. 248, no. 1, pp. 38–47, 2001.
- [397] W. H. Harris, "The problem is osteolysis.," *Clinical orthopaedics and related research*, vol. 311, pp. 46–53, 1995.
- [398] T. Schmalzried, M. Jasty, and W. H. Harris, "Periprosthetic bone loss in total hip arthroplasty. polyethylene wear debris and the concept of the effective joint space.," *J Bone Joint Surg Am*, vol. 74, no. 6, pp. 849–863, 1992.
- [399] L. Knight, A. Galvin, J. Jeffers, A. Hopkins, J. Fisher, and M. Taylor, "Influence of cross-shear on the wear of polyethylene: A finite element study," *Transactions of the Orthopaedic Research Society*, p. 0987, 2005.

-
- [400] A. Wang, C. Stark, and J. Dumbleton, “Mechanistic and morphological origins of ultra-high molecular weight polyethylene wear debris in total joint replacement prostheses,” *Proceedings of the Institution of Mechanical Engineers, Part H: Journal of Engineering in Medicine*, vol. 210, no. 3, pp. 141–155, 1996.
- [401] C. Bragdon, D. O’Connor, J. Lowenstein, M. Jasty, and W. Syniuta, “The importance of multidirectional motion on the wear of polyethylene,” *Proceedings of the Institution of Mechanical Engineers, Part H: Journal of Engineering in Medicine*, vol. 210, no. 3, pp. 157–165, 1996.
- [402] A. Galvin, L. Kang, J. Tipper, M. Stone, E. Ingham, Z. Jin, and J. Fisher, “Wear of crosslinked polyethylene under different tribological conditions,” *Journal of Materials Science: Materials in Medicine*, vol. 17, no. 3, pp. 235–243, 2006.
- [403] B. S. Ramamurti, C. R. Bragdon, D. O. O’Connor, J. D. Lowenstein, M. Jasty, D. M. Estok, and W. H. Harris, “Loci of movement of selected points on the femoral head during normal gait: three-dimensional computer simulation,” *The Journal of arthroplasty*, vol. 11, no. 7, pp. 845–852, 1996.
- [404] P. Barbour, M. Stone, and J. Fisher, “A hip joint simulator study using simplified loading and motion cycles generating physiological wear paths and rates,” *Proceedings of the Institution of Mechanical Engineers, Part H: Journal of Engineering in Medicine*, vol. 213, no. 6, pp. 455–467, 1999.
- [405] D. B. Bennett, J. F. Orr, and R. Baker, “Movement loci of selected points on the femoral head for individual total hip arthroplasty patients using three-dimensional computer simulation,” *The Journal of arthroplasty*, vol. 15, no. 7, pp. 909–915, 2000.
- [406] J. Sinclair, J. Hebron, H. Hurst, and P. Taylor, “The influence of different cardan sequences on three-dimensional cycling kinematics,” *Human Movement*, vol. 14, no. 4, pp. 334–339, 2013.
- [407] S. H. J. Sinclair, S. Atkins Taylor, “The influence of cardan rotation sequence on 3-d kinematic parameters and planar cross-talk during maximal out of hand rugby kicking,” 2014. (2014) Bases 2013 Abstracts, *Journal of Sports Sciences*, 32:sup1, s4-s116, DOI: 10.1080/02640414.2014.896604.
- [408] S. Davey, J. Orr, F. Buchanan, J. Nixon, and D. Bennett, “Measurement of molecular orientation in retrieved ultra-high-molecular-weight polyethylene (uhmwpe) hip sockets using fourier-transform infrared spectroscopy,” *Strain*, vol. 40, no. 4, pp. 203–210, 2004.

-
- [409] B. J. Hamrock, “Fluid film lubrication with applications to machine elements,” in *Fundamentals of Tribology and Bridging the Gap Between the Macro-and Micro/Nanoscales*, pp. 747–765, Springer, 2001.
- [410] T. Stewart, “Tribology of artificial joints,” *Orthopaedics and Trauma*, vol. 24, no. 6, pp. 435–440, 2010.
- [411] G. Higginson, “Squeeze films between compliant solids,” *Wear*, vol. 46, no. 2, pp. 387–395, 1978.
- [412] Z. Jin, D. Dowson, and J. Fisher, “Analysis of fluid film lubrication in artificial hip joint replacements with surfaces of high elastic modulus,” *Proceedings of the Institution of Mechanical Engineers, Part H: Journal of Engineering in Medicine*, vol. 211, no. 3, pp. 247–256, 1997.
- [413] “<http://docs.exdat.com/docs/index138520.html>,” Accessed June 2016.
- [414] T. Foti, J. R. Davids, and A. Bagley, “A biomechanical analysis of gait during pregnancy*,” *The Journal of Bone & Joint Surgery*, vol. 82, no. 5, pp. 625–625, 2000.
- [415] S. P. Nair, S. Gibbs, G. Arnold, R. Abboud, and W. Wang, “A method to calculate the centre of the ankle joint: A comparison with the vicon plug-in-gait model,” *Clinical Biomechanics*, vol. 25, no. 6, pp. 582–587, 2010.
- [416] “<https://www.motion-labs.com/>,” Accessed November 2016.
- [417] “<http://www.analisedemarcha.com/papers/manutencao/manuais/>,” Accessed November 2016.
- [418] “<http://www.footache.com/anatomyofthefootankle.html>,” Accessed February 2016.
- [419] “<http://www.nanda-books.com/2012/11/why-pelvis-in-men-and-women-different.html>,” Accessed March 2016.
- [420] M. S. Andersen, M. Damsgaard, B. MacWilliams, and J. Rasmussen, “A computationally efficient optimisation-based method for parameter identification of kinematically determinate and over-determinate biomechanical systems,” *Computer methods in biomechanics and biomedical engineering*, vol. 13, no. 2, pp. 171–183, 2010.
- [421] “<http://medical-dictionary.thefreedictionary.com/oxford+hip+score>,” Accessed November 2015.

-
- [422] F. Pierchon, H. Migaud, A. Duquennoy, and C. Fontaine, “[radiologic evaluation of the rotation center of the hip],” *Revue de chirurgie orthopedique et reparatrice de l’appareil moteur*, vol. 79, no. 4, pp. 281–284, 1992.
- [423] C. S. Ranawat, L. D. Dorr, and A. E. Inglis, “Total hip arthroplasty in protrusio acetabuli of rheumatoid arthritis,” *The Journal of Bone & Joint Surgery*, vol. 62, no. 7, pp. 1059–1065, 1980.
- [424] E. Genda, N. Iwasaki, G. Li, B. A. MacWilliams, P. J. Barrance, and E. Y. Chao, “Normal hip joint contact pressure distribution in single-leg standing effect of gender and anatomic parameters,” *Journal of Biomechanics*, vol. 34, no. 7, pp. 895–905, 2001.
- [425] J. A. Bjarnason and O. Reikeras, “Changes of center of rotation and femoral offset in total hip arthroplasty,” *Annals of Translational Medicine*, vol. 3, no. 22, 2015.
- [426] A. Durandet, P.-L. Ricci, A. H. Saveh, Q. Vanat, B. Wang, I. Esat, and M. Chizari, “Radiographic analysis of lower limb axial alignments,” in *Proceedings of the World Congress on Engineering*, vol. 2, 2013.
- [427] E. Pluot, E. Davis, M. Revell, A. Davies, and S. James, “Hip arthroplasty. part 2: normal and abnormal radiographic findings,” *Clinical radiology*, vol. 64, no. 10, pp. 961–971, 2009.
- [428] S. O’Brien, “Femoral offset in total hip replacement: A study of anatomical offset in the northern ireland population,” *International Journal of Orthopaedic and Trauma Nursing*, vol. 18, no. 3, pp. 162–169, 2014.
- [429] B. McGrory, B. Morrey, T. Cahalan, K. An, and M. Cabanela, “Effect of femoral offset on range of motion and abductor muscle strength after total hip arthroplasty,” *Journal of Bone & Joint Surgery, British Volume*, vol. 77, no. 6, pp. 865–869, 1995.
- [430] D. P. Sakalkale, P. F. Sharkey, K. Eng, W. J. Hozack, and R. H. Rothman, “Effect of femoral component offset on polyethylene wear in total hip arthroplasty,” *Clinical orthopaedics and related research*, vol. 388, pp. 125–134, 2001.
- [431] G. Pasquier, G. Ducharne, E. S. Ali, F. Giraud, A. Mouttet, and E. Durante, “Total hip arthroplasty offset measurement: is ct scan the most accurate option?,” *Orthopaedics & Traumatology: Surgery & Research*, vol. 96, no. 4, pp. 367–375, 2010.

-
- [432] H. Davies, J. Foote, and R. F. Spencer, "Accuracy of femoral templating in reproducing anatomical femoral offset in total hip replacement.," *Hip international: the journal of clinical and experimental research on hip pathology and therapy*, vol. 17, no. 3, pp. 155–159, 2006.
- [433] I. Charlton, P. Tate, P. Smyth, and L. Roren, "Repeatability of an optimised lower body model," *Gait & Posture*, vol. 20, no. 2, pp. 213–221, 2004.
- [434] N. Pennington, A. Redmond, T. Stewart, and M. Stone, "The impact of surgeon handedness in total hip replacement," *The Annals of The Royal College of Surgeons of England*, vol. 96, no. 6, pp. 437–441, 2014.
- [435] S. B. Michaud, S. A. Gard, and D. S. Childress, "A preliminary investigation of pelvic obliquity patterns during gait in persons with transtibial and transfemoral amputation," *Journal of rehabilitation research and development*, vol. 37, no. 1, pp. 1–10, 2000.
- [436] A. Obialor, C. Ihentuge, and F. Akpuaka, "Determination of height using femur length in adult population of oguta local government area of imo state nigeria," *The FASEB Journal*, vol. 29, no. 1 Supplement, p. LB19, 2015.
- [437] R. Robinson, W. Herzog, and B. Nigg, "Use of force platform variables to quantify the effects of chiropractic manipulation on gait symmetry.," *Journal of manipulative and physiological therapeutics*, vol. 10, no. 4, pp. 172–176, 1987.
- [438] "<http://www.discussfastpitch.com/softball-hitting-technical/12372-rear-leg-7.html>," Accessed November 2015.
- [439] "<http://sustainableexercise.com/2014/08/11/exercise-of-the-week-hip-flexor-pulses/>," Accessed November 2015.
- [440] <http://forums.sherdog.com/forums/f12/williams-guard-compendium-gif-image-heavy-long-post-2650585/>. Accessed November 2015.
- [441] "<http://www.gla.ac.uk/t4/fbls/files/fab/images/anatomy/kneeflex.gif>," Accessed November 2015.
- [442] "www.thinglink.com," Accessed November 2015.
- [443] G. Bovi, M. Rabuffetti, P. Mazzoleni, and M. Ferrarin, "A multiple-task gait analysis approach: kinematic, kinetic and emg reference data for healthy young and adult subjects," *Gait & posture*, vol. 33, no. 1, pp. 6–13, 2011.

-
- [444] D. Davis, S. Öunpuu, P. DeLuca, and M. Romness, “Clinical gait analysis and its role in treatment decision-making,” *Medscape General Medicine*, 2002.
- [445] M. C. Morais Filho, R. A. d. Reis, and C. M. Kawamura, “Evaluation of ankle and knee movement pattern during maturation of normal gait,” *Acta Ortopédica Brasileira*, vol. 18, no. 1, pp. 23–25, 2010.
- [446] S. Singer, S. Klejman, E. Pinsker, J. Houck, and T. Daniels, “Ankle arthroplasty and ankle arthrodesis: gait analysis compared with normal controls,” *The Journal of Bone & Joint Surgery*, vol. 95, no. 24, p. e191, 2013.
- [447] Á. Illyés, Z. Bejek, I. Szlávik, R. Paróczai, and R. Kiss, “Three-dimensional gait analysis after unilateral cemented total hip arthroplasty,” *Physical Education and Sport*, vol. 4, no. 1, pp. 27–34, 2006.
- [448] R. M. Queen, J. S. Appleton, R. J. Butler, E. T. Newman, S. S. Kelley, D. E. Attarian, and M. P. Bolognesi, “Total hip arthroplasty surgical approach does not alter postoperative gait mechanics one year after surgery,” *PM&R*, vol. 6, no. 3, pp. 221–226, 2014.
- [449] M. Pospischill, A. Kranzl, B. Attwenger, and K. Knahr, “Minimally invasive compared with traditional transgluteal approach for total hip arthroplasty,” *The Journal of Bone & Joint Surgery*, vol. 92, no. 2, pp. 328–337, 2010.
- [450] N. Hashimoto, M. Ando, T. Yayama, K. Uchida, S. Kobayashi, K. Negoro, and H. Baba, “Dynamic analysis of the resultant force acting on the hip joint during level walking,” *Artificial organs*, vol. 29, no. 5, pp. 387–392, 2005.
- [451] “<http://www.clinicalgaitanalysis.com/faq/hayes/>,” Accessed January 2016.
- [452] D. Kiernan, A. Malone, T. O’Brien, and C. Simms, “The clinical impact of hip joint centre regression equation error on kinematics and kinetics during paediatric gait,” *Gait & posture*, vol. 41, no. 1, pp. 175–179, 2015.
- [453] A. Chohan, P. Dey, C. Sutton, D. Thewlis, and J. Richards, “Do different methods of hip joint centre location impact on kinetics and kinematics in obese adults?,” *Gait & Posture*, no. 38, p. S109, 2013.
- [454] R. Stagni, A. Leardini, A. Cappozzo, M. G. Benedetti, and A. Cappello, “Effects of hip joint centre mislocation on gait analysis results,” *Journal of Biomechanics*, vol. 33, no. 11, pp. 1479–1487, 2000.

-
- [455] R. Mahaffey, *Biomechanics of the paediatric foot and lower limb: associations with adiposity*. PhD thesis, Citeseer, 2013.
- [456] S. I. Kim and T. S. Suh, *World Congress of Medical Physics and Biomedical Engineering 2006: August 27-September 1, 2006 COEX Seoul, Korea*, vol. 14. Springer Science & Business Media, 2007.
- [457] J. Barnett, “Motions in Space,” Master’s thesis, School of Mechanical Engineering, UK, 2009.
- [458] M. Turell, A. Wang, and A. Bellare, “Quantification of the effect of cross-path motion on the wear rate of ultra-high molecular weight polyethylene,” *Wear*, vol. 255, no. 7, pp. 1034–1039, 2003.
- [459] D. Bennett, L. Humphreys, S. O’Brien, C. Kelly, J. Orr, and D. E. Beverland, “The influence of wear paths produced by hip replacement patients during normal walking on wear rates,” *Journal of Orthopaedic Research*, vol. 26, no. 9, pp. 1210–1217, 2008.
- [460] D. Bennett, L. Humphreys, S. O’Brien, C. Kelly, J. Orr, and D. Beverland, “Wear paths produced by individual hip-replacement patients: a large-scale, long-term follow-up study,” *Journal of biomechanics*, vol. 41, no. 11, pp. 2474–2482, 2008.
- [461] Q. Meng, F. Liu, J. Fisher, and Z. Jin, “Contact mechanics and lubrication analyses of ceramic-on-metal total hip replacements,” *Tribology International*, vol. 63, pp. 51–60, 2013.
- [462] H. D. Atkinson, K. S. Johal, C. Willis-Owen, S. Zadow, and R. D. Oakeshott, “Differences in hip morphology between the sexes in patients undergoing hip resurfacing,” *Journal of orthopaedic surgery and research*, vol. 5, no. 1, p. 1, 2010.
- [463] “<http://www.bonepreservation.com/download/welshbhs2015lld.pdf>,” Accessed December 2015.
- [464] A. Sykes, J. Hill, J. Orr, P. Humphreys, A. Rooney, E. Morrow, and D. Beverland, “Patients’ perception of leg length discrepancy post total hip arthroplasty,” *Hip international: the journal of clinical and experimental research on hip pathology and therapy*, vol. 25, no. 5, pp. 452–456, 2015.
- [465] J. V. Bono, *Revision total hip arthroplasty*. Springer Science & Business Media, 1999.
- [466] J. Li, *Computational Biomechanics/Biotribological Modelling of Natural and Artificial Hip Joints*. PhD thesis, University of Leeds, 2013.

- [467] D. Laroche, A. Duval, C. Morisset, J.-N. Beis, P. dAthis, J.-F. Maillefert, and P. Ornetti, "Test-retest reliability of 3d kinematic gait variables in hip osteoarthritis patients," *Osteoarthritis and cartilage*, vol. 19, no. 2, pp. 194–199, 2011.
- [468] V. Maynard, A. Bakheit, J. Oldham, and J. Freeman, "Intra-rater and inter-rater reliability of gait measurements with coda mpx30 motion analysis system," *Gait & posture*, vol. 17, no. 1, pp. 59–67, 2003.
- [469] A. Bhave, D. Paley, and J. E. Herzenberg, "Improvement in gait parameters after lengthening for the treatment of limb-length discrepancy*," *The Journal of Bone & Joint Surgery*, vol. 81, no. 4, pp. 529–34, 1999.
- [470] T. P. Schmalzried, H. C. Amstutz, and F. J. Dorey, "Nerve palsy associated with total hip replacement. risk factors and prognosis.," *J Bone Joint Surg Am*, vol. 73, no. 7, pp. 1074–1080, 1991.
- [471] A. Bhave, M. Mont, S. Tennis, M. Nickey, R. Starr, and G. Etienne, "Functional problems and treatment solutions after total hip and knee joint arthroplasty," *The Journal of Bone & Joint Surgery*, vol. 87, no. suppl 2, pp. 9–21, 2005.
- [472] B. Neville and R. Goodman, *Congenital hemiplegia*. Cambridge University Press, 2000.

15 Appendix I

Table 24: LLI and Happy THR patients demographics and anthropometrics

Patient ID	Sex	BMI	Height (m)
LLI 1	f	23.8	1.64
LLI 2	m	28.8	1.79
LLI 3	f	28.8	1.52
LLI 4	f	28.3	1.51
LLI 5	m	27.6	1.70
LLI 6	f	31.2	1.55
LLI 7	f	20.1	1.61
LLI 8	f	22.1	1.72
LLI 9	f	24.6	1.59
LLI 10	f	30.6	1.64
LLI 11	f	29.7	1.51
LLI 12	f	38.6	1.60
LLI 13	No Data	No Data	No Data
LLI 14	f	24.6	1.58
LLI 15	f	28.3	1.56
LLI 16	f	26.0	1.57
LLI 17	f	27.5	1.52
LLI 18	f	33.3	1.71
LLI 19	f	29.6	1.55
LLI 20	m	24.3	1.74
LLI 21	f	24.4	1.62
LLI 22	f	27.4	1.62
LLI 23	m	30.9	1.68
LLI 24	m	29.1	1.65
LLI 25	f	36.3	1.62
LLI 26	f	37.4	1.75
Happy THR 1	m	30.8	1.86
Happy THR 2	m	23.5	1.77
Happy THR 3	m	32.6	1.80
Happy THR 4	m	31.7	1.61
Happy THR 5	f	26.9	1.60
Happy THR 6	m	33.2	1.74
Happy THR 7	m	44.1	1.64
Happy THR 8	f	25.2	1.57
Happy THR 9	m	26.0	1.77
Happy THR 10	f	22.1	1.66
Happy THR 11	f	28.7	1.54
Happy THR 12	m	27.1	1.84
Happy THR 13	m	37.0	1.74
Happy THR 14	m	37.3	1.70

Table 25: Normal patients demographics and anthropometrics

Patient ID	Sex	BMI	Height (m)
N1	m	21.0	1.76
N2	m	20.1	1.76
N3	f	27.4	1.67
N4	m	31.8	1.73
N5	f	25.1	1.64
N6	m	21.9	1.76
N7	f	23.3	1.70
N8	m	24.0	1.87
N9	m	26.6	1.83
N10	f	24.9	1.65
N11	f	25.0	1.56
N12	f	24.5	1.63
N13	f	22.6	1.63
N14	f	25.4	1.59
N15	m	24.1	1.82
N16	m	25.1	1.68
N17	f	23.5	1.66
N18	m	26.9	1.73
N19	m	28.4	1.68
N20	f	24.2	1.66
N21	m	21.9	1.78
N22	m	26.9	1.80
N23	f	27.3	1.69
N24	f	21.3	1.53
N25	f	22.1	1.68
N26	f	21.0	1.57
N27	m	28.5	1.84
N28	m	30.0	1.78
N29	m	22.0	1.79
N30	m	26.5	1.72
N31	f	20.8	1.60
N32	f	23.4	1.60
N33	m	24.8	1.72
N34	f	27.7	1.70
N35	f	26.7	1.76
N36	m	27.8	1.77
N37	f	21.4	1.56
N38	m	23.3	1.78

11/12/2009

Dr Derrick White
Research Fellow
Leeds Institute for Molecular Disease
Section of Musculoskeletal Disease
2nd Floor
Chapel Allerton Hospital

Research & Development
Leeds Teaching Hospitals NHS Trust

34 Hyde Terrace
Leeds
LS2 9LN

Tel: 0113 392 2878
Fax: 0113 392 6397

r&d@leedsth.nhs.uk
www.leedsteachinghospitals.com

Dear Dr White

Re: LTHT R&D Approval of: Leg length discrepancy following total hip arthroplasty.
LTHT R&D Number: RR09/9076
CLRN ID: 23474/WY
MREC: 09/H1307/63

I confirm that this study has R&D approval and the study may proceed at The Leeds Teaching Hospitals NHS Trust (LTHT). This organisational level approval is given based on the information provided in the documents listed below.

In undertaking this research you must comply with the requirements of the *Research Governance Framework for Health and Social Care* which is mandatory for all NHS employees. This document may be accessed on the R&D website http://www.leedsth.nhs.uk/sites/research_and_development/

R&D approval is given on the understanding that you comply with the requirements of the *Framework* as listed in the attached sheet "Conditions of Approval".

If you have any queries about this approval please do not hesitate to contact the R&D Department on telephone 0113 392 2878.

Indemnity Arrangements

The Leeds Teaching Hospitals NHS Trust participates in the NHS risk pooling scheme administered by the NHS Litigation Authority 'Clinical Negligence Scheme for NHS Trusts' for: (i) medical professional and/or medical malpractice liability; and (ii) general liability. NHS Indemnity for negligent harm is extended to researchers with an employment contract (substantive or honorary) with the Trust. The Trust only accepts liability for research activity that has been managerially approved by the R&D Department.

Chairman Martin Buckley Chief Executive Maggie Boyle

The Leeds Teaching Hospitals incorporating: Chapel Allerton Hospital Leeds Dental Institute Seacroft Hospital
St James's University Hospital The General Infirmary at Leeds Wharfedale Hospital

The Trust therefore accepts liability for the above research project and extends indemnity for negligent harm to cover you as principal investigator and the researchers listed on the Site Specific Information form. Should there be any changes to the research team please ensure that you inform the R&D Department and that s/he obtains an employment contract with the Trust if required.

Yours sincerely



Dr D R Norfolk
Associate Director of R&D

Approved documents

The documents reviewed and approved are listed as follows

<i>Document</i>	<i>Version</i>	<i>Date of document</i>
NHS R&D Form	2.2	02/09/09
SSI Form	2.2	24/11/09
Directorate Approval		04/11/09
Protocol	0.4	17/07/09
REC Letter confirming favourable opinion		15/10/09
Insurance letter		02/10/08
Patient information sheet (MREC Approved) - control	0.4	17/07/09
Consent form (MREC Approved)-Control	0.5	20/10/09
Patient information sheet (MREC Approved) - group i	0.4	17/07/09
Consent form (MREC Approved)-group I to iii	0.5	20/10/09
Patient information sheet (MREC Approved) - group ii & iii	0.4	17/07/09
Oxford Hip Score (MREC Approved)		April 09
Health Questionnaire (MREC Approved)		April 09
Leg length Score (MREC Approved)		-

Participant Information Sheet (control group)

Leg length discrepancy following total hip arthroplasty.

You are being invited to take part in a research study. The study is making an assessment of lower limb function. This means we are using special equipment to look at how people walk.

Before you decide, it is important for you to understand why the research is being done and what it will involve. Please take time to read the following information carefully and discuss it with your friends, relatives, and GP if you would like. Phone us if there is anything that is not clear or you would like further information. Take time to decide whether or not you wish to take part.

Q: What is the purpose of this study?

A: This study is looking at how well people walk after hip surgery.

Q: Why have I been chosen?

A: You have been asked to take part because we would like to compare information from people who have no walking problems with data we are collecting from patients who do have walking problems after hip surgery. Information on the way you walk will help researchers decide how best to look after some individuals before and after hip surgery.

Q: Do I have to take part?

A: It is up to you to decide if you would like to take part. If you decide to take part you are still free to withdraw at any time without giving a reason. A decision to withdraw at any time, or decision not to take part, will not affect the standard of care of the person you are accompanying or any care that you may receive in the future.

Q: What will happen if I choose to take part?

A: If you decide that you want to take part, the researchers will ask you to complete some questions. These questions will take no more than 10 minutes to complete.

Once the questions are complete the researchers will take some clinical measurements and look at how you walk using special equipment. This part should take no more than 30 minutes in total.

The equipment uses a number of cameras, the cameras record pictures of reflective markers that are attached to you. These markers are fixed around your feet, legs and pelvis with the help of special tape. For the cameras to 'see' all of the markers the researchers suggest that you wear shorts and close fitting clothes during your visit to the gait laboratory. There is somewhere private for you to get changed in the gait laboratory.

With the markers in place you will be asked to walk short distances. Once the cameras have recorded how you walk you may be asked to walk a short distance on a special walkway that also examines how you walk.

Q: What do I have to do?

A: You will be asked to complete some questionnaires, get changed, have a number of measurements taken, have a number of markers fixed to you and you will be asked to walk a short distance a number of times.

Q: What are the possible disadvantages and risks of taking part?

A: Apart from the time taken (which should be no more than 40 minutes) there are no disadvantages of taking part in this study. However, in the unlikely event of you being dissatisfied with the way the researchers have behaved you can contact Dr Anthony Redmond on 0113 3924914.

If you are harmed by taking part in this research project, there are no special compensation arrangements. If you are harmed due to someone's negligence, the normal NHS indemnity arrangements will apply. Regardless of this, if you wish to complain about any aspect of the way you have been approached or treated during the course of this study the normal National Health Service complaints mechanism will be available to you.

Q: What are the possible benefits of taking part?

A: There are no direct benefits to you taking part. However this research is very important to help us learn more about how people walk after hip surgery.

Q: Will my taking part in this study be confidential?

A: All information collected will be strictly confidential. Any information will have your name and address removed so you can not be recognised from it.

Q: What will happen to the results of this research study?

A: Once completed the results of this study will be published in appropriate medical journals and presented at conferences where the information can be used by other clinicians to improve their treatment of people who have had or are about to undergo hip replacement surgery.

All published material will be anonymous, with all names and addresses removed so you will not be identifiable in any way.

Q: Who is organising and funding this study?

A: This study is being funded by the LMBRU (Leeds Musculoskeletal Biomedical Research Unit) which has been established by the NIHR (National Institute for Health Research). The LMBRU has been set up to undertake translational clinical research in priority areas of disease: Leeds was identified as an international leader in musculoskeletal disease research.

Contact for further information:

Should you wish to discuss any aspect of this project please contact;
Dr Derrick White on 0113 3923064 or Dr Anthony Redmond on 0113 3924914.

**Thank you very much for taking the time to read this information sheet.
Please keep a copy of this information sheet with your signed consent form**

Participant Information Sheet (group ii & iii)

Leg length discrepancy following total hip arthroplasty

You are being invited to take part in a research study. The study is making an assessment of lower limb function. This means we are using special equipment to look at how people walk.

Before you decide, it is important for you to understand why the research is being done and what it will involve. Please take time to read the following information carefully and discuss it with your friends, relatives, and GP if you would like. Phone us if there is anything that is not clear or you would like further information. Take time to decide whether or not you wish to take part.

Q: What is the purpose of this study?

A: This study is looking at how well people walk after hip surgery.

You will not be required to undergo any treatment that is different to what you would normally do. You will be asked to answer some short questions and to walk short distances along special walkways that measure how you walk.

Q: Why have I been chosen?

A: You have been asked to take part because we would like to compare information from people who have no walking problems with data we are collecting from patients who do have walking problems after hip surgery. Information on the way you walk, along with the x-ray images of your hip/pelvis will help researchers decide how best to look after some individuals before and after hip surgery.

Q: Do I have to take part?

A: It is up to you to decide if you would like to take part. If you decide to take part you are still free to withdraw at any time without giving a reason. A decision to withdraw at any time, or decision not to take part, will not affect the standard of care you receive.

Q: What will happen if I choose to take part?

A: If you decide that you want to take part, the researchers will ask you to complete some questions. These questions will take no more than 10 minutes to complete.

Once the questions are complete the researchers will take some clinical measurements and look at how you walk using special equipment. This part should take no more than 30 minutes in total.

The equipment uses a number of cameras, the cameras record pictures of reflective markers that are attached to you. These markers are fixed around your feet, legs and pelvis with the help of special tape. For the cameras to 'see' all of the markers the researchers suggest that you wear shorts and close fitting clothes during your visit to the gait laboratory. There is somewhere private for you to get changed in the gait laboratory.

With the markers in place you will be asked to walk short distances. Once the cameras have recorded how you walk you may be asked to walk a short distance on a special walkway that also examines how you walk.

The researchers will also review the x-ray images of your hip/pelvis. You will not be asked to have any extra x-rays of your hip or pelvis.

Q: What do I have to do?

A: You will be asked to complete some questionnaires, get changed, have a number of measurements taken, have a number of markers fixed to you and you will be asked to walk a short distance a number of times.

Q: What are the possible disadvantages and risks of taking part?

A: Apart from the time taken (which should be no more than 40 minutes) there are no disadvantages of taking part in this study. However, in the unlikely event of you being dissatisfied with the way the researchers have behaved you can contact Dr Anthony Redmond on 0113 3924914.

If you are harmed by taking part in this research project, there are no special compensation arrangements. If you are harmed due to someone's negligence, the normal NHS indemnity arrangements will apply. Regardless of this, if you wish to complain about any aspect of the way you have been approached or treated during the course of this study the normal National Health Service complaints mechanism will be available to you.

Q: What are the possible benefits of taking part?

A: There are no direct benefits to you taking part. However this research is very important to help us learn more about how people walk after hip surgery.

Q: Will my taking part in this study be confidential?

A: All information collected will be strictly confidential. Any information will have your name and address removed so you can not be recognised from it.

Q: What will happen to the results of this research study?

A: Once completed the results of this study will be published in appropriate medical journals and presented at conferences where the information can be used by other clinicians to improve their treatment of people who have had or are about to undergo hip replacement surgery.

All published material will be anonymous, with all names and addresses removed so you will not be identifiable in any way.

Q: Who is organising and funding this study?

A: This study is being funded by the LMBRU (Leeds Musculoskeletal Biomedical Research Unit) which has been established by the NIHR (National Institute for Health Research). The LMBRU has been set up to undertake translational clinical research in priority areas of disease: Leeds was identified as an international leader in musculoskeletal disease research.

Contact for further information:

Should you wish to discuss any aspect of this project please contact;
Dr Derrick White on 0113 3923064 or Dr Anthony Redmond on 0113 3924914.

**Thank you very much for taking the time to read this information sheet.
Please keep a copy of this information sheet with your signed consent form**

Leg length discrepancy following total hip arthroplasty.

Lead Researcher: A. Redmond

PARTICIPANT CONSENT FORM

*Please
initial box
to confirm*

1. I confirm that I have read and understand the Patient Information Sheet for the above study, dated 15th July 2009. I have had the opportunity to consider the information, ask questions and have the questions answered satisfactorily.
2. I understand that I am free to withdraw from the study at any time without having a reason and without my medical care or legal rights being affected.
3. I agree to take part in the above study.
4. I give permission for the data collected in this study to be used in this and future related studies.

Name of Patient _____ Date _____

Signature _____

Name of Person taking consent _____ Date _____

Signature _____

Leg length discrepancy following total hip arthroplasty

Lead Researcher: A. Redmond

PARTICIPANT CONSENT FORM

*Please
initial box
to confirm*

1. I confirm that I have read and understand the Patient Information Sheet for the above study, dated 17^h July 2009. I have had the opportunity to consider the information, ask questions and have the questions answered satisfactorily.
2. I understand that I am free to withdraw from the study at any time without having a reason and without my medical care or legal rights being affected.
3. I understand that relevant sections of my medical notes, including x-rays, CT scans and data collected during the study may be looked at by individuals from the University of Leeds, from regulatory authorities or from the NHS Trust, where it is relevant to my taking part in this research. I give permission for these individuals to have access to my records.
4. I agree to take part in the above study.
5. I give permission for the data collected in this study to be used in this and future related studies.

Name of Patient _____ Date _____

Signature _____

Name of Person taking consent _____ Date _____

Signature _____

17 Appendix III

Performance, Governance and Operations
 Research & Innovation Service
 Charles Thackrah Building
 101 Clarendon Road
 Leeds LS2 9LJ
 Tel: 0113 343 4873
 Email: j.m.blajkie@leeds.ac.uk



UNIVERSITY OF LEEDS

Ammar Wahid
 School of Mechanical Engineering
 University of Leeds
 Leeds, LS2 9JT

**MEEC Faculty Research Ethics Committee
 University of Leeds**

22 December 2016

Dear Ammar

Title of study **The Biomechanical Effects of Marker Placement and EMG
 for Gait Analysis – on Student volunteers only**
Ethics reference **MEEC 12-004**

I am pleased to inform you that the application listed above has been reviewed by the MaPS and Engineering joint Faculty Research Ethics Committee (MEEC FREC) and following receipt of your response to the Committee's initial comments, I can confirm a favourable ethical opinion as of the date of this letter. The following documentation was considered:

<i>Document</i>	<i>Version</i>	<i>Date</i>
MEEC 12-004 2012 November MEEC 12-004 Committee Provisional.doc	1	05/11/12
MEEC 12-004 2012 ethics.doc	1	05/11/12
MEEC 12-004 Health and Safety Wahid 2012.doc	1	05/11/12
MEEC 12-004 sample e-mail.docx	1	05/11/12
MEEC 12-004 Example_participant_consent_form.doc	2	05/11/12
MEEC 12-004 Information for Subjects_consent_screen.docx	2	05/11/12
MEEC 12-004 e-mail to be sent around.docx	1	22/10/12
MEEC 12-004 Health and Safety Wahid 2012.doc	1	22/10/12
MEEC 12-004 UNIVERSITY OF LEEDS MEDIC QU ver 02.docx	1	22/10/12
MEEC 12-004 2012 ethics.doc	1	22/10/12
MEEC 12-004 2012 AMMAR WAHID Ethical_Review_Form Stewart Messenger.doc	1	01/10/12

Please notify the committee if you intend to make any amendments to the original research as submitted at date of this approval, including changes to recruitment methodology. All changes must receive ethical approval prior to implementation. The amendment form is available at

http://researchsupport.leeds.ac.uk/index.php/academic_staff/good_practice/managing_approved_projects-1/applying_for_an_amendment-1.

Please note: You are expected to keep a record of all your approved documentation, as well as documents such as sample consent forms, and other documents relating to the study. This should be kept in your study file, which should be readily available for audit purposes. You will be given a two week notice period if your project is to be audited. There is a checklist listing examples of documents to be kept which is available at

http://researchsupport.leeds.ac.uk/index.php/academic_staff/good_practice/managing_approved_projects-1/ethics_audits-1.

Yours sincerely

Jennifer Blaikie

Senior Research Ethics Administrator, Research & Innovation Service

On behalf of Professor Gary Williamson, Chair, [MEEC FREC](#)

CC: Student's supervisor(s)

INFORMATION FOR PARTICIPANTS

Title of the study: The Biomechanical Effects of Marker Placement on Gait Analysis

Introduction

We are inviting you to take part in a research study. Before you decide whether you would like to take part, it is important for you to understand why the research is being done and what it will involve. Please take time to read the following information carefully and discuss it with friends and relatives if you wish. Ask us if there is anything that is not clear, or if you would like more information (a contact number and address are at the end of this information sheet). Take time to decide whether or not you wish to take part.

Background to and purpose of the study

Research requires the use of a gait laboratory, used for examining the walking pattern of an individual, in a clinical and/or academic setting. The volunteer will have fluorescent spherical markers placed at various joints from the pelvis down to the ankle. Different sets/types of marker sets will be used with markers being placed at various locations.

The volunteer will firstly stand static in a comfortable position wearing markers whilst their arms are spread out. They will then walk down the gait platform (a set walking path) and will place their foot purposely onto a force platform which will be located along the walk-way. This will be repeated between 6-12 times with the individual alternating placing their left and right foot onto the platform during each repeat trial. The spherical markers will be picked up by infrared cameras located at specific points across the room. This will then allow a 3-D image to be developed onto the technicians computer showing the movement of the volunteer whilst walking down the pathway, together with their pose when static. The data will then be exported into a software program for analysis of hip motions and loads during walking. Data will be anonymised and will not contain any video files for the volunteer.

Am I a suitable participant for the study?

The study will analyse the gait of healthy individuals who are free from musculoskeletal disease. There are no other suitability criteria for the study.

Do I have to take part?

Participants will have 2 weeks from volunteering to taking part and can withdraw at any time. If following the study students no longer wish for their data to be used for research it will be discarded through the deletion of all relevant files.

What will happen if I take part?

Volunteers will visit the gait laboratory at the Miall Building in the University of Leeds and/or the laboratory at Chapel Allerton Hospital. Travel to the former will be on foot whilst the latter will use a Taxi service. Students will have to change into clothing provided by the department (t-shirt and shorts) and walk barefoot across a gait platform. The volunteers will however be required to bring suitable footwear i.e trainers. The joints from the hip down to the ankle will have fluorescent markers placed onto them which will be picked up by infrared cameras placed around the laboratory.

The data produced will be in regards to joint motion and moments in all three planes for the pelvis, hip, knee and ankle together with hip joint forces. Data will also be produced with regards to temporal-spatial parameters (i.e. gait velocity, stride length, cycle time). All studies are non-invasive, will be anonymised and will not contain any video files of the student. Participants will have 2 weeks from volunteering to taking part and can withdraw at any time before or after the study

What do I have to do?

See above

How often will the test be?

The test will be carried out only once in the Miall Building and/or at Chapel Allerton Hospital. On both occasions multiple sources of data will be acquired through the volunteer repeating the walk down the gait platform between 6-12 times

What are the possible benefits of taking part in this study?

Volunteers will be able to learn about the clinical measuring techniques carried out in the gait laboratory and the uncertainty/multiple sources of error which are unavoidable in motion analysis. As many of the student volunteers will be a part of the iMBE (Institute of Medical and Biological Engineering), the research could aid in their understanding of joint motion and may aid in their research projects.

What happens if something goes wrong?

Both laboratories have a healthy and safety protocol which will be adhered to in case of an accident or an emergency

Will taking part in this study be kept confidential?

The data outlined by the 1998 Data Protection Act in terms of sensitive information will not be recorded. The students volunteering will have their names anonymised through having all data recorded in terms of patient number and trial number. The data will be stored on a CD and be accessible to the research instigator and the supervisors

What will happen to the results of the study?

This study will investigate the differences in joint motions, moments and forces. Results will be used to analyse the variations present with the use of different marker systems together with assessing the effects of marker misplacement. These will form a part of a PhD thesis and may be published in medical/biomechanics journals and/or presented to experts at conferences in the future.

Contact for further information

Ammar Wahid Room
X302
iMBE
School of Mechanical Engineering
Department of Engineering
mnaw@leeds.ac.uk

Consent Form

Title: The Biomechanical Effects of Marker Placement on Gait Analysis

Please delete as applicable

- | | | |
|---|--|--------|
| 1 | I have read the Participant Information Sheet. | Yes/No |
| 2 | I have had the opportunity to ask questions and discuss the research study. | Yes/No |
| 3 | I am satisfied with the answers to my questions. | Yes/No |
| 4 | I have received enough information about this study. | Yes/No |
| 5 | I have spoken to Mr Ammar Wahid | Yes/No |
| 6 | I understand that I am free to withdraw from the study at any time without giving reason and without affecting my future care. | Yes/No |
| 7 | I agree to take part in this research study. | Yes/No |

Signature.....

Name (block capitals).....

Date.....

Signature of person taking consent.....

Name (block capitals).....

Date.....

Screening Questionnaire

Please read the following questions very carefully and answer each one honestly by deleting as applicable.

- | | | |
|----|---|--------|
| 1 | Has your doctor ever said that you have a heart condition <u>and</u> that you should only do physical activity recommended by a doctor? | Yes/No |
| 2 | Do you feel pain in your chest when you do physical activity? | Yes/No |
| 3 | In the past month, have you had chest pain when you were not doing physical activity? | Yes/No |
| 4 | Has your doctor ever said that you have high blood pressure? | Yes/No |
| 5 | Does exercise cause you to feel dizzy or faint or do you ever lose consciousness? | Yes/No |
| 6 | Do you ever have nausea when you exercise? | Yes/No |
| 7 | Do you ever feel short of breath when you exercise? | Yes/No |
| 8 | Do you have any bone, joint, or muscular problem(s) that could be made worse by exercising? | Yes/No |
| 9 | Is your doctor currently prescribing drugs for you? | Yes/No |
| 10 | Do you smoke? | Yes/No |
| 11 | Do you drink excessive amounts of alcohol on a regular basis? | Yes/No |
| 12 | Do you know of any other reason why you should not do vigorous physical activity? | Yes/No |

I have read, understood and completed the questionnaire to the best of knowledge

Name _____

Signature _____

Date _____